Technische Universität Kaiserslautern
Fachbereich Chemie
Fachrichtung Lebensmittelchemie / Toxikologie

Impact of 'Dioxins' on Gene Expression In Mouse Liver *in vivo*, and in both Rat Liver Cells and Human Blood Cells *In Culture*.

Vom Fachbereich Chemie der Technischen Universität Kaiserslautern
zur Verleihung des akademischen Grades
„Doktor der Naturwissenschaften“
Genehmigte

Dissertation
(D386)

vorgelegt von
Diplom-Lebensmittelchemikerin
Sylke Neser

Betreuer der Arbeit: Prof. Dr. Dr. Dieter Schrenk

Kaiserslautern 2014

Eröffnung des Promotionsverfahrens: 27. Juni 2012

Tag der wissenschaftlichen Aussprache: 7. November 2014

Promotionskommission:

Vorsitzender: Prof. Dr. H. Sitzmann

1. Berichterstatter: Prof. Dr. Dr. D. Schrenk

2. Berichterstatter: Prof. Dr. M. van den Berg

Der experimentelle Teil der vorliegenden Arbeit entstand im Zeitraum von Mai 2009 bis Oktober 2012 im Fachbereich Chemie, Fachrichtung Lebensmittelchemie und Toxikologie an der Technischen Universität Kaiserslautern im Arbeitskreis von Prof. Dr. Dr. Dieter Schrenk.

Table of Contents

Index of figures

Index of tables

Abbreviations

A-value	signal intensity
ADME	absorption, distribution, metabolism, and excretion
AHH	aryl hydrocarbon hydroxylase
AhR	aryl hydrocarbon receptor
AhRR	aryl hydrocarbon receptor repressor
ALDH	aldehyde dehdrogenase
ANOVA	one-way analysis of variance
ARNT	aryl hydrocarbon nuclear translocator
ATSDR	Agency for Toxic Substances and Disease Registry
BCA	bicinchoninic acid
bHLH/PAS	basic-helix-loop-helix Per-ARNT-Sim
BMDC	bone marrow-derived dendritic cell
BSA	bovine serum albumin
bw	body weight
CAR	constitutive androstane receptor
CDU	collagenase digestion units
CI	confidence interval
CLRTAP	Convention on Long-Range Transboundary Air Pollution
CoMFA	comparative molecular field analysis
CT	threshold cycle
CTL	cytotoxic T lymphocyte
Cy	cyanine
CYP	cytochrome P450-dependent monooxygenase
DC	dendritic cell
DL	dioxin-like
DPBS	Dulbecco’s phosphate-buffered saline
EAE	experimental autoimmune encephalomyelitis
EC	effective concentration
EROD	7-ethoxyresorufin-*O*-deethylase
FACS	fluorescence-activated cell sorting
FDR	false discovery rate
FSC	forward scatter
GST	glutathion *S*-transferase
GIT	gastrointestinal tract
GO	gene ontology
HDAC	histone deacetylase
HFM	hepatocyte functional medium
HSD	hydroxysteroid dehydrogenase
HSM	hepatocyte seeding medium
i.p.	*intraperitoneal*
i1-4	individual(s) 1-4
IARC	International Agency for Research on Cancer
IBWF	Institute of Biotechnology and Drug Research
IDO	indoleamine 2,3-dioxygenase
IEB	isotonic extraction buffer
IEL	intraepithelial lymphocytes
Ig	immunoglobulin G
IRAS	Institute for Risk Assessment Sciences
JECFA	Joint FAO/WHO Expert Committee on Food Additives

lfc	logarithmic (log 2) fold change
LOAEL	lowest observed adverse effect level
LPS	lipopolysaccharide
MHC	major histocompatibility complex
NDL	non dioxin-like
NLS	nuclear localization sequence
OR	odds ratio
PAGE	polyacrylamide gel electrophoresis
PAH	polycyclic aromatic hydrocarbon
PBMC	peripheral blood mononuclear cell
PBS^{--}	phosphate buffered saline (without Mg^{2+} and Ca^{2+})
PCA	principal component analysis
PCB	polychlorinated biphenyls
PCDD	polychlorinated dibenzo-*p*-dioxins
PCDF	polychlorinated dibenzofurans
PCR	polymerase chain reaction
PHA	phytohemagglutinin
POP	persistent organic pollutant
PPAR	peroxisome proliferator-activated receptor
PRH	primary rat hepatocytes
PTMI	provisional tolerable monthly intake
PVDF	polyvinylidene difluoride
PXR	pregnane X receptor
QRT-PCR	quantitative real-time polymerase chain reaction
QSAR	quantitative structure-activity relationship
REP	relative effect potency
RFU	relative fluorescence unit
ROS	reactive oxygen species
RR	relative risk
RXR	retinoid X receptor
SCF	Scientific Committee on Food
SD	standard deviation
SSC	sideward scatter
SULT	sulfotransferase
t-TWI	temporary tolerable weekly intake
TBS	Tris-buffered saline
TBS-T	Tris-buffered saline with Tween-20
TDI	tolerable daily intake
TDO	tryptophan-2,3-dioxygenase
TEF	toxic equivalency factor
TEQ	toxic equivalent
Th cell	helper T cell
TIPARP	TCDD-inducible poly(ADP-ribose) polymerase
TLR	Toll-like receptor
Treg	regulatory T cell
TWI	tolerable weekly intake
UGT	uridine 5'-diphospho (UDP)-glucuronosyltransferase
UNECE	United Nations Economic Commission for Europe
UNEP	United Nations Environment Programme
WB	Western Blot
WHO	World Health Organization
XRE	xenobiotic responsive element

Abstract

‘Dioxin-like’ (DL) compounds occur ubiquitously in the environment. Toxic responses associated with specific dibenzo-*p*-dioxins (PCDDs), dibenzofurans (PCDFs), and polychlorinated biphenyls (PCBs) include dermal toxicity, immunotoxicity, liver toxicity, carcinogenicity, as well as adverse effects on reproduction, development, and endocrine functions. Most, if not all of these effects are believed to be due to interaction of these compounds with the aryl hydrocarbon receptor (AhR).
With tetrachlorodibenzo-*p*-dioxin (TCDD) as representatively most potent congener, a toxic equivalency factor (TEF) concept was employed, in which respective congeners were assigned to a certain TEF-value reflecting the compound’s toxicity relative to TCDD’s.
The EU-project ‘SYSTEQ’ aimed to develop, validate, and implement human systemic TEFs as indicators of toxicity for DL-congeners. Hence, the identification of novel quantifiable biomarkers of exposure was a major objective of the SYSTEQ project.
In order to approach to this objective, a mouse whole genome microarray analysis was applied using a set of seven individual congeners, termed the ‘core congeners’. These core congeners (TCDD, 1-PeCDD, 4-PeCDF, PCB 126, PCB 118, PCB 156, and the non dioxin-like PCB 153), which contribute to approximately 90% of TEQs in the human food chain, were further tested *in vivo* as well as *in vitro*. The mouse whole genome microarray revealed a conserved list of differentially regulated genes and pathways associated with ‘dioxin-like’ effects.

A definite data-set of *in vitro* studies was supposed to function as a fundament for a probable establishment of novel TEFs. Thus, CYP1A induction measured by EROD activity, which represents a sensitive and yet best known marker for dioxin-like effects, was used to estimate potency and efficacy of selected congeners. For this study, primary rat hepatocytes and the rat hepatoma cell line H4IIE were used as well as the core congeners and an additional group of compounds of comparable relevance for the environment: 1,6-HxCDD, 1,4,6-HpCDD, TCDF, 1,4-HxCDF, 1,4,6-HpCDF, PCB 77, and PCB 105.

Besides, a human whole genome microarray experiment was applied in order to gain knowledge with respect to TCDD’s impact towards cells of the immune system. Hence, human primary blood mononuclear cells (PBMCs) were isolated from individuals and exposed to TCDD or to TCDD in combination with a stimulus (lipopolysaccharide (LPS), or phytohemagglutinin (PHA)). A few members of the AhR-gene batterie were found to be regulated, and minor data with respect to potential TCDD-mediated immunomodulatory effects were given. Still, obtained data in this regard was limited due to great inter-individual differences.

1

Theoretical Background

1.1. Aryl hydrocarbon Receptor (AhR)

Induction of drug-metabolizing enzymes due to polycyclic aromatic hydrocarbon (PAH)-exposure has been reviewed earlily in literature (Nebert and Gelboin, 1968a; Nebert and Gelboin, 1968b; Nebert *et al.*, 1977; Nebert *et al.*, 1975). Verified by specific binding of [^{3}H]TCDD to hepatic cytosol from C57BL/6J mice, Poland *et al.* (1976) ascertained that aromatic hydrocarbon responsiveness was determined by a single locus, providing evidence for the presence of a ligand-dependent receptor, and proposing the requirement of a receptor-ligand-complex initiating the expression of respective genes (Poland *et al.*, 1976). Within this study, the authors found an overall correspondence between potencies of 23 tested halogenated dibenzo-*p*-dioxins and dibenzofurans to induce aryl hydrocarbon hydroxylase (AHH) *in vivo* and their affinities for the proposed receptor which became known as aryl hydrocarbon receptor (AhR).

1.1.1. AhR-ligands

Halogenated aromatic hydrocarbons (HAHs) like polyhalogenated dibenzo-*p*-dioxins (PCDDs), dibenzofurans (PCDFs), and biphenyls (PCBs), as well as polycyclic aromatic hydrocarbons (PAHs) such as dibenz[*a*,*h*]anthracene, benzo[*a*]pyrene, 3-methylcholanthrene, or chrysene, accomplish high affinity for AhR (Bandiera *et al.*, 1982; Bandiera *et al.*, 1984; Bigelow and Nebert, 1982; Okey and Vella, 1982; Sawyer *et al.*, 1983). Further synthetic AhR-ligands are *β*-naphthoflavone, or carbaryl, for instance (Denison *et al.*, 1998; Sugihara *et al.*, 2008). Exemplary chemicals exhibiting lower AhR-affinity are *N*,*N*'-Diphenyl-*p*-phenylendiamine, 2-Mercapto-5-methoxybenzimidazole, or primaquine (Backlund and Ingelman-Sundberg, 2004; Sugihara *et al.*, 2008). To date, several naturally occurring and even endogenous AhR-ligands are known. Among these are indoles (indole-3-carbinol, tryptophan, e.g.), arachidonic acid metabolites (prostaglandin G2, e.g.), and tetrapyrroles (bilirubin, biliverdin) (Bjeldanes *et al.*, 1991; Heath-Pagliuso *et al.*, 1998; Phelan *et al.*, 1998; Seidel *et al.*, 2001). Notably, yet found natural ligands bear comparable low affinities for the AhR, whereas some metabolites of weak agonists (indole-3-carbinol, tryptophan) were found to yield higher affinities, exemplifying indolo[3,2-*b*]carbazole (ICZ) with a relative binding affinity of $3.7*10^{-2}$ compared to TCDD's relative binding affinity for the receptor, which was detemined in the course of Bjeldanes and co-workers' study using AhR prepared from

mouse livers (Bjeldanes *et al.*, 1991; Perdew and Babbs, 1991). Recently, the tryptophan metabolites kynurenine and kynurenic acid were as well identified to be endogenous AhR-ligands (DiNatale *et al.*, 2010; Opitz *et al.*, 2011). However, for several weak ligands, which were reported to induce AhR-dependent gene expression, varying results were determined regarding their ability to competitively bind the AhR. Omeprazole, e.g., for which Backlund and Ingelman-Sundberg (2004) failed to determine its potential AhR-binding affinity, did competitively bind the receptor in a study by Hu *et al.* (2007).

Quantitative structure-activity relationship (QSAR) analyses propose steric and lipophilic properties, as well as chemical softness, electrophilicity index, hydrogen bonding capacity, and dispersion and electrostatic interaction are crucial properties attributing AhR-binding affinities of chemicals (Arulmozhiraja and Morita, 2004; Kafafi *et al.*, 1992a/b; Poso *et al.*, 1993; Safe *et al.*, 1986; Waller and McKinney, 1992; Zhao *et al.*, 2008b). Chlorination patterns of HAHs affect their ability to interact with the receptor. Laterally chlorinated molecules possess highest polarizabilities along the lateral direction and exhibit maximum AhR-binding properties (Kafafi *et al.*, 1993; Mhin *et al.*, 2002). By comparative molecular field analysis (CoMFA), a threedimensional QSAR paradigm, Waller and McKinney determined the AhR binding site size (maximal van der Waal's dimensions) to measure 14 Å x 12 Å x 5 Å (Waller and McKinney, 1995).

1.1.2. Transcriptional activation by the AhR

In the organism, the AhR is expressed in many types of cells and tissues with considerable expression levels found in liver, lung, and thymus (De Montellano *et al.*, 2005). AhR function is proposed to be connected to toxicological as well as physiological functions. In this regard, the AhR is involved in hepatic growth and development, teratogenesis, immune function, cell proliferation and differentiation, nephrogenesis, apoptosis, adipogenesis, tumor promotion, and reproductive function (Alexander *et al.*, 1996; Chopra *et al.*, 2009; Chopra *et al.*, 2010a; Falahatpisheh *et al.*, 2011; Fernandez-Salguero *et al.*, 1995; Hernández-Ochoa *et al.*, 2009; Ma and Whitlock, 1996; Mimura *et al.*, 1997; Moennikes *et al.*, 2004; Puga *et al.*, 2009; Schmidt *et al.*, 1996).

The mechanism for transcriptional activation by the AhR is demonstrated schematically in figure 1.

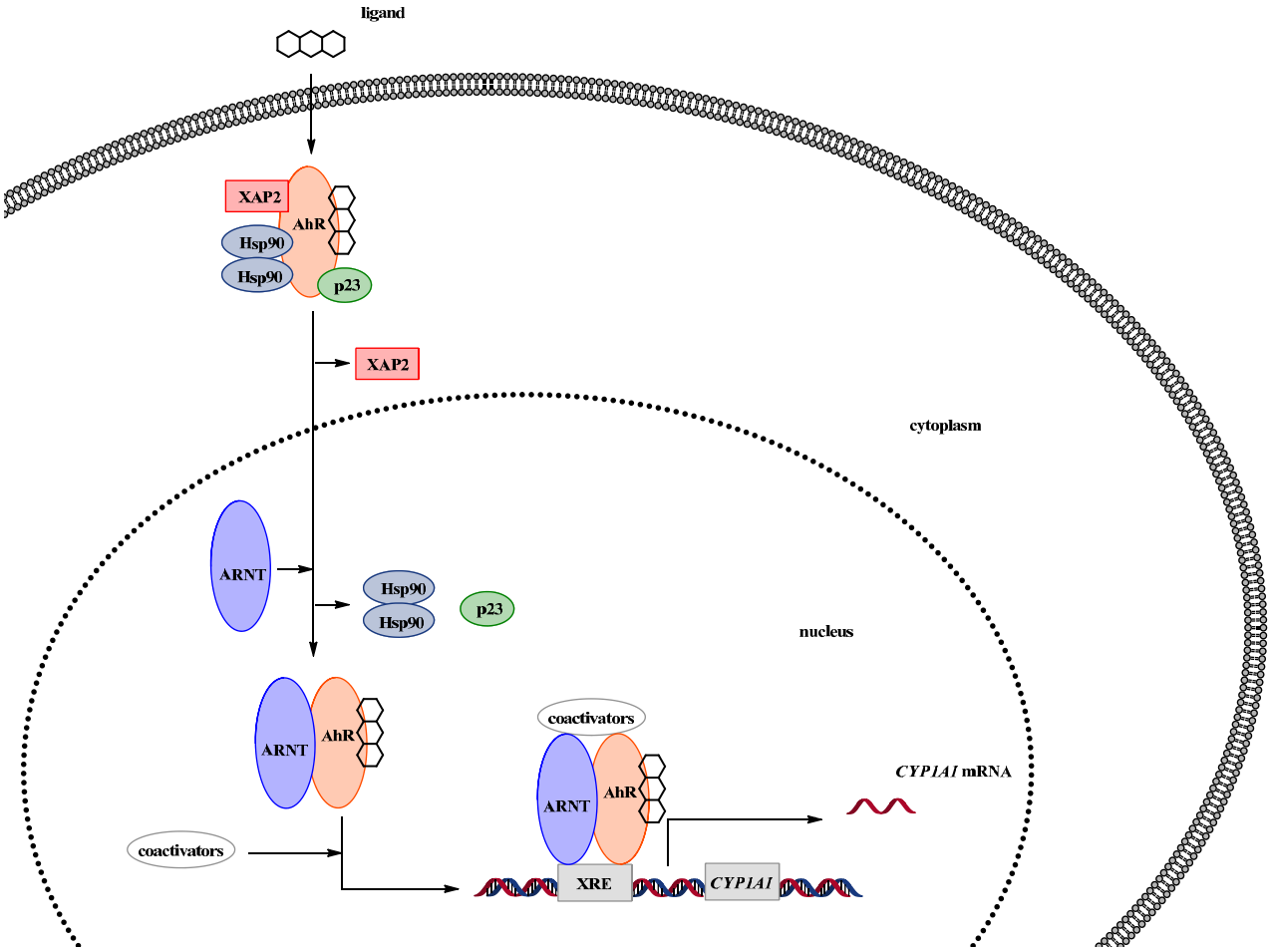

Figure 1: Transcriptional activation by the AhR, schematically demonstrated (according to Denison *et al.*, 2011; Kawajiri and Fujii-Kuriyama, 2007).

The AhR is a ligand-activated basic-loop-helix (bHLH)/Periodic (PER)-aryl hydrocarbon receptor nuclear translocator (ARNT)-single minded (SIM) (PAS) transcription factor. In a latent state, the AhR is associated with a 90-kDa heat shock protein (HSP90) dimer, the AhR interacting protein (AIP; also: immunophilin-like hepatitis B virus X-associated protein 2 (XAP2), or Ah receptor-associated protein (ARA9)), and the co-chaperone phosphoprotein p23 in cytoplasm (Carver and Bradfield, 1997; Carver *et al.*, 1998; Kazlauskas *et al.*, 1999; Ma and Whitlock, 1997; Meyer *et al.*, 1998; Nair *et al.*, 1996; Perdew, 1988). The potentially inducing compound diffuses across the plasma membrane and ligates the AhR. Upon ligand-binding, the AhR is presumed to undergo a conformational change, which exposes its N-terminal nuclear localization sequence (NLS) and leads to translocation of the complex into the nucleus (Ikuta *et al.*, 1998; Ikuta *et al.*, 2000). In the nucleus, chaperone proteins are displaced by ARNT, and the resulting ligand-AhR/ARNT-complex is generated. Following recruitment of coactivators like steroid receptor coactivator 1 (SCR-1), nuclear coactivator 2, SRC-2 (NcoA2), p300/CBP cointagrator protein, SRC-3 (p/CIP), and

receptor-interacting protein 140 (RIP 140), engenders the transcriptional activator complex (reviewed in Hankinson, 2005). The AhR/ARNT-complex specifically recognizes nucleotide sequences referred to as xenobiotic-responsive elements (XREs; also: dioxin-responsive elements (DREs)), which contain the core sequence 5'-*TNG*CGTG-3' (Bacsi *et al.*, 1995; Denison *et al.*, 1988; Shen and Whitlock, 1992). The transcriptional activator complex binds to and activates transcription from XRE-containing promoters, for which the gene encoding cytochrome P450 1A1 (CYP1A1) represents one of the best characterized. Expression of *CYP1A1* is regulated through at least three kinds of regulatory DNA elements: the TATA box sequence, XREs, and the basic transcription element (BTE), a GC box sequence located in the gene's proximal promoter (Kobayashi *et al.*, 1996; Yanagida *et al.*, 1990; AhR activation reviewed in Denison *et al.*, 2002; Denison *et al.*, 2011; Fujii-Kuriyama and Kawajiri, 2010; Hankinson, 1995).

Upon AhR-activation, a further bHLH-PAS protein termed AhR repressor (AhRR) represses AhR's transcription activity by competing with AhR for heterodimer formation with ARNT and preventing the AhR/ARNT-complex from binding XREs. Enhanced SUMOylation of both ARNT and AhRR, as well as recruitment of the corepressor Ankyrin repeat family A protein 2 (ANKRA2), and histone deacetylases (HDACs) HDAC4, and/or HDAC5 results in formation of the transcriptional repressor complex. Since AhRR's expression is induced by AhR-activation through binding to the XRE upstream of the *AhRR* gene, AhR function is regulated by feedback inhibition. Secondly, AhR signaling can be down-regulated by proteasomal degradation in cytoplasm (Baba *et al.*, 2001; Ma and Baldwin, 2000; Mimura *et al.*, 1999; Oshima *et al.*, 2007; Oshima *et al.*, 2009).

Of peculiar interest is AhR's function in organisms in absence of exogen ligands, and quite a few endogen AhR-agonists were figured out, as quoted above. An approach within this scientific section using $AhR^{-/-}$-mice indicated various implications of the AhR. In these animals, a range of physiological defects was displayed, including slower growth rates associated with decreased body weight, reduced liver size, immune system impairment, the appearance of a patent ductus venosus – a portocaval vascular shunt, which postnatally closes during the first 48 h in wild-type mice, portal tract fibrosis, and reduced fertility (Baba *et al.*, 2005; Fernandez-Salguero *et al.*, 1995; Lahvis *et al.*, 2000; Lahvis *et al.*, 2005; Schmidt *et al.*, 1996).

The understanding of endogenous AhR-ligands together with obvious and considerable physiological alterations in $AhR^{-/-}$-mice substantially support relevance of research on role and impact of AhR-regulation with respect to physiological function(s).

1.1.3. Cytochrome P450 Isoenzymes

Among yet predicted AhR-target gene products, such as UDP-glucuronosyltransferase 1a6 (UGT1A6), Glutathion *S*-transferase (GST) Ya subunit, or NAD(P)H (quinone) dehydrogenase 1 (NQO1), CYP1A-isoenzymes were excessively studied (Favreau and Pickett, 1991; Jaiswal, 1991; Owens, 1977; Rushmore and Pickett, 1990).

Cytochromes P450 (CYPs) constitute a superfamily of heme enzymes. CYP enzymes, which possess at least 40% homology in their amino acid sequence, are classified in different families and are designated by Arabic numerals (CYP1, e.g.). The further division into subfamilies is delineated by ≥ 55% sequence homology in mammalians and is denoted by capital letters (CYP1A, e.g). Within subfamilies, proteins exhibiting more than 3% divergence are assigned individual CYP members (CYP1A1, e.g), unless (i) functional differences have been ascertained, or (ii) nontranslated regions are clearly divergent, indicating distinct genes (Nelson *et al.*, 1993; Rendic and Di Carlo, 1997).

The CYP family of isoenzymes represents an important class of phase I xenobiotic-metabolizing enzymes (‘monooxygenases’), which catalyze the introduction of functional groups to lipophilic compounds. In CYPs, the prosthetic group is constituted of an iron(III) protoporphyrin-IX covalently coupled to the protein by the sulfur atom of a proximal cysteine ligand. Characteristic reactions catalyzed by CYPs are hydroxylations of saturated carbon-hydrogen bonds, epoxidations of CC-double bonds, oxidations of heteroatoms, and oxidations of aromatics. The appropriate CYP enzyme uses molecular oxygen, inserts one oxygen atom into the substrate, and reduces the second oxygen to water, applying two electrons, which are provided by nicotinamide adenine dinucleotide (phosphate) (NAD(P)H) via cytochrome P450 reductase (Meunier *et al.*, 2004).

Transcripts of relevant AhR-responsive genes are the three members of the CYP1 gene family: CYP1A1, CYP1A2, and CYP1B1 (Nebert *et al.*, 2000; Tsuchiya *et al.*, 2003; Zhang *et al.*, 1998). CYP1A1 is expressed in many mammalian tissues including lung, liver, brain gastrointestinal tract (GIT), lymphocytes, and heart, whereas CYP1A2 is mainly a hepatic enzyme. CYP1B1 was found in skin, brain, heart, lung, placenta, liver, kidney, GIT, and spleen (reviewed in Anzenbacher and Anzenbacherova, 2001).

For CYP1A2 as well as for CYP1B1, AhR-independent mechanisms for transcriptional regulation were established. It was discussed that CYP1A2 might as well be regulated by constitutive androstane receptor (CAR), whereas CYP1B1 was demonstrated to be regulated via estrogen receptor (Lee *et al.*, 2007; Tsuchiya *et al.*, 2004).

So far, it is not proven, if CYP1A1-expression is exclusively regulated by the AhR. Sérée *et al.* (2004) reported evidence for a regulation pathway involving peroxisome proliferator-activated receptor α (PPARα), and two peroxisome proliferators response elements (PPREs) in an *in vitro*-model (Sérée *et al.*, 2004). However, the AhR was neither antagonized nor was its response silenced in the course of this study. Therefore, and in particular due to findings from Wang *et al.* (2011), who postulated an AhR-mediated route for *Ppara*-expression, a general AhR-involvement regarding CYP1A1-induction cannot be excluded (Wang *et al.*, 2011).

CYP-isoenzyme members of the subfamilies CYP2B and CYP3A, which are inducible by non dioxin-like (NDL-)PCBs, are regulated by CAR, and/or pregnane X receptor (PXR), both of which are discussed to be involved in diverging contribution (Gährs *et al.*, 2013; Timsit and Negeshi, 2007; Wei *et al.*, 2002; Xie *et al.*, 2000).

1.2. Polychlorinated dibenzo-*p*-dioxins, dibenzofurans, and biphenyls

Polychlorinated dibenzo-*p*-dioxins (PCDDs) and polychlorinated dibenzofurans (PCDFs) are lipophilic, highly persistent compounds, which are inadvertently formed by-products in thermal processes such as waste incineration, residential combustion, metallurgical processes, and upon the chlorine bleaching of paper pulp (Swanson *et al.*, 1988; UNECE, 2010). Furthermore relevant is the formation of PCDDs and PCDFs (figure 2) during the production of chlorophenols and chlorophenoxy herbicides (Fuhrmann, 2006; Homberger *et al.*, 1979; Suskind, 1985).

Seven of 75 (PCDDs), and ten of 135 (PCDFs) congeners are classified as dioxin-like (DL) due to their chlorine substitution pattern and associated AhR-mediated activities, which demand chlorine atoms at (lateral) positions 2,3,7, and 8 in respective molecules (Bandiera *et al.*, 1984; Harris *et al.*, 1990; van den Berg *et al.*, 1994).

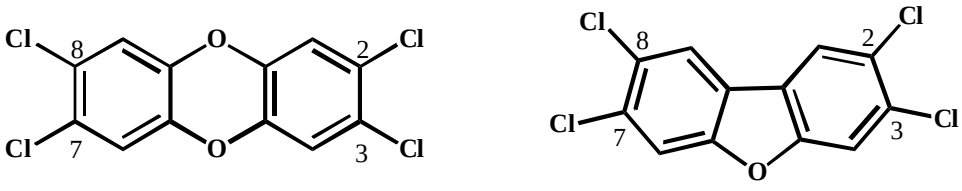

Figure 2: Chemical structures of PCDDs (TCDD, left), and PCDFs (TCDF, right), chlorinated at positions 2,3,7, and 8.

A further class of compounds is considered in terms of DL-mode of action. Of 209 possible polychlorinated biphenyl (PCB)-congeners (figure 3), twelve appeared to reveal binding affinities towards the AhR and thus were termed ‘dioxin-like’ (DL) PCBs. Of them, four are non-*ortho*-chlorinated, and eight are mono-*ortho*-substituted PCBs, with 3,3’,4,4’,5-pentaCB (PCB 126), correspondent to a WHO-TEF of 0.1, being the most potent congener (Bandiera *et al.*, 1982; van den Berg *et al.*, 2006).

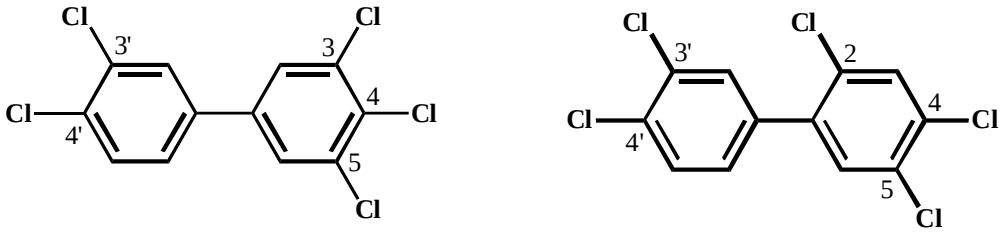

Figure 3: Chemical structures of a non-*ortho* (PCB 126, left), and a mono-*ortho* substituted PCB (PCB 118, right)

In non-*ortho*-substituted PCB-congeners, the two phenyl rings are able to rotate more easily about the shared bond, leading to a higher probability to reach a planar conformation, which further yields in higher binding affinities towards the AhR (reviewed in De Voogt *et al.*, 1990). In accordance, the remaining congeners, which do not share DL-mechanisms through binding to the AhR, are termed ‘non dioxin-like’ (NDL)-PCBs, and are known to exert their biochemical and toxicological effects via other cellular factors, namely constitutive androstane receptor (CAR), and/or pregnane X receptor (PXR) (Al-Salman and Plant, 2012). For industrial purposes, complex mixtures of PCBs formerly were produced to be used as dielectric insulating fluids for transformators or capacitors. Beyond, PCBs were applied in paints, plastics, and hydraulic fluids, and were produced in dimensions of thounds of tons, e.g. under the trade name Aroclor® (Monsanto Corporation, St. Louis, Missouri, USA) (Breivik *et al.*, 2002; IARC, 2012; Safe, 1994).

1.2.1. Risk estimation and the toxic equivalency factor (TEF)-concept

Although the international community has called for actions to reduce the emission of DL-chemicals employing two legally binding instruments, namely 'The Protocol on the regional UNECE Convention on Long-Range Transboundary Air Pollution (CLRTAP) on persitent organic pollutants (POPs) (The 1998 Aarhus protocol on POPs)', and 'The Stockholm convention on POPs', their occurrence in the environment is still of concern since these chemicals represent a class of higly persistent chemicals and remain in the environment for a long time (Denier van der Gon *et al.*, 2007; Karlaganis *et al.*, 2001; UNECE, 2010; UNEP, 1013).

In 1997, the International Agency for Research on Cancer (IARC) classified TCDD as a group 1 human carcinogen (IARC, 1997). By this time, there was only limited evidence for its carcinogenicity towards humans, which was reinforced in the course of IARC's reevalution in 2012. The most important studies for the evaluation of TCDD's carcinogenicity in 1997 were four cohort studies, one each in the United States (Fingerhut *et al.*, 1991), the Netherlands (Hooiveld *et al.*, 1996), and two in Germany (Becher *et al.*, 1996; Ott and Zober, 1996), and further one cohort of residents living in the in 1976 contaminated area from Seveso, Italy (Bertazzi *et al.*, 1993; Bertazzi *et al.*, 1996). Contribution of novel epidemiological data regarding these cohort studies (Bertazzi *et al.*, 2001; Boers *et al.*, 2010; Pesatori *et al.*, 2009; Steenland *et al.*, 1999; Steenland *et al.*, 2001), the IARC again proposed sufficient evidence for the carcinogenicity of TCDD towards humans (group 1) in 2012 (IARC, 2012). Strongest evidence in this regard was for all cancers combined. A positive correlation was as well observed between TCDD-exposure and soft-tissue sarcoma, non-Hodgkin lymphoma, and lung cancer (IARC, 2012). According to the IARC Working Group, TCDD was supposed to be a human carcinogen with tumor-promoting properties which operates through modifications of cell replication and apoptosis, associating secondary mechanisms involving increased oxidative stress and accompanied DNA damage (IARC, 2012).

Along with respective IARC reevaluation in 2012, 4-PeCDF, and PCB 126 were as well categorized as group 1 human carcinogens. This classification was based upon evidence of carcinogenicity in laboratory animals as well as upon exhibiting activity identical to TCDD for each step of TCDD's proposed mechanism for carcinogenesis including binding to the AhR, changes of protein-activity, cellular replication, and oxidant/antioxidant imbalance (IARC, 2012).

According to the IARC evaluation in 1997, PCDDs and PCDFs except for TCDD and 4-PeCDF were not classifiable as to their carcinogenicity to humans (Group 3; IARC, 1997). Referred to the currently valid evaluation from 1987 (IARC 1987), PCBs except for PCB 126 were classified as probably carcinogenic agents to humans (Group 2A). Suggested evidence for increased hepatobiliar

cancer risk associated with PCB-exposure was considered to be limited due to insufficient data including lack of dose-response relationship evaluations, and the enabled exclusion of other compounds' potential roles (IARC, 1987; Robertson and Ruder, 2009). In IARC's Monograph Volume 107, which currently is in preparation, PCBs are supposed to be upgraded to Group 1 based on strong supporting evidence from other relevant data (IARC-List of classifications 2014; Lauby-Secretan *et al.*, 2013).

Based on lowest observed adverse effect levels (LOAELs) for the most sensitive responses in animal studies, namely hormonal, reproductive, and developmental effects, which were associated with budy burdens from which a range of estimated long-term human intakes of 14-37 pg TCDD/kg bw/day was calculated, a tolerable daily intake (TDI) range of 1-4 pg TEQs/kg bw was established. For TCDD, a half-life of 7.5 yrs was assumed (Van Leeuwen *et al.*, 2000; WHO, 2000). In 2001, the Scientific Committee on Food (SCF) revised the previous established temporary tolerable weekly intake (t-TWI) from 2000 of 7 pg TEQ/kg bw/week (SCF, 2000), and decided on a TWI of 14 pg TEQ/kg bw/week (SCF, 2001). A further provisional tolerable monthly intake (PTMI) of 70 pg TEQ/kg bw/month was established by the Joint FAO/WHO Expert Committee on Food Additives (JECFA) in 2001 (JECFA, 2001).

During a World Health Organization (WHO)-International Programme on Chemical Safety expert meeting in 2005, the toxic equivalency factors (TEFs) for DL-compounds, which were valid since 1998, were reevaluated (Van den Berg *et al.*, 2006). For inclusion of a certain compound in the TEF concept, a compound had to (a) show a structural relationship to the PCDDs and PCDFs, (b) bind to the AhR, (c) elicit AhR-mediated biochemical and toxic responses, and to (d) be persistent and accumulate in the food chain (Ahlborg *et al.*, 1994; Van den Berg *et al.*, 1998; Van den Berg *et al.*, 2006). In the TEF concept, relative effect potencies (REPs) determined for individual congeners regarding their biological or toxic effect(s) relative to a reference compound, usually TCDD, were used. Due to their combination of both toxicokinetic and toxicodynamic aspects, *in vivo* studies were attributed to the highest priority and are preferably used for setting TEFs. In accordance with a generally accepted additivity in mixtures, the total toxic equivalent (TEQ) was defined by the sum of the products of the concentration of each compound multiplied by its TEF value and represents an estimate of total 'TCDD-like' activity of a mixture. In table 1 (following page), WHO-TEFs from 1998 are compared to those from 2005 (Van den Berg *et al.*, 1998; Van den Berg *et al.*, 2006).

Table 1: Dioxin-like PCDDs, PCDFs and PCBs compiled with their corresponding WHO-TEFs (1998; 2005).

	WHO-TEF (1998) Van den Berg *et al.*, 1998	WHO-TEF (2005) Van den Berg *et al.*, 2006
Chlorinated Dibenzo-*p*-dioxins		
TCDD	1	1
1-PeCDD	1	1
1,4-HxCDD	0.1	0.1
1,6-HxCDD	0.1	0.1
1,9-HxCDD	0.1	0.1
1,4,6-HpCDD	0.01	0.01
OCDD	0.0001	0.0003
Chlorinated Dibenzofurans		
TCDF	0.1	0.1
1-PeCDF	0.05	0.03
4-PeCDF	0.5	0.3
1,4-HxCDF	0.1	0.1
1,6-HxCDF	0.1	0.1
1,9-HxCDF	0.1	0.1
4,6-HxCDF	0.1	0.1
1,4,6-HpCDF	0.01	0.01
1,4,9-HpCDF	0.01	0.01
OCDF	0.0001	0.0003
Non-*ortho*-substituted PCBs		
PCB 77 (3,3',4,4'-tetraCB)	0.0001	0.0001
PCB 81 (3,4,4',5-tetraCB)	0.0001	0.0003
PCB 126 (3,3',4,4',5-pentaCB)	0.1	0.1
PCB 169 (3,3',4,4',5,5'-hexaCB)	0.01	0.03
Mono-*ortho*-substituted PCBs		
PCB 105 (2,3,3',4,4'-pentaCB)	0.0001	0.00003
PCB 114 (2,3,4,4',5-pentaCB)	0.0005	0.00003
PCB 118 (2,3',4,4',5-pentaCB)	0.0001	0.00003
PCB 123 (2',3,4,4',5-pentaCB)	0.0001	0.00003
PCB 156 (2,3,3',4,4',5-hexaCB)	0.0005	0.00003
PCB 157 (2,3,3',4,4',5'-hexaCB)	0.0005	0.00003
PCB 167 (2,3',4,4',5,5'-hexaCB)	0.00001	0.00003
PCB 189 (2,3,3',4,4',5,5'-heptaCB)	0.0001	0.00003

1.2.2. Intake and absorption of dioxin-like compounds

Due to their high lipophilicity and low biodegradation rate, PCDDs, PCDFs, and PCBs ubiquitously occur in soil, sediments, and air. Besides occupational or accidental exposures, food represents the major source for DL-compounds towards humans. Approximately 90% of daily intake is derived from the diet, with foods of animal origin and fish being the predominat sources. The remaining dose for instance originates from inhalation, or dermal contact rates (Liem *et al.*, 2000).

Dietary intake (lower bound estimates) ranges from 0.57 pg TEQ/kg bw/day (France; Sirot *et al.*, 2012), over 0.7 pg TEQ/kg bw/day (Sweden; Törnkvist *et al.*, 2011), and 0.8 pg TEQ/kg bw/day (The Netherlands; De Mul *et al.*, 2008) to 1.8 pg TEQ/kg bw/day (Belgium; Windal *et al.*, 2010, and Germany; BFR, 2010), and 2.86 pg TEQ/kg bw/day (Spain; Marin *et al.*, 2011) for adults. As for the last-mentioned, some parts of the population still exceed the TWI and/or PTMI; e.g. higher consumers (69.4-73.6 pg TEQ/ kg bw/month in China (Zhang *et al.*, 2013); 22.04 pg TEQ/kg bw/week in Germany (BFR, 2010)), or concerning upper bound estimates (15.96 pg TEQ/kg bw/week in Italy (Fattore *et al.*, 2006); 16.89 pg TEQ/kg bw/week in Germany (BFR, 2010)). Anyhow, TEQ-exposure by dietary intake decreased over the past years of inquiries, whereby, in accordance with the prohibition of PCB-production, a larger decrease regarding DL-PCBs was reported compared to PCDD/PCDF-reductions (Baars *et al.*, 2004; De Mul *et al.*, 2008; Sirot *et al.*, 2012; Tard *et al.*, 2007). DL-PCB-contribution to TEQ-exposure by food intake amounts to about 50-80% of TEQ-exposure (BFR 2010; De Mul *et al.*, 2008; Sirot *et al.*, 2012; Windal *et al.*, 2010).

Rates of absorption in organisms, as well as tissue distribution and elimination of DL-compounds are mostly controlled by their lipophilicity. Predominating limiting factors for the absorption from the GIT appear to be solubility and molecular size (Van den Berg *et al.*, 1994). Accordingly, congeners containing 4, 5, or 6 chlorine-substituents are reportedly well absorbed, whereas hepta-or octa-chlorinated compounds tend to be absorbed to a lesser extent (Abraham *et al.*, 1994; Abraham *et al.*, 1996; Moser and McLachlan, 2001).

Uptake, which is proposed to occur primarily through passive diffusion in the GIT, is dependent on both the administered matrix and the respective compound concentration(s) (Budinsky *et al.*, 2008; Kitamura *et al.*, 2005; Schlummer *et al.*, 1998). Furthermore, absorption rates are assumed to be dependent on present blood level(s) and budy burden (Harrad *et al.*, 2003; Moser and McLachlan, 2001; Schlummer *et al.*, 1998). Information regarding DL-compounds and associated absorption, distribution, metabolism, and excretion (ADME) in humans is limited. In the course of a self-

experiment, Poiger and Schlatter (1986) reported on an absorption of more than 87% after ingestion of a single dose (1.14 ng/kg bw) of [^{3}H]TCDD administered in corn oil. Moser and McLachlan (2001) reported on a net absorption of around 80% of 2,3,7,8-tetra-, penta-, and hexachlorinated PCDDs and PCDFs, as well as PCBs including PCB 77, 105, 118, and 126, and the NDL-PCB 153, e.g., in five male volunteers who ingested toxic equivalents of less than 2% of their body burden by consumption of naturally contaminated eggs. Net absorption rates decreased in line with increasing number of chlorine-substituents accounting for ~70% regarding heptachlorinated PCDDs/PCDFs, and for ~50% relating octachlorinated congeners, respectively (Moser and McLachlan, 2001). Further data declared particularly high excretion levels – most notably regarding higher chlorinated compounds – partially exceeding uptake levels, which were correlated with elevated blood concentrations, and therefore indicated the possibility of facilitated TEQ-elimination due to diminished TEQ-intake (Rohde *et al.*, 1999; Schlummer *et al.*, 1998; Schrey *et al.*, 1998). The authors concluded strong evidence that contaminant concentrations in blood lipids are the major factor of influence determining absorption (Schlummer *et al.*, 1998).

1.2.3. Tissue-distribution of dioxin-like compounds

Liver and adipose tissue constitute the major compartments for the disposition of PCDDs, PCDFs, and PCBs (Carrier *et al.*, 1995a+b; Gasiewicz *et al.*, 1983; Piper *et al.*, 1973; Van Ede *et al.*, 2013a). Thereby, hepatic sequestration of DL-congeners was reported to be distinct in rodent experimental animals (DeVito *et al.*, 1998; Hakk *et al.*, 2009; Van Ede *et al.*, 2013b). Tissue distribution was observed to appear in a dose-dependent manner in both mouse (Dilberto *et al.*, 2001) and rat (Abraham *et al.*, 1988), whereas at lower doses distribution to adipose tissue was greater than to liver, shifting to a greater distribution of congeners to liver compared to adipose tissue for higher doses.

Within the framework of SYSTEQ-project, three days studies with female Sprague Dawley and female C57BL/6 mice were performed (Van Ede *et al.*, 2013b). Dose-dependent hepatic sequestration of TCDD, 1-PeCDD, 4-PeCDF, or PCB 126 was observed subsequent to oral administration of single doses for both species. The investigations with rats revealed highest liver/adipose concentration ratios between 4.7 and 58 for 4-PeCDF within the range of applied doses of 5 to 1000 µg/kg bw. No significant hepatic sequestration was observed for mono-*ortho* PCBs 118 or 156, or NDL-PCB 153 at doses ranging from 5 to 500 mg/kg bw (Van Ede *et al.*, 2013b). Chen *et al.* (2001) observed comparable findings. The authors additionally did not determine hepatic sequestration for non-*ortho* substituted PCB 77, and TCDF, which were orally administered as components of a mixture containing seven further DL-compounds, in female Long-

Evans rats in single doses of 0.67-13.3 µg/kg bw (PCB 77), and 6.10-128 ng/kg bw (TCDF), as parts of total doses of 0.05-1.0 µg TEQ/kg bw (Chen *et al.*, 2001).
Following subchronic treatment (five days/week for 13 weeks), dose-dependent increases in the liver/fat concentration ratios were found for several DL-compounds including TCDD, 4-PeCDF, TCDF, OCDF, and PCB 126 in female B6C3F1 mice (DeVito *et al.*, 1998). Excepting PCB 126, no hepatic sequestration was obtained for further DL-PCBs (mono-*ortho* substituted PCBs 105, 118, and 156) investigated in the course of this study. While non-*ortho* PCB 169 as well retained in adipose tissue to a greater extent than in animals' livers, the liver/fat concentration ratios in contrast appeared to increase with doses of up to 3.9 mg/kg bw/day (DeVito *et al.*, 1998).

Regarding humans, the issue of potential hepatic sequestration of DL-compounds is yet not fully understood due to limited data. The topic was recently reviewed by van Ede and co-workers (Van Ede *et al.*, 2013b). On grounds of evaluated liver/adipose concentration ratios of DL-compounds based on autopsy samples from the general population (Iida *et al.*, 1999; Schecter *et al.*, 1991; Thoma *et al.*, 1990; Watanabe *et al.*, 2013; Weistrand and Norén, 1998), the authors concluded little or no hepatic sequestration in humans at environmental exposure levels (Van Ede *et al.*, 2013b).

As indicated by means of animal experiments including studies on CYP1A2 k/o-mice, hepatic sequestration is believed to mainly be attributable to CYP1A2 and binding affinities of respective compound to this inducible hepatic protein (DeVito *et al.*, 1998; Dilberto *et al.*, 1997; Hakk *et al.*, 2009; Santostefano *et al.*, 1996). In consistence, higher CYP1A2-induction owing to impact by high affinity congeners results in greater extent of hepatic sequestration of respective chemical (Chen *et al.*, 2001; Dilberto *et al.*, 1999). Both dose-dependency and interspecies differences referred to hepatic sequestration might as well - at least in parts - be attributable to higher senstitivity and inducibility of CYP1A2 in rodent hepatocytes compared to human cells (Budinsky *et al.*, 2010; Schrenk *et al.*, 1995; Silkworth *et al.*, 2005; Xu *et al.*, 2000; Zeiger *et al.*, 2001). In consequence, further need for clarification exists regarding degree of availability of chemicals linked to hepatic CYP1A2 for AhR-interaction and resulting extent of biological and toxic responses (Dilberto *et al.*, 1999; Van Ede *et al.*, 2013b). Subsequent to hepatic retention of respective congeners, redistribution into adipose tissue with time was proposed to impact the accessibility for metabolic degradation and elimination, which was discussed in the context of observations regarding CYP1A2 and its role as inducible binding protein (Dilberto *et al.*, 1995; Wang *et al.*, 1997).

1.2.4. Metabolism, elimination and half-lives of dioxin-like compounds

Fecal excretion represents major elimination pathway for DL-compounds in mammals (Gasiewicz *et al.*, 1983; Lutz *et al.*, 1984; Piper *et al.*, 1973; Poiger and Schlatter, 1986; Rohde *et al.*, 1999). Interestingly, cutaneous elimination is as well reported (Geusau *et al.*, 2001). Data on two severely intoxicated women (initial TCDD-concentrations of 144,000 pg/g blood fat, and 26,000 pg/g blood fat, respectively) from unknown source excreted 1-2% of the overall daily TCDD elimination rate via skin (Geusau *et al.*, 2001).

Apparent half-lives vary from few weeks for rodents up to several years in humans (Gasiewicz *et al.*, 1983; Piper *et al.*, 1973; Poiger and Schlatter, 1986). As mentioned above, for estimation of a TDI range of 1-4 pg TEQs/kg bw, a half-life of 7.5 yrs for TCDD was assumed (Van Leeuwen *et al.*, 2000; WHO, 2000). As a matter of fact, experimental data actually indicated a dose-dependency for TCDD's half-life in organisms (Aylward *et al.*, 2005; Emond *et al.*, 2006). By means of a concentration-dependent toxicokinetic model, Aylward *et al.* (2005) proposed half-lives for TCDD ranging from less than three years at serum lipid levels above 10,000 ppt to more than ten years at serum lipid levels below 50 ppt (Aylward *et al.*, 2005). Calculations on elimination kinetics for PCBs in humans were accomplished by Ogura in 2004 and outlined by Milbrath *et al.* (2009). Estimated half-lives ranged from 0.1 year for PCB 77, over 2.7 yrs for PCB 126, to 5.35 yrs for PCB 156, and 10.4 yrs for PCB 169 (Milbrath *et al.*, 2009; Ogura, 2004).

Although there is general consensus that metabolism appears to be limited as well as slow, several worthwile findings have been reported regarding metabolic modifications of DL-compounds.

As part of the self-experiment reported by Poiger and Schlatter, half-life for [^{3}H]TCDD accounted for 5.8 yrs after administration of a dose of 1.14 ng/kg bw (Poiger and Schlatter, 1986). Exhibiting levels of 108,000 pg TCDD/g lipid weight in blood serum about four months subsequent to poisoning in Victor Yushchenko, a half-life of 15.4 months was calculated following three years of monitoring of the patient's TCDD levels in blood serum and subcutaneous fat (Sorg *et al.*, 2009). In the course of this study, the authors analyzed samples from blood serum, adipose tissue, faeces, skin, urine, and sweat using gas chromatography and high-resolution mass spectrometry, and detected two metabolites - 2,3,7-trichloro-8-hydroxydibenzo-*p*-dioxin (OH-TrCDD), and 1,3,7,8-tetrachloro-2-hydroxydibenzo-*p*-dioxin (OH-TCDD) - in faeces, blood serum, and urine, with faeces being the main route of elimination. These metabolites accounted for 38% of total TCDD eliminated. Furthermore, the authors confirmed previous findings with regards to correlative serum lipid-, and adipose tissue-concentrations of TCDD. An equibrilium between these two compartments was already declared in 1988 along with a study by Patterson *et al.* with 50

participants from Missouri (Patterson *et al.*, 1988). Upon aforementioned self-experiment reported by Poiger and Schlatter (1986), a minimum, although not farther specified, metabolism of 50% of radiolabeled TCDD was observed (Wendling *et al.*, 1990).

As investigated by means of animal studies, metabolic transformation of PCDDs and PCDFs includes oxidation and hydrolytic or reductive dechlorination (Poiger *et al.*, 1982; Poiger *et al.*, 1989). In the bile of a dog, who converts the chemical at a higher rate compared to rats, six metabolites were found after administration of a lethal dose of [^{3}H]TCDD with 1,3,7,8-tetrachloro-2-hydroxydibenzo-*p*-dioxin (OH-TCDD) representing the major metabolite (Poiger *et al.*, 1982). Rearrangement of a chlorine substituent from a lateral to a peri-position, which is established for aromatic compounds as an NIH-shift, indicates metabolic transformation via an arene oxide. Additionally, two dihydroxy-TrCDDs, one of them as well being a major compound, were found. Further relevant metabolic pathway represents oxygen bridge cleavage, yielding a tetrachloro-dihydroxy-diphenylether. Continuation of this pathway could explain the appearance of 1,2-dichloro-4,5-dihydroxybenzene identified in the course of this study. Furthermore, 2,7,8-trichloro-3-hydroxydibenzo-*p*-dioxin was detected as a metabolite in dog's bile (Poiger *et al.*, 1982). Hydroxylated PCDDs and ring-cleaved metabolites were as well identified from biles of rats, which were, in comparison to the dog, present as phase II-conjugates (Poiger and Buser, 1984). In contrast to absent sulfates, glucuronide-conjugates were found in biles of [^{14}C]TCDD-treated rats, which was as well determined in *in vitro* studies using primary rat hepatocytes (Ramsey *et al.*, 1982; Wroblewski and Olson, 1985).

Although for most cases the precise attribution to the responsible enzyme triggering degradation of DL-compounds remains unresolved issue, CYP1A1 was established to mediate metabolism of TCDF in rat and human hepatocytes (Tai *et al.*, 1990). Burka *et al.* (1991) identified 4-hydroxy-2,3,7,8-TCDF and 3-hydroxy-2,3,8-TrCDF as biliary metabolites in the rat. Observation of trace amounts of 2,2'-dihydroxy-4,4',5,5'-tetrachlorobiphenyl supported evidence that oxygen bridge cleavage is only of minor relevance for PCDFs (Burka *et al.*, 1991). This hypothesis was confirmed by Kuroki *et al.* (1990) subsequent to administration of a mixture of 1,2,7,8-TCDF, 2,3,7,8-TCDF, and 1,2,3,7,8-PeCDF to rat (Kuroki *et al.*, 1990). In contrast, for 4-PeCDF, ether-bond cleavage was obtained to be an important mechanism for degradation in rat livers. Major metabolites were hydroxy-, and dihydroxy-pentachlorobiphenyl in this regard (Poiger *et al.*, 1989). Furthermore, hexa- and hepta-CDFs examined in the same study were poorly metabolized, if at all. Apart from one hydroxy-PeCDF formed from 1,6-HxCDF, no metabolites were detected for 1,4,6-HpCDF

(Poiger *et al.*, 1989). In concordance with enhanced steric shielding by bulky substituents, no metabolites were found for OCDD or OCDF in *in vivo* experiments with rats (Tulp and Hutzinger, 1978; Veerkamp *et al.*, 1981).
Hakk and Dilberto found hydroxylated metabolites in feces of [^{14}C]TCDD-, and 1-[^{14}C]PeCDD-treated mice. They further investigated glucuronide ether-, and sulfate ester-conjugates in the urine of single-dose treated animals (Hakk and Dilberto, 2002; Hakk and Dilberto, 2003). Regarding PCBs, hydroxylated and methyl sulfone derivates emerged to represent the most important metabolites to be retained in biota (Letcher *et al.*, 2000).

1.3. Toxicological relevance of TCDD

Among DL-compounds, TCDD still represents the most extensively studied congener regarding its toxicological relevance. Biological and toxic responses attributed to TCDD and presumably other DL-compounds, of which most, if not all, are believed to be mediated through the AhR, include dermal, hepatotoxic, endocrine, immunological, reproductive, developmental, and carcinogenic effects (ATSDR 2012; Van den Berg *et al.*, 1994).

After the industrial accident in the Seveso, Italy, area in 1976, upon which a large residential population was exposed to substantial amounts of TCDD, chloracne was the earliest effect established with definite exposure dependence (Bertazzi *et al.*, 1998; Caramaschi *et al.*, 1981). Characterized by hyperkeratinization of the stratum corneum and disappearance of sebaceous gland follicles in the formation of keratin cysts, chloracne is the most commonly reported effect attributable to TCDD-exposure in humans (Suskind, 1985). In the heaviest contaminated zone of the Seveso area, lipid-adjusted serum concentrations in samples of children from 1976 suffering chloracne ranged from 1,688 to 56,000 ppt TCDD, and from 54 to 8,750 ppt TCDD for those without chloracne. Notably, TCDD concentration ranges of these two groups overlap, which elucidates that the absence of chloracne subsequent to exposure does not necessarily imply low serum TCDD levels (Needham *et al.*, 1997/98).

Subsequent to poisoning of Victor Yushchenko, 108,000 ppt TCDD was measured in the politician's blood lipids (Sorg *et al.*, 2009). In his face, severe edemas appeared two weeks after poisoning, followed by development of cystic lesions termed harmatomas, which became widespread over the entire body with a peak clinical manifestation at month eleven. Thereafter, symptoms declined gradually but generation of novel hamartomatous lesions progressed until month 28 after the poisoning (Saurat *et al.*, 2012).

Though comprehensive adjustment for confounding factors is sensitive topic, several epidemiological studies are available with respect to proposed adverse health effects in cohorts occupationally or accidentially exposed to TCDD including hepatic, cardiovascular, neurological, reproductive, and developmental effects (Baccarelli *et al.*, 2008; Heilier *et al.*, 2005; Neuberger *et al.*, 1999; Pelclová *et al.*, 2007; Steenland *et al.*, 1999; Thömke *et al.*, 1999). The role of TCDD as endocrine disruptor is as well of relevant concern, with potential alterations in glucose metabolism and thyroid function as important issues (Baccarelli *et al.*, 2008; Kang *et al.*, 2006; Pesatori *et al.*, 2009; Trnovec *et al.*, 2013).

Findings regarding thyroid function were discussed with respect to a population living in an organochlorine-polluted area in eastern Slovakia (Trnovec *et al.*, 2013). Trnovec and co-workers' purpose was to determine relative effect potencies (REPs) for systemic DL-concentrations in humans using thyroid volume and serum free thyroxine (FT4), observing regression coefficient-derived REPs correlating with the WHO-TEF-values for both endpoints (Trnovec *et al.*, 2013). These observations were investigated in the course of the EU-project 'PCBRISK' (EU Grant No. QLK4-CT-2000-00488), in which the main objective was the evaluation of human health risks of low-dose and long-term exposure to a group of POPs, including PCDDs, PCDFs, as well as PCBs and their metabolites (Trnovec *et al.*, 2004). As part of the PCBRISK-project, further evidence was observed regarding antiestrogenic effects correlated with high exposure to DL-chemicals (Machala *et al.*, 2004; Plíšková *et al.*, 2005). Besides a significant suppression of human placental aromatase (CYP19) activity found in placental samples, a decrease of 17β-estradiol (E2)-blood levels in male serum was observed, which, however, appeared to be not statistically significant (Machala *et al.*, 2004; Plíšková *et al.*, 2005). Induction of appropriate enzymes metabolically inactivating E2, namely CYP1A1, CYP1A2, CYP1B1, and CYP3A4, was discussed as presumable mechanism responsible for antiestrogenic effects (Plíšková *et al.*, 2005).

Furthermore, exposure to DL-compounds was discussed relating to increased risk of endometriosis (Eskenazi *et al.*, 2002; Heilier *et al.*, 2005). According to the authors, their results regarding increased risks correlating with an increment of 10 pg total TEQ-levels/g lipids accounting for endometriotic nodules (odds ratio (OR) = 3.3; 95% confidence interval (CI): 1.4-7.6), and for peritoneal endometriosis (OR = 1.9; 95% CI: 0.9-3.8), provided the first statistically significant evidence of an association between increased total TEQ-body burden and endometriosis (Heilier *et al.*, 2005).

A respectable volume of data concerned with TCDD's impact on the organism comprises a broad spectrum of biochemical and toxic effects in experimentally treated animals. Implied consequences correlated with TCDD-exposure, which are of substantial concern, range from tissue weight changes – in particular, increased liver weight, and decreased thymus weight, decreased body weight ('wasting syndrome'), through to teratogenic and carcinogenic effects (DeCaprio *et al.*, 1986; Kociba *et al.*, 1976; Kociba *et al.*, 1978; NTP, 1982; Seefeld *et al.*, 1984; Smith *et al.*, 1976; Sparschu *et al.*, 1971).

Predicted hypotheses regarding TCDD-mediated carcinogenicity and its tumor-promoting properties include AhR-dependent impact on gene expression of networks of genes, which are involved in cell growth, differentiation, or senescence, induction of CYP-catalyzed activation pathways and potentially implied DNA-damages, as well as expansion of preneoplastic lesions by inhibition of apoptosis, positive modulation of extra- or intracellular growth-stimuli, or disruption of immune control and function (Dragan and Schrenk, 2000; IARC,1997; Ray and Swanson, 2009; Safe, 2001). Biochemical effects mediated by TCDD and selected structurally related compounds are basically classifiable as either altered metabolism due to enzyme induction, altered homeostasis as a result from changes in hormones and their receptors, or altered growth and differentiation as a result from changes in growth factors and their receptors. Further, these effects appear to be species-, as well as tissue-specific, and mechanisms are often not (fully) understood (Birnbaum, 1994).

1.4. Proposed AhR-dependent immunological effects

1.4.1. Epidemiological investigations

Inquiries into TCDD's impact on the immune system on the basis of epidemiological data bear not only various, but also controversial and even opposing findings throughout available literature.

About 20 years after the Seveso incident, Baccarelli *et al.* (2002) investigated potential TCDD-induced immunologic effects in 62 randomly selected subjects from the highest exposed zones in comparison to 59 individuals from the surrounding non-contaminated area. Dependent on lipid-adjusted TCDD-plasma-concentrations, median plasma immunoglobulin G (IgG)-concentration decreased from 1,526 mg/dL in the group with lowest (< 3.5 ppt) TCDD-levels to 1,163 mg/dL in the group with highest TCDD-levels (20.1-89.9 ppt). Results were statistically significant ($p = 0.0004$) even after adjustment of several confounding factors (Baccarelli *et al.*, 2002).

In a further examination by Landi *et al.* (2003), gene expression analysis in peripheral blood mononuclear cells (PBMCs) obtained from TCDD-exposed Seveso residents was accomplished. Mean *AHR*-expression was statistically significantly ($p < 0.05$) higher (14.5*100,000 copies/µg) in PBMCs from individuals with lower plasma TCDD-levels (1.0-7.9 ppt) compared to those with higher plasma TCDD-levels (8.0-89.9 ppt; mean *AHR*-expression: 9.1*100,000 copies/µg) in uncultered, as well as in mitogen-stimulated cells (mean *AHR*-expression lower TCDD-levels: 39.0*100,000 copies/µg; mean *AHR*-expression higher TCDD-levels: 30.9*100,000 copies/µg; $p < 0.05$). In mitogen-stimulated PBMCs, mean *CYP1A1*-expression was slightly, but statistically significantly ($p < 0.05$) higher (6.9*100,000 copies/µg) in cells from subjects from the highest exposed zones compared to *CYP1A1*-expression in cells from persons from the non-contaminated area (5.0*100,000 copies/µg).

In contrast, lack of an association with AhR-dependent gene expression was observed for plasma (TEQ)-levels in *in vitro* mitogen-stimulated PBMCs from subjects, which were treated with TCDD (10 nM; 72 h). Plasma TCDD-levels further were negatively correlated with EROD-activity in those cells. These conflicting results led to the suggestion that long-term exposure to TCDD might perturb AhR-pathway regulation (Landi *et al.*, 2003).

The most notable result regarding mortality studies and the Seveso incident was an excess of lymphatic and hematopoietic neoplasms with increasing risk with time (Consonni *et al.*, 2008). In the most recent evaluation reflecting 25 years of follow-up, a relative risk (RR) of 2.23 (95% CI: 1.00-4.97) for people living in the most polluted zone was established. Highest risks were obtained for non-Hodgkin's lymphomas (RR = 3.35; 95% CI: 1.07-10.46) (Consonni *et al.*, 2008). Enhanced risks of developing non-Hodgkin's lymphomas were also reported for other TCDD-exposed cohorts (Floret *et al.*, 2003; Kogevinas *et al.*, 1997).

The thymus is an early established target organ for TCDD's AhR-dependent impact in experimental animals (Fernandez-Salguero *et al.*, 1996; Kociba *et al.*, 1976). In several studies, the thymus was in fact described to represent the most sensitive target organ as indicated by its perceptably reduced weight in response to TCDD-treatment (Harris *et al.*, 1973; Kociba *et al.*, 1976).

1.4.2. Proposed role(s) of the AhR in immune cells and AhR-ligands' impact

Whereas epidemiological investigations on cellular level of immune response either reveal inconsistent, marginal or insignificant findings regarding exposure to TCDD, the *in vitro* and especially the *in vivo* research using provides clearer evidence in this regard, which approaches to verify mechanism(s) potentially mediated by TCDD – or even by AhR in particular.

In organisms, epithelial or endothelial barriers provide the first line of defense against external pathogens. Within respective organs such as skin, lung, or gut, AhR is expressed in appropriate localized cells, as reported for keratinocytes, melanocytes, fibroblasts, Langerhans cells, or specialized intraepithelial lymphocytes (IELs), e.g. (Di Meglio *et al.*, 2014; Jux *et al.*, 2009; Luecke *et al.*, 2010; Li *et al.*, 2011; Martey *et al.*, 2005; Potapovich *et al.*, 2011).
There, the AhR is believed to be involved in cell differentiation processes and cell cycle regulation, hence potentially affecting the formation of respective barrier. Dependent on the ligand's properties and presence of AhR, the receptor is proposed to either promote cell cycle progression (endogen ligand/ transient activation), or to lead to growth arrest (exogen ligand/ sustained activation, or AhR absence) (Kalmes *et al.*, 2011; Mitchell and Elferink, 2008).

1.4.2.1. Innate immune cells

Among cells composing the innate immune system, macrophages, dendritic cells (DCs), human NK-22 cells, and murine lymphoid tissue inducer (LTi)-like cells were reported to express the AhR (Cella *et al.*, 2009; Colonna, 2009; Frericks *et al.*, 2007; Kimura *et al.*, 2009).

DCs and macrophages are antigen presenting cells linking innate immune response with adaptive immunity (reviewed in Moser and Leo, 2010). Macrophages and DCs promote T cell responses and express receptors, such as members of the Toll-like receptor (TLR) family, through which they are able to recognize pathogen-associated molecular patterns (PAMPs) or endogenous adjuvants and signals released by dying cells. To link innate to adaptive immune response, activated DCs and macrophages present high levels of particular major histocompatibility complex (MHC), molecules loaded with pathogen-derived peptides, express costimulatory molecules and secrete cytokines (Akira *et al.*, 2001; Joffre *et al.*, 2009).

In figure 4, a schematically demonstrated excerpt of proposed involvement of the AhR and its ligands in immune signaling is presented.

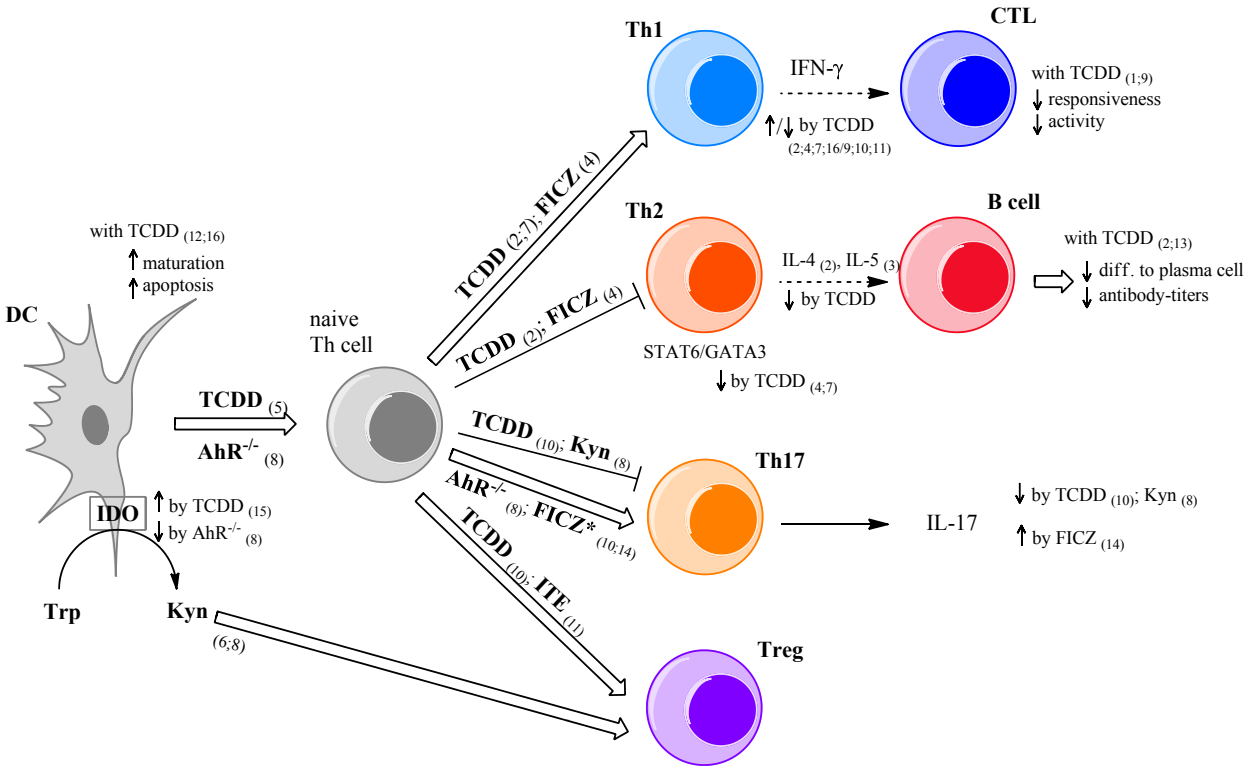

Figure 4: Proposed complex network of AhR-ligands' effects on immune signaling; schematically demonstrated excerpt. For detailed description, see text below. According to De Krey and Kerkvliet, 1995 [1]; Fujimaki *et al.*, 2002 [2]; Inouye *et al.*, 2005 [3]; Jeong *et al.*, 2012 [4]; Lee *et al.*, 2007 [5]; Mezrich *et al.*, 2010 [6], Negishi *et al.*, 2005 [7]; Nguyen *et al.*, 2010 [8]; Prell *et al.*, 2000 [9]; Quintana *et al.*, 2008 [10]; Quintana *et al.*, 2010 [11]; Ruby *et al.*, 2004 [12]; Tucker *et al.*, 1986 [13]; Veldhoen *et al.*, 2008 [14]; Vogel *et al.*, 2008 [15]; Vorderstrasse and Kerkvliet, 2001 [16]. FICZ*: Incubation of cells with FICZ under Th17-inducing conditions [10, 14].

Dendritic cells and macrophages

In mice, DCs were reported to be activated due to TCDD-exposure indicated by dose-, and AhR-dependent elevated expression levels of ICAM-1, CD-24, B7-2, CD40 (Vorderstrasse and Kerkvliet, 2001). This activation was further accompanied by a significant decrease in numbers of splenic DCs in TCDD-treated wild-type mice, whereas TCDD-treatment in $AhR^{-/-}$-mice did not alter the quantity of DCs recovered from the spleen. These findings were discussed in the context of an early loss of DCs correlated with immune suppression by enhanced maturation and apoptosis of DCs due to exaggerated activation of DCs by TCDD (Ruby *et al.*, 2004; Vorderstrasse and Kerkvliet, 2001).

Studying the effect of *in vivo* TCDD-exposure in mice on DC-function *ex vivo*, DCs obtained from TCDD-treated mice mediated enhanced ability to activate T cells, which was demonstrated by augmented T cell-proliferation (Vorderstrasse and Kerkvliet, 2001). Similarly, enhanced tumor necrosis factor-α (TNF-α)-induced maturation of DCs impacted by TCDD was obtained *in vitro* in primary bone marrow-derived DCs (BMDCs) from C57BL/6 mice. These findings were indicated by increased expression-levels of MHCII, CD86, CD40, and CD54 on surfaces of cells (Ruby *et al.*, 2004).

In vitro AhR-expression in BMDCs, splenic DCs, as well as peritoneal macrophages was demonstrated to be stimulated by the TLR-ligand LPS in cells obtained from mice (Kimura *et al.*, 2009; Nguyen *et al.*, 2010). In macrophages from $AhR^{-/-}$-mice, mRNA-expression levels of interleukin (IL)-6 (*Il6*), TNF-α (*Tnf*), and IL-12 (*Il12b*) were significantly elevated by LPS in comparison to those in wild-type mice, which was furthermore accompanied by significantly altered kinetics for IL-6-, and TNF-α production, reflecting an enhanced LPS-induced proinflammatory cytokine production in $AhR^{-/-}$-mice. Thus, the AhR was discussed to be involved in the negative regulation of LPS-responses (Kimura *et al.*, 2009). The authors demonstrated that the AhR negatively regulates the LPS signaling pathway by cooperating with signal transducer and activator of transcription 1 (STAT1) and nuclear factor-κB (NF-κB). In LPS-stimulated macrophages from wild-type mice, the AhR is able to form a complex with STAT1, which binds to NF-κB and as a result implicates the inhibition of the promoter activity of IL-6 (Kimura *et al.*, 2009).
It remains unresolved, which role (a) potentially present chemical(s) in the applied test system might play as (an) AhR-ligand(s). On the other hand, the AhR was reported to synergistically lead to induction of IL-6 expression in *in vitro* tumor cell systems, as its activation was coupled with inflammatory signals (DiNatale *et al.*, 2010; Hollingshead *et al.*, 2008). These findings were

observed, when the AhR was activated by its ligands TCDD or kynurenic acid, which was postulated to be an AhR-ligand just within respective study, and co-treated with IL-1β. According to the authors, these effects were 'largely' (but presumably not exclusively) dependent on the AhR (DiNatale *et al.*, 2010; Hollingshead *et al.*, 2008).

Enhanced IL-6 expression is discussed along with the stimulation of tumor progression as well as an involvement in the pathophysiology of autoimmune diseases and chronic inflammatory proliverative diseases (Ishihara and Hirano, 2002; Pollard, 2004). Further, IL-6 was revealed to synergistically induce indoleamine 2,3-dioxygenase (IDO) expression in concert with other cytokines (Fujigaki *et al.*, 2006). Thus, the activated AhR and accompanied IL-6 induction were suggested to play a role allowing tumor cells to escape immune surveillance and might be involved in molecular mechanisms related to immune mediated diseases (DiNatale *et al.*, 2010).

Indoleamine 2,3-dioxygenase (IDO)

In BMDCs and splenic DCs from $AhR^{-/-}$-mice, IL-10 production, as well as the expression of IDO, was inhibited by LPS compared to respective expression in cells from wild-type mice (Nguyen *et al.*, 2010). IL-10 production was also inhibited in LPS-stimulated peritoneal macrophages from $AhR^{-/-}$-mice compared to wild-type mice (Kimura *et al.*, 2009). Since regulatory DCs, specialized subsets of DCs, function their T cell-activating ability by mediation of regulatory factors like IL-10 and IDO, the authors speculated the AhR to play an anti-inflammatory role in BMDCs and splenic DCs (Nguyen *et al.*, 2010). Investigations by means of $AhR^{-/-}$-models further revealed an AhR-dependency of IDO-induction, which was determined *in vitro* in murine primary Langerhans cells and BMDCs, as well as *in vivo* in spleen and lung of mice (Jux *et al.*, 2009; Vogel *et al.*, 2008).

IDO, which is induced in the presence of TLR-ligands or proinflammatory cytokines by either an interferon-γ (IFN-γ)-dependent pathway via STAT1-α and interferon regulatory factor (IRF)-1, or through an IFN-γ-independent mechanism involving p38 mitogen-activated protein kinase (MAPK) and NF-κB (Fujigaki *et al.*, 2006; Taylor and Feng, 1991). The enzyme catalyzes the essential amino acid tryptophan (Trp) into kynurenine (Kyn), which represents, like the aforementioned kynurenic acid, another IDO-catabolite, which was quite recently identified to be an AhR-agonist (Opitz, *et al.*, 2011; Taylor and Feng, 1991).

IDO is often referred to as immunosuppressive enzyme and is discussed regarding its role in the regulation of naïve T cell-differentation. IDO-induced Trp-metabolites suppress T cell-response,

and IDO-induction in macrophages has been shown to lead to inhibition of T cell-proliferation (Bauer *et al.*, 2004; Munn *et al.*, 1999). DCs are able to directly and IDO-dependently activate (resting) mature regulatory T cells (Tregs) (Sharma *et al.*, 2007). The enzyme both activates Tregs and blocks their conversion into Th17-like T cells (Baban *et al.*, 2009). In reverse, when IDO is blocked, DCs were found to be stimulated to express IL-6, which represents a 'pro T helper 17 (Th17) cell-stimulus' (Baban *et al.*, 2009; Jetten, 2009). In the fashion of a feedback loop, dendritic IDO expression was revealed to be synergistically inducible in combination with IL-6, TNF-α, or IL-1β (Fujigaki *et al.*, 2006).

Tryptophan-2,3-dioxygenase (TDO)

Protein biosynthesis of tryptophan-2,3-dioxygenase (TDO), which degrades Trp to Kyn like IDO does, was also reported to be impacted by the AhR. Although usually predominantly expressed in the liver, Opitz *et al.* (2011) detected TDO in several human tumor tissues with increasing TDO protein levels corresponding to malignancy and to the proliferation index of respective tumor specimens. TDO-derived Kyn was correlated to lowered infiltration of immune cells in tumor tissue sections with elevated TDO-expression, and thus to suppression of antitumor immune responses. This was further demonstrated by a decreased release of IFN-γ by tumorspecific T cells and tumor cell lysis by spleen cells of mice afflicted with TDO-expressing tumors compared to mice bearing TDO-deficient tumors. The latter, as well as promoted tumor cell survival and motility, appeared in dependence of the AhR in an autocrine/paracrine fashion. The authors suggested that TDO-expression might be a general trait of cancer and that the activation of Trp catabolism may represent an endogenous feedback loop to AhR-mediated restriction of inflammation (Opitz *et al.*, 2011).

Recently, studies by Bessede and co-workers discovered that an initial exposure of mice to LPS activated the AhR and TDO, providing Kyn as an activating ligand of the AhR. On LPS-rechallenge, the AhR engaged in long-term regulation of inflammation, pointing a role for the AhR contributing to disease tolerance and correspondent ability of a host to reduce effects caused by infections on host fitness. Responses to primary LPS-challenge were mitigated by AhR and TDO-dependent Trp catabolism, whereas endotoxin tolerance required combined effects of AhR, IDO, and TGF-β (Bessede *et al.*, 2014).

1.4.2.2. Adaptive immune cells

Among adaptive immune cells, the AhR was reported to be expressed (and to be partially inducible) in B cells, $CD4^+$ helper T (Th) cells, and in $CD8^+$ cytotoxic T lymphocytes (CTLs) (Green *et al.*, 2011; Kerkvliet *et al.*, 2002; Sherr and Monti, 2013, Veldhoen *et al.*, 2008). Differentiation of $CD4^+$ T cells proceeds along transcription-factor-specific pathways including the T-box transcription factor T-bet and STAT4 for Th1 cells, GATA-binding protein 3 (GATA3) and STAT6 for Th2, retinoid related orphan receptor (ROR) γt and STAT3 for Th17, and forkhead box protein P 3 (FoxP3) and STAT5 for Tregs (reviewed in Chen *et al.*, 2011; Jetten, 2009; Kanhere *et al.*, 2012).

Th1 and Th2 cells

Th1 and Th2 cells direct different immune response pathways, and either pathway is able to down-regulate the other. Th1 cells (’cellular immunity’) secrete IFN-γ and activate inflammatory pathways mainly via macrophage activation and fight viruses and other intracellular pathogens, stimulate delayed-type hypersensitivity skin reactions, and eliminate cancerous cells. By contrast, Th2 cells (IgE-mediated ’humoral immunity’) proceed against extracellular organisms, and attribute to tolerance of xenografts and of the fetus during pregnancy, secreting cytokines IL-4 and IL-5, which upregulate antibody formation via B lymphocytes, eosinophils, mast cells, and other pathways (reviewed in Kidd, 2003).

In several reports, AhR agonists, namely TCDD, *β*-naphthoflavone, M50354 (an active metabolite of M50367, an antiallergic agent), or 6-formylindolo[3,2-*b*]carbazole (FICZ) shifted Th1/Th2 balance towards Th1 dominance in mouse experimental models *in vitro* and *in vivo* (Fujimaki *et al.*, 2002; Inouye *et al.*, 2005; Jeong *et al.*, 2012; Negishi *et al.*, 2005). These AhR agonists suppressed GATA3-expression and STAT6-activation, and reduced production of IL-4 and IL-5 in naïve Th cells, overall leading to suppression of Th2 differentiation (Fujimaki *et al.*, 2002; Inouye *et al.*, 2005; Jeong *et al.*, 2012; Negishi *et al.*, 2005). By use of AhR-deficient mice, Negishi *et al.* (2005) determined the modulating effects on Th1/Th2 balance to be AhR-dependent, even though AhR’s exact role in this regard remains largely unresolved.

B cells

Reduced secretion of IgE, IgG_1, and IgM, and accordant impaired humoral immune response are effects attributed to impact of AhR ligands (Fujimaki *et al.*, 2002; Yoshida *et al.*, 2012). Repressed IgM secretion in activated B cells by TCDD for instance, just as suppression of B cell differentiation by TCDD were found to appear AhR-dependently (Sulentic *et al.*, 1998; Tucker *et al.*, 1986).

The reduction of Th2-derived IL-5 production, which apparently was thought to represent a considerably sensitive endpoint for detection of TCDD's immunotoxicity, was proposed to mechanistically be due to impaired T cell function, suggesting that TCDD-induced suppression of T cell-derived cytokine production is involved in the impairment of antigen-specific antibody production (Inouye *et al.*, 2005; Ito *et al.*, 2002).

Immune response from B lymphocytes therefore at least secondarily seems to be affected by the AhR or by AhR-ligands, respectively. Interestingly, AhR expression in B cells is inducible by LPS, or by the Th2-type cytokine IL-4 *in vitro* in murine and human cell systems (Marcus *et al.*, 1998; Tanaka *et al.*, 2005).

Cytotoxic T cells (CTLs)

Despite the shift of Th1/Th2 balance towards Th1 dominance, Th1-dependent $CD8^+$ cytotoxic T cell (CTL)-mediated responses were found to be suppressed, and priming of naïve CTL-precursors was inhibited by TCDD *in vivo* (De Krey and Kerkvliet, 1995; Prell *et al.*, 2000). Interestingly, expression of the AhR is required in both $CD4^+$ and $CD8^+$ T cells in this regard, and both cell subsets contribute to the full suppressive effect of TCDD (Kerkvliet *et al.*, 2002).

Differential results, which at least partially might be explainable by diverging study designs and endpoints, regarding excretion of IFN-γ were reported. Correspondent to facilitated Th1 differentiation by TCDD, production of IFN-γ significantly increased in several studies (Fujimaki *et al.*, 2002; Jeong *et al.*, 2012; Negishi *et al.*, 2005; Vorderstrasse and Kerkvliet, 2001), whereas agreeing with the further occurring suppression of CTLs by TCDD, IFN-γ levels were found to be significantly decreased in other investigations (Prell *et al.*, 2000; Quintana *et al.*, 2008).

Th17 cells and Tregs

A considerable quantum of information is available regarding AhR's influence on differentiation, development, and function of Th17 vs. Treg cells. Differentiation and function of Tregs and Th17 cells are reciprocally controlled, as Th17 cells secrete the proinflammatory cytokines IL-17 and IL-22 mediating exacerbation of inflammation and autoimmunity, whereas opposing Tregs produce TGF-β and IL-10 playing an indispensable role regarding immune tolerance and suppression of excessive immune responses (Hanieh, 2014; Sakaguchi *et al.*, 2008).

In the course of an experimental autoimmune encephalomyelitis (EAE), activation of the AhR by TCDD *in vivo* leads to enhanced production of TGF-β and reduced secretion of IL-17 in lymph node cells and to an increased frequency of Tregs in spleens of mice (Quintana *et al.*, 2008). *In vivo* treatment with 2-(1'H-indole-3'-carbonyl)-thiazole-4-carboxylic acid methyl ester (ITE), an endogenous AhR ligand isolated from porcine lung in 2002, resulted in a higher frequency of Tregs and led to a lowered percentage of Th17 cells in murine splenocytes in an EAE model (Quintana *et al.*, 2010; Song *et al.*, 2002). *Ex vivo*, immunized lymph node cells secreted reduced amounts of IL-17, whereas secretion of IL-10 and TGF-β was enhanced (Quintana *et al.*, 2010).
Nguyen *et al.* (2010) demonstrated that AhR-absence in BMDCs skewed naïve T-cell-differentiation into Treg-cells ($Foxp3^+$), facilitating Th17-cell development. In turn, addition of synthetic L-Kyn to the applied coculture system using BMDCs and naïve T cells from $AhR^{-/-}$-mice reversed the T-cell-differentiation to Tregs rather than Th17-cells (Nguyen *et al.*, 2010).

The AhR ligand FICZ, on the other hand, promotes Th17 cell differentiaton *in vitro* and *in vivo* (Quintana *et al.*, 2008; Veldhoen *et al.*, 2008). In murine $CD4^+$ T cells cultured unter Th17 conditions, the presence of FICZ (0-500 nM, 96 h) led to concentration-dependent up-regulation of IL-17 (*Il17a*, *Il17f*) and IL-22 (*Il22*) mRNA expression (Veldhoen *et al.*, 2008). Besides its inhibitory effects on Treg cell differentiation, FICZ synergized with TGF-β1, IL-6, and IL-23 to drive Th17 cell differentiation and augmented the secretion of IL-17, IL-21, and IL-22 *in vitro*. *In vivo*, treatment with FICZ (1 µg/mouse) was associated with decreased frequency of $CD4^+Foxp3^+$ Treg cells, increased frequencies of $CD4^+IL\text{-}17^+$ T cells and $CD4^+IFN\text{-}\gamma^+$ T cells, and enhanced secretion of IL-17 and IFN-γ subsequent to *in vitro* stimulation (Quintana *et al.*, 2008). Further, the absolute number of $CD4^+IL\text{-}17A^+$ and of $CD4^+IL\text{-}22^+$ cells in the spinal cord of immunized mice significantly elevated after treatment with FICZ (600 ng/mouse) on day 18 of an EAE-response compared to the control group. This effect was inverted in $AhR^{-/-}$-mice (Veldhoen *et al.*, 2008).
Since Th17 cells represent a driving force of pathogenesis for some autoimmune diseases, AhR activation potentially exacerbates Th17-mediated autoimmunity (Esser *et al.*, 2009).

1.4.2.3. AhR and immune cells – critical view

Based on available studies, it occasionally remains uncleared issue whether effects, e.g. shifts of cell (sub-)populations, are due to a primary 'true induction' of a cell type. Cell type specific inhibition of apoptosis by a ligand might simulate this outcome, or other cell types may be reduced by mechanisms like cell subset-specific cytotoxity or apoptosis. Impacted functionality of cells or cell counts and hence imbalanced cell subsets might emerge as a 'feigned induction' of a definite cell type (Prell *et al.*, 2000; Ruby *et al.*, 2004).

Conclusively, the presence of the AhR itself and the receptor in collaboration with its endogenous or exogenous ligands is proposed to be interlocked in several sections of the complex network of immune reactions. To date, precise attribution of pathways impacted by the AhR and its ligands remains complex and involves inconsistency in a number of cases. The manner and course of effect directed in particular appears to be dependent on the occurrence and on the type of a ligand, and might also be contingent on the type of exposure and applied dose as well as the physiological or pathological condition of regarded organism.
Of further relevance are inter-species differences as well as respective binding affinities of exogen vs. endogen ligands to the AhR. Although rodent AhR generally exhibits higher affinities towards exogen ligands than human AhR does, a reversed situation was found for several endogen ligands like kynurenic acid or indirubin (DiNatale *et al.*, 2010; Flaveny *et al.*, 2009; Ramadoss and Perdew, 2004). Further on, widely used $AhR^{-/-}$-models on one hand are of relevant informative content but are still difficult to interpret, since estimation of impact of the receptor's absence itself represents complex issue.

Overall, AhR seems to play considerable but intricate role in immune response implying feasible divergence across species, ligand properties, dose and type of exposure.

1.4.3. Expression and induction of CYP1-isoenzymes in PBMCs

As indicated in the previous chapter, expression of the Ah receptor was described in several blood cells like macrophages, DCs, T cells, and B cells, it is not all that surprising that several authors report on inducibility of CYP1-isoenzymes in immune cells (Frericks *et al.*, 2007; Kerkvliet *et al.*, 2002; Kimura *et al.*, 2009; Sherr and Monti, 2013).

CYP1-induction *in vivo* – mouse

In vivo experiments with rodents provide prelusive information in this regard. In immature $CD4^-$ $CD8^-$-thymocytes and thymic emigrants from mice treated with TCDD (10 mg/kg bw; single *i.p.* dose) for seven days, *Cyp1b1* was up-regulated (cut-off: ≥2fold change) in the course of a microarray gene expression analysis (Frericks *et al.*, 2006). *Cyp1b1* was also up-regulated in fetal thymic emigrants, for which fetal thymic lobes were taken from mouse embryos and cultivated for six days in the presence of 10 nM TCDD. Interestingly, *Cyp1a1* was only up-regulated in fetal emigrants but not in adult immune cells, although the AhR – at least on mRNA-level – was markedly expressed in these cells. This was also the case subsequent to a short *in vivo* TCDD-exposure of 24 h. As part of the latter investigation, *Cyp1a1* and *Ahrr* were obtained to be up-regulated in DCs from TCDD-treated mice (Frericks *et al.*, 2006). In a further gene expression microarray experiment with mice using lower TCDD-concentrations (20 µg/kg bw, oral) and shorter treatment durations, *Cyp1a1* was up-regulated (cutoff: ≥2 fold change) in $CD4^+$-T cells (3 h or 24 h) and B cells (3 h) from spleens of *in vivo* exposed and Ovalbumin (OVA)-immunized mice (Nagai *et al.*, 2005). In addition, mRNAs encoding TIPARP or AhRR appeared to be up-regulated in B cells (3 h, or 24 h), and in $CD4^+$-T cells (24 h), respectively (Nagai *et al.*, 2005).

CYP1-induction *in vivo* – rat

In PBMCs received in the course of studies with rats *in vivo* exposed to AhR ligands (3-methylcholanthrene, or β-naphthoflavone), induction of EROD-activity in response to these ligands was obtained (Dey *et al.*, 2001; Saurabh *et al.*, 2010). Regarding WB analyses (CYP1A1, CYP1A2) and investigations examining mRNA-levels (*Cyp1a1*, *Cyp1a2*, and *Cyp1b1*) included in these trials, effects generally appeared to be slight, and respective AhR ligands were consistently less effective in PBMCs compared to their responses in livers of treated animals (up to seven times higher fold-induction of EROD-activity). However, in a recent *in vivo* study with rats using doses of a PAH-mixture accounting for 6 or 600 µg (of each of phenanthrene, pyrene, benzo[*a*]pyrene) per day for

28 days, the authors revealed dose- and time-dependent EROD inductions in PBMCs with maximal absolute values of around 90 or 200 pmol resorufin/min*mg protein, which was at least approaching comparable dimensions measured in liver samples (~440 or 970 resorufin/min*mg protein) (Chahin *et al.*, 2013).

CYP1-induction *in vitro*

In concentration-dependent manner, CYP1A1 and CYP1B1 are also inducible by AhR-ligands *in vitro* in rodent PBMCs, which was investigated on both mRNA and protein level, while CYP1A2 was not reported to be targeted (Lawrence *et al.*, 1996; Mezrich *et al.*, 2010; Nohara *et al.*, 2006). In human PMBCs, *CYP1A1* and *CYP1B1* are constitutively expressed, whereas *CYP1A2* expression appears to be detectable only sporadically and not in PBMCs from every investigated individual (Finnström *et al.*, 2002; Krovat *et al.* 2000, Siest *et al.*, 2008). On the basis of current information, CYP1A2 is also not inducible by AhR ligands *in vitro* in human blood cells.

CYP1A1 – human blood cells

In 1974, Kouri *et al.* already reported on concentration-dependent TCDD-inducible EROD (or CYP1A) activity in primary human PBMCs. At exposure duration of 24 h and TCDD-concentrations ranging from 0.3 to 300 nM, they received a half maximal effective concentration (EC50) of 8 nM TCDD (Kouri *et al.*, 1974). To date, a couple of articles on this subject are accessible, in which most of the experiments show great inter- and intra-individual variety and overall comparably low absolute induction values both on gene transcription and on protein level. Such results diverge considerably, as results from investigations using TCDD ranged from ~3fold (100 nM, 6 h) over ~20fold (10 nM, 72 h), and ~60fold (10 nM, 48 h) to ~160fold (10 nM, 48 h) *CYP1A1*-induction on mRNA-level in primary human PBMCs (Nohara *et al.*, 2006; Vanden Heuvel *et al.*, 1993; Van Ede *et al.*, 2014b). In several studies, *CYP1A1* mRNA- and EROD-induction by AhR ligands occurred concentration-dependently, implicating diverging EC50-values of ~800 pM (72 h) as well as the aforementioned value of 8 nM (24 h) for EROD-induction, and ~400 pM (48 h) and 1.4 nM TCDD (6 h), with respect to *CYP1A1* mRNA-induction (Kouri *et al.*, 1974; Nohara *et al.*, 2006; Van Duursen *et al.*, 2005; Van Ede *et al.*, 2014b).

CYP1B1 – human blood cells

CYP1B1 was as well reported to be up-regulated in response to TCDD. Respective maximum mRNA-levels achieved after TCDD-treatment varied from ~2-3fold (5 nM, 6 h; 5 nM, 72 h; or 10 nM, 48 h), to around 5-8fold (1 nM, 48 h) induction in PBMCs (De Waard *et al.*, 2008; Van Duursen *et al.*, 2005; Van Ede *et al.*, 2014b). Recently, van Ede *et al.* published data on concentration-dependent elevation of *CYP1B1* mRNA in human PBMCs, implicating diverging effective concentration 20% (EC20)-values ranging from 77 to 164 pM (48 h treatment), dependent on the donor (Van Ede *et al.*, 2014b). *CYP1B1*-induction has also been shown to vary contingent upon exposure duration. In respective investigation by Spencer *et al.* (1999), elevation of mRNA-levels concentration-dependently increased with time until it peaked at 72 h of treatment, whereupon it continuously decreased up to the limit of the test series at five days of culture.

AhR ligands other than TCDD and CYP1-induction

Further exogen and endogen AhR-ligands lead to induction of CYP1-isoenzymes in primary human PBMCs, as indolo[3,2-*b*]carbazole (ICZ, 100 nM, 48 h) or 6-formylindolo[3,2-*b*]carbazole (FICZ, 10 nM, 3 h) elevated *CYP1B1* gene expression (~2fold or ~5fold), benzo[*a*]pyrene (1 µM, 12 h) or 3-methylcholanthrene (0.1-1 µM, 12 h) enhanced *CYP1A1* mRNA levels in these cells (De Waard *et al.*, 2008; Komura *et al.*, 2001; Tuominen *et al.*, 2003). Two other members of the AhR-gene batterie, namely *AhRR* and *TIPARP*, were reported to be up-regulated in response to AhR-agonists in human PBMCs, which was shown to appear concentration-dependently regarding *AhRR* on mRNA-level by van Ede *et al.* (De Waard *et al.*, 2008; Van Ede *et al.*, 2014b; Wens *et al.*, 2011). In this regard, around 10-14fold maximum *AhRR*-induction by TCDD with EC20s ranging 120-240 pM was achieved after 48 h of incubation, whereas treatment with 1-PeCDD resulted in EC20s ranging 110-620 pM, and 4-PeCDF gained ~80 pM for EC20 (Van Ede *et al.*, 2014b).

Overall, treatment of human PBMCs with AhR-ligands leads to rather low absolute values and induction levels and of CYP1-isoenzymes. Besides considerable inter-species diversity, responses vary greatly among different individuals and deviate respectably regarding both efficacy and potency in different cell systems. Applying human PBMCs and their properties regarding induction of CYP1-isoenzymes as biomarker of exposure remains contentious issue, as it shows to represent a parameter, which so far appears difficult to adjust and reproduce (De Waard *et al.*, 2008; Nohara *et al.*, 2006; Spencer *et al.*, 1999; Van Duursen *et al.*, 2005).

2

Assignment of tasks

Within the framework of SYSTEQ project, seven individual congeners termed the ‘core congeners’ were chosen: TCDD, 1-PeCDD, 4-PeCDF, PCB 118, PCB 126, PCB 156, and the NDL-PCB 153. Core congeners, contributing approximately 90% of TEQs in the human food chain (Liem *et al.*, 2000), were tested *in vivo* as well as *in vitro*. A further, regarding environmental relevance likewise important, set of seven congeners was included for *in vitro* experiments of the present study: 1,6-HxCDD, 1,4,6-HpCDD, TCDF, 1,4-HxCDF, 1,4,6-HpCDF, PCB 77, and PCB 105.

Three major investigations were applied. In *in vitro* liver cell systems using both primary rat hepatocytes and the rat hepatoma cell line H4IIE, impact of the core congeners as well as the group of seven further compounds was investigated by means of EROD-induction. CYP1A-induction measured by EROD-activity represents a sensitive marker for dioxin-like effects, and was used to estimate potency and efficacy of selected chemicals. A definite data-set of *in vitro* studies was supposed to serve as a fundament for a probable establishment of novel TEFs with respect to the SYSTEQ project.

One further important objective within the SYSTEQ project was to find potential novel biomarkers of exposure. Hence, a mouse whole genome microarray experiment using the seven core congeners was implemented. Of these compounds, five were investigated within present study: 1-PeCDD, 4-PeCDF, PCB 118, PCB 126, and PCB 156. Though the microarray experiment was realized as one project, TCDD and PCB 153 were examined in a previous study by C. Lohr (Lohr, 2013).

In order to gain knowledge with respect to TCDD-mediated effects towards immune cells, a further whole genome microarray experiment by use of human PBMCs was applied. To approach to this objective, freshly isolated PBMCs were characterized by flow cytometry and exposed to TCDD ‘alone’ or combined with a stimulus (LPS, or PHA).

Along with several experiments within the SYSTEQ project, a concluded compilation of eight ‘potential’ AhR-target genes encoding CYP1A1, CYP1A2, CYP1B1, AHRR, TIPARP, ALDH3A1, CD36, and HSD17B2, was chosen and investigated in the course of all three models – mouse liver, rat liver cells, and human blood cells.

3
Methods

Test compounds were provided by The Dow Chemical Company (Midland, Michigan, USA). For *in vitro* experiments, congeners were dissolved in DMSO and added to respective incubation media constantly yielding final DMSO-concentrations of 0.1% (v/v). As part of *in vivo* studies, which were performed at the animal facility of the Utrecht University (Institute for Risk Assessment Sciences (IRAS), Utrecht, The Netherlands), congeners were diluted in corn oil. Accordingly, controls examined were either DMSO-, or corn oil-treated vehicles.

Purity and quality of test compounds PCBs 118, 153, and 156, as well as the vehicles DMSO and corn oil, were checked at Umeå University (Department of Chemistry, Umeå, Sweden) using a carbon fractionation method in combination with a gas chromatography/high-resolution mass spectrometry (GC-HRMS)-analysis. PCB 118, formerly containing 85 ng/g TEQs, was cleaned to a final concentration of 6.6 ng/g TEQs, whereas PCB 156, initially containing 201 ng/g TEQs, was purified to 36 ng/g TEQs. PCB 153 was marginally contaminated with 0.41 ng/g TEQs (correspondence with P. Andersson, Umeå University, SE-901 87 Umeå, Sweden; Van Ede *et al.*, 2013a).

Chemicals and reagents were obtained from Roth (Karlsruhe, Germany), or from Merck (Darmstadt, Germany). Fine-chemicals were from Sigma-Aldrich (Steinheim, Germany), unless otherwise stated. The same applies to all consumables, which were purchased from Greiner Bio-one (Frickenhausen, Germany). Buffers and solutions were aqueous, if not differently specified.

3.1. H4IIE cells

The rat hepatoma cell line H4IIE (Rat hepatoma Reuber H35, ATCC® CRL-1548™; figure 5, following page) was established in 1964 (Pitot *et al.*, 1964), and was purchased from The European Collection of Cell Cultures (ECACC; Public Health England, Salisbury, UK). The adherent, morphologically epithelial cell line originally was derived by the strain *Rattus norvegicus*, and is characterized by both low basal CYP1A-expression and high CYP1A-inducibility, and is useful for detection of picogram levels of AhR-ligands (Sawyer and Safe, 1982; Tillitt *et al.*, 1991).

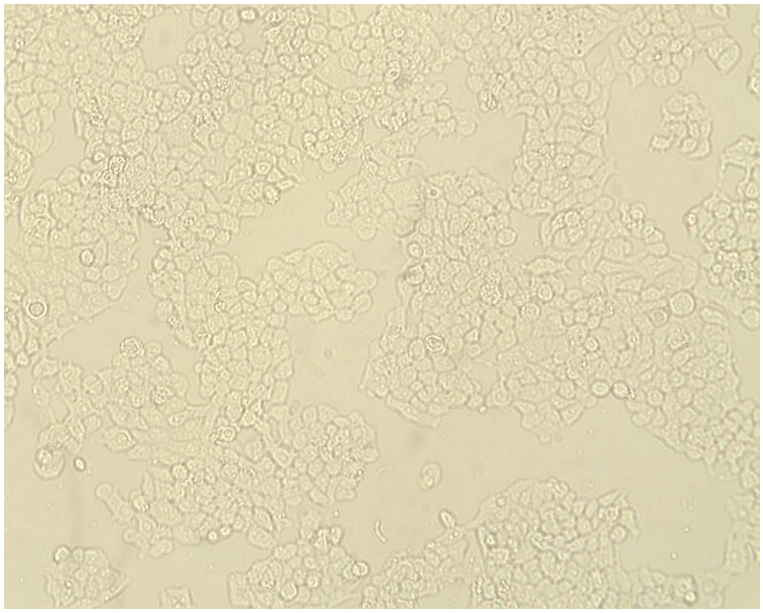

Figure 5: Light microscopic photograph of H4IIE-cells (magnification 100x).

H4IIE cells were grown in Dulbecco's modified Eagle medium (DMEM) high glucose (4.5 g/L) with L-glutamine, without phenol-red (PAA Laboratories, Coelbe, Germany), supplemented with 10% (v/v) fetal bovine serum (PAA Laboratories), 1% (v/v) penicillin/streptomycin (PAA Laboratories), and dexamethasone (100 nM) in 75 cm^2-, or 175 cm^2 cell culture flasks. Cells were cultured at 37°C, 95% relative humidity, and 5% CO_2, and cell culture medium was renewed every 2-3 days. Subculture was performed by use of trypsin/EDTA (PAA Laboratories) according to Lindl (2002). To be used within experiments, viable cells were counted using a Neubauer counting chamber via trypan blue (trypan blue solution, 0.4%) exclusion test (Evans and Schulemann, 1914; Rous and Jones, 1916), and seeded on either 24-well cell culture plates ($1.2*10^5$ cells/1 mL/well), 60 mm cell culture dishes ($1.3*10^6$ cells/4 mL/dish), or 100 mm cell culture dishes ($4*10^6$ cells/7 mL/dish). Cells were allowed to grow for 24 h. For incubation, medium was removed and incubation medium (DMEM high glucose (4.5 g/L) with L-glutamine, without phenol-red, supplemented with 10% (v/v) charcoal stripped fetal bovine serum (PAA Laboratories), 1% (v/v) penicillin/streptomycin, and dexamethasone (100 nM)) was applied. For details regarding tested compound concentrations in respective assays examined, see appropriate chapters.

3.2. Primary rat hepatocytes

Primary rat hepatocytes (PRH, figure 6) were obtained from male Sprague Dawley® rats weighing 150-250 g (Charles River, Sulzfeld, Germany) applying a collagenase-based, modified method originally established by Seglen in 1972 (Schrenk *et al.*, 1992).

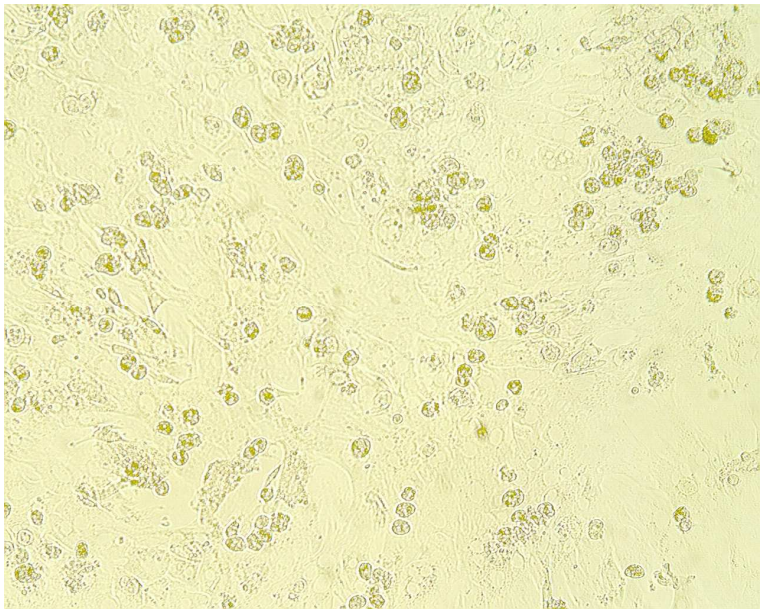

Figure 6: Light microscopic photograph of primary rat hepatocytes (magnification 100x).

Isolation of primary rat hepatocytes

Prior to isolation of cells, required perfusion-solutions were preheated to 42°C. The particular animal was anesthetized by *intraperitoneal* (*i.p.*) injection of sodium pentobarbital (100 mg/kg bw), and full narcosis was verified via tail pinch response test. After the animal was fixed on the work bench, the abdomen was sprayed with 70% Ethanol, and the abdominal cavity was opened. Two loose ligatures were placed: One around *vena porta* ca. 1 cm beneath liver entry just above the branch to the spleen, and one around *vena cava inferior* just above the branch to the right kidney. 100 µL of a heparin-solution (1000 U/mL in 0.9% NaCl) was injected into the *vena cava inferior* to prevent blood coagulation. About 1-2 cm below the ligation, *vena porta* was punctured with a cannula, through which Ethylenglykol-bis(*β*)-Aminoethylether-*N*,*N*,*N'*,*N'*-Tetraacetat (EGTA)-containing perfusion buffer 1 (PB1) was poured (3.6 mL/min). The ligature was fixed, and flow rate was sped up to 40 mL/min for 10 min, after the *vena cava inferior* was cut through ca. 2 cm below the ligation point. The liver exsanguinated, and due to EGTA-induced Ca^{2+}-loss, desmosomal connections between hepatocytes loosened. During this perfusion step, the diaphragm was opened, whereby the lung collapsed and the animal died. By puncturing the right atrium, another cannula,

which was fixed with a further ligature, was inserted into the *vena cava superior*. Hence, perfusate flowed recirculating. Liver was flushed with PB2 containing freshly dissolved collagenase (100 CDU/mL) for 10 min (20 mL/min), leading to disintegration of the extracellular matrix structure. The liver was carefully cut out, put on a nylon-net (mesh size 250 µm) spanned over a 250 mL-beaker, and the liver capsule was opened. Rinsing with washing buffer, hepatocytes were washed out and the procedure repeated with a nylon-net of mesh size 100 µm. The total volume of ca. 200 mL cell suspension was filled in four 50 mL-falcons, and centrifuged (20 g, 3-4 min, RT). Cells were washed twice with washing buffer, cautiously resuspended in ca. 25 mL washing buffer, and counted with the help of a Fuchs-Rosenthal counting chamber (Lindl, 2002) via trypan blue (trypan blue solution, 0.4%) exclusion test (Evans and Schulemann, 1914; Rous and Jones, 1916). Cell viability always exceeded 85% (modified method according to Seglen, 1972; Schrenk *et al.*, 1992). The components of perfusion buffers and required solutions, and respective storage conditions are summarized in table 2.

Table 2: Solutions required for isolation of primary rat hepatocytes.

Perfusion buffer 1 (PB1)	Hank's balanced salt solution (HBSS)[1] without Ca & Mg without phenol-red HEPES (10 mM) EGTA (0.1 mM) 4°C
Perfusion buffer 2 (PB2)	DMEM low glucose (1 g/L) with L-glutamine[1] HEPES (10 mM) 4°C prior to use: collagenase (100 CDU/mL), freshly dissolved
Washing buffer	DMEM high glucose (4.5 g/L) with L-glutamine[1] without phenol-red 1% (v/v) penicillin/streptomycin[1] 0.2% (v/v) bovine serum albumin (BSA; 30% solution[1]) HEPES (10 mM) 4°C
HEPES	HEPES (1 M) pH 7.4 4°C
EGTA	EGTA (100 mM) pH 8.0 4°C
Heparin-solution	1000 U/mL in 0.9% NaCl 4°C
Sodium pentobarbital-solution	33 mg/mL freshly prepared

[1]PAA Laboratories, Coelbe, Germany

PRH were seeded on rat-tail collagen-coated cell culture vessels. Cells were seeded in hepatocyte seeding medium (HSM) on either 24-well plates ($2*10^5$ cells/1 mL/well), 60 mm dishes ($2*10^6$ cells/4 mL/dish), or 100 mm dishes ($6*10^6$ cells/7 mL/dish). Cells were allowed to attach for 2 h before medium was changed to hepatocyte functional medium (HFM). After further 24 h, medium was replaced by fresh HFM, and PRH were incubated with test compounds. For details regarding tested compound concentrations in respective assays examined, see appropriate chapters. Composition of culture media and media additives are compiled in table 3 (following page).

Preparation of collagen-solution and coating of cell culture vessels

Ca. 20 rat tails were used to yield around 2 g collagen fibers. Rat tails were disinfected (70% ethanol), and skinned under the hood. Collagen fibers were drawn out from the tail tip, dried over night under UV light, hackled, and dried again under UV light. Collagen fibers were washed with purified water (1 h) and transferred into sterile filtered acetic acid (0.1%, 500 mL). After 24 h of stirring, undissolved fibers were separated (2300 g, 3 h, RT), and protein content of obtained collagen-solution was measured according to bicinchoninic acid (BCA) protein assay (Pierce® BCA Protein Assay Kit; Thermo Fisher Scientific, Karlsruhe, Germany), according to the manufacturer's protocol. Collagen working solution was prepared (0.5 mg protein/mL; storage: 4°C), and used to coat cell culture vessels (modified method according to Elsdale and Bard, 1972). Freshly coated vessels were dried over night under UV light, and were hence ready to be used for cell seeding.

Table 3: Culture media and media additives used for cultivation of primary rat hepatocytes.

Hepatocyte seeding medium (HSM)	DMEM + Ham's F12 (1+1): DMEM high glucose (4.5 g/L) with L-glutamine[1] without phenol-red Ham's F12 medium with L-glutamine[2] without phenol-red with 1.176 g/L $NaHCO_3$ 5% (v/v) fetal bovine serum[1] HEPES (10 mM) gentamicin[1] (50 µg/mL) insulin (100 nM) sodium selenite (100 nM) 4°C
Hepatocyte functional medium (HFM)	DMEM + Ham's F12 (1+1): DMEM high glucose (4.5 g/L) with L-glutamine[1] without phenol-red Ham's F12 medium with L-glutamine[2] without phenol-red with 1.176 g/L $NaHCO_3$ BSA/linoleic acid (5 µg/mL BSA, 0.5 mg/mL) HEPES (10 mM) dexamethasone (100 nM) gentamicin[1] (50 µg/mL) insulin (100 nM) sodium selenite (100 nM) transferrin (5 µg/mL) 4°C
HEPES	HEPES (1 M) pH 7.4 4°C
BSA/linoleic acid	BSA (10% in DPBS) 50 mg linoleic acid 4°C
Dexamethasone working solution	Dexamethasone stock solution (25 mg/6.3 mL Ethanol, p.a.) diluted 1:100 with sterile filtered, purified water final concentration: 100 µM -20°C
Insulin working solution	Insulin stock solution (10 mg/mL in 25 mM HEPES) diluted with DMEM high glucose (4.5 g/L) with L-glutamine (without phenol-red)[1] final concentration: 100 µM -20°C
Transferrin working solution	5 mg/mL in DMEM high glucose (4.5 g/L) with L-glutamine (without phenol-red)[1] -20°C

[1]PAA Laboratories, Coelbe, Germany
[2]PAN-Biotech, Aidenbach, Germany

3.3. Alamar Blue® assay

Alamar Blue® assay was used to determine viability of cells. The test is based on the reduction of non-fluorescent resazurin to fluorescent resorufin in the presence of $NADH/H^+$ (O'Brien *et al.*, 2000). Although it has been proposed that mitochondrial, cytosolic, as well as microsomal enzymes are able to reduce resazurin (Gonzalez and Tarloff, 2001), it remains unclear, whether this occurs intracellularly or in the medium as a chemical reaction (O'Brien *et al.*, 2000).

H4IIE cells or PRH were seeded and incubated with test compounds in 24-well plates as described. Final concentrations of congeners are specified in table 4.
Samples and controls (medium, DMSO 0.1%) were performed as doublets, and saponine (final concentration 0.1%) was used as positive-control for cytotoxic effects (reviewed in Podolak *et al.*, 2010). Subsequent to the incubation period of 24 h, incubation medium was removed, and cells were washed twice with phosphate buffered saline (PBS^{--}, without Ca and Mg, 37°C). Resazurin working solution (37°C) was added and incubated for 1 h at 37°C, 95% relative humidity, and 5% CO_2. Afterwards, fluorescence was measured in a preheated (37°C) microplate fluorometer (ex, 544 nm; em, 590 nm; Fluoroskan Ascent FL, Thermo Fisher Scientific, Karlsruhe, Germany). Blank values were subtracted from measured values, and viabilities were displayed in per cent related to appendant solvent controls (DMSO 0.1%). For details regarding composition of Alamar Blue® assay reagents, PBS^{--}, and respective storage conditions see tables 4 and 5.

Table 4: Final congener-concentrations tested in Alamar Blue® assay (H4IIE, PRH).

TCDD,		
1-PeCDD	H4IIE, PRH	10^{-10} M - 10^{-8} M
1,6-HxCDD	H4IIE, PRH	$5*10^{-10}$ M - $3*10^{-8}$ M
1,4,6-HpCDD	H4IIE, PRH	$5*10^{-9}$ M - $4.56*10^{-7}$ M
TCDF	H4IIE, PRH	10^{-8} M - $9.84*10^{-7}$ M
4-PeCDF	H4IIE, PRH	10^{-9} M - 10^{-7} M
1,4-HxCDF	H4IIE, PRH	$5*10^{-9}$ M - $3*10^{-7}$ M
1,4,6-HpCDF	H4IIE, PRH	$5*10^{-9}$ M - $1.58*10^{-7}$ M
PCB 126	H4IIE	$5*10^{-9}$ M - 10^{-7} M
	PRH	10^{-8} M - 10^{-6} M
PCBs		
77, 105, 118, 153, 156	H4IIE, PRH	10^{-8} M - 10^{-6} M

Table 5: Alamar Blue® assay reagents, and PBS^{--}-components.

Resazurin stock solution	Resazurin (440 mM in DMF) diluted (1:1000) with NaPi-buffer (440 µM resazurin) 4°C; four weeks
Resazurin working solution	Resazurin stock solution diluted (1:10) with respective culture medium (without supplements) prepared immediately prior to use (37°C)
NaP_i-buffer	NaCl (154 mM) $Na_2HPO_4*H_2O$ (3.7 mM) KH_2PO_4 (1.1 mM) 4°C
Phosphate buffered saline (without Ca and Mg) PBS^{--}	NaCl (137 mM) NaH_2PO_4 (6.5 mM) KCl (2.7 mM) KH_2PO_4 (1.5 mM) pH 7.4 RT

3.4. 7-Ethoxyresorufin *O*-deethylase (EROD)-assay

As a parameter for AhR-activation, induction of CYP1A-mediated 7-ethoxyresorufin *O*-deethylase (EROD)-activity was determined in H4IIE cells and PRH (Burke and Mayer, 1974; Kennedy *et al.*, 1993). EROD-activity was measured according to van Duursen *et al.* (2005) with modifications. As described, cells were seeded and incubated with compounds in 24-well plates. Final concentrations of congeners applied are noted in table 6.

Samples and controls (medium, DMSO 0.1%) were performed as doublets, whereas TCDD (1 nM) was used as positive-control for EROD induction. After 24 h of exposure, incubation medium was removed, and cells were washed twice with PBS^{--} (37°C). EROD medium (37°C; see table 7) was added, and plates were placed in a preheated (37°C) microplate fluorometer (Fluoroskan Ascent FL, Thermo Fisher Scientific, Karlsruhe, Germany), and fluorescence was measured at an excitation wavelength of 544 nm, and an emission wavelength of 590 nm, every 90 s for 30 min. Resorufin-content was quantified with the help of a calibration curve (0-1000 nM resorufin).

After measurement and removal of EROD medium, cells were washed twice with PBS^{--} and frozen to -80°C over night. Cells were cracked through a freeze-thaw-cycle (thawing: 3x, 15 min, RT; freezing in between: 3 h at least), and protein content was measured by BCA assay (Pierce® BCA Protein Assay Kit), according to the manufacturer's protocol.

Kinetics of resorufin-formation due to impact of congeners was used as basis for calculation of EROD-activities. Values were indicated as pmol resorufin/min*mg protein (method modified according to van Duursen *et al.*, 2005).

Table 6: Ranges of final congener-concentrations tested in EROD-assay (H4IIE, PRH).

TCDD	H4IIE	$5*10^{-13}$ M - 10^{-9} M
	PRH	10^{-14} M - 10^{-8} M
1-PeCDD	H4IIE	10^{-12} M - $5*10^{-10}$ M
	PRH	10^{-13} M - 10^{-8} M
1,6-HxCDD	H4IIE	$5*10^{-12}$ M - $5*10^{-9}$ M
	PRH	10^{-12} M - $3*10^{-8}$ M
1,4,6-HpCDD	H4IIE	$5*10^{-12}$ M - $5*10^{-9}$ M
	PRH	$5*10^{-12}$ M - 10^{-7} M
TCDF	H4IIE	10^{-11} M - 10^{-7} M
	PRH	10^{-12} M - 10^{-8} M
4-PeCDF	H4IIE	10^{-13} M - 10^{-9} M
	PRH	10^{-12} M - 10^{-8} M
1,4-HxCDF	H4IIE	10^{-12} M - 10^{-9} M
	PRH	$5*10^{-12}$ M - $5*10^{-8}$ M
1,4,6-HpCDF	H4IIE	$5*10^{-11}$ M - $5*10^{-8}$ M
	PRH	10^{-11} M - $1.58*10^{-7}$ M
PCB 126	H4IIE	$5*10^{-12}$ M - $5*10^{-9}$ M
	PRH	$5*10^{-12}$ M - 10^{-7} M
PCBs 105, 118, 153	H4IIE, PRH	10^{-10} M - 10^{-6} M
PCB 77	H4IIE	10^{-10} M - 10^{-6} M
	PRH	$5*10^{-11}$ M - 10^{-6} M
PCB 156	H4IIE	$5*10^{-9}$ M - 10^{-6} M
	PRH	10^{-10} M - 10^{-6} M

Table 7: EROD medium components.

EROD medium	25 mL respective culture medium (without supplements)
	125 µL $MgCl_2$ (1 M)
	25 µL Dicumarol (10 mM in 0.2 M NaOH)
	125 µL 7-ethoxyresorufin (1 mM in DMSO)
	prepared immediately prior to use (37°C)

3.5. SDS-PAGE and Western Blot

For investigations on CYP1A1-protein via Western Blot (WB) analysis, H4IIE cells, or PRH, which were seeded on 100 mm cell culture dishes as described, were exposed to congener-concentrations depicted in table 8.

Table 8: Final congener-concentrations tested via SDS-PAGE/Western Blot (H4IIE, PRH).

TCDD	H4IIE	$5*10^{-12}$ M - 10^{-8} M
	PRH	10^{-13} M - 10^{-9} M
1-PeCDD	H4IIE	10^{-13} M - $5*10^{-10}$ M
	PRH	10^{-13} M - 10^{-8} M
1,6-HxCDD	H4IIE	$5*10^{-12}$ M - $5*10^{-9}$ M
	PRH	10^{-12} M - $3*10^{-8}$ M
1,4,6-HpCDD	H4IIE	$5*10^{-12}$ M - $5*10^{-9}$ M
	PRH	10^{-12} M - 10^{-7} M
TCDF	H4IIE	10^{-11} M - 10^{-7} M
	PRH	10^{-13} M - 10^{-8} M
4-PeCDF	H4IIE	10^{-13} M - 10^{-9} M
	PRH	10^{-12} M - 10^{-8} M
1,4-HxCDF	H4IIE	10^{-12} M - 10^{-9} M
	PRH	10^{-12} M - $5*10^{-8}$ M
1,4,6-HpCDF	H4IIE	$5*10^{-11}$ M - $5*10^{-8}$ M
	PRH	10^{-12} M - 10^{-7} M
PCB 126	H4IIE	10^{-12} M - $5*10^{-9}$ M
	PRH	10^{-12} M - 10^{-7} M
PCBs 77, 105, 118, 153, 156	H4IIE, PRH	10^{-9} M - 10^{-6} M

After incubation of congeners for 24 h, cells were washed and scraped off from dishes using ice-cold isotonic extraction buffer (IEB, 1 mL) containing protease inhibitor cocktail (0.1%). Cells were homogenized using an ultrasonic probe, and proteins were separated (12,000 g, 15 min, 4°C). From protein-containing supernatants, microsomes were isolated per ultracentrifugation (100,000 g, 1 h, 4°C; Ultracentrifuge Optima TL, Beckman Coulter, Krefeld, Germany), and dissolved in NaP_i-buffer (100 µL, 50 mM). Protein content was measured by BCA assay (Pierce® BCA Protein Assay Kit) according to the manufacturer's protocol.

To microsomes (20 µg protein/15 µL), Laemmli loading buffer (6x, 3 µL) was added, and proteins were denatured at 95°C for 5 min. Samples were stored at -20°C until used for SDS-PAGE. Microsomes were held at -80°C. Details regarding composition and storage conditions of required solutions are summarized in table 9.

Table 9: Solutions required for protein sample preparation for SDS-PAGE/Western Blotting.

Isotonic extraction buffer IEB	Saccharose (250 mM) KCl (25 mM) HEPES (10 mM) EGTA (1 mM) pH 7.8 4°C added prior to use: protease inhibitor cocktail (0.1%) P8340, Sigma-Aldrich
NaP_i-buffer 50 mM	$Na_2HPO_4*H_2O$ (43.5 mM) NaH_2PO_4 (6.5 mM) pH 7.6 4°C
Laemmli loading buffer (6x)	50 mL Tris/HCl (0.5 M, pH 6.8) 40 mL glycerin 5 mL 2-mercaptoethanol 1.24 g SDS 160 mg bromphenol blue ad 100 mL -20°C

Discontinuous sodium dodecyl sulfate-polyacrylamide gel electrophoresis (disc SDS-PAGE) and Western Blot was performed according to Laemmli (1970), and Towbin (1979) as described previously (Chopra *et al.*, 2010b) with modifications. Discontinuous gels composed of separating gels (10% acrylamide) and stacking gels (4% acrylamide) were poured (table 10), placed in vertical electrophoresis apparatuses (Bio-Rad Laboratories GmbH, Munich, Germany), and proteins of samples (20 µg protein/18 µL) were electrophoretically separated (140 V).

Protein standards (#161-0375) were purchased from Bio-Rad Laboratories GmbH. Proteins were blotted onto polyvinylidene difluoride (PVDF)-membranes (pore size 0.2 µm, Bio-Rad Laboratories GmbH) by semi-dry blotting (figure 7; Semi-Dry Blotter TE77, Hoefer, Inc.; San Francisco, California, USA).

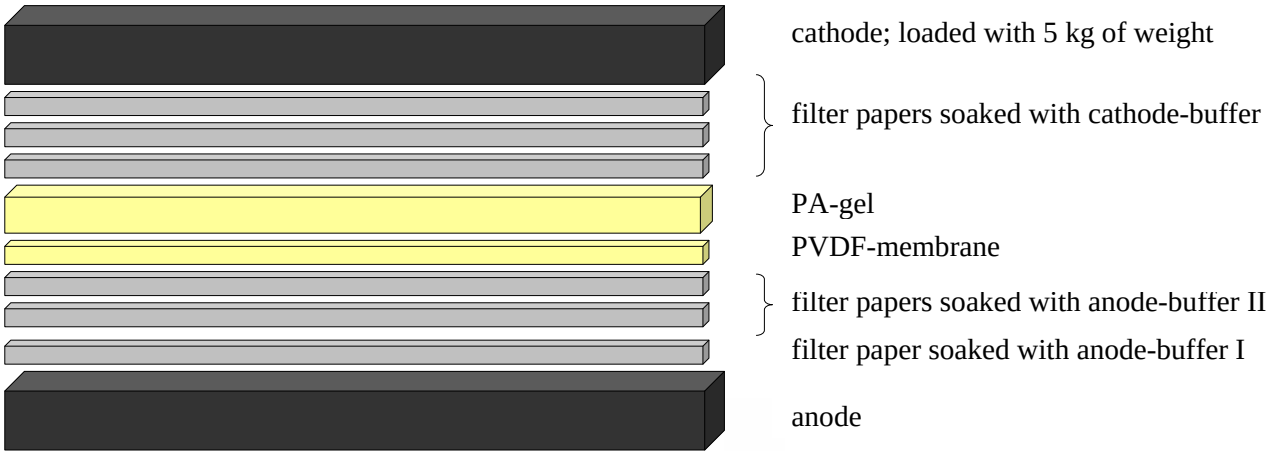

Figure 7: Semi-dry blotting procedure, schematic view.

Subsequent to blotting for 75 min and 45 mA per membrane (7 x 9.5 cm), membranes were blocked (5% lowfat powdered milk in Tris-buffered saline with Tween-20 (TBS-T)) for 1 h at RT, or at 4°C over night. Appropriate membrane parts were incubated with rabbit anti-CYP1A1 (1:1000 in TBS-T; sc-20772, Santa Cruz Biotechnology, Inc., Heidelberg, Germany), or rabbit anti-voltage-dependent anion channel (VDAC, 1:1000 in TBS-T; #4866, Cell Signaling Technology, Inc., Frankfurt on the Main, Germany), for 1 h at RT, or over night at 4°C. VDAC served as loading control. Membranes were washed (3 x 5 min) with TBS-T, and incubated with goat anti-rabbit IgG horseradish peroxidase (HRP) (1:5000 in TBS-T, sc-2004, Santa Cruz Biotechnology) for 1 h at RT.

After washing of membranes (3 x 5 min with TBS-T, 1 x 5 min with TBS), CYP1A1 (56 kDa)-, and VDAC (32 kDa)-protein bands were visualized by means of chemoluminescence detetection. Therefor, 100 µL reagent B were added to containing reagent A, and membranes were incubated for 1 min prior to detetection via Lumi Imager (Roche, Mannheim, Germany) and Lumi Analyst Software (Version 3.1, Roche). See table 10 for detailed information regarding required reagents (method modified according to Chopra *et al.*, 2010b).

Table 10: Gel components and buffers used for disc SDS-PAGE/Western Blot, and reagents for chemoluminescence detection.

Separating gel	Formulation per gel:	
(% acrylamide)	purified water	2 mL
	acrylamide (30%)	1.64 mL
	1.5 M Tris/HCl (pH 8.8)	1.23 mL
	sodium dodecyl sulfate (SDS, 10%)[1]	50 µL
	ammonium persulfate (APS, 10%)	50 µL
	N,*N*,*N′*,*N′*-Tetramethylethylenediamine (TEMED)	5 µL
Stacking gel	Formulation per gel:	
(% acrylamide)	purified water	1.2 mL
	acrylamide (30%)	0.25 mL
	0.5 M Tris/HCl (pH 6.8)	0.5 mL
	SDS (10%)[1]	20 µL
	APS (10%)	20 µL
	TEMED	4 µL
Electrophoresis-buffer	Glycine (200 mM)	
	Tris/HCl (25 mM)	
	SDS (0.1%)[1]	
Tris-buffered saline	NaCl (130 mM)	
TBS	Tris/HCl (20 mM)	
	pH 7.4	
TBS with Tween-20	TBS	
TBS-T	Tween-20 (0.1%)[1]	
Anode-buffer I	Tris (300 mM)	
	methanol (10%)	
	pH 10.4	
Anode-buffer II	Tris (25 mM)	
	methanol (10%)	
	pH 10.4	
Cathode-buffer	Glycine (40 mM)	
	Tris (25 mM)	
	methanol (20%)	
	SDS (0.005%)[1]	
	pH 9.4	
Reagent A	Luminol (50 mg in 100 mM Tris/HCl, pH 8.6)	10 mL
	p-coumaric acid (11 mg/10 mL DMSO)	1 mL
Reagent B	100 mM Tris/HCl, pH 8.6	1 mL
	H_2O_2 (30%)	50 µL

[1]Applichem GmbH, Darmstadt, Germany

3.6. Quantitative real-time PCR

For determination of core congeners' properties on gene transcription *in vitro*, definite mRNA-levels in exposed H4IIE-cells, or PRH, were investigated via quantitative real-time polymerase chain reaction (qRT-PCR). To approach to this objective, transcription of eight potential AhR-target genes (*Cyp1a1*, *Cyp1a2*, *Cyp1b1*, *Ahrr*, *Aldh3a1*, *Cd36*, *Hsd17b2*, and *Tiparp*), were examined using TCDD-treated H4IIE-cells, or PRH (0.1 pM-1 nM TCDD, 24 h). Furthermore, effects on *Cyp1a1*, *Cyp1a2*, *Cyp1b1*, and *Aldh3a1* after 24 h of treatment (H4IIE, PRH) were analyzed more extensively, studying effects of the complete set of core congeners (TCDD, 1-PeCDD, 4-PeCDF, PCBs 118, 126, 153, and 156), applying compound concentrations noted in table 11.

Table 11: Final congener-concentrations used for investigations via qRT-PCR (H4IIE, PRH).

TCDD	H4IIE	10^{-13} M - 10^{-9} M
	PRH	10^{-14} M - 10^{-8} M
1-PeCDD	H4IIE	10^{-13} M - 10^{-9} M
	PRH	10^{-13} M - 10^{-8} M
4-PeCDF	H4IIE	10^{-13} M - 10^{-9} M
	PRH	10^{-12} M - 10^{-8} M
PCB 126	H4IIE	10^{-12} M - $5*10^{-9}$ M
	PRH	10^{-12} M - 10^{-6} M
PCB 118	H4IIE, PRH	10^{-9} M - 10^{-6} M
PCB 153	H4IIE, PRH	$5*10^{-9}$ M - 10^{-6} M
PCB 156	H4IIE	$5*10^{-9}$ M - 10^{-6} M
	PRH	10^{-9} M - 10^{-6} M

From H4IIE cells, PRH, PBMCs, and mouse-, or rat liver tissues, mRNA was isolated using Qiagen RNeasy Mini Kit (Qiagen GmbH, Hilden, Germany) according to the manufacturer's protocol. For details regarding PBMC-, mouse-, and rat liver samples, see respective chapters. Prior to use in microarray analysis, integrity of mRNA was checked applying Agilent RNA 6000 Pico Kit (Agilent Technologies GmbH, Waghaeusel-Wiesental, Germany), by means of 2100 Bioanalyzer (Agilent Technologies GmbH, Waldbronn, Germany), using 2100 Expert software (Agilent Technologies GmbH, Waldbronn, Germany).

For qRT-PCR, mRNA was transcribed to cDNA in a MyCycler™ Thermo Cycler (Bio-Rad, Munich, Germany). To accomplish reverse transcription, iScript™ cDNA Synthesis Kit (Bio-Rad) was applied according to the manufacturer's protocol, using 1 µg mRNA per sample (NanoDrop ND-1000 Spectrophotometer, Wilmington, Delaware, USA). IQ™ SYBR® Green Supermix (Bio-Rad) was used for dye-based quantitative PCR (Mastermix: 1 µL sample cDNA, 12.5 µL IQ™ SYBR® Green Supermix, 9.5 µL nuclease-free H_2O, 1 µL forward primer, 1 µL reverse primer), whereas measurement of fluorescence was carried out in an iCycler iQ™ Thermal Cycler (Bio-Rad) according to the manufacturer's protocol. For each experiment, gene transcripts of the housekeeping gene encoding β-actin were measured. Referring to Pfaffl (2001), ratios were calculated on the basis of the crossing point (CP), where the threshold fluorescence is crossed. The threshold fluorescence is defined as the point at which fluorescence appreciably rises above background fluorescence. Ratios were calculated with the aid of the 'delta-delta-method' (Pfaffl, 2001). Primer validations were implemented to investigate qRT-PCR-efficacies, unless primers were already established in the laboratory (Dörr, 2010; Lohr, 2013; Roos, 2011). Sequences of primers are listed in table 12 (following page).

Table 12: Primer sequences used for qRT-PCR (for, forward; rev, reverse; Ta, annealing temperature).

Gene name	RefSeq accession number	Primer sequences (5'→ 3')	T_a	Reference
Human				
ACTB	NM_001101	for: CGTGCGTGACATTAAGGAGAA; rev: CAATGCCAAGGAAGGAAGG	55.7°C	Dörr, 2010
AHRR	NM_020731	for: CTTCATCTGCCGTGTGCGCT; rev: ATGAGTGGCTCGGGACAGCAGA	57°C	Lohr, 2013
ALDH3A1	NM_001135168	for: GCAAGCAAGTAAGGGAGCGGA; rev: ACCCGAGTCCTAAGCCGAACTG	60°C	Lohr, 2013
CD36	NM_001001547	for: AGATGCAGCCTCATTTCCAC; rev: CGTCGGATTCAAATACAGCA	60°C	Chuang *et al.*, 2009
CYP1A1	NM_000499	for: CAGAAGATGGTCAAGGAGCA; rev: GACATTGGCGTTCTCATCC	60°C	Andersson *et al.*, 2011
CYP1A2	NM_000761	for: CCCAGAATGCCCTCAACA; rev: CCACTGACACCACCACCTGAT	60°C	Ooi *et al.*, 2011
CYP1B1	NM_000104	for: CGGCCACTATCACTGACATC; rev: CTCGAGTCTGCACATCAGGA	60°C	Andersson *et al.*, 2011
HSD17B2	NM_002153	for: CTGAGGAATTGCGAAGAACC; rev: AAGAAGCTCCCCATCAGTTG	52°C	Su *et al.*, 2007
TIPARP	NM_001184717	for: GCGCACAAGTCTTCGTCTTCCTCC; rev: AAAAATCCTCCCGAGGAGCGTCCAA	60°C	Lohr, 2013
Rat				
Actb	NM_031144	for: AGCCATGTACGTAGCCATCCA; rev: TCTCCGGAGTCCATCACAATG	58°C	Roos, 2011
Ahrr	NM_001024285	for: GGGGACAGAGAAGAGGACGATCAGA; rev: ACTTCGCTGCTCTGTGCTCCA	65.4°C	Validated primers
Aldh3a1	NM_031972	for: TATCCCCCAAGCCCAGCCAAGA; rev: AGGACGGCAGGTGGGAATAAGC	60.1°C	Validated primers
Cd36	NM_031561	for: GGCTGTGTTTGGAGGCATTCT; rev: CCCGTTTTCACCCAGTTTTTG	59°C	Dalgaard *et al.*, 2011
Cyp1a1	NM_012540	for : CCTCTTTGGAGCTGGGTTTG; rev: CCTGTGGGGGATGGTGAA	55°C	Roos, 2011
Cyp1a2	NM_012541	for: GCAAGGACTTTGTGGAGAATGT; rev: GTGATGTCCTGGATACTGTTCTTGT	64°C	*Mirek*
Cyp1b1	NM_012940	for: CTCATCCTCTTTACCAGATACCCG; rev: GACGTATGGTAAGTTGGGTTGGTC	58°C	*Mirek*
Cyp2b1	NM_001134844	for: ATGGAGAAGGAGAAGTCGAACC; rev: CTTGAGCATCAGCAGGAAACC	64°C	Roos, 2011
Cyp3a1	NM_013105	for: CCAGCAGCACACTTTCCTTTG; rev: GGTGGGAGGTGCCTTATTGG	52°C	Roos, 2011
Hsd17b2	NM_024391	for: TCGGTGTCCTGCTTCTTCCTTCTG; rev: CCCTCTTTATCCAGCACTCCAGCAA	64°C	Validated primers
Tiparp	XM_003753596	for: TTGGAAATTCTTCTGTAGAGACCAC; rev: TTCAATTAGTCGAACAACAGACTCA	57°C	Validated primers

3.7. Peripheral Blood Mononuclear Cells

To approach novel findings regarding AhR's role in immune cells, investigations on TCDD-treated human peripheral blood mononuclear cells (PBMCs) were performed. For this purpose, PBMCs (figure 8) were isolated from freshly drawn blood from four subjects, and characterized by fluorescence activated cell sorting (FACS) analysis. Cells were exposed to TCDD alone or co-incubated with either lipopolysaccharide (LPS) or phytohemagglutinine (M Form; PHA), and mRNA was isolated after 24 h of treatment. Impact on transcription of eight potential AhR-target genes (*CYP1A1*, *CYP1A2*, *CYP1B1*, *AHRR*, *ALDH3A1*, *CD36*, *HSD17B2*, and *TIPARP*) was examined. Furthermore, human whole genome microarray analysis was performed.

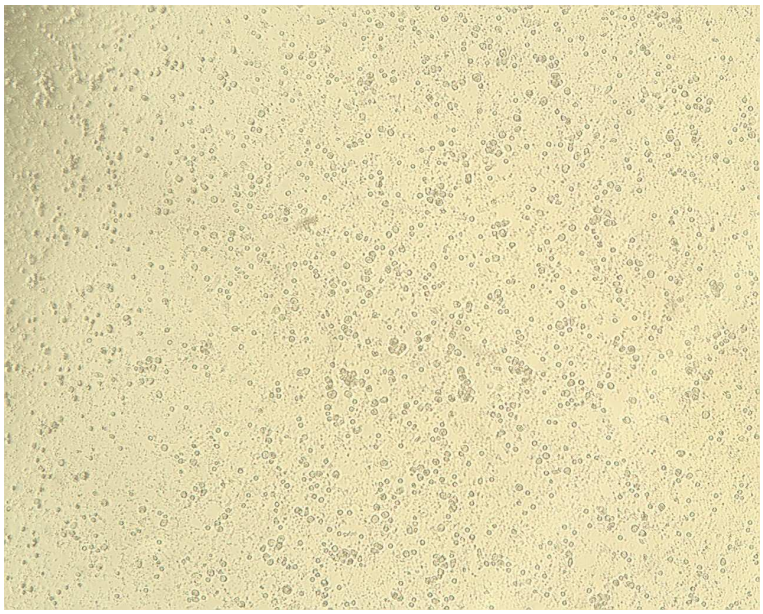

Figure 8: Light microscopic photograph of human PBMCs stimulated with LPS (1 µg/mL) for 24 h (magnification 100x).

3.7.1. Isolation and treatment of human PBMCs

Venous blood (40-45 mL) of four healthy, non-smoking individuals (two female, two male; 23-29 years of age) was collected in EDTA-monovettes (Sarstedt, Nuernbrecht, Germany), carefully layered on Ficoll-Paque™ PLUS solution (GE Healthcare Europe GmbH, Freiburg, Germany; blood:Ficoll (v:v) = 3:4), and centrifuged at 400 g for 30 min at RT in 15 mL falcons (isolation method modified according to Bøyum, 1964). PBMC-layers were transferred to PBS^{--}, washed (300 g, 5 min, RT), and resuspended in PBMC culture medium (RPMI 1640 with L-glutamine, without phenol-red (PAA Laboratories, Coelbe, Germany), supplemented with 10% (v/v) charcoal stripped fetal bovine serum (PAA Laboratories), 25 mM HEPES, 1% (v/v) penicillin/streptomycin (PAA

Laboratories)), or PBMC culture medium containing PHA (1.5%). Cells were counted with the aid of a Neubauer counting chamber via trypan blue (trypan blue solution, 0.4%) exclusion test (Evans and Schulemann, 1914; Rous and Jones, 1916), yielding 1.2 (±0.5)*10^6 cells/mL blood. PBMCs were seeded on 6-well cell culture plates (6*10^6 cells/3 mL/well) in appropriate PBMC culture medium, and incubated (see table 13) for 24 h at 37°C, 95% relative humidity, and 5% CO_2.

Table 13: *In vitro* treatment of human PBMCs.

Control I	DMSO 0.1%	Incubation I	TCDD 10 nM
Control II	DMSO 0.1% LPS[1] 1 µg/mL	Incubation II	TCDD 10 nM LPS[1] 1 µg/mL
Control III	DMSO 0.1% PHA[2] 1.5%	Incubation III	TCDD 10 nM PHA[2] 1.5%

[1]LPS from *E. coli* 0111:B4 (L3012); Sigma-Aldrich, Steinheim, Germany
[2]Gibco® Life Technologies GmbH, Darmstadt, Germany

After incubation, PBMCs were separated from medium (300 g, 10 min, RT), and mRNA was isolated using Qiagen RNeasy Mini Kit (Qiagen GmbH, Hilden, Germany) according to the manufacturer's protocol. Further preparations of samples accomplished prior to qRT-PCR-, or human whole genome microarray analysis are explained in respective chapters.

3.7.2. Characterization of PBMCs by Flow Cytometry

Isolated PBMCs were characterized by FACS analysis. Cells were washed (300 g, 5 min, 4°C), and resuspended in ice-cold Stain Buffer (BD Pharmingen™, Heidelberg, Germany). To cells (10^6 cells/100 µL each), antibodies (20 µL) were added, and incubated on ice for 20 min (protected from light). Unstained cells, as well as cells stained with respective isotyp control antibodies (see table 14 for antibody details; following page), were used for control measurements. Subsequent to antibody-incubation, cells were washed twice (Stain Buffer; 300 g, 5 min, 4°C), and resuspended in 100 µL ice-cold Stain Buffer per sample. Samples were measured using a BD FACS Canto II flow cytometer (BD Biosciences, Heidelberg, Germany).

Cell populations were identified per forward scatter (FSC)/sideward scatter (SSC) dot blots, and distinguished via light detection from the 633 nm (red) laser enabled by a trigon detector array (bandpass filter: 660/20 nm). Required solutions for FACS analysis are listed in table 14 (following page).

Table 14: List of antibodies and solutions used in the course of FACS analysis for human PBMCs.

APC Mouse Anti-human CD3	555335; BD Pharmingen™ (1)
APC Mouse Anti-human CD14	561708; BD Pharmingen™ (1)
APC Mouse Anti-human CD19	555415; BD Pharmingen™ (1)
APC Mouse IgG_1, κ isotyp control	555751; BD Pharmingen™ (1)
APC Mouse IgG_{2a}, κ isotyp control	555576; BD Pharmingen™ (1)
BD FACS Clean Solution	340345; BD FACS™ (1)
BD FACSFlow Sheath Fluid	342003; BD FACSFlow™ (1)
BD FACS Shutdown Solution	334224; BD FACS™ (1)

(1)Heidelberg, Germany

The CD3 monoclonal antibody specifically binds to the human CD3ε-chain, a 20 kD subunit of the CD3/T cell receptor complex. CD19 is specifically expressed on B cells, and respective CD19 monoclonal antibody binds to the 95 kDa type I transmembrane CD19 glycoprotein. The CD14 monoclonal antibody specifically binds to CD14, a 53-55 kDa glycosylphosphatidylinositol-anchored single chain glycoprotein expressed at high levels on the surface of monocytes and macrophages (information was taken from technical data sheets of antibodies; BD Pharmingen™, Heidelberg, Germany). After FACS analysis, from relative fluorescence units (RFUs) of samples stained with CD3-, CD14-, or CD19-antibody, RFUs of respective isotyp control-stained cells were subtracted. For investigations of $CD3^+$-, and $CD19^+$-cells, IgG_1, κ isotyp control was used, whereas for analysis of $CD14^+$-cells, IgG_{2a}, κ isotyp control was applied.

Resulting ΔRFUs exceeding 4,000 referred to positively stained cells and were termed CDX^+. Hence, $CD3^+$-cells indicated the presence of T-lymphocytes, $CD19^+$-cells designated B-lymphocytes, and $CD14^+$-cells indicated the presence of monocytes/macrophages.

3.8. Whole Genome Microarrays – human & mouse

To reveal novel findings regarding potential AhR-dependent-, and AhR-independent impact of DL-chemicals on gene transcription, mouse whole genome microarray analysis was performed. Within the framework of SYSTEQ project, female C57BL/6J mice were exposed to single doses of one of the seven core congeners (TCDD, 1-PeCDD, 4-PeCDF, PCB 118, PCB 126, PCB 153, or PCB 156) for three days. In the course of the entire experiment, impact of TCDD, and PCB 153 was closely studied by Dr. Christiane Lohr (Lohr, 2013). For the purposes of the work in hand, respective data obtained by courtesy of Christiane Lohr was partially required to attain reasonable considerations and findings, or to draw comparisons between congeners, which especially was inevitable regarding TCDD.

To approach both potential effects of TCDD towards humans and to disclose its possible impact on immune system, *in vitro* studies on human PBMCs were implemented. From four subjects (one female, two male), mRNA of *in vitro*-treated PBMCs exposed to TCDD for 24 h was examined in terms of whole genome microarray analysis.

From each treatment group within the mouse experiment, samples of all six treated animals as well as three controls were analyzed. Referring to PBMCs, incubations I, II, and III were included. Regarding both variants of starting material, procedure was performed as follows.

From PBMCs and mouse liver samples, mRNA was isolated and checked on integrity as described and used for two-color microarray-based gene expression analysis, which was processed implementing dye-swop procedures. According to the manufacturer's protocol (G4140-90050, version 6.5, 2010; Agilent Technologies, Waldbronn, Germany), 100 ng of mRNA per sample was applied. By means of low input quick amp labeling kit (Agilent Technologies GmbH, Waghaeusel-Wiesental, Germany), fluorescent cRNA was generated. This method involved T7 RNA polymerase, which simultaneously amplified target material and incorporated cyanine (Cy)3-, or Cy5-labeled CTP.

All used reagents and buffers used for two-color microarray-based gene expression analysis are listed in table 15.

Table 15: List of reagents und buffers used in the course of two-color microarray-based gene expression analysis.

Low Input Quick Amp Labeling Kit, two-color	5190-2306; Agilent Technologies GmbH [(1)]
RNA Spike In Kit, two-color	5188-5279; Agilent Technologies GmbH [(1)]
Gene Expression Hybridization Kit	5188-5242; Agilent Technologies GmbH [(1)]
Gene Expression Wash Buffer Kit	5188-5327; Agilent Technologies GmbH [(1)]
Hybridization Gasket Slide Kit	G2534-60011; Agilent Technologies GmbH [(1)]
Human GE 4x44K v2 Microarray Kit	G4845A; Agilent Technologies GmbH [(1)]
Mouse GE 4x44K v2 Microarray Kit	G4846A; Agilent Technologies GmbH [(1)]
RNeasy Mini Kit	Qiagen GmbH, Hilden, Germany
Ethanol (absolute, reag. ISO, reag. Ph. Eur)	Sigma Aldrich, Steinheim, Germany

[(1)]Waghaeusel-Wiesental, Germany

Hybridized microarray slides were scanned using Agilent Microarray Scanner System (Scanner Model G2505B, Agilent Technologies Scan Control Software Version A.7.0.1; Agilent Technologies GmbH, Waldbronn, Germany). Preliminary processing of data was made by means of Agilent Technologies Feature Extraction Software (9.5.1.1; Agilent Technologies GmbH). Data normalization and statistical analyses were performed using Bioconductor (Gentleman *et al.*, 2004) R (version 2.15.1) package limma (version 3.12.3) (Smyth, 2004). Raw signals were background corrected subtracting local spot background. Two normalization steps were applied: firstly within arrays using the global loess method, and secondly between the arrays using the Aquantile method. Differential expression was assessed with the help of empirical Bayes moderated t-tests carried out in limma (Smyth, 2005) on the dataset. Cutoff criteria for further functional analysis were logarithmic (log2) fold change $|\text{lfc}| \geq 1$, and p-value < 0.05, corrected by false discovery rate (FDR) using the Benjamini-Hochberg method (Benjamini and Hochberg, 1995), and an A-mean value $A \geq 2^7$. The clipped list was subjected to Gene Ontology (GO) analysis using the TopGO (version 2.8.0) package in R (Alexa *et al.*, 2006). Classical enrichment analysis by testing over-representation of GO terms within the group of differentially expressed genes was performed using Fisher's exact test (correspondence with Karsten Andresen, Institute of Biotechnology and Drug Research (IBWF), Kaiserslautern).

3.9. Animal experiments

All animal experiments were performed at the animal facility of the Utrecht University (Institute for Risk Assessment Sciences (IRAS), Utrecht, The Netherlands) with permission of the Animal Ethical Committee, and according to Dutch law on animal experiments (http://wetten.overheid.nl/BWBR0003081). Nine-week-old female C57BL/6 mice, and Sprague Dawley rats (Harlan laboratories, Venray, The Netherlands) were randomly assigned to treatment groups (six animals per group), and allowed to acclimate for 1.5 weeks. Animals were housed in groups in standard cages and conditions (temperature 23 (±2)°C, 50-60% relative humidity, 12 h dark and light cycle) with free access to food and water. Mice and rats received single doses (table 16) of core congeners (TCDD, 1-PeCDD, 4-PeCDF, PCB 118, PCB 126, PCB 153, or PCB 156), which were administered in corn oil at a dosing volume of 10 mL/kg bw by oral gavage. Dependent on the congener and its current TEF, five different dosages (L, M, N, O, or P) were administered. Animals were sacrificed at day three after dosing by CO_2/O_2. One dose group (O-group) of each compound was added for an exposure time of 14 days (Van Ede *et al.*, 2013a; Van Ede *et al.*, 2011). For the work in hand, livers (snap frozen and stored at -80°C) were used as starting material for microarray or qRT-PCR experiments. The P-group was excluded from examinations and is therefore not displayed in table 16.

Table 16: Overview of animal experiments (mouse, rat) performed at IRAS and administered doses; six animals per dose group; three days, and 14 days study.

Congener	Single dose (µg/kg bw)					WHO-TEF (2005)[a]
	K[b]	L	M	N	O[b]	
TCDD	0	0.5	2.5	10	25	1
1-PeCDD	0	0.5	2.5	10	25	1
4-PeCDF	0	5	25	100	250	0.1
PCB 126	0	5	25	100	250	0.1
PCB 118	0	5000	15000	50000	150000	0.00003
PCB 156	0	5000	15000	50000	150000	0.00003
PCB 153	0	5000	15000	50000	150000	-

[a]Van den Berg *et al.*, 2006
[b]Doses for both three days & 14 days study

3.10. Calculation of relative effect potencies and statistical analysis

Half maximal effective concentration (EC50)-values of congeners as part of *in vitro*-studies were received by sigmoid fitting using Origin software (OriginLab 6.0, Microcal Software, Inc.; Northampton, Massachusetts, USA). Concerning EROD-measurements, EROD-activities in solvent controls were considered as background level, and subtracted from data. For effective concentration 20% (EC20)-values, the upper limit of the respective TCDD-derived curve was set 100%, and test compound concentrations attaining its fifth part were defined as EC20. In accordance with the TEF-concept, respective relative effect potencies (REPs) revealed the compounds' potencies relative to the reference compound TCDD.

Essentially, all models are wrong, but some are useful (George E. P. Box).

Statistical significant differences of means (control vs. treatment group(s)) were determined using one-way analysis of variance (ANOVA) followed by either two-tailed unpaired t-test with Welch-correction (applied for two groups), or Dunnett's Post-Test (applied for ≥ three groups). Statistically significant values were marked with * (p-value < 0.05; significant), ** (p-value < 0.01; very significant), or *** (p-value < 0.001; extremely significant). Calculations were performed using GraphPad InStat version 3.00 (GraphPad Software, San Diego, California, USA). For detailed information regarding evaluation and statistical analysis of microarray experiments, see respective chapter.

4

Results

4.1. *In vivo* – animal experiments

In the course of the SYSTEQ project, mouse and rat studies were performed in order to establish AhR-dependent effects. Mice and rats received single doses of TCDD, 1-PeCDD, 4-PeCDF, PCB 118, PCB 126, or PCB 156 and were sacrificed after three days or 14 days of exposure. Treatment of animals with PCB 153 was used to specify AhR-independent effects.

For the purposes of the work in hand, mRNA of liver samples of mouse three days study was isolated, checked on purity via Bioanalyzer, and applied to whole genome microarray analysis. TCDD-and PCB 153-derived effects on gene expression in mouse liver were closely studied by Christiane Lohr (Lohr, 2013), whereas impact of 1-PeCDD, 4-PeCDF, PCB 118, PCB 126, or PCB 156 were analyzed in the following. According to the TEF-concept, contrasting effects due to these DL-congeners to TCDD's was essential and required for evaluation within the framework of the SYSTEQ project. By courtesy of Christiane Lohr, raw-data referring to TCDD's impact on gene expression in mouse liver was used in this regard. Besides heat maps, principal component analyses (PCAs), and gene lists, pathway analyses by means of TopGO analysis were performed in order to gain further information regarding mechanism(s) of action among core congeners.

Furthermore, liver samples of rat studies (three days, 14 days) were analyzed regarding AhR-, CAR-, and PXR-dependent effects of core congeners. To approach to these objectives, mRNA was examined via qRT-PCR with respect to *Cyp1a1*, *Cyp2b1*, and *Cyp3a4*.

4.1.1. Mouse whole genome microarray analysis

Subsequent to verification of purity of mRNA isolated from liver samples of treated animals, two-color microarray-based gene expression analysis followed applying Mouse GE 4x44K v2 Microarray Kits (Agilent Technologies GmbH, Waghaeusel-Wiesental, Germany). Of each treatment group, samples of all six treated animals and three controls were included, and processed individually implementing dye-swop procedures. Data normalization and statistical analyses were performed using Bioconductor R package Limma (Smyth, 2004), whereas data of the entire study was analyzed globally, including TCDD-, and PCB 153-derived data obtained by courtesy of Christiane Lohr (Lohr, 2013). Results were filtered by cutoff values for signal intensity $A \geq 2^7$, logarithmic (log2) fold change $|lfc| \geq 1$, and p-value < 0.05.

4.1.1.1. Heat maps and Principal Components Analysis

Initial inspection of microarray data implied clustering of information to reduce data dimensionality. To at first approximate variability of data, and to verify exhibited trends, principal component analyses (PCAs) were performed.

Figure 9 shows PCA-results regarding whole genome microarray analysis and effects of core congeners on gene expression in mouse livers after three days of single dose exposure.

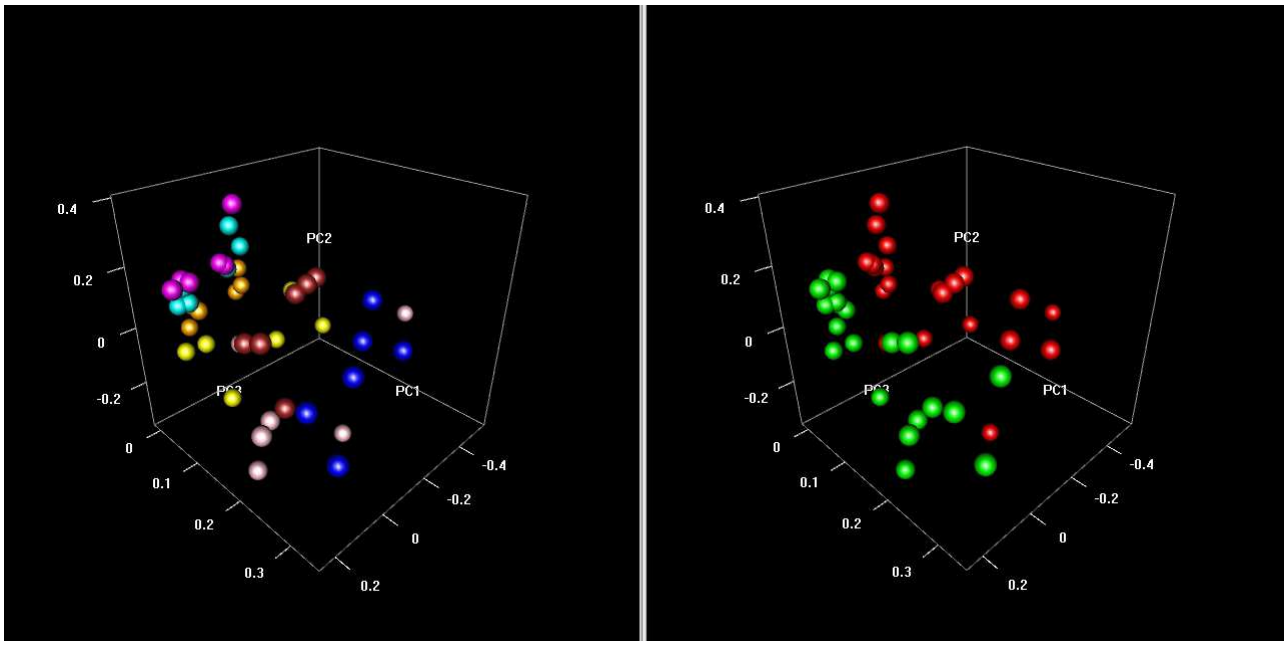

Figure 9: PCA mouse whole genome microarray analysis (*in vivo*, three days). Examination of RNA of livers from mice treated with TCDD (cyan), 1-PeCDD (magenta), 4-PeCDF (blue), PCB 118 (yellow), PCB 126 (pink), PCB 153 (orange), or PCB 156 (brown), focusing on treatment groups (left), and contrasting dyes (right; red: control dyed Cy3, green: control dyed Cy5). 3D scatter plot view of data with respect to their correlation to the first three principal components (PCs 1-3).

By means of PCA-results regarding mouse whole genome microarrays, reasonable clustering of data among animals of one treatment group was observed (figure 9, left). PCB 126 (pink), 4-PeCDF (blue), or PCB 118 (yellow) affected gene transcription in broader diversifying degree among treatment groups compared to TCDD's, 1-PeCDD's, or PCB 156's effects. Clustering between treatment groups appeared less prominent referred to differently affected gene expression in mouse livers due to compound treatments but yet indicated consistency of mRNA integrity.

Varying properties of samples referable to applied dye (figure 9, right) resulted in homogenous, but not highly deviated clustering of Cy3 (red, w.r.t. control)-, and Cy5 (green, w.r.t. control)-dyed samples. Adopted dye-swop was used in order to reduce diverging dye properties delineated in figure 9.

Microarray data visualized by means of a (bi)cluster visualization technique generated heat maps, which reflect congeners' effects on gene expression in mouse livers. With the aid of heat maps, indication of congeners' impact, including overlaps or distinctions among these, affecting gene expression may be outlined in this regard.

Figure 10 presents a heat map regarding mouse microarray data and $|lfc| \geq 1$ (p-value < 0.05), comprising results of the entire study with all seven core congeners, including data by courtesy of Christiane Lohr (Lohr, 2013), observed by examination of TCDD-, and PCB 153-treated mice.

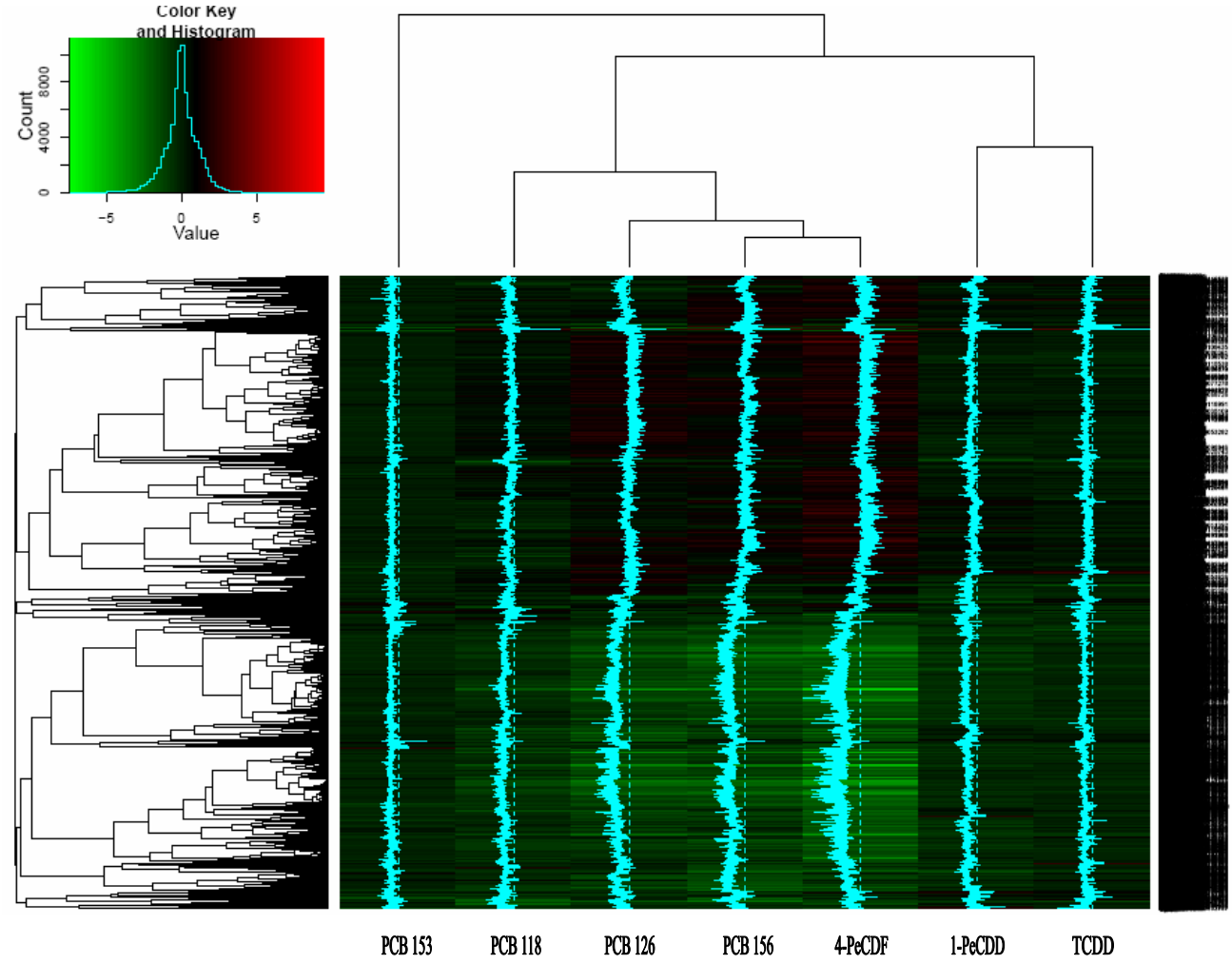

Figure 10: Heat map (I) mouse whole genome microarray analysis (*in vivo*, three days). Examination of RNA of livers from mice treated with TCDD, 1-PeCDD, 4-PeCDF, PCB 118, PCB 126, PCB 153, or PCB 156. For degree of up-regulation (red), and down-regulation (green) see Color Key and Histogram; $|lfc| \geq 1$, p-value < 0.05. Treatment groups (horizontal) vs. regulated genes (vertical).

The heat map presented in figure 10 gives initial impressions concerning core congeners' impact on gene expression in mouse livers considering $|lfc| \geq 1$. Correlating degree of red-, and green-coloring, 4-PeCDF, PCB 126, or PCB 156 led to more pronounced effects regarding number and

extent of up-, and down-regulation of genes compared to TCDD, 1-PeCDD, PCB 118, or PCB 153. Interrelations between impact of TCDD and 1-PeCDD was indicated, as well as between PCB 156 and 4-PeCDF, furthermore between these two congeners and PCB 126, continuing with a coherence of PCB 118 and the correlating group of PCB 126/PCB 156/4-PeCDF, and finally, to less prominent extent among DL-compounds, conforming TCDD/1-PeCDD to PCB 118/PCB 126/PCB 156/4-PeCDF. Weakest compliance was obtained between DL-congeners and the NDL PCB 153.

Specifying focus on highly regulated genes ($|lfc| \geq 5$; p-value < 0.05) led to a heat map, which is presented in figure 11. Results comprise data obtained by courtesy of Christiane Lohr (Lohr, 2013), regarding mRNA-analysis of TCDD-, and PCB 153-treated mice.

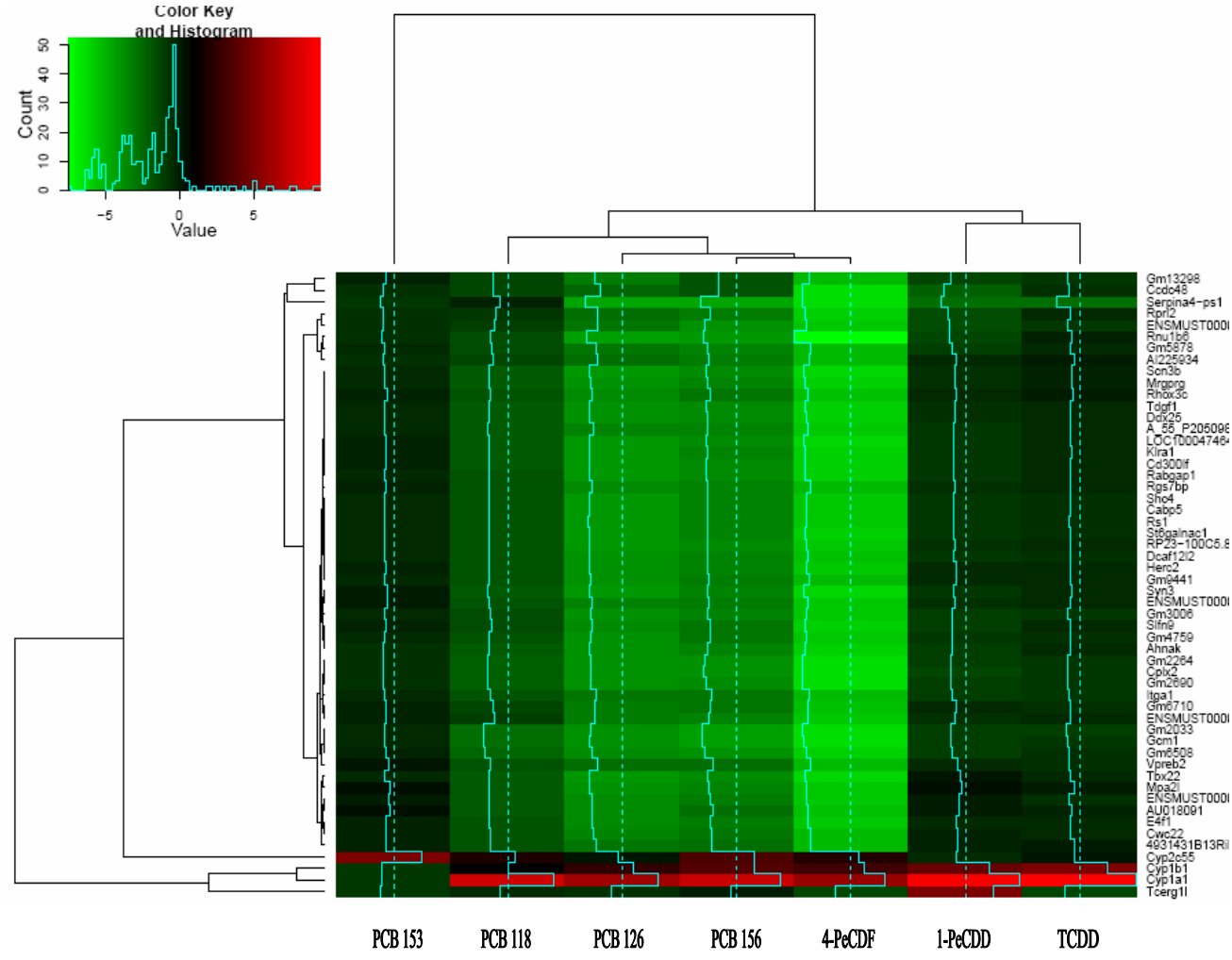

Figure 11: Heat map (II) mouse whole genome microarray analysis (*in vivo*, three days). Examination of RNA of livers from mice treated with TCDD, 1-PeCDD, 4-PeCDF, PCB 118, PCB 126, PCB 153, or PCB 156. For degree of up-regulation (red), and down-regulation down-regulation (green) see Color Key and Histogram; $|lfc| \geq 1$, p-value < 0.05. Treatment groups (horizontal) vs. regulated genes (vertical).

Since a low number of genes was affected to higher extent ($|lfc| \geq 5$) throughout the entire study, closer examination of regulated genes depicted in heat map in figure 11 was feasible. Most prominent degree of regulated genes was obtained due to 4-PeCDF-treatment, followed by PCB 126, PCB 156, and PCB 118. Regarding coherence as well as distinctions between congeners' effects, stronger correlations even by means of visual perception was given. Coherencies between congeners foreseen in figure 10 appeared in stronger dimensions.

Coherent groups were TCDD/1-PeCDD; 4-PeCDF/PCB 156; PCB 126/PCB 156/4-PeCDF; PCB 118/PCB 126/PCB 156/4-PeCDF, and least of all, clustering of all DL-congeners lightly concurred with NDL-PCB 153's effects. Interestingly, most obvious up-regulated genes due to treatment with all DL-congeners were *Cyp1a1*, and *Cyp1b1*, except for PCB 118, where the strict cutoff of $|lfc| \geq 5$ may have restrained *Cyp1b1*-inducing effects in the diagram. In contrast, NDL-PCB 153 slightly repressed *Cyp1a1*, and *Cyp1b1*, but distinctly induced another *Cyp* (*Cyp2c55*).

4.1.1.2. Regulated genes

In terms of examination of genes, which were affected regarding their transcription rates due to congeners' impact, data normalization and statistical analyses were performed using Bioconductor R package Limma (Smyth, 2004). In this regard, data of the entire study was analyzed globally, including TCDD-, and PCB 153-derived data by courtesy of Christiane Lohr (Lohr, 2013). Results were filtered by cutoff values for signal intensity $A \geq 2^7$, $|lfc| \geq 1$ and p-value < 0.05.

TCDD

Relevant with regard to purposes of the work in hand were effects on gene transcription due to single dose-exposure (25 µg/kg bw, three days) of mice with TCDD. Taking account of defined cutoff values ($A \geq 2^7$, $|lfc| \geq 1$, p-value < 0.05), the number of ≥ 2fold regulated genes by TCDD was 125 (up-regulated), and 95 (down-regulated), respectively. Top three up-regulated genes in descendant order were *Cyp1a1* (NM_009992, $A = 2^{10.23}$, lfc = 9.478, fold induction = 713.12), *Cyp1b1* (NM_009994, $A = 2^{7.16}$, lfc = 5.169, fold induction = 35.98), and *Cyp1a2* (NM_009993, $A = 2^{13.33}$, lfc = 3.985, fold induction = 15.83). Top three down-regulated genes in descendant order were *Klf10* (NM_013692, $A = 2^{8.11}$, lfc = -2.846, fold induction = 0.1391), *Rgs16* (NM_011267, $A = 2^{8.35}$, lfc = -2.601, fold induction = 0.1648), and *Serpina4-ps1* (BC031891, $A = 2^{9.43}$, lfc = -2.573, fold induction = 0.1681).

4.1.1.2.1. 1-PeCDD – impact on gene transcription in mouse livers

In figure 12, numbers of genes regulated in mouse livers subsequent to single-dose treatments with 1-PeCDD (25 µg/kg bw) and three days of exposure are depicted. Comparison to data obtained by TCDD-treatment by courtesy of Christiane Lohr was included (Lohr, 2013).

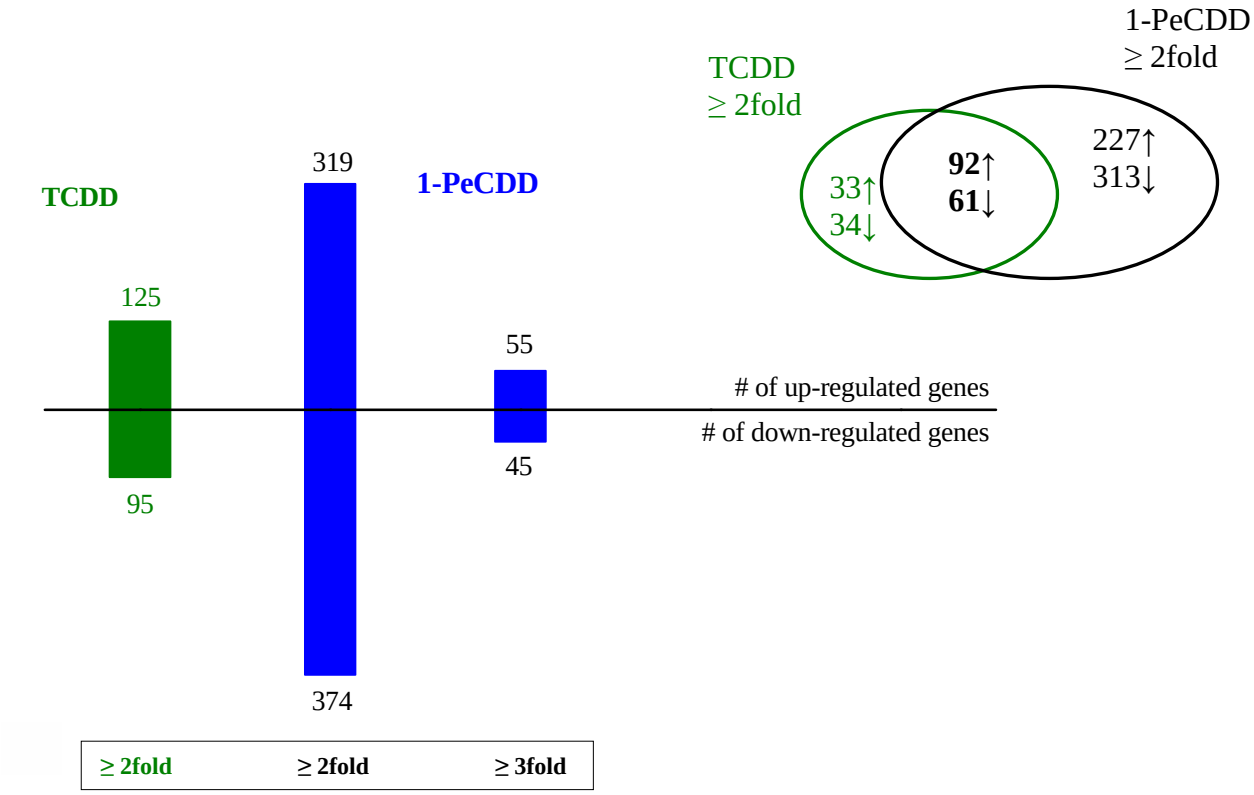

Figure 12: Mouse whole genome microarray analysis. Numbers of regulated genes in mouse livers by 1-PeCDD (25 µg/kg bw, three days) compared to numbers of genes regulated by TCDD (25 µg/kg bw, three days), and numbers of genes regulated both by 1-PeCDD and TCDD (TCDD-raw data by courtesy of C. Lohr; Lohr, 2013). A ≥ 27, p-value < 0.05.

Choosing cutoff values for signal intensity A ≥ 2^7, logarithmic (log2) fold change $|lfc| \geq 1$, and p-value < 0.05, transcription of genes in mouse livers was up-regulated concerning 319, and down-regulated for 374 genes (figure 12). Scaling up cutoff value to $|lfc| \geq 1.585$ (≥ 3fold induction), 55 up-, and 45 down-regulated genes were impacted by 1-PeCDD. From 125 up-, and 95-down-regulated genes due to TCDD-treatment, which were induced ≥ 2fold, 92 (up), and 61 (down) genes were accordantly affected by 1-PeCDD.

In order to gain an insight into types of genes regulated in mouse livers subsequent to 1-PeCDD-exposure, the Top 20 of 319 up-regulated genes (≥ 2fold) are compiled in table 17.

Table 17: Mouse whole genome microarray analysis. Top 20 up-regulated genes in mouse livers by 1-PeCDD (25 µg/kg bw, three days); descending order. Cutoff values: A ≥ 27, lfc ≥ 1, p-value < 0.05.

1-PeCDD lfc	Gene systematic name	Gene description	**Gene name**
9.092	NM_009992	cytochrome P450, family 1, subfamily a, polypeptide 1	*Cyp1a1*
4.440	NM_009994	cytochrome P450, family 1, subfamily b, polypeptide 1	*Cyp1b1*
3.975	NM_009993	cytochrome P450, family 1, subfamily a, polypeptide 2	*Cyp1a2*
3.212	NM_027872	solute carrier family 46, member 3	*Slc46a3*
2.871	NM_016865	HIV-1 tat interactive protein 2, homolog (human)	*Htatip2*
1.754-2.870	NM_201640	cytochrome P450, family 4, subfamily a, polypeptide 31	*Cyp4a31*
2.798	NM_017379	tubulin, alpha 8	*Tuba8*
2.747	NM_010210	fragile histidine triad gene	*Fhit*
2.641	NM_025557	Purkinje cell protein 4-like 1	*Pcp4l1*
2.526	NM_012006	acyl-CoA thioesterase 1	*Acot1*
2.516	NM_201641	UDP glycosyltransferase 1 family, polypeptide A10	*Ugt1a10*
2.476	NM_013786	hydroxysteroid (17-beta) dehydrogenase 6	*Hsd17b6*
2.360	NM_026791	F-box and WD-40 domain protein 9	*Fbxw9*
1.314-2.336	NM_206537	cytochrome P450, family 2, subfamily c, polypeptide 54	*Cyp2c54*
2.231/1.466	NM_025341	abhydrolase domain containing 6	*Abhd6*
2.174/1.104	NM_145079	UDP glucuronosyltransferase 1 family, polypeptide A6A	*Ugt1a6a*
2.172/1.081	NM_007618	serine (or cysteine) peptidase inhibitor, clade A, member 6	*Serpina6*
2.135/1.134	NM_021282	cytochrome P450, family 2, subfamily e, polypeptide 1	*Cyp2e1*
2.126	XM_885022	predicted pseudogene 6168	*Gm6168*
1.721-2.123	NM_010011	cytochrome P450, family 4, subfamily a, polypeptide 10	*Cyp4a10*

Values b/a from oligo b/oligo a; values a-n: value range of more than two (n) oligos.

The top three up-regulated and concurrently typical AhR-responsive genes in mouse livers responding to 1-PeCDD-treatment were *Cyp1a1* (NM_009992; lfc = 9.092), *Cyp1b1* (NM_009994; lfc = 4.440), and *Cyp1a2* (NM_009993; lfc = 3.975) (table 17). Further up-regulated gene transcripts encoding CYP-enzymes within the Top 20-table were *Cyp4a31* (lfc = 1.754-2.870), *Cyp2c54* (lfc = 1.314-2.336), *Cyp2e1* (lfc = 2.135/1.134), and *Cyp4a10* (lfc = 1.721-2.123).

Denoted CYP-enzymes share relevant roles regarding oxidation-reduction processes and are involved in lipid and fatty acid metabolism, as CYPs of the 4A subfamily catalyze ω-hydroxylations of fatty acids, e.g. (Gibson *et al.*, 1982; Hardwick *et al.*, 1987; Tamburini *et al.*,

1984). CYP2C54 and CYP4A10 are proteins further correlated to arachidonic acid metabolism and are hence potentially able to play a role regarding prostaglandin-biosynthesis (Binns *et al.*, 2009; Dimmer *et al.*, 2012; Varvas *et al.*, 2009). The encoded monooxygenases were discussed with respect to lipid peroxidation and oxidative stress and were further linked to hepatic steatosis and steatohepatitis (Chitturi and Farrell, 2001; Leclercq *et al.*, 2000).

By heterodimerization with the retinoic acid receptor α (RXRα), peroxisome proliferator-activated receptor *α* (PPAR*α*) regulates *Cyp4a*-gene transcription (Keller *et al.*, 1993; Kliewer *et al.*, 1992; Muerhoff *et al.*, 1992), and as well regulates gene transcription of *Cyp4a10*, and *Cyp4a31* (Bumpus and Johnson, 2011). Being inducible by fatty acids, eicosanoids, or peroxisome proliferators like clofibrate (Krey *et al.*, 1997; Lee *et al.*, 1995; Sharma *et al.*, 1988), PPAR*α*-activation participates in the regulation of biological processes including lipid metabolism, cell cycle control, as well as inflammatory response (reviewed in Vanden Heuvel, 1999; Wahli *et al.*, 1995). In particular, this transcription factor governs both microsomal (via CYP4A) and peroxisomal (β-oxidation) pathways of lipid oxidation and ultimate production of reactive oxygen species (ROS) (Chitturi and Farrell, 2001). Though *Ppara*-responsive genes appeared up-regulated, *Ppara*-mRNA itself was not regulated by 1-PeCDD according to two of three oligos (NM_011144; lfc = 0.424), and was down-regulated regarding the third of three available oligos on the microarray-slides (NM_011144; lfc = -1), however.

Further genes indicating altered lipid metabolism and transport within and beyond the Top-20 gene-list, which were up-regulated by 1-PeCDD in the course of the study in hand, were acyl-CoA thioesterase 1 (*Acot1*, NM_012006; lfc = 2.526), hydroxysteroid (17-*β*) dehydrogenase 6 (*Hsd17b6*, NM_013786; lfc = 2.476), abhydrolase domain containing 6 (*Abhd6*, NM_025341; lfc = 2.231 (max.)), CD36 antigen (*Cd36*, NM_007643, long chain fatty acid translocase family; lfc = 1.792), *Cyp4a14* (‘lauric acid *ω*-hydroxylase 3’, NM_007822; lfc = 1.674), and *Cyp8b1* (‘sterol 12-*α*-hydroxylase’, NM_010012; lfc = 1.480) (Binns *et al.*, 2009; Dimmer *et al.*, 2012; Hunt *et al.*, 2000; Muerhoff *et al.*, 1992; Post *et al.*, 2001).

Up-regulation of these genes further might hint towards 1-PeCDD’s probable impact on eicosanoid biosynthetic processes (*Abhd6, Cyp4a14*) and involvement in bile acid synthesis (*Cyp8b1*) (Binns *et al.*, 2009; Dimmer *et al.*, 2012). *Abhd6*-induction was discussed in terms of macrophage activation in conjunction with the endocannabinoid system (Alhouayek *et al.*, 2013). The endocannabinoid system is a lipid signaling system, which outside the brain crucially modulates physiological functions including the endocrine network, the immune system, and microcirculation (Rodríguez de Fonseca *et al.*, 2005). The enzyme ABHD6 is able to hydrolyze the endocannabinoid

2-arachidonoyl glycerol (2-AG), which potentially leads to a decrease of 2-AG in the cell and subsequent macrophage activation in case not only *Abhd6* mRNA was induced by 1-PeCDD but also the ABHD6 protein itself (Alhouayek *et al.*, 2013). Induction of *Hsd17b6* might indicate 1-PeCDD's impact to alter steroid hormone metabolism, as respective HSD17B6 protein is capable of conversion of 5*α*-androstan-3*α*, 17*β*-diol to androsterone and of estradiol to estrone (Su *et al.*, 1999). Another gene-product within the Top 20-list related to endocrine function was serine (or cysteine) peptidase inhibitor, clade A, member 6 (*Serpina6*, NM_007618; max. lfc = 2.172), of which the translated protein is involved in pathways of chemical reactions with glucocorticoids including their metabolism and their regulatory function in carbohydrate and protein metabolism (Binns *et al.*, 2009; Dimmer *et al.*, 2012). F-box and WD-40 domain protein 9 (*Fbxw9*, NM_026791; lfc = 2.360), was also up-regulated by 1-PeCDD in mouse livers. The respective protein takes part in ubiquitin-dependent protein catabolic processes (Binns *et al.*, 2009; Dimmer *et al.*, 2012).

Besides aforementioned transcripts encoding CYP-enzymes, further affected oligos within the Top 20-list, which are involved or proposed to be involved in (xenobiotic) metabolism, were UDP-glycuronosyltransferase 1 family, polypeptide A10 (*Ugt1a10*, NM_201641; lfc = 2.516), *Ugt1a6a* (NM_145079; lfc = max. 2.174), and the predicted pseudogene 6168 (*Gm6168*, XM_885022; lfc = 2.126). The latter pseudogene lies within a cluster of sulfotransferase family 2A genes on chromosome 7 A1 (Binns *et al.*, 2009; Dimmer *et al.*, 2012). Another indication regarding transcriptionally and metabolically active liver cells gave the up-regulation of solute carrier family 46, member 3 (*Slc46a3*, NM_027872; lfc = 3.212). The encoded protein participates in transmembrane transport mechanisms including transport of nucleotides, peptides, steroids, carbohydrates, and hydrogen peroxide (Binns *et al.*, 2009; Dimmer *et al.*, 2012).

HIV-1 tat interactive protein 2 (*Htatip2*, NM_016865; lfc = 2.871) constitutes a tumor suppressor protein acting as a repressive transcription factor in the nucleus. Among a number of other mechanisms, HTATIP2 was discussed in correlance with induction of apoptosis under oxidative stress through stabilization of p53 mRNA (Zhao *et al.*, 2008a). Fragile histidine triad gene (*Fhit*, NM_010210; lfc = 2.747) represents another pro-apoptotic tumor suppressor gene induced by 1-PeCDD-treatment. Tubulin, alpha 8 (*Tuba8*, NM_017379; lfc = 2.798), as the encoding tubulin represents a major constituent of microtubules, is at present annotated to biological processes including microtubule cytoskeleton organization, GTP catabolic processes, and protein polymerization (Binns *et al.*, 2009; Dimmer *et al.*, 2012).

The results obtained by means of classical enrichment analysis by testing over-representation of GO terms within the group of differentially expressed genes due to 1-PeCDD-treatment in mouse livers are presented in table 18 and in figure 13.

Table 18: Mouse whole genome microarray analysis – TopGO analysis (1-PeCDD), Fisher's exact test. Top 20 GO terms identified by the classic algorithm for scoring GO terms for enrichment regarding up-regulated genes; descending order. Mouse liver, 1-PeCDD (25 µg/kg bw, three days). Top five GO terms indicated in bold.

1-PeCDD GO term	GO ID	sign./annot. probes	raw p-value
oxidation-reduction process	**GO:0055114**	**86/1237**	**1.6E-15**
long-chain fatty acid metabolic process	**GO:0001676**	**16/68**	**2.8E-11**
cellular ketone metabolic process	**GO:0042180**	**61/948**	**5.3E-10**
lipid metabolic process	**GO:0006629**	**72/1221**	**6.6E-10**
terpenoid metabolic process	**GO:0006721**	**12/42**	**7.5E-10**
carboxylic acid metabolic process	GO:0019752	58/918	2.8E-09
oxoacid metabolic process	GO:0043436	58/918	2.8E-09
xenobiotic metabolic process	GO:0006805	11/38	3.3E-09
cellular response to xenobiotic stimulus	GO:0071466	11/38	3.3E-09
organic acid metabolic process	GO:0006082	58/937	5.8E-09
response to xenobiotic stimulus	GO:0009410	11/41	8.0E-09
monoterpenoid metabolic process	GO:0016098	5/5	1.4E-08
cellular lipid metabolic process	GO:0044255	54/876	2.3E-08
monocarboxylic acid metabolic process	GO:0032787	38/511	2.6E-08
small molecule metabolic process	GO:0044281	125/2829	3.4E-08
isoprenoid metabolic process	GO:0006720	13/75	1.0E-07
very long-chain fatty acid metabolic process	GO:0000038	10/43	1.7E-07
drug metabolic process	GO:0017144	8/25	2.0E-07
coenzyme metabolic process	GO:0006732	23/250	3.9E-07
cofactor metabolic process	GO:0051186	26/311	4.5E-07

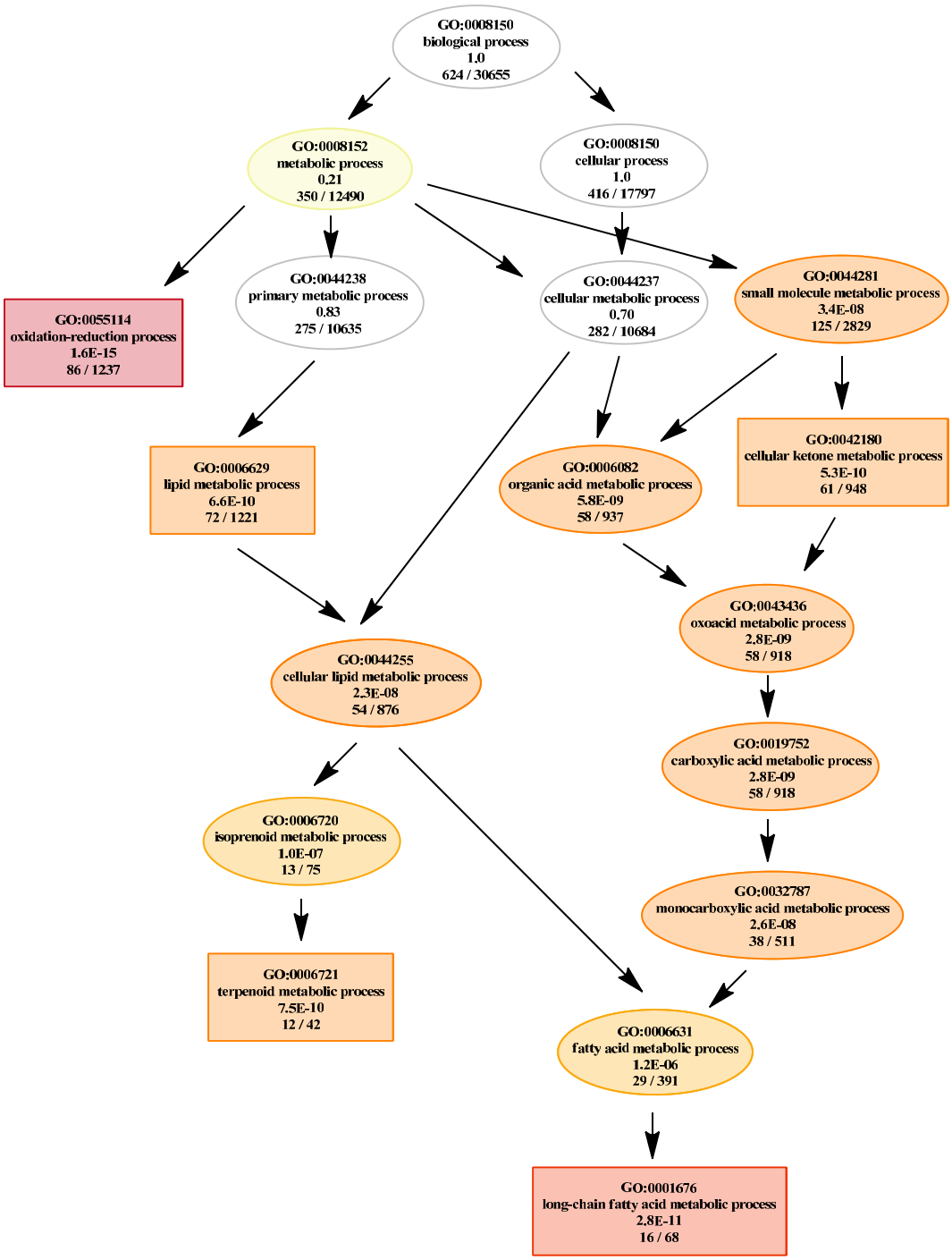

Figure 13: Mouse whole genome microarray analysis – TopGO analysis (1-PeCDD, 25 µg/kg bw, three days; mouse liver): The GO subgraph plot induced by the top five GO terms identified by the classic algorithm for scoring GO terms for enrichment regarding up-regulated genes. Boxes indicate the five most significant GO terms. Box color represents relative significance ranging from dark red (most significant) to light yellow (least significant).

The top five GO terms (indicated in bold in table 18) inducing the subgraph presented in figure 13, are linked to ‘oxidation-reduction processes’ (GO:0055114) and lipid metabolism (GO:0001676, GO:0042180, GO:0006629, GO:0006721). ‘Oxidation-reduction process’ is as well connected with metabolism and actually represents a parent term from lipid oxidation (GO:0034440), for instance, which in turn has child terms such as fatty acid beta-oxidation (GO:0006635). Another child term from ‘oxidation-reduction process’ is ‘oxidoreductase activity’ (GO:0016491) followed by inferred ‘monooxygenase activity’ (GO:0004497). Among annotated genes up-regulated by 1-PeCDD within ‘oxidation-reduction processes’ (GO:0055114; 86/1237 significant probes), 29 probes (21 genes) encoded CYP-enzymes of families 1, 2, 3, 4, 8, and 26. Further significantly up-regulated genes annotated to this GO term were *Cd36* (NM_007643), hydroxysteroid (17-beta) dehydrogenase 2 (*Hsd17b2*, NM_008290), tryptophan 2,3-dioxygenase (*Tdo2*, NM_019911), and kynurenine 3-hydroxylase (*Kmo*, NM_133809).

Obtained by testing over-representation of GO terms within the group of differentially expressed genes, further relevant biological processes significantly switched on by 1-PeCDD in mouse livers were related to drug and xenobiotic metabolism (GO:0017144, GO:0006805) as well as ancestral terms including coenzyme/cofactor metabolic processes (GO:0006732, GO:0051186) (Ashburner *et al.*, 2000; Binns *et al.*, 2009).

Along the whole experiment, high correlation between 1-PeCDD-, and TCDD-derived effects was revealed. Of 43020 oligos (excluding intern controls), 13312 were assigned to signal intensities $A \geq 2^7$ throughout the entire study concerning all seven core congeners. From these, lfc-expressing coefficients belonging to 1-PeCDD’s impact, which diverged at most ±1 from TCDD’s, were 13170, 11322 lay in a range of ±0.5 TCDD’s lfcs, 3270 oligos were not exceeding ±0.1 TCDD’s lfcs, 1674 varied less or equal than ±0.05 from TCDD’s lfc’s, and 372 oligos conformed with TCDD’s lfcs to ±0.01. As mentioned above, of 319 up-regulated genes by 1-PeCDD, and 125 up-regulated genes by TCDD, 92 genes were induced in response to both treatments in livers of mice. The respective Top 20-list (sorted referring to TCDD-derived effects) of up-regulated genes is presented in table 19. Raw data pertaining to TCDD-treatment was obtained by courtesy of Christiane Lohr (Lohr, 2013).

Table 19: Mouse whole genome microarray analysis. Top 20 genes (totaling 92) accordantly up-regulated in mouse livers by 1-PeCDD (25 µg/kg bw, three days), and TCDD (25 µg/kg bw, three days). Sorted based on TCDD-derived effects. TCDD-raw data by courtesy of Lohr (2013). Cutoff values: A ≥ 27, lfc ≥ 1, p-value < 0.05.

1-PeCDD & TCDD lfc	lcf	Gene systematic name	Gene description	Gene name
9.092	9.478	NM_009992	cytochrome P450 family 1 subfamily a polypeptide 1	*Cyp1a1*
4.440	5.169	NM_009994	cytochrome P450 family 1 subfamily b polypeptide 1	*Cyp1b1*
3.975	3.985	NM_009993	cytochrome P450 family 1 subfamily a polypeptide 2	*Cyp1a2*
2.747	3.582	NM_010210	fragile histidine triad gene	*Fhit*
2.798	3.379	NM_017379	tubulin alpha 8	*Tuba8*
3.212	3.103	NM_027872	solute carrier family 46 member 3	*Slc46a3*
1.349	2.903	NM_178892	TCDD-inducible poly(ADP-ribose) polymerase	*Tiparp*
1.725	2.819	NM_008181	glutathione S-transferase alpha 1 (Ya)	*Gsta1*
2.117	2.722	XM_001477458	predicted gene ENSMUSG00000054044	*Gm9933*
2.871	2.678	NM_016865	HIV-1 tat interactive protein 2, homolog (human)	*Htatip2*
2.641	2.518	NM_025557	Purkinje cell protein 4-like 1	*Pcp4l1*
1.831	2.386	NM_013872	phosphomannomutase 1	*Pmm1*
1.351	2.153	NM_023440	transmembrane protein 86B	*Tmem86b*
2.360	2.123	NM_026791	F-box and WD-40 domain protein 9	*Fbxw9*
1.427	1.978	NM_028747	RIKEN cDNA 0610012H03 gene	*0610012H03Rik*
2.172/ 1.081	1.931/ 1.039	NM_007618	serine (or cysteine) peptidase inhibitor clade A member 6	*Serpina6*
1.606/ 1.054	1.857/ 1.362	NM_013541	glutathione S-transferase pi 1	*Gstp1*
1.251	1.853	NM_001122660	predicted gene 10639	*Gm10639*
1.792	1.758	NM_007643	CD36 antigen	*Cd36*
1.919	1.702	NM_007689	chondroadherin	*Chad*

Values b/a from oligo b/oligo a.

As suggestible due to the appropriate correlation regarding numbers of accordantly up-regulated genes by both 1-PeCDD and TCDD, the Top 20-list of up-regulated genes (table 19) in the main reflected 1-PeCDD's Top 20-list of up-regulated genes. Gene transcripts of the top three CYPs were induced in the same ranking order (*Cyp1a1* > *Cyp1b1* > *Cyp1a2*) and to a highly correlative degree. In total, ten out of 20 genes appeared in both the 1-PeCDD-Top 20-list and the 1-PeCDD&TCDD-Top 20-list.

TCDD-inducible poly(ADP-ribose) polymerase (*Tiparp*), of which TCDD-induced transcription was reported to be AhR-dependent, was up-regulated by both congeners (Ma, 2002; Ma *et al.*, 2001). Since *Tiparp*-inducing effects due to 1-PeCDD-treatment were less efficient compared to TCDD's impact (lfc (1-PeCDD) = 1.349 vs. lfc (TCDD) = 2.903), and the Top 20 list in table 19 for 1-PeCDD&TCDD was sorted referring to TCDD-derived effects, *Tiparp* did occur in table 19, but not in the Top 20-list of 1-PeCDD-up-regulated genes (table 17). The NAD^+-ADP-ribosyltransferase was proposed to be involved in several biological processes including estrogen metabolism or hemopoiesis (Binns *et al.*, 2009; Dimmer *et al.*, 2012).

Another up-regulated gene related to immune response affected by 1-PeCDD as well as TCDD was *Cd36* (NM_007643; lfc (1-PeCDD) = 1.792, lfc (TCDD) = 1.758), which is also linked to lipid metabolism. Further hints regarding both compounds' effects on lipid metabolism were given due to effects on transmembrane protein 86B (*Tmem86b*, NM_023440; lfc (1-PeCDD) = 1.351, lfc (TCDD) = 2.153). The encoded enzyme lysoplasmalogenase catalyzes the degradation of lysoplasmalogens, which are formed by the hydrolysis of the abundant membrane glycerophospholipids plasmalogens (Binns *et al.*, 2009; Dimmer *et al.*, 2012).

A dominating result within the Top 20-table (figure 19) of both examined dibenzo-*p*-dioxins was their impact on genes implicated in phase II metabolism: the glutathione *S*-transferases (GSTs) *Gsta1* and *Gstp1*, as well as a transcript (NM_001122660) encoding a GST named protein Gm10639 (Binns *et al.*, 2009; Dimmer *et al.*, 2012).

Table 20 presents the Top 20-list of down-regulated genes in mouse livers in respond to single doses of 1-PeCDD (25 µg/kg bw). In total, transcription of 374 genes was inhibited by 1-PeCDD-treatment according to chosen cutoff values ($A \geq 2^7$, lfc ≤ -1, p-value < 0.05).

Table 20: Mouse whole genome microarray analysis. Top 20 down-regulated genes in mouse livers by 1-PeCDD (25 µg/kg bw, three days); descending order. Cutoff values: A ≥ 27, lfc ≤ -1, p-value < 0.05.

1-PeCDD lfc	Gene systematic name	Gene description	Gene name
-2.797-(-2.009)	NM_007706	suppressor of cytokine signaling 2	*Socs2*
-2.535/ -2.537	BC031891/ NR_002861	serine (or cysteine) peptidase inhibitor clade A member 4 pseudogene 1	*Serpina4-ps1*
-2.531	NM_001081141	gamma-aminobutyric acid B receptor 2	*Gabbr2*
-2.381/-2.129	NM_134037	ATP citrate lyase	*Acly*
-2.244-(-2.138)	NM_207655	epidermal growth factor receptor	*Egfr*
-2.123	NM_007988	fatty acid synthase	*Fasn*
-2.087	NM_001111110	cytidine monophospho-N-acetylneuraminic acid hydroxylase	*Cmah*
-2.070	NM_145148	FERM domain containing 4B	*Frmd4b*
-2.040/-1.148	NM_029389	family with sequence similarity 35 member A	*Fam35a*
-2.031	ENSMUST00000 099037	Unknown	*ENSMUST0000 0099037*
-2.027	NM_007606	carbonic anhydrase 3	*Car3*
-2.013	XM_001480325	similar to hepatocyte nuclear factor 6 beta	*LOC100048479*
-2.010/-1.856	ENSMUST00000 099683	Unknown	*ENSMUST0000 0099683*
-1.980/-1.922	ENSMUST00000 099050	Unknown	*ENSMUST0000 0099050*
-1.964	NM_146153	thyroid hormone receptor associated protein 3	*Thrap3*
-1.955/-1.586	NM_133904	acetyl-Coenzyme A carboxylase beta	*Acacb*
-1.894	NM_009723	ATPase Ca++ transporting plasma membrane 2	*Atp2b2*
-1.889	XM_001003154	similar to Glucose phosphate isomerase 1 transcript variant 2	*LOC676974*
-1.888	NM_020507	transducer of ERBB2, 2	*Tob2*
-1.888	NM_013490	choline kinase alpha	*Chka*

Values b/a from oligo b/oligo a; values a-n: value range of more than two (n) oligos.

Suppressor of cytokine signaling 2 (*Socs2*, NM_007706; lfc (max) = -2.797) was the most efficiently down-regulated gene-transcript in livers from mice treated with 1-PeCDD (table 20). SOCS family proteins belong to a class of negative regulators of the Janus kinase/signal transducers and activators of transcription (JAK/STAT) pathway, which is a principal signaling mechanism for a wide array of cytokines and growth factors stimulating cell proliferation, cell migration and apoptosis. SOCS2 was proposed to play a role in mediating ubiquitination and subsequent proteasomal degradation of target proteins (Binns *et al.*, 2009; Dimmer *et al.*, 2012; Rawlings *et al.*, 2004).

The two serine (or cysteine) peptidase inhibitor clade A member 4 pseuogene 1 (*Serpina4-ps1*, BC031891/NR_002861; lfc (max) = -2.537) gene transcripts representing the second highest down-regulating effect on gene transcription by 1-PeCDD are non-protein coding. Other cysteine- or serine-type peptidase inhibitor proteins are involved in apoptotic processes or response(s) to cytokines (Binns *et al.*, 2009; Dimmer *et al.*, 2012). The down-regulated transcription of gamma-aminobutyric acid (GABA) B receptor 2 (*Gabbr2*, NM_001081141; lfc = -2.531) might be correlated to reduced GABBR2-mediated coupling to G proteins and correlated G-protein coupled receptor signaling pathways, since GABBR2 together with GABBR1 builds the heterodimeric G-protein coupled receptor for GABA (Binns *et al.*, 2009; Dimmer *et al.*, 2012).

An enzyme, which is involved in the citric acid cycle, is encoded by another down-regulated gene transcript, namely ATP citrate lyase ('ATP citrate synthase', *Acly*, NM_134037; lfc (max) = -2.381). Shortened, the enzyme catalyzes the reaction of acetyl-CoA and oxalacetate to form citrate and Coenzyme A (CoA). A central role in *de novo* lipid synthesis is attributed to ACLY since the ability of citrate to leave the mitochondria allows transferring acetyl-CoA into cytoplasm, where it is required for fatty acid synthesis (Srere and Bhaduri, 1962). An inhibition of ACLY is therefore negatively correlated to lipid biosynthesis. Inhibition of lipid biosynthesis by 1-PeCDD was also indicated by down-regulation of fatty acid synthase (*Fasn*, NM_007988; lfc = -2.123), and acetyl-CoA carboxylase beta (*Acacb*, NM_133904; lfc (max) = -1.955). During fatty acid biosynhesis, *Acacb* catalyzes the carboxylation of acetyl-CoA to malonyl-CoA, whereas *Fasn* catalyzes the formation of long-chain fatty acids from acetyl-CoA, malonyl-CoA, and NADPH (Binns *et al.*, 2009; Dimmer *et al.*, 2012). Beyond the top 20 list, further genes related to lipid metabolism were down-regulated by 1-PeCDD in mouse livers including acyl-Coenzyme A oxidase 3 (*Acox3*, NM_030721; lfc = -1.063), apolipoprotein C-III (*Apoc3*, NM_023114; lfc = -1.155), apolipoprotein A-I (*Apoa1*, NM_009692; lfc (max) = -1.165) (Staels *et al.*, 1992; Tugwood *et al.*, 1992).

Among the Top 20-list, genes down-regulated by 1-PeCDD in mouse livers involved in altered carbohydrate- and glucose-metabolism were FERM domain containing 4B (*Frmd4b*, NM_145148; lfc = -2.070) and potentially 'similar to hepatocyte nuclear factor 6 beta' (*LOC100048479*, XM_001480325; lfc = -2.013). *Frmd4b* is a member of general receptor for 3-phosphoinositides 1 (GRP1) signaling complexes, which are recruited to plasma membrane ruffles in response to insulin receptor signaling. GRP1 was further identified to play a key role in linking insulin signaling to glucose transporter type 4 GLUT4 recycling (Binns *et al.*, 2009; Dimmer *et al.*, 2012; Li *et al.*, 2012). *Glut4* itself was regulated by neither investigated DL-congener in the course of the study in hand. The similarity of *LOC100048479* to hepatocytes nuclear factor 6 (*Hnf6*) might hint a role of 1-PeCDD in terms of glucose metabolism (Binns *et al.*, 2009; Dimmer *et al.*, 2012). Further, *Hnf6* and *Fasn* both are related to immune response. In particular, *Fasn* is involved in the cellular response to IL-4, whereas *Hnf6* plays a role in B cell differentiation and spleen development, which together might hint towards 1-PeCDD-mediated suppression of B cell differentiation and B cell response (Binns *et al.*, 2009; Dimmer *et al.*, 2012).

Regarding endocrine function, thyroid hormone receptor associated protein 3 (*Thrap3*, NM_146153; lfc = -1.964) was part of the Top 20-list of down-regulated gene transcripts. *Thrap3* is involved in thyroid hormone receptor binding processes (Binns *et al.*, 2009; Dimmer *et al.*, 2012). Down-regulated genes within the Top 20-list related to oxidative stress were epidermal growth factor receptor (*Egfr*, NM_207655; lfc (max) = -2.244) and carbonic anhydrase 3 (*Car3*, NM_007607; lfc = -2.027). EGFR is able to activate signaling cascades including RAS-RAF-MEK-ERK pathway or the STAT modules and may also activate the NF-κB signaling cascade (Binns *et al.*, 2009; Dimmer *et al.*, 2012).

Setting chosen cutoff levels, the list for down-regulated genes by 1-PeCDD was examined performing classical enrichment analysis by testing over-representation of GO terms within the group of differentially expressed genes using Fisher's exact test. The Top 20 GO terms obtained by means of this TopGO analysis is presented in table 21 (following page).

Table 21: Mouse whole genome microarray analysis – TopGO analysis (1-PeCDD), Fisher's exact test. Top 20 GO terms identified by the classic algorithm for scoring GO terms for enrichment regarding down-regulated genes; descending order. Mouse liver, 1- PeCDD (25 µg/kg bw, three days). Top five GO terms indicated in bold.

1-PeCDD GO term	GO ID	sign./annot. genes	Raw p-value
triglyceride metabolic process	**GO:0006641**	**15/109**	**1.1E-09**
triglyceride biosynthetic process	**GO:0019432**	**11/55**	**3.2E-09**
acylglycerol metabolic process	**GO:0006639**	**15/125**	**7.6E-09**
neutral lipid biosynthetic process	**GO:0046460**	**11/60**	**8.5E-09**
acylglycerol biosynthetic process	**GO:0046463**	**11/60**	**8.5E-09**
glycerol ether metabolic process	GO:0006662	16/147	1.0E-08
neutral lipid metabolic process	GO:0006638	15/128	1.1E-08
glycerol ether biosynthetic process	GO:0046504	11/62	1.2E-08
organic ether metabolic process	GO:0018904	16/150	1.4E-08
lipid biosynthetic process	GO:0008610	29/572	6.5E-07
glycerolipid metabolic process	GO:0046486	20/308	8.9E-07
fatty acid biosynthetic process	GO:0006633	15/181	1.0E-06
gland development	GO:0048732	21/344	1.3E-06
glycerolipid biosynthetic process	GO:0045017	14/162	1.4E-06
fatty acid metabolic process	GO:0006631	22/391	2.8E-06
regulation of lipid metabolic process	GO:0019216	16/226	3.6E-06
monocarboxylic acid metabolic process	GO:0032787	25/511	7.1E-06
regulation of biological quality	GO:0065008	73/2614	7.5E-06
small molecule biosynthetic process	GO:0044283	23/448	7.5E-06
cell development	GO:0048468	52/1660	8.6E-06

The most significant GO terms affected by 1-PeCDD regarding down-regulation of gene transcription were to highest degree related to lipid-biosynthesis and metabolism (table 21). Formally, these were divided into seven biosynthetic and nine metabolic processes among the Top 20 GO terms. As the general structure of metabolic process terms correlates 'cellular substance biosynthetic process' and 'cellular substance catabolic process' as child terms of 'cellular substance metabolic process', several genes are often annotated to both biosynthetic and metabolic processes.

For instance, the term ‘triglyceride metabolic process’ (GO:0006641) represents a parent term to ‘triglyceride biosynthetic process’ (GO:0019432).

Accordingly, the down-regulated gene *Fasn* (lfc = -2.123) by 1-PeCDD is assigned to ‘fatty acid biosynthetic process(es)’ (GO:0006633) as well as to ‘fatty acid metabolic process(es)’ (GO:0006631). Consequently, the majority of most significantly clustering GO terms in response to *in vivo* treatment was related to inhibitory effects on gene expression correlated with lipid biosynthetic processes in mouse livers.

With lowered significance (≥ 1.3E-06), further biological processes negatively regulated by 1-PeCDD included ‘gland development’ (GO:0048732), ‘cell development’ (GO:0048468), and ‘regulation of biological quality’ (GO:0065008). Among significantly affected probes belonging to ‘gland development’ (21/344), the majority was not exclusively related to gland development including insulin receptor substrate 2 (*Irs2*, NM_001081212), *Socs2* (NM_007706), apolipoprotein A-1 (*Apoa1*, NM_009692), *Atp2b2* (NM_009723), and *Egfr* (NM_207655). A probe, which was down-regulated by 1-PeCDD-treatment and is more specifically involved in this process, was netrin 1 (*Ntn1*, NM_008744). Though belonging to a highly conserved family of axonal guidance signals, *Ntn1* was proposed to serve as a survival factor to prevent the initiation of apoptosis (Ashburner *et al.*, 2000; Binns *et al.*, 2009; Püschel, 1999).
GO-terms ‘cell development’ (GO:0048468), and ‘regulation of biological quality’ (GO:0065008) represent more comprehensive processes with many subordinated child terms. Significant probes (52/1660) within GO:0048468 partly coincided with those mentioned with respect to ‘gland development’ (*Socs2*, *Apoa1*, *Atp2b2*, *Egfr*, *Ntn1*), and further include Kruppel-like factor 10 (*Klf10*, NM_013692), B-cell leukemia/lymphoma 6 (*Bcl6*, NM_009744), or mitogen-activated protein kinase 9 (*Mapk9*, NM_207692), for instance.
A ‘biological quality’ represents a measurable attribute of an organism or part of an organism, such as size, mass, or shape (Ashburner *et al.*, 2000; Binns *et al.*, 2009). In terms of ‘biological quality’, 73 of 2614 probes were inhibited by 1-PeCDD-treatment in mouse livers (*Cd4* (NM_013488), complexin 2 (*Cplx2*, NM_009946), *Socs2*, *Apoa1*, *Atp2b2*, *Bcl6*, *Ntn1*, e.g.), whereas 57 probes were up-regulated, by contrast. Interestingly, these 57 probes contained *Cyp1a1*, *Cyp1a2*, *Cyp1b1*, *Tiparp*, *Cd36*, and *Hsd17b2*.

The table presenting down-regulated genes affected accordingly by 1-PeCDD- or TCDD-treatment in mouse livers three days subsequent to single dose exposures is shown in the attachments.

4.1.1.2.2. 4-PeCDF – impact on gene transcription in mouse livers

Numbers of genes regulated in livers due to single-dose treatment of mice with 4-PeCDF (250 µg/kg bw) and three days of exposure are compiled in figure 14. Contrasting with data obtained by TCDD-treatment by courtesy of Christiane Lohr (Lohr, 2013) was included.

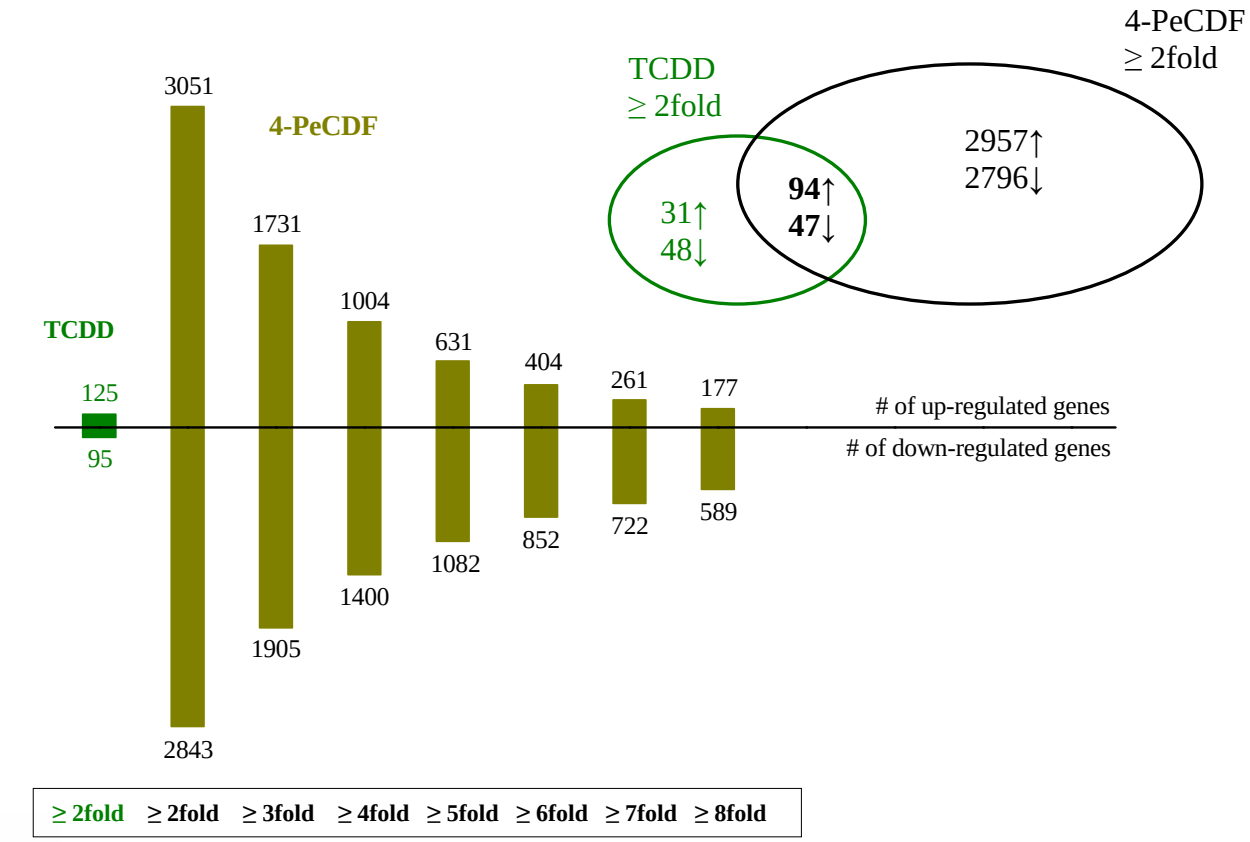

Figure 14: Mouse whole genome microarray analysis. Numbers of regulated genes in mouse livers by 4-PeCDF (250 µg/kg bw, three days) compared to numbers of genes regulated by TCDD (25 µg/kg bw, three days), and numbers of genes regulated both by 4-PeCDF and TCDD (TCDD-raw data by courtesy of C. Lohr; Lohr, 2013). A ≥ 27, p-value < 0.05.

Subsequent to three days of exposure of single-dose treated mice with 4-PeCDF (250 µg/kg bw), vast numbers of genes were affected in livers (figure 14). Regarding selected cutoff values for signal intensity $A \geq 2^7$, logarithmic (log2) fold change $|lfc| \geq 1$ (≥ 2fold induction/repression), and p-value < 0.05, 3051 genes were up-, and 2843 genes were down-regulated. Proceeding to raise cutoff value concerning lfc, levels below 1000 genes for up-, as well as down-regulation were gained beginning with ≥ 6fold induction/repression ($|lfc| \geq 2.585$; 404 genes up-, 852 genes down-regulated).

Continuing examination up to $|lfc| \geq 3$ ($\geq$ 8fold), at least regarding number of up-regulated genes (177 genes), orders of magnitude comparable to effects induced by TCDD (125 genes) was reached. Overlap between TCDD- and 4-PeCDF- derived effects accounted for 94 up- and 47 accordantly down-regulated genes.

In table 22, attention was directed to types of genes affected in mouse livers after three days of exposure. Top 20 genes up-regulated by 4-PeCDF are overviewed.

Table 22: Mouse whole genome microarray analysis. Top 20 up-regulated genes in mouse livers by 4-PeCDF (250 µg/kg bw, three days). Cutoff values: A ≥ 27, lfc ≥ 1, p-value < 0.05.

4-PeCDF lfc	Gene systematic name	Gene description	**Gene name**
5.994	NM_009992	cytochrome P450, family 1, subfamily a, polypeptide 1	*Cyp1a1*
4.576/2.433	NM_011034	peroxiredoxin 1	*Prdx1*
3.506-4.357	NM_031164	coagulation factor XIII beta subunit	*F13b*
4.356	NM_008618	malate dehydrogenase 1 NAD (soluble)	*Mdh1*
4.334	NM_145925	pituitary tumor-transforming 1 interacting protein	*Pttg1ip*
4.303	NM_009028	RAS-like family 2 locus 9	*Rasl2-9*
4.279/2.334	NM_008211	H3 histone family 3B	*H3f3b*
4.227	NM_007643	CD36 antigen transcript variant 2	*Cd36*
4.174	A_55_P2125868	Unknown	*A_55_P2125868*
4.143	NM_026503	RIKEN cDNA 1110058L19 gene	*1110058L19Rik*
4.137	NM_153798	polymerase (RNA) II (DNA directed) polypeptide B	*Polr2b*
4.129	NM_001040396	RIKEN cDNA 2810407C02 gene	*2810407C02Rik*
4.102	NAP029947-1	Unknown	*NAP029947-1*
4.077	NM_175255	Sec24 related gene family member A (S. cerevisiae)	*Sec24a*
4.041	NM_025535	SAR1 gene homolog B (S. cerevisiae)	*Sar1b*
4.022	NM_013778	aldo-keto reductase family 1 member C13	*Akr1c13*
3.996	NM_001113413	ring finger protein 13	*Rnf13*
3.904	NM_023418	phosphoglycerate mutase 1	*Pgam1*
3.902/2.030	NM_009725	ATP synthase H+ transporting mitochondrial F0 complex subunit b	*Atp5f1*
3.882	NR_003625	RIKEN cDNA 1700073E17 gene	*1700073E17Rik*

Values b/a from oligo b/oligo a; values a-n: value range of more than two (n) oligos.

The most effectively up-regulated gene in mouse livers due to 4-PeCDF-exposure was *Cyp1a1* (NM_009992; lfc = 5.994). AhR-dependent genes encoding CYP1A2, and CYP1B1 were absent within the Top 20 up-regulated genes list (table 22). Within chosen cutoff-values, *Cyp1b1* (NM_009994, lfc = 2.926) was lightly higher up-regulated than was *Cyp1a2* (NM_009993, lfc = 2.414).

Highest up-regulated target gene in mouse livers for 4-PeCDF-treatment *Cyp1a1* was followed by peroxiredoxin 1 (*Prdx1*, NM_011034; lfc (max) = 4.576), and coagulation factor XIII, beta subunit (*F13b*, NM_031164; lfc (max) = 3.506). PRDX 1 is involved in regulation of intracellular H_2O_2-concentrations, using reducing equivalents provided through the thioredoxin system to reduce peroxides (Chae *et al.*, 1994a; Chae *et al.*, 1994b; Iwahara *et al.*, 1995). Furthermore, PRDX 1 was linked to inhibition of apoptosis (Berggren *et al.*, 2001; Egler *et al.*, 2005; Kim *et al.*, 2000; Kim *et al.*, 2008).
Though not integrated in the Top 20 gene list shown in table 22, further members of the thioredoxin/thioredoxin reductase redox system were up-regulated within cutoff values. Besides thioredoxin 1 (*Txn1*, NM_153162), which was enhanced to 1.311 lfc, thioredoxin reductases 1 and 3 were up-regulated reaching lfc values of 1.544 (*Txnrd1*, NM_001042523), and 2.642 (*Txnrd3*, NM_153162), respectively. *Prdx1*, *Txn*, and *Txnrd* were found to be overexpressed in a number of human cancers (Lincoln *et al.*, 2003; Yanagawa *et al.*, 1999), whereas *Txn* concurrently was correlated with enhanced cell proliferation and inhibition of apoptosis *in vitro* and *in vivo* (Baker *et al.*, 1997; Gadaska *et al.*, 1995; Grogan *et al.*, 2000). In accordance, nuclear factor, erythroid derived 2, like 2 (*Nfe2l2*, NM_010902) was up-regulated (lfc = 2.473). NFE2l2 constitutes a transcription factor, which binds to antioxidant response elements and leads to hemin (ferriprotoporphyrin IX)-induced activation of the thioredoxin gene (Kim *et al.*, 2001).

Coagulation factor XIII (plasma transglutaminase, fibrin stabilizing factor) is a glycoprotein, which constitutes a tetramer consisting of two A and two B chains. In the course of blood coagulation, activated factor XIII covalently cross-links fibrin-monomers resulting in stable fibrin-clots. The B chain (F13B) is not catalytically active, but possesses influence on the rate of activation by thrombin (Chung *et al.*, 1974; Ichinose and Davie, 1988). Two different probes for analysis of gene transcripts for coagulation factor XIII A1 subunit (*F13a1*, NM_028784) were spotted on the array, but neither was within set cutoff values for all congeners investigated.

Malate dehydrogenase 1 (*Mdh1*, NM_008618; lfc = 4.356) was up-regulated by 4-PeCDF. Besides its involvement in the tricarboxylic acid cycle, MDH1 was further considered to serve as biomarker for hepatocellular carcinomas and the severity of acute hepatitis (Amacher *et al.*, 2005; Kawai and Hosaki, 1990), and was associated with hepatotoxicity and liver necrosis (Clifford and Rees, 1967; Zieve *et al.*, 1985). Further, a 4-PeCDF-induced gene related to glycolytic processes was found within the Top 20-list: phosphoglycerate mutase 1 (*Pgam1*, NM_023418; lfc = 3.904) (Binns *et al.*, 2009; Dimmer *et al.*, 2012).

The protein encoded by pituitary tumor-transforming 1 interacting protein (*Pttg1ip*, NM_145925; lfc = 4.334), which was up-regulated in mouse livers after 4-PeCDF-treatment, specifically interacts with the oncogene pituitary tumor-transforming gene 1 (PTTG1) *in vitro* and *in vivo*, and facilitates PTTG1 nuclear translocation, subsequently enhancing its force as transcription factor (Chien and Pei, 2000; Li *et al.*, 2013; Pei and Melmed, 1997). *Pttg1* was also examined in the course of microarray analysis in hand. The presence of two different probes was intended to identify alterations of respective mRNA-levels, but no significant effect was observed throughout the complete mouse microarray experiment.
Ras-like, family 2, locus 9 (*Rasl2-9*, NM_009028; lfc = 4.303), also referred to as encoding the GTP-binding nuclear protein RAN, was up-regulated within the mouse microarray-experiment by 4-PeCDF. The Ras superfamily of small guanosine triphosphatases (GTPases) represent GTP-binding proteins involved in nucleocytoplasmic transport of both proteins and RNA (Kadowaki *et al.*, 1993; Melchior *et al.*, 1993; Schlenstedt *et al.*, 1995; Weis, 2003).

Within the mouse microarray experiment, probes for H3 histone, family 3B (histone H3.3, *H3f3b*, NM_008211; lfc (max) = 4.279) revealed up-regulated levels of gene transcripts in mouse livers due to 4-PeCDF-treatment. As deposited at sites of nucleosomal displacement throughout transcribed genes, H3.3 was proposed to represent an epigenetic imprint of transcriptionally active chromatin (Dimmer *et al.*, 2012; Wirbelauer *et al.*, 2005). The number of oligos included within the present microarray analysis involved in histone-regulation amounted to 168. Among these, with due regard to cutoff values ($A \geq 2^7$, $|lfc| \geq 1$, p-value < 0.05), 29 genes were affected in mouse livers by treatment with 4-PeCDF, of which 10 were up-, and 19 down-regulated. Besides discussed regulation of *H3f3b*, up-regulated genes comprised further histones and histone clusters. Down-regulated oligos included genes encoding class II histone deacetylases (HDACs) (*Hdac5*, NM_001077696; *Hdac6*, NM_010413; *Hdac7*, NM_019572) (class II HDACs reviewed in Bertos *et al.*, 2001; Yang and Grégoire, 2005).

In addition, and not least besides the high number of genes significantly induced, further evidence for 4-PeCDF's role as a inducer of transcription and activator of cellular machinery were given by up-regulated genes within the Top 20-list (Binns *et al.*, 2009; Dimmer *et al.*, 2012): polymerase (RNA) II (DNA directed) polypeptide B (*Polr2b*, NM_153798; lfc = 4.137), Sec24 related gene family member A (*Sec24a*, NM_175255; lfc = 4.077; encoded protein involved in promotion of secretory, plasma membrane, and vacuolar proteins from the endoplasmic reticulum to the Golgi complex), and SAR1 gene homolog B (*Sar1b*, NM_025535; lfc = 4.041; encoded protein involved in intracellular protein transport), ATP synthase H+ transporting mitochondrial F0 complex subunit b (*Atp5f1*, NM_009725; lfc (max) = 3.902; encoded protein produces ATP from ADP, member of electron transport complex of the respiratory chain).

Genes correlated with lipid metabolism obtained within the Top 20 of up-regulated genes by 4-PeCDF were CD36 antigen transcript variant 2 (*Cd36*, NM_007643; lfc = 4.227), and aldo-keto reductase family 1 member C13 (*Akr1c13*, NM_013778; lfc = 4.022). The protein aldo-keto reductase 1C13 represents an oxidoreductase implicated in xenobiotic metabolic processes, and is able to catalyze the dehydrogenation of 17-beta-hydroxysteroids (Binns *et al.*, 2009; Dimmer *et al.*, 2012).

According to NCBI BLAST (BLASTN 2.2.28, Zhang *et al.*, 2000), Probe A_55_P2125868 (lfc = 4.174) might match with tyrosine 3-monooxygenase/tryptophan 5-monooxygenase activation protein, theta polypeptide (*Ywhaq*, NM_011739; 54/60 identities, 90%). Regulation of *Ywhaq* was examined by means of five different probes on applied array slides, of which three revealed up-regulations ranging from 1.375 to 2.507 lfc, and one declared down-regulation of 2.124 lfc.
14-3-3 protein theta belongs a family of proteins, which mediate signal transduction by specific phosphoserine/phosphothreonine binding activities (Morrison, 2009; Yaffe *et al.*, 1997), being connected with cell cycle regulation, apoptosis, or signaling molecules including members of the protein kinase C family (Meller *et al.*, 1996; Peng *et al.*, 1997; Zha *et al.*, 1996).

Data on up-regulation of genes by 4-PeCDF in mouse livers was studied performing classical enrichment analysis by testing over-representation of GO terms using Fisher's exact test. By respective TopGO analysis, a Top 20 list, which is illustrated in table 23, of most significant GO terms was revealed. Respective subgraph induced by the top five GO terms is depicted in figure 15.

Table 23: Mouse whole genome microarray analysis – TopGO analysis (4-PeCDF): Fisher's exact test. Top 20 GO terms identified by the classic algorithm for scoring GO terms for enrichment regarding up-regulated genes; descending order. Mouse liver, 4-PeCDF (250 µg/kg bw, three days). Top five GO terms indicated in bold.

4-PeCDF GO term	GO ID	sign./annot. genes	Raw p-value
metabolic process	**GO:0008152**	**2714/12490**	**3.8E-25**
cellular metabolic process	**GO:0044237**	**2353/10684**	**5.0E-24**
oxidation-reduction process	**GO:0055114**	**355/1237**	**6.8E-18**
small molecule metabolic process	**GO:0044281**	**703/2829**	**8.4E-17**
primary metabolic process	**GO:0044238**	**2277/10635**	**2.9E-16**
cellular catabolic process	GO:0044248	487/1853	3.7E-16
catabolic process	GO:0009056	553/2156	5.0E-16
translation	GO:0006412	205/658	1.4E-14
cofactor metabolic process	GO:0051186	113/311	2.6E-13
cellular ketone metabolic process	GO:0042180	268/948	5.4E-13
RNA processing	GO:0006396	232/798	9.5E-13
RNA splicing	GO:0008380	146/451	3.7E-12
cellular protein metabolic process	GO:0044267	924/4045	6.3E-12
intracellular transport	GO:0046907	295/1088	7.7E-12
coenzyme metabolic process	GO:0006732	92/250	1.8E-11
carboxylic acid metabolic process	GO:0019752	254/918	2.5E-11
oxoacid metabolic process	GO:0043436	254/918	2.5E-11
organic acid metabolic process	GO:0006082	257/937	5.0E-11
protein metabolic process	GO:0019538	1058/4764	1.7E-10
protein catabolic process	GO:0030163	176/603	3.7E-10

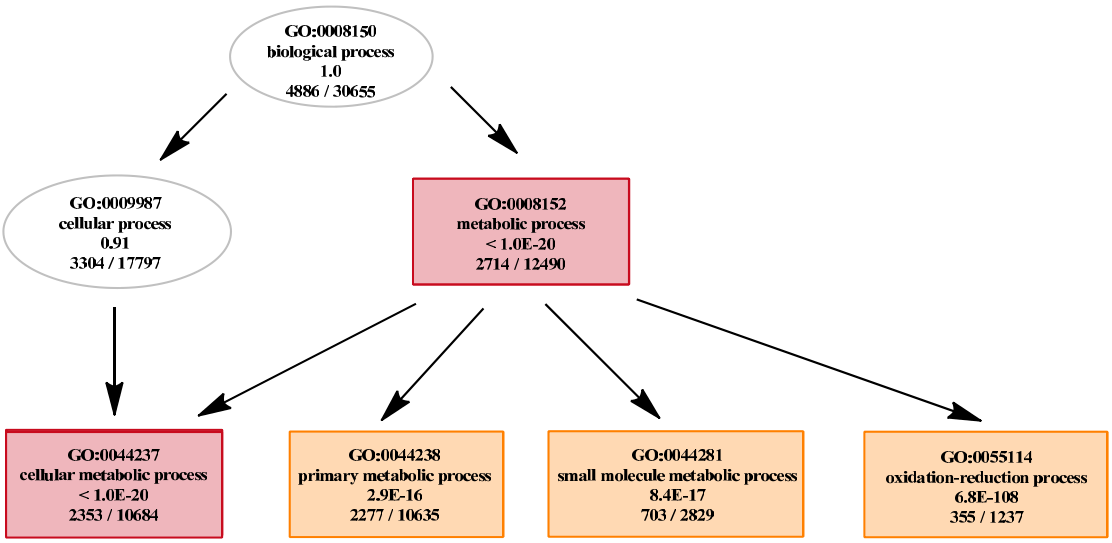

Figure 15: Mouse whole genome microarray analysis – TopGO analysis (4-PeCDF, 250 µg/kg bw, three days; mouse liver): The GO subgraph plot induced by the top five GO terms identified by the classic algorithm for scoring GO terms for enrichment regarding up-regulated genes. Boxes indicate the five most significant GO terms. Box color represents relative significance ranging from dark red (most significant) to orange (less significant).

With a respectable statistical significance (3.8E-25) and more than 20% of 12490 significant annotated probes, the Top 20-list of biological processes for up-regulated genes by 4-PeCDF-treatment (table 23) was headed and hallmarked by the GO term ‘metabolic process’ (GO:0008152). The Top 20-list comprised 16 GO terms involved in metabolic and catabolic processes plus four GO terms correlated with transcription/translation and processing of proteins (translation, GO:0006412; RNA processing, GO:0006396; RNA splicing, GO:0008380; intracellular transport, GO:0046907). The top five most significant GO terms were closely related to each other, hence leading to the very compact subgraph displayed in figure 15.

Respective GO terms ‘cellular metabolic process’ (GO:0044237), ‘oxidation-reduction process’ (GO:0055114), ‘small molecule metabolic process’ (GO:0044281), and ‘primary metabolic process’ (GO:0044238) all represent direct child terms from the most significant GO term ‘metabolic process’ (Ashburner *et al.*, 2000; Binns *et al.*, 2009).

In table 24, the Top 20 list of 2843 genes ≥ 2fold down-regulated in mouse livers by treatment with 4-PeCDF (250 µg/kg bw, three days) is presented.

Table 24: Mouse whole genome microarray analysis. Top 20 down-regulated genes in mouse livers by 4-PeCDF (250 µg/kg bw, three days). Cutoff values: A ≥ 2^7, lfc ≤ -1, p-value < 0.05.

4-PeCDF lfc	Gene systematic name	Gene description	Gene name
-7.474	NR_004413	U1b6 small nuclear RNA	*Rnu1b6*
-6.294	XM_001474429	similar to cyclic nucleotide gated channel beta 1	*Gm2690*
-6.278-(-3.710)	NM_009946	complexin 2	*Cplx2*
-6.185/ -6.176	BC031891/ NR_002861	serine (or cysteine) peptidase inhibitor clade A member 4 pseudogene 1	*Serpina4-ps1*
-6.180	XM_001472970	similar to R10D12.10 (LOC100039488)	*Gm2264*
-6.149	XM_001472203	similar to Ubtf protein	*Gm2033*
-6.118-(-4.014)	NM_008103	glial cells missing homolog 1	*Gcm1*
-5.987	NM_153522	sodium channel voltage-gated type III beta	*Scn3b*
-5.943	AK036325	16 days neonate cerebellum cDNA RIKEN full-length enriched library	*Syn3*
-5.926	XM_001478202	hypothetical protein LOC100047464	*LOC100047464*
-5.914	NM_181319	T-box 22 (Tbx22) transcript variant 2	*Tbx22*
-5.852	NM_001033960	RAB GTPase activating protein 1	*Rabgap1*
-5.851	NM_016659	killer cell lectin-like receptor subfamily A member 1	*Klra1*
-5.846	NM_001039959	AHNAK nucleoprotein (desmoyokin)	*Ahnak*
-5.820	NM_011562	teratocarcinoma-derived growth factor 1	*Tdgf1*
-5.815	NM_001169153	CD300 antigen like family member F	*Cd300lf*
-5.801	NM_203492	MAS-related GPR member G	*Mrgprg*
-5.768	NR_004439	ribonuclease P RNA-like 2	*Rprl2*
-5.751	NM_011371	ST6 (alpha-N-acetyl-neuraminyl-2,3-beta-galactosyl-1,3)-N-acetylgalactosaminide alpha-2,6-sialyltransferase 1	*St6galnac1*
-5.74	NM_172796	schlafen 9	*Slfn9*

Values b/a from oligo b/oligo a; values a-n: value range of more than two (n) oligos.

The Top 20 gene list representing most efficiently and apparently down-regulating effects of 4-PeCDF on gene expression in mouse livers (table 24) comprises several gene segments of unknown or partly unresolved function, which complicates understanding and weighing the relevance of respective down-regulating effects.

Still, a considerable number of genes participating in immune function were down-regulated by 4-PeCDF: complexin 2 (*Cplx2*, NM_009946; lfc (max) = -6.278; proposed involvement in mast cell degranulation), *Serpina4-ps1* (BC031891/NR_002861; lfc (max) = -6.185), T-box 22 transcript variant 2 (*Tbx22*, NM_181319; lfc = -5.914; encodes a probable transcriptional regulator involved in developmental processes; major determinant crucial to palatogenesis), killer cell lectin-like receptor subfamily A member 1 (*Klra1*, NM_016659; lfc = -5.851; encodes T-cell surface glycoprotein YE1/48, a MHC class I receptor), teratocarcinoma-derived growth factor 1 (*Tdgf1*, NM_011562; lfc = -5.820), CD300 antigen like family member F (*Cd300lf*, NM_001169153; lfc = -5.815; encoded protein participates in osteoclast differentiation), and schlafen 9 (*Slfn9*, NM_172796; lfc = -5.74). *Serpina4-ps1* and *Tdgf1* are also implicated in apoptotic processes (Binns *et al.*, 2009; Bustos *et al.*, 2009; Dimmer *et al.*, 2012). Further, *Cplx2* was reported to be essential for normal neurological function in mice (Glynn *et al.*, 2003). Down-regulated ST6 (alpha-N-acetyl-neuraminyl-2,3-beta-galactosyl-1,3)-N-acetylgalactosaminide alpha-2,6-sialyltransferase 1 (*St6galnac1*, NM_011371; lfc = -5.751) encodes a glycosyltransferase, which plays a role with respect to protein glycosylation (Binns *et al.*, 2009; Dimmer *et al.*, 2012).

RAB GTPase activating protein 1 (*Rabgap1*, NM_001033960; lfc = -5.852; encoded protein possesses Rab GTPase activator activity; might be involved in cell cycle regulation), and MAS-related GPR member G (*Mrgprg*, NM_203492; lfc = -5.801; G-protein coupled receptor activity) are implicating G-proteins, of which gene transcription was inhibited by 4-PeCDF (Binns *et al.*, 2009; Dimmer *et al.*, 2012).

Implicated in cell-cell junctions, AHNAK nucleoprotein (*Ahnak*, NM_001039959; lfc = -5.846) was down-regulated by 4-PeCDF (Binns *et al.*, 2009; Dimmer *et al.*, 2012).

In terms of classical enrichment analysis by testing over-representation of GO terms with Fisher's exact test, down-regulated genes were analyzed in view of potential 4-PeCDF-derived effects on biological processes in mouse livers. In appendant table 25, the Top 20 GO terms obtained by this analysis are listed.

Table 25: Mouse whole genome microarray analysis – TopGO analysis (4-PeCDF), down-regulated genes: Fisher's exact test. Top 20 GO terms identified by the classic algorithm for scoring GO terms for enrichment; descending order. Mouse livers, 4-PeCDF (250 µg/kg bw, three days). Top five GO terms indicated in bold.

4-PeCDF GO term	GO ID	sign./annot. genes	Raw p-value
regulation of RNA metabolic process	**GO:0051252**	**587/3478**	**5.0E-10**
regulation of gene expression	**GO:0010468**	**657/3952**	**5.4E-10**
regulation of RNA biosynthetic process	**GO:2001141**	**574/3403**	**8.9E-10**
regulation of transcription, DNA-templated	**GO:0006355**	**573/3402**	**1.2E-09**
RNA biosynthetic process	**GO:0032774**	**588/3507**	**1.4E-09**
transcription, DNA-templated	GO:0006351	587/3503	1.6E-09
reg. of nucleobase-containing compound metab. pr.	GO:0019219	656/4018	1.1E-08
reg. of nitrogen compound metabolic process	GO:0051171	659/4055	2.1E-08
reg. of cellular macromolecule biosynthetic process	GO:2000112	608/3707	2.2E-08
negative regulation of transcription, DNA-templated	GO:0045892	203/1052	4.1E-08
regulation of macromolecule biosynthetic process	GO:0010556	615/3789	8.2E-08
neg. reg. of nucleobase-containing compound metab. pr.	GO:0045934	224/1196	1.0E-07
regulation of biosynthetic process	GO:0009889	649/4036	1.4E-07
negative regulation of nitrogen compound metab. pr.	GO:0051172	225/1208	1.5E-07
negative regulation of RNA metabolic process	GO:0051253	204/1076	1.5E-07
regulation of cellular biosynthetic process	GO:0031326	642/3993	1.6E-07
negative regulation of gene expression	GO:0010629	216/1161	2.8E-07
neg. reg. of transcription from RNA polymerase II promoter	GO:0000122	133/650	3.5E-07
reg. of transcription from RNA polymerase II promoter	GO:0006357	260/1455	5.9E-07
positive regulation of gene expression	GO:0010628	249/1387	7.0E-07

As both 'regulation of gene expression' (GO:0010468) and 'regulation of RNA biosynthetic process' (GO:2001141) represent direct parent terms from 'regulation of transcription, DNA-templated' (GO:0006355), and GO:2001141 is a child term of both 'RNA biosynthetic process' (GO:0032771) and the most significantly occurring GO term 'regulation of RNA metabolic process' (GO:0051252), the top five GO terms appeared to be closely connected with each other (table 25). Besides these top five GO terms, all other GO terms within the Top 20 list for down-

regulation by 4-PeCDF were members of the same path in which they issued into, namely ‘regulation of transcription, DNA-templated’.

Regulation of transcription and, due to view on down-regulated genes in this regard, regulation of RNA biosynthesis might implicate both initiation, resulting from 4-PeCDF exposure, and termination of RNA synthesis, which might be feasible three days after single dose exposures according to feedback mechanims.

4.1.1.2.3. PCB 118 – impact on gene transcription in mouse livers

Numbers of genes affected by PCB 118 in mouse livers after three days of treatment with a single dose of 150000 µg/kg bw are illustrated and compared to TCDD-derived effects in figure 16. Raw data for treatment with TCDD (25 µg/kg bw) was received by courtesy of Christiane Lohr (Lohr, 2013).

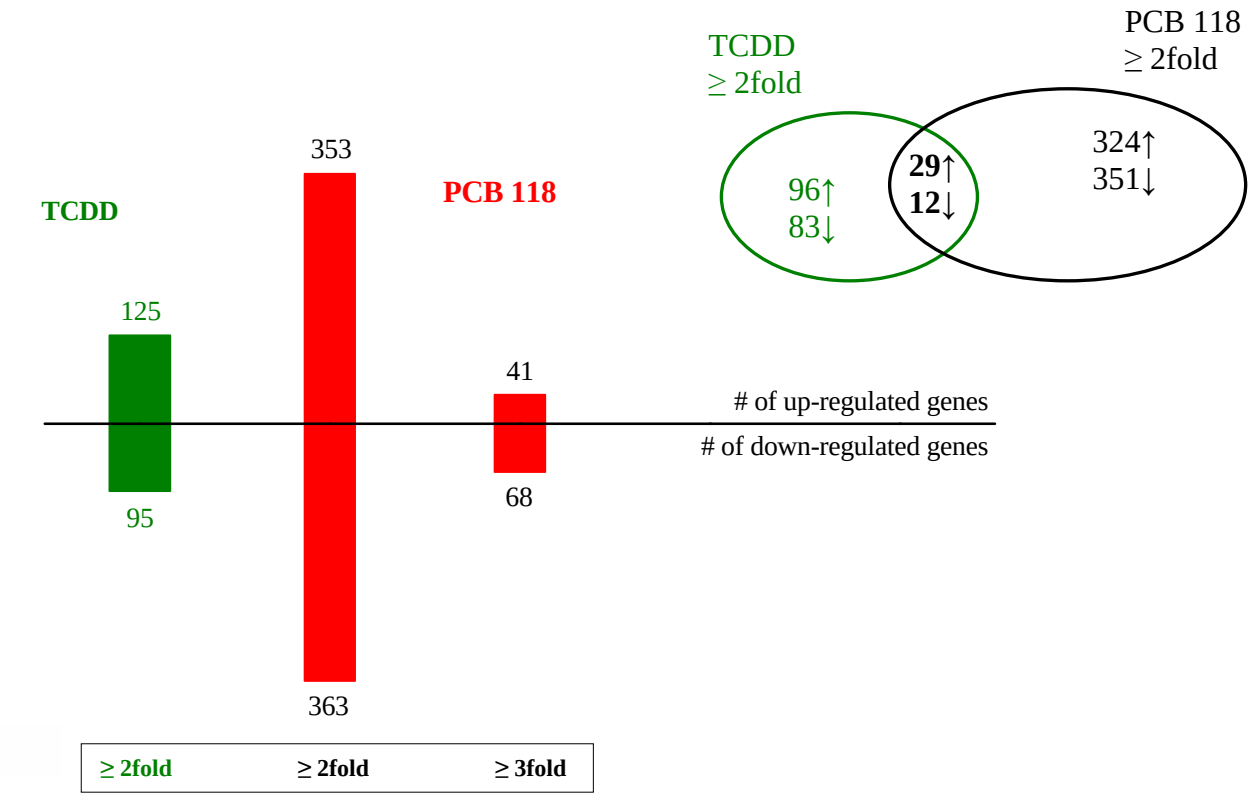

Figure 16: Mouse whole genome microarray analysis. Numbers of regulated genes in mouse livers by PCB 118 (150000 µg/kg bw, three days) compared to numbers of genes regulated by TCDD (25 µg/kg bw, three days), and numbers of genes regulated both by PCB 118 and TCDD (TCDD-raw data by courtesy of C. Lohr; Lohr, 2013). A ≥ 2^7, p-value < 0.05.

Numbers of genes, which were regulated by PCB 118-treatment in mouse livers with respect to set cutoff-values, accounted for 353 up- and 363 down-regulated genes regarding ≥ 2fold induction and repression, respectively. Raise of cutoff to ≥ 3fold regulation (lfc ≥ 1.58) reduced the quantity to 41 up- and 68 down-regulated genes. Although numbers of genes tended to appear in a comparable order of magnitude, the consensus with genes affected by TCDD emerged least substantial. A conserved group of 29 up- and 12 down-regulated genes remained.

Table 26 gives an overview of PCB 118-affected genes and presents the Top 20-list for up-regulation.

Table 26: Mouse whole genome microarray analysis. Top 20 up-regulated genes in mouse livers by PCB 118 (150000 µg/kg bw, three days). Cutoff values: A ≥ 2^7, lfc ≥ 1, p-value < 0.05.

PCB 118 lfc	Gene systematic name	Gene description	**Gene name**
7.799	NM_009992	cytochrome P450, family 1, subfamily a, polypeptide 1	*Cyp1a1*
3.998	NM_008181	glutathione S-transferase alpha 1 (Ya)	*Gsta1*
3.631/2.279	NM_001122660	predicted gene 10639	*Gm10639*
3.311	NM_009993	cytochrome P450 family 1 subfamily a polypeptide 2	*Cyp1a2*
2.697	NM_008182	glutathione S-transferase alpha 2 (Yc2)	*Gsta2*
1.102-2.621	NM_145603	carboxylesterase 2	*Ces2*
2.603	NM_198171	cDNA sequence BC015286	*BC015286*
2.310/1.775	NM_013541	glutathione S-transferase pi 1	*Gstp1*
2.282/1.990	NM_010358	glutathione S-transferase mu 1	*Gstm1*
2.276/1.398	NM_206537	cytochrome P450 family 2 subfamily c polypeptide 54	*Cyp2c54*
2.227	NM_023440	transmembrane protein 86B	*Tmem86b*
2.162	NM_010002	cytochrome P450 family 2 subfamily c polypeptide 38	*Cyp2c38*
2.101	NM_134144	cytochrome P450 family 2 subfamily c polypeptide 50	*Cyp2c50*
2.095	NM_025797	cytochrome b-5	*Cyb5*
2.027/1.751	NM_181796	glutathione S-transferase pi 2	*Gstp2*
2.018	NM_027872	solute carrier family 46 member 3	*Slc46a3*
1.997/1.450	NM_020559	aminolevulinic acid synthase 1	*Alas1*
1.990/1.112	NM_175224	methionyl aminopeptidase 1	*Metap1*
1.984	NM_025647	cytidine monophosphate (UMP-CMP) kinase 1	*Cmpk1*
1.956	NM_023429	OCIA domain containing 1	*Ociad1*

Values b/a from oligo b/oligo a; values a-n: value range of more than two (n) oligos.

Highest up-regulated target gene for treatment of mice with PCB 118 (150000 µg/kg bw; three days) in livers was *Cyp1a1* (NM_009992; lfc = 7.799). Within PCB 118's list of up-regulated genes, *Cyp1a2* (NM_009993; lfc = 3.311) ranked fourth (table 26). Effects on *Cyp1b1*-transcription were scarcely excluded from the Top 20-list by the lfc-cutoff of 1. Still, PCB 118 enhanced *Cyp1b1* (NM_009994) gene expression to an lfc of 0.935 corresponding to a 1.9-fold change.

Prominent targets affected by PCB 118 obviously were genes encoding glutathione *S*-transferases (GSTs). Besides the second-highest up-regulated gene by PCB 118, *Gsta1* (NM_008181; lfc = 3.998) was followed by another five *Gsts* within the Top 20-list including the predigted gene 10639 (*Gm10639*, NM_001122660; lfc (max) = 3.631), which encodes a protein (protein Gm10639) exhibiting GST activity (Dimmer *et al.*, 2012). In total, thirteen different *Gsts* were up-regulated by PCB 118 within chosen cutoff-levels.

Up-regulated genes involved in lipid metabolism and transport within the Top 20-list were *Tmem86b* (NM_023440; lfc = 2.227) and carboxylesterase 2 (*Ces2*, NM_145603; lfc (max) = 2.621). *Ces2* encodes an acylcarnitine hydrolase releasing fatty acids coupled to L-carnitine after entering the cell (Furihata *et al.*, 2003). Genes related to arachidonic acid metabolism affected by PCB 118 in mouse livers were *Cyp2c54* (NM_206537; lfc (max) = 2.276), *Cyp2c38* (NM_010002; lfc = 2.162), and *Cyp2c50* (NM_134144; lfc = 2.101) (Binns *et al.*, 2009; Dimmer *et al.*, 2012).
Further up-regulated genes linked to enhanced transport, metabolism, and transcription in cells within the Top 20-list were represented by cytochrome b-5 (*Cyb5*, NM_025797; lfc = 2.095), *Slc46a3* (NM_027872; lfc = 2.018), methionyl aminopeptidase 1 (*Metap1*, NM_175224; lfc (max) = 1.990), and cytidine monophosphate (UMP-CMP) kinase 1 (*Cmpk1*, NM_025647; lfc = 1.984) (Binns *et al.*, 2009; Dimmer *et al.*, 2012).

For examination of pathways affected by PCB 118, classical enrichment analysis by testing over-representation of GO terms using Fisher's exact test was performed. The Top 20-list of most significant GO terms regarding biological processes obtained by means of TopGO analysis for PCB 118 and it's up-regulating effects on gene expression is shown in table 27, whereas respective subgraph induced by the top five GO terms is presented in figure 17.

Table 27: Mouse whole genome microarray analysis – TopGO analysis (PCB 118): Fisher's exact test. Top 20 GO terms identified by the classic algorithm for scoring GO terms for enrichment regarding up-regulated genes; descending order. Mouse liver, PCB 118 (150000 µg/kg bw, three days). Top five GO terms indicated in bold.

PCB 118 GO term	GO ID	sign./annot. genes	Raw p-value
glutathione metabolic process	**GO:0006749**	**16/48**	**6.6E-14**
xenobiotic metabolic process	**GO:0006805**	**14/38**	**5.0E-13**
cellular response to xenobiotic stimulus	**GO:0071466**	**14/38**	**5.0E-13**
xenobiotic catabolic process	**GO:0042178**	**9/12**	**1.4E-12**
response to xenobiotic stimulus	**GO:0009410**	**14/41**	**1.7E-12**
peptide metabolic process	GO:0006518	16/84	7.6E-10
sulfur compound metabolic process	GO:0006790	21/189	4.7E-08
oxidation-reduction process	GO:0055114	67/1237	5.7E-08
cellular modified amino acid metabolic process	GO:0006575	18/164	5.1E-07
drug metabolic process	GO:0017144	7/25	3.1E-06
cellular ketone metabolic process	GO:0042180	49/948	1.2E-05
secondary metabolic process	GO:0019748	7/32	1.9E-05
carboxylic acid metabolic process	GO:0019752	47/918	2.4E-05
oxoacid metabolic process	GO:0043436	47/918	2.4E-05
response to oxidative stress	GO:0006979	19/244	3.8E-05
organic acid metabolic process	GO:0006082	47/937	3.9E-05
exogenous drug catabolic process	GO:0042738	4/10	9.6E-05
cellular amino acid metabolic process	GO:0006520	24/382	1.2E-04
drug catabolic process	GO:0042737	4/11	1.5E-04
hydrogen peroxide metabolic process	GO:0042743	7/44	1.6E-04

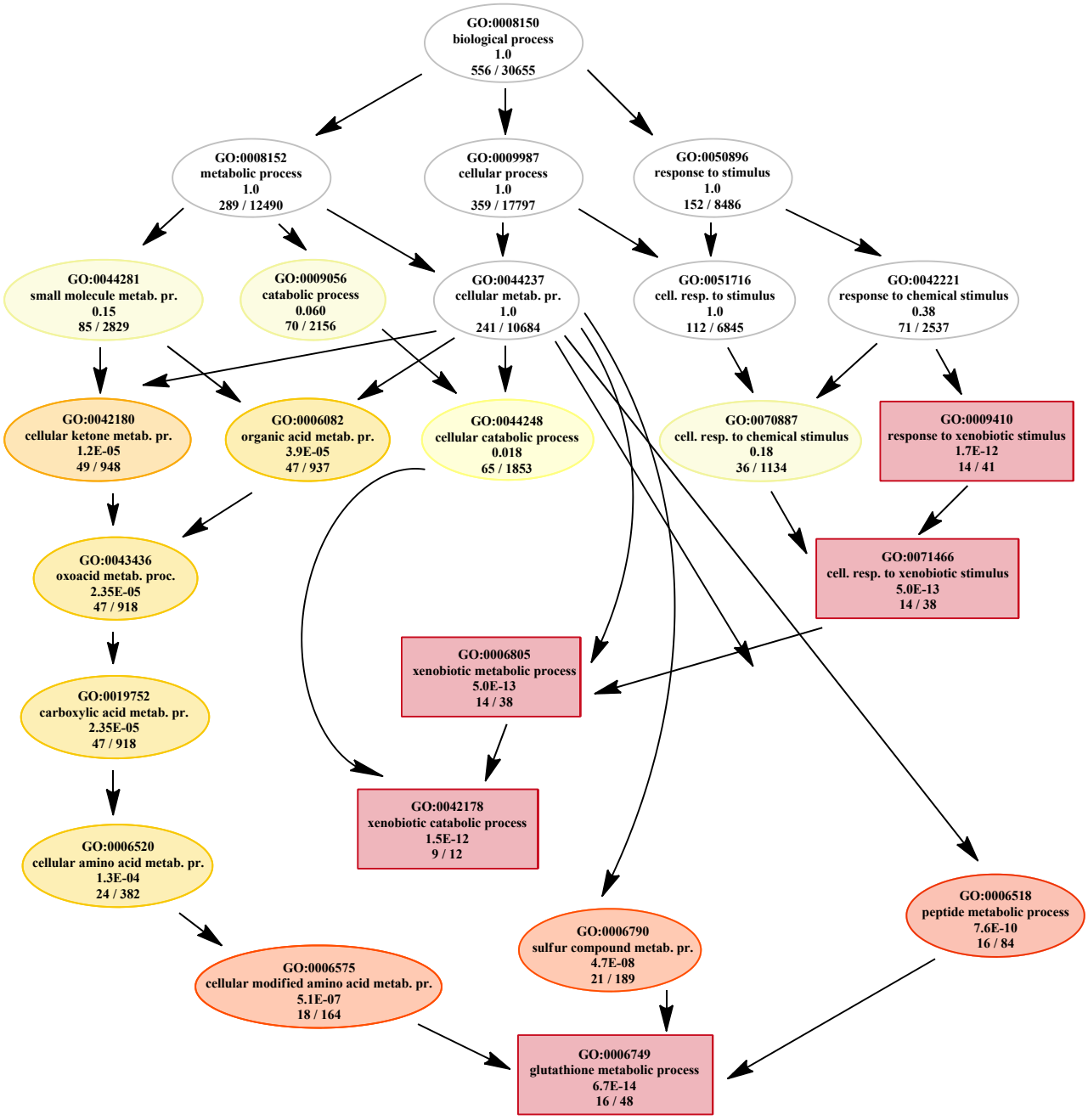

Figure 17: Mouse whole genome microarray analysis – TopGO analysis (PCB 118, 150000 µg/kg bw, three days; mouse liver): The GO subgraph plot induced by the top five GO terms identified by the classic algorithm for scoring GO terms for enrichment regarding up-regulated genes. Excerpt. Boxes indicate the five most significant GO terms. Box color represents relative significance ranging from dark red (most significant) to light yellow (least significant).

According to results from gene ontology analysis illustrated in figure 17 and table 27, impact of PCB 118 in view of up-regulated expression of genes was almost exclusively related to xenobiotic metabolism. Over several further significantly involved nodes within the gene tree (figure 17) like ‘cellular modified amino acid metabolic process’ (GO:0006575), ‘cellular ketone metabolic process’ (GO:0042180), and ‘carboxylic acid metabolic process’ (GO:0019752), members of the top five biological processes switched on by PCB 118 issued into the most significant term ‘glutathione metabolic process’ (GO:0006749), and into ‘xenobiotic catabolic process’ (GO:0042178). Induced targets behind these top five GO terms included seven different glutathione *S*-transferases (*Gsta1*, NM_008181; *Gstm1*, NM_010358; *Gstm2*, NM_008183; *Gstm3*, NM_010359; *Gstp1*, NM_013541; *Gstp2*, NM_181796; *Gstt3*, NM_133994), glutathione peroxidase 3 (*Gpx3*, NM_008161), and glutathione reductase (*Gsr*, NM_010344). The GO term ‘cellular response to xenobiotic stimulus’ (GO:0071466) further included *Cyp1a1*, *Ugt2b1*, and aldo-keto reductase family 1 member 13 (*Akr1c13*, NM_013778).

Affected probes according to ‘carboxylic acid metabolic process’ (GO:0019752) implicated several *Gsts*, as well as *Cyp1a2*, *Htatip2* (NM_016865), abhydrolase domain containing 5 (*Abhd5*, NM_026179), fatty acid desaturase 2 (*Fads2*, ENSMUST00000025567), and *Cyb5* (NM_025797), for instance.

Connected to initiated metabolic processes and induced monooxygenases, two biological processes related to redox-homeostasis were among PCB 118’s Top 20-list for up-regulation of gene transcription. Formally, ‘hydrogen peroxide metabolic process’ (GO:0042743) not directly represents a child term of ‘response to oxidative stress’ (GO:0006979), but both pathways are consequences due to an imbalanced redox state apparently occurring in the cells. Consequently, annotated probes are similar for both GO terms. Up-regulated genes impacted by PCB 118 within these two processes were peroxiredoxin 1, (*Prdx1*, NM_011034), *Prdx3* (NM_007452), glutathione peroxidase 3 (*Gpx3*, NM_008161), thioredoxin reductase 1 (*Txnrd1*, NM_001042523), *Cyp1a1*, and *Cyp1a2*, whereas the *Cyps* were annotated only for GO:0042743.

In table 28 (following page), the Top 20 of 363 down-regulated genes in response to PCB 118-treatment in mouse livers is depicted.

Table 28: Mouse whole genome microarray analysis. Top 20 down-regulated genes in mouse livers by PCB 118 (150000 µg/kg bw, three days). Cutoff values: A ≥ 2^7, lfc ≤ -1, p-value < 0.05.

PCB 118			
lfc	Gene systematic name	Gene description	**Gene name**
-3.057	NM_008341	insulin-like growth factor binding protein 1	*Igfbp1*
-2.607--1.415	NM_008103	glial cells missing homolog 1 (Drosophila)	*Gcm1*
-2.558	XM_001472203	similar to Ubtf protein (LOC100039072)	*Gm2033*
-2.449	XM_889044	Mus musculus predicted gene EG624491	*Gm6508*
-2.270	BC052524	RIKEN cDNA 4833411C07 gene	*4833411C07Rik*
-2.255	NM_001081212	insulin receptor substrate 2	*Irs2*
-2.184	NR_001463	inactive X specific transcripts	*Xist*
-2.149	AK017575	8 days embryo whole body cDNA RIKEN full-length enriched library clone:5730419F03	*5730419F03Rik*
-2.119	NM_009744	B-cell leukemia/lymphoma 6	*Bcl6*
-2.114--1.339	NM_009946	complexin 2	*Cplx2*
-2.105	ENSMUST00000115107	cDNA clone MNCb-1768cDNA sequence AB041803	*ENSMUST00000115107*
-2.096	XM_001472970	similar to R10D12.10 (LOC100039488)	*Gm2264*
-2.070	XM_001474429	similar to cyclic nucleotide gated channel beta 1	*Gm2690*
-2.040	NM_011817	growth arrest and DNA-damage-inducible 45 gamma	*Gadd45g*
-2.033	AK017236	adult male pituitary gland cDNA RIKEN full-length enriched library clone:5330406M23	*5330406M23Rik*
-1.955	A_55_P2050988	Unknown	*A_55_P2050988*
-1.943	AK036325	16 days neonate cerebellum cDNA RIKEN full-length enriched library clone:9630056N24	*Syn3*
-1.912	NM_203492	MAS-related GPR member G	*Mrgprg*
-1.906	NM_153522	sodium channel voltage-gated type III beta	*Scn3b*
-1.904	NM_016659	killer cell lectin-like receptor subfamily A member 1	*Klra1*

Values b/a from oligo b/oligo a; values a-n: value range of more than two (n) oligos.

Of 363 genes in total, the most efficiently down-regulated gene by PCB 118 (table 28) named insulin-like growth factor binding protein 1 (*Igfbp1*, NM_008341; lfc = -3.057) represents an inhibited gene involved in insulin receptor signaling pathways, which was also proposed to be implicated in regulation of cell growth and tissue regeneration (Binns *et al.*, 2009; Dimmer *et al.*, 2012). Further down-regulated genes related to insulin receptor signaling were insulin receptor substrate 2 (*Irs2*, NM_001081212; lfc = -2.255), and insulin-like growth factor 1 (*Igf1*, NM_184052; lfc = -1.502; not part of the Top 20-list).

Inhibited expression of the gene B-cell leukemia/lymphoma 6 (*Bcl6*, NM_009744; lfc = -2.119) hinted towards repressive properties with regard to type 2 immune response and B cell differentiation (Binns *et al.*, 2009; Dimmer *et al.*, 2012). Further genes implicated in immune response within PCB 118's Top 20-list of down-regulated genes were growth arrest and DNA-damage inducible 45 gamma (*Gadd45g*, NM_011817; lfc = -2.040), and killer cell lectin-like receptor subfamily A member 1 (*Klra1*, NM_016659; lfc = -1.904). *Gadd45g*, an intermediate upstream of p38 MAPK, has shown to be able to induce STAT4 serine phosphorylation and was thus discussed to be involved in correlated IFN-γ production and Th1-differentiation (Morinobu *et al.*, 2002). *Klra1* encodes a MHC class I receptor protein named T cell surface glycoprotein YE1/48 (Binns *et al.*, 2009; Dimmer *et al.*, 2012).

The Top 20-list of down-regulated genes in mouse livers affected by PCB 118 contained several gene products or solely predicted genes with insufficient experimental evidence at transcription level, for which information is rare and no GO terms are annotated to date. An appropriate interpretation was thus even more intricate.

Classical enrichment analysis by testing over-representation of GO terms using Fisher's exact test was applied. For down-regulated probes, the Top 20-list of GO terms presented in table 29 (following page), was obtained.

Table 29: Mouse whole genome microarray analysis – TopGO analysis (PCB 118): Fisher's exact test. Top 20 GO terms identified by the classic algorithm for scoring GO terms for enrichment regarding down-regulated genes; descending order. Mouse liver, PCB 118 (150000 µg/kg bw, three days). Top five GO terms indicated in bold.

PCB 118 GO term	GO ID	sign./annot. genes	Raw p-value
positive regulation of synaptic plasticity	**GO:0031915**	**4/10**	**8.0E-05**
astrocyte fate commitment	**GO:0060018**	**3/6**	**3.2E-04**
carbohydrate mediated signaling	**GO:0009756**	**2/2**	**6.6E-04**
hexose mediated signaling	**GO:0009757**	**2/2**	**6.6E-04**
sugar mediated signaling pathway	**GO:0010182**	**2/2**	**6.6E-04**
glucose mediated signaling pathway	GO:0010255	2/2	6.6E-04
negative regulation of oxidative phosphorylation	GO:0090324	2/2	6.6E-04
glial cell differentiation	GO:0010001	12/160	9.0E-04
endothelial cell proliferation	GO:0001935	8/88	1.9E-03
regulation of oxidative phosphorylation	GO:0002082	2/3	1.9E-03
astrocyte differentiation	GO:0048708	6/54	2.5E-03
cell diff. involved in embryonic placenta development	GO:0060706	4/23	2.6E-03
neg. reg. of blood vessel endothelial cell migration	GO:0043537	3/12	3.1E-03
branching involved in labyrinthine layer morphogenesis	GO:0060670	3/12	3.1E-03
regulation of endothelial cell proliferation	GO:0001936	7/77	3.6E-03
negative regulation of hair follicle development	GO:0051799	2/4	3.8E-03
gliogenesis	GO:0042063	12/192	4.2E-03
blood vessel remodeling	GO:0001974	5/43	4.7E-03
cell fate commitment	GO:0045165	15/272	4.7E-03
endocrine hormone secretion	GO:0060986	4/28	5.4E-03

Overall, the over-representation of GO terms as well as correspondent statistical significances regarding appearance of clustered GO terms was limited for down-regulating effects of PCB 118 on gene expression (table 29). Three principal pathways induced by the top five GO terms included 'positive regulation of synaptic plasticity' (GO:0031915), 'astrocyte fate commitment' (GO:0060018), and 'hexose mediated signaling' (GO: 0009757). The direct parent term from the latter, 'sugar mediated signaling pathway' (GO:0010182), and its parent term 'carbohydrate

mediated signaling' (GO:0009756), were both among the top five GO terms for down-regulating effects of PCB 118. Annotated and significantly occurring probes behind this hexose mediated pathway both encoded MLX-interacting protein-like (*Mlxipl*, NM_021455). *Mlxipl* is annotated to several further processes like 'glucose homeostasis' (GO:0042593), 'positive regulation of glycolytic process' (GO:0045821), 'fatty acid homeostasis' (GO:0055089), 'positive regulation of fatty acid biosynthetic process' (GO:0045723). Encoded carbohydrate-responsive element-binding protein (ChREBP) is a transcriptional repressor, which was reported to reduce *de novo* lipogenesis as well as glycolysis *in vivo*. In a ChREBP$^{-/-}$ mouse model, ChREBP was shown to be required for basal and carbohydrate-induced expression of liver enzymes essential for these processes, such as liver-type pyruvate kinase, ATP citrate lyase, acetyl-CoA carboxylase 1, or fatty acid synthase (Binns *et al.*, 2009; Dimmer *et al.*, 2012; Iizuka *et al.*, 2004).

In addition to *Mlxipl*, regarding GO terms 'glucose homeostasis' (GO:0042593), and 'positive regulation of glycolytic process' (GO:0045821), five genes among 99, and one among 17 annotated probes, respectively, were down-regulated by PCB 118. These included glucose-6-phosphatase (*G6pc*, NM_008061), transcription factor 7-like 2 (*Tcf7l2*, NM_001142920), adrenergic receptor, alpha 1b (*Adra1b*, NM_007416), and insulin-like growth factor 1 (*Igf1*, NM_184052). None of the further aforementioned genes related to carbohydrate metalism were affected by PCB 118.

Significantly affected regarding 'positive regulation of synaptic plasticity' (GO:0031915) were four out of ten probes, which represented two genes: complexin 2 (*Cplx2*, NM_009946), and the predicted gene EG628080 (*Gm6837*, XM_900336; '*This record was removed as a result of standard genome annotation processing*' (NCBI)). Besides its involvement in mast cell degranulation, *Cplx2* was indicated to locally act at presynaptic sites by mediation of neurogenic differentiation 2 (NeuroD2) to suppress presynaptic differentiation (Yang *et al.*, 2009).

'Astrocyte fate commitment' (GO:0060018) was also observed in the Top 20-list containing potentially inhibited biological processes by PCB 118. Three out of six annotated probes were affected, whereas all of the three were specific for one gene: glial cells missing homolog 1 (*Gcm1*, NM_008103). The mammalian homolog of *Drosophila gcm*, mouse *Gcm1*, was reported to exhibit potential to induce gliogenesis, but might function in the generation of a minor subpopulation of glial cells (Iwasaki *et al.*, 2003). In this regard, as also concerning related processes 'glial cell differentiation' (GO:0010001), astrocyte differentiation (GO:0048708), and 'gliogenesis' (GO:0042063), for interpretation of these results and accordant biological processes, tissue

specifities would need to be considered and discussed to assess relevance of them and their probable role for a PCB 118-exposed organism, as not least liver was investigated for the work in hand.

Four GO terms involved in blood vessel-related processes and endothelial cells were members of the Top 20-list for PCB 118 and its inhibitory effects on gene expression. With respect to 'endothelial cell proliferation' (GO:0001935) and its direct child term 'regulation of endothelial cell proliferation' (GO:0001936), around ten per cent of probes annotated were down-regulated by PCB 118, including *Jun* (NM_010591), fibroblast growth factor 2 (*Fgf2*, NM_008006), and vasohibin 1 (*Vash1*, NM_177354) for both GO terms. In related GO term 'negative regulation of blood vessel endothelial cell migration' (GO:0043537), down-regulated genes were also represented by *Fgf2* and *Vash1*. The protein Vasohibin 1 represents an angiogenesis inhibitor, which selectively inhibits migration, proliferation, and network formation by endothelial cells. Besides its ability to inhibit macrophage infiltration, it was proposed to inhibit tumor growth and tumor angiogenesis acting in an autocrine manner (Ashburner *et al.*, 2000; Binns *et al.*, 2009; Dimmer *et al.*, 2012).

With a comparably low significance (5.4E-03), a GO term named 'endocrine hormone secretion' (GO:0060986) occurred within the Top 20 of biological processes probably suppressed by PCB 118 in mouse livers. Four out of 28 probes were negatively affected by the compound in this regard: inhibin beta-A (*Inhba*, NM_008380), maternally expressed 3 (*Meg3*, NR_027652), urocortin 2 (*Ucn2*, NM_145077), and leukemia inhibitory factor (*Lif*, NM_008501). These genes and their gene products, respectively, possess diverging functions from involment in erythroid differentiation or insulin secretion (*Inhba*), over suppression of food intake and delayed gastric emptying (*Ucn2*), to stimulation of acute-phase protein synthesis in hepatocytes (*Lif*) (Ashburner *et al.*, 2000; Binns *et al.*, 2009; Dimmer *et al.*, 2012). The low number of genes and the limited correlation among themselves related to endocrine function exacerbates the interpretation of their occurrence as part of a suppressed biological process responding to PCB 118-treatment.

4.1.1.2.4. PCB 126 – impact on gene transcription in mouse livers

Female C57BL/6 mice were treated with single doses of PCB 126 (250 µg/kg bw), or TCDD (25 µg/kg bw) for three days each. Using mRNA isolated from livers, whole genome microarray experiments were performed. The numbers of genes affected by PCB 126 and/or TCDD treatments are summarized in figure 18. Raw data from experiments with TCDD was received by courtesy of Christiane Lohr (Lohr, 2013).

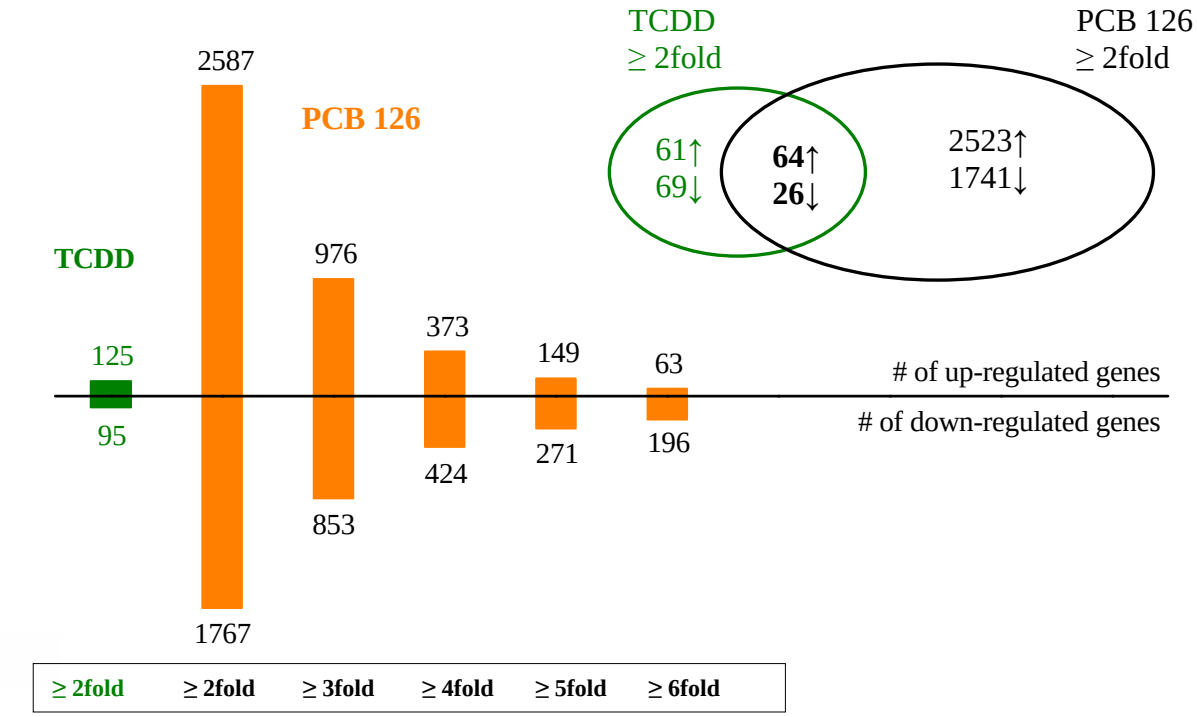

Figure 18: Mouse whole genome microarray analysis. Numbers of regulated genes in mouse livers by PCB 126 (250 µg/kg bw, three days) compared to numbers of genes regulated by TCDD (25 µg/kg bw, three days), and numbers of genes regulated both by PCB 126 and TCDD (TCDD-raw data by courtesy of C. Lohr; Lohr, 2013). A ≥ 2^7, p-value < 0.05.

Treatment with PCB 126 (250 µg/kg bw) exerted a highly inductive effect on gene expression in mouse livers (figure 18). In numbers, transcription of 2587 genes was up-, and transcription of 1767 genes was down-regulated by PCB 126 according to set cutoff-levels (A ≥ 2^7, $|lfc| \geq 1$ (≥ 2fold), p-value < 0.05). Raise of cutoff-values reduced numbers of affected genes from 976/853 (up/down-regulated genes) for ≥ 3fold induction, over 373/424 (≥ 4fold), and 149/271 (≥ 5fold) to 63/196 (≥ 6fold). By contrast, TCDD led to an increased transcription of genes accounting for 125 up-, and 95 down. About half of the genes induced by TCDD were as well up-regulated by PCB 126, whereas overlap with respect to down-regulated genes turned out to be even smaller. From 95 genes repressed by TCDD, 26 were also down-regulated by PCB 126.

In table 30, the Top 20-list of genes, which were up-regulated by PCB 126 in mouse livers, is displayed.

Table 30: Mouse whole genome microarray analysis. Top 20 up-regulated genes in mouse livers by PCB 126 (250 µg/kg bw, three days). Cutoff values: A ≥ 2^7, lfc ≥ 1, p-value < 0.05.

PCB 126 lfc	Gene systematic name	Gene description	Gene name
6.292	NM_009992	cytochrome P450 family 1 subfamily a polypeptide 1	*Cyp1a1*
3.873	A_55_P2097048	Unknown	*A_55_P2097048*
3.417	XM_001477211	similar to Major urinary protein 1 (LOC100048884)	*CU104690.1*
3.250	NM_198171	cDNA sequence BC015286	*BC015286*
3.195	NM_008618	malate dehydrogenase 1 NAD (soluble)	*Mdh1*
3.184	NM_172054	thioredoxin domain containing 9	*Txndc9*
3.172	NM_027872	solute carrier family 46 member 3	*Slc46a3*
3.163	XM_985615	similar to NADH dehydrogenase (ubiquinone) 1 subcomplex unknown 2	*LOC675851*
3.159	NM_025535	SAR1 gene homolog B (S. cerevisiae)	*Sar1b*
3.134/2.086	NM_011034	peroxiredoxin 1	*Prdx1*
3.129	NM_007451	solute carrier family 25 (mitochondrial carrier adenine nucleotide translocator) member 5	*Slc25a5*
3.123	NM_145925	pituitary tumor-transforming 1 interacting protein	*Pttg1ip*
1.845-3.097	NM_172588	serine incorporator 5	*Serinc5*
3.095	NM_008181	glutathione S-transferase alpha 1 (Ya)	*Gsta1*
3.085	NM_031170	keratin 8	*Krt8*
3.049/2.144	NM_001122660	predicted gene 10639	*Gm10639*
3.016/1.175	NM_009725	ATP synthase H+ transporting mitochondrial F0 complex	*Atp5f1*
2.989	NM_001101534	predicted gene 5584	*Gm5584*
2.972	NM_029814	chromatin modifying protein 5	*Chmp5*
2.971	NM_025615	RIKEN cDNA 2810004N23 gene	*2810004N23Rik*

Values b/a from oligo b/oligo a; values a-n: value range of more than two (n) oligos.

The Top 20-list of genes up-regulated by PCB 126 (table 30) was headed by *Cyp1a1* (NM_009992; lfc = 6.292). Although not among the Top 20 of induced genes, *Cyp1a2* and *Cyp1b1* were up-regulated by PCB 126 in mouse livers. With regards to extent of induction, *Cyp1b1* (NM_009994; lfc = 2.557) was very closely followed by *Cyp1a2* (NM_009993; lfc = 2.555).

Further affected genes and predicted genes associated with xenobiotic metabolism were *Gsta1* (NM_008181; lfc = 3.095), predicted gene 10639 (*Gm110639*, NM_0011226600; lfc (max) = 3.049), and predicted gene 5584 (*Gm5584*, NM_001101534; lfc = 2.989). Corresponding encoded predicted proteins were proposed to bear GST (Protein GM10639), and SULT (predicted gene 5584, MCG8002; *Sult2a4*) activity, respectively (Binns *et al.*, 2009; Dimmer *et al.*, 2012).

Indications of altered lipid metabolism and biosynthesis in livers of PCB 126-treated mice gave reduced transcription of cDNA sequence BC015286 (*BC015286*; NM_198171; lfc = 3.250), and serine incorporator 5 (*Serinc5*, NM_172588; lfc = 3.097). The protein product of *BC015286* (MCG142671, isoform CRA_B; *Ces2b*) clusters with an acylcarnitine hydrolase. Acylcarnitine hydrolases release fatty acids coupled to L-carnitine after entering the cell (Binns *et al.*, 2009; Dimmer *et al.*, 2012; Furihata *et al.*, 2003).

Another gene, of which transcription was induced by PCB 126, was malate dehydrogenase 1 (*Mdh1*, NM_008618; lfc = 3.195). The protein MDH1 is involved in the tricarboxylic acid cycle, and was further discussed in the context of hepatotoxicity and liver necrosis (Clifford and Rees, 1967; Zieve *et al.*, 1985). In this regard, MDH1 was proposed to serve as biomarker for hepatocellular carcinomas and the severity of acute hepatitis (Amacher *et al.*, 2005; Kawai and Hosaki, 1990).

As its encoded protein plays major role within electron transport complexes of the respiratory chain, the induction of ATP synthase H+ transporting mitochondrial F0 complex (*Atp5f1*, NM_009725; lfc = 3.016) gave indication of a high energy turnover in hepatocytes from PCB 126-treated mice (Dimmer *et al.*, 2012). Further hints towards trancriptionally and metabolically active conditions in mouse livers were given by inhibited transcription of *Slc46a3* (NM_027872; lfc = 3.172; transmembrane transport mechanisms including transport of nucleotides, peptides, steroids, carbohydrates, and hydrogen peroxide), SAR1 gene homolog B (*Sar1b*, NM_025535; lfc = 3.159; intracellular transport), and chromatin modifying protein 5 (*Chmp5*, NM_029814; lfc = 2.972; protein transport/endosome to lysosome transport) (Binns *et al.*, 2009; Dimmer *et al.*, 2012).

Thioredoxin domain containing 9 (*Txndc9*; NM_172954; lfc = 3.184), and peroxiredoxin 1 (*Prdx1*; NM_011034; lfc (max) = 3.134) are genes related to oxidative stress and are involved in redox regulation of cells. A number of further members belonging to the thioredoxin/thioredoxin reductase redox system were induced by PCB 126: *Txndc17* (NM_026559; lfc = 1.985), Thioredoxin reductase 3 (*Txnrd3*, NM_153162; lfc = 1.821), *Txnrd1* (NM_001042523; lfc = 1.747), *Txn1* (NM_011660; lfc = 1.55), Thioredoxin-interacting protein (*Txnip*, NM_001009935; lfc = 1.521), *Txndc15* (NM_175150; lfc = 1.459), and *Txndc12* (NM_025334; lfc = 1.156). Gene transcription of members belonging to the thioredoxin/thioredoxin reductase redox system was shown to be enhanced in a number of human cancers (Lincoln *et al.*, 2003; Yanagawa *et al.*, 1999). TXN and PRDX 1 were also found to be implicated in processes inhibiting apoptosis (Baker *et al.*, 1997; Egler *et al.*, 2005; Kim *et al.*, 2000).

Beyond, PCB 126 induced further genes correlated with apoptosis: *Slc25a5* (NM_007451; lfc = 3.129), and keratin 8 (*Krt8*, NM_031170; lfc = 3.085) were members of the Top 20-list. The protein Keratin-8 (K8) potentially moderates TNF-α-induced, c-Jun N-terminal kinase (JNK; member of the MAPK family) intracellular signaling as well as NF-κB activation and hence the apoptotic effects of TNF-α. These effects were discussed in association with K8's feasible functions regarding liver regeneration, hepatotoxin sensitivity, and its diagnostic, persistent expression in several carcinomas (Caulin *et al.*, 2000).

Within current mouse whole genome microarray experiment, neither TNF-α, nor NF-κB gene products were regulated by any of the tested DL-congeners, whereas transcription of genes encoding the proteins MAPK 1 and MAPK 11 was significantly affected by PCB 126: *Mapk1* (NM_011949; lfc (max) = 2.027) was up-regulated, while *Mapk11* (NM_011161; lfc = -1.833) was down-regulated in response to treatment with PCB 126 in mouse livers.

Pituitary tumor-transforming 1 interacting protein (*Pttg1ip*, NM_145925; lfc = 3.123) was up-regulated by PCB 126. Encoded protein specifically interacts with the oncogene pituitary tumor-transforming gene 1 (PTTG1) *in vitro* and *in vivo*, and facilitates PTTG1 nuclear translocation, subsequently enhancing its force as transcription factor (Chien and Pei, 2000; Li *et al.*, 2013; Pei and Melmed, 1997). *Pttg1* was not affected by any tested congener throughout the entire mouse microarray experiment.

TopGO analysis provided the list of 20 most significant GO terms displayed in table 31, which were over-representated within the group of differentially expressed genes. This classical enrichment analysis was performed using Fisher's exact test. The TopGO subgraph is shown in figure 19.

Table 31: Mouse whole genome microarray analysis – TopGO analysis (PCB 126): Fisher's exact test. Top 20 GO terms identified by the classic algorithm for scoring GO terms for enrichment regarding up-regulated genes; descending order. Mouse liver, PCB 126 (250 µg/kg bw, three days). Top five GO terms indicated in bold.

PCB 126			
GO ID	GO term	sign./annot. genes	Raw p-value
oxidation-reduction process	**GO:0055114**	**262/1237**	**7.6E-21**
translation	**GO:0006412**	**165/658**	**8.1E-21**
cellular catabolic process	**GO:0044248**	**341/1853**	**1.2E-16**
translational elongation	**GO:0006414**	**74/225**	**1.3E-16**
cellular ketone metabolic process	**GO:0042180**	**201/948**	**2.7E-16**
carboxylic acid metabolic process	GO:0019752	193/918	2.6E-15
oxoacid metabolic process	GO:0043436	193/918	2.6E-15
organic acid metabolic process	GO:0006082	195/937	5.3E-15
cofactor metabolic process	GO:0051186	85/311	1.4E-13
catabolic process	GO:0009056	367/2156	8.6E-13
coenzyme metabolic process	GO:0006732	71/250	1.9E-12
small molecule metabolic process	GO:0044281	459/2829	2.1E-12
cellular metabolic process	GO:0044237	1469/10684	1.2E-11
metabolic process	GO:0008152	1686/12490	5.0E-11
glutathione metabolic process	GO:0006749	24/48	1.3E-10
peptide metabolic process	GO:0006518	33/84	1.7E-10
intracellular transport	GO:0046907	201/1088	2.0E-10
sulfur compound metabolic process	GO:0006790	55/189	2.0E-10
establishment of protein localization	GO:0045184	247/1406	2.9E-10
protein transport	GO:0015031	240/1358	2.9E-10

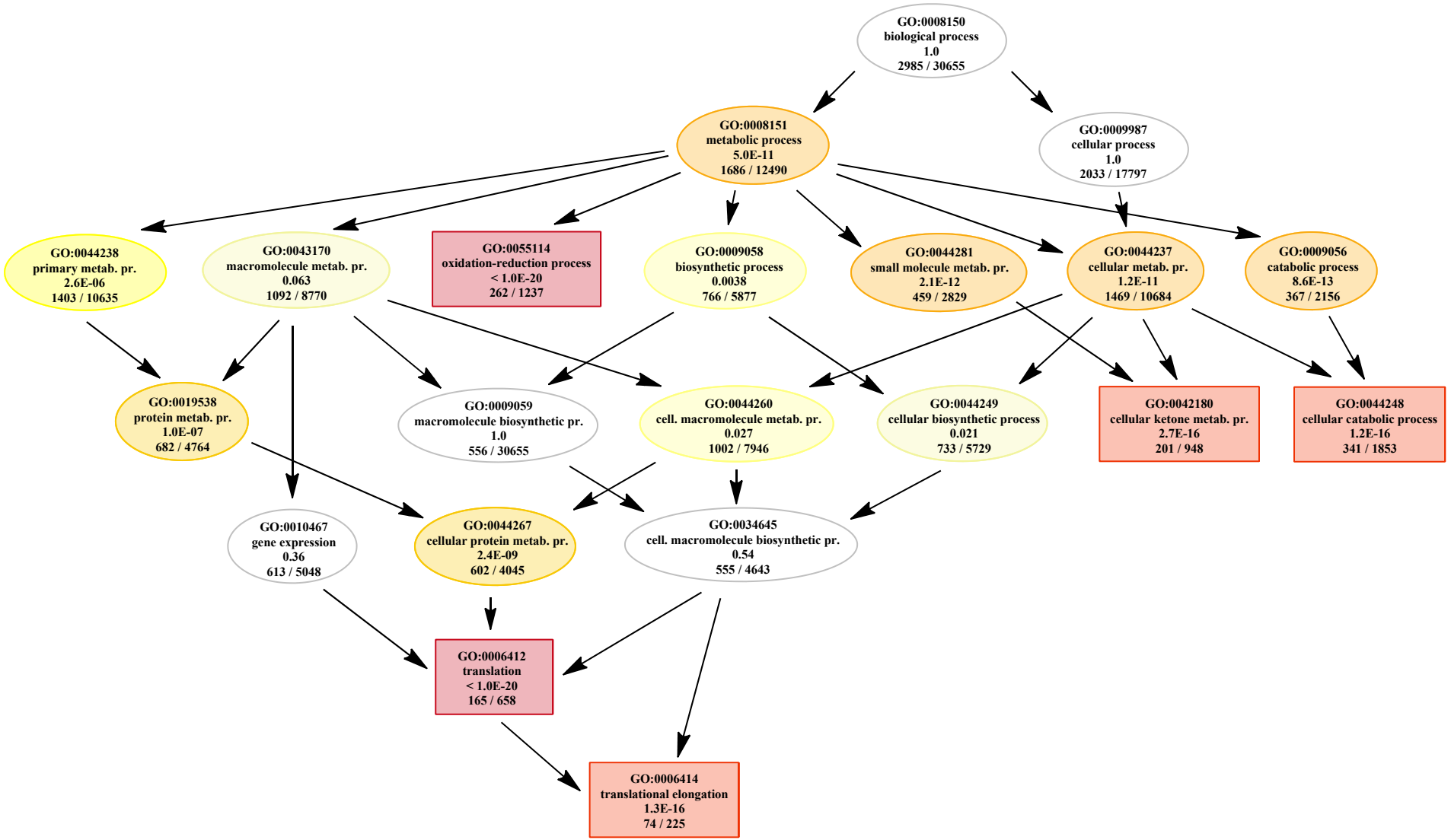

Figure 19: Mouse whole genome microarray analysis – TopGO analysis (PCB 126, 250 µg/kg bw, three days; mouse liver): The GO subgraph plot induced by the top five GO terms identified by the classic algorithm for scoring GO terms for enrichment regarding up-regulated genes. Boxes indicate the five most significant GO terms. Box color represents relative significance ranging from dark red (most significant) to light yellow (least significant).

Pathway analyis respecting up-regulated genes in mouse livers in response to *in vivo* treatment with PCB 126 predominantly was related with metabolic, in particular catabolic (GO:0044248), processes most significantly including ‘oxidation-reduction processes’ (GO:0055114), and translation (‘translational elongation’, GO:0006414) corresponding to the inductive effect of the congener (table 31, figure 19). Out of 20 GO-terms, 13 were associated with metabolism and included GO terms correlated with lipid metabolism like ‘carboxylic acid metabolic process’ (GO:0019752), or ‘peptide metabolic process’ (GO:0006518). Besides, highly processive hepatocytes were as well indicated by up-regulated genes annotated to ‘intracellular transport’ (GO:0046907), ‘establishment of protein localization’ (GO:0045184), and ‘protein transport’ (GO:0015031).

Half of the probes (24 out of 48) annotated to ‘glutathione metabolic process’ (GO:0006749) were up-regulated by PCB 126 in mouse livers. Among them, ten encoded GSTs plus several genes involved in GSH-regeneration or protection of cells from oxidative damage, such as superoxide dismutase 2 (*Sod2*, NM_013671), glutathione peroxidases (*Gpx1*, NM_008160; *Gpx3*, NM_008161; *Gpx4*, NM_001037741), and glutathione reductase (*Gsr*, NM_010344).
Altogether, the subgraph induced by the top five GO terms regarding up-regulated genes responding to PCB 126-treatment showed fairly clustering genes uncovering the congener’s impact on gene transcription and metabolism.

PCB 126 inhibited transcription of 1767 genes (≥ 2fold) in mouse livers subsequent to three days of single dose exposure (250 µg/kg bw). The Top 20 of down-regulated genes is displayed in table 32.

Table 32: Mouse whole genome microarray analysis. Top 20 down-regulated genes in mouse livers by PCB 126 (250 µg/kg bw, three days). Cutoff values: A ≥ 2^7, lfc ≤ -1, p-value < 0.05.

PCB 126 lfc	Gene systematic name	Gene description	Gene name
-4.502/ -4.480	BC031891/ NR_002861	serine (or cysteine) peptidase inhibitor clade A member 4 pseudogene 1	*Serpina4-ps1*
-4.207	NR_004413	U1b6 small nuclear RNA	*Rnu1b6*
-4.029	NM_011302	retinoschisis (X-linked juvenile) 1 (human)	*Rs1*
-3.951	NM_013877	calcium binding protein 5	*Cabp5*
-3.949	NM_199022	SHC (Src homology 2 domain containing) family member 4	*Shc4*
-3.941	NM_197945	ProSAPiP1 protein	*RP23-100C5.8*
-3.940	NM_011371	ST6 (alpha-N-acetyl-neuraminyl-2,3-beta-galactosyl-1,3)-N-acetylgalactosaminide alpha-2,6-sialyltransferase 1	*St6galnac1*
-3.936	XM_001478202	hypothetical protein LOC100047464	*LOC100047464*
-3.925	NM_181319	T-box 22 (Tbx22) transcript variant 2	*Tbx22*
-3.900	NM_001169153	CD300 antigen like family member F	*Cd300lf*
-3.892	NM_016659	killer cell lectin-like receptor subfamily A member 1	*Klra1*
-3.892	XM_981891	predicted gene EG665802 transcript variant 6	*Gm7792*
-3.889	NM_001033960	RAB GTPase activating protein 1	*Rabgap1*
-3.889	AK036325	16 days neonate cerebellum cDNA *RIKEN full-length enriched library clone:9630056N24*	*Syn3*
-3.880	NM_153522	sodium channel voltage-gated type III beta	*Scn3b*
-3.826	NM_194336	macrophage activation 2 like	*Mpa2l*
-3.823	NM_011562	teratocarcinoma-derived growth factor 1	*Tdgf1*
-3.822	NM_010418	hect (homologous to the E6-AP (UBE3A) carboxyl terminus) domain and RCC1 (CHC1)-like domain (RLD) 2	*Herc2*
-3.807- -2.754	NM_008103	glial cells missing homolog 1 (Drosophila)	*Gcm1*

Value range of more than two (n) oligos: values a-n.

Most effectively down-regulated *Serpina4-ps1* (BC031891/NR_002861; lfc (max) = -4.502) by PCB 126 represented one of six genes within the Top 20-list (table 32) implicated in immune function (Binns *et al.*, 2009; Dimmer *et al.*, 2012): *Tbx22* (NM_181319; lfc = -3.925; encodes a probable transcriptional regulator involved in developmental processes; major determinant crucial to palatogenesis), *Cd300lf* (NM_001169153; lfc = -3.900; encoded protein participates in osteoclast differentiation), *Klra1* (NM_016659; lfc = -3.892; encodes T-cell surface glycoprotein YE1/48, a MHC class I receptor), and *Tdgf1* (NM_011562; lfc = -3.823). *Serpina4-ps1* and *Tdgf1* are also involved in apoptotic processes (Binns *et al.*, 2009; Bustos *et al.*, 2009; Dimmer *et al.*, 2012).

Notably and not only regarding these immune-related genes, PCB 126's list of down-regulated genes resembled the Top 20-list for inhibitory effects on transcription for 4-PeCDF-treatment with respect to several genes. Two more examples represented *St6galnac1* (NM_011371; lfc = -3.940; encodes a glycosyltransferase, which plays a role in glycosylation of proteins), and *Rabgap1*, NM_001033960; lfc = -3.889; encodes a protein possessing Rab GTPase activator activity; proposed involvement in cell cycle regulation) (Binns *et al.*, 2009; Dimmer *et al.*, 2012).

Further down-regulated genes within PCB 126's Top 20-list were involved in forming cell junctions (ProSAPiP1 protein, *RP23-100C5.8*, NM_197945; lfc = -3.941), or DNA repair (hect (homologous to the E6-AP (UBE3A) carboxyl terminus) domain and RCC1 (CHC1)-like domain (RLD) 2, *Herc2*, NM_010418; lfc = -3.822) (Binns *et al.*, 2009; Dimmer *et al.*, 2012).

Table 33 presents results regarding TopGO analysis with respect to down-regulated genes in mouse livers subsequent to PCB 126-treatment.

Table 33: Mouse whole genome microarray analysis – TopGO analysis (PCB 126): Fisher's exact test. Top 20 GO terms identified by the classic algorithm for scoring GO terms for enrichment regarding down-regulated genes; descending order. Mouse liver, PCB 126 (250 µg/kg bw, three days). Top five GO terms indicated in bold.

PCB 126 GO term	GO ID	sign./annot. genes	Raw p-value
positive regulation of synaptic plasticity	**GO:0031915**	**6/10**	**3.1E-05**
cell fate commitment	**GO:0045165**	**40/272**	**4.5E-05**
diencephalon development	**GO:0021536**	**15/76**	**1.6E-04**
endocrine system development	**GO:0035270**	**21/132**	**3.9E-04**
cytotoxic T cell differentiation	**GO:0045065**	**2/3**	**4.4E-04**
ethanolamine metabolic process	GO:0006580	5/10	4.6E-04
phosphatidylethanolamine biosynthetic process	GO:0006646	5/10	4.6E-04
ethanolamine biosynthetic process	GO:0046335	5/10	4.6E-04
positive regulation of epithelial cell proliferation	GO:0050679	23/144	5.5E-04
ameboidal cell migration	GO:0001667	20/119	6.3E-04
pituitary gland development	GO:0021983	11/48	7.8E-04
regulation of cartilage development	GO:0061035	11/48	7.8E-04
phosphatidylethanolamine metabolic process	GO:0046337	5/11	7.9E-04
positive regulation of histone methylation	GO:0031062	5/12	1.3E-03
skeletal muscle tissue development	GO:0007519	29/210	1.3E-03
histone H3-K4 methylation	GO:0051568	8/30	1.4E-03
positive regulation of cAMP-mediated signaling	GO:0043950	3/4	1.7E-03
CDP-choline pathway	GO:0006657	4/8	1.8E-03
S-adenosylmethioninamine metabolic process	GO:0046499	4/8	1.8E-03
spinal cord development	GO:0021510	14/77	1.8E-03

According to the top five GO terms identified by the classic algorithm for scoring GO terms for enrichment regarding down-regulated genes, low correlation between these processes was observed (table 33). Overall, significances regarding over-representation of GO terms for down-regulated genes and accordant clusters among the Top 20 GO terms by means of PCB 126-treatment were low (raw p-values ≥ 3.1E-05).

Statistically slightly dominating paths within the top five and correlated GO terms among the Top 20-list issued into ‘positice regulation of synaptic plasticity’ (GO:0031915), ‘cytotoxic T cell differentiation’ (GO:0045065), and ‘diencephalon development’ (GO:0021536). The path issuing into the latter also involved another top five GO term: ‘endocrine system development’ (GO:0035270). Within, 21 out of 132 annotated probes were negatively affected by PCB 126. Respective genes are listed in table 34.

Table 34: Mouse whole genome microarray analysis. Down-regulated genes by PCB 126 (250 µg/kg bw, three days) annotated to the GO term ‘endocrine system development’ (GO:0035270); mouse liver. Cutoff values: A ≥ 27, lfc ≤ -1, p-value < 0.05.

PCB 126

Gene name	Gene systematic name	Gene description
Nog	NM_008711	noggin
Fgf2	NM_008006	fibroblast growth factor 2
Apoa1	NM_009692	apolipoprotein A-I
LOC100044968	XM_001473421	Mus musculus similar to modulator recognition factor 2
Drd2	NM_010077	dopamine receptor 2
Nkx6-1	NM_144955	NK6 homeobox 1
Onecut1	NM_008262	one cut domain family member 1
Nkx2-2	NM_010919	NK2 transcription factor related
Pou1f1	NM_008849	POU domain
Tcf7l2	NM_001142920	transcription factor 7-like 2
Lhx3	NM_001039653	LIM homeobox protein 3
Il6ra	NM_010559	interleukin 6 receptor
Nf1	NM_010897	neurofibromatosis 1
ENSMUST00000089855	ENSMUST00000089855	oxidase 2
Foxe3	NM_015758	forkhead box E3
Smo	NM_176996	smoothened homolog
Tcf7l2	NM_001142923	transcription factor 7-like 2
Bmp4	NM_007554	bone morphogenetic protein 4
Pbx1	NM_183355	pre B-cell leukemia transcription factor 1
Onecut2	NM_194268	one cut domain family member 2
LOC100048479	XM_001480325	similar to hepatocyte nuclear factor 6 beta

The genes and respective encoded proteins listed in table 34 are involved in several diverging processes within ‘endocrine system development’ (GO:0035270). These included lipid metabolism, glucose homeostasis, steroidogenesis, immune response, acute-phase reactions and hematopoiesis. For instance, the protein encoded by apolipoprotein A-I (*Apoa1*, NM_009692) participates in the transport of cholesterol from tissues to the liver for excretion by promoting cholesterol efflux from tissues and by acting as a cofactor for lecithin cholesterol acyltransferase (*Lcat*). *Lcat* (NM_008490) was not regulated by any of the tested congeners. Ten probes out of significantly down-regulated probes annotated to ‘endocrine system development’ (GO:0035270; sign./annot.: 21/132 in total) matched those annotated to ‘diencephalon development’ (GO:0021536) sign./annot.: 15/76 in total). Both of these subsets of genes did not clearly appear obviously straight-lined regarding their specific roles in respective process (Ashburner *et al.*, 2000; Binns *et al.*, 2009; Dimmer *et al.*, 2012).

Processes involved in lipid biosynthesis with correlating significant annotated genes were ‘phosphatidylethanolamine biosynthetic process’ (GO:0006646), ‘phosphatidylethanolamine metabolic process’ (GO:0046337), and ‘CDP-choline pathway’ (GO:0006657). To these processes, solute carrier family 27, member 1 (*Slc27a1*, NM_011977; fatty acid transporter), cholin kinase alpha (*Chka*, NM_013490), and *Chkb* (NM_007692) represented significantly down-regulated genes by PCB 126-treatment. These genes and respective GO terms are of relevance with respect to biosynthesis of glycerophospholipids, especially of phosphatidylcholin (Ashburner *et al.*, 2000; Binns *et al.*, 2009; Dimmer *et al.*, 2012).

Within GO term ‘cytotoxic T cell differentiation’ (GO:0045065), two out of three probes annotated were affected significantly by PCB 126, representing both annotated genes (one of the genes was tested with two different probes): CD8 antigen (*Cd8a*, NM_009857), and aquamous cell carcinoma antigen recognized by T-cells 1 (*Sart1*, NM_016882). These genes are required for both development and activity of cytotoxic T cells (Fung-Leung *et al.*, 1991; Kikuchi *et al.*, 1999).

A few epigenetic processes were included in the Top 20-list for down-regulating effects on gene expression by PCB 126: ‘S-adenosylmethioninamine metabolic process’ (GO:0046499), ‘positive regulation of histone methylation’ (GO:0031062), and ‘histone H3-K4 methylation’ (GO:0051568). To these processes, DNA methyltransferases (*Dnmt1*, NM_010066; *Dnmt3b*, NM_001003961), histone-lysine N-methyltransferases (*Kmt2d* (*MII2*), NM_001033276, encoded protein methylates ‘Lys-4’ of histone 3; *Kmt2e* (*MII5*), NM_026984, encoded methyltransferase specifically mono- and dimethylates ‘Lys-4’ of histone H3), O-linked N-acetylglucosamine transferase (*Ogt*,

NM_139144; encoded protein glycosylates diverse proteins including histone H2B, AKT1, or 6-phosphofructokinase), and dpy-30 homolog (*Dpy30*, NM_001146224; encoded protein is part of the MLL1/MLL complex, involved in the methylation of histone H3 at ‘Lys-4’, particularly trimethylation) were annotated and significantly down-regulated by the congener.

Histone H3 'Lys-4' methylation represents a specific tag for epigenetic transcriptional activation and is associated with active genes. Besides their denoted general impact on epigenetics, information on more specific roles is available for some of the described genes. *MII2* and *Ogt* are concerned with insulin sensitivity and glucose tolerance, whereas KMT2E represents a key regulator of hematopoiesis involved in terminal myeloid differentiation and in the regulation of hematopoietic stem cell self-renewal by a DNA methylation-dependent mechanism (Ashburner *et al.*, 2000; Binns *et al.*, 2009; Dimmer *et al.*, 2012; Goldsworthy *et al.*, 2013; Heuser *et al.*, 2009; Jiang *et al.*, 2011; Santos-Rosa *et al.*, 2002).

4.1.1.2.5. PCB 156 – impact on gene transcription in mouse livers

Treatment with single doses of PCB 156 (150000 µg/kg bw) for three days exerted highly inductive effects on gene expression in mouse livers. Observations regarding ≥ 2fold up to ≥ 6fold inductive/repressive effects by PCB 156 on gene transcription in comparison to ≥ 2fold effects by TCDD is illustrated in figure 20.

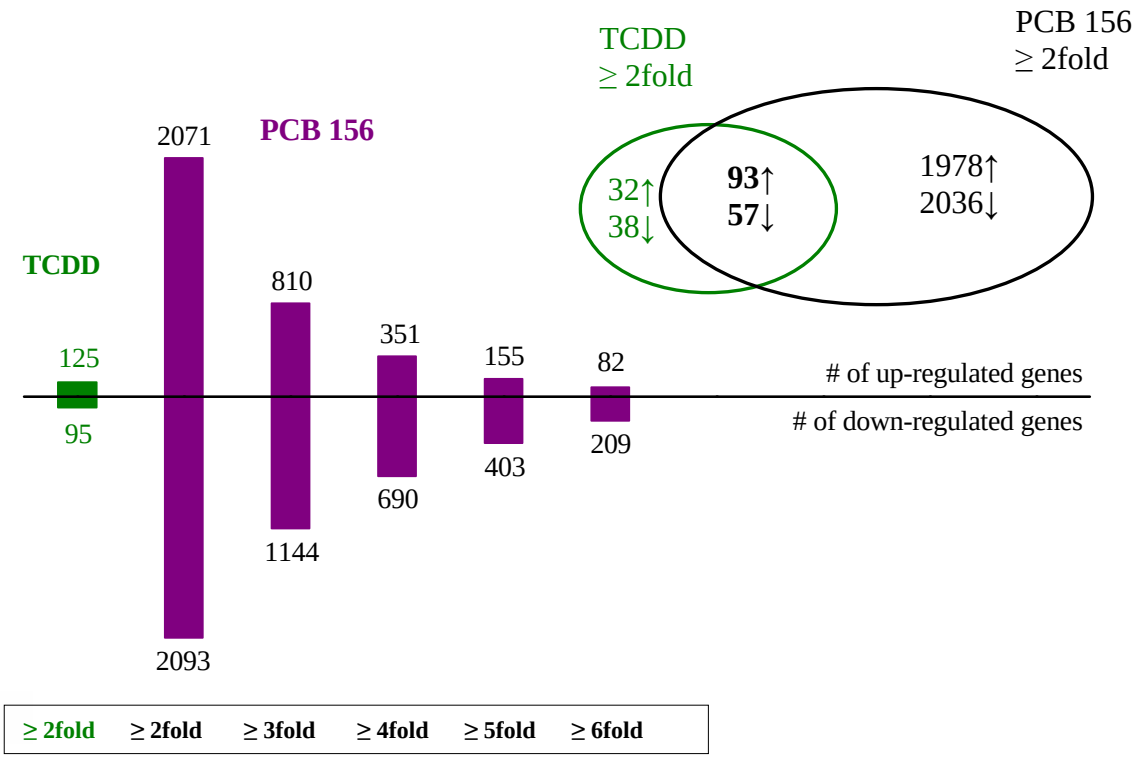

Figure 20: Mouse whole genome microarray analysis. Numbers of regulated genes in mouse livers by PCB 156 (150000 µg/kg bw, three days) compared to numbers of genes regulated by TCDD (25 µg/kg bw, three days), and numbers of genes regulated both by PCB 156 and TCDD (TCDD-raw data by courtesy of C. Lohr; Lohr, 2013). A ≥ 2^7, p-value < 0.05. 2071;

In mouse livers, *in vivo* treatment with PCB 156 led to both induction and respression of more than 2000 genes each (figure 20) within set cutoff-values (A ≥ 2^7, $|lfc| \geq 1$ (≥ 2fold); p-value < 0.05). By change of cutoff-levels to effects, numbers of affected genes constantly reduced from 810 (up), and 1144 (down) (≥ 3fold) to 82 (up), and 209 (down) (≥ 6fold). Overlap of PCB 156-, and TCDD-affected genes (125 up-, and 95 down-regulated genes) accounted for 93 up-, and 57 down-regulated genes accordantly regulated with respect to ≥ 2fold effects.

In table 35 (following page), the Top 20-list of genes, which were up-regulated in response to treatment with PCB 156 (150000 µg/kg bw, three days) in mouse livers is depicted.

Table 35: Mouse whole genome microarray analysis. Top 20 up-regulated genes in mouse livers by PCB 156 (150000 µg/kg bw, three days). Cutoff values: A ≥ 2^7, lfc ≥ 1, p-value < 0.05.

PCB 156 lfc	Gene systematic name	Gene description	Gene name
7.467	NM_009992	cytochrome P450 family 1 subfamily a polypeptide 1	*Cyp1a1*
4.006	NM_008181	glutathione S-transferase alpha 1 (Ya)	*Gsta1*
3.939/2.268	NM_001122660	predicted gene 10639	*Gm10639*
3.861	NM_010210	fragile histidine triad gene	*Fhit*
3.816	NM_009028	RAS-like family 2 locus 9	*Rasl2-9*
3.796	NM_010002	cytochrome P450 family 2 subfamily c polypeptide 38	*Cyp2c38*
3.718	NAP029947-1	Unknown	*NAP029947-1*
3.671/1.734	NM_011034	peroxiredoxin 1	*Prdx1*
3.652	NM_009994	cytochrome P450 family 1 subfamily b polypeptide 1	*Cyp1b1*
3.584	NM_198171	cDNA sequence BC015286	*BC015286*
3.549/2.267	NM_172881	UDP glucuronosyltransferase 2 family polypeptide B35	*Ugt2b35*
3.493	NM_008030	flavin containing monooxygenase 3	*Fmo3*
3.463	NM_017475	Ras-related GTP binding C	*Rragc*
3.429/3.387	NM_145603	carboxylesterase 2	*Ces2*
3.402	NM_009993	cytochrome P450 family1 subfamily a polypeptide 2	*Cyp1a2*
3.368	NM_025535	SAR1 gene homolog B (S. cerevisiae)	*Sar1b*
3.270	XM_902301	predicted gene EG546797 transcript variant 1	*Gm5978*
3.246	A_55_P2168781	Unknown	*A_55_P2168781*
3.234	NR_003625	RIKEN cDNA 1700073E17 gene	*1700073E17Rik*
3.209	NM_001081325	predicted gene 6957	*Gm6957*

Values b/a from oligo b/oligo a; values a-n: value range of more than two (n) oligos.

The highest up-regulated gene in mouse livers in response to treatment with PCB 156 was *Cyp1a1* (NM_009992; lfc = 7.467). *Cyp1b1* (NM_009994; lfc = 3.652), and *Cyp1a2* (NM_009993; lfc = 3.402) were also within the Top 20-list of up-regulated genes (table 35). Transcription of further genes implicated in (drug) metabolism was disctinctly enhanced by PCB 156: *Gsta1* (NM_008181; lfc = 4.006), *Gm10639* (NM_001122660; lfc (max) = 3.939; encoded protein exhibits GST activity), *Ugt2b35* (NM_172881; lfc (max) = 3.549), flavin containing monooxygenase 3 (*Fmo3*, NM_008030; lfc = 3.493), and predicted gene 6957 (*Gm6957*,

NM_001081325; lfc = 3.209; encoded protein exhibits SULT-activity) were affected and listed among the Top 20-list (Binns *et al.*, 2009; Dimmer *et al.*, 2012).

Indications regarding altered lipid and fatty acid metabolism were given by up-regulation of *Cyp2c38* (NM_010002; lfc = 3.796; encodes an arachidonic acid metabolism), cDNA sequence BC015286 (*BC015286*, NM_198171; lfc = 3.584; encodes an acylcarnitine hydrolase), and *Ces2* (NM_145603; lfc (max) = 3.429; encodes an acylcarnitine hydrolase) (Binns *et al.*, 2009; Dimmer *et al.*, 2012).

Treatment with PCB 156 appeared to impact transcriptional and metabolical activity in mouse livers, which was further hinted by up-regulation of *Sar1b* (NM_025535; lfc = 3.368; encoded protein involved in intracellular transport), and *Rasl2-9* (NM_009028; lfc = 3.816; encoded GTP-binding protein involved in nucleocytoplasmatic transport of proteins and RNA) (Binns *et al.*, 2009; Dimmer *et al.*, 2012; Kadowaki *et al.*, 1993; Melchior *et al.*, 1993).

A member of the Top 20-list of up-regulated genes implicated in the redox status represented *Prdx1* (NM_011034; lfc (max) = 3.671). By use of reducing equivalents provided through the thioredoxin system, PRDX 1 enables the reduction of peroxides (Chae *et al.*, 1994a; Chae *et al.*, 1994b; Iwahara *et al.*, 1995). Besides, PRDX 1 was discussed related to inhibition of apoptosis (Berggren *et al.*, 2001; Egler *et al.*, 2005; Kim *et al.*, 2000; Kim *et al.*, 2008).
Several further members of the thioredoxin/thioredoxin reductase redox system were up-regulated by PCB 156 in the course of current study: *Txnip* (NM_001009935; lfc = 1.742), *Txndc12* (NM_025334; lfc = 1.719), thioredoxin-like 4A (*Txnl4a*, NM_025299; lfc = 1.539), *Txndc15* (NM_175150; lfc = 1.137), *Txndc17* (NM_026559; lfc = 1.107), and *Txn1* (NM_011660; lfc = 1.053). Another up-regulated gene implicated in apoptotic processes was *Fhit* (NM_010210; lfc = 3.861). *Fhit* represents a pro-apoptotic tumor suppressor gene playing a role in p53/TP53-mediated apoptosis (Binns *et al.*, 2009; Dimmer *et al.*, 2012).

Transcription of Ras-related GTP binding C (*Rragc*, NM_017475; lfc = 3.463) was as well up-regulated by PCB 156 in mouse livers. Rags are GTPases, which function as heterodimers consisting of RagA or B bound to RagC or D. These heterodimeric complexes are required for amino acid-induced relocalization of mechanistic target of rapamycin complex 1 (mTORC1) to lysosomes and its subsequent activation by the GTPase Ras homolog enriched in brain (RHEB). Consisting of TORC1 and TORC2, TOR is a key regulatory kinase regulating cellular growth and

metabolism. RagC/D was shown to be a key regulator in the activation of the TOR signaling cascade by amino acids (Russell *et al.*, 2011; Tsun *et al.*, 2013). Further, hepatic mTORC1 was reported to be involved in the control of locomotor activity and lipid metabolism (Cornu *et al.*, 2014).

Besides *Rragc*, genes which are concerned with TOR signaling and were up-regulated by PCB 156 in mouse livers were *Rraga* (NM_178376; lfc = 2.338), and Rheb (NM_053075; lfc = 1.573). *Mtor* (NM_020009) appeared slightly below cutoff regarding signal intensity ($A \geq 2^7$), though tendentiously adverting to an up-regulation ($A \geq 2^{5.91}$, lfc = 2.106) by PCB 156.

By classical enrichment analysis performed using Fisher's exact test, over-representation of GO terms within the group of differentially expressed genes was assessed. The 20 most significant GO terms in terms of up-regulation by PCB 156 is presented in table 36.

Table 36: Mouse whole genome microarray analysis – TopGO analysis (PCB 156): Fisher's exact test. Top 20 GO terms identified by the classic algorithm for scoring GO terms for enrichment regarding up-regulated genes; descending order. Mouse liver, PCB 156 (150000 µg/kg bw, three days). Top five GO terms are indicated in bold.

PCB 156 GO ID	GO term	sign./annot. genes	Raw p-value
oxidation-reduction process	**GO:0055114**	**262/1237**	**1.2E-24**
cellular ketone metabolic process	**GO:0042180**	**197/948**	**7.5E-18**
translation	**GO:0006412**	**148/658**	**9.8E-17**
carboxylic acid metabolic process	**GO:0019752**	**185/918**	**1.8E-15**
oxoacid metabolic process	**GO:0043436**	**185/918**	**1.8E-15**
organic acid metabolic process	GO:0006082	186/937	6.8E-15
cofactor metabolic process	GO:0051186	81/311	3.1E-13
coenzyme metabolic process	GO:0006732	68/250	2.8E-12
small molecule metabolic process	GO:0044281	431/2829	1.4E-11
intracellular transport	GO:0046907	196/1088	1.6E-11
metabolic process	GO:0008152	1585/12490	2.1E-10
cellular catabolic process	GO:0044248	291/1853	1.9E-09
glutathione metabolic process	GO:0006749	22/48	1.9E-09
protein transport	GO:0015031	224/1358	2.5E-09
translational elongation	GO:0006414	57/225	2.9E-09
establishment of protein localization	GO:0045184	228/1406	7.9E-09
cellular amino acid metabolic process	GO:0006520	81/382	1.4E-08
cellular metabolic process	GO:0044237	1355/10684	1.8E-08
response to xenobiotic stimulus	GO:0009410	19/41	1.9E-08
catabolic process	GO:0009056	324/2156	2.5E-08

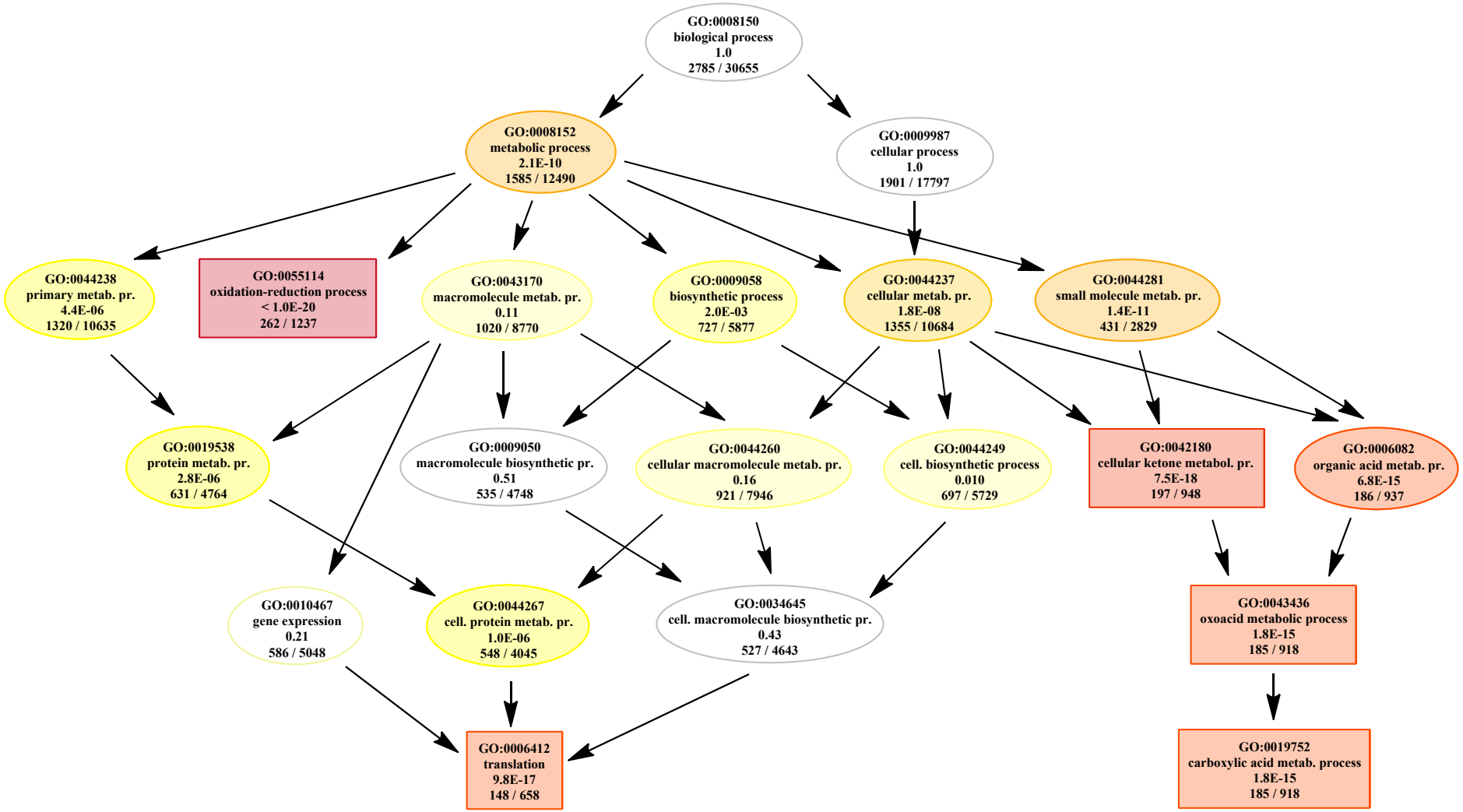

Figure 21: Mouse whole genome microarray analysis – TopGO analysis (PCB 156, 150000 µg/kg bw, three days; mouse liver): The GO subgraph plot induced by the top five GO terms identified by the classic algorithm for scoring GO terms for enrichment regarding up-regulated genes. Boxes indicate the five most significant GO terms. Box color represents relative significance ranging from dark red (most significant) to light yellow (least significant).

The Top 20 GO terms assigned to TopGO pathway analysis investigating up-regulated genes by PCB 156 in mouse livers most prominently and statistically very significantly were related to metabolic processes including ‘oxidation-reduction process’ (GO:0055114), ‘carboxylic acid metabolic process’ (GO:0019752), and ‘translation’ (GO:0006412) (see table 36, figure 21).
Paths included xenobiotic metabolism (*Cyp1a1*; *Ahr*, NM_013464; *Ahrr*, NM_009644; *Ugt2b1*, NM_152811, e.g.; annotated to ‘response to xenobiotic stimulus’, GO:0009410), and accordant ‘glutathione metabolic process’ (GO:0006749; annotated genes: *Sod2*, NM_013671; *Gpx3*, NM_08161; *Gsr*, NM_010344; *Gsta1*, NM_008181; *Gstm1*, NM_010358; *Gstp2*, NM_181796; *Gstt3*, NM_133994, e.g.), as well as lipid metabolism (*Aldh1a1*, NM_013467; *Aldh1a7*, NM_011921; hydroxyacid oxidase 2, *Hao2*, NM_019545; fatty acid binding protein 2, *Fabp2*, NM_007980; *Slc27a5*, NM_009512; phospholipase A2, *Pla2g15*, NM_133792; annotated to ‘carboxylic acid metabolic process’, GO:0019752, and ‘lipid metabolic process’, GO:0006629, 191 significant probes out of 1245 annotated).

Indications of transcriptionally and metabolically active cells in general were given by aforementioned top five GO term ‘translation’ (GO:0006412), as well as by ‘translational elongation’ (GO:0006414), ‘protein transport’ (GO:0015031), and ‘establishment of protein localization’ (GO:0045184).

In table 37, the Top 20 genes of 2093 down-regulated genes affected in mouse livers subsequent to PCB 156-treatment are listed.

Table 37: Mouse whole genome microarray analysis. Top 20 down-regulated genes in mouse livers by PCB 156 (150000 µg/kg bw, three days). Cutoff values: A ≥ 2^7, lfc ≤ -1, p-value < 0.05.

PCB 156 lfc	Gene systematic name	Gene description	Gene name
-4.481/ -4.279	BC031891/ NR_002861	serine (or cysteine) peptidase inhibitor clade A member 4 pseudogene 1	*Serpina4-ps1*
-4.098- -2.451	NM_008103	glial cells missing homolog 1 (Drosophila)	*Gcm1*
-4.094	XM_001472203	similar to Ubtf protein (LOC100039072)	*Gm2033*
-3.964	NR_004413	U1b6 small nuclear RNA	*Rnu1b6*
-3.839- -2.362	NM_009946	complexin 2	*Cplx2*
-3.788	XM_001472970	similar to R10D12.10 (LOC100039488)	*Gm2264*
-3.754	NM_008341	insulin-like growth factor binding protein 1	*Igfbp1*
-3.714	ENSMUST0000 0106778	Probable ATP-dependent RNA helicase DDX5 (DEAD box protein 5)	*ENSMUST00000 106778*
-3.645	XM_889044	predicted gene EG624491	*Gm6508*
-3.629	XM_001474429	similar to cyclic nucleotide gated channel beta 1	*Gm2690*
-3.556	XM_001480348	similar to gag (LOC100043516)	*Gm4492*
-3.547	NM_153522	sodium channel voltage-gated type III beta	*Scn3b*
-3.537	A_55_P1986743	Unknown	*A_55_P1986743*
-3.509	AK017236	adult male pituitary gland cDNA RIKEN full-length enriched library clone:5330406M23	*5330406M23Rik*
-3.495	NM_001169153	CD300 antigen like family member F	*Cd300lf*
-3.470	NM_001033960	RAB GTPase activating protein 1	*Rabgap1*
-3.459	XM_001478202	hypothetical protein LOC100047464	*LOC100047464*
-3.451	NM_011562	teratocarcinoma-derived growth factor	*Tdgf1*
-3.419	NM_197945	ProSAPiP1 protein	*RP23-100C5.8*
-3.410	NM_013932	DEAD (Asp-Glu-Ala-Asp) box polypeptide 25	*Ddx25*
-3.407	NM_181319	T-box 22 (Tbx22) transcript variant 2 mRNA	*Tbx22*

Values b/a from oligo b/oligo a; values a-n: value range of more than two (n) oligos.

Among down-regulated genes by PCB 156 (table 37), several representatives implying a potential role of the congener on immune function and/or response included *Serpina4-ps1* (BC031891/NR_002861; lfc (max) = -4.481), *Cplx2* (NM_009946; lfc (max) = -3.839; proposed involvement in mast cell degranulation), *Cd300lf* (NM_001169153; lfc = -3.495; encoded protein participates in osteoclast differentiation), *Tdgf1* (NM_011562; lfc = -3.451), and *Tbx22* (NM_181319; lfc = -3.407; encodes a probable transcriptional regulator involved in developmental

processes; major determinant crucial to palatogenesis) (Binns *et al.*, 2009; Dimmer *et al.*, 2012). Besides, *Serpina4-ps1* and *Tdgf1* are also involved in apoptotic processes (Binns *et al.*, 2009; Bustos *et al.*, 2009; Dimmer *et al.*, 2012).

A further down-regulated gene transcript by PCB 156 was *Igfbp1* (NM_008341; lfc = -3.754). The encoded protein is implicated in insulin receptor signaling pathways and is further proposed to be involved in regulation of cell growth and tissue regeneration (Binns *et al.*, 2009; Dimmer *et al.*, 2012). With respective proteins supposedly playing roles in cell cycle regulation or in formation of cell junctions, *Rabgap1* (NM_001033960; lfc = -3.470), and *RP23-100C5.8* (NM_197945; lfc = -3.419; encoding ProSAPiP1 protein) were among the Top 20 of down-regulated genes by PCB 156 (Binns *et al.*, 2009; Dimmer *et al.*, 2012).

Down-regulated DEAD (Asp-Glu-Ala-Asp) box polypeptide 25 (*Ddx25*, NM_013932; lfc = -3.410), and 'probable' ATP-dependent RNA helicase DEAD box protein 5 (*Ddx5*; *ENSMUST00000106778*; lfc = -3.714) ('probably') encode RNA helicases from the DEAD-box family, which use energy from ATP hydrolysis and are associated with many processes ranging from RNA synthesis to RNA degradation. Connection of DEAD-box proteins to these processes includes p53-dependent apoptosis (DDX5, e.g.), innate immune response (esp. DDX1, DDX3, DDX5, DDX9, DDX17, and DDX41), and regulation of ER-α dependent transcription (DDX17, e.g) (Bates *et al.*, 2005; Fuller-Pace, 2013; Rocak and Linder, 2004; Soulat *et al.*, 2008; Worthham *et al.*, 2009).

Including mentioned members of the Top 20-list, several DEAD-box protein gene transcripts were affected by PCB 156-treatment: six were up-regulated (*Ddx51*, NM_027156; lfc = 1.821; *Ddx54*, NM_028041; lfc = 1.435; *Ddx20*, NM_017397; lfc = 1.4; *Ddx41*, NM_134059; lfc =1.274; *Ddx27*, NM_153065; lfc = 1.106; *Ddx21*, NM_019553; lfc = 1.078), and four were down-regulated (*ENSMUST00000106778* (*Ddx5*), lfc = -3.714; *Ddx25*, NM_013932; lfc = -3.410; *Ddx5*, NM_007840; lfc = -2.058; *Ddx1*, NM_134040; lfc = -1.21) within set cutoff-values.

Table 38 shows TopGO results with respect to down-regulated genes by PCB 156.

Table 38: Mouse whole genome microarray analysis – TopGO analysis (PCB 156): Fisher's exact test. Top 20 GO terms identified by the classic algorithm for scoring GO terms for enrichment regarding down-regulated genes. Mouse liver, PCB 156 (150000 µg/kg bw, three days). Top five GO terms are indicated in bold.

PCB 156 GO term	GO ID	sign./annot. genes	Raw p-value
regulation of RNA metabolic process	**GO:0051252**	**382 / 3478**	**1.8E-08**
regulation of nitrogen compound metabolic process	**GO:0051171**	**434 / 4055**	**4.0E-08**
transcription, DNA-dependent	**GO:0006351**	**382 / 3503**	**4.1E-08**
regulation of gene expression	**GO:0010468**	**424 / 3952**	**4.5E-08**
RNA biosynthetic process	**GO:0032774**	**382 / 3507**	**4.7E-08**
regulation of nucleobase-containing compound metabolic pr.	GO:0019219	429 / 4018	6.4E-08
regulation of biosynthetic process	GO:0009889	430 / 4036	8.0E-08
regulation of transcription, DNA-templated	GO:0006355	370 / 3402	9.2E-08
regulation of RNA biosynthetic process	GO:2001141	370 / 3403	9.5E-08
regulation of cellular biosynthetic process	GO:0031326	425 / 3993	1.1E-07
regulation of cellular macromolecule biosynthetic process	GO:2000112	393 / 3707	5.4E-07
cellular developmental process	GO:0048869	352 / 3271	5.6E-07
regulation of macromolecule biosynthetic process	GO:0010556	399 / 3789	8.7E-07
cell differentiation	GO:0030154	335 / 3106	8.9E-07
negative regulation of nitrogen compound metabolic pr.	GO:0051172	150 / 1208	9.7E-07
negative regulation of nucleobase-containing metabolic pr.	GO:0045934	148 / 1196	1.4E-06
negative regulation of cellular biosynthetic process	GO:0031327	155 / 1267	1.5E-06
negative regulation of biosynthetic process	GO:0009890	157 / 1287	1.6E-06
triglyceride biosynthetic process	GO:0019432	17 / 55	1.6E-06
RNA metabolic process	GO:0016070	443 / 4300	2.1E-06

Most of the Top 20 GO terms, and especially respective top five GO terms, obtained by view on down-regulated genes by PCB 156 were related to 'regulation of gene expression' (GO:0010468), 'transcription' (DNA-dependent, GO:0006351), and 'regulation of RNA metabolic processes' (GO:0051252) (see table 38). In addition, these processes appeared to be closely connected to each other, indicating a quite defined mode of action regarding inhibited processes in mouse livers.

These observations might be a result of PCB 156's high inducing effect in mouse livers, since excessively and probably redundantly synthezised gene transcripts might be catabolized. Further,

these results might represent a feedback-regulation after three days of the single dose treatment with the DL-congener.

Besides, ‘triglyceride biosynthetic process’ (GO:0019432) as a more specified biological process occured in the Top 20-list of GO terms obtained via investigation of down-regulated genes by PCB 156. Exemplarily, among significantly affected probes annotated to this GO term (17 out of 55), fatty acid synthase (*Fasn*, NM_007988), 1-acylglycerol-3-phosphate O-acyltransferase 6 (*Agpat6*, NM_018743), elongation of very long chain fatty acids 2, and 4 (*Elovl2*, NM_019423; *Elovl4*, NM_148941), and acyl-CoA synthetase long-chain family member 5 (*Acsl5*, NM_027976) were located.

4.1.1.3. Mouse microarrays – Investigations among congeners

Of particular interest with respect to understanding mechanisms of action of different DL-congeners and potential degree of involvement of the AhR, might be an examination of mouse whole genome microarray results among congeners. To primarily approach to this topic, correlations of gene lists between congeners and 'together' regulated genes were investigated, as already indicated in respective congener-specific chapters.

Table 39 (following page) gives an overview of numbers of genes regulated by individual congeners, as well as 'together' regulated genes considering several combinations. Implied cutoff values were $A \geq 2^7$ regarding signal intensity, $|lfc| \geq 1$ with respect to (log2) fold change (≥ 2fold induction/repression), and p-value < 0.05, as applied throughout mouse whole genome microarray analysis.

Table 39: Mouse whole genome microarray analysis. Numbers of 'together' regulated genes in mouse livers by treatment with TCDD, 1-PeCDD, 4-PeCDF, PCB 118, PCB 126, or PCB 156 (three days); several correlations among congeners. TCDD-raw data by courtesy of Christiane Lohr (Lohr, 2013). A ≥ 2^7, | lfc | ≥ 1, p-value < 0.05.

congener or correlation	# of significantly affected genes		congener or correlation	# of significantly affected genes		congener or correlation	# of significantly affected genes	
TCDD*	125↑	95↓				**TCDD** &		
1-PeCDD	319↑	374↓	**TCDD** &			1-PeCDD 4-PeCDF	74↑	32↓
4-PeCDF	3051↑	2843↓	1-PeCDD	92↑	61↓			
PCB 118	353↑	363↓	4-PeCDF	94↑	47↓	**TCDD** &		
PCB 126	2587↑	1767↓	PCB 118	29↑	12↓	PCB 118 PCB 126		
			PCB 126	64↑	26↓	PCB 156	25↑	7↓
PCB 156	2071↑	2093↓	PCB 156	93↑	57↓			
TCDD & 1-PeCDD 4-PeCDF PCB 118 PCB 126 PCB 156	22↑	5↓	**TCDD** & 1-PeCDD 4-PeCDF PCB 126 PCB 156	48↑	19↓	**TCDD** & PCB 126 PCB 156	58↑	26↓
1-PeCDD & 4-PeCDF	220↑	304↓	**1-PeCDD** & PCB 118			**1-PeCDD** &		
PCB 118	44↑	37↓	PCB 126			PCB 126		
PCB 126	141↑	223↓	PCB 156	37↑	32↓	PCB 156	132↑	218↓
PCB 156	215↑	305↓						
4-PeCDF & PCB 118	321↑	346↓	**4-PeCDF** & PCB 118			**4-PeCDF** & PCB 126		
PCB 126	2229↑	1660↓	PCB 126			PCB 156	1500↑	1487↓
PCB 156	1884↑	1952↓	PCB 156	276↑	328↓			
PCBs PCB 118 PCB 126	314↑	345↓	PCB 118 PCB 156	305↑	344↓	PCB 126 PCB 156	1548↑	1513↓
PCB 118 PCB 126 PCB 156	283↑	332↓						

*raw data regarding TCDD-treatment was obtained by courtesy of Christiane Lohr (Lohr, 2013).

Oral treatment of mice with TCDD, 1-PeCDD, 4-PeCDF, PCB 118, PCB 126, or PCB 156 led to highly diverging numbers of regulated genes in livers among congeners. Ranging around 100 to 400 up-, and down-regulated genes, TCDD, 1-PeCDD, or PCB 118 regulated comparable amounts of genes in mouse livers. By contrast, treatments with 4-PeCDF, PCB 126, or PCB 156 affected very high numbers of around 2000, up to more than 3000 genes.

Overlap between TCDD-derived effects (125↑ 95↓) and those obtained by 1-PeCDD, or 4-PeCDF, was by tendency most prominent among congeners, but was still limited to around half/up to three quarters of genes regulated by TCDD (TCDD & 1-PeCDD: 92↑ 61↓; TCDD & 4-PeCDF: 94↑ 47↓). The amount of accorantly regulated genes was limited regarding DL-PCBs and TCDD. By view on all DL-PCBs compared with TCDD, 25 accordantly up-, and 7 down-regulated genes remained, which slightly increased by exception of PCB 118 (58↑ 26↓). Hence, overlap was minor for the correlation TCDD & PCB 118 (29↑ 12↓); less than 10% of PCB 118-regulated genes were as well affected by TCDD-treatment.

Generally, overlap between PCB 118-derived effects and impact of the remaining DL-compounds was limited excepting the correlation 4-PeCDF & PCB 118 (321↑ 346↓). Overall, 4-PeCDF-derived effects quite well correlated with those obtained with DL-PCBs. Around 90% of genes affected by each PCB were accordantly regulated by 4-PeCDF in mouse livers. Among DL-PCBs, modes of action appeared to be fairly comparable in view of numbers and percentage of ‘together’ regulated genes.

Correlating 1-PeCDD-impacted genes (319↑ 374↓) with other DL-congeners, strongest overlap was revealed together with 4-PeCDF (220↑ 304↓). For the remaining compounds, the consent tended to be slightly higher than with TCDD with around twice as much ‘together’ regulated genes each.

In the attachments, the Top 20-gene lists containing accordantly up-, and down-regulated genes for 1-PeCDD & TCDD, 4-PeCDF & TCDD, PCB 126 & TCDD, and PCB 156 & TCDD are shown. Further, the gene-list containing accordantly regulated genes (48↑ 19↓) of DL-congeners excepting PCB 118 is found in the attachments.

4.1.1.3.1. Mouse microarrays – ‘all’ DL-congeners

The number of genes, which were regulated by every investigated DL-congener (TCDD, 1-PeCDD, 4-PeCDF, PCB 118, PCB 126, or PCB 156; ‘all’ DL-congeners), was limited to 22 up-regulated and five down-regulated genes (compare table 39). Respective list of genes is presented in table 40. Raw-data on TCDD-derived effects was obtained by courtesy of Christiane Lohr (Lohr, 2013).

The list of up-regulated genes impacted by ‘all’ DL-congeners was headed by *Cyp1a1*, and *Cyp1a2*. *Cyp1b1* was missing in this table, since lfc for PCB 118 was slightly below cutoff (lfc (PCB 118, *Cyp1b1*) = 0.935). The majority of regulated genes by DL-compounds was related to (xenobiotic) metabolism (*Gsta1*, *Gsta2*, *Gstp1*, *Gstp2*, *Fmo3*, *Gm10639*, and *Ugt2b35*), followed by genes involved in lipid metabolism (*Tmem86b*, *Cyb5*, *Ces2*, *BC015286*, *Apoa1*, and *Etnk2*), carbohydrate metabolic processes (*Pgk1*, *Ugdh*, *LOC676974*, and *G6pc*) or other cellular processes implicating highly processive cells and metabolically active conditions (*Slc46a3* and *Car2*).
Fhit and *Htatip2* both represent tumor suppressor genes, and were correlated with apoptotic processes (Binns *et al.*, 2009; Dimmer *et al.*, 2012; Zhao *et al.*, 2008a).

‘Dioxin’-mediated effects were further investigated by TopGO pathway analysis. By classical enrichment analysis performed using Fisher’s exact test, over-representation of GO terms within the group of up-regulated genes was assessed. The 20 most significant GO terms in terms of up-regulation by ‘all’ DL-congeners are presented in table 41. The GO subgraph induced by the top five GO terms is depicted in figure 22 (for table 41 and figure 22, see following pages).

Table 40: Mouse whole genome microarray analysis. 22 accordantly up-regulated and five down-regulated genes in mouse livers by treatment with DL-congeners TCDD, 1-PeCDD, 4-PeCDF, PCB 118, PCB 126, or PCB 156. Listed in descending order according to TCDD-derived effects. TCDD-raw data by courtesy of Christiane Lohr (Lohr, 2013). Cutoff values: A ≥ 2^7, |lfc| ≥ 1, p-value < 0.05.

lfc (TCDD)	Gene systematic name	Gene description	DL-congeners Gene name
		up	
9.478	NM_009992	cytochrome P450 family 1 subfamily a polypeptide 1	*Cyp1a1*
3.985	NM_009993	cytochrome P450 family 1 subfamily a polypeptide 2	*Cyp1a2*
3.582	NM_010210	fragile histidine triad gene	*Fhit*
3.379	NM_017379	tubulin alpha 8	*Tuba8*
3.103	NM_027872	solute carrier family 46 member 3	*Slc46a3*
2.819	NM_008181	glutathione S-transferase alpha 1 (Ya)	*Gsta1*
2.678	NM_016865	HIV-1 tat interactive protein 2 homolog (human)	*Htatip2*
2.518	NM_025557	Purkinje cell protein 4-like 1	*Pcp4l1*
2.153	NM_023440	transmembrane protein 86B	*Tmem86b*
1.857/1.362	NM_013541	glutathione S-transferase pi 1	*Gstp1*
1.853	NM_001122660	predicted gene 10639	*Gm10639*
1.696/1.65	NM_145603	carboxylesterase 2	*Ces2*
1.63	NM_198171	cDNA sequence BC015286	*BC015286*
1.559	NM_181796	glutathione S-transferase pi 2	*Gstp2*
1.481	NM_008030	flavin containing monooxygenase 3	*Fmo3*
1.441	NM_009150	selenium binding protein 1	*Selenbp1*
1.394	NM_172881	UDP glucuronosyltransferase 2 family polypeptide B35	*Ugt2b35*
1.391	NM_009466	UDP-glucose dehydrogenase	*Ugdh*
1.297	NM_008182	glutathione S-transferase alpha 2 (Yc2)	*Gsta2*
1.156	NM_008828	phosphoglycerate kinase 1	*Pgk1*
1.105	NM_025797	cytochrome b-5	*Cyb5*
1.093	NM_009801	carbonic anhydrase 2	*Car2*
		down	
-1.821	XM_001003154	similar to Glucose phosphate isomerase 1 transcript variant 2	*LOC676974*
-1.425	NM_008061	glucose-6-phosphatase catalytic	*G6pc*
-1.387--1.328	NM_009692	apolipoprotein A-I	*Apoa1*
-1.113	XM_001471861	hypothetical protein LOC100044148	*Etnk2*
-1.103	XM_001481023	hypothetical protein LOC100043770	*Gm4635*

Values b/a from oligo b/oligo a; values a-n: value range of more than two (n) oligos.

(1-PeCDD, 4-PeCDF, PCB 118, PCB 126, PCB 156) & TCDD

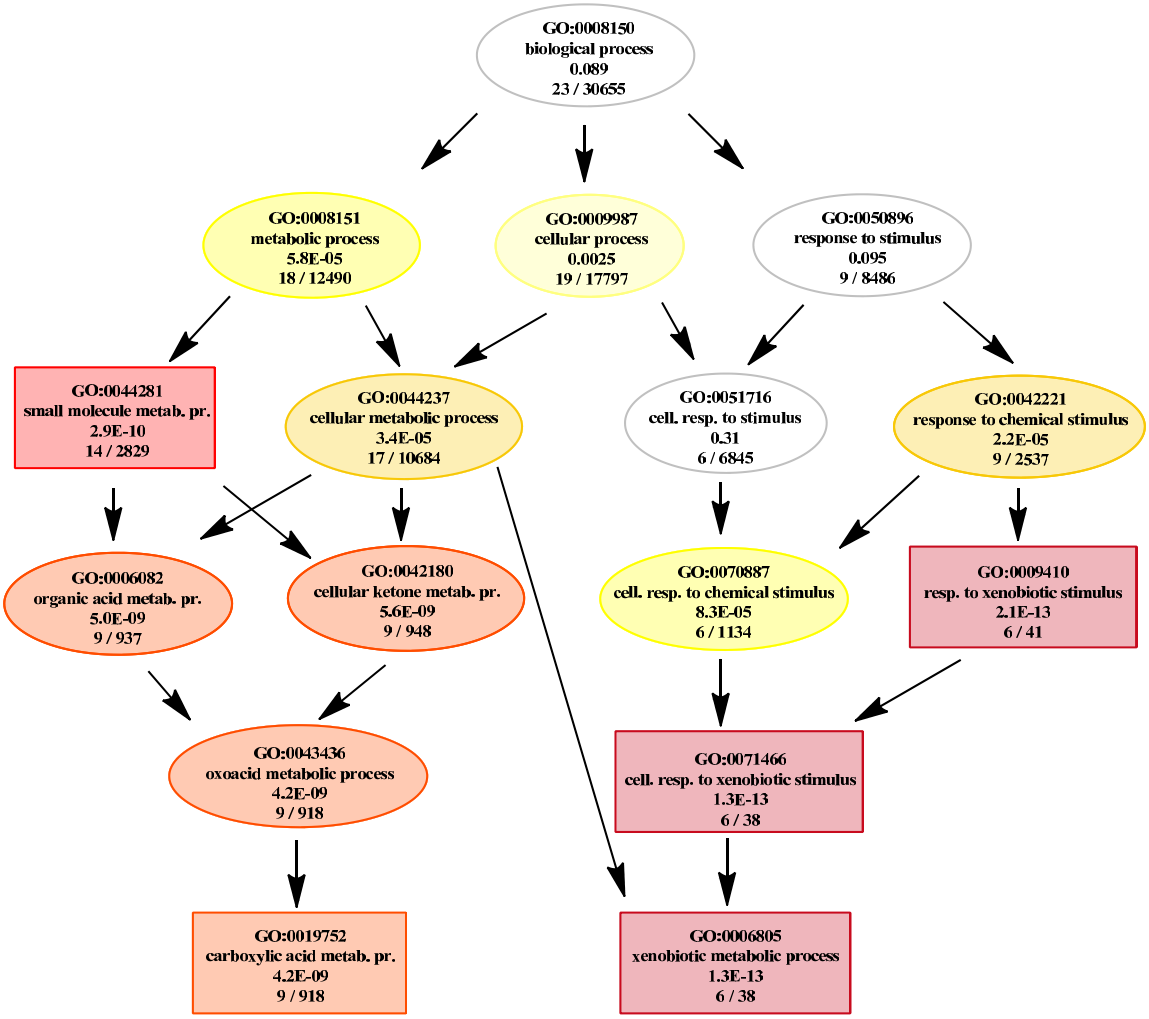

Figure 22: Mouse whole genome microarray analysis – TopGO analysis for 'all' DL-congeners (1-PeCDD, 4-PeCDF, PCB 118, PCB 126, PCB 156) & TCDD: The GO subgraph plot induced by the top five GO terms identified by the classic algorithm for scoring GO terms for enrichment regarding up-regulated genes. Boxes indicate the five most significant GO terms. Box color represents relative significance ranging from dark red (most significant) to light yellow (least significant). Mouse liver; three days of treatment. TCDD-raw data obtained by courtesy of Christiane Lohr (Lohr, 2013).

Table 41: Mouse whole genome microarray analysis – TopGO analysis for 'all' DL-congeners (1-PeCDD, 4-PeCDF, PCB 118, PCB 126, PCB 156) & TCDD: Fisher's exact test. Top 20 (+8) GO terms identified by the classic algorithm for scoring GO terms for enrichment regarding up-regulated genes; descending order. Mouse liver, three days of treatment. Top five GO terms are indicated in bold. TCDD-raw data obtained by courtesy of Christiane Lohr (Lohr, 2013).

(1-PeCDD, 4-PeCDF, PCB 118, PCB 126, PCB 156) & TCDD		
GO term	GO ID	**Rank**
xenobiotic metabolic process	**GO:0006805**	**I**
cellular response to xenobiotic stimulus	**GO:0071466**	**II**
response to xenobiotic stimulus	**GO:0009410**	**III**
small molecule metabolic process	**GO:0044281**	**IV**
carboxylic acid metabolic process	**GO:0019752**	**V**
oxoacid metabolic process	GO:0043436	VI
organic acid metabolic process	GO:0006082	VII
cellular ketone metabolic process	GO:0042180	VIII
glutathione metabolic process	GO:0006749	IX
xenobiotic catabolic process	GO:0042178	X
peptide metabolic process	GO:0006518	XI
common myeloid progenitor cell proliferation	GO:0035726	XII
neutrophil aggregation	GO:0070488	XIII
negative regulation of monocyte chemotactic protein-1 production	GO:0071638	XIV
regulation of neutrophil aggregation	GO:2000428	XV
negative regulation of neutrophil aggregation	GO:2000429	XVI
regulation of peroxidase activity	GO:2000468	XVII
negative regulation of peroxidase activity	GO:2000469	XVIII
drug metabolic process	GO:0017144	XIX
reactive oxygen species metabolic process	GO:0072593	XX
response to chemical stimulus	GO:0042221	> XX_a
cellular metabolic process	GO:0044237	> XX_b
metabolic process	GO:0008152	> XX_c
cellular response to chemical stimulus	GO:0070887	> XX_d
cellular process	GO:0009987	> XX_e
biological process	GO:0008150	> XX_f
response to stimulus	GO:0050896	> XX_g
cellular response to stimulus	GO:0051716	> XX_h

Viewing results on pathway analysis revealed by assessment of over-represented GO terms within the group of up-regulated genes, two biological processes issuing in two related pathways predominated ‘dioxin-like’ effects: ‘xenobiotic metabolic process’ (GO:0006805), and ‘carboxylic acid metabolic process’ (GO:0019752) (figure 22).
Annotated and significantly impacted genes with respect to ‘xenobiotic metabolic process’ were *Cyp1a1*, *Gstp1*, *Gstp2*, *Gsta1*, and *Gsta2* (analyzed by six probes in total). Similar genes were as well represented by significantly occurring annotated probes within ‘carboxylic acid metabolic process’: *Cyp1a1*, *Cyp1a2*, *Gstp1*, *Gstp2*, *Gsta1*, *Ugdh*, *Cyb5*, and *Htatip2*. Accordingly, the majority of GO terms obtained by pathway analysis were involved in xenobiotic or carboxylic acid metabolism (table 41). Further correlated biological processes involved ‘reactive oxygen species metabolic process’ (GO:0072593). Annotated, and significantly affected by ‘all’ DL-congeners were *Cyp1a1*, *Cyp1a2*, and *Gstp1*.

Four GO terms within the Top 20-list were implicated in ‘neutrophil aggregation’ (GO:0070488), or ‘negative regulation of monocyte chemotactic protein-1 production’ (GO:0071638). Closer investigation of annotated genes exhibited that significance with respect to these four GO terms was solely due to up-regulation of *Gstp1* (analyzed by two probes in total). GSTP1 was reported to attenuate acute inflammation in mice. In this regard, GSTP1 was shown to prevent LPS-induced TNF-α, IL-1β, monocyte chemotactic protein 1 (MCP-1), and nitric oxide (NO) production (Luo *et al.*, 2009). Relevance of an up-regulation of *Gstp1* with respect to this, reflecting its role among a high amount of further genes involved in metabolism, needs to be considered, though.

Interestingly, the TopGO-graph regarding up-regulating effects of ‘all’ DL-congeners together almost matched the GO subgraph plot for effects by PCB 126 & TCDD together. The comparison is shortly shown in figure 23.

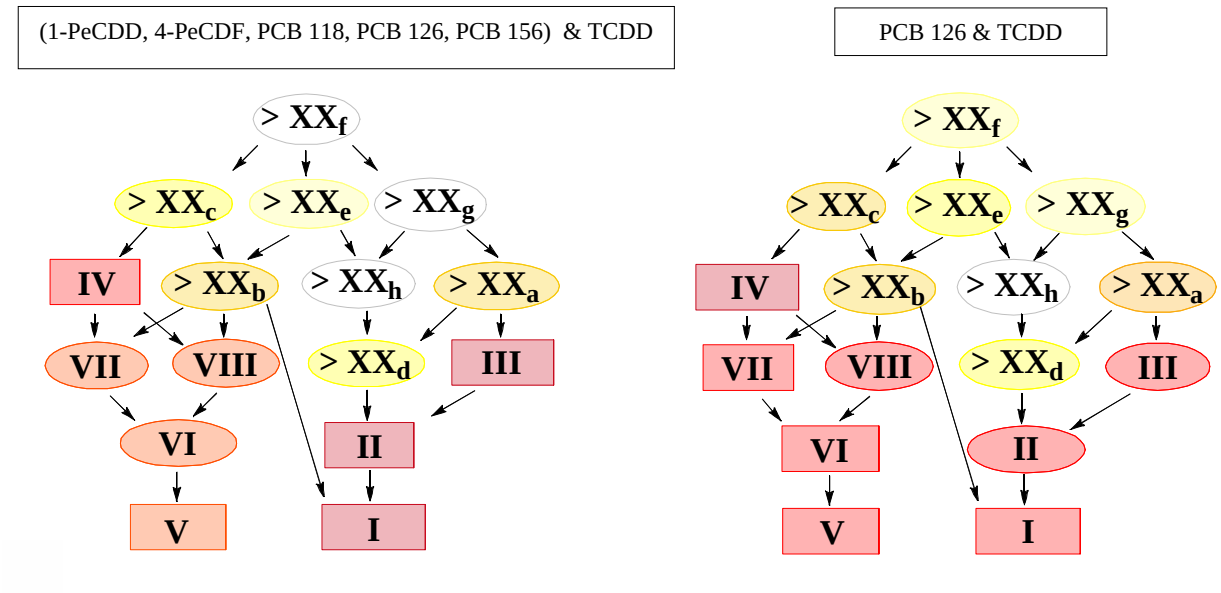

Figure 23: Mouse whole genome microarray analysis – Comparison of TopGO analysis for all DL-congeners (1-PeCDD, 4-PeCDF, PCB 118, PCB 126, PCB 156) & TCDD (left), and PCB 126 (right): GO subgraph plots induced by the top five GO terms each identified by the classic algorithm for scoring GO terms for enrichment regarding up-regulated genes. Boxes indicate the five most significant GO terms including ranks (I-XX). Box color represents relative significance ranging from dark red (most significant) to light yellow (least significant). Mouse liver, three days of treatment. GO term ranks I-XX; XX_a-XX_h according to table 41. TCDD-raw data by courtesy of Christiane Lohr (Lohr, 2013).

Even with similar ranking, the TopGO subgraph for TCDD & PCB 126-'together' derived effects closely resembled the TopGO subgraph induced by 'all' DL-congeners 'together'. For comparison and identification of GO terms, as well as in figure 23 coded rankings, see table 41, and figure 22. For the study in hand, PCB 126 seems to represent a 'prototype' for DL-response regarding enhancement of pathways.

4.1.1.3.2. Mouse microarrays – TCDD & PCB 118

As indicated above, with the exception of the correlation 4-PeCDF & PCB 118, smallest overlaps between investigated DL-congeners were obtained, as soon as PCB 118 was involved. Hence, the overlap with TCDD-derived effects might potentially represent one of significance understanding AhR-dependent response with relevance for low-affinity ligands.

Comparison of up-regulating effects towards mouse livers regarding PCB 118-treatment with effects induced by TCDD yielded 29 accordantly up-regulated genes in total. Respective gene-list, which was sorted by TCDD-mediated effects, is figured in table 42. Raw data for TCDD's impact was obtained by courtesy of Christiane Lohr (Lohr, 2013).

Table 42: Mouse whole genome microarray analysis. 29 genes accordantly up-regulated in mouse livers by PCB 118 (150000 µg/kg bw, three days), and TCDD (25 µg/kg bw, three days). TCDD-raw data by courtesy of Christiane Lohr (Lohr, 2013). Cutoff values: A ≥ 2^7, lfc ≥ 1, p-value < 0.05.

PCB 118 & lfc	TCDD lcf	Gene systematic name	Gene description	Gene name
7.799	9.478	NM_009992	cytochrome P450 family 1 subfamily a polypeptide 1	*Cyp1a1*
3.311	3.985	NM_009993	cytochrome P450 family 1 subfamily a polypeptide 2	*Cyp1a2*
1.622	3.582	NM_010210	fragile histidine triad gene	*Fhit*
1.654	3.379	NM_017379	tubulin alpha 8	*Tuba8*
2.018	3.103	NM_027872	solute carrier family 46 member 3	*Slc46a3*
3.998	2.819	NM_008181	glutathione S-transferase alpha 1 (Ya)	*Gsta1*
1.503	2.678	NM_016865	HIV-1 tat interactive protein 2 homolog (human)	*Htatip2*
1.398	2.518	NM_025557	Purkinje cell protein 4-like 1	*Pcp4l1*
2.227	2.153	NM_023440	transmembrane protein 86B	*Tmem86b*
1.775/ 2.310	1.857/ 1.362	NM_013541	glutathione S-transferase pi 1	*Gstp1*
3.631/ 2.279	1.853/ 1.036	NM_001122660	predicted gene 10639	*Gm10639*
1.609	1.702	NM_007689	chondroadherin	*Chad*
2.560/ 2.621	1.696/ 1.650	NM_145603	carboxylesterase 2	*Ces2*
2.603	1.630	NM_198171	cDNA sequence BC015286	*BC015286*
2.027/ 1.751	1.559/ 1.187	NM_181796	glutathione S-transferase pi 2	*Gstp2*
1.194	1.481	NM_008030	flavin containing monooxygenase 3	*Fmo3*
1.500	1.452	NM_008183	glutathione S-transferase mu 2	*Gstm2*
1.014	1.441	NM_009150	selenium binding protein 1	*Selenbp1*
1.533	1.394	NM_172881	UDP glucuronosyltransferase 2 family polypeptide B35	*Ugt2b35*
1.897	1.391	NM_009466	UDP-glucose dehydrogenase	*Ugdh*
1.398	1.366	NM_206537	cytochrome P450 family 2 subfamily c polypeptide 54	*Cyp2c54*
2.697	1.297	NM_008182	glutathione S-transferase pi 1	*Gsta2*
1.096	1.156	NM_008828	glutathione S-transferase alpha 2 (Yc2)	*Pgk1*
1.050	1.146	NM_172928	doublecortin-like kinase 3	*Dclk3*
2.095	1.105	NM_025797	cytochrome b-5	*Cyb5*
1.133	1.093	NM_009801	carbonic anhydrase 2	*Car2*
1.296	1.088	NM_009286	RIKEN cDNA C730007P19 gene	*C730007P19Rik*
1.149	1.059	NM_133738	anthrax toxin receptor 2	*Antxr2*
1.234	1.048	NM_016956	hemoglobin beta adult minor chain	*Hbb-b2*

Values b/a from oligo b/oligo a.

Though the overlap between PCB 118-, and TCDD-derived effects was limited regarding 'together' regulated genes (29↑ 12↓; see table 42), various genes highly affected by TCDD were induced by PCB 118 as well. In numbers, eleven genes out of the Top 20 genes, which were up-regulated by TCDD-treatment, were as well induced by PCB 118-treatment: *Cyp1a1*, *Cyp1a2*, *Fhit*, *Tuba8*, *Slc46a3*, *Gsta1*, *Htatip2*, *Pcp4l1*, *Tmem86b*, *Gstp1*, and *Gm10639*. For further information regarding TCDD's impact on mouse livers, see Lohr (2013). The twelve accordantly down-regulated genes by treatment with TCDD or PCB 118 are presented in the attachments.

To gain a further insight into correlative impact by TCDD together with PCB 118, pathway analysis was applied. By classical enrichment analysis performed using Fisher's exact test, over-representation of GO terms within the group of up-regulated genes was assessed regarding PCB 118 alone, TCDD alone, and PCB 118 together with TCDD (PCB 118 & TCDD). The obtained subgraphs induced by the top five GO terms each, are presented in figure 24. Corresponding top five GO terms are listed in subsequent table 43 (for table 43 and figure 24, see following pages).

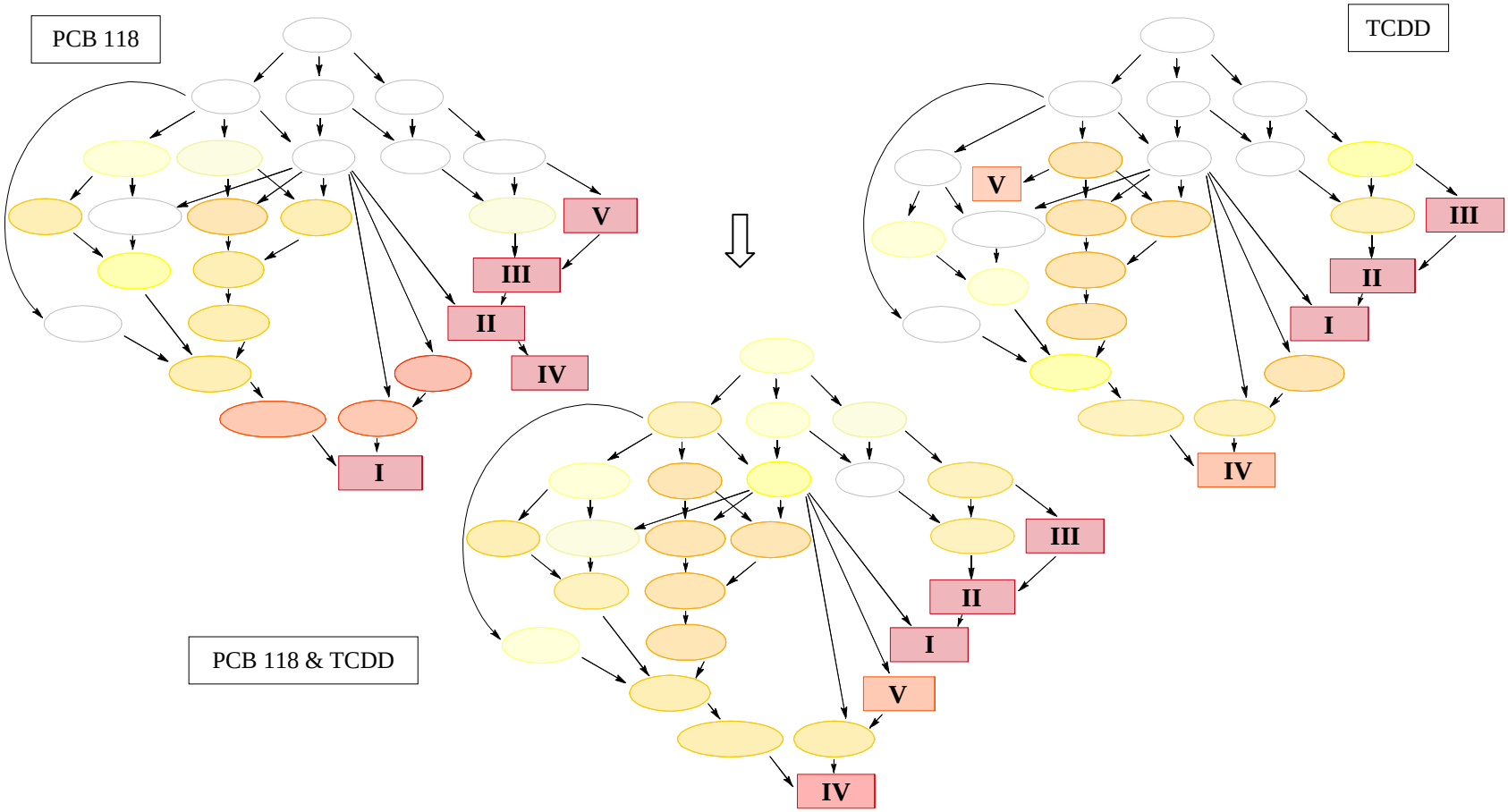

Figure 24: Mouse whole genome microarray analysis – Comparison of TopGO analysis for PCB 118, TCDD, or PCB 118 & TCDD. GO subgraph plots induced by the top five GO terms each identified by the classic algorithm for scoring GO terms for enrichment regarding up-regulated genes. Boxes indicate the five most significant GO terms including ranks (I-V). Box color represents relative significance ranging from dark red (most significant) to light yellow (least significant). Mouse liver, three days of treatment. GO term ranks I-V according to table 43 (following page). TCDD-raw data by courtesy of Christiane Lohr (Lohr, 2013).

Table 43: Mouse whole genome microarray analysis – TopGO analysis for PCB 118, TCDD, or PCB 118 & TCDD: Fisher's exact test. Top five GO terms identified by the classic algorithm for scoring GO terms for enrichment regarding up-regulated genes; descending order. Mouse liver, three days of treatment. TCDD-raw data by courtesy of Christiane Lohr (Lohr, 2013).

		TCDD	PCB 118	PCB118 & TCDD
GO term	GO ID	Rank	Rank	Rank
xenobiotic metabolic process	GO:0006805	**I**	**II**	**I**
cellular response to xenobiotic stimulus	GO:0071466	**II**	**III**	**II**
response to xenobiotic stimulus	GO:0009410	**III**	**V**	**III**
glutathione metabolic process	GO:0006749	**IV**	**I**	**IV**
organic ether metabolic process	GO:0018904	**V**	n.a.	n.a.

n.a.: not analyzed.

As visuable in figure 24 and with regard to GO terms listed in table 43, most efficiently affected pathways were accordantly regulated by PCB 118 & TCDD with respect to induction of expression of genes involved in xenobiotic metabolism in mouse livers. In contrast to a quite low overlap for PCB 118 & TCDD regarding numbers of 'together' regulated genes – a proportion of about 25% of TCDD-induced genes (125 up-regulated genes by TCDD) was up-regulated by PCB 118-treatment (29 'together' up-regulated genes by PCB 118 & TCDD) – PCB 118 appeared to share relevant properties with TCDD; at least regarding major TCDD-derived effects.

4.1.1.3.3. Mouse microarrays – 'all' DL-congeners excepting PCB 118

As described above, PCB 118 generally exhibited diverging impact on gene transcription in mouse livers compared to the remaining DL-congeners studied in the course of present mouse whole genome microarray experiment. Hence, and besides investigations implementing 'all' DL-congeners, PCB 118 was disregarded from one further examination.

Pathway analysis was performed in order to gather information on predominating accordant modes of action for 1-PeCDD, 4-PeCDF, PCB 126, and PCB 156 together with TCDD. The gene-lists containing accordantly regulated genes (48↑ 19↓) of DL-congeners except for PCB 118 are shown in the attachments.

Figure 25 represents GO subgraphs with respect to investigations on (1-PeCDD, 4-PeCDF, PCB 126, PCB 156) & TCDD, 1-PeCDD & TCDD, 4-PeCDF & TCDD, and PCB 156 & TCDD. Corresponding GO terms are declared in table 44 (following page).

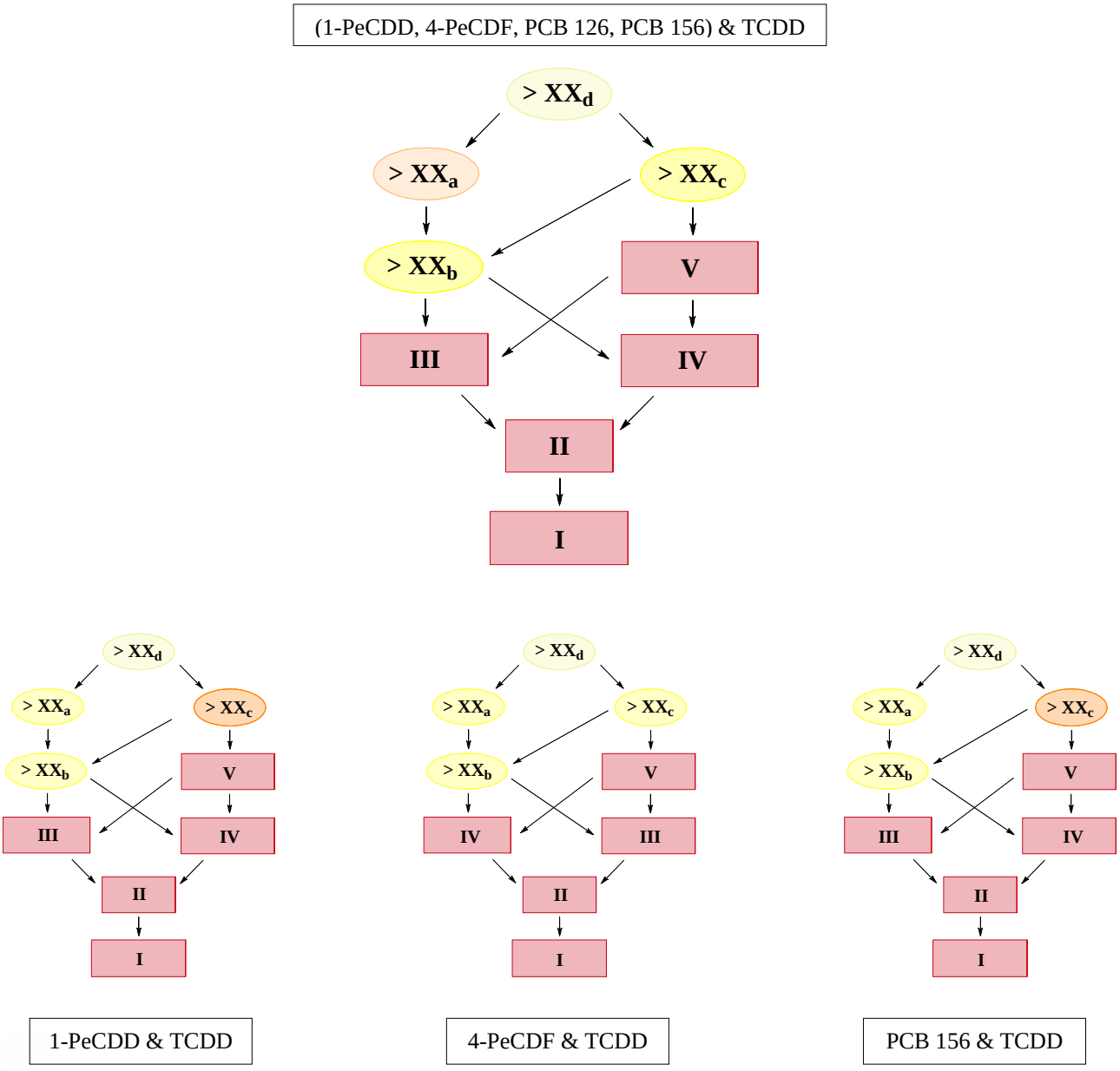

Figure 25: Mouse whole genome microarray analysis – Comparison of TopGO analysis for DL-congeners (1-PeCDD, 4-PeCDF, PCB 126, PCB 156) & TCDD, 1-PeCDD & TCDD, 4-PeCDF & TCDD, and PCB 156 & TCDD: GO subgraph plots induced by the top five GO terms each identified by the classic algorithm for scoring GO terms for enrichment regarding up-regulated genes. Boxes indicate the five most significant GO terms including ranks. Box color represents relative significance ranging from dark red (most significant) to light yellow (least significant). Mouse liver, three days of treatment. GO terms and ranks I-XX; XX_a-XX_d according to table 44. TCDD-raw data by courtesy of Christiane Lohr (Lohr, 2013).

Table 44: Mouse whole genome microarray analysis – TopGO analysis for (1-PeCDD, 4-PeCDF, PCB 126, PCB 156) & TCDD: Fisher's exact test. Top 20 GO terms identified by the classic algorithm for scoring GO terms for enrichment regarding up-regulated genes; descending order. Mouse liver, three days of treatment. TCDD-raw data by courtesy of Christiane Lohr (Lohr, 2013).

(1-PeCDD, 4-PeCDF, PCB 126, PCB 156) & TCDD GO term (significant/annotated genes; raw p-value)	GO ID	**Rank**
carboxylic acid metabolic process	**GO:0019752**	**I**
oxoacid metabolic process	**GO:0043436**	**II**
organic acid metabolic process	**GO:0006082**	**III**
cellular ketone metabolic process	**GO:0042180**	**IV**
small molecule metabolic process	**GO:0044281**	**V**
xenobiotic metabolic process	GO:0006805	VI
cellular response to xenobiotic stimulus	GO:0071466	VII
response to xenobiotic stimulus	GO:0009410	VIII
dibenzo-p-dioxin metabolic process	GO:0018894	IX
glutathione metabolic process	GO:0006749	X
monocarboxylic acid metabolic process	GO:0032787	XI
endocannabinoid signaling pathway	GO:0071926	XII
regulation of endocannabinoid signaling pathway	GO:2000124	XIII
ether metabolic process	GO:0018904	XIV
oxidation-reduction process	GO:0055114	XV
response to chemical	GO:0042221	XVI
peptide metabolic process	GO:0006518	XVII
toxin metabolic process	GO:0009404	XVIII
response to reactive oxygen species	GO:0000302	XIX
regulation of superoxide metabolic process	GO:0090322	XX
cellular process	GO:0009987	$> XX_a$
cellular metabolic process	GO:0044237	$> XX_b$
metabolic process	GO:0008152	$> XX_c$
biological process	GO:0008150	$> XX_d$

GO subgraphs demonstrated in figure 25 show greatly correlating effects regarding most prominently affected pathways concerning 'together' up-regulated genes with respect to (1-PeCDD, 4-PeCDF, PCB 126, PCB 156) & TCDD, 1-PeCDD & TCDD, 4-PeCDF & TCDD, and PCB 156 & TCDD. For all four investigations, the same GO terms represented the top five GO terms occurring in only lightly divergent order, if at all. The most significantly occurring GO term 'carboxylic acid metabolic process' (GO:0019752) for all four examinations, in which the remaining of the top five GO terms issued into, included up-regulated genes *Cyp1a1*, *Gstp1*, *Cd36*, *Hpgd* (NM_008278), *Htatip2*, *Cyp1a2*, *Cth* (NM_145953), *Gstp2*, *Gsta1*, *Pkm2* (NM_011099), *MgII*, and *Cyb5*, with respect to the investigation (1-PeCDD, 4-PeCDF, PCB 126, PCB 156) & TCDD.

Besides further processes related to (xenobiotic) metabolism (table 44), two rather unexpected GO terms were found, which are involved in endocannabinoid signaling. To both occurring GO terms (GO:0071926, and GO:2000124), two genes were annotated and significantly up-regulated by the DL-congeners 1-PeCDD, 4-PeCDF, PCB 126, and PCB 156: monoglyceride lipase (*MgII*, NM_001166250), and abhydrolase domain containing 6 (*Abhd6*, NM_025341). Both of them encode potentially degradative enzymes for the endocannabinoid 2-arachidonoyl glycerol (2-AG). ABHD6 was reported to control accumulation and efficacy of 2-AG at cannabinoid receptors, and to be involved in macrophage activation subsequent to a decrease of 2-AG in the cell (Alhouayek *et al.*, 2013; Marrs *et al.*, 2010; Schlosburg *et al.*, 2010). Though obviously regulated by all DL-congeners except for PCB 118, these observations need to be estimated carefully, thinking about the dominating metabolism-related mechanisms.

Referring to the gene-lists containing accordantly regulated genes (48↑ 19↓) of DL-congeners excepting PCB 118 (see attachments; tables 64, and 65) compared to the (22↑ 5↓)-list for 'all' DL-congeners (including PCB 118; table 40) investigated, more proposed AhR-target genes were listed: *Cyp1b1*, and *Tiparp* in addition to *Cyp1a1*, and *Cyp1a2*, which were also impacted by PCB 118. Further genes within the (48↑ 19↓)-list were generally involved in the same processes as were those of the (22↑ 5↓)-list. Decisively different in this regard was the number of genes involved in these processes. In addition to those tabled in the (22↑ 5↓)-list, *Cd36*, *Hsd17b2*, *Hpgd*, *Tiparp*, *MgII* (up-regulated), *Pnpla3*, *Acly*, and *Acaca* (down-regulated) were implicated in altered lipid metabolic processes. Additionally assigned genes led to higher significance with respect to TopGO investigations and to more conserved, and more specific GO-subgraphs (compare figures 22 and 25), which was most prominently reflecting impact of DL-congeners on xenobiotic and lipid metabolism.

One further member of the AhR-gene batterie should be mentioned, namely *Ahrr* (NM_009644). This gene was not regulated by any DL-congener investigated within the study in hand. *Ahrr*-expression was analyzed by means of two probes on the microarray slides.

Regarding one of these probes ('A_55_P2128388'), measured values were not significant with respect to all set cutoffs ($A \geq 2^7$, $|lfc| \geq 1$, p-value < 0.05).

With respect to the second probe ('A_51_P254425'), results were below cutoff-level for signal-intensity ($A = 2^{5.65}$). Hints towards up-regulating effects for *Ahrr* by congener-treatment was given for all DL-compounds except for PCB 118 (lfc = 0.158, p-value = 0.656); lfc (TCDD) = 3.906, lfc (1-PeCDD) = 2.996, lfc (4-PeCDF) = 2.89, lfc (PCB 126) = 1.54, and lfc (PCB 156 = 1.912). Regarding the FDR, the potentially up-regulating effects were not excluded for TCDD, 1-PeCDD, 4-PeCDF, PCB 126, or PCB 156. Raw-data for TCDD-treatment was obtained by courtesy of Christiane Lohr (Lohr, 2013).

4.1.2. Quantitative real-time PCR – *in vivo* rat studies

Within the framework of SYSTEQ, rat studies, which were constructed equivalently to mouse studies, were performed at IRAS (Van Ede *et al.*, 2013; Van Ede *et al.*, 2011). Dependent on current TEF-values, animals were exposed to varying single doses (L, M, N, O, or P) of the core congeners TCDD, 1-PeCDD, 4-PeCDF, PCB 118, PCB 126, PCB 153, or PCB 156, and sacrificed either after three, or 14 days. With regard to 14 days-studies, RNA of livers of second-highest dose groups (O-groups) and corresponding control groups (K-groups) were examined via qRT-PCR analysis. Concerning three days-studies, the following groups were analyzed: TCDD, 1-PeCDD, and PCB 126 – K, L, M, N; 4-PeCDF – K, L, N; PCB 118, PCB 153, and PCB 156 – K, O. To unravel AhR-, CAR-, and PXR-dependent effects of congeners, focused genes investigated at TU Kaiserslautern were *Cyp1a1*, *Cyp2b1*, and *Cyp3a1*, whereby *Actb* (encoding β-actin) was used as housekeeping gene.

4.1.2.1. QRT-PCR *in vivo*, rat studies – *Cyp1a1*

Figure 26 illustrates results for qRT-PCR-analysis concerning *Cyp1a1*-mRNA for liver samples derived from three days-rat studies and treatment with core congeners.

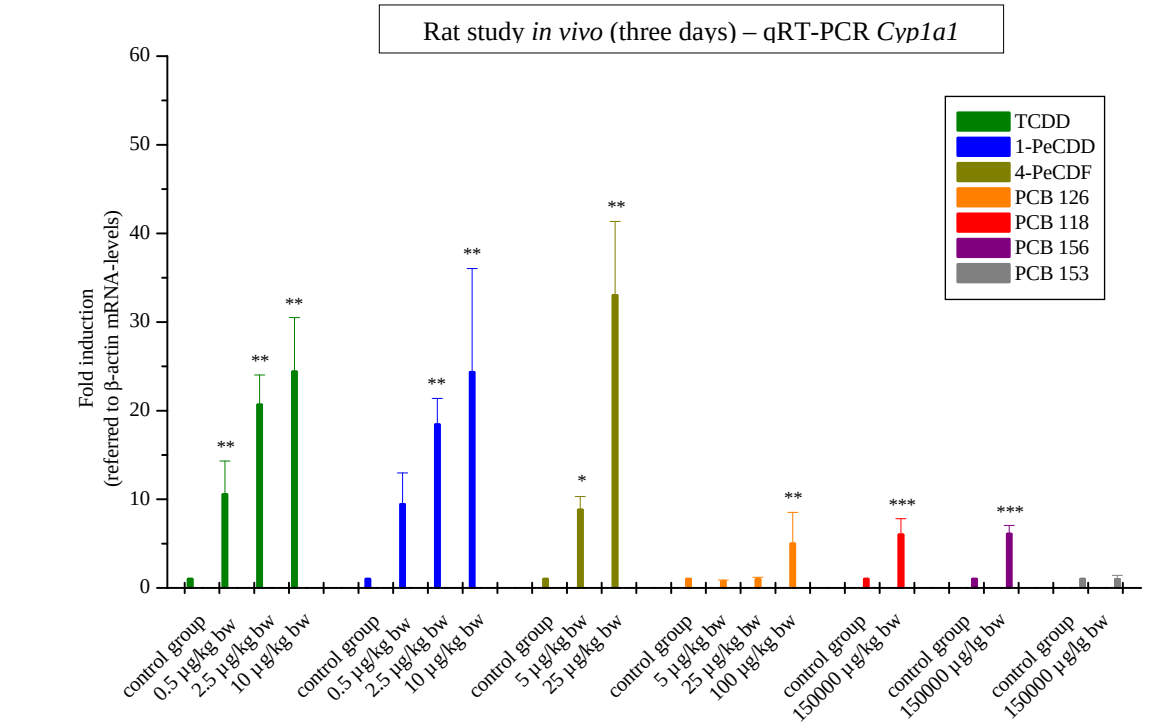

Figure 26: QRT-PCR (*Cyp1a1*) rat study *in vivo* (three days). Rats treated with single doses of TCDD, 1-PeCDD, 4-PeCDF, PCB 118, PCB 126, PCB 153, or PCB 156 for three days. Abscissa: Treatment; ordinate: Fold induction (referred to β-actin mRNA-levels). One-way ANOVA with Dunnett's post test (control vs. treatment groups); Two-tailed unpaired t-test (control vs. one treatment group). Six animals per group.*: p-value < 0.05, **: p-value < 0.01, ***: p-value < 0.001.

Concentration-dependently, *Cyp1a1*-mRNA-levels in livers increased due to exposure of rats with TCDD, 1-PeCDD, or 4-PeCDF for three days (figure 26). With this regard, statistically significant (p-value < 0.05) deviation from respective control group was obtained for 5 µg/kg bw 4-PeCDF (8.8±1.5-fold induction, L-group), whereas statistically very significant (p-value < 0.01) *Cyp1a1*-inductions were gained from 0.5 µg/kg bw TCDD (10.5±3.8-fold, L-group), 2.5 µg/kg bw 1-PeCDD (18.4±3-fold, M-group), yielding up to 33.0(±8.4)-fold induction with 25 µg/kg bw 4-PeCDF (N-group). In livers of rats exposed to 100 µg/kg bw PCB 126 (N-group), statistically very significant (p-value < 0.01) *Cyp1a1*-induction of 5.0(±3.5)-fold was revealed. Treatment of rats with PCB 118, or PCB 156 (150000 µg/kg bw, O-groups) led to statistically extremely (p-value < 0.001) significant *Cyp1a1*-inductions in livers accounting for 6.0(±1.8)-fold (PCB 118), and 6.1(±1.0)-fold (PCB 156), respectively. No effect on *Cyp1a1*-mRNA-levels in livers of PCB 153-treated rats was obtained using 150000 µg/kg bw of the congener.

In figure 27, *Cyp1a1*-qRT-PCR results obtained by analysis of livers from rats treated with core congeners for 14 days are compiled.

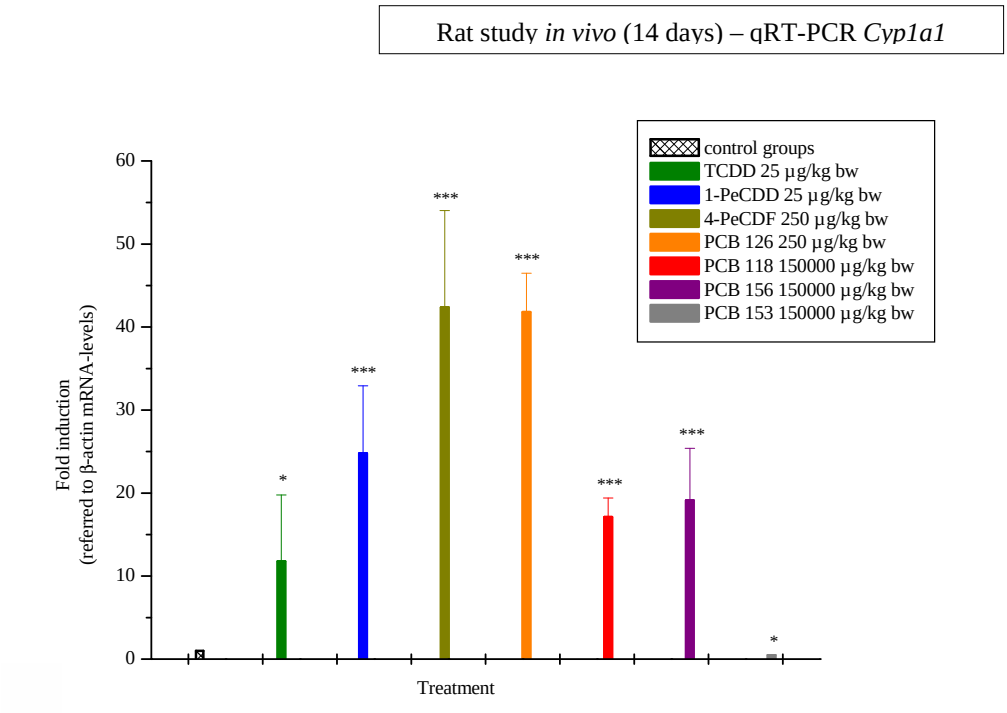

Figure 27: QRT-PCR (*Cyp1a1*) rat study *in vivo* (14 days). Rats treated with single doses of TCDD, 1-PeCDD, 4-PeCDF, PCB 118, PCB 126, PCB 153, or PCB 156 for 14 days. Abscissa: Treatment; ordinate: Fold induction (referred to β-actin mRNA-levels). Two-tailed unpaired t-test (control vs. treatment group). Six animals per group.*: p-value < 0.05, ***: p-value < 0.001.

Subsequent to 14 days of exposure of rats with TCDD (25 µg/kg bw), *Cyp1a1*-mRNA levels in livers statistically significantly (p-value < 0.05) raised to 11.8(±8.0)-fold (figure 27). Comparable high standard deviation was manifested due to two of six animals, barely responding (0.57-, to 0.75-fold induction). Regarding residual four animals, *Cyp1a1*-induction on mRNA-level consistently ranged from 14.8-, to 19.5-fold in livers. With the exception of PCB 153, treatment with the remaining core congeners led to statistically extremely significant (p-value < 0.001) *Cyp1a1*-inductions in following ascending ranking order: 150000 µg/kg bw PCB 118 (17.1±2.3-fold), 150000 µg/kg bw PCB 156 (19.1±6.3-fold), 25 µg/kg bw 1-PeCDD (24.8±8.1-fold), 250 µg/kg bw PCB 126 (41.8±4.7-fold), 250 µg/kg bw 4-PeCDF (42.4±11.7-fold). From statistical point of view, exposure to PCB 153 (150000 µg/kg bw) caused significant (p-value < 0.05) decrease of *Cyp1a1*-mRNA-levels to 0.4(±0.1)-fold in rat livers.

4.1.2.2. QRT-PCR (*in vivo*, rat) – *Cyp2b1*

Figure 28 overviews qRT-PCR-results concerning *Cyp2b1*, gained from examination of livers from rats, which were exposed to single doses of core congeners and sacrificed after three days.

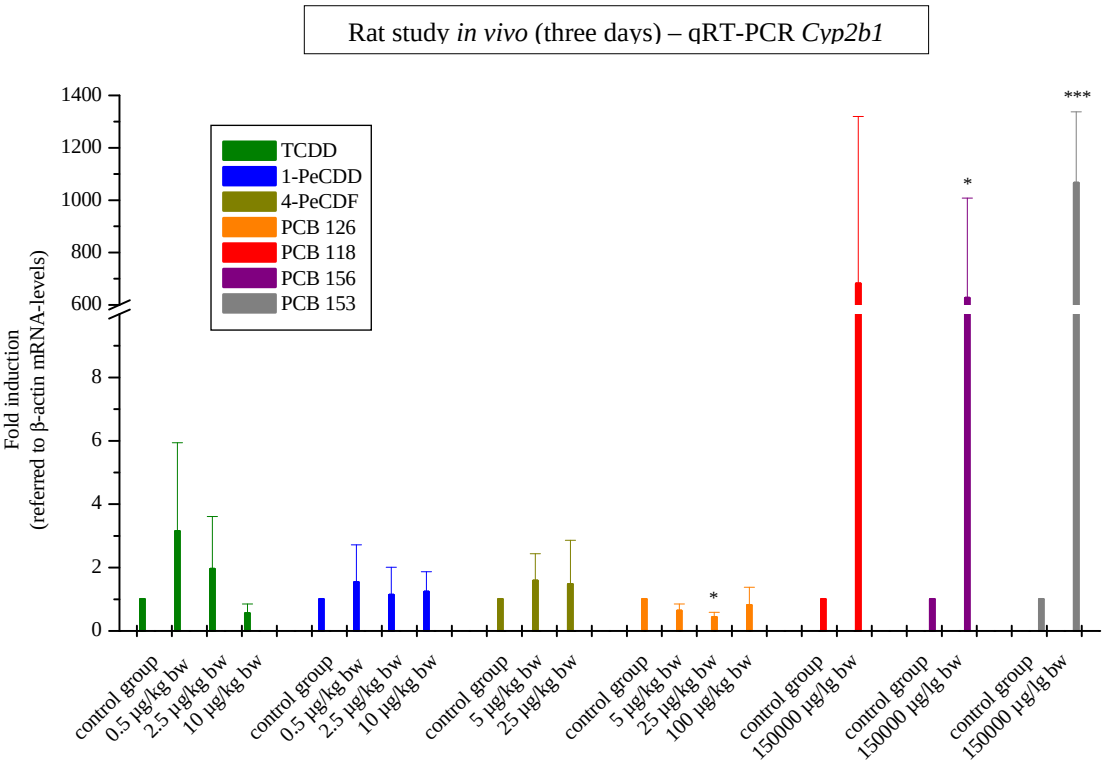

Figure 28: QRT-PCR (*Cyp2b1*) rat study *in vivo* (three days). Rats treated with single doses of TCDD, 1-PeCDD, 4-PeCDF, PCB 118, PCB 126, PCB 153, or PCB 156 for three days. Abscissa: Treatment; ordinate: Fold induction (referred to β-actin mRNA-levels). One-way ANOVA with Dunnett's post test (control vs. treatment groups); Two-tailed unpaired t-test (control vs. one treatment group). Six animals per group.*: p-value < 0.05, ***: p-value < 0.001.

Slight increase of *Cyp2b1*-mRNA-levels in rat livers (figure 28) was obtained after three days of treatment with TCDD (2.5 µg/kg bw; 3.1±2.8-fold). TCDD's impact was not considered statistically significant ($P > 0.05$). No distinct deviation from control groups was received due to exposure to 1-PeCDD (0.5-10 µg/kg bw), or 4-PeCDF (5-25 µg/kg bw) in tested ranges of doses. Along individuals with values in general ranging around those of respective control group, PCB 126 in total led to light reduction of *Cyp2b1*-mRNA, whereas from statistical point of view, 25 µg/kg bw PCB 126 caused significant (p-value < 0.05) decrease (0.4±0.2-fold) of respective gene transcription. Regarding these effects, no concentration-dependency was indicated.

PCB 118, PCB 153, or PCB 156 induced *Cyp2b1*-mRNA in livers of treated rats (150000 µg/kg bw each). Concerning PCB 156, statistically significant (p-value < 0.05) value of 626.1(±381.8)-fold

was gained, while PCB 153 statistically extremely significantly (p-value < 0.001) increased *Cyp2b1*-mRNA to 1065.5(±272.0)-fold. In consequence of a high standard deviation, PCB 118's effect (680.3±639.4-fold) statistically was not emphasized. The high standard deviation came about considerable differential responses, in the course of two of six animals intensely reacting from 1290.2-, to 1824.6-fold induction. Effect of PCB 118 towards remaining four animals ranged from 198.5-, to 262.0-fold *Cyp2b1*-induction in livers.

In figure 29, qRT-PCR results concerning effects of core congeners on *Cyp2b1* in livers of treated rats (14 days) are displayed.

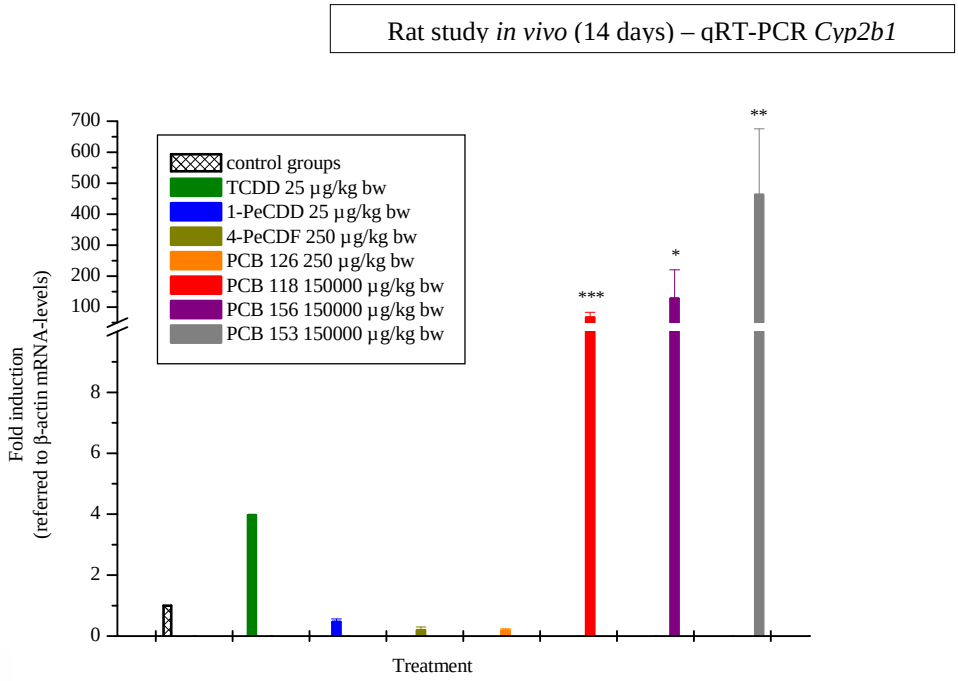

Figure 29: QRT-PCR (*Cyp2b1*) rat study *in vivo* (14 days). Rats treated with single doses of TCDD, 1-PeCDD, 4-PeCDF, PCB 118, PCB 126, PCB 153, or PCB 156 for 14 days. Abscissa: Treatment; ordinate: Fold induction (referred to β-actin mRNA-levels). Two-tailed unpaired t-test (control vs. treatment group). Six animals per group.*: p-value < 0.05, **: p-value < 0.01, ***: p-value < 0.001.

Subsequent to 14 days of TCDD-exposure (25 µg/kg bw), slight, statistically not significant *Cyp2b1*-induction in rat-livers averaging 4.0(±7.0)-fold was examined (figure 29). This induction cohered with a discordant value belonging to one animal, which accounted for 19.5-fold induction, whereas levels of the remainder ranged from 0.3-, to 1.6-fold induction. In mouse livers, *Cyp2b1*-mRNA-levels due to 1-PeCDD-exposure (25 µg/kg bw, 0.5±0.1-fold) did not differ distinctly from respective control group.

Regarding 4-PeCDF, or PCB 126 (250 µg/kg bw each), light deduction (0.2±0.1-fold) of *Cyp2b1*–mRNA was received. Two-tailed p-value of applied unpaired t-tests was 0.0731 for both congeners, which statistically was considered not quite significant. Doses of 150000 µg/kg bw of PCB 118, PCB 153, or PCB 156 induced *Cyp2b1*-levels in rat livers. Statistically significant (p-value < 0.05) value of 127.3(±93.5)-fold was obtained regarding PCB 156, whereby PCB 153 led to statistically very significant (p-value < 0.01) *Cyp2b1*-induction of 462.1(±213.5)-fold, and PCB 118 yielded statistically extremely significant (p-value < 0.001) increase of *Cyp2b1*-mRNA-levels of 65.8(±17.4)-fold in rat livers.

4.1.2.3. QRT-PCR (*in vivo*, rat) – *Cyp3a1*

Figure 30 overviews qRT-PCR-results concerning *Cyp3a1*-mRNA in livers of rats, which were exposed to single doses of TCDD, 1-PeCDD, 4-PeCDF, PCB 118, PCB 126, PCB 153, or PCB 156 for three days.

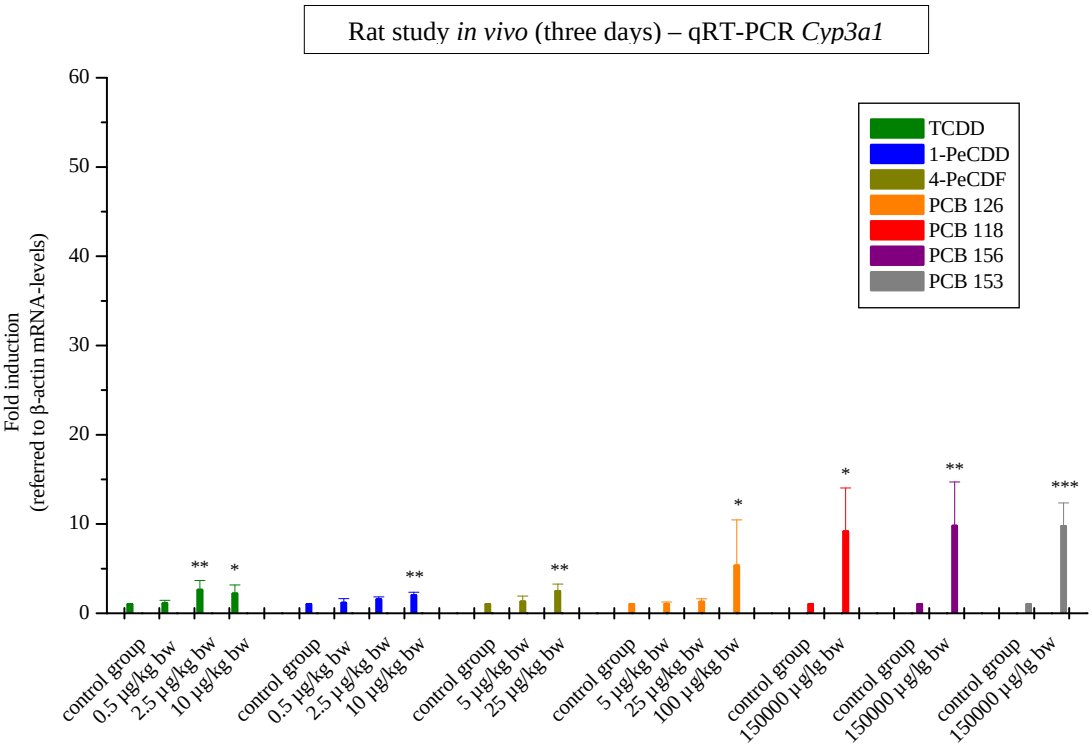

Figure 30: QRT-PCR (*Cyp3a1*) rat study *in vivo* (three days). Rats treated with single doses of TCDD, 1-PeCDD, 4-PeCDF, PCB 118, PCB 126, PCB 153, or PCB 156 for three days. Abscissa: Treatment; ordinate: Fold induction (referred to β-actin mRNA-levels). One-way ANOVA with Dunnett's post test (control vs. treatment groups); Two-tailed unpaired t-test (control vs. one treatment group). Six animals per group.*: p-value < 0.05, **: p-value < 0.01, ***: p-value < 0.001.

Cyp3a1-mRNA was marginally induced in rat livers subsequent to TCDD-exposure (figure 30). Statistically very significant (p-value < 0.01), or significant (p-value < 0.05) values were obtained using 2.5 µg/kg bw TCDD (2.6±1.1-fold), or 10 µg/kg bw TCDD (2.2±1.0-fold), respectively. Highest analyzed dose groups (N-groups) of 1-PeCDD, and 4-PeCDF led to slight, statistically very significant (p-value < 0.01) *Cyp3a1*-inductions of 2.0(±0.4)-fold (10 µg/kg bw 1-PeCDD), and 2.4(±0.8)-fold (25 µg/kg bw 4-PeCDF). Also, samples of the N-group for PCB 126-treatment (100 µg/kg bw) showed slight, statistically significant (p-value < 0.05) *Cyp3a1*-induction in rat livers, accounting for 5.3(±5.1)-fold. Respectable standard deviation was originated from a discordant value belonging to one animal (16.2-fold induction), whereby five animals exhibited *Cyp3a1*-values ranging from 1.1-, to 6.6-fold in livers.

Treatment of rats with PCBs 118, 153, or 156 (150000 µg/kg bw each) led to increase of *Cyp3a1*-mRNA-levels in livers. With respect to PCB 118, statistically significant (p-value < 0.05) value of 9.1(±4.9)-fold was obtained. PCB 156 statistically very significantly (p-value < 0.01) induced *Cyp3a1* 9.8(±4.9)-fold, whereas PCB 153 statistically extremely significantly (p-value < 0.01) enhanced *Cyp3a1*-mRNA-levels (9.7±2.6-fold) compared to respective control group.

In figure 31, results of qRT-PCR analysis regarding *Cyp3a1* and 14 days-studies with rats exposed to single doses of core congeners are depicted.

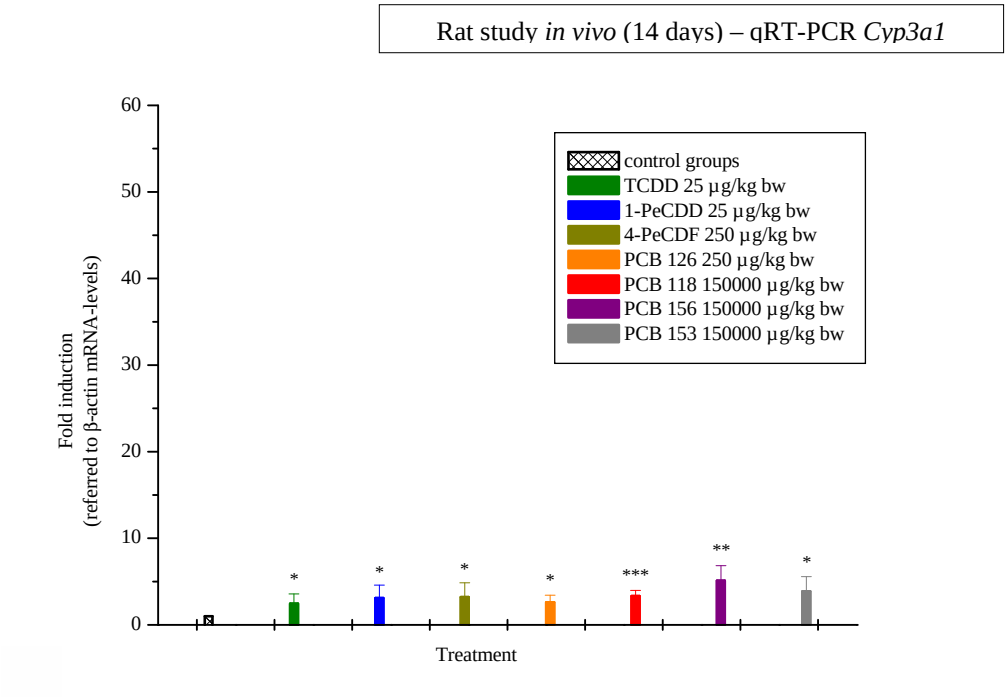

Figure 31: QRT-PCR (*Cyp3a1*) rat study *in vivo* (14 days). Rats treated with single doses of TCDD, 1-PeCDD, 4-PeCDF, PCB 118, PCB 126, PCB 153, or PCB 156 for 14 days. Abscissa: Treatment; ordinate: Fold induction (referred to β-actin mRNA-levels). Two-tailed unpaired t-test (control vs. one treatment group). Six animals per group.*: p-value < 0.05, **: p-value < 0.01, ***: p-value < 0.001.

Throughout core congeners, light inducing effects on *Cyp3a1*-mRNA-levels in rat livers were obtained subsequent to 14 days of single dose-exposures (figure 31). Smallest effects, which were statistically significant (p-value < 0.05), were achieved due to TCDD-, 1-PeCDD-, 4-PeCDF-, or PCB 126-treatment, and accounted for 2.5(±1.1)-fold (25 µg/kg bw TCDD), 3.1(±1.5)-fold (25 µg/kg bw 1-PeCDD), 3.2(±1.7)-fold (250 µg/kg bw 4-PeCDF), or 2.6(±0.8)-fold (250 µg/kg bw PCB 126), respectively.

Slightly higher *Cyp3a1*-inducing effects were gained by use of 150000 µg/kg bw of PCB 118, PCB 153, or PCB 156. PCB 153 led to statistically significantly (p-value < 0.05) enhanced *Cyp3a1*-mRNA-levels of 3.9(±1.7)-fold in rat livers, whereas treatment with PCB 156 statistically very significantly (p-value < 0.01) induced *Cyp3a1* to 3.9(±1.7)-fold. From statistical point of view, extremely significantly (p-value < 0.001) increased number of *Cyp3a1*-gene transcripts in rat livers (3.3±0.7-fold) were gained with PCB 118.

4.2. *In vitro* – Liver Cell Systems

4.2.1. Alamar Blue® assay

Before testing compounds regarding their AhR-interacting potential, substances were profiled with respect to cytotoxity. For this purpose, the Alamar Blue® assay was performed after primary rat hepatocytes as wells as H4IIE cells were incubated with compounds for 24 h. Statistically, saponin (0.1%), which was used as positive control for cytotoxic effects (reviewed in Podolak *et al.*, 2010), extremely significantly (p-value < 0.0001) reduced cell viability to 2.0±2.3% (n = 47) in H4IIE cells, and to 0.50±0.46% (n = 48) in Sprague Dawley primary rat hepatocytes, respectively. Viabilities are displayed in per cent related to appendant solvent controls (DMSO 0.1%). Figure 32 overviews Alamar Blue® assay results regarding H4IIE cells treated with PCDDs for 24 h.

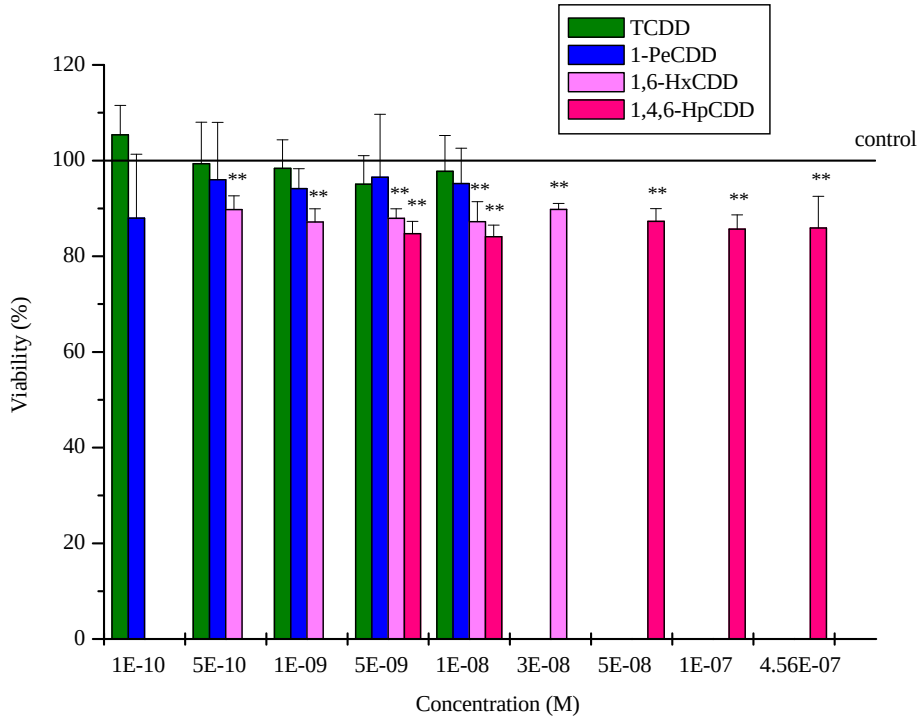

Figure 32: Alamar Blue® assay H4IIE. Cells treated with PCDDs for 24 h. Abscissa: Concentration (M); ordinate: Viability (%). Viabilities displayed relative to respective solvent controls (DMSO 0.1%). Results from at least three independent experiments each. One-way ANOVA with Dunnett's post test (control vs. treatments). **: p-value < 0.01.

Incubation with TCDD or 1-PeCDD for 24 h led to no cytotoxic effects in H4IIE cells (figure 32) in applied concentrations (100 pM-10 nM). For both 1,6-HxCDD and 1,4,6-HpCDD, minor but statistically very significant (p-value < 0.01) cytotoxic effects were determined in used range of

concentrations. 1,6-HxCDD maximally reduced viability of H4IIE cells to 87,2(±2.8)% (1 nM 1,6-HxCDD) after 24 h. 1,4,6-HpCDD-treated H4IIE cells were viable from 84.1(±2.4)% to 87.3(±2.7)% (5-456 nM 1,4,6-HpCDD). Concerning 1,6-HxCDD, as well as 1,4,6-HpCDD, determined cytotoxicities in H4IIE cells showed no concentration dependence.

In figure 33, Alamar Blue® assay results for H4IIE cells treated with PCDFs (24 h) are summarized.

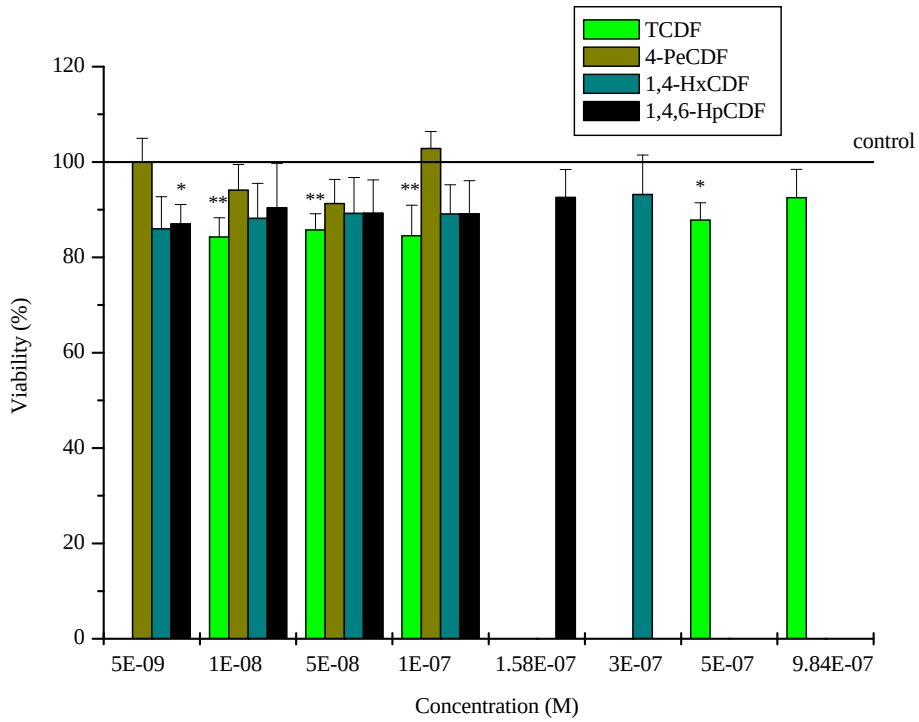

Figure 33:Alamar Blue® assay H4IIE. Cells treated with PCDFs for 24 h. Abscissa: Concentration (M); ordinate: Viability (%). Viabilities displayed relative to respective solvent controls (DMSO 0.1%). Results from at least three independent experiments each. One-way ANOVA with Dunnett's post test (control vs. treatments). *: p-value < 0.05; **: p-value < 0.01.

TCDF-incubated H4IIE cells possessed statistically significant (p-value < 0.05) and very significant (p-value < 0.01) reductions of viability (figure 33). The significant effect (500 nM TCDF) amounted to 87.8(±3.6)%, whereas very significant cytotoxicities accounted for 84.3(±4.1)% to 85.8(±3.4)% viable cells (1-100 nM TCDF). Mentioned cytotoxicities showed no concentration dependence. The highest used TCDF concentration (984 nM) was not cytotoxic in this cell system, as well. With regard to 1,4,6-HpCDF, incubation with 5 nM for 24 h resulted in a statistically significant (p-value < 0.05) reduction of cell viability to 87.0(±4.1)%. However, higher

concentrations of this compound showed no cytotoxicity. No cytotoxic effects in H4IIE cells were revealed subsequent to cell-treatment with 4-PeCDF, or 1,4-HxCDF, respectively.

Figure 34 compares Alamar Blue® assay results with respect to H4IIE cells, which were treated with PCBs for 24 h.

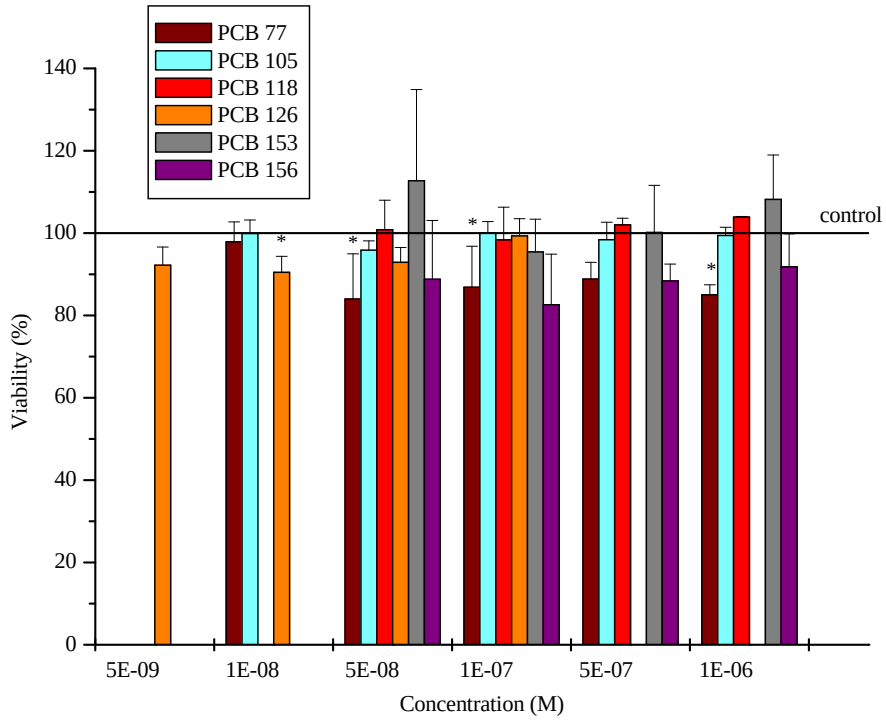

Figure 34: Alamar Blue® assay H4IIE. Cells treated with PCBs for 24 h. Abscissa: Concentration (M); ordinate: Viability (%). Viabilities displayed relative to respective solvent controls (DMSO 0.1%). Results from at least three independent experiments each. One-way ANOVA with Dunnett's post test (control vs. treatments). *: p-value < 0.05.

Figure 34 reveals no statistically significant concentration-dependent effects on viability in H4IIE cells resulting from PCBs in used range of concentrations after 24 h of treatment. For PCB 126, a statistically significant (p-value < 0.05) cytotoxic effect (90.5(±3.9)% viable cells) was found for the lowest determined concentration (5 nM). Incubation with PCB 77 in concentrations between 5 nM and 1 µM statistically significantly (p-value < 0.05) reduced cell viability to a minimum of 84.0(±11.0)%. PCBs 105, 118, 153, or 156 did not show any cytotoxic effect on H4IIE cells in the Alamar Blue® assay.

Figure 35 illustrates Alamar Blue® assay results regarding Sprague Dawley primary rat hepatocytes treated with PCDDs for 24 h.

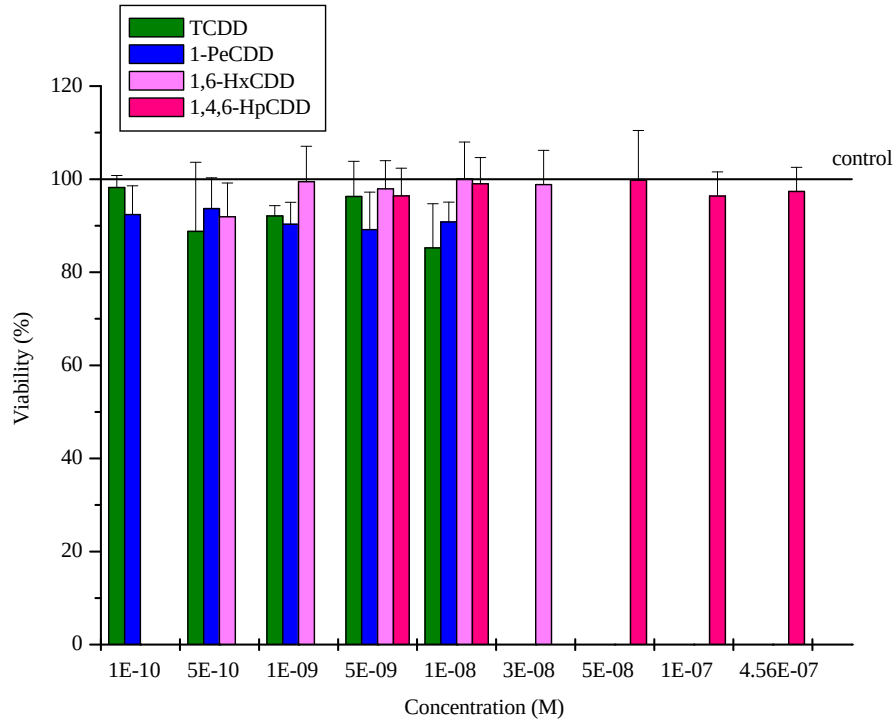

Figure 35: Alamar Blue® assay PRH. Cells treated with PCDDs for 24 h. Abscissa: Concentration (M); ordinate: Viability (%). Viabilities displayed relative to respective solvent controls (DMSO 0.1%). Results from at least three independent experiments each. One-way ANOVA with Dunnett's post test (control vs. treatments).

Incubation with TCDD, 1-PeCDD, 1,6-HxCDD, or 1,4,6-HpCDD did not lead to any statistically significant cytotoxic effect in primary rat hepatocytes attained from male Sprague Dawley rats (figure 35).

Alamar Blue® assay results concerning Sprague Dawley primary rat hepatocytes incubated with PCDFs for 24 h are portrayed in figure 36.

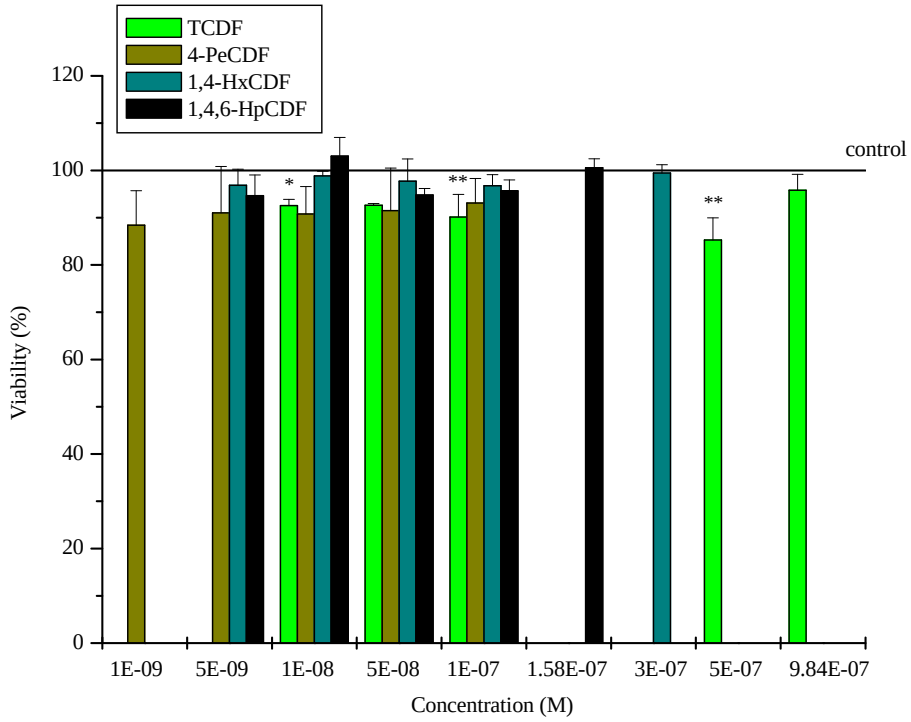

Figure 36: Alamar Blue® assay PRH. Cells treated with PCDFs for 24 h. Abscissa: Concentration (M); ordinate: Viability (%). Viabilities displayed relative to respective solvent controls (DMSO 0.1%). Results from at least three independent experiments each. One-way ANOVA with Dunnett's post test (control vs. treatments). *: p-value < 0.05; **: p-value < 0.01

Figure 36 bears no statistically significant concentration-dependent effect on viability of primary rat hepatocytes subsequent to incubation with polychlorinated dibenzofurans for 24 h. However, several TCDF-concentrations led to statistically significant incidences. The maximum effect (p-value < 0.01) added up to 85.3(±4.7)% viable cells for 500 nM TCDF. In turn, the highest TCDF-concentration 984 nM did not impact any statistical relevance regarding cytotoxicity in Alamar Blue® assay. The same applied to 4-PeCDF, 1,4-HxCDF, as well as 1,4,6-HpCDF for all examined concentrations.

Figure 37 illustrates Alamar Blue® assay data received from PCB-incubated Sprague Dawley primary rat hepatocytes.

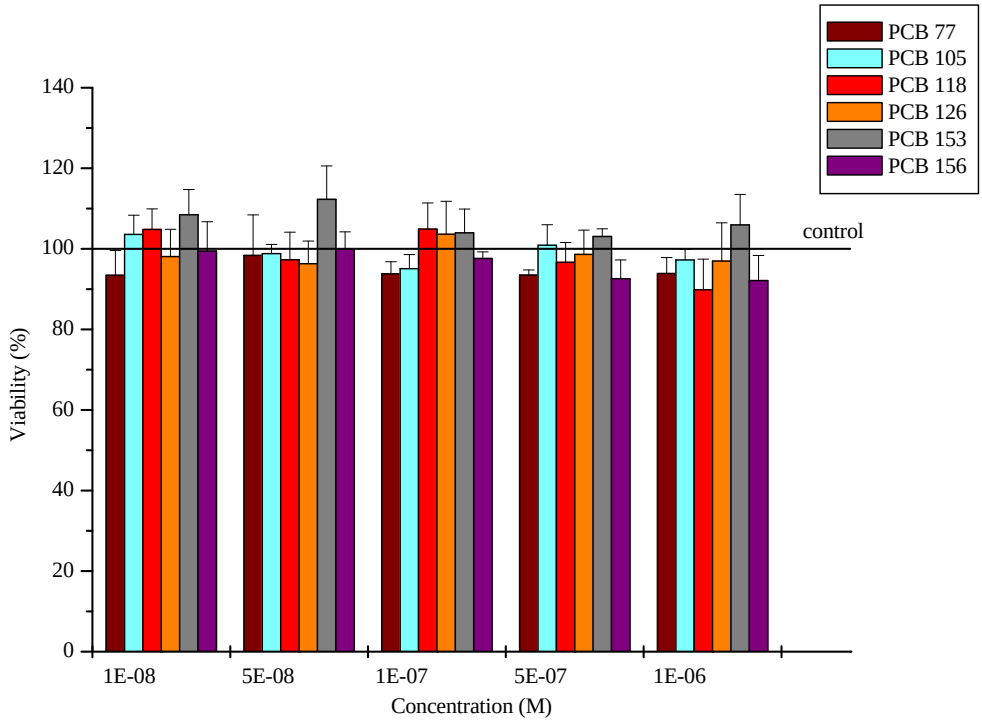

Figure 37: Alamar Blue® assay PRH. Cells treated with PCBs for 24 h. Abscissa: Concentration (M); ordinate: Viability (%). Viabilities displayed relative to respective solvent controls (DMSO 0.1%). Results from at least three independent experiments each. One-way ANOVA with Dunnett's post test (control vs. treatments).

No statistically significant cytotoxic effect is depicted in figure 37. Incubation of primary rat hepatocytes with PCBs 77, 105, 118, 126, 153, or 156 did not affect cell viability in the present test system.

4.2.2. Ethoxyresorufin Deethylase (EROD) assay and Western Blot

Defining congeners' AhR-interacting properties towards H4IIE cells and Sprague Dawley primary rat hepatocytes after 24 h of exposure, CYP1A-induction was examined. To approach to this objective, CYP1A1- and CYP1A2-induction was studied using EROD assay. Besides, CYP1A1 protein levels were analyzed semi-quantitatively via Western Blotting. Up to 13 diverse concentrations of congeners were analyzed to yield concentration-response-relations, which supposed to enable comparisons both among compounds and with TCDD-derived effects.

4.2.2.1. EROD assay and Western Blot – H4IIE cells

For measurement of CYP1A1 and CYP1A2-induction on protein level by use of Western Blotting as well as EROD-induction, TCDD (1 nM) served as positive control for AhR-dependent enzyme-induction in H4IIE cells. With respect to Western Blots, VDAC was measured as loading control in microsomes derived from treated H4IIE cells. From EROD-activities induced by congeners, background levels (DMSO 0.1%) were subtracted.

In figure 38, the concentration-response slope illustrating EROD induction in H4IIE cells subsequent to 24 h of incubation with TCDD is compared to a correspondent representative CYP1A1-Western Blot.

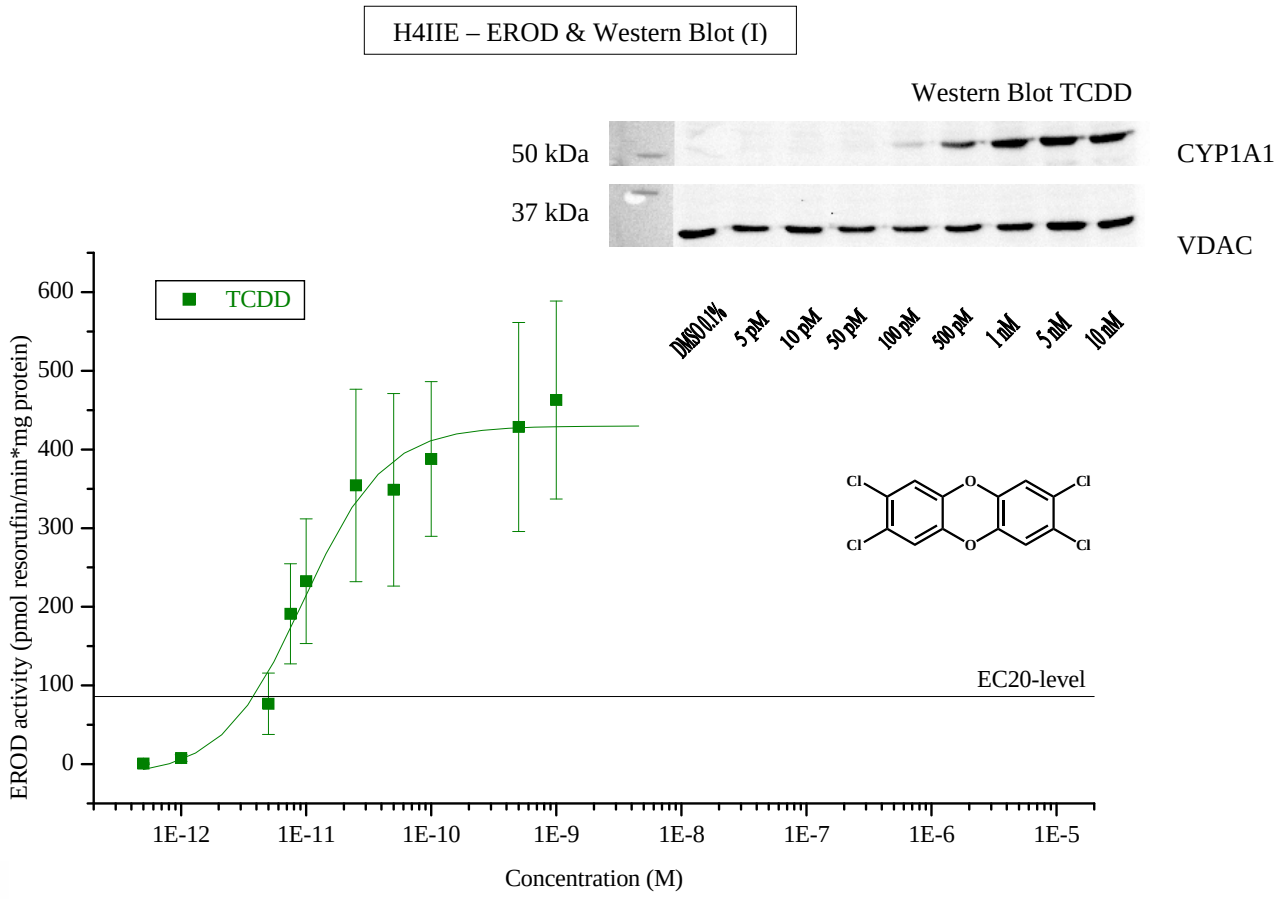

Figure 38: EROD assay and Western Blot H4IIE (I). Cells treated with TCDD for 24 h. Concentration (M) logarithmically plotted against EROD-activity (pmol resorufin/min*mg protein). EC20-level (86.0 pmol resorufin/min*mg protein) represents 20% of TCDD-induced maximum response. Exemplary CYP1A1-and VDAC-Western Blot from microsomes. Results from at least three independent experiments each.

To generate a concentration-response slope concerning TCDD-derived EROD-inducing effects in H4IIE cells, concentrations from $5*10^{-13}$ to 10^{-9} M were incubated for 24 h (figure 38).

With $5*10^{-13}$ M TCDD, EROD-activity in H4IIE cells basically remained at background level (0.6±0.9 pmol resorufin/min*mg protein). From 10^{-12} M TCDD, a slight (7.7±4.3 pmol resorufin/min*mg protein), followed by an exponential increase of EROD-induction was given. Hence, $5*10^{-12}$ M TCDD led to an EROD-activity of 76.7(±39.0) pmol resorufin/min*mg protein in H4IIE cells subsequent to 24 h of incubation. Statistically (One-way ANOVA with Dunnett's post test; control vs. treatments), a significant increase (p-value < 0.05) of EROD-activity (232.6±79.3 pmol resorufin/min*mg protein) compared to control (DMSO 0.1%, not shown) was observed for 10^{-11} M TCDD. This significance, which was accompanied by transition from an exponential to a logarithmical ascent of curve, passed into a statistically very significant value (p-value < 0.05) for $2.5*10^{-11}$ M TCDD with 354.3(±122.4) pmol resorufin/min*mg protein. Concentration-dependently, the increase of EROD-activity pursued, until a plateau was reached at 429.8(±21.4) pmol resorufin/min*mg protein, given by the maintained concentration-response slope. The TCDD-derived EC50 amounted to $9.49(\pm1.71)*10^{-12}$ M TCDD under present conditions. 20% of maximum effect was calculated for $3.80*10^{-12}$ M TCDD. The respective EROD-activity of 86.0 pmol resorufin/min*mg protein was defined as EC20-level and used for further EROD-investigations with H4IIE cells. Per definition, REP values (REP (EC20); REP (EC50)) for TCDD with respect to EROD-induction were 1.

The Western Blot membrane pictured in figure 38 constitutes a representative example of four independent experiments. H4IIE cells were treated with eight different concentrations of TCDD, varying from $5*10^{-12}$ M to 10^{-8} M. The loading control VDAC (32 kDA) consistently was measured regularly for each incubation. Isolated microsomes contained no detectable CYP1A1-protein from solvent control (DMSO 0.1%) to $5*10^{-11}$ M TCDD.
By use of 10^{-10} M TCDD, the protein CYP1A1 (56 kDa) marginally appeared on the membrane. With greater concentrations of TCDD, the CYP1A1-bands emerged more pronounced, which balanced at a maximal level for the highest tested concentrations, $5*10^{-9}$ M and 10^{-8} M TCDD.

Comparing both methods for verification of CYP1A on protein level in H4IIE cells, different limits for detection were indicated by use of TCDD. Even though a statistically relevant EROD-induction was seen from 10^{-11} M TCDD, an obvious increase of EROD-activity was given even with concentrations from around $5*10^{-12}$ M TCDD, whereas for Western Blotting, CYP1A1 was not detectable below 10^{-10} M TCDD in the present test system.

Figure 39 compares EROD-induction in H4IIE cells due to treatment with 1-PeCDD, 1,6-HxCDD, or 1,4,6-HpCDD for 24 h with TCDD-derived effects. Besides, representative examples of Western Blot membranes, which semi-quantitatively show CYP1A1-induction in microsomes obtained from H4IIE cells incubated with 1-PeCDD, 1,6-HxCDD, or 1,4,6-HpCDD, are presented in figure 39.

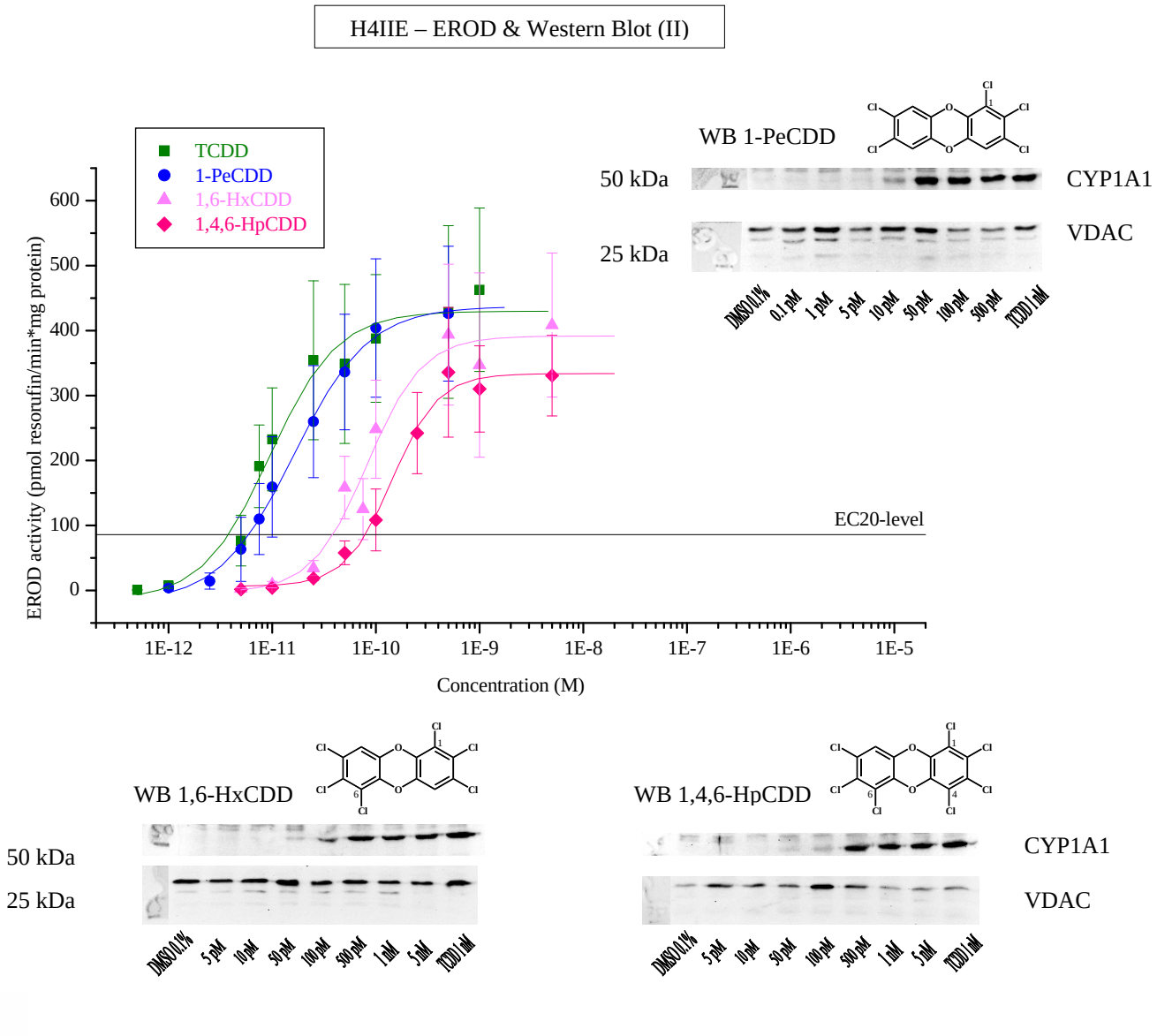

Figure 39: EROD assay and Western Blot H4IIE (II). Cells treated with TCDD, 1-PeCDD, 1,6-HxCDD, or 1,4,6-HpCDD, 24 h. Abscissa (logarithm.): Concentration (M); ordinate: EROD-activity (pmol resorufin/min*mg protein). EC20-level represents 20% of TCDD-induced maximum response. Exemplary CYP1A1-and VDAC-Western Blots from microsomes. Results from at least three independent experiments each.

Tested 1-PeCDD concentrations for EROD assay were 10^{-12} to $5*10^{-10}$ M. Subsequent to incubation of 10^{-12} M 1-PeCDD for 24 h, EROD-activity (3.8±3.4 pmol resorufin/min*mg protein) mostly remained at background level (figure 39). From $2.5*10^{-12}$ M 1-PeCDD, an initial slow increase of active CYP1A advanced exponentially with higher concentrations. On account of this, statistically

very significant (p-value < 0.01; One-way ANOVA with Dunnett's post test; control vs. treatments) distinctions compared to solvent control (DMSO 0.1%, not shown) appeared from $2.5*10^{-11}$ to $5*10^{-10}$ M 1-PeCDD (426.1±103.7 pmol resorufin/min*mg protein). According to the obtained concentration-response slope, EC50 for 1-PeCDD-derived EROD-induction in H4IIE cells was $1.62*10^{-11}(\pm 1.52*10^{-12})$ M 1-PeCDD, which led to a REP (EC50) of 0.58. The calculated EC20 value was $5.98*10^{-12}$ M, which brought forth a REP (EC20) of 0.64 for 1-PeCDD. The maximum extent of EROD-activity induced by 1-PeCDD (437.2±13.3 pmol resorufin/min*mg protein) highly correlated with the TCDD-derived upper level (429.8±21.4 pmol resorufin/min*mg protein).

Compared to TCDD- and 1-PeCDD-derived curves reflecting EROD-induction in H4IIE cells, curves obtained by 1,6-HxCDD, or by 1,4,6-HpCDD were sparsely shifted to higher concentrations. Lowest concentrations leading to statistically very significant (p-value < 0.01) increases of EROD-induction were 10^{-10} M 1,6-HxCDD (248.2±75.6 pmol resorufin/min*mg protein), or $2.5*10^{-10}$ M 1,4,6-HpCDD (242.3±62.6 pmol resorufin/min*mg protein), respectively.

In a concentration-range from $5*10^{-10}$ M to $5*10^{-9}$ M, upper limits of EROD-induction were accomplished for both the six-and the seven-fold chlorine-substituted dioxin. Upper asymptotes of sigmoid curves counted to 391.7(±28.1) pmol resorufin/min*mg protein for 1,6-HxCDD, and to 333.8(±13.1) pmol resorufin/min*mg protein for 1,4,6-HpCDD. In correspondence to similar concentration-response slopes, EC50-values of these congeners lay close together and amounted to $8.25*10^{-11}(\pm 1.69*10^{-11})$ M 1,6-HxCDD, or $1.43*10^{-10}(\pm 1.64*10^{-11})$ M 1,4,6-HpCDD. Respective REPs (EC50) were 0.12 (1,6-HxCDD), and 0.066 (1,4,6-HpCDD). Related instances were given for EC20-values, which added up to $3.88*10^{-11}$ M 1,6-HxCDD, or $7.98*10^{-11}$ M 1,4,6-HpCDD, and correlated with REPs for EC20 of 0.10 (1,6-HxCDD), and 0.048 (1,4,6-HpCDD), respectively.

Although transported slightly to higher concentrations, the run of the EROD-induction concentration-response curve belonging to 1-PeCDD rather reflected the TCDD-derived curve regarding ascent and value of the upper asymptote. Mentioned shift to higher concentrations appeared more prominent for six-and seven-fold chlorine-substituted dioxins. Regarding analyzed congeners, a higher number of chlorine-substituents correlated with a higher extent of shift to higher concentrations, deriving the most prominent effect for six chlorine-substituents instead of five. Furthermore, upper limits of EROD-induction in H4IIE cells lay in an order of magnitude for all tested dioxins, whereas along with lowering efficacy of compounds, the potency decreased with increasing number of chlorine-substituents.

Exemplary Western Blot membranes obtained after analysis of microsomes gained by dioxin-incubated H4IIE cells showed consistent appearance of VDAC-loading controls (32 kDa) for all plotted samples. Distinct CYP1A1-inductions (56 kDa) were seen for positive controls (TCDD 10^{-9} M). From solvent control (DMSO 0.1%) to a 1-PeCDD concentration of $5*10^{-12}$ M, no CYP1A1 protein was detectable, whereas a minimal induction initiated with 10^{-11} M 1-PeCDD. From $5*10^{-11}$ M to $5*10^{-10}$ M of the congener, an almost indistinguishable degree of CYP1A1-induction was manifested. In contrast, for both 1,6-HxCDD and 1,4,6-HpCDD, compound concentrations of $5*10^{-11}$ M led to a minor CYP1A1-induction detectable via Western Blotting, which initially increased using 10^{-10} M of respective congener, and reached maximum levels within a concentration range of $5*10^{-10}$ M to $5*10^{-9}$ M.

The progressivity of concentration-dependent CYP1A1-induction was more pronounced by use of 1,6-HxCDD compared to 1,4,6-HpCDD. Maximum effects due to PCDD-exposure to H4IIE cells induced CYP1A1-protein levels possessing similar extents compared to TCDD-controls. Regarding required concentrations of 1-PeCDD, 1,6-HxCDD, or 1,4,6-HpCDD, a light correlation between passing the EC20-level of EROD-induction and detectable CYP1A1-protein in Western Blot was observed.

Both used methods gave comparable ranges of PCDD-concentrations for relevant, and according to EROD-measurement, even statistically relevant, levels of CYP1A(1)-protein in H4IIE cells:
10^{-11}-$2.5*10^{-11}$ M 1-PeCDD; $5*10^{-11}$-10^{-10} M 1,6-HxCDD; and $5*10^{-11}$-$2.5*10^{-10}$ M 1,4,6-HpCDD.

Following figure summarizes results for EROD-induction and appendant CYP1A1-Western Blots obtained after analyzing effects of PCDFs on H4IIE cells.

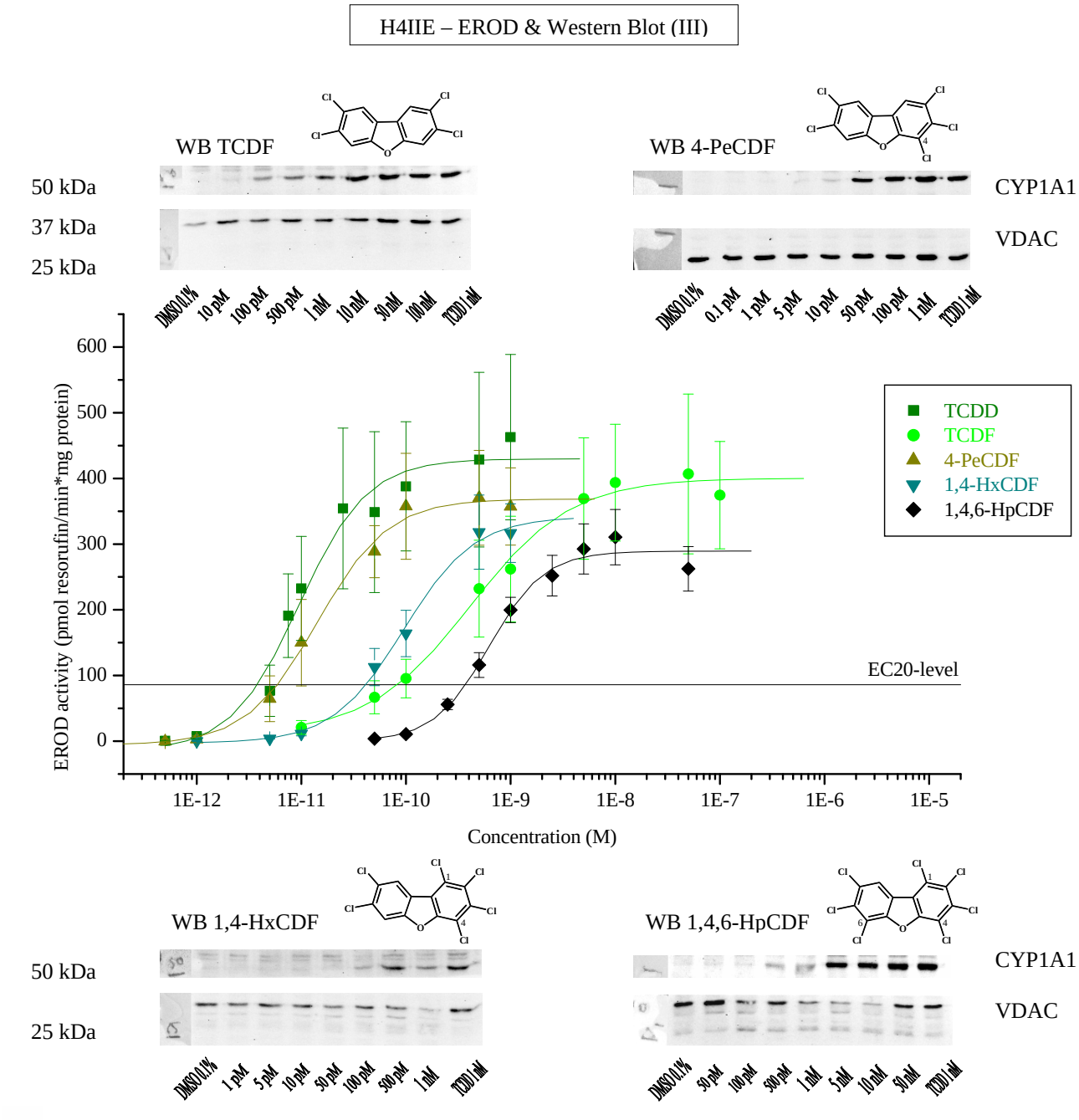

Figure 40: EROD assay and Western Blot H4IIE (III). Cells treated with TCDD, TCDF, 4-PeCDF, 1,4-HxCDF, or 1,4,6-HpCDF for 24 h. Abscissa (logarithm.): Concentration (M); ordinate: EROD-activity (pmol resorufin/min*mg protein). EC20-level represents 20% of TCDD-induced maximum response. Exemplary CYP1A1-and VDAC-Western Blots from microsomes. Results from at least three independent experiments each.

Studying PCDFs regarding their EROD-inducing properties after 24 h, EROD-activity in H4IIE cells increased in concentration-dependent manners, as it has been shown for TCDD. Referring to run and their position on the abscissa, the concentration-response slope received for 4-PeCDF

represented the most accordant of the curves for PCDFs compared to the TCDD-derived curve (figure 40). Subsequent to a slight increase of EROD-activity along with lowest used concentrations (10^{-13}-10^{-12} M 4-PeCDF), the increase amplified to 64.6(±34.8) pmol resorufin/min*mg protein for $5*10^{-12}$ M 4-PeCDF, and was followed by statistically very significant (p-value < 0.01, One-way ANOVA with Dunnett's post test; control vs. treatments) EROD-inducing values starting from 10^{-11} M 4-PeCDF with 150(±65.9) pmol resorufin/min*mg protein. The growth of EROD-induction asymptotically reached maximum levels of 368.7(±10.4) pmol resorufin/min*mg protein at around 10^{-10}-10^{-9} M 4-PeCDF.
EC50 was $1.43*10^{-11}$($\pm 1.73*10^{-11}$) M 4-PeCDF, whereas the EC20 value at 86 pmol resorufin/min*mg protein was calculated as $5.92*10^{-12}$ M 4-PeCDF. Corresponding REPs were 0.67 (REP (EC50)), and 0.64 (REP (EC20)).

Considering the constraint of a shift to higher concentrations, a similar run of the concentration-response slope was obtained by use of 1,4-HxCDF. Statistically very significant (p-value < 0.01) values were gained from $5*10^{-11}$ M of the compound, and the upper asymptote level reached 341.8(±22.7) pmol resorufin/min*mg protein.
EC values, which both varied to an extent of a factor of ten to higher concentrations compared to the pentafuran's EC values, were $9.48*10^{-11}$($\pm 1.52*10^{-11}$) M 1,4-HxCDF for EC50, and $4.16*10^{-11}$ M 1,4-HxCDF for EC20. Respective REPs were 0.10 for EC50, and 0.091 referring to EC20.

The concentration-response slope gained by use of 1,4,6-HpCDF was shifted approximately another factor of ten to higher concentrations compared to the hexafuran's. With this regard, REPs expressing EROD-inducing properties of the heptafuran were 0.015 (REP (EC50); EC50: $6.25*10^{-10}$($\pm 9.24*10^{-11}$) M 1,4,6-HpCDF), and 0.010 (REP (EC20); EC20: $3.72*10^{-19}$ M 1,4,6-HpCDF).
Statistically very significant EROD-inductions (p-value < 0.01) were obtained with $5*10^{-10}$ M 1,4,6-HpCDF (115.9±18.8 pmol resorufin/min*mg protein). Furthermore, the maximally achieved EROD-activity received by treating H4IIE cells with 1,4,6-HpCDF for 24 h was 289.4(±11.9) pmol resorufin/min*mg protein.

In contrast, the concentration-response curve deduced from incubation of H4IIE cells with TCDF differed concerning growth und run from the TCDD-derived curve, as well as from the curves of the other tested furans. The flatter ascent of slope combined with an upper asymptotic level of

400.5(±12.3) pmol resorufin/min*mg protein led to an EC50 value of $4.12*10^{-10}$($\pm 8.81*10^{-11}$) M TCDF, and an EC20 of $8.34*10^{-11}$ M TCDF. Yielded REPs were 0.023 (EC50), and 0.046 (EC20), respectively. Statistically very significant increases of EROD-activities (p-value < 0.01) from solvent control (DMSO 0.1%, not shown) were indicated from $5*10^{-10}$ M TCDF and 232.2(±73.7) pmol resorufin/min*mg protein.

Regarding exemplary CYP1A1 Western Blots pictured in figure 40, the protein VDAC (32 kDa) served as loading control and was detected rather uniformly for all analyzed microsomes. Positive controls (TCDD 1 nM) showed intense bands of CYP1A1-protein (56 kDa) in each case.
Light CYP1A1-bands were detected for 10^{-10} M TCDF, $5*10^{-12}$-10^{-11} M 4-PeCDF, 10^{-10} M 1,4-HxCDF, or $5*10^{-10}$-10^{-9} M 1,4,6-HpCDF. These findings as well as subsequent exponential increases of CYP1A1-band-intensities with higher concentrations for 4-PeCDF, 1,4-HxCDF, or 1,4,6-HpCDF mirrored conditions foreseen in EROD-measurements. Furthermore, listed concentrations of PCDFs generating light CYP1A1-bands approximated respective EC20-values. Highest tested concentrations of congeners depicted CYP1A1-band-intensities in comparable extents to those of positive controls.
Maximum and barely indistinguishable CYP1A1-inductions were gained using following concentrations of compounds: 10^{-8}-10^{-7} M TCDF, $5*10^{-11}$-10^{-9} M 4-PeCDF, $5*10^{-10}$-10^{-9} M 1,4-HxCDF, or $5*10^{-9}$-$5*10^{-8}$ M 1,4,6-HpCDF.

On the whole, among tested PCDFs, microsomes obtained by incubation of H4IIE cells with 1,4-HxCDF established minor CYP1A1-band-intensities correlating with an overall lower protein content of samples indicated by slight VDAC-bands. Reflecting results of EROD-measurements, analysis of microsomes from TCDF-treated H4IIE cells exhibited less rapid exponential increases of CYP1A1-band-intensities compared to results obtained by TCDD or previously discussed furans, visible in an exemplary Western Blot membrane in figure 40. Mentioned increases proceeded over a concentration-range of 10^{-10}-10^{-8} M TCDF, whereas such increases were completed within a half-logarithmical modification of concentrations regarding the other PCDFs.

In figure 41, results for EROD measurement and CYP1A1-Western Blotting using non-*ortho*-substituted PCBs (PCB 77, or PCB 126), or the mono-*ortho*-substituted PCB 156 compared to TCDD-derived effects towards H4IIE cells are compiled.

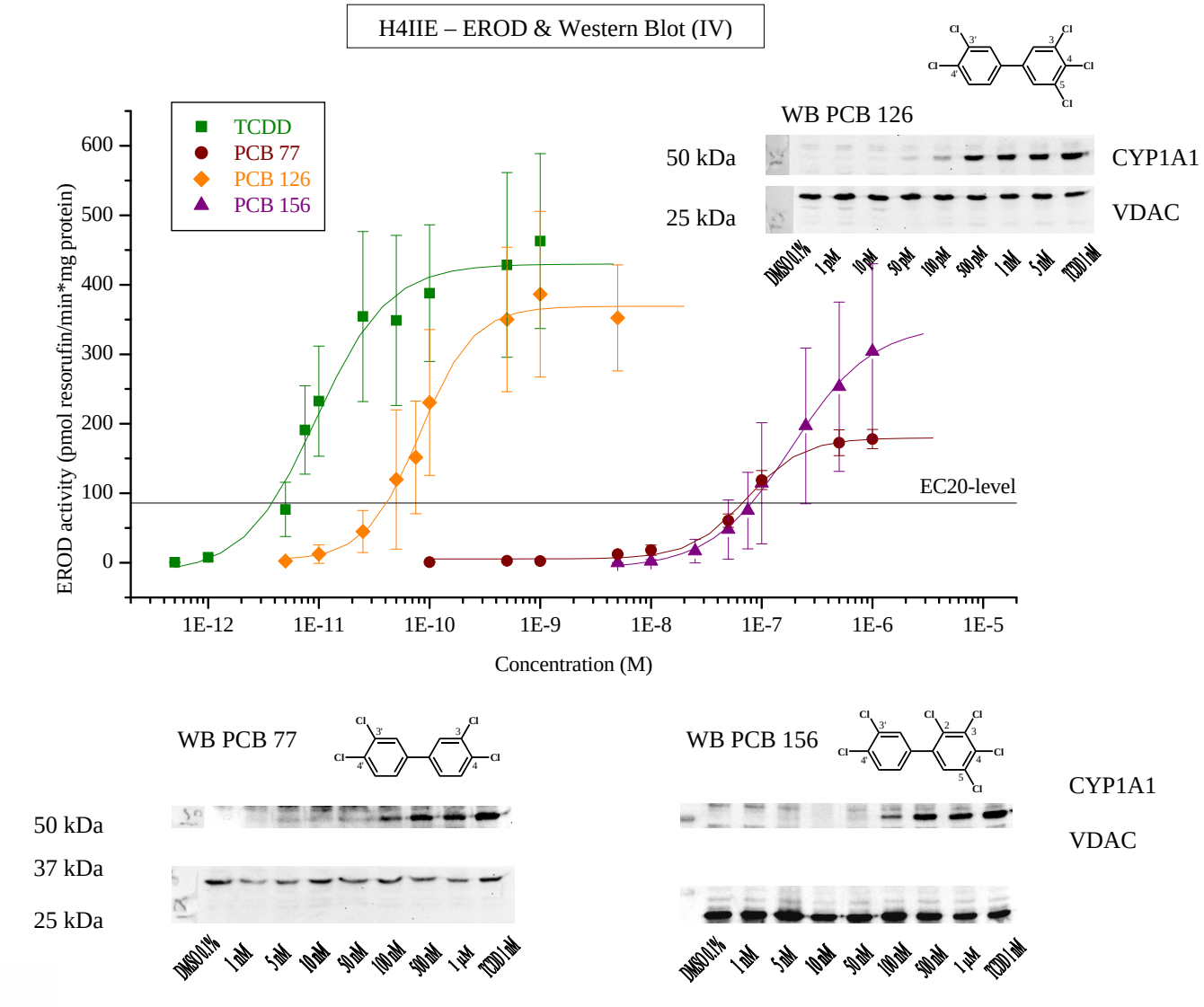

Figure 41: EROD assay and Western Blot H4IIE (IV). Cells treated with TCDD, PCB 77, PCB 126, or PCB 156 for 24 h. Abscissa (logarithm.): Concentration (M); ordinate: EROD-activity (pmol resorufin/min*mg protein). EC20-level represents 20% of TCDD-induced maximum response. Exemplary CYP1A1-and VDAC-Western Blots from microsomes. Results from at least three independent experiments each.

Studying PCB-mediated EROD-activities in H4IIE cells, PCB 126 most notably exhibited conformable characteristics compared to effects induced by TCDD (figure 41). Application of this 3,3',4,4',5-pentaCB led to concentration-dependent EROD-induction in sigmoid manner subsequent to 24 h of incubation. Passing statistically significant (p-value < 0.05; 10^{-10} M PCB 126, 230.6±104.9 pmol resorufin/min*mg protein; One-way ANOVA with Dunnett's post test; control vs. treatments), and successive statistically very significant (p-value < 0.01) values from

$5*10^{-10}$ M PCB 126 with 350.1(±103.9) pmol resorufin/min*mg protein, EROD-induction culminated in an asymptotic level of 369.1(±11.5) pmol resorufin/min*mg protein. Deduced from the concentration-response slope, EC50 was $8.18*10^{-11}$($\pm 7.12*10^{-12}$) M PCB 126, whereas EC20 value was $4.12*10^{-11}$ M PCB 126 with corresponding REPs of 0.12 (REP (EC50)), and 0.092 (REP (EC20)), respectively.

Transported to higher concentrations combined with a shift to lower maximum EROD-activities of 179.7(±5.0) pmol resorufin/min*mg protein, treatment with PCB 77 engendered an EC50 of $7.30*10^{-8}$($\pm 5.21*10^{-9}$) M PCB 77, and an EC20 of $6.69*10^{-8}$ M PCB 77. Respective REPs were 0.00013 (REP (EC50)), and 0.000057 (REP (EC20)). Use of 3,3',4,4'-tetraCB scored statistically very significant (p-value < 0.01) EROD inductions from $5*10^{-8}$ M PCB 77 (60.6±9.5 pmol resorufin/min*mg protein) to 10^{-6} M PCB 77 (177.9±13.8 pmol resorufin/min*mg protein).

Yielding similar potency but higher efficacy, incubation with PCB 156 afforded an EC50 of $1.87*10^{-7}$($\pm 2.08*10^{-8}$) M PCB 156, and an EC20 of $8.13*10^{-8}$ M PCB 156 in H4IIE cells. Associated REPs were 0.000051 for EC50, and 0.000047 for EC20.
Statistically very significant (p-value < 0.01) deviations from solvent control (DMSO 0.1%, not shown) were available from $5*10^{-7}$ to 10^{-6} M PCB 156, preceding a statistical significant (p-value < 0.05) value of 197.0(±112.0) pmol resorufin/min*mg protein for $2.5*10^{-7}$ M PCB 156. Focusing on the concentration-response slope gained by use of PCB 156 and EROD measurement, the upper asymptote was not yet reached under experimental conditions. Anyhow, according to progress of EROD-induction, the degree of logarithmical ascent initially lowered from around $5*10^{-7}$ M PCB 156, mathematically indicating the approaching asymptote. Applying sigmoid fitting extrapolated an upper asymptotic level of 342.1(±18.4) pmol resorufin/min*mg protein.

VDAC-loading controls (32 kDa) on Western Blot membranes obtained by analysis of microsomes from H4IIE cells incubated with PCBs for 24 h appeared consistently (figure 41). Furthermore, microsomes from positive control-treated (TCDD 1 nM) H4IIE cells engendered distinct CYP1A1-protein-bands (56 kDa).
Light CYP1A1-bands were detected due to impact of $5*10^{-11}$-10^{-10} M PCB 126, $5*10^{-8}$-10^{-7} M PCB 77, or 10^{-7} M PCB 156, which constituted ranges of concentration correlating with respective EC20 values for EROD-induction. With this regard, the shift amounted to three orders of magnitude concerning varying efficacies between PCB 77 and PCB 126, observed by means of EROD-measurement, was reinforced by Western Blotting. Likewise, effects of PCB 77, or PCB 156

approximated implying a slightly higher potency of PCB 77 in terms of both methods measuring CYP1A-protein. Light CYP1A1-inductions concentration-dependently merged into stronger protein-bands from $5*10^{-10}$ M PCB 126, $5*10^{-7}$ M PCB 77, or $5*10^{-7}$ M PCB 156, comparable regarding extent to those affected by positive controls (TCDD 1 nM).

Mono-*ortho*-substituted PCBs 105, or 118, as well as the NDL-PCB 153 were analyzed regarding their CYP1A-affecting properties towards H4IIE cells. Consequential results for EROD-measurements and CYP1A1-Western Blots are assembled in figure 42.

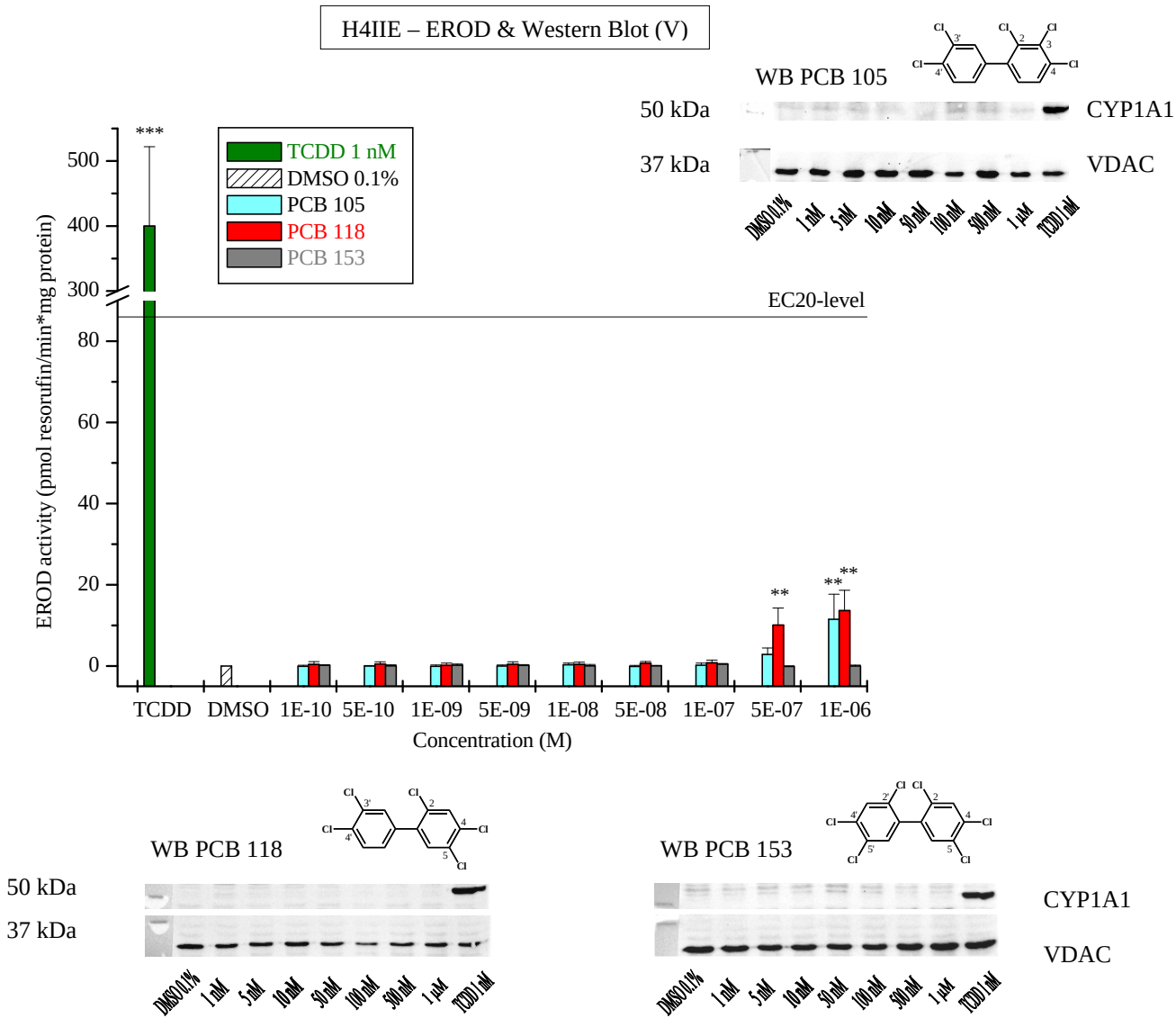

Figure 42: EROD assay and Western Blot H4IIE (V). Cells treated with TCDD, PCB 105, PCB 118, or PCB 153 for 24 h. Abscissa: Concentration (M); ordinate: EROD-activity (pmol resorufin/min*mg protein). EC20-level represents 20% of TCDD-induced maximum response. Exemplary CYP1A1-and VDAC-Western Blots from microsomes. Results from at least three independent experiments each. One-way ANOVA with Dunnett's post test (control vs. treatment groups); Two-tailed unpaired t-test (control vs. TCDD 1 nM; n = 42). **: p-value < 0.01; ***: p-value < 0.0001.

In figure 42, effects of the positive control TCDD (1 nM) on EROD-activity in H4IIE cells are illustrated. Average EROD-induction value was 400(±122) pmol resorufin/min*mg protein (n = 42) after 24 h, which statistically was considered extremely significant (p-value < 0.0001) compared to solvent-control (DMSO 0.1%).

Mono-*ortho*-substituted PCB 105 had no influence on EROD-activity from 10^{-10} to 10^{-7} M of the compound. Using $5*10^{-7}$ M of the 2,3,3',4,4'-pentaCB, EROD-activity slightly increased to 2.8(±1.6) pmol resorufin/min*mg protein. Mentioned increase enforced with the highest tested concentration of 10^{-6} M PCB 105, possessing a statistically very significant (p-value < 0.01) EROD-induction of 11.5(±6.2) pmol resorufin/min*mg protein compared to solvent control (DMSO 0.1%). Although marginally exhibiting higher efficacy, related conditions were obtained testing mono-*ortho*-substituted PCB 118 on H4IIE cells, whereby statistically very significant (p-value < 0.01) EROD-levels were yielded from $5*10^{-7}$ to 10^{-6} M 2,3,4,4',5-pentaCB amounting to 10.1(±4.2), and 13.6(±5.0) pmol resorufin/min*mg protein, respectively. Assaying mono-*ortho*-substituted PCBs 105, or 118 under present conditions, minor effects on EROD-activity remaining explicitly below EC20-level (86.0 pmol resorufin/min*mg protein) were gained.
NDL-PCB 153 (2,2',4,4',5,5'-hexaCB) had no effect on EROD levels in any of the administered concentrations ranging from 10^{-10} to 10^{-6} M PCB 153.

Western Blots of microsomes from PCB-treated H4IIE cells revealed a consistent appearance of VDAC-loading controls (32 kDa) for each plotted sample (figure 42). Analysis of microsomes from H4IIE cells incubated with the positive control (TCDD 1 nM) additionally resulted in pronounced CYP1A1-protein-bands (56 kDa). For PCB 105, 118, or 153, no CYP1A1-protein was detectable via Western Blotting in tested range of concentrations (10^{-10}-10^{-6} M).

4.2.2.2. EROD assay liver cell systems – summary H4IIE cells

Table 45 summarizes results obtained by analysis of H4IIE cells regarding EROD-inducing properties of 14 congeners. EC50- and EC20-values as well as correspondent REPs are opposed to current TEFs from 2005 (Van den Berg *et al.*, 2006).

Table 45: EC50-, and EC20-values and respective REPs derived from EROD-measurements with H4IIE cells subsequent to incubation with 14 congeners for 24 h compared to WHO-TEFs (Van den Berg *et al.*, 2006).

H4IIE	EC50 (M)	REP (EC50)	EC20 (M)	REP (EC20)	WHO-TEF (2005)
TCDD	**9.49E-12**	**1**	**3.80E-12**	**1**	1
1-PeCDD	**1.62E-11**	**0.58**	**5.98E-12**	**0.64**	1
1,6-HxCDD	**8.25E-11**	**0.12**	**3.88E-11**	**0.10**	0.1
1,4,6-HpCDD	**1.43E-10**	**0.066**	**7.98E-11**	**0.048**	0.01
TCDF	**4.12E-10**	**0.023**	**8.34E-11**	**0.046**	0.1
4-PeCDF	**1.43E-11**	**0.67**	**5.92E-12**	**0.64**	0.3
1,4-HxCDF	**9.48E-11**	**0.10**	**4.16E-11**	**0.091**	0.1
1,4,6-HpCDF	**6.25E-10**	**0.015**	**3.72E-10**	**0.010**	0.01
PCB 77	**7.30E-08**	**0.00013**	**6.69E-08**	**0.000057**	0.0001
PCB 126	**8.18E-11**	**0.12**	**4.12E-11**	**0.092**	0.1
PCB 105					0.00003
PCB 118					0.00003
PCB 156	**1.87E-07**	**0.000051**	**8.13E-08**	**0.000047**	0.00003
PCB 153					-

4.2.2.3. EROD assay and Western Blot – primary rat hepatocytes

For analysis of selected congeners' effects on CYP1A on protein-level, primary rat hepatocytes (PRH) were obtained from male Sprague Dawley rats according to Seglen (1972). Subsequent to cultivation, cells were incubated with compounds for 24 h. TCDD (1 nM) served as positive control for AhR-dependent CYP1A-induction in primary rat hepatocytes with respect to both EROD-measurements and Western Blotting. Referring to the latter, VDAC was detected as loading control in microsomes derived from treated hepatocytes. Solvent-control-accompanied background levels (DMSO 0.1%) were subtracted from EROD-activities induced by congeners.

In figure 43, results for EROD-measurements obtained by incubation of PRH with TCDD, arranged with a correspondent representative CYP1A1-Western Blot, are assembled.

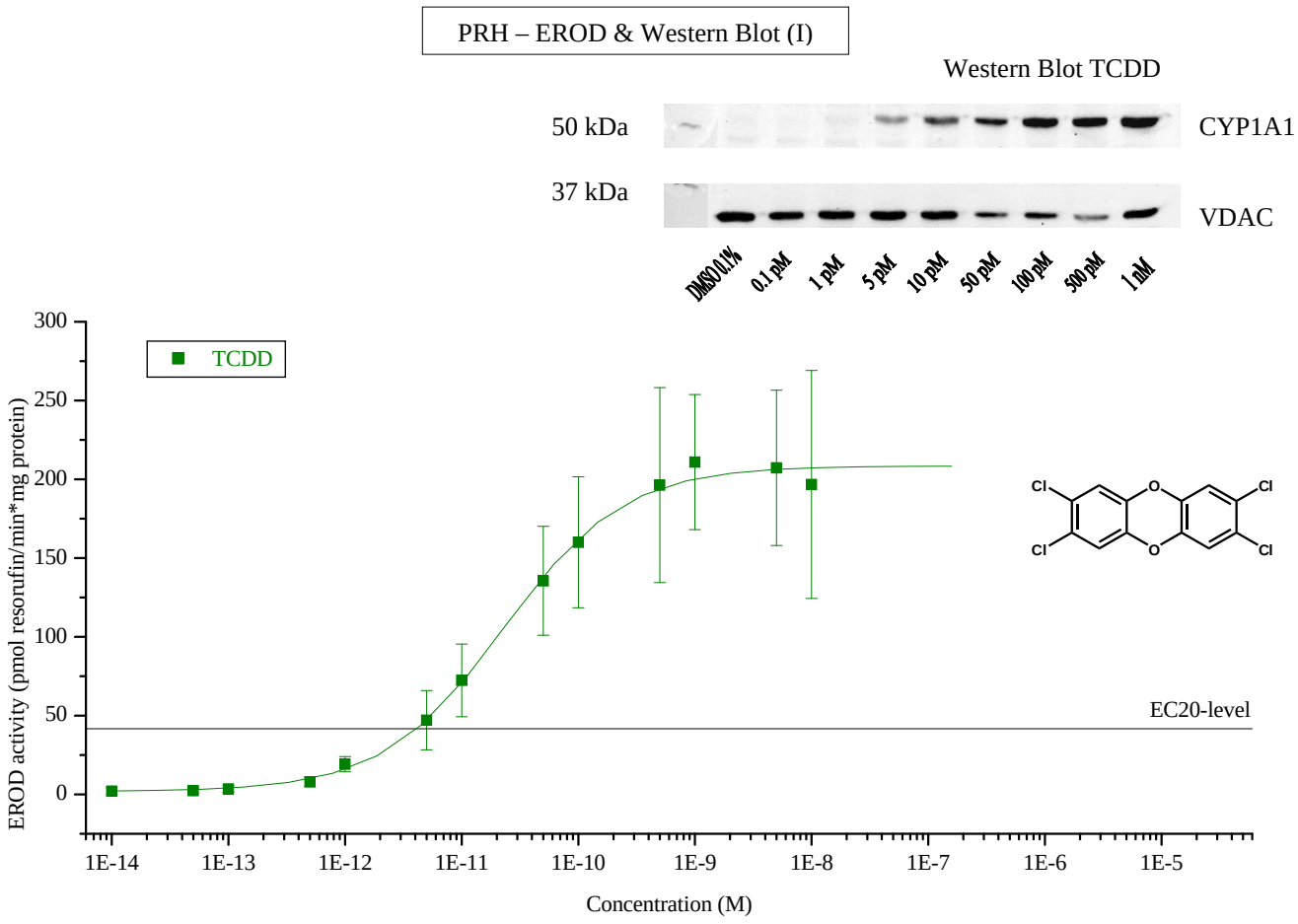

Figure 43: EROD assay and Western Blot PRH (I). Cells treated with TCDD for 24 h. Concentration (M) logarithmically plotted against EROD-activity (pmol resorufin/min*mg protein). EC20-level (41.7 pmol resorufin/min*mg protein) represents 20% of TCDD-induced maximum response. Exemplary CYP1A1-and VDAC-Western Blot from microsomes. Results from three independent experiments each.

To develop a concentration-response-relationship regarding TCDD's EROD-inducing properties towards Sprague Dawley primary rat hepatocytes after 24 h, TCDD-concentrations from 10^{-14} M to 10^{-8} M were investigated (figure 43). Subsequent to a slight increase within a concentration-range of 10^{-13}-10^{-12} M TCDD, an exponential increase of EROD-induction was present as far as a conversion into a logarithmical ascent followed around $5*10^{-12}$-10^{-10} M TCDD. Converging to an upper asymptote from ca. $5*10^{-10}$ M TCDD, EROD-levels of 208.5(±3.6) pmol resorufin/min*mg protein were approached. Summarized, the concentration-dependent increase of EROD-activity in PRH due to incubation with TCDD constituted a sigmoid run of curve.
Received EC50 was $2.28*10^{-11}$(±$2.39*10^{-12}$) M TCDD. Obtained EC20-level, representing 20% of maximum induction by TCDD, was 41.7 pmol resorufin/min*mg protein, while appendant EC20 was calculated as $4.14*10^{-12}$ M TCDD. Per definition, REP-values were 1 in each case.
Statistically very significant deviations (p-value < 0.01) from solvent control (DMSO 0.1%, not shown) were yielded from $5*10^{-11}$ M to 10^{-8} M TCDD scoring from 135.6(±34.6) pmol resorufin/min*mg protein to 196.7(±72.4) pmol resorufin/min*mg protein (One-way ANOVA with Dunnett's post test; control vs. treatments).

Exemplary Western Blot membrane in figure 43 comprised results from three independently implemented repetitions and showed consistent occurrence of VDAC-loading controls (32 kDa) for all samples. Starting from microsomes obtained by incubation of PRH with solvent-control (DMSO 0.1%) for 24 h, and followed by samples for treatment with 10^{-13}-10^{-12} M TCDD, no further protein-band was detectable on membranes.
Initiated from $5*10^{-12}$ M TCDD, a concentration-dependently amplifying appearance of CYP1A1-protein (56 kDa) was measured. Progressivity of this protein's appearance ended in almost indistinguishably occurring CYP1A1-band-intensities from about 10^{-10}-$5*10^{-10}$ M to 10^{-9} M TCDD. The initial band of CYP1A1-protein for treatment with $5*10^{-12}$ M TCDD highly correlated with the EC20 ($4.14*10^{-12}$ M TCDD) obtained by EROD-measurements. Further, the range of TCDD-concentrations regarding enhancement of CYP1A1-protein and subsequent indistinguishable band-intensities approximated the run of EROD-induction's associated concentration-dependent sigmoid curve.

Usage of TCDD (1 nM, 24 h) as positive control for further investigations resulted in ascent of EROD-activity in statistically extremely significant (p-value < 0.0001) manner to 162(±37) pmol resorufin/min*mg protein (Two-tailed unpaired t-test (control vs. TCDD 1 nM; n = 43) in PRH.

An assembly of results from EROD-measurements and CYP1A1-Western Blots referring to 24 h of incubation of PRH with 1-PeCDD, 1,6-HxCDD, or 1,4,6-HpCDD, compared to TCDD-derived EROD-induction, is shown in figure 44.

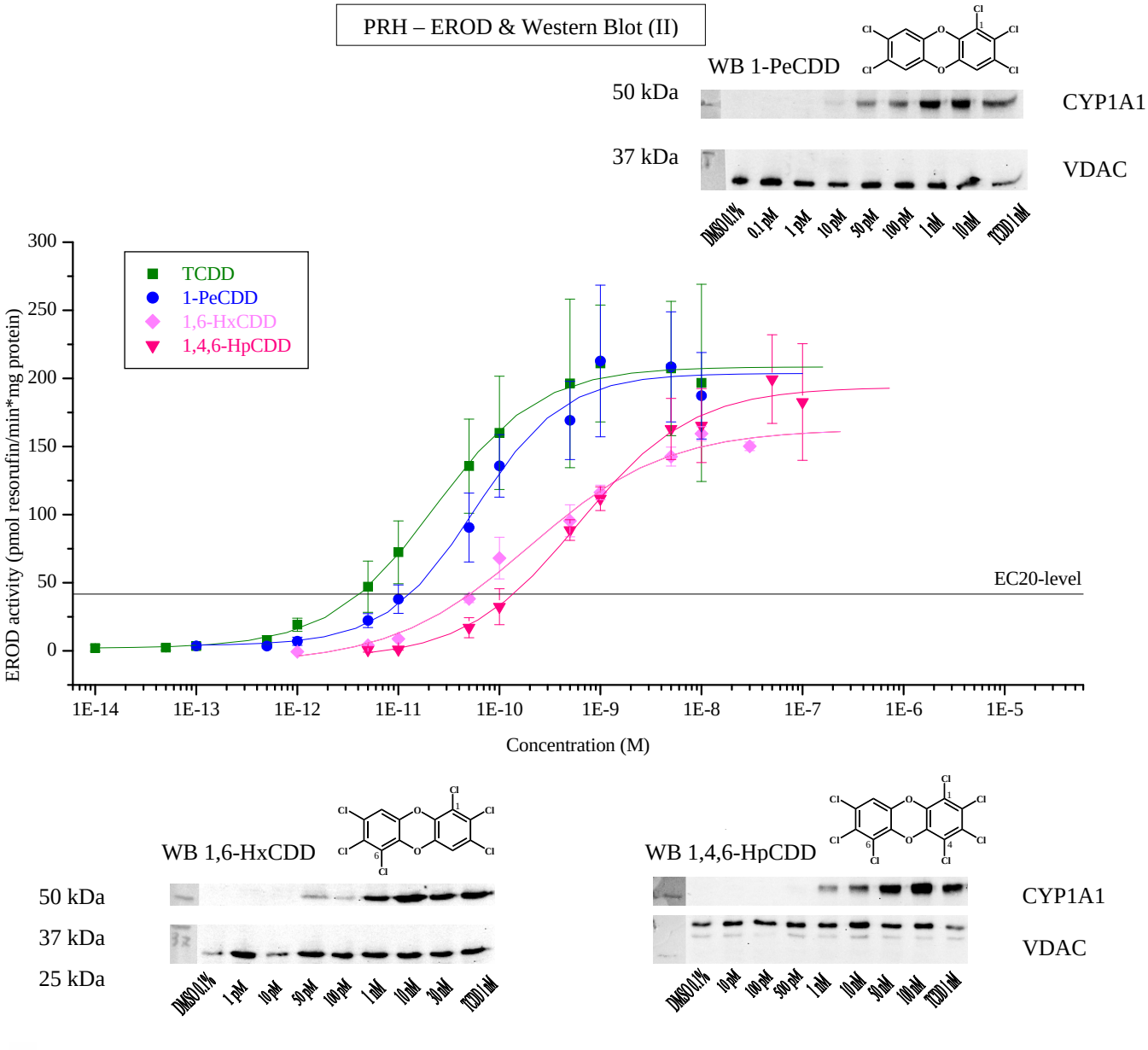

Figure 44: EROD assay and Western Blot PRH (II). Cells treated with TCDD, 1-PeCDD, 1,6-HxCDD, or 1,4,6-HpCDD for 24 h. Abscissa (logarithm.): Concentration (M); ordinate: EROD-activity (pmol resorufin/min*mg protein). EC20-level represents 20% of TCDD-induced maximum response. Exemplary CYP1A1-and VDAC-Western Blots from microsomes. Results from three independent experiments each.

Incubation of PRH with PCDDs resulted in EROD-inductions in concentration-dependent manners (figure 44). Comparing the TCDD-derived curve to effects caused by 1-PeCDD, the combination of an exponential ascent of EROD-activity slightly shifted to higher concentrations (10^{-12}-10^{-11} M 1-PeCDD) with a lightly enhanced gradient in the logarithmical part of the slope,

whereas the upper asymptotic level of 203.7(±8.5) pmol resorufin/min*mg protein was reached around $5*10^{-10}$-10^{-9} M 1-PeCDD, highly correlating with the TCDD-gained asymptote. Since the logarithmical section of curve was slightly shifted to higher concentrations, EC50 for 1-PeCDD of $5.73*10^{-11}$($\pm1.21*10^{-11}$) M led to a correspondent REP (EC50) of 0.40. The EC20-level of 41.7 pmol resorufin/min*mg protein was accomplished with $1.32*10^{-11}$ M 1-PeCDD, bearing a REP (EC20) of 0.31. Statistically very significant (p-value < 0.01; One-way ANOVA with Dunnett's post test; control vs. treatments) EROD-inductions were present from $5*10^{-11}$ M 1-PeCDD with 90.5(±25.3) pmol resorufin/min*mg protein.

Transported about one order of magnitude to higher concentrations, incubation with 1,4,6-HpCDD brought forth a sigmoid regarding EROD-induction in PRH, comprising a logarithmical ascent approximately reflecting conditions in the TCDD-derived slope. Yielding an upper EROD-inducing level of 193.6(±6.5) pmol resorufin/min*mg protein, the curve passed through an EC20 of $1.38*10^{-10}$ M (REP (EC20): 0.030), and an EC50 of $6.13*10^{-10}$($\pm1.05*10^{-10}$) M (REP (EC50): 0.037). From $5*10^{-10}$ M 1,4,6-HpCDD (88.7±7.6 pmol resorufin/min*mg protein), induced EROD-activities were considered statistically very significant (p-value < 0.01).
Closely located to the 1,4,6-HpCDD-derived concentration-response curve, whereby connected with flatter ascent of slope lightly moved to lower concentrations and establishing efficacy to a lesser extent, usage of 1,6-HxCDD led to statistically very significant (p-value < 0.01) EROD-inductions in PRH from $5*10^{-11}$ M of the congener (38.2±2.8 pmol resorufin/min*mg protein). Reaching an asymptotic value of 162.8(±9.1) pmol resorufin/min*mg protein, EC50 for 1,6-HxCDD scored $1.98*10^{-10}$($\pm5.32*10^{-11}$) M, correlating to a REP (EC50) of 0.12. EC20 amounted to $5.14*10^{-11}$ M 1,6-HxCDD, affording a REP (EC20) of 0.081.

Western Blot membranes, exemplarily pictured in figure 44, revealed reasonably uniformly occurring protein-bands constituting loading controls (VDAC, 32 kDa). Examination of positive controls from microsomes of PRH incubated with TCDD (1 nM, 24 h) resulted in appearances of obvious bands (56 kDa) representing CYP1A1-protein. Using PCDDs, respective microsomes revealed slight CYP1A1-protein-bands from 10^{-11}-$5*10^{-11}$ M 1-PeCDD, $5*10^{-11}$ M 1,6-HxCDD, or $5*10^{-10}$ M 1,4,6-HpCDD. Growing band-intensities within ranges of about two orders of magnitude in concentration were followed by stable CYP1A1-band-intensities for around 10^{-9}-10^{-8} M 1-PeCDD, 10^{-8}-$3*10^{-8}$M 1,6-HxCDD, or 10^{-8}-10^{-7} M 1,4,6-HpCDD.

Any finding regarding CYP1A-inducing properties of PCDD-concentrations closely resembled among both examined methods, most significantly noting correlations between EROD's EC20-values and initial CYP1A1-protein-bands.

In figure 45, results for EROD-measurements and Western Blotting derived by incubation of PRH with PCDFs are shown.

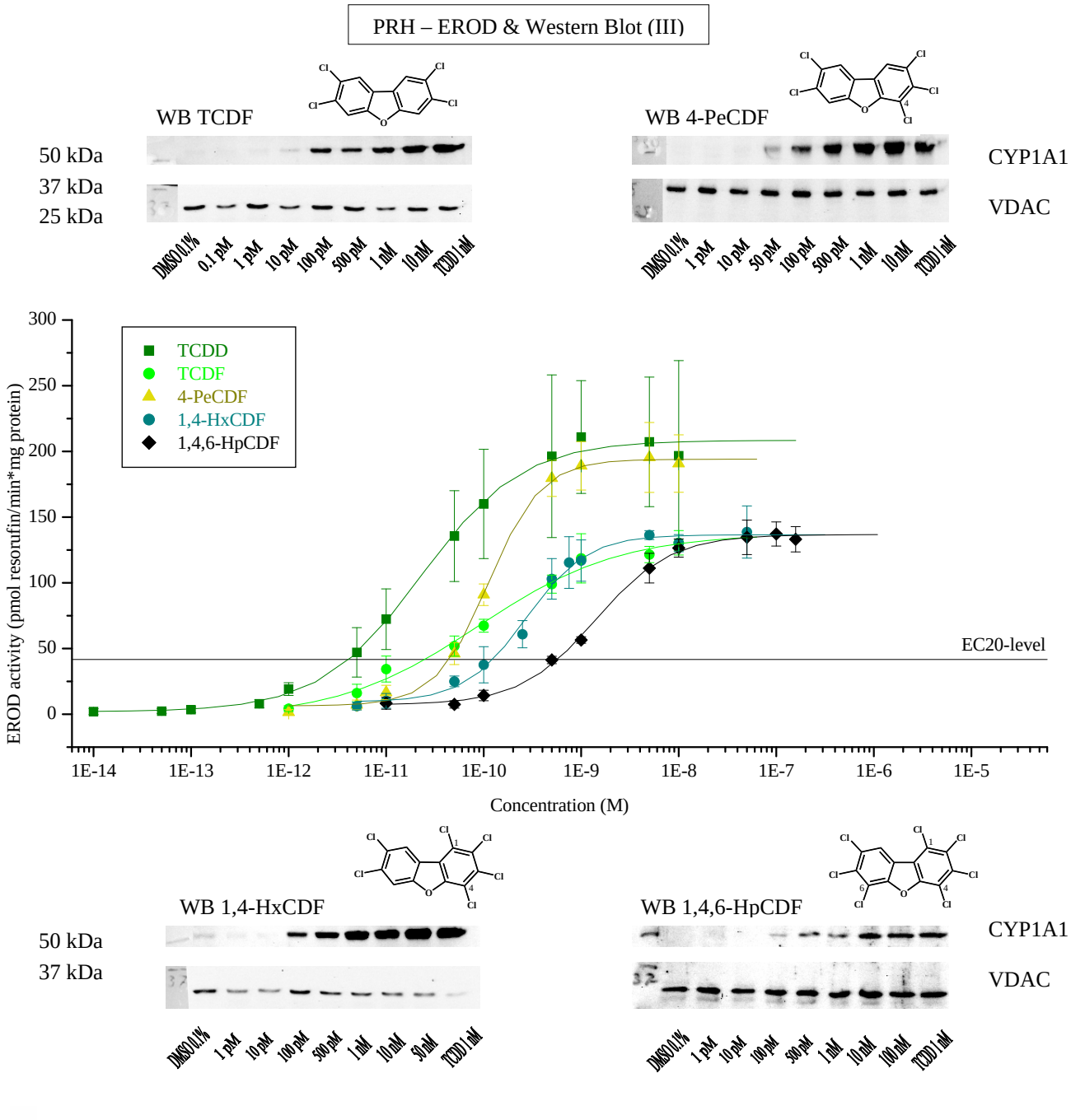

Figure 45: EROD assay and Western Blot PRH (III). Cells treated with TCDD, TCDF, 4-PeCDF, 1,4-HxCDF, or 1,4,6-HpCDF for 24 h. Abscissa (logarithm.): Concentration (M); ordinate: EROD-activity (pmol resorufin/min*mg protein). EC20-level represents 20% of TCDD-induced maximum response. Exemplary CYP1A1-and VDAC-Western Blots from microsomes. Results from three independent experiments each.

Measuring EROD-activity in PRH due to 4-PeCDF-incubation, subsequent to a rapid, but compared to effects caused by TCDD delayed, exponential increment, the logarithmical growth of EROD-values implied the steepest ascent among results plotted in figure 45, including the TCDD-derived concentration-response-relationship. From $5*10^{-11}$ M 4-PeCDF and 46.1(±8.3) pmol resorufin/min*mg protein, statistically very significant (p-value < 0.01; One-way ANOVA with Dunnett's post test; control vs. treatments) EROD-inductions were obtained.
The sigmoid curve passed an EC20 of $4.50*10^{-11}$ M 4-PeCDF (REP (EC20): 0.092), and an EC50-value of $1.12*10^{-10}(\pm 6.52*10^{-12})$ M 4-PeCDF (REP (EC50): 0.20), approaching an asymptote of 194.1(±2.7) pmol resorufin/min*mg protein, which lay close to TCDD's asymptote regarding both value of abscissa and value of ordinate.

The concentration-response slope referring to 1,4-HxCDF's properties towards PRH was proceeded about one order of magnitude to higher concentrations compared to the curve obtained by TCDD, but revealed similar degree of ascent within the logarithmical section.
Values from 10^{-10} M 1,4-HxCDF and 37.6(±13.7) pmol resorufin/min*mg protein were considered statistically very significant (p-value < 0.01), whereas upper asymptotic level was 136.6(±3.3) pmol resorufin/min*mg protein. 1,4-HxCDF's sigmoid curve intersected the EC20-level at $1.25*10^{-10}$ M, and EC50-value was $2.71*10^{-10}(\pm 2.83*10^{-11})$ M 1,4-HxCDF, correspondent to REPs of 0.033 (REP (EC20), and 0.084 (REP (EC50), respectively.

Transferred another order of magnitude to higher concentrations, 1,4,6-HpCDF led to a sigmoid regarding EROD-inducing properties in PRH with less intense ascent compared to the TCDD-derived slope. Initial statistically very significant (p-value < 0.01) deviations from solvent control (DMSO 0.1%, not shown) were present from $5*10^{-10}$ M 1,4,6-HpCDF (41.3±2.8 pmol resorufin/min*mg protein), closely followed by a calculated EC20 of $5.74*10^{-10}$ M 1,4,6-HpCDF, which associated a REP (EC20) of 0.0072. EC50 scored $1.41*10^{-9}(\pm 1.05*10^{-10})$ M 1,4,6-HpCDF, revealing a REP (EC50) of 0.016. Maximum EROD-inductions obtained by 1,4,6-HpCDF in PRH were 136.7(±1.9) pmol resorufin/min*mg protein.

Possessing an even flatter ascent across the entire concentration-response curve, TCDF led to statistically very significant (p-value < 0.01) EROD-activities from 10^{-11} M TCDF with 34.4(±9.9) pmol resorufin/min*mg protein. Running through an EC20 of $2.49*10^{-11}$ M TCDF (REP (EC20): 0.17), and an EC50 of $8.89*10^{-11}(\pm 2.93*10^{-11})$ M TCDF (REP (EC50): 0.26), upper limit of EROD-induction by TCDF was 137.5(±9.4) pmol resorufin/min*mg protein.

According to Western Blot analysis represented in figure 45, detection of VDAC-loading-controls (32 kDa) was considered as constant. Microsomes obtained by PRH incubated with TCDD 1 nM for 24 h served as positive controls, and brought forth considerable bands indicating the protein CYP1A1 (56 kDa).

Correlating with EROD-derived EC20-values, initial CYP1A1-protein-bands slightly appeared by use of 10^{-11} M TCDF, $5*10^{-11}$ M 4-PeCDF, 10^{-10} M 1,4-HxCDF, or 10^{-10}-$5*10^{-10}$ M 1,4,6-HpCDF. Further strengthening of CYP1A1-band-intensities with higher concentrations of congeners proceeded in course of around two orders of magnitude in concentration.

Blotting of microsomes from hepatocytes exposed to highest concentrations of PCDFs (10^{-8} M TCDF, 10^{-9}-10^{-8} M 4-PeCDF, 10^{-9}-$5*10^{-8}$ M 1,4-HxCDF, or 10^{-8}-$*10^{-7}$ M 1,4,6-HpCDF) revealed thick CYP1A1-protein-bands comparable concerning extent to those of positive controls.

The mono-*ortho*-substituted PCB 156, as well as non-*ortho*-substituted PCBs 77, or 126, were examined regarding their CYP1A-inducing properties in PRH and contrasted with TCDD-originated characteristics. Results of EROD-measurements and CYP1A1-Western Blots are summarized in figure 46.

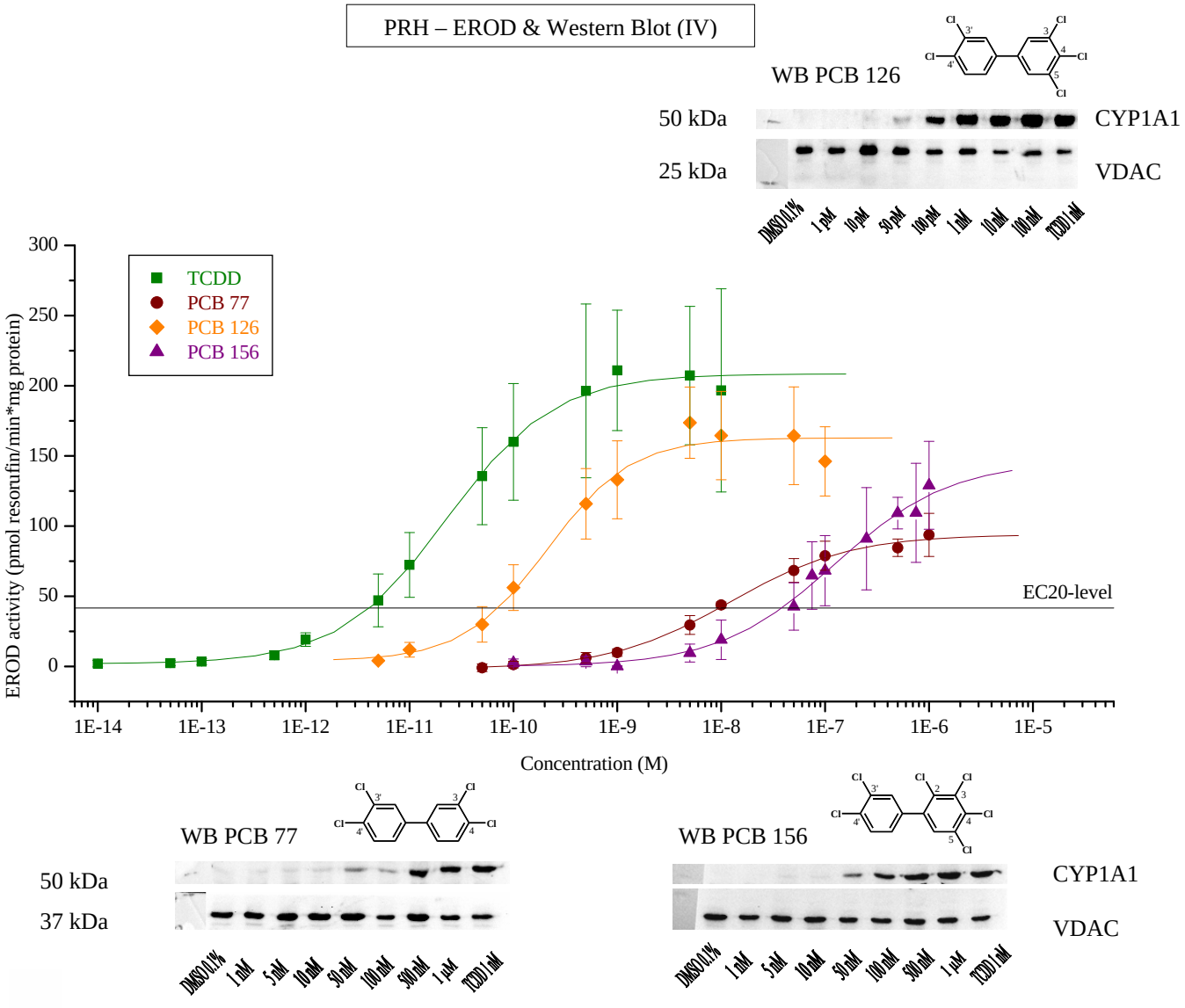

Figure 46: EROD assay and Western Blot PRH (IV). Cells treated with TCDD, PCB 77, PCB 126, or PCB 156 for 24 h. Abscissa (logarithm.): Concentration (M); ordinate: EROD-activity (pmol resorufin/min*mg protein). EC20-level represents 20% of TCDD-induced maximum response. Exemplary CYP1A1-and VDAC-Western Blots from microsomes. Results from three independent experiments each.

In an almost parallel course, quite accurately shifted one order of magnitude to higher concentrations, the sigmoid curve describing CYP1A-inducing effects in PRH due to incubation with PCB 126 for 24 h reached an upper asymptotic level of 162.8(±5.8) pmol resorufin/min*mg protein (figure 46). Considering statistical relevance, a significant (p-value < 0.05; One-way

ANOVA with Dunnett's post test; control vs. treatments) value of 56.2(±16.3) pmol resorufin/min*mg protein using 10^{-10} M PCB 126 was followed by very significant (p-value < 0.01) inductions from $5*10^{-10}$ M PCB 126 (115.9±25.1 pmol resorufin/min*mg protein). EC20-value scored $7.20*10^{-11}$ M PCB 126, and EC50 was $2.11*10^{-10}(\pm 5.11*10^{-11})$ M PCB 126, constituting respective REPs of 0.058 (REP (EC20)), and 0.11 (REP (EC50).

A farther transfer of curve of about two orders of magnitude on the x-axis in combination with a flatter degree of ascent pictured concentration-dependent EROD-induction due to PCB 77 in PRH. Passed EC20- and EC50-values of $9.63*10^{-9}$ M PCB 77 (REP (EC20): 0.00043), and $1.22*10^{-8}(\pm 1.56*10^{-9})$ M PCB 77 (REP (EC50): 0.0019), respectively, asymptotically margined 94.0(±2.7) pmol resorufin/min*mg protein. PCB 77 led to statistically very significant ($P<0.01$) deviations from $5*10^{-9}$ M (29.5±6.7 pmol resorufin/min*mg protein) regarding EROD-activity in PRH.
Furthermore, slightly moved to higher concentrations, but with respect to the curve derived by PCB 77 exhibiting a steeper ascent, treatment with PCB 156 resulted in a concentration-response slope yielding an asymptote, mathematically indicated due to reducing degree of ascent for around $5*10^{-7}$-10^{-6} M PCB 156, of 146.1(±16.7) pmol resorufin/min*mg protein of EROD-activity in PRH. Attaining statistically very significant (p-value < 0.01) EROD-values from $7.5*10^{-8}$ M PCB 156 (64.8±42.1 pmol resorufin/min*mg protein), the sigmoid ran through an EC20 of $3.85*10^{-8}$ M PCB 156 (REP (EC20): 0.00011), and an EC50 of $1.24*10^{-7}(\pm 4.16*10^{-8})$ M PCB 156 (REP (EC50): 0.00018).

Focusing on exemplary Western Blot membranes in figure 46, loading controls (VDAC, 32 kDa) were detected in consistent manner. Bold CYP1A1-protein-bands (56 kDa) were visible analyzing positive controls gained by microsomes from TCDD-treated (1 nM, 24 h) PRH.
With 10^{-8}-$5*10^{-8}$ M PCB 77, $5*10^{-11}$ M PCB 126, or $5*10^{-8}$ M PCB 156, light CYP1A1-bands appeared on Western Blot membranes, linking respective concentrations to EC20-values of congeners in EROD-measurements. Subsequent to an ascent throughout 1-1.5 orders of magnitude of PCB 77-, PCB 126-, or PCB 156-concentration, CYP1A1-band-intensities succeeded proportions comparable to those of TCDD-positive controls ($5*10^{-7}$-10^{-6} M PCB 77, 10^{-9}-10^{-7} M PCB 126, or $5*10^{-7}$-10^{-6} M PCB 156).

In figure 47, EROD-assay- and Western Blot-results derived by analysis of NDL-PCB 153, and mono-*ortho*-substituted PCBs 105, or 118, on PRH are contrasted.

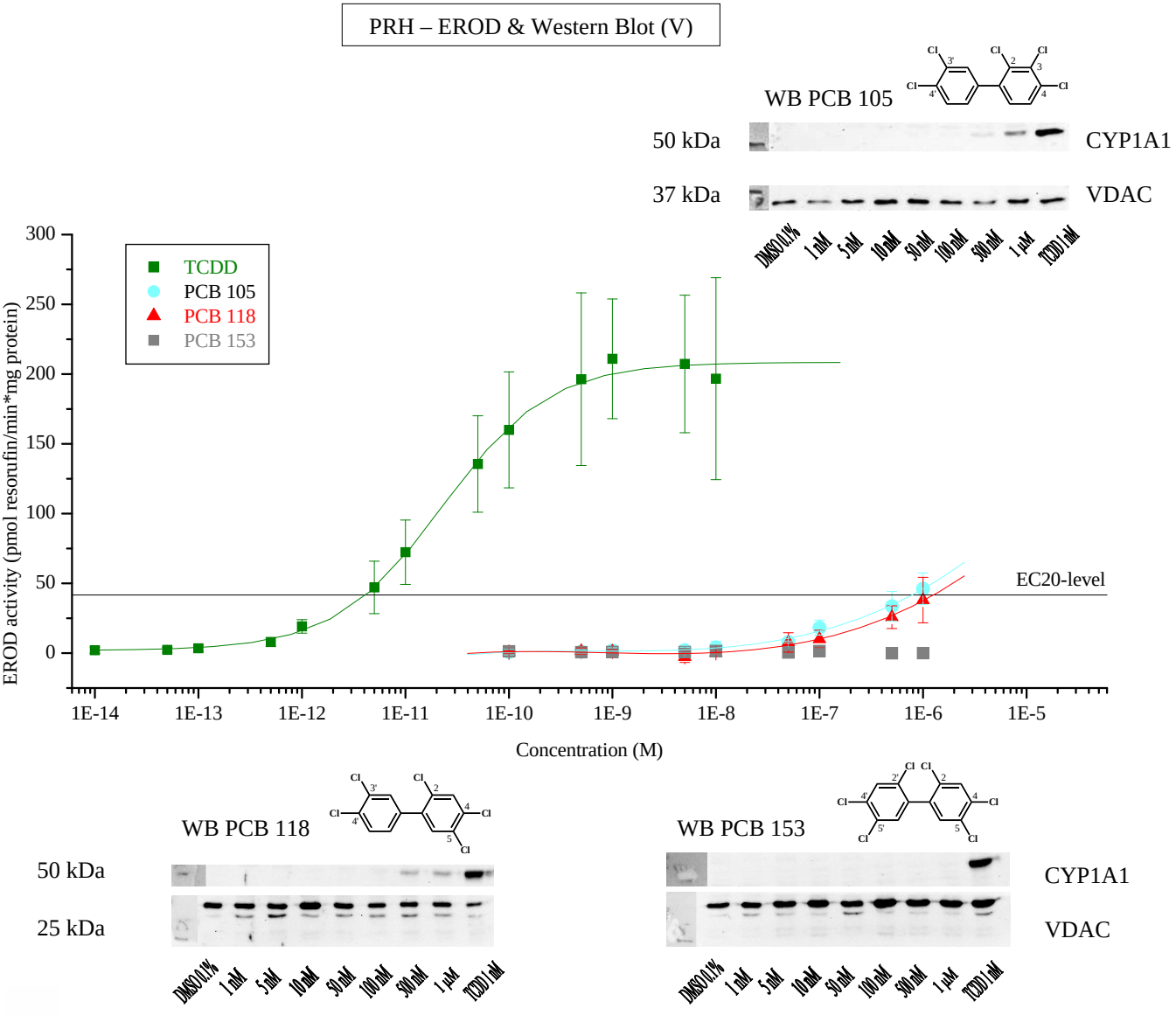

Figure 47: EROD assay and Western Blot PRH (V). Cells treated with TCDD, PCB 105, PCB 118, or PCB 153 for 24 h. Abscissa (logarithm.): Concentration (M); ordinate: EROD activity (pmol resorufin/min*mg protein). EC20-level represents 20% of TCDD-induced maximum response. Exemplary CYP1A1-and VDAC-Western Blots from microsomes. Results from three independent experiments each.

Incubation of PRH with mono-*ortho*-substituted PCB 105 for 24 h led to a slight increase of EROD-activity from about $5*10^{-8}$ M (8.0±0.6 pmol resorufin/min*mg protein), which enhanced and yielded statistically very significant (p-value < 0.01; One-way ANOVA with Dunnett's post test; control vs. treatments) EROD-induction levels from 10^{-7} M PCB 105 with 18.2(±5.4) pmol resorufin/min*mg protein (figure 47). Using highest tested concentration of 10^{-6} M PCB 105,

maximum EROD-activity of 46.2(±11.3) pmol resorufin/min*mg protein was achieved. Due to polynomial fitting, an EC20 of $7.86*10^{-7}$ M PCB 105 was evolvable, corresponding to a REP scoring 0.0000053.

Comparable findings were obtained by analysis of PCB 118-derived EROD-inducing effects, whereby polynomial fitting generated a concentration-response-relationship positioned slightly below PCB 105's fit.
Subsequent to slightly increasing EROD-activities from $5*10^{-8}$ M PCB 118 (8.0±0.6 pmol resorufin/min*mg protein), statistically very significant (p-value < 0.01) enzyme-inductions were gained from $5*10^{-7}$ M PCB 118 amounting to 25.8(±8.1) pmol resorufin/min*mg protein. Maximally reached EROD-activity examining 10^{-6} M PCB 118 amounted to 38.0(±16.3) pmol resorufin/min*mg protein. Being located minimally above this highest concentration, deduced EC20 was $1.25*10^{-6}$ M, correlating with a REP of 0.0000032.
Compared to effects caused by PCB 105, EC20 and statistically relevant values due to treatment of PRH with PCB 118 were transferred about half an order of magnitude to higher concentrations.

Focusing on Western Blot membranes obtained by analysis of microsomes from primary rat hepatocytes exposed to PCBs 105, or 118, both substances slightly induced CYP1A1-protein (56 kDa) using $5*10^{-7}$ M of respective congener, sparsely intensifying with 10^{-6} M. As well as for the exemplary Western Blot-membrane referring to PCB 153, membranes showed regularly occurring bands indicating the VDAC-loading-control (32 kDa). Constantly, TCDD-positive-controls generated distinct CYP1A1-bands. Regarding NDL-PCB 153, effects on CYP1A-levels were observed attempting neither method.

4.2.2.4. EROD assay liver cell systems – summary primary rat hepatocytes

In table 46, EC-values and correspondent REPs obtained by EROD-measurements in Sprague Dawley primary rat hepatocytes exposed to polychlorinated dibenzo-*p*-dioxins, polychlorinated dibenzofurans, or polychlorinated biphenyls, are compared to current TEF (2005)-values (Van den Berg et al., 2006).

Table 46: EC50-and EC20-values and respective REPs derived from EROD-measurements with PRH subsequent to incubation with 14 congeners for 24 h compared to WHO-TEFs (Van den Berg *et al.*, 2006).

PRH	EC50 (M)	REP (EC50)	EC20 (M)	REP (EC20)	WHO-TEF (2005)
TCDD	**2.28E-11**	**1**	**4.14E-12**	**1**	1
1-PeCDD	**5.73E-11**	**0.40**	**1.32E-11**	**0.31**	1
1,6-HxCDD	**1.98E-10**	**0.12**	**5.14E-11**	**0.081**	0.1
1,4,6-HpCDD	**6.13E-10**	**0.037**	**1.38E-10**	**0.030**	0.01
TCDF	**8.89E-11**	**0.26**	**2.49E-11**	**0.17**	0.1
4-PeCDF	**1.12E-10**	**0.20**	**4.50E-11**	**0.092**	0.3
1,4-HxCDF	**2.71E-10**	**0.084**	**1.25E-10**	**0.033**	0.1
1,4,6-HpCDF	**1.41E-09**	**0.016**	**5.74E-10**	**0.0072**	0.01
PCB 77	**1.22E-08**	**0.0019**	**9.63E-09**	**0.00043**	0.0001
PCB 126	**2.11E-10**	**0.11**	**7.20E-11**	**0.058**	0.1
PCB 105			**7.86E-07**	**0.0000053**	0.00003
PCB 118			**1.25E-06**	**0.0000032**	0.00003
PCB 156	**1.24E-07**	**0.00018**	**3.85E-08**	**0.00011**	0.00003
PCB 153					-

4.2.2.5. EROD assay liver cell systems – H4IIE cells vs. PRH

Summarizing EROD assay results derived from both used liver cells systems, varying EROD-inducing properties using primary rat hepatocytes, or the cell-line H4IIE, were remarkable. Exemplarily, in figure 48, sigmoid curves reflecting EROD-inducing effects of TCDD in both cell types are contrasted.

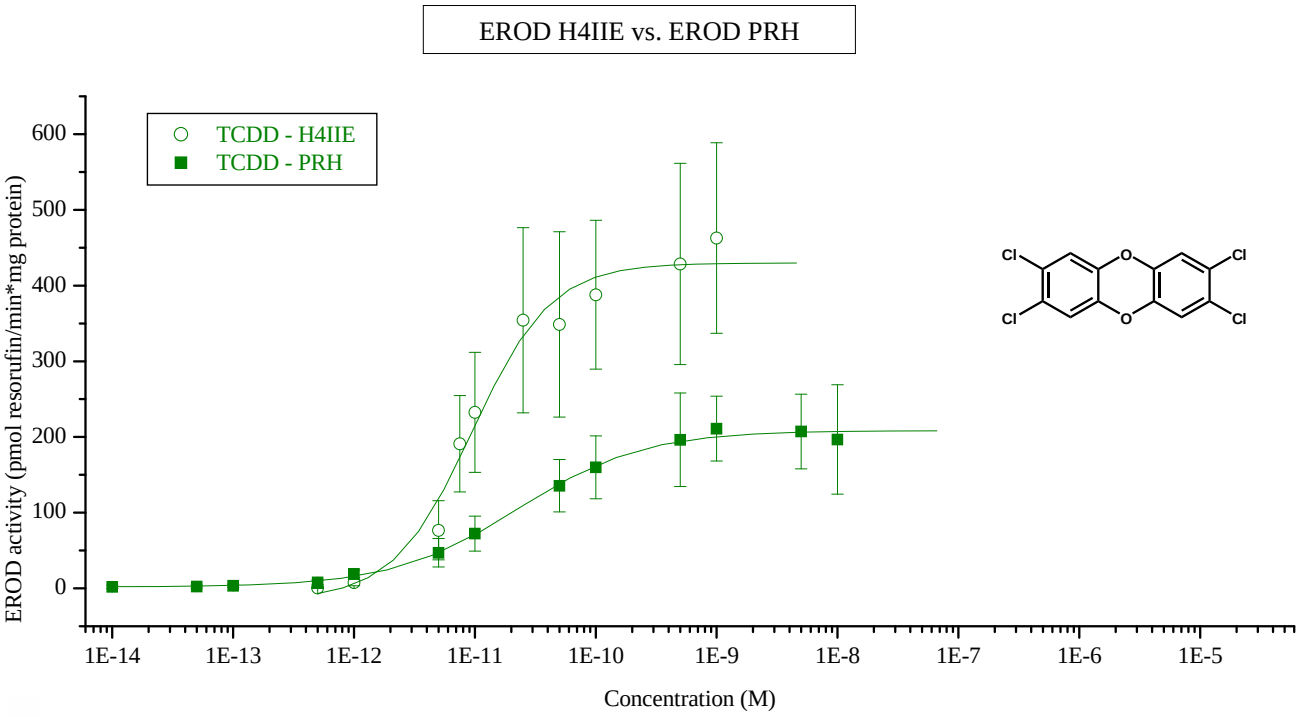

Figure 48: EROD assay H4IIE vs. PRH. Cells treated with TCDD for 24 h. Abscissa (logarithm.): Concentration (M); ordinate: EROD-activity (pmol resorufin/min*mg protein). Results from three independent experiments each.

The exponential increase of EROD-activity using low TCDD-concentrations comprised an equal range of concentration (10^{-12}-$5*10^{-12}$ M) for both cell systems displayed in figure 48.

Yet, differences concerning degree of exponential increase existed, with H4IIE-cells revealing a higher extent accompanied by a slightly sooner transition into the logarithmical section of the curve. This logarithmical segment furthermore exhibited a steeper ascent using H4IIE-cells instead of PRH. In addition, the upper asymptote of the sigmoid curve was both reached with about 0.5 orders of magnitude lower TCDD-concentration, and, most remarkably, at a higher absolute level. Precisely, the maximum EROD-level due to TCDD-treatment doubled switching from PRH to H4IIE cells. Taken together, mentioned deviations of sigmoid curves were associated with varying EC-values. Whereas EC20-values for TCDD differed less than ten percent, the shift regarding EC50 appeared more prominent, being twice as high for PRH compared to H4IIE.

Throughout tested compounds, differing properties towards H4IIE-cells and PRH explained above emerged by trend. Exceptionally, mono-*ortho*-substituted PCBs 105, or 118 yielded minor EROD-inductions in H4IIE-cells barely distinguishable from background levels, whereat EROD-activities due to these PCBs at least reached the respective EC20-level in primary rat hepatocytes.

Table 47 overviews REPs acquired by EROD-measurements using H4IIE cells or primary rat hepatocytes, and opposes these to valid WHO-TEFs from 2005 (Van den Berg *et al.*, 2006).

Table 47: REPs derived from EROD-measurements with PRH and H4IIE cells subsequent to incubation with 14 congeners for 24 h compared to WHO-TEFs (Van den Berg *et al.*, 2006).

EROD	REP (EC50) PRH	REP (EC50) H4IIE	REP (EC20) PRH	REP (EC20) H4IIE	WHO-TEF (2005)
TCDD	**1**	**1**	**1**	**1**	1
1-PeCDD	**0.40**	**0.58**	**0.31**	**0.64**	1
1,6-HxCDD	**0.12**	**0.12**	**0.081**	**0.10**	0.1
1,4,6-HpCDD	**0.037**	**0.066**	**0.030**	**0.048**	0.01
TCDF	**0.26**	**0.023**	**0.17**	**0.046**	0.1
4-PeCDF	**0.20**	**0.67**	**0.092**	**0.64**	0.3
1,4-HxCDF	**0.084**	**0.10**	**0.033**	**0.091**	0.1
1,4,6-HpCDF	**0.016**	**0.015**	**0.0072**	**0.010**	0.01
PCB 77	**0.0019**	**0.00013**	**0.00043**	**0.000057**	0.0001
PCB 126	**0.11**	**0.12**	**0.058**	**0.092**	0.1
PCB 105			**0.0000053**		0.00003
PCB 118			**0.0000032**		0.00003
PCB 156	**0.00018**	**0.000051**	**0.00011**	**0.000047**	0.00003
PCB 153					-

4.2.3. *In vitro* Liver Cell Systems – qRT-PCR

To approach to the objective to distinguish properties of chlorinated compounds, besides enzyme-activity measurements and protein analysis, investigations on mRNA-level were processed. Even though gene transcription is necessarily required for translation, the presence of mRNA in a cell merely constitutes a sufficient condition for transcribing mRNA to protein. Confining strategy to protein analysis might implicate losses on information regarding potency and/or efficacy of substances. Hence, several genes were examined on mRNA-level to focus congeners' impact on the fundamental process of gene transcription in liver cell systems.

4.2.3.1. QRT-PCR *in vitro* – TCDD & eight potential target genes

Based on several investigations within the SYSTEQ project, eight potential AhR-target genes were chosen. Genes supposed to be determined were those encoding CYP1A1, CYP1A2, CYP1B1, AhRR, ALDH3A1, CD36, HSD17B2, and TIPARP. For this purpose, H4IIE cells as well as primary rat hepatocytes were incubated with eight different TCDD-concentrations for 24 h. Yielded mRNA was transcribed to cDNA and analyzed by qRT-PCR using SYBR Green, whereby *ACTB* encoding β-actin served as housekeeping gene.

4.2.3.1.1. QRT-PCR *in vitro – Cyp1a1, Cyp1a2, Cyp1b1*

Focused CYP-enzymes, whose gene transcripts were measured via qRT-PCR, were *Cyp1a1*, *Cyp1a2*, and *Cyp1b1*. Effects of TCDD on respective mRNA-levels in PRH, or H4IIE cells after 24 h of incubation are overviewed in figure 49.

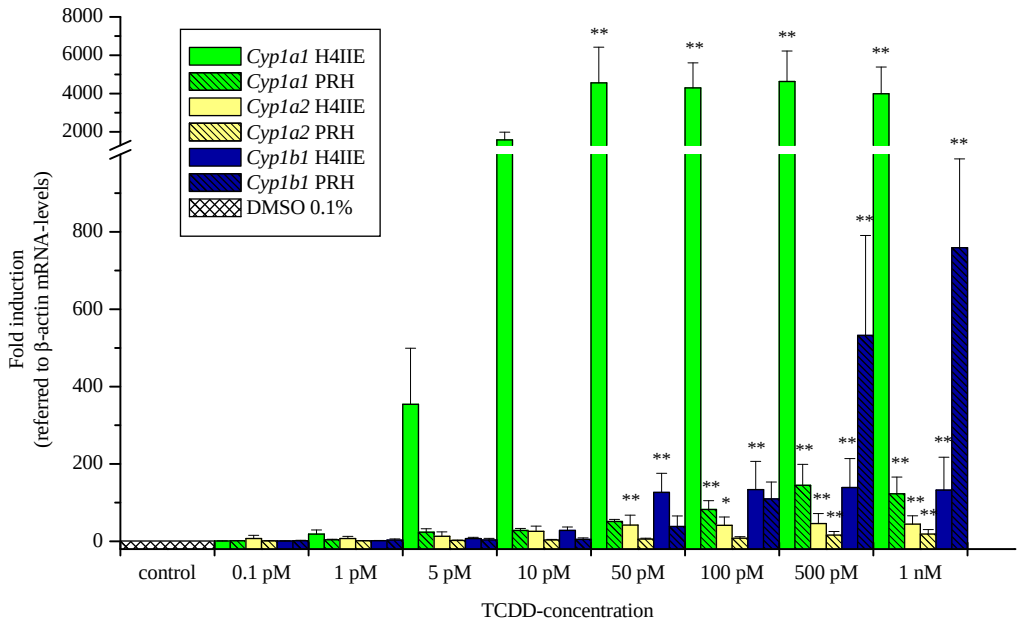

Figure 49: QRT-PCR (*Cyp1a1, Cyp1a2, Cyp1b1*) H4IIE vs. PRH. Cells treated with TCDD for 24 h. TCDD-concentration (M) plotted against fold induction (referred to β-actin mRNA-levels). Results from four independent experiments each. One-way ANOVA with Dunnett's post test (control vs. treatments). *: p-value < 0.05; **: p-value < 0.01.

Slight *Cyp1a1*-inductions in H4IIE cells on mRNA-level (figure 49) were detectable from 10^{-12} M TCDD (18.0±11.0-fold), getting more prominent from $5*10^{-12}$ M (354.1±144.9-fold). Concentration-dependently increasing, fold induction reached statistically very significant upper values (p-value < 0.01) from $5*10^{-11}$-10^{-9} M TCDD with 3544.8(±543.8)-4626.8(±1594.4)-fold enhanced mRNA-levels.

In contrast, maximum effects analyzing PRH were 145.0(±54.0)-fold *Cyp1a1*-inductions ($5*10^{-10}$ M TCDD), concentration-dependently increasing from $5*10^{-11}$ M TCDD (23.6±8.8-fold). Statistically very significant (p-value < 0.01) *Cyp1a1*-inductions in PRH were obtained from 10^{-10} M TCDD (82.3±22.8-fold).

Regarding enhancement and highest mRNA-levels, *Cyp1a1*-fold inductions measured in H4IIE cells were shifted about 0.5-1 order of magnitude to lower concentrations, and in around 30-fold higher extent than in PRH.

In contrast, *Cyp1b1*-qRT-PCR-measurements resulted in a reverse order concerning yielded efficacies in liver cells systems. Using PRH, highest and statistically very significant inductions (p-value < 0.01) of 532.5(±258.3)-759.1(±229.2)-fold were gained with $5*10^{-10}$-10^{-9} M TCDD. More than five times lower upper induction-levels (statistically very significant; p-value < 0.01) were obtained in H4IIE cells testing a TCDD-concentration-rage of $5*10^{-11}$-10^{-9} M (126.3(±49.4) to 138.9(±74.9)-fold induction). Progress of *Cyp1b1*-induction retained in concentration-dependent manner for both cell systems, distinctly increasing from $5*10^{-12}$ to 10^{-11} M TCDD (H4IIE), or from 10^{-11} to $5*10^{-11}$ M TCDD (PRH), representing potencies about 0.5-1 order of magnitude higher in H4IIE cells than in PRH.

Regarding *Cyp1a2*-mRNA-levels, smallest concentration-dependent effects among focused CYP-enzymes were obtained, yielding statistically very significant (p-value < 0.01) inductions scoring 16.2(±9.6)-, and 19.0(±11.4)-fold in PRH using $5*10^{-10}$ M, or 10^{-9} M TCDD.
Being around twice as efficient in H4IIE cells, TCDD led to statistically very significant elevations (p-value < 0.01) accounted for 42.1(±25.7)- to 45.9(±26.0)-fold within a concentration-range of $5*10^{-11}$-10^{-9} M TCDD. Statistically significant (p-value < 0.05) value of 41.4(±21.5)-fold was measured incubating H4IIE cells with 10^{-10} M TCDD.

Constantly, TCDD-derived potencies regarding examined *Cyp*-mRNA-levels were greater in H4IIE cells than in PRH. Analogical findings were obtained comparing TCDD's efficacies towards liver cell models, excepting *Cyp1b1*-inductions, being more excessive in PRH.

4.2.3.1.2. QRT-PCR *in vitro – Ahrr*

In figure 50, qRT-PCR-data concerning TCDD-treated PRH, or H4IIE cells and corresponding *Ahrr*-mRNA-levels are summarized.

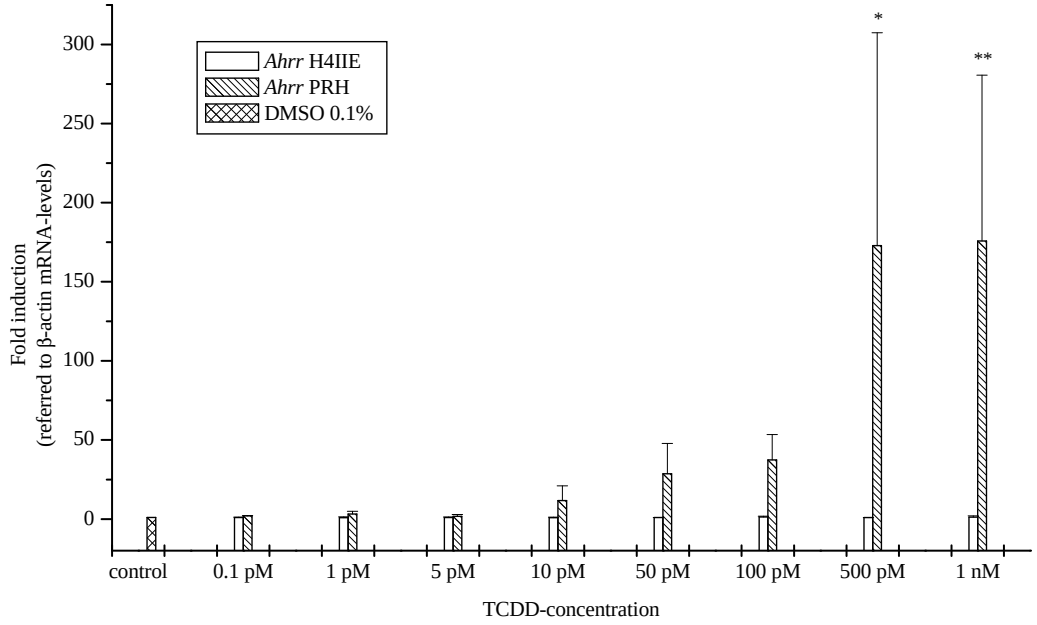

Figure 50: QRT-PCR (*Ahrr*) H4IIE vs. PRH. Cells treated with TCDD for 24 h. TCDD-concentration (M) plotted against fold induction (referred to β-actin mRNA-levels). Results from three independent experiments each. One-way ANOVA with Dunnett's post test (control vs. treatments). *: p-value < 0.05; **: p-value < 0.01.

Incubation with TCDD for 24 h led to a concentration-dependent enhancement of *AhRR*-mRNA-levels in PRH (figure 50). Beginning from 10^{-11} M TCDD, increase progressed passing a statistically significant (p-value < 0.05) value of 172.9(±134.6)-fold ($5*10^{-10}$ M TCDD), and achieved maximal, statistically very significant (p-value < 0.01) induction of 175.8(±104.8)-fold (10^{-9} M TCDD). Sigmoid fitting (not shown) educed an EC50 of $1.79*10^{-10}$($\pm 4.16*10^{-11}$) M TCDD, and respective upper asymptotic value was 183.1(±13.1)-fold.

Usage of H4IIE cells, response with regard to *Ahrr*-induction on mRNA-level was absent by use of tested TCDD-concentrations (10^{-13}-10^{-9} M).

4.2.3.1.3. QRT-PCR *in vitro – Aldh3a1*

Results of qRT-PCR-investigations regarding *Aldh3a1* in PRH, or H4IIE subsequent to treatment with TCDD for 24 h are compiled in figure 51.

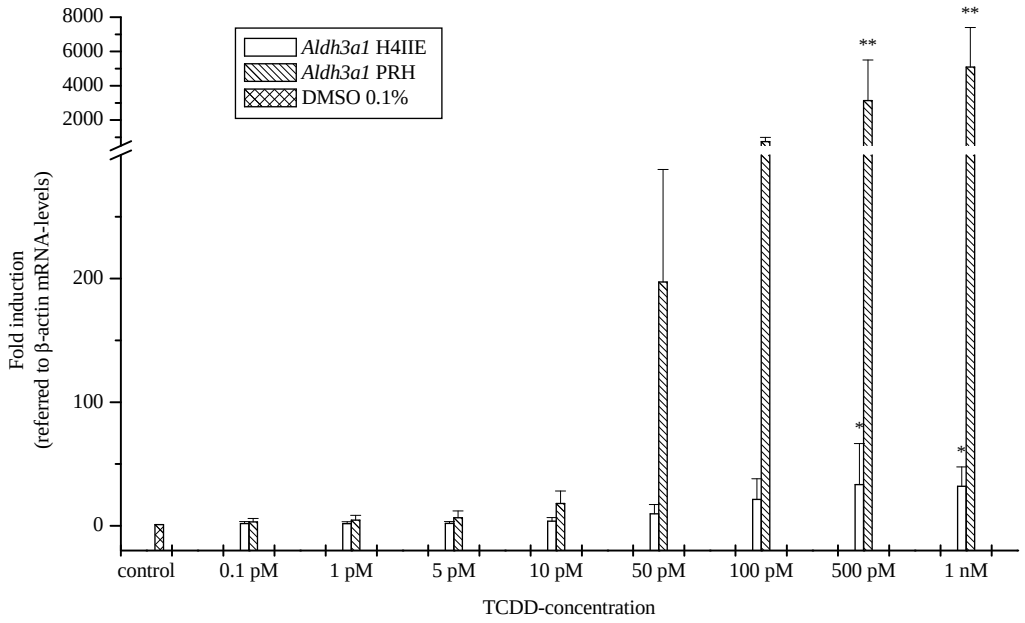

Figure 51: QRT-PCR (*Aldh3a1*) H4IIE vs. PRH. Cells treated with TCDD for 24 h. TCDD-concentration (M) plotted against fold induction (referred to β-actin mRNA-levels). Results from four independent experiments each. One-way ANOVA with Dunnett's post test (control vs. treatments). *: p-value < 0.05; **: p-value < 0.01.

Concentration-dependently, *Aldh3a1*-mRNA-levels in H4IIE cells increased after incubation with TCDD (figure 51). Statistically relevant (p-value < 0.05) inductions were obtained with $5*10^{-10}$-10^{-9} M TCDD, scoring 33.3(±33.1)-32.0(±15.7)-fold.

With more than 10-fold higher efficacy, revealed inductions in PRH due to TCDD-exposure ($5*10^{-10}$-10^{-9} M) amounted to statistically very significant (p-value < 0.01) values of 3134.1(±2373.0)-, and 5093.4(±2302.2)-fold.

Progress of mRNA-level-enhancement proceeded resembled among both tested cell-types, implying conformable potencies responding to TCDD.

4.2.3.1.4. QRT-PCR *in vitro – Cd36*

Presented qRT-PCR-results in figure 52 display relative *Cd36*-mRNA-levels obtained from H4IIE cells or PRH after 24 h of TCDD-exposure.

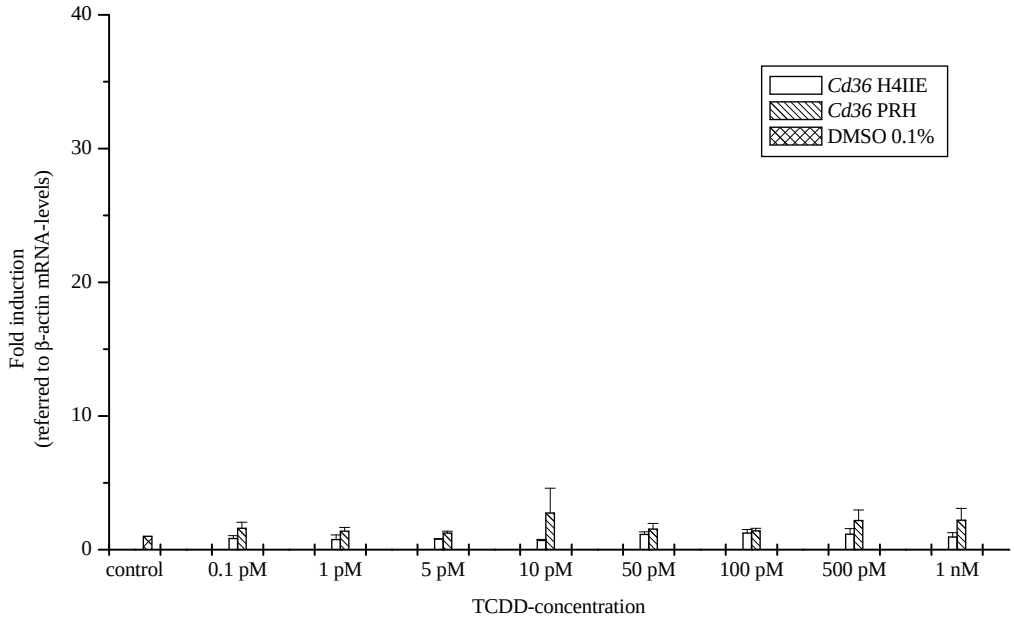

Figure 52: QRT-PCR (*Cd36*) H4IIE vs. PRH. Cells treated with TCDD for 24 h. TCDD-concentration (M) plotted against fold induction (referred to β-actin mRNA-levels). Results from three independent experiments each. One-way ANOVA with Dunnett's post test (control vs. treatments).

Incubation of H4IIE cells, or PRH, with TCDD in a range of concentration of 10^{-13}-10^{-9} M, led to no deviations regarding count of mRNA-transcripts of the gene encoding *Cd36* compared to control (figure 52).

4.2.3.1.5. QRT-PCR *in vitro – Hsd17b2*

Assembly of qRT-PCR-results obtained by analysis of gene-transcripts encoding *Hsd17b2* in PRH, and H4IIE cells treated with TCDD for 24 h is shown in figure 53.

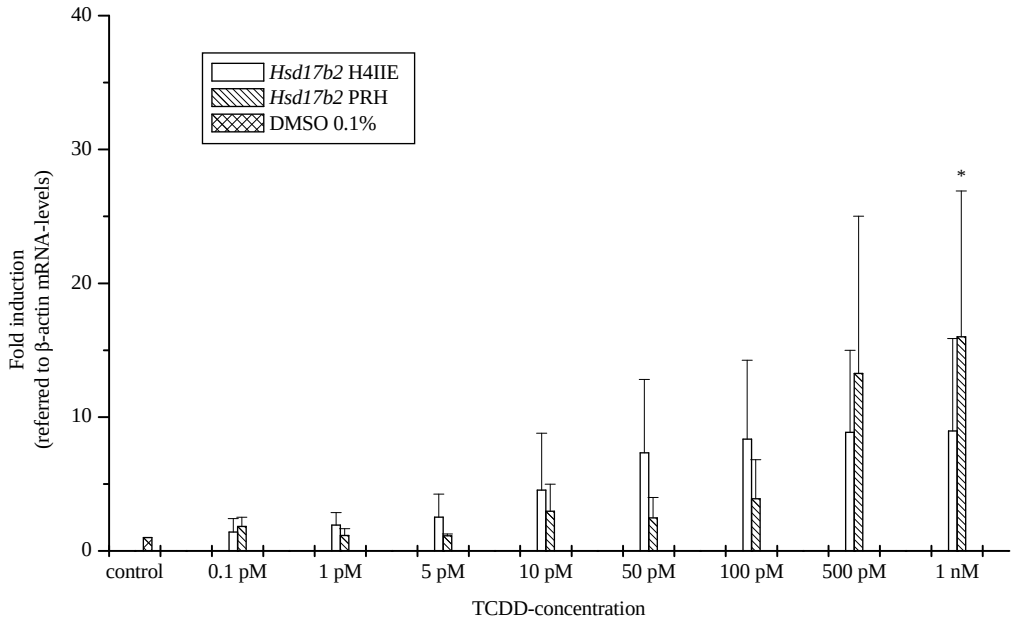

Figure 53: QRT-PCR (*Hsd17b2*) H4IIE vs. PRH. Cells treated with TCDD for 24 h. TCDD-concentration (M) plotted against fold induction (referred to β-actin mRNA-levels). Results from three independent experiments each. One-way ANOVA with Dunnett's post test (control vs. treatments). *: p-value < 0.05.

Incubation of PRH with TCDD resulted in concentration-dependently increasing *Hsd17b2*-mRNA-levels after 24 h (figure 53). Comparably light enhancement peaked with the highest tested TCDD-concentration of 10^{-9} M at a statistically significant (p-value < 0.05) value of 16.0(±10.9)-fold induction.

In contrast, TCDD-exposure to H4IIE cells led to no statistically relevant deviation of respective mRNA-levels from controls. Slight concentration-dependent increase in H4IIE cells maximally achieved *Hsd17b2*-induction of 9.0(±6.9)-fold using 10^{-9} M TCDD.

4.2.3.1.6. QRT-PCR *in vitro* - *Tiparp*

Subsequent figure gives summary of results concerning measurement of *Tiparp*-mRNA-levels in PRH, or H4IIE-cells exposed to TCDD for 24 h (figure 54).

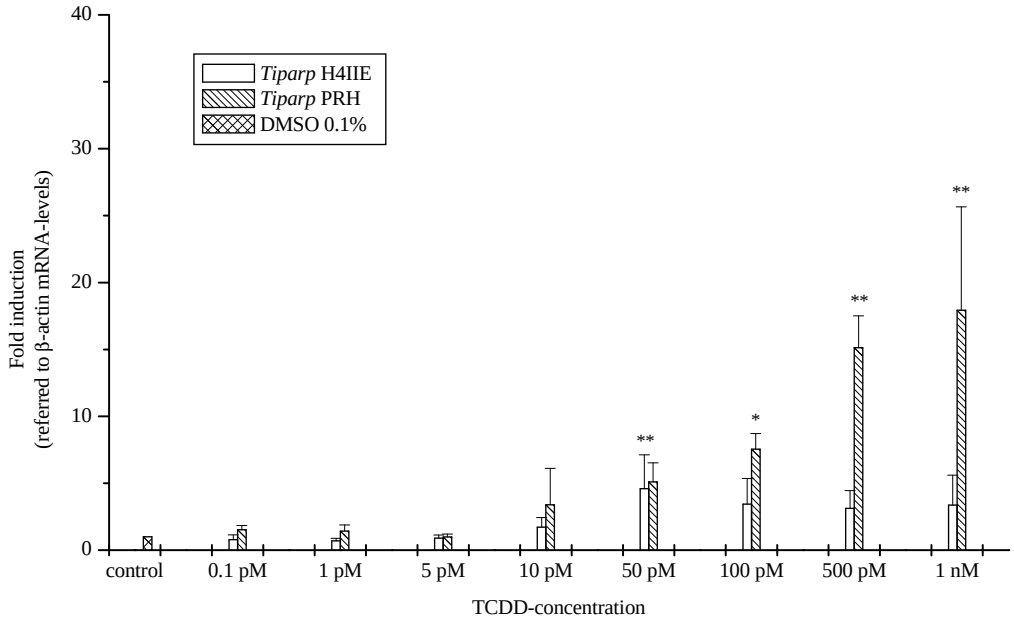

Figure 54: QRT-PCR (*Tiparp*) H4IIE vs. PRH. Cells treated with TCDD for 24 h. TCDD-concentration (M) plotted against fold induction (referred to β-actin mRNA-levels). Results from four independent experiments each. One-way ANOVA with Dunnett's post test (control vs. treatments). *: p-value < 0.05; **: p-value < 0.01.

Consequence of incubation with TCDD for 24 h was a concentration-dependent increase of *Tiparp*-mRNA-levels in PRH (figure 54). Slightly enhancing from $5*10^{-11}$ M TCDD, fold induction gained statistically significant (p-value < 0.05; 10^{-10} M TCDD, 7.6±1.2-fold) value, and reached statistically very significant (p-value < 0.01) heights of 15.1(±2.4)-, and 17.9(±7.7)-fold from $5*10^{-10}$ to 10^{-9} M TCDD.

Sigmoid fitting (not shown) generated an EC50 of $1.51*10^{-10}(\pm 2.93*10^{-11})$ M TCDD, and an upper limit of 18.4(±0.9)-fold induction.

Count of gene-transcripts according to *Tiparp* was not affected concentration-dependently in H4IIE cells due to TCDD-exposure. However, a slight, statistically significant (p-value < 0.05) fold induction of 4.6(±2.5) was attained using $5*10^{-11}$ M TCDD.

4.2.3.2. QRT-PCR *in vitro* – core congeners & four potential AhR-target genes

Based on findings derived from qRT-PCR-analysis regarding impact of TCDD on eight potential AhR-target genes in PRH and H4IIE cells, a further selection was made due to responsiveness and concentration-dependence in both tested liver cell systems. Hence, *Cyp1a1*, *Cyp1a2*, *Cyp1b1*, and *Aldh3a1* were chosen, and effects of core congeners (TCDD, 1-PeCDD, 4-PeCDF, PCB 118, PCB 126, PCB 153, and PCB 156) on both H4IIE cells and PRH were investigated via q-RT-PCR.

4.2.3.2.1. QRT-PCR H4IIE cells – *Cyp1a1*

In figure 55, impact of TCDD, 1-PeCDD, or 4-PeCDF on *Cyp1a1*-mRNA-levels in H4IIE cells are contrasted. Cells were incubated with compounds for 24 h.

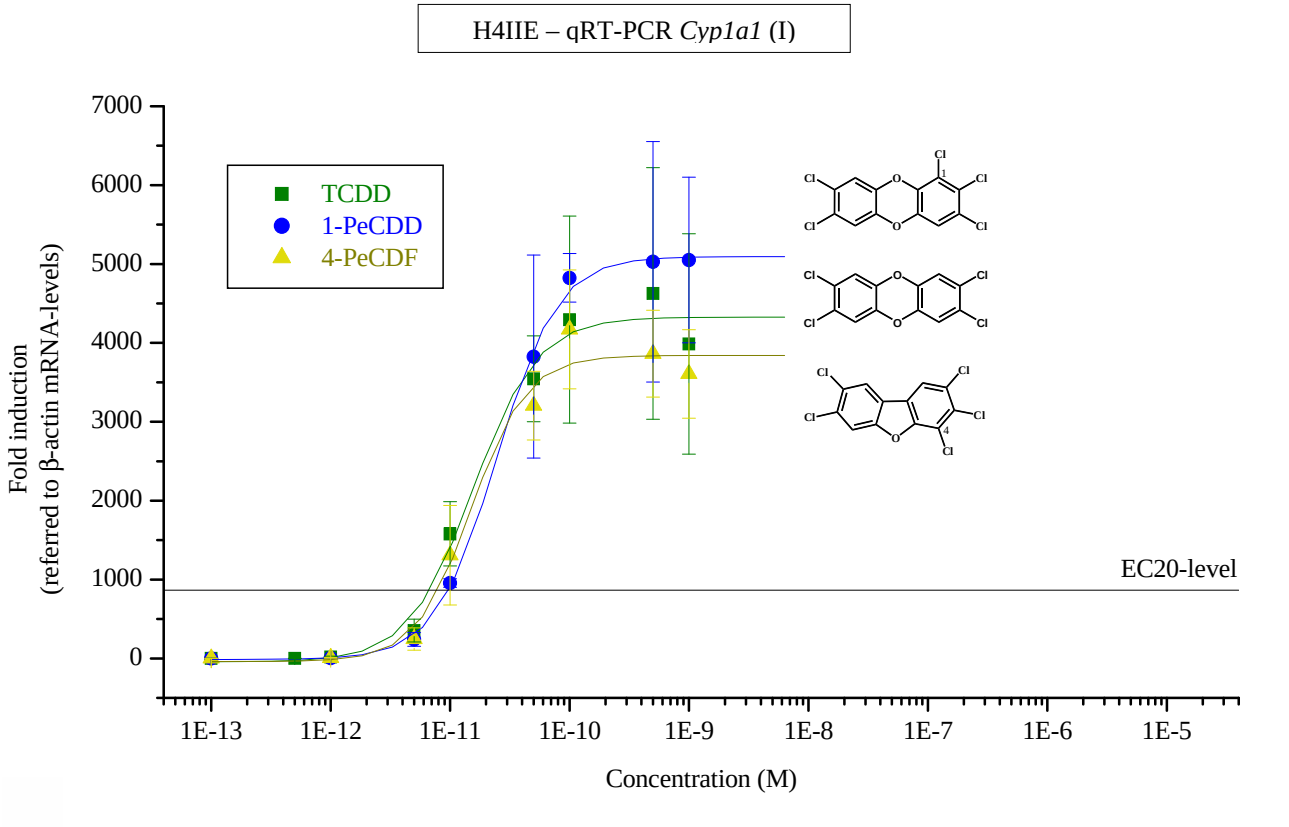

Figure 55: QRT-PCR (*Cyp1a1*) H4IIE (I). Cells treated with TCDD, 1-PeCDD, or 4-PeCDF for 24 h. Abscissa (logarithm.): Concentration (M); ordinate: Fold induction (referred to β-actin mRNA-levels). EC20-level represents 20% of TCDD-induced maximum response (865-fold). Results from at least three independent experiments each.

QRT-PCR-measurements regarding effects of TCDD, 1-PeCDD, or 4-PeCDF on *Cyp1a1* revealed quite comparable output among these congeners (figure 55). Concentration-dependently, incubation with each substance for 24 h led to an increase of relative *Cyp1a1*-mRNA-levels in H4IIE cells,

asymptotically yielding maximum levels, and accordingly outlining sigmoid curves. Upper asymptote obtained subsequent to TCDD-exposure was 4327.3(±188.0)-fold, bearing an EC20-level of 865-fold, and a correspondent EC20 of $6.76*10^{-12}$ M TCDD. Respective EC50 amounted to $1.55*10^{-11}(\pm 2.92*10^{-12})$ M TCDD.
Statistically very significant (p-value < 0.01; One-way ANOVA with Dunnett's post test; control vs. treatments) deviations from solvent control (DMSO 0.1%, not shown) were present from $5*10^{-11}$ M TCDD (3544.8±543.8-fold).

Being almost as potent as was TCDD, 4-PeCDF gained an EC50 of $1.51*10^{-11}(\pm 3.46*10^{-12})$ M (REP (EC50): 1.0), and was furthermore about ten per cent less efficient, compared to TCDD's properties (upper asymptote (4-PeCDF): 3841.6±196.8-fold). Calculated EC20 scored $7.99*10^{-12}$ M 4-PeCDF, correlating with a REP (EC20) of 0.85.
Statistically significant (p-value < 0.05) value was accomplished with 10^{-11} M 4-PeCDF (1308.8±630.9-fold), followed by statistically very significant (p-value < 0.01) inductions starting from $5*10^{-10}$ M 4-PeCDF (3204.8±436.2-fold).

1-PeCDD attained further, slightly lower potency, yielding an EC50 of $2.46*10^{-11}(\pm 1.62*10^{-12})$ M 1-PeCDD, corresponding with a REP (EC50) of 0.63. On the other hand, accompanied by a slightly steeper ascent in the logarithmical segment of the curve, maximum *Cyp1a1*-induction due to 1-PeCDD-incubation in H4IIE cells amounted to 5095.2(±75.6)-fold, which was more than 15% higher compared to the TCDD-derived maximum. Reflecting the lightly delayed ascent, EC20 scored $9.80*10^{-12}$ M 1-PeCDD and resulted in a REP (EC20) of 0.69.
Statistically very significant (p-value < 0.01) *Cyp1a1*-inductions were obtained from $5*10^{-11}$ M 1-PeCDD (3826.9±1285.8-fold).

A comparison of qRT-PCR-results analyzing effects of PCB 118, PCB 126, PCB 153, PCB 156, or TCDD on *Cyp1a1*-mRNA in H4IIE cells is imaged in figure 56.

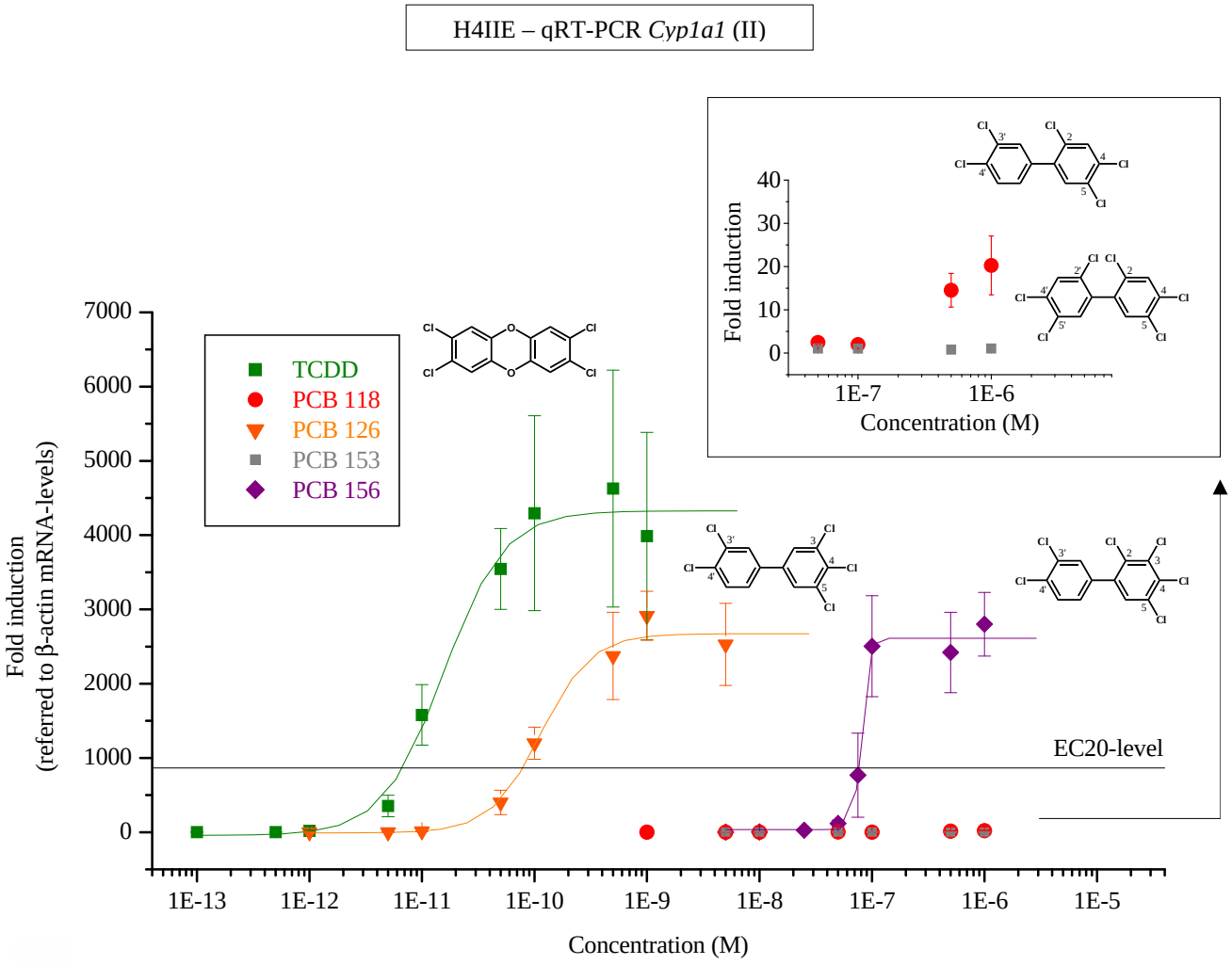

Figure 56: QRT-PCR (*Cyp1a1*) H4IIE (II). Cells treated with TCDD, PCB 118, PCB 126, PCB 153, or PCB 156 for 24 h. Axes with varying scales. Abscissae (logarithm.): Concentration (M); ordinates: Fold induction (referred to β-actin mRNA-levels). EC20-level represents 20% of TCDD-induced maximum response (865-fold). Results from at least three independent experiments each.

Shifted around one order of magnitude to higher concentrations compared to TCDD-derived effects, concentration-dependent increase of *Cyp1a1*-mRNA-levels in H4IIE cells due to incubation with PCB 126 appeared in sigmoid manner (figure 56).

EC50 was $1.14*10^{-10}(\pm 1.96*10^{-11})$ M PCB 126, bringing forth a REP (EC50) of 0.14, whereas upper asymptote lay at 2672.5(±134.0)-fold induction, consequently exhibiting almost 40% lower efficacy than TCDD. Ascending in lightly less extent, EC20-level was reached with $7.86*10^{-11}$ M PCB 126 (REP (EC20): 0.086).

Statistically very significant increases of *Cyp1a1*-mRNA were obtained from 10^{-10} M PCB 126 (1197.9±216.7-fold; p-value < 0.01; One-way ANOVA with Dunnett's post test; control vs. treatments).

Contrasted with PCB 126, the additionally substituted chlorine atom at position 2 in PCB 156 led to a further shift on the abscissa of around three orders of magnitude. Respective EC50 accounted for $8.01*10^{-08}$($\pm 2.59*10^{-9}$) M PCB 156, revealing a REP (EC50) of 0.00019. Running along an even steeper ascent compared to the TCDD-curve, the upper limit of sigmoid scored 2612.6(±100.6)-fold induction, scaling consistent efficacy of PCBs 126 and 156.
An EC20 of $7.60*10^{-8}$ M PCB 156 rendered a REP (EC20) of 0.000089, whereby statistically very significant (p-value < 0.01) *Cyp1a1*-inductions were gained beginning with 10^{-7} M PCB 156 (2504.0±679.2-fold).

Due to minor effects towards H4IIE cells, PCB 118-induced modifications were hidden in the main diagram in figure 56. With the aid of varied scaling, an additional display detail elaborated *Cyp1a1*-induction referable to PCB 118-exposure.
Among tested concentrations, slight increase of mRNA-levels was obtained for $5*10^{-7}$ M PCB 118 (14.5±3.9-fold), enhancing with the highest concentration of 10^{-6} M PCB 118 to 20.3(±6.8)-fold. Noted values statistically very significantly (p-value < 0.05) differed from solvent control (DMSO 0.1%, not shown). Hypothetically constructing PCB 118 from PCB 156, under abstraction of the chlorine substituent at position 3, led to inaccessibility concerning EC50-, as well as EC20-values under present conditions.

Cyp1a1-mRNA in H4IIE cells remained at base levels after application of PCB 153 throughout tested concentrations ($5*10^{-9}$-10^{-6} M).

4.2.3.2.2. QRT-PCR H4IIE cells – *Cyp1a2*

Investigations of *Cyp1a2*-mRNA in H4IIE cells affected by core congeners were evaluated and summarized in figure 57.

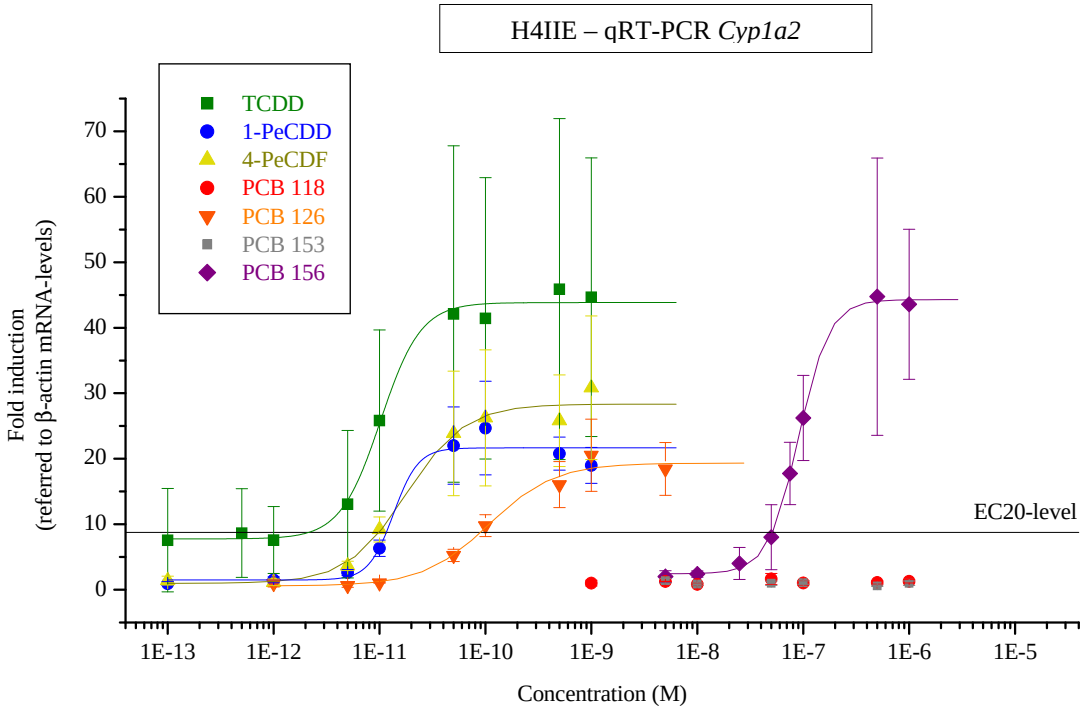

Figure 57: QRT-PCR (*Cyp1a2*) H4IIE. Cells treated with TCDD, 1-PeCDD, 4-PeCDF, PCB 118, PCB 126, PCB 153, or PCB 156 for 24 h. Abscissa (logarithm.): Concentration (M); ordinate: Fold induction (referred to β-actin mRNA-levels). EC20-level represents 20% of TCDD-induced maximum response (8.77-fold). Results from at least three independent experiments each.

As seen in figure 57, incubation of H4IIE cells with TCDD led to a concentration-dependent increase of *Cyp1a2*-mRNA in sigmoid manner. Running through an EC20 of $2.16*10^{-12}$ M TCDD, and an EC50 of $1.02*10^{-11}(\pm 8.46*10^{-13})$ M TCDD, an asymptote limited maximum induction level at 43.9(±0.8)-fold.

Statistically significant (p-value < 0.05; One-way ANOVA with Dunnett's post test; control vs. treatments) *Cyp1a2*-induction was obtained for 10^{-10} M TCDD (41.4±21.5-fold). Statistically very significant (p-value < 0.01) values were present for $5*10^{-11}$ M TCDD (42.1±25.7-fold), and from $5*10^{-10}$ M TCDD.

Attention should be paid to the lower limit of TCDD-derived effects on *Cyp1a2*-mRNA-levels, which with 7.8(±0.9)-fold induction lay quite high and additionally very close to the appropriate

EC20-level of 8.77-fold. Concurring with all other tested compounds' lower limits, which lay in a range of 0.6-2.4-fold induction, a reduction of congeners' EC20-REPs was affected.

Treatment with 4-PeCDF caused concentration-dependently increased formation of *Cyp1a2*-mRNA in H4IIE cells, whereas the appendant sigmoid function featured shorter and lightly flatter ascent in the logarithmical part of the curve compared to the TCDD-derived.
Furthermore, the slope was transferred to higher concentrations almost by a factor of two, revealing an EC50 of $1.79*10^{-11}(\pm 3.83*10^{-12})$ M (REP (EC50): 0.57) and yielding an upper limit of 28.3(±1.3)-fold induction. Associated with a lower extent regarding exponential ascent initiating the sigmoid, EC20-level was crossed with $9.94*10^{-12}$ M 4-PeCDF (REP (EC20): 0.22).
Statistically very significant (p-value < 0.01) fold induction was gained from $5*10^{-11}$ M 4-PeCDF (23.9±9.5-fold). Contrasted with TCDD, 4-PeCDF rendered about 35% less efficacy and around 40-80% (depending on the focused segment of curve) less potency towards H4IIE cells after 24 h of incubation.

Using 1-PeCDD, revealed concentration-response curve concerning *Cyp1a2*-induction on mRNA-level spanned a shorter excerpt on the ordinate, yielding an upper asymptote at 21.7(±1.1)-fold induction. Hence being about 50% less efficient than TCDD, relative potency referring to EC-levels added up to REP (EC50): 0.76 (EC50: $1.35*10^{-11}\pm 6.88*10^{-12}$ M 1-PeCDD), or REP (EC20): 0.19 (EC20: $1.16*10^{-11}$ M 1-PeCDD). Lying close together, depicted EC-values reflected a run of curve located close to the 4-PeCDF-derived, which was slightly delayed regarding initiation of ascent, combined with the steepest incline of slope among tested compounds.
Statistically very significant (p-value < 0.05) deviations of *Cyp1a2*-mRNA-levels compared to control (DMSO 0.1%, not shown) were obtained from $5*10^{-11}$ M 1-PeCDD (22.0±5.9-fold induction).

Moved to higher concentrations more than one order of magnitude, and proceeding less steep ascending, the concentration-response curve belonging to PCB 126's effects on *Cyp1a2*-mRNA-levels in H4IIE cells asymptotically reached 19.3(±1.2)-fold induction, thus being slightly less efficient than 1-PeCDD.
EC50 was $1.08*10^{-10}(\pm 2.35*10^{-11})$ M PCB 126, whereas EC20 scored $8.98*10^{-11}$ M PCB 126, corresponding to respective REPs of 0.095 (REP (EC50)), and 0.024 (REP (EC20)). Statistically very significant (p-value < 0.01) *Cyp1a2*-inductions were present from 10^{-10} M PCB 126 (9.8±1.7-fold).

Following a further shift about three orders of magnitude on the x-axis, the sigmoid representing concentration-dependent increase of *Cyp1a2*-mRNA-levels in H4IIE cells due to PCB 156-exposure delineated.

Ascending in comparable degree to the TCDD-derived curve within the logarithmical section, upper asymptotic value approached 44.3(±0.5)-fold induction, depicting TCDD-equivalent efficacy. EC50 amounted to $9.09*10^{-8}(\pm 1.83*10^{-9})$ M PCB 156, whereas EC20 scored $5.12*10^{-8}$ M PCB 156, revealing corresponding REPs of 0.00011 (REP (EC50)), and 0.000042 (REP (EC20)).

Statistically significant (p-value < 0.05) *Cyp1a2*-induction was obtained for 10^{-7} M PCB 156 (26.2±6.5-fold), followed by statistically very significant deviations from $5*10^{-7}$ M PCB 156 (44.7±21.2-fold; p-value < 0.01).

Subsequent to incubation of H4IIE cells with PCB 118, or PCB 153, relative quantity of *Cyp1a2*-mRNA remained on levels indistinguishable from those of solvent control.

4.2.3.2.3. QRT-PCR H4IIE cells – *Cyp1b1*

In figure 58, effects of core congeners on *Cyp1b1*-mRNA-levels in H4IIE cells measured by qRT-PCR are compiled.

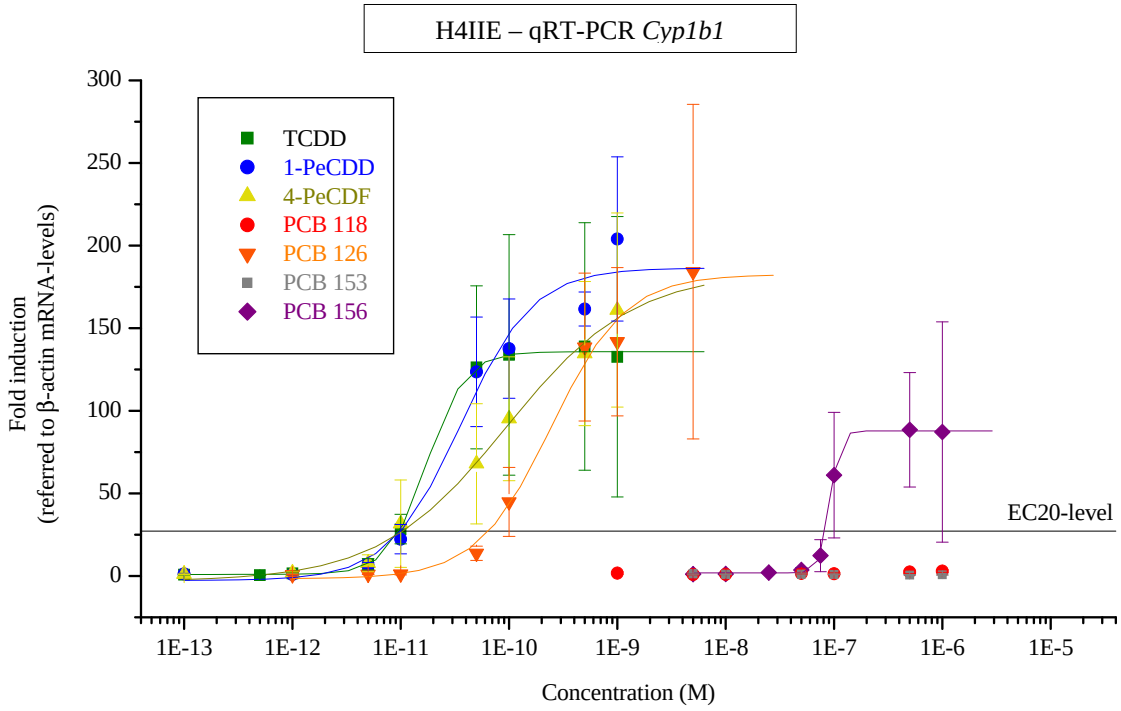

Figure 58: QRT-PCR (*Cyp1b1*) H4IIE. Cells treated with TCDD, 1-PeCDD, 4-PeCDF, PCB 118, PCB 126, PCB 153, or PCB 156 for 24 h. Abscissa (logarithm.): Concentration (M); ordinate: Fold induction (referred to β-actin mRNA-levels). EC20-level represents 20% of TCDD-induced maximum response (27.2-fold). Results from at least three independent experiments each.

Cyp1b1-induction in H4IIE cells due to TCDD-exposure indicated in figure 58 described a concentration-dependent increase asymptotically limited at 135.8(±1.3)-fold induction. Sigmoid curve ran through an EC20 of $9.76*10^{-12}$ M at 27.2-fold induction, and an EC50 of $1.75*10^{-12}(\pm 8.41*10^{-13})$ M TCDD. Statistically very significant (p-value < 0.01; One-way ANOVA with Dunnett's post test; control vs. treatments) deviations from solvent control (DMSO 0.1%, not shown) were achieved from $5*10^{-11}$ M TCDD (126.3±49.4-fold).

The sigmoid curve figuring *Cyp1b1*-mRNA-enhancing impact of 1-PeCDD ran through the EC20-level at a point very close to the TCDD-derived curve, precisely at $9.96*10^{-12}$ M, affording a REP (EC20) of 0.98. Since 1-PeCDD with maximal induction of 186.5(±14.2)-fold yielded higher efficacy (ca. 35%), and the slope ascended to slightly less extent, EC50 accounted for $3.60*10^{-11}(\pm 1.04*10^{-11})$ M 1-PeCDD, generating a respective REP (EC50) of 0.49.

From $5*10^{-11}$ M 1-PeCDD (123.6±33.1-fold), statistically very significant (p-value < 0.01) *Cyp1b1*-inductions were obtained.

At $1.04*10^{-11}$ M, as well crossing the EC20-level close to TCDD's sigmoid curve, treatment of H4IIE cells with 4-PeCDF engendered a REP (EC20) of 0.93 regarding *Cyp1b1*-induction on mRNA-level. Describing a flatter curve, sigmoid fitting unveiled an upper asymptotic value of 184.0(±23.3)-fold induction due to 4-PeCDF-exposure, being related to 1-PeCDD's upper induction level. EC50 scored $9.50*10^{-11}(\pm 3.82*10^{-11})$ M 4-PeCDF, corresponding to a REP (EC50) of 0.18. Statistically, significant (p-value < 0.05) *Cyp1b1*-induction was obtained by use of 10^{-10} M 4-PeCDF, amounting to 95.2(±37.5)-fold, whereas very significant (p-value < 0.01) inductions were present from $5*10^{-10}$ M 4-PeCDF.

Proceeding rather parallel to the 1-PeCDD-derived curve, the concentration-response curve depicting increase of *Cyp1b1*-mRNA-levels in H4IIE cells due to PCB 126-influence was shifted almost one order of magnitude to higher concentrations. Respective EC50 was $2.46*10^{-10}(\pm 5.11*10^{-11})$ M PCB 126 (REP (EC50): 0.071), whereas EC20 valued $6.49*10^{-11}$ M PCB 126, providing a REP (EC20) of 0.15. From statistical point of view, very significant *Cyp1b1*-inductions were gained beginning with $5*10^{-10}$ M PCB 126 at 138.5(±44.7)-fold (p-value < 0.01).

Contrasting with results for TCDD, 1-PeCDD, 4-PeCDF, or PCB 126, the sigmoid describing *Cyp1b1*-inducing effects of PCB 156 was both transferred to higher concentrations and yielded a lower asymptotic level at 87.8(±0.7)-fold induction. Being hence about 35% less efficient than TCDD, relative potencies of PCB 156 regarding *Cyp1b1*-induction in H4IIE cells based on EC-values were 0.00012 (EC20: $8.41*10^{-8}$ M PCB 156), and 0.00019 (EC50: $9.21*10^{-8}\pm 5.68*10^{-10}$ M PCB 156). Statistically very significant (p-value < 0.01) deviations from control were given from $5*10^{-7}$ M PCB 156 (88.5±34.6-fold induction).

Incubation with PCB 118 led to minor *Cyp1b1*-induction in H4IIE cells after 24 h. Usage of $5*10^{-7}$ M PCB 118 caused slight, but statistically significant increase to 2.5(±1.1)-fold *Cyp1b1*-mRNA-levels (p-value < 0.05). Under present conditions, maximal and statistically very significant value was reached with 10^{-6} M PCB 118 and scored 3.0(±0.7)-fold induction (p-value < 0.01).

PCB 153 did not affect *Cyp1b1*-mRNA-levels in H4IIE cells within the tested range of concentration ($5*10^{-9}$-10^{-6} M PCB 153).

4.2.3.2.4. QRT-PCR H4IIE cells – *Aldh3a1*

An assembly of qRT-PCR results regarding impact of core congeners on *Aldh3a1*-mRNA-levels in H4IIE cells is pictured in figure 59.

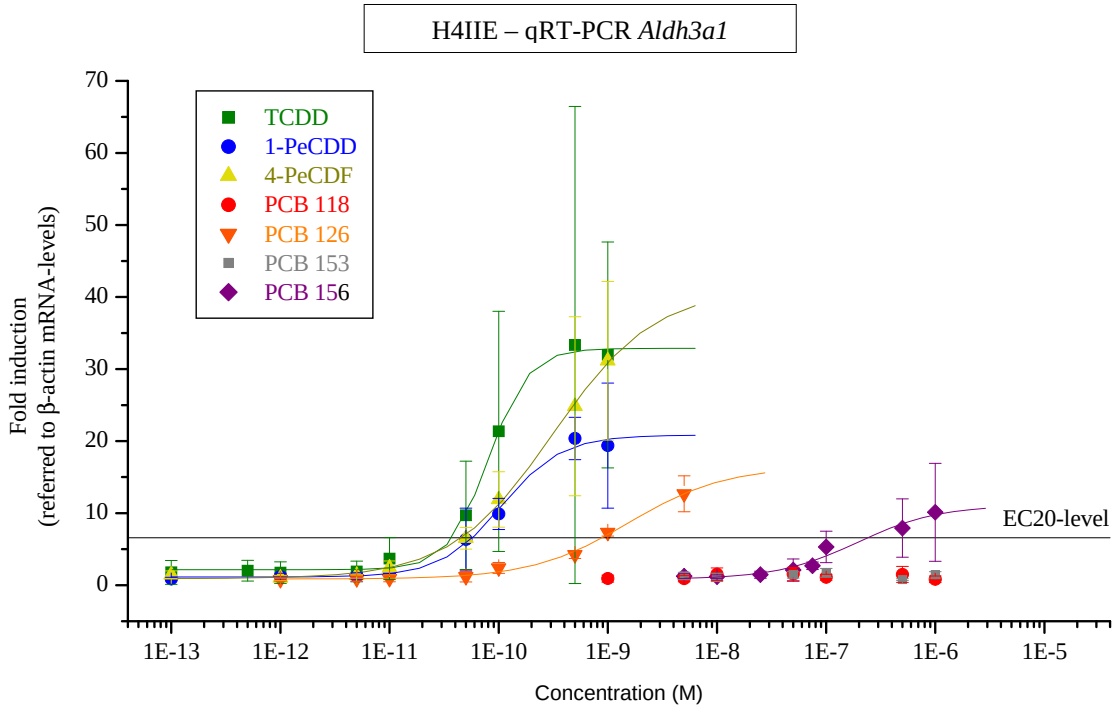

Figure 59: QRT-PCR (*Aldh3a1*) H4IIE. Cells treated with TCDD, 1-PeCDD, 4-PeCDF, PCB 118, PCB 126, PCB 153, or PCB 156 for 24 h. Abscissa (logarithm.): Concentration (M); ordinate: Fold induction (referred to β-actin mRNA-levels). EC20-level represents 20% of TCDD-induced maximum response (6.58-fold). Results from at least three independent experiments each.

Concentration-dependent effects of TCDD on *Aldh3a1*-mRNA-levels in H4IIE cells comprised elevated standard deviations (figure 59). Anyway, process of enhancement approved sigmoid fitting and revealed an EC50 of $8.03*10^{-11}(\pm 3.79*10^{-12})$ M TCDD, and an upper asymptote at 32.9(±0.7)-fold induction. 20% of TCDD-induced maximum response was yielded with $3.76*10^{-11}$ M TCDD, and respective EC20-level cut the ordinate at 6.58-fold induction.
Statistically significant (p-value < 0.05; One-way ANOVA with Dunnett's post test; control vs. treatments) increase of *Aldh3a1*-mRNA was obtained for $5*10^{-10}$ M TCDD (33.3±33.1-fold), and 10^{-9} M TCDD (32.0±15.7-fold).

Exhibiting a flatter ascent in the logarithmical segment, the concentration-response curve derived by 1-PeCDD-exposure gained an upper limit of 20.8(±1.2)-fold induction and an EC50 of

$1.06*10^{-10}$ M 1-PeCDD (REP (EC50): 0.76) regarding *Aldh3a1*-mRNA-levels in H4IIE cells. EC20 scored $5.74*10^{-11}$ M 1-PeCDD, accompanying a REP (EC20) of 0.66.
Relevant data concerning statistical analysis were obtained for 10^{-10} M 1-PeCDD (p-value < 0.05), and beginning from $5*10^{-10}$ M 1-PeCDD (p-value < 0.01; 20.4±2.9-fold induction).

Presumably being located within the upper section of the logarithmical part of curve testing up to 10^{-9} M 4-PeCDF, sigmoid fitting under weighting of standard deviations extrapolated an upper value regarding *Aldh3a1*-induction of (32.3±12.5)-fold for this congener. Referring sigmoid implied an EC20 of $5.03*10^{-11}$ M 1-PeCDF, and an EC50 of $1.59*10^{-10}(\pm1.07*10^{-10})$ M 1-PeCDF, leading to REPs of 0.75 (REP (EC20)), and 0.50 (REP (EC50)).
Statistically very significant deviations (p-value < 0.01) from solvent-control (DMSO 0.1%, not shown) were gained for $5*10^{-10}$ M 4-PeCDF (24.8±12.4-fold), and 10^{-9} M 4-PeCDF, scoring 31.2(±11.0)-fold.

Ascending an even flatter slope, sigmoid function illustrating PCB 126-induced increase of *Aldh3a1*-mRNA-levels approached an asymptote at 16.5(±3.0)-fold induction. Being about half as efficient as TCDD, relative potencies based on EC-values scored 0.052 (REP (EC50)), regarding an EC50 of $1.55*10^{-9}(\pm7.28*10^{-10})$ M PCB 126, and 0.042 (REP (EC20)), respecting the EC20 of $8.88*10^{-10}$ M PCB 126.
Statistically very significant (p-value < 0.01) induction of *Aldh3a1*-mRNA in H4IIE cells was present from $5*10^{-10}$ M PCB 126, amounting up to 12.7(±2.5)-fold (10^{-9} M PCB 126).

Depicting an approximately parallel course, the sigmoid delineating concentration-response relations of *Aldh3a1*-induction in H4IIE cells due to PCB 156-exposure was shifted about two orders of magnitude to higher concentrations compared to the PCB 126-derived. Respective EC50 was $1.95*10^{-7}(\pm1.44*10^{-7})$ M PCB 156, and REP (EC50) scored 0.00041. EC20-level was crossed with $2.40*10^{-7}$ M PCB 156 (REP (EC20): 0.00016), and upper limit added up to 11.1(±3.2)-fold induction of *Aldh3a1*.
Statistically relevant values were obtained for $5*10^{-7}$ M PCB 156 (p-value < 0.05; 7.9±4.0-fold), and 10^{-6} M PCB 156 (p-value < 0.01), yielding 10.1(±6.8)-fold induction.

Regarding PCB 118, or PCB 153, no effects on *Aldh3a1*-mRNA-levels in H4IIE cells were determined after 24 h of incubation.

4.2.3.2.5. QRT-PCR H4IIE cells – summary

Table 48 assembles qRT-PCR results regarding core congeners' effects on transcription of genes encoding CYP1A1, CYP1A2, CYP1B1, or ALDH3A1 in H4IIE cells. EC-values and respective REPs are contrasted with current WHO-TEFs from 2005 (Van den Berg *et al.*, 2006).

Table 48: EC50-, EC20-values and respective REPs derived from qRT-PCR analysis (*Cyp1a1, Cyp1a2, Cyp1b1, Aldh3a1*) with H4IIE cells subsequent to incubation with core congeners for 24 h compared to WHO-TEFs (Van den Berg *et al.*, 2006).

H4IIE	EC50 (M)	REP (EC50)	EC20 (M)	REP (EC20)	WHO-TEF (2005)
Cyp1a1					
TCDD	**1.55E-11**	**1**	**6.76E-12**	**1**	1
1-PeCDD	**2.46E-11**	**0.63**	**9.80E-12**	**0.69**	1
4-PeCDF	**1.51E-11**	**1.0**	**7.99E-12**	**0.85**	0.3
PCB 126	**1.14E-10**	**0.14**	**7.86E-11**	**0.086**	0.1
PCB 118					0.00003
PCB 156	**8.01E-08**	**0.00019**	**7.60E-08**	**0.000089**	0.00003
PCB 153					-
Cyp1a2					
TCDD	**1.02E-11**	**1**	**2.16E-12**	**1**	1
1-PeCDD	**1.35E-11**	**0.76**	**1.16E-11**	**0.19**	1
4-PeCDF	**1.79E-11**	**0.57**	**9.94E-12**	**0.22**	0.3
PCB 126	**1.08E-10**	**0.095**	**8.98E-11**	**0.024**	0.1
PCB 118					0.00003
PCB 156	**9.09E-08**	**0.00011**	**5.12E-08**	**0.000042**	0.00003
PCB 153					-
Cyp1b1					
TCDD	**1.75E-11**	**1**	**9.76E-12**	**1**	1
1-PeCDD	**3.60E-11**	**0.49**	**9.96E-12**	**0.98**	1
4-PeCDF	**9.50E-11**	**0.18**	**1.04E-11**	**0.93**	0.3
PCB 126	**2.46E-10**	**0.071**	**6.49E-11**	**0.15**	0.1
PCB 118					0.00003
PCB 156	**9.21E-08**	**0.00019**	**8.41E-08**	**0.00012**	0.00003
PCB 153					-
Aldh3a1					
TCDD	**8.03E-11**	**1**	**3.76E-11**	**1**	1
1-PeCDD	**1.06E-10**	**0.76**	**5.74E-11**	**0.66**	1
4-PeCDF	**1.59E-10**	**0.50**	**5.03E-11**	**0.75**	0.3
PCB 126	**1.55E-09**	**0.052**	**8.88E-10**	**0.042**	0.1
PCB 118					0.00003
PCB 156	**1.95E-07**	**0.00041**	**2.40E-07**	**0.00016**	0.00003
PCB 153					-

4.2.3.2.6. QRT-PCR primary rat hepatocytes – *Cyp1a1*

QRT-PCR results according to incubation of PRH with TCDD, 1-PeCDD, or 4-PeCDF for 24 h and affected *Cyp1a1*-mRNA-levels are presented in figure 60.

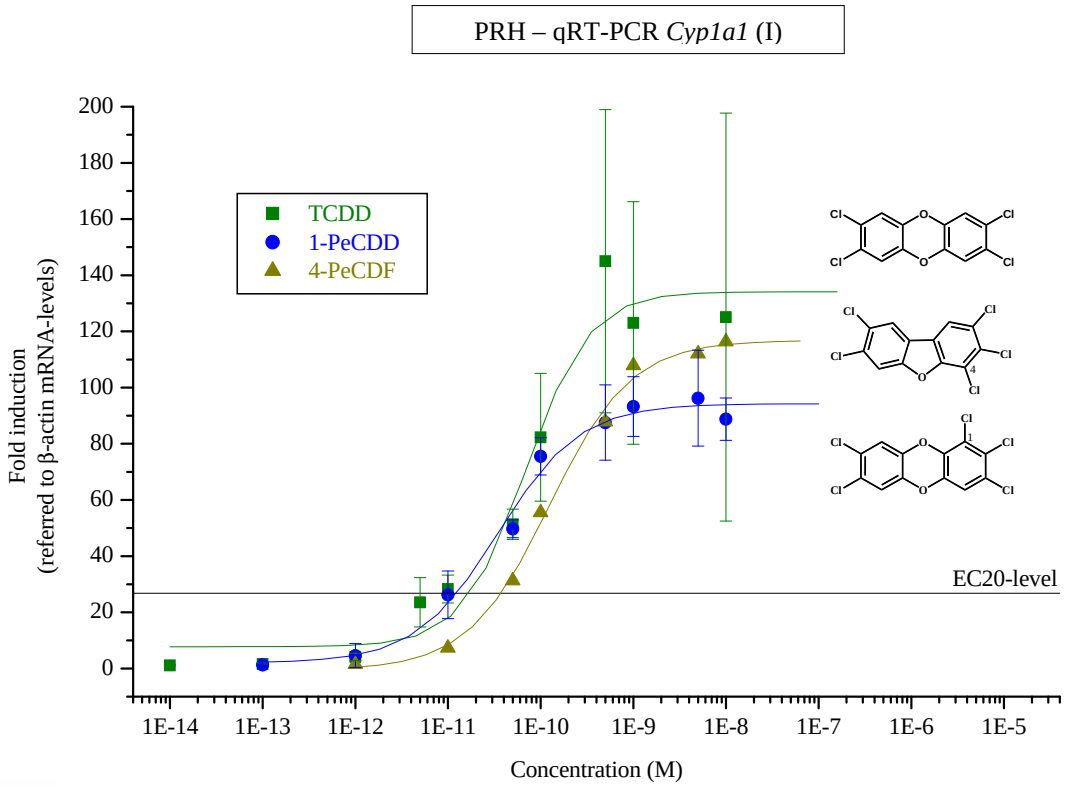

Figure 60: QRT-PCR (*Cyp1a1*) PRH (I). Cells treated with TCDD, 1-PeCDD, or 4-PeCDF for 24 h. Abscissa (logarithm.): Concentration (M); ordinate: Fold induction (referred to β-actin mRNA-levels). EC20-level represents 20% of TCDD-induced maximum response (26.8-fold). Results from at least three independent experiments each.

Concentration-dependent increase of *Cyp1a1*-mRNA-levels in PRH (figure 60) due to TCDD-exposure for 24 h delineated a sigmoid course. Under test conditions, maximal effects were confined to 134.1(±10.0)-fold induction. Consequential EC20-level amounted to 26.8-fold induction, implicating an EC20 of $1.78*10^{-11}$ M TCDD. EC50 was $6.94*10^{-11}(\pm 1.99*10^{-11})$ M TCDD. Statistically very significant (p-value < 0.01; One-way ANOVA with Dunnett's post test; control vs. treatments) *Cyp1a1*-elevations were obtained beginning from 10^{-10} M TCDD with 82.3(±22.8)-fold induction.

Increasing with slightly lower concentrations compared to TCDD, the concentration-response curve representing 1-PeCDD's effects on *Cyp1a1*-mRNA cut the EC20-level with $1.25*10^{-11}$ M 1-PeCDD, generating a REP (EC20) of 1.4. Accompanied by a flattened ascent in the logarithmical

segment, and passing an EC50 of $3.45*10^{-11}(\pm 7.32*10^{-12})$ M 1-PeCDD, the sigmoid approached 94.2(±3.3)-fold induction, evincing about 70% of TCDD's efficacy. REP (EC50) expressed a potency of 2.0 in relation to TCDD.

Statistically significant (p-value < 0.05) deviation from solvent control (DMSO 0.1%, not shown) was obtained with 10^{-11} M 1-PeCDD, (26.3±8.5-fold) whereas from $5*10^{-11}$ M 1-PeCDD, statistically very significant (p-value < 0.01) inductions up to 96.2(±17.1)-fold were yielded.

Slightly shifted to higher concentrations, the sigmoid curve illustrating concentration-responsiveness regarding *Cyp1a1*-mRNA in PRH due to 4-PeCDF-treatment reached the EC20-level at $3.73*10^{-11}$ M 4-PeCDF (REP (EC20): 0.48) and yielded 116.8(±3.8)-fold induction. Hence, 4-PeCDF's efficacy was situated lower than TCDD's, but higher than 1-PeCDD's. EC50 amounted to $1.25*10^{-10}(\pm 1.90*10^{-11})$ M 4-PeCDF, revealing a REP (EC50) of 0.56.

From statistical point of view, 4-PeCDF led to significant (P< 0.05) *Cyp1a1*-induction using $5*10^{-10}$ M of the congener (87.9±24.5-fold), and very significant (p-value < 0.01) inductions from 10^{-10} M 4-PeCDF (107.9±48.6-fold) in PRH after 24 h of incubation.

Figure 61 presents *Cyp1a1*-qRT-PCR results referable to incubation of PRH with TCDD, PCB 118, PCB 126, PCB 153, or PCB 156 for 24 h.

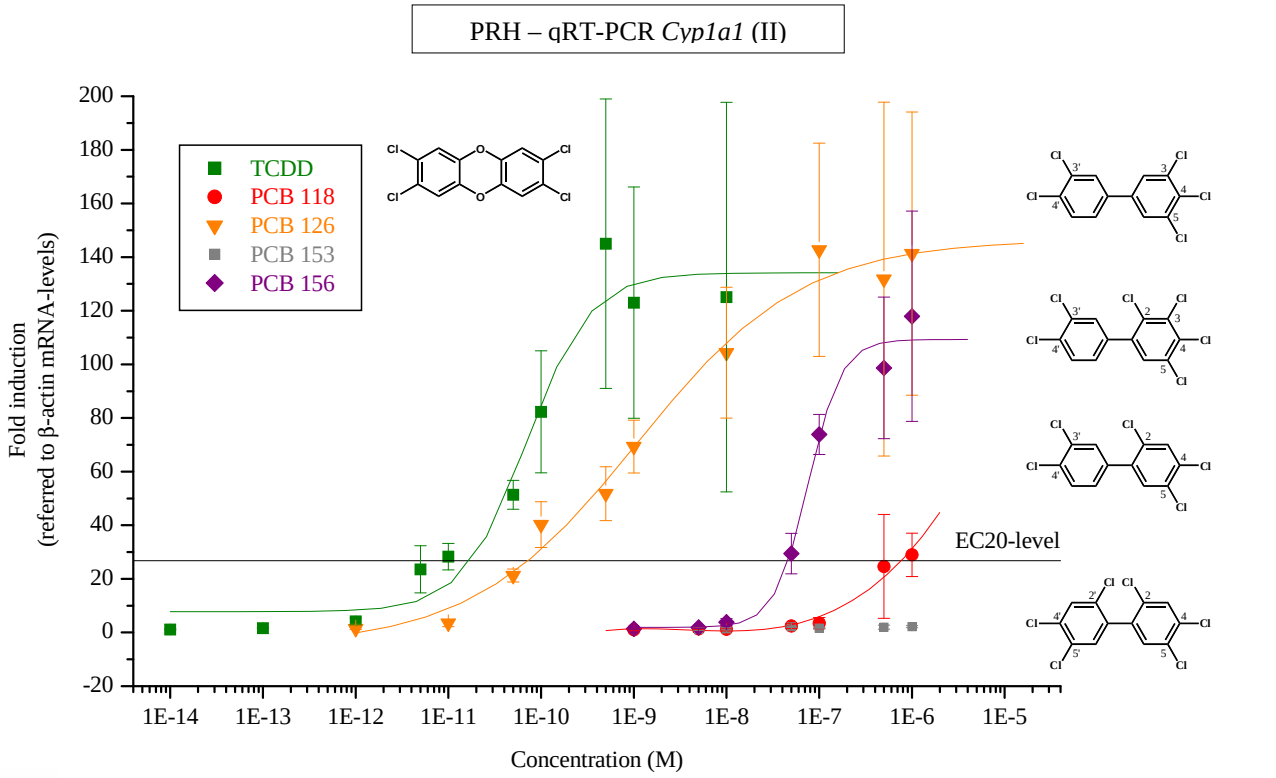

Figure 61: QRT-PCR (*Cyp1a1*) PRH (II). Cells treated with TCDD, PCB 118, PCB 126, PCB 153, or PCB 156 for 24 h. Abscissa (logarithm.): Concentration (M); ordinate: Fold induction (referred to β-actin mRNA-levels). EC20-level represents 20% of TCDD-induced maximum response (26.8-fold). Results from at least three independent experiments each.

Treatment of PRH with PCB 126 led to concentration-dependently increasing *Cyp1a1*-mRNA-levels (figure 61). Compared to TCDD's effects, sigmoid fitting generated a curve exhibiting a less steep slope across the entire graph, further transferred about 1.5 orders of magnitude to higher concentrations. This shift respecting the middle of the curve implied an EC50 of $1.10*10^{-9}(\pm 4.50*10^{-10})$ M PCB 126 (REP (EC50): 0.063). EC20-level was crossed with $7.28*10^{-11}$ M PCB 126, bringing forth a REP (EC20) of 0.24. Maximally achieved *Cyp1a1*-indcution in PRH due to PCB 126-treatment was 146.5(±8.7)-fold under present conditions. Statistically very significant (p-value < 0.01; One-way ANOVA with Dunnett's post test; control vs. treatments) deviations from control (DMSO 0.1%, not shown) were given from 10^{-8} M PCB 126 (104.3±24.4-fold).

Shifted about three orders of magnitude to higher concentrations and attaining almost 20% less efficacy scoring 109.3(±5.7)-fold induction compared to the curve derived by TCDD-exposure, the sigmoid reflecting PCB 156-induced effects implied an EC50 of $7.61*10^{-8}$($\pm 9.12*10^{-9}$) M PCB 156 (REP (EC50): 0.00091). EC20 amounted to $4.64*10^{-8}$ M PCB 156, revealing a respective REP (EC20) of 0.00038.
Statistically very significant (p-value < 0.01) *Cyp1a1*-inductions in PRH due to PCB 156-treatment were gained from 10^{-7} M PCB 156 (73.9±7.5-fold). Comparing PCB 156 to PCB 126, the additional chlorine atom in position 2 led to decreased potency (2-3 orders of magnitude), as well as reduced efficacy (75%) regarding *Cyp1a1*-induction in PRH.

Cyp1a1-mRNA-levels lightly increased beginning with around 10^{-7} M PCB 118 (3.5±2.1-fold), by exponential enhancement reaching statistically very significant values from $5*10^{-7}$ to 10^{-6} M PCB 118, not exceeding 29.0(±8.1)-fold induction (p-value < 0.01). By means of polynomial fitting, an EC20 of $7.62*10^{-7}$ M PCB 118 was established, correspondent to a REP (EC20) of 0.000023.
Respecting *Cyp1a1*-induction in PRH, hypothetical abstraction of the chlorine atom in position 3 implicated decreased potency (~1.5 orders of magnitude regarding EC20-values) and, under given test conditions, a lack of knowledge regarding maximal effects and accessible EC50, comparing PCB 118 with PCB 156.
Contrasting PCB 118 to PCB 126, potency lowered about 4 orders of magnitude (applying EC20-values) along with a theoretical exchange of chlorine substituents from position 3 to 2.

No effect on *Cyp1a1*-mRNA-levels was obtained due to PCB 153-exposure ($5*10^{-9}$-10^{-6} M) to PRH.

4.2.3.2.7. QRT-PCR primary rat hepatocytes – *Cyp1a2*

In figure 62, qRT-PCR results regarding *Cyp1a2*-mRNA and effects of core congeners after 24 h of incubation towards PRH are summarized.

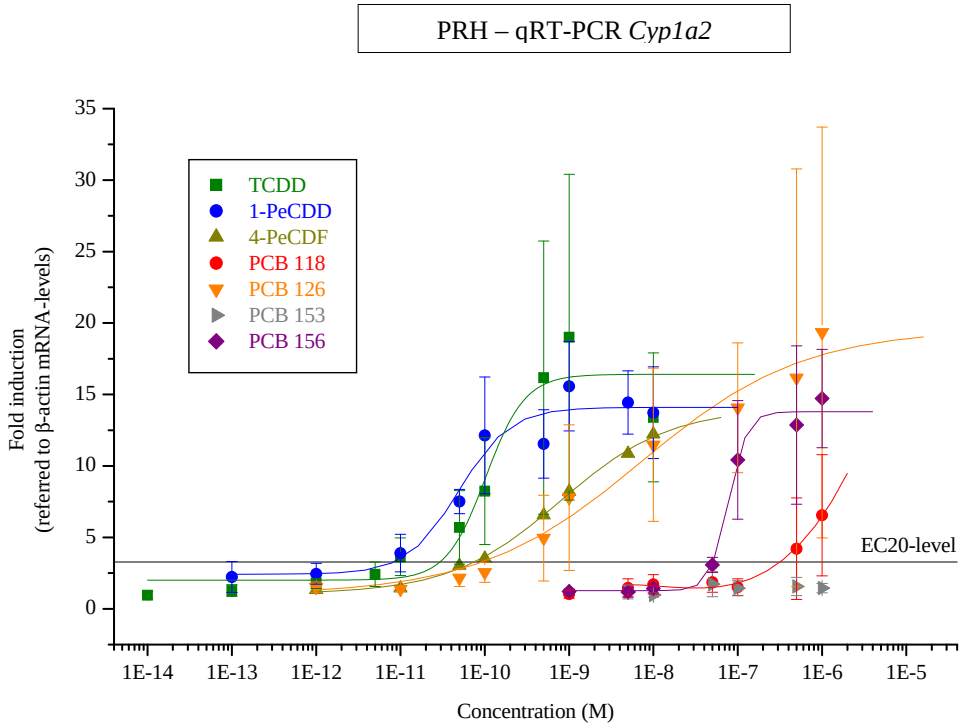

Figure 62: QRT-PCR (*Cyp1a2*) PRH. Cells treated with TCDD, 1-PeCDD, 4-PeCDF, PCB 118, PCB 126, PCB 153, or PCB 156 for 24 h. Abscissa (logarithm.): Concentration (M); ordinate: Fold induction (referred to β-actin mRNA-levels). EC20-level represents 20% of TCDD-induced maximum response (3.28-fold). Results from at least three independent experiments each.

Increase of *Cyp1a2*-mRNA in PRH due to TCDD-treatment indicated a concentration-response-relationship in sigmoid manner (figure 62). Correspondent fitted curve passed an EC50 of $1.03*10^{-10}(\pm 3.28*10^{-11})$ M TCDD and was asymptotically limited at 16.4(±1.4)-fold induction. 20% of maximum induction (3.28-fold) was obtained with $2.94*10^{-11}$ M TCDD.

Regarding statistical aspects, very significant (p-value < 0.01; One-way ANOVA with Dunnett's post test; control vs. treatments) *Cyp1a2*-inductions were gained using $\geq 5*10^{-10}$ M TCDD (≤19.0±11.4-fold).

Slightly orientated to lower concentrations, the sigmoid depicting 1-PeCDD's effects on *Cyp1a2*-mRNA in PRH exhibited a slightly flattened ascent and approached an asymptote at 14.1(±0.8)-fold induction. EC50 accounted for $4.91*10^{-11}(\pm 1.61*10^{-11})$ M 1-PeCDD, whereby EC20 scored

$8.40*10^{-12}$ M 1-PeCDD. Respective REPs amounted to 2.1 (REP (EC 50), and 3.5 (REP (EC20)). Statistically significant (p-value < 0.05) *Cyp1a2*-induction of 7.5(±0.8)-fold was yielded with $5*10^{-11}$ M 1-PeCDD, and very significant (p-value < 0.01) values, beginning from 10^{-10} M 1-PeCDD, achieved up to 15.6(±3.1)-fold induction.
Thus, compared to TCDD, 1-PeCDD manifested slightly lower (~15%) efficacy towards PRH, but higher potency according to revealed REPs.

Transferred about one order of magnitude to higher concentrations (REP (EC50): 0.13), and furthermore showing less ascent, the sigmoid curve displaying effects of 4-PeCDF on *Cyp1a2*-mRNA ran through an EC50 of $7.84*10^{-10}(\pm 1.89*10^{-10})$ M 4-PeCDF, and yielded an upper level at 14.0(±0.9)-fold induction, representing an efficacy equal to 1-PeCDD's. EC20-level was cut at $7.55*10^{-11}$ M 4-PeCDF, generating a REP (EC20) of 0.39.
Statistically, values regarded significant (p-value < 0.05), and very significant (p-value < 0.01), were obtained by use of 10^{-9} M 4-PeCDF (8.2±4.3-fold), and from $5*10^{-9}$-10^{-8} M 4-PeCDF (up to 12.2±4.7-fold), respectively.

Ascending in comparable extent, but shifted about one order of magnitude to higher concentrations regarding EC50 ($7.19*10^{-9}\pm 5.55*10^{-9}$ M PCB 126), the concentration-response curve illustrating PCB 126's *Cyp1a2*-inducing effects gained around 40% greater efficacy (19.6±2.0-fold) than did 4-PeCDF. Calculated EC20 was $9.37*10^{-11}$ M PCB 126. REPs representing potencies relative to TCDD accounted for 0.31 (REP (EC20)), and 0.014 (REP (EC50), whereas PCB 126 yielded almost 20% higher efficacy than TCDD.
Due to comparatively high standard deviations, statistically significant (p-value < 0.05) *Cyp1a2*-induction of 19.3(±14.4)-fold was given with 10^{-6} M PCB 126.

With respect to effects of PCB 156, incubation of PRH with this compound led to *Cyp1a2*-induction on mRNA-level in a concentration-dependent manner, apart from a slightly steeper slope resembling the TCDD-derived sigmoid, but located approximately three orders of magnitude at higher concentrations. EC50 scored $7.79*10^{-8}(\pm 6.14*10^{-9})$ M PCB 156, revealing a REP (EC50) of 0.0013. Upper asymptote lay at 13.8(±0.5)-fold induction, implying efficacy similar to 4-PeCDF's, or PCB 126's. The curve crossed the EC20-level with $5.15*10^{-8}$ M PCB 156, revealing a REP (EC20) of 0.00057.
Respecting statistical analysis, PCB 156-concentrations beginning from 10^{-7} M (10.4±4.1-fold) very significantly (p-value < 0.01) induced *Cyp1a2*.

Due to minor potency of PCB 118 to induce *Cyp1a2* in PRH within 24 h and tested range of concentration, only an initiating exponential course of increase was examined. Polynomial fitting unveiled an EC20 of $3.16*10^{-7}$ M PCB 118, respecting a REP (EC20) of 0.000093, hence extrapolating more than four orders of magnitude lesser potency of PCB 118 compared to TCDD's. Statistically, testing 10^{-6} M PCB 118, the *Cyp1a2*-induction amounting to 6.5(±4.2)-fold was regarded significant (p-value < 0.05).

PCB 153 showed no *Cyp1a2*-induction accessible via qRT-PCR measurements towards PRH under present test conditions.

4.2.3.2.8. QRT-PCR primary rat hepatocytes – *Cyp1b1*

Results of qRT-PCR-analysis regarding *Cyp1b1* in PRH incubated with core congeners for 24 h are compiled in figure 63.

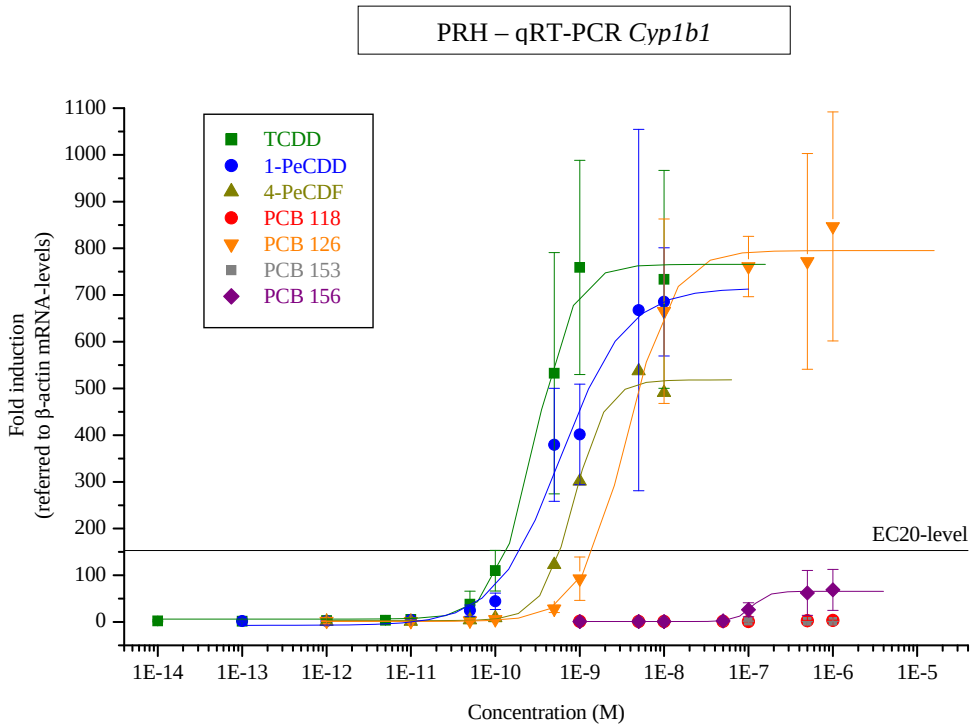

Figure 63: QRT-PCR (*Cyp1b1*) PRH. Cells treated with TCDD, 1-PeCDD, 4-PeCDF, PCB 118, PCB 126, PCB 153, or PCB 156 for 24 h. Abscissa (logarithm.): Concentration (M); ordinate: Fold induction (referred to β-actin mRNA-levels). EC20-level represents 20% of TCDD-induced maximum response (153-fold). Results from at least three independent experiments each.

Incubation of PRH with TCDD led to a concentration-dependently increasing level of *Cyp1b1*-mRNA (figure 63). The respective sigmoid comprised a steep slope, ran through an EC50 of $2.91*10^{-10}(\pm 3.68*10^{-11})$ M TCDD, and yielded maximal effects of 765.8(±29.4)-fold induction. EC20, which crossed an induction-level of 153-fold, accounted for $1.38*10^{-10}$ M TCDD. Considering statistical aspects, very significant (p-value < 0.01; One-way ANOVA with Dunnett's post test; control vs. treatments) *Cyp1b1*-inductions from $5*10^{-10}$ M TCDD (532.5±258.3-fold) were emphasized.

Comparing these findings with 1-PeCDD-affected mRNA-levels in PRH, the sigmoid illustrating *Cyp1b1*-induction depicted a lightly less steep ascent approaching an asymptote at 714.9(±52.0)-fold converging to the TCDD-derived upper level. EC50 amounted to $5.98*10^{-10}(\pm 1.29*10^{-10})$ M 1-PeCDD, revealing a REP (EC50) of 0.49, whereas EC20 scored $1.97*10^{-10}$ M 1-PeCDD, yielding a REP (EC20) of 0.70.
Statistically significant (p-value < 0.05) *Cyp1b1*-inductions were obtained with $5*10^{-10}$ to 10^{-9} M 1-PeCDD, and very significant (p-value < 0.01) effects of up to 685.4(±115.7)-fold were given with $5*10^{-9}$-10^{-8} M 1-PeCDD.

With regard to TCDD's sigmoid, the curve reflecting impact of 4-PeCDF on *Cyp1b1* in PRH was transferred about one third order of magnitude to higher concentrations, and possessed an EC50 of $8.57*10^{-10}(\pm 5.73*10^{-11})$ M 4-PeCDF (REP (EC50): 0.34), reaching up to 518.4(±15.0)-fold induction. Hence affording about 30% lower efficacy than TCDD, treatment of PRH with 4-PeCDF disclosed an EC20 of $5.83*10^{-10}$ M 4-PeCDF and a correspondent REP (EC20) of 0.24.
Statistically relevant were very significant (p-value < 0.01) deviations from control samples (DMSO 0.1%, not shown) starting from 10^{-9} M 4-PeCDF (301.3±122.6-fold) with respect to *Cyp1b1*-induction.

In contrast to TCDD-derived concentration-response curve, the sigmoid displaying PCB 126's impact on *Cyp1b1*-mRNA-levels was shifted about one order of magnitude to higher concentrations, slightly surpassing TCDD's upper level with maximally 795.3(±15.5)-fold induction. Assigned EC50 was $3.63*10^{-9}(\pm 5.09*10^{-10})$ M PCB 126 (REP (EC50): 0.080), whereas EC20-level was cut with $1.47*10^{-10}$ M PCB 126, revealing a REP (EC20) of 0.094.
From 10^{-8} M PCB 126 (665.3±197.4-fold), statistically very significant (p-value < 0.01) *Cyp1b1*-inductions were obtained in PRH.

Minor efficacy of PCB 156 towards *Cyp1b1*-induction on mRNA-level led to a flat sigmoid curve distinctly lying below the EC20-level. Upper asymptote yielded 65.6(±1.8)-fold induction, indicating more than 90% less efficacy than TCDD, whereas potency referring to EC50 ($1.10*10^{-7}$±$7.34*10^{-9}$ M PCB 156) accounted for 0.0026 (REP (EC50).
Statistically significant *Cyp1b1*-induction in PRH was obtained for $5*10^{-7}$-10^{-6} M PCB 156 scoring 62.4(±48.1)-68.8(±44.0)-fold (p-value < 0.01).

In tested concentrations, PCB 118 led to marginal increase of *Cyp1b1*-mRNA in PRH after 24 h. From statistical point of view, significant (p-value < 0.05) deviation from control was obtained with $5*10^{-7}$ M PCB 118 (2.6±1.1-fold), whereby very significant enhancement using 10^{-6} M PCB did not exceed (3.4±0.6)-fold induction (p-value < 0.01).

NDL-PCB 153 did not alter *Cyp1b1*-mRNA-levels in PRH within 24 h and applied range of concentration ($5*10^{-9}$-10^{-6} M PCB 153).

4.2.3.2.9. QRT-PCR primary rat hepatocytes – *Aldh3a1*

QRT-PCR results focusing *Aldh3a1* and analysis of PRH incubated with core congeners for 24 h are diagramed in figure 64.

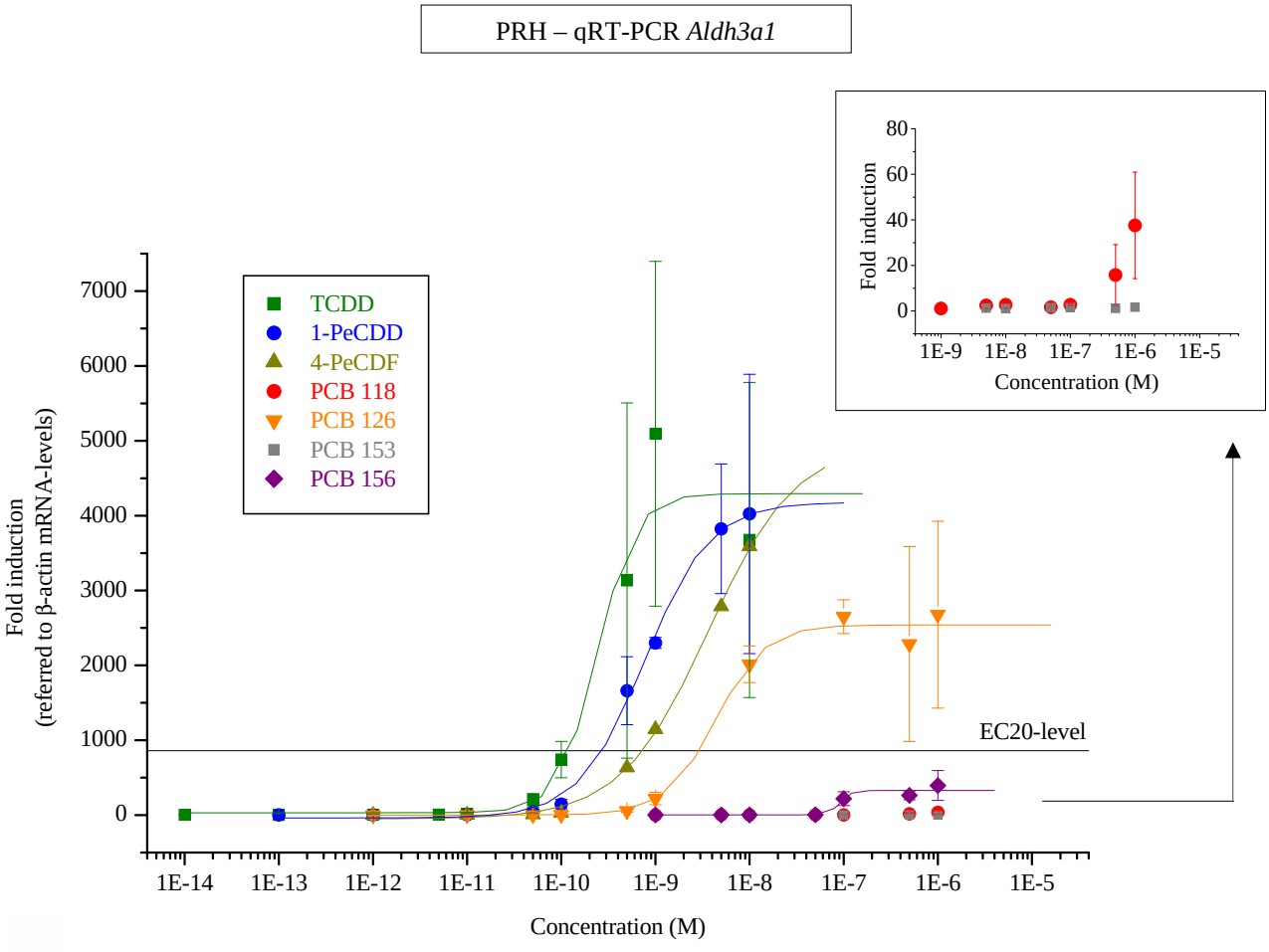

Figure 64: QRT-PCR (*Aldh3a1*) PRH. Cells treated with TCDD, 1-PeCDD, 4-PeCDF, PCB 118, PCB 126, PCB 153, or PCB 156 for 24 h. Axes with varying scales. Abscissae (logarithm.): Concentration (M); ordinates: Fold induction (referred to β-actin mRNA-levels). EC20-level represents 20% of TCDD-induced maximum response (859-fold). Results from at least three independent experiments each.

Concentration-dependent increase of *Aldh3a1* due to TCDD-treatment for 24 h was highly responsive in PRH, revealing a sigmoid function, which comprised a steep slope and approached 4293.6(±446.6)-fold induction (figure 64). Passed EC50 amounted to $2.41*10^{-10}$($\pm 9.16*10^{-11}$) M TCDD, and the EC20-level of 859-fold induction led to an EC20 of $1.24*10^{-10}$ M TCDD.

From statistical point of view, very significant (p-value < 0.01; One-way ANOVA with Dunnett's post test; control vs. treatments) enhancement of *Aldh3a1*-mRNA-levels was obtained from $5*10^{-10}$ M TCDD (3134.1±2373.0-fold).

Concentration-dependent *Aldh3a1*-induction in PRH by 1-PeCDD described a course with slightly lower degree of ascent. Fitted sigmoid implicated an EC50 of $7.71*10^{-10}(\pm 7.05*10^{-11})$ M 1-PeCDD (REP (EC50): 0.31), and an upper asymptote at 4180.1(±144.7)-fold induction.
Statistically significant value was indicated with 10^{-9} M 1-PeCDD (1661.0±453.9-fold; p-value < 0.05), whereas from $5*10^{-9}$ M 1-PeCDD (2300.0±74.3-fold), very significant *Aldh3a1*-inductions were obtained (p-value < 0.01). EC20-level was crossed with $2.72*10^{-10}$ M 1-PeCDD, bringing forth a REP (EC20) of 0.46.

4-PeCDF led to concentration-dependent increase of *Aldh3a1*-mRNA-levels in PRH indicating a sigmoid manner, although under test conditions, upper induction limit was not reached yet. Assuming that 4-PeCDF's properties would not exceed TCDD's efficacy, sigmoid fitting revealed an EC50 of $2.55*10^{-9}(\pm 1.34*10^{-10})$ M 4-PeCDF, corresponding to a REP (EC50) of 0.094. REP (EC20) added up to 0.17, calculated by an EC20 of $7.35*10^{-10}$ M 4-PeCDF.
Statistically significant (p-value < 0.05) *Aldh3a1*-induction of 1145.4(±477.1)-fold was gained with 10^{-9} M 4-PeCDF, and very significant (p-value < 0.01) values were examined from $5*10^{-9}$ M 4-PeCDF (2786.5±943.4-fold).

Providing an around 1.5 orders of magnitude lesser potency than TCDD based on REPs (REP (EC50): 0.055; REP (EC20): 0.043), the sigmoid reflecting *Aldh3a1*-inducing effects by PCB 126 approximated an upper level at (2541.2±76.0)-fold induction, implying an efficacy of the compound about 60% of TCDD's. Respective EC50 scored $4.37*10^{-9}(\pm 9.43*10^{-10})$ M PCB 126, and EC20 amounted to $2.90*10^{-9}$ M PCB 126.
Starting from 10^{-8} M PCB 126, and 2015.4(±244.0)-fold induction, statistically very significant elevation of *Aldh3a1*-mRNA-levels was obtained (p-value < 0.01).

PCB 156 affected transcription of gene encoding ALDH3A1 in concentration-dependent, sigmoid manner, revealing almost three orders of magnitude lower potency compared to TCDD. Yielding minor efficacy among tested compounds, sigmoid's upper asymptote approached 329.3(±38.0)-fold induction. Hence, rendering less than 10% of TCDD's efficacy, EC20-level of 859-fold induction was not achieved. EC50 scored $9.09*10^{-8}(\pm 2.77*10^{-8})$ M PCB 156, implying a REP (EC50) of 0.0026.
Statistical analysis characterized *Aldh3a1*-induction in PRH of 219.7(±91.7)-fold due to usage of 10^{-7} M PCB 156 as significant (p-value < 0.05), and very significant from $5*10^{-7}$ M PCB 156 (263.4±58.9-fold; p-value < 0.01).

Incubation of PRH with PCB 118 led to a slight concentration-dependent increase of *Aldh3a1*-mRNA-levels adding up to 15.8(±13.4)-fold induction with $5*10^{-7}$ M PCB 118, yielding statistically significant value of 37.6(±23.4)-fold testing the highest concentration of 10^{-6} M PCB 118.

Aldh3a1-mRNA-levels in PRH treated with PCB 153 for 24 h ($5*10^{-9}$-10^{-6} M PCB 153) remained indistinguishable from those of solvent controls.

4.2.3.2.10. QRT-PCR primary rat hepatocytes – summary

Table 49 summarizes QRT-PCR results concerning impact of core congeners on the genes *CYP1A1*, *CYP1A2*, *CYP1B1*, and *ALDH3A1* in PRH. Obtained EC20-, and EC50-values and corresponding REPs are collated and compared to WHO-TEFs from 2005 (Van den Berg *et al.*, 2006).

Table 49: EC50-, EC20-values and respective REPs derived from qRT-PCR analysis (*Cyp1a1, Cyp1a2, Cyp1b1, Aldh3a1*) with PRH subsequent to incubation with core congeners for 24 h compared to WHO-TEFs (Van den Berg *et al.*, 2006).

PRH	EC50 (M)	REP (EC50)	EC20 (M)	REP (EC20)	WHO-TEF (2005)
Cyp1a1					
TCDD	**6.94E-11**	**1**	**1.78E-11**	**1**	1
1-PeCDD	**3.45E-11**	**2.0**	**1.25E-11**	**1.4**	1
4-PeCDF	**1.25E-10**	**0.56**	**3.73E-11**	**0.48**	0.3
PCB 126	**1.10E-09**	**0.063**	**7.28E-11**	**0.24**	0.1
PCB 118			**7.62E-07**	**0.000023**	0.00003
PCB 156	**7.61E-08**	**0.00091**	**4.64E-08**	**0.00038**	0.00003
PCB 153					-
Cyp1a2					
TCDD	**1.03E-10**	**1**	**2.94E-11**	**1**	1
1-PeCDD	**4.91E-11**	**2.1**	**8.40E-12**	**3.5**	1
4-PeCDF	**7.84E-10**	**0.13**	**7.55E-11**	**0.39**	0.3
PCB 126	**7.19E-09**	**0.014**	**9.37E-11**	**0.31**	0.1
PCB 118			**3.16E-07**	**0.000093**	0.00003
PCB 156	**7.79E-08**	**0.0013**	**5.15E-08**	**0.00057**	0.00003
PCB 153					-
Cyp1b1					
TCDD	**2.91E-10**	**1**	**1.38E-10**	**1**	1
1-PeCDD	**5.98E-10**	**0.49**	**1.97E-10**	**0.70**	1
4-PeCDF	**8.57E-10**	**0.34**	**5.83E-10**	**0.24**	0.3
PCB 126	**3.63E-09**	**0.080**	**1.47E-09**	**0.094**	0.1
PCB 118					0.00003
PCB 156	**1.10E-07**	**0.0026**			0.00003
PCB 153					-
Aldh3a1					
TCDD	**2.41E-10**	**1**	**1.24E-10**	**1**	1
1-PeCDD	**7.71E-10**	**0.31**	**2.72E-10**	**0.46**	1
4-PeCDF	**2.55E-09**	**0.094**	**7.35E-10**	**0.17**	0.3
PCB 126	**4.37E-09**	**0.055**	**2.90E-09**	**0.043**	0.1
PCB 118					0.00003
PCB 156	**9.09E-08**	**0.0026**			0.00003
PCB 153					-

4.2.3.2.11. QRT-PCR H4IIE vs. QRT-PCR PRH – summary

Figure 65 compares qRT-PCR results for *Cyp1a1*, *Cyp1a2*, *Cyp1b1*, and *Aldh3a1* regarding TCDD-treatment of H4IIE to respective results concerning PRH.

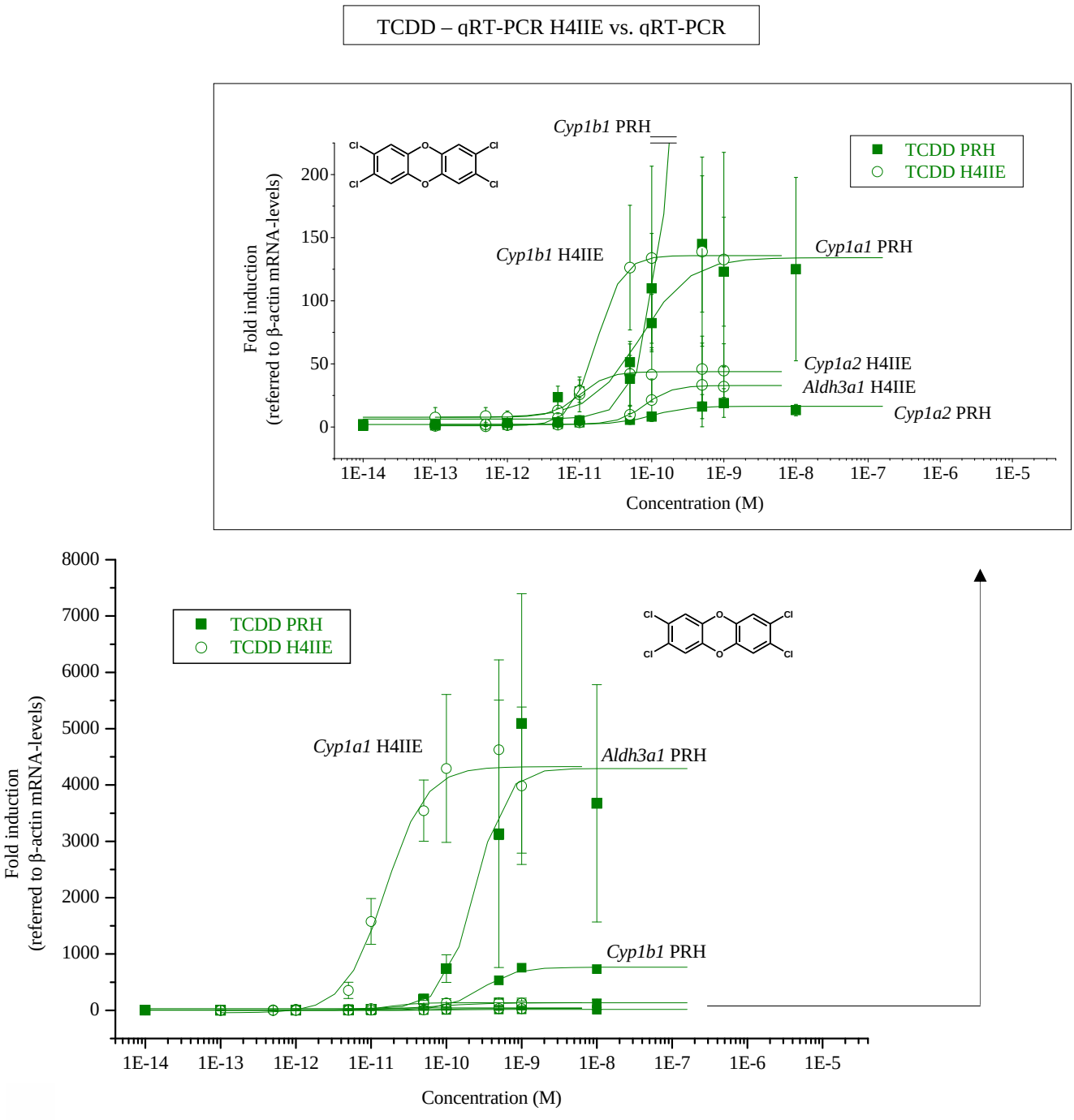

Figure 65: QRT-PCR (*Cyp1a1, Cyp1a2, Cyp1b1, Aldh3a1*) H4IIE vs. PRH. Cells treated with TCDD for 24 h. Axes with varying scales. Abscissae (logarithm.): Concentration (M); ordinates: Fold induction (referred to β-actin mRNA-levels). Results from four independent experiments each.

Contrasting effects on *Cyp1a1* in H4IIE cells with impact on *Aldh3a1* in PRH by means of qRT-PCR measurements (figure 65), TCDD-treatment yielded comparable efficacy but almost 1.5 orders of magnitude lower potency (REP [*Cyp1a1* (H4IIE)/ *Aldh3a1* (PRH)]: 0.064). Similar findings, but extenuated regarding differing potencies [REP *Cyp1b1* (H4IIE)/*Cyp1a1* (PRH): 0.25] were obtained comparing *Cyp1b1* (H4IIE) with *Cyp1a1* (PRH). Further correlation was indicated between TCDD's efficacy towards *Cyp1a2*, and *Aldh3a1* in H4IIE cells, where measured upper induction limits lay close together.

Focusing TCDD's efficacy in both liver cell systems in general, impact on *Cyp1a1*, or *Cyp1a2* was higher in H4IIE cells compared to PRH, whereas concerning *Cyp1b1*, or *Aldh3a1*, TCDD-treatment yielded greater efficacy in PRH than in H4IIE cells. Ranking order of TCDD-yielded efficacies in total was

Cyp1a1 (H4IIE) ≈ *Aldh3a1* (PRH) >> *Cyp1b1* (PRH) >> *Cyp1b1* (H4IIE) ≈ *Cyp1a1* (PRH)
> *Cyp1a2* (H4IIE) ≥ *Aldh3a1* (H4IIE) > *Cyp1a2* (PRH),
regarding treatment of cells for 24 h under present test conditions.

Taking account of relative potencies regarding attained EC-values, TCDD constantly revealed higher potency towards H4IIE cells compared to its impact on PRH. With this regard, contrasting EC-values for all genes among each other, REPs (H4IIE/PRH) were consistently below 1. Exceptions of this outcome, whereat TCDD's efficacy was situated conversely, were received considering subsequent potencies in descending order:
REP (EC20) [*Aldh3a1* (H4IIE)/ *Cyp1a1* (PRH)]: 2.12,
REP (EC20) [*Aldh3a1* (H4IIE)/ *Cyp1a2* (PRH)]: 1.28,
REP (EC50) [*Aldh3a1* (H4IIE)/ *Cyp1a1* (PRH)]: 1.16.

Comparing impact on same genes in different cell systems, a ranking order regarding degree of distinction between cell systems and respective EC50-values of
REP [*Cyp1b1* (H4IIE/PRH): 0.060] > REP [*Cyp1a2* (H4IIE/PRH): 0.10]
> REP [*Cyp1a1* (H4IIE/PRH): 0.060] > REP [*Aldh3a1* (H4IIE/PRH): 0.33] was obtained.

With respect to EC20-values, similar ranking order was established:
REP [*Cyp1b1* (H4IIE/PRH): 0.071] > REP [*Cyp1a2* (H4IIE/PRH): 0.073]
> REP [*Aldh3a1* (H4IIE/PRH): 0.30] > REP [*Cyp1a1* (H4IIE/PRH): 0.38].

REPs (H4IIE/PRH) concerning EC50-values scored from
0.035 (REP [*Cyp1a2* (H4IIE)/ *Cyp1b1* (PRH)]) to
0.78 (REP [*Aldh3a1* (H4IIE)/ *Cyp1a2* (PRH)]), whereas regarding EC20-values, REPs ranged from
0.016 (REP [*Cyp1a2* (H4IIE)/ *Cyp1b1* (PRH)]) to
0.55 (REP [*Cyp1b1* (H4IIE)/ *Cyp1a2* (PRH)]).

Assessed based on EC50-values, responsivity of genes beginning with lowest TCDD-concentrations ranked from
EC50 (*Cyp1a2* H4IIE) < EC50 (*Cyp1a1* H4IIE) < EC50 (*Cyp1b1* H4IIE) < EC50 (*Cyp1a1* PRH) < EC50 (*Aldh3a1* H4IIE) < EC50 (*Cyp1a2* PRH) < EC50 (*Aldh3a1* PRH) < EC50 (*Cyp1b1* PRH).

Responsivity regarding EC20-values rated
EC20 (*Cyp1a2* H4IIE) < EC20 (*Cyp1a1* H4IIE) < EC20 (*Cyp1b1* H4IIE) < EC20 (*Cyp1a1* PRH) < EC20 (*Cyp1a2* PRH) < EC20 (*Aldh3a1* H4IIE) < EC20 (*Aldh3a1* PRH) < EC20 (*Cyp1b1* PRH).

An assembly of REPs obtained by qRT-PCR analysis with H4IIE cells and PRH is compared to current WHO-TEFs from 1005 in table 50 (Van den Berg *et al.*, 2006).

Table 50: REPs derived from qRT-PCR measurements with PRH and H4IIE cells subsequent to incubation with core congeners for 24 h compared to WHO-TEFs (Van den Berg *et al.*, 2006).

QRT-PCR	REP (EC50) pRH	REP (EC50) H4IIE	REP (EC20) pRH	REP (EC20) H4IIE	WHO-TEF (2005)
Cyp1a1					
TCDD	**1**	**1**	**1**	**1**	1
1-PeCDD	**2.0**	**0.63**	**1.4**	**0.69**	1
4-PeCDF	**0.56**	**1.0**	**0.48**	**0.85**	0.3
PCB 126	**0.063**	**0.14**	**0.24**	**0.086**	0.1
PCB 118			**0.000023**		0.00003
PCB 156	**0.00091**	**0.00019**	**0.00038**	**0.000089**	0.00003
PCB 153					-
Cyp1a2					
TCDD	**1**	**1**	**1**	**1**	1
1-PeCDD	**2.1**	**0.76**	**3.5**	**0.19**	1
4-PeCDF	**0.13**	**0.57**	**0.39**	**0.22**	0.3
PCB 126	**0.014**	**0.095**	**0.31**	**0.024**	0.1
PCB 118			**0.000093**		0.00003
PCB 156	**0.0013**	**0.00011**	**0.00057**	**0.000042**	0.00003
PCB 153					-
Cyp1b1					
TCDD	**1**	**1**	**1**	**1**	1
1-PeCDD	**0.49**	**0.49**	**0.70**	**0.98**	1
4-PeCDF	**0.34**	**0.18**	**0.24**	**0.93**	0.3
PCB 126	**0.080**	**0.071**	**0.094**	**0.15**	0.1
PCB 118					0.00003
PCB 156	**0.0026**	**0.00019**		**0.00012**	0.00003
PCB 153					-
Aldh3a1					
TCDD	**1**	**1**	**1**	**1**	1
1-PeCDD	**0.31**	**0.76**	**0.46**	**0.66**	1
4-PeCDF	**0.094**	**0.50**	**0.17**	**0.75**	0.3
PCB 126	**0.055**	**0.052**	**0.043**	**0.042**	0.1
PCB 118					0.00003
PCB 156	**0.0026**	**0.00041**		**0.00016**	0.00003
PCB 153					-

Throughout tested core congeners, differing properties in particular regarding responsiveness towards H4IIE-cells and PRH explained above for TCDD emerged by trend for 1-PeCDD, 4-PeCDF, and PCB 126 (table 50).
Comparing impact on same genes in different cell systems, comparable findings as revealed for TCDD were obtained concerning 1-PeCDD, 4-PeCDF, or PCB 126, revealing higher potency towards H4IIE cells compared to its effect on PRH. With this regard, contrasting EC-values for all genes among each other, REPs (H4IIE/PRH) were consistently below 1, involving exceptionally higher potency of 1-PeCDD regarding *Cyp1a2* (REP EC20 1-PeCDD [*Cyp1a2* (H4IIE/PRH): 1.4]), and of 4-PeCDF towards PRH regarding *Cyp1a1* than in H4IIE (REP EC20 PCB 126 [*Cyp1a1* (H4IIE/PRH): 1.1]).

1-PeCDD revealed potency comparable to TCDD's, gaining the lowest among examined genes concerning *Aldh3a1* with a REP (EC50) of 0.31. Excepting *Cyp1a1*, and *Cyp1a2* in PRH, 1-PeCDD yielded higher potency than TCDD. In general, 1-PeCDD's efficacy approached TCDD's, but with respect to *Cyp1a1*, and *Cyp1a2* in PRH, or *Cyp1a2*, and *Aldh3a1* in H4IIE, the congener attained lightly lower efficacy than TCDD. In contrast, 1-PeCDD was more efficient regarding *Cyp1a1*, and *Cyp1b1* in H4IIE cells compared to TCDD.

Except for its impact on *Cyp1a1* in H4IIE cells (REP (EC50): 1.0), 4-PeCDF attained slightly lower potency than TCDD, accomplishing REPs of 0.094 (REP (EC50), *Aldh3a1* PRH) at the least. 4-PeCDF's efficacy tended to approach TCDD's efficacy regarding *Aldh3a1* (H4IIE, PRH), and *Cyp1b1* in H4IIE cells, but revealed lightly lower efficacy concerning remained genes in both cell types.

Deriving still less potency, PCB 126 yielded REPs scoring from 0.014 (REP (EC50) *Cyp1a2*, PRH) to 0.31 (REP (EC20) *Cyp1a2* PRH). By trend achieving efficacy comparable to TCDD's (PRH: *Cyp1a1*, *Cyp1a2*, *Cyp1b1*; H4IIE: *Cyp1b1*), lower efficacy of PCB 126 was received concerning *Aldh3a1* (H4IIE, PRH), *Cyp1a1* (H4IIE), and *Cyp1a2* (H4IIE).

Responsivity of liver cell systems due to PCB 156-incubation differed from those of TCDD or previously described core congeners. Assessed based on EC50-values, responsiveness of genes beginning with lowest PCB 156-concentrations ranked from
EC50 (*Cyp1a1* PRH) < EC50 (*Cyp1a2* PRH) < EC50 (*Cyp1a1* H4IIE) < EC50 (*Cyp1a2* H4IIE)
= EC50 (*Aldh3a1* PRH) < EC50 (*Cyp1b1* H4IIE) < EC50 (*Cyp1b1* PRH) < EC50 (*Aldh3a1* H4IIE).

Overall, deviation of PCB 156's EC50-values, which lay close together, ranged from $7.61*10^{-8}$ M PCB 156 (EC50 (*Cyp1a1* PRH)) to $1.95*10^{-7}$ M PCB 156 (EC50 (*Aldh3a1* H4IIE)). This contrasted with effects induced by TCDD, whose EC50-values comprised an about one order of magnitude wider range of concentration.

Comparing impact on same genes in different cell systems, except for REP (EC50) *Cyp1b1* (REP EC50 PCB 156 [*Cyp1b1* (H4IIE/PRH): 0.83]), potency attained by PCB 156 was higher towards PRH than in H4IIE cells, consistently resulting in REPs (H4IIE/PRH) ≥ 1. According to these findings, PCB 156 revealed higher potency towards PRH, which was even accompanied by efficacies comparable to TCDD's regarding *Cyp1a1*, and *Cyp1a2*.

Controversially, mRNA-levels of *Cyp1b1*, and *Aldh3a1* in PRH were marginally affected by PCB 156 and yielded less than 10% of TCDD's efficacy, hence retaining below corresponding EC20-levels. Regarding H4IIE cells, depending on respective genes, PCB 156 gained 34-65% of TCDD's efficacy (*Cyp1a1*, *Cyp1b1*, *Aldh3a1*), whereas *Cyp1a2* in H4IIE was equally efficiently affected by PCB 156 than by TCDD.

So far, core congeners induced gene transcription in present liver cell systems in sigmoid manner, whereas DL-PCB 118 in tested range of concentrations of up to 10^{-6} M PCB 118 comparably led to minor effects within 24 h of incubation.

Slightly increasing mRNA-levels in PRH beginning from 0.44% (*Cyp1b1*), over 0.88% of maximum TCDD-induced response for *Aldh3a1*, PCB 118-derived effects initially trespassed respective EC20-level at 21.6% (*Cyp1a1*), and culminated in maximal effects regarding *Cyp1a2* yielding 39.9% of TCDD's maximum response. *Cyp1a1* in H4IIE cells was slightly affected (0.47%) by PCB 118, which was closely followed by effects on *Cyp1b1*, accomplishing 2.2% of TCDD's upper limit.

With respect to *Cyp1a2*, and *Aldh3a1* in H4IIE cells, response due to PCB 118-treatment was absent under given test conditions.

Incubation with NDL-PCB 153 did not modify mRNA-levels of tested genes in both used liver cell systems.

4.3. *In vitro* investigations using human PBMCs

In order to gain information on potential impact of TCDD on cells of the immune system, freshly isolated primary human PBMCs were exposed to the compound. After characterization of applied cells by flow cytometry and subsequent incubation for 24 h in presence or in absence of a defined stimulus, mRNA of cells was isolated and investigated by use of whole genome microarray experiments as well as qRT-PCR. Aim of these examinations was to presumably disclose TCDD's mechanism(s) and mode(s) of action towards these immune cells and to identify possible overlap(s) with genes identified by mouse whole genome microarray analysis. Such observations could help understanding TCDD's immunotoxic effects and the role of the AhR in this regard, and might be feasible in view of a future establishment of potential novel biomarker(s).

4.3.1. Characterization of PBMCs by Flow Cytometry

Freshly isolated human PBMCs from four individuals were analyzed by means of flow cytometry (BD FACSCanto II, BD Biosciences, Heidelberg, Germany) in order to gain an insight into the composition of obtained cell suspensions.

Using monoclonal antibodies specifically binding CD3, CD19, or CD14 on the surface of cells, definite subsets of cells were identified as T lymphocytes ($CD3^+$), B lymphocytes ($CD19^+$), or monocytes/macrophages ($CD14^+$).

Cell populations were identified per forward scatter (FSC)/sideward scatter (SSC) dot blots according to their properties regarding cell size (FSC) and granularity (SSC). In figure 66, an exemplary dot plot for a flow cytometric analysis of freshly isolated human PBMCs is presented.

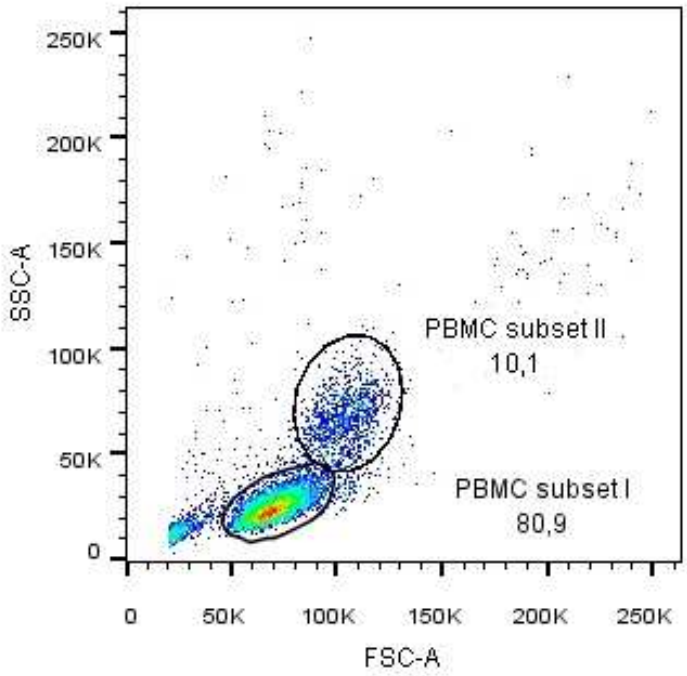

Figure 66: FACS analysis. Dot plot obtained by measurement of human PBMCs; FSC plotted against SSC. Two populations of cells were identified: PBMC subset I (80.9%), and PBMC subset II (10.1%). Sample from individual 2 (male). 10,000 events. Threshold count: 20,000.

As exemplarily shown in figure 66, two obvious populations of cells were identified by view on dot plots during FACS measurement of PBMCs.

A first subset of cells ('PBMC subset I') represented around 80% of sample particles analyzed by the flow cytometer. According to measured intensities for FSC and SSC, cells' properties added up to comparably low size and granularity, as compared to the second population of cells ('PBMC subset II'). This population accounted for about 10% of 10,000 events measured in total. Cell debris and other particles of smaller size and of low granularity constituted the majority of the remaining 10%. A few single events detected at higher levels for FSC and SSC might indicate scattered neutrophiles and/or granulocytes.

Proportions ranged from around 72 to 90% for PBMC subset I and from 5 to 16% for PBMC subset II of totally measured events. There was no gender-specific significant difference between samples from male and female individuals.

By means of specifically binding monoclonal antibodies and flow cytometry, $CD3^+$-, $CD19^+$-, or $CD14^+$-cells were identified within the two populations PBMC subset I and II. Figure 67 exemplarily shows verifications of $CD3^+$-, and $CD19^+$-cells.

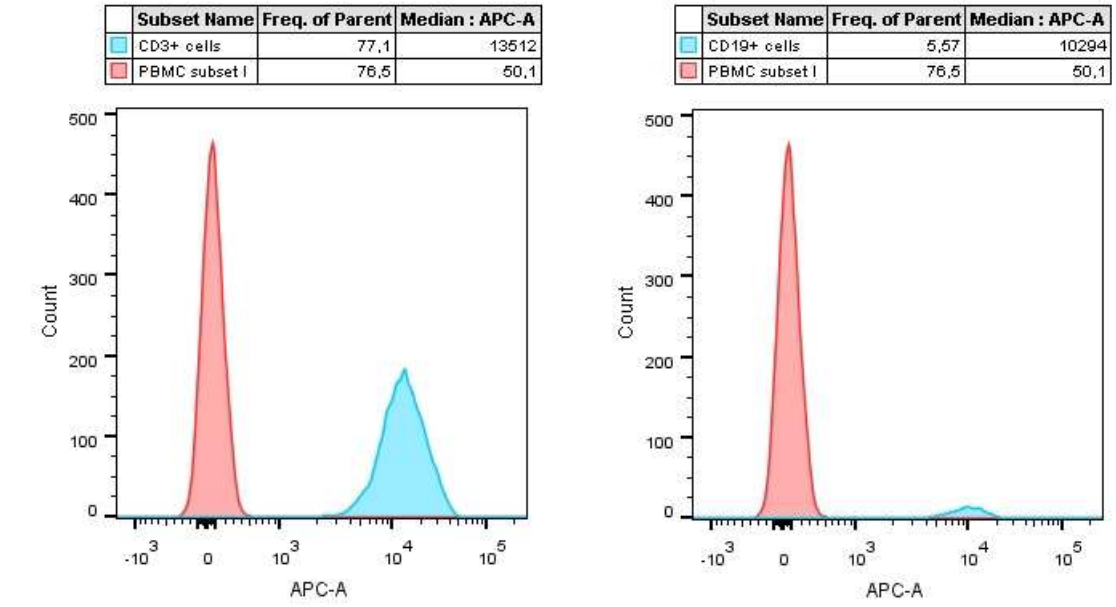

Figure 67: FACS analysis. Histograms (I) obtained by measurement of human PBMCs treated with antibodies. Relative fluorescence units (RFU; APC) logarithmically plotted against number of cells exhibiting respective fluorescence intensity. $CD3^+$-cells (left, light blue), and $CD19^+$-cells (right, light blue), plus respective isotyp control (IgG_1, κ; red). Relative frequencies within parent cell subsets and median APC-values shown in legends. Samples from individual 4 (female). 10'000 events each. Threshold count: 20,000.

For exclusion and hence implication of yet emergent non-specific binding of antibodies, cells were exposed to respective isotyp control antibodies; IgG_1, κ in case of CD3-, and CD19-antibodies. Relative fluorescence units (RFUs) were plotted as histograms versus those obtained by measurement of CD3-, or CD19-stained cells (figure 67). Occurring with diverging frequence, RFUs of both CD3-, and CD19-antibody-stained cells were shifted to great extent to higher fluorescence intensities (more than 10,000 each, light blue) compared to cells stained with isotyp control antibody (median APC-A: 50, red). Among samples from individuals, ΔRFUs ranged from 8,300 to 28,000 for $CD3^+$-stained cells, and from 4,100 to 21,000 for $CD19^+$-stained cells.

$CD3^+$-cells represented around three quarters of PBMC subset I ('frequ. of parent'), which itself represented around three quarters of the total amount of particles measured by the flow cytometer each sample. $CD19^+$-cells were present to a lower extent, accounting for around 5% of PBMC subset I.

With respect to the whole flow cytometry experiment, proportions of $CD3^+$-cells within PBMC subset I ranged from 70 to 87%, whereas proportions of $CD19^+$-cells within PBMC subset I ranged from 4 to 7%.

In figure 68, an example for the characterization of $CD14^+$-cells within freshly isolated human PBMCs is illustrated.

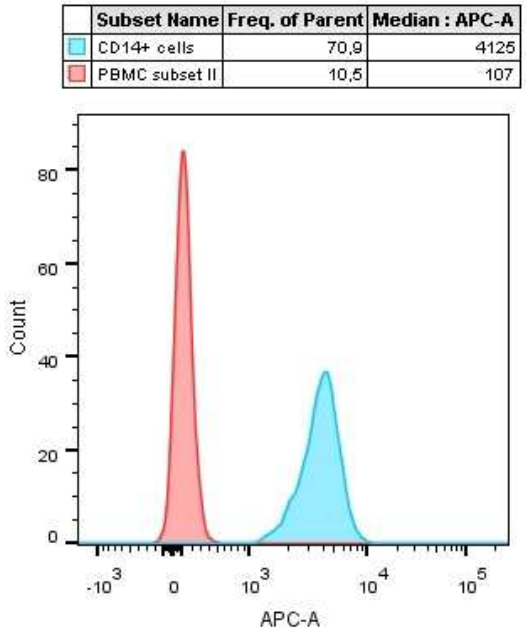

Figure 68: FACS analysis. Histogram (II) obtained by measurement of human PBMCs treated with antibodies. Relative fluorescence units (RFU; APC) logarithmically plotted against number of cells exhibiting respective fluorescence intensity. $CD14^+$-cells (light blue), plus respective isotyp control (IgG_{2a}, κ; red). Relative frequencies within parent cell subsets and median APC-values shown in legend. Samples from individual 4 (female). 10,000 events each. Threshold count: 20,000.

Figure 68 represents a typical histogram obtained by measurement of $CD14^+$-cells within isolated PBMC-suspension. $CD14^+$-cells were located within PBMC subset II to around 70%, and the shift to greater RFU-values compared to required isotyp control (IgG_{2a}, κ) measurement amounted to about 4,000. Dependent on the individual, ΔRFUs ranged from around 4,000 to 11,000 for characterization of $CD14^+$-cells without gender-specific differences.
Frequency of $CD14^+$-cells within PBMC subset II accounted for 81-98% throughout the complete FACS analysis.

Taken together, yielding 1.2 (±0.5)*10^6 cells/mL blood, obtained PBMC-suspensions, which were used for further gene expression measurements, constituted of 70 (±12)% $CD3^+$-cells (T lymphocytes), 6.0 (±1.0)% $CD19^+$-cells (B lymphocytes), and 10 (±3)% $CD14^+$-cells (monocytes/macrophages).

4.3.2. Human whole genome microarray analysis

Freshly isolated and characterized human PBMCs composed of 70 (±12)% $CD3^+$-cells, 6.0 (±1.0)% $CD19^+$-cells, and 10 (±3)% $CD14^+$-cells, were exposed to either TCDD alone (10 nM TCDD), TCDD and LPS (10 nM TCDD + 1 µg/mL LPS), or TCDD combined with PHA (10 nM TCDD + 1.5% PHA) for 24 h, corresponding to control treatments (DMSO 0.1%; 1 µg/mL LPS; 1.5% PHA). Subsequently, mRNA was isolated and checked on integrity (2100 Bioanalyzer, Agilent Technologies GmbH, Waldbronn, Germany), and two-color microarray-based gene expression analysis was perfomed applying Human GE 4x44K v2 Microarray Kits (Agilent Technologies GmbH, Waghaeusel-Wiesental, Germany) by implementation of dye-swop procedures to reduce potential artifactual effects due to diverging dye properties. Data normalization and statistical analyses were performed using Bioconductor R package Limma (Smyth, 2004). Results were filtered by cutoff values for signal intensity $A \geq 2^7$, logarithmic (log2) fold change $|lfc| \geq 1$, and p-value < 0.05.

4.3.2.1. Principal component analysis

An initial step examining microarray data was represented by view on principal component analysis (PCA). By clustering of information to reduce data dimensionality, a first insight into identification of general properties of individual samples was enabled by this method.

In figure 69 (following page), PCA-results concerning human whole genome microarray analysis and effects of TCDD alone, TCDD + LPS, or TCDD + PHA on gene expression *in vitro* in human PBMCs are presented.

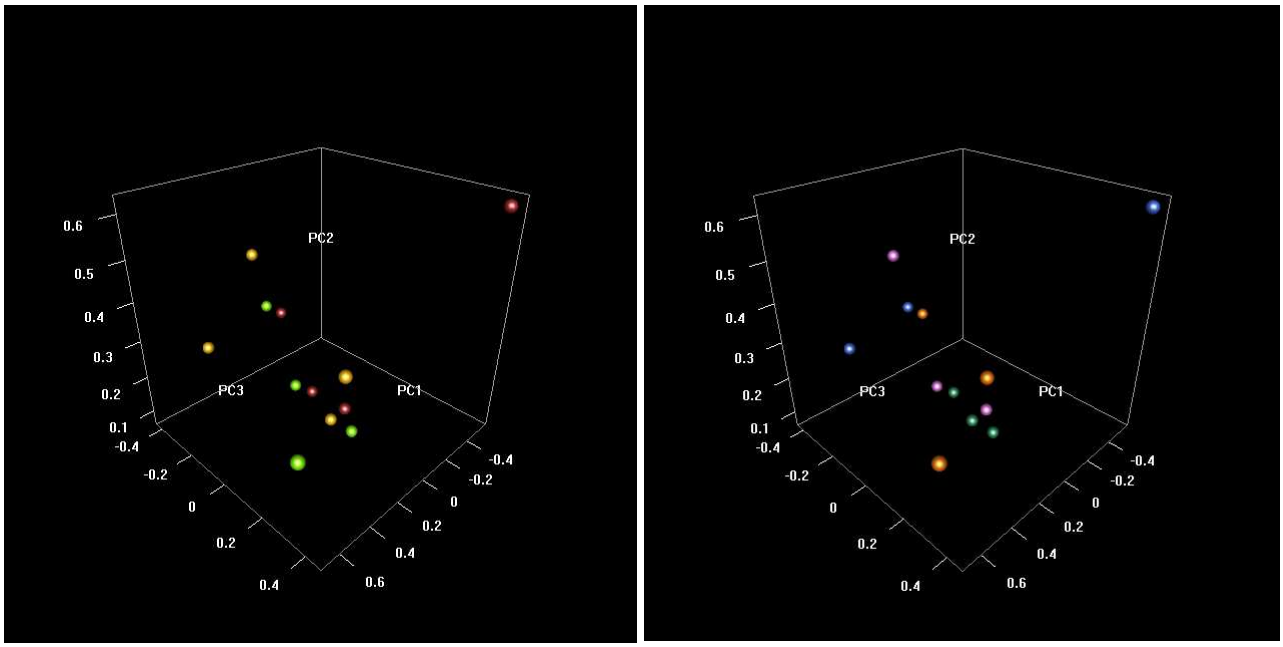

Figure 69: PCA human whole genome microarray analysis (human primary PBMCs, *in vitro*, 24 h, n = 4). Examination of RNA from human PBMCs treated with TCDD (light green), TCDD + LPS (red), or TCDD + PHA (yellow), focusing on treatment groups (left), and individuals (right; green: individual 1 (female, f); pink: individual 2 (male, m); orange: individual 3 (m), blue: individual 4 (f)). 3D scatter plot view of data with respect to their correlation to the first three principal components (PC1-3).

Presented PCA-results focused on different treatment groups (left, figure 69) and individuals (right, figure 69). Among treatment groups (light green, red, and yellow colored), the clustering of principal components appeared limited. Treatment with TCDD + PHA (yellow) or with TCDD alone (light green) to lightly lesser extent, slightly contrasted with the treatment TCDD + LPS (red). Inter-individual differences obviously emerged in reference to the image on the right hand side in figure 69.

By view on these PCA results, individual 4 (f) diverged most significantly from the other individuals, indicating to represent an explicit outlier. Closer examinations of raw data led to the conclusion to discard individual 4 from most of further investigations of the microarray analysis, as corresponding results differed greatly from individuals 1, 2, and 3, even if taking account of considerable present inter-individual differences overall. Though a reduction of sample size was implied by this decision, it was an important one to enforce from both statistical and biological point of view, in order to improve relevance of data regarding the complete human whole genome microarray experiment.

4.3.2.2. Human whole genome microarray analysis – regulated genes

Three treatment groups (*in vitro* for 24 h) were investigated by whole genome microarray analysis of human PBMCs: TCDD (10 nM), TCDD+LPS (10 nM TCDD + 1 µg/mL LPS), or TCDD+PHA (10 nM TCDD + 1.5% PHA). The analysis was prepared by direct, internal correlation of treatment on control samples, whereas respective mRNA was obtained from PBMCs treated with either the solvent (DMSO 0.1%), or respective stimulus (1 µg/mL LPS, or 1.5% PHA).

As indicated in preceding chapter, considerable inter-individual differences were revealed by whole genome investigations. Hence, data was not analyzed globally, as it was carried out regarding mouse whole genome microarrays. Still, if setting identical cutoff criteria as for the mouse whole genome microarray experiment (logarithmic (log2) fold change $|\text{lfc}| \geq 1$, p-value < 0.05; corrected by false discovery rate (FDR) using the Benjamini-Hochberg method (Benjamini and Hochberg, 1995), A-mean value $\geq 2^7$), no single gene was affected by two out of three treatments, namely TCDD, as well as TCDD+LPS, for neither up-, nor down-regulation regarding both treatments. With respect to treatment of human PBMCs with TCDD+PHA, 16 genes were up-, and three genes were down-regulated within these cutoff-levels.

In order to gain an insight with respect to potential tendencies of TCDD or TCDD+LPS-treatment-derived effects on gene expression in human PBMCs, one of the cutoffs was eased. The false discovery rate (FDR), representing a method for identification of false positive hypotheses, was disregarded to approach to this objective (Benjamini and Hochberg, 1995). The remaining cutoffs ($|\text{lfc}| \geq 1$, p-value < 0.05, A-mean value $\geq 2^7$) were maintained.

4.3.2.3. Human whole genome microarray analysis – TCDD

If FDR was disregarded, *in vitro* treatment of human PBMCs with TCDD (10 nM, 24 h) tendencially led to up-regulation of seven genes, and to down-regulation of twelve genes, respectively. These genes are listed in table 51.

Table 51: Human whole genome microarray analysis. Up-, and down-regulated genes in human PBMCs treated with TCDD (10 nM), *in vitro*, 24 h, n = 4. Descending order each. Cutoff values: A ≥ 27, lfc ≥ 1, p-value < 0.05. FDR disregarded.

TCDD			PBMCs
lfc	Gene systematic name	Gene description	**Gene name**
up			
1.798	NM_000499	cytochrome P450, family 1, subfamily a, polypeptide 1	*CYP1A1*
1.585	NM_002981	chemokine (C-C motif) ligand 1	*CCL1*
1.102	NM_138451	IQ motif containing D	*IQCD*
1.055	NM_025139	armadillo repeat containing 9	*ARMC9*
1.042	NM_020731	aryl-hydrocarbon receptor repressor	*AHRR*
1.023	NM_004694	solute carrier family 16 member 6	*SLC16A6*
1.003	NM_000160	glucagon receptor	*GCGR*
down			
-2.056	NM_001565	chemokine (C-X-C motif) ligand 10	*CXCL10*
-1.463	NM_001710	complement factor B	*CFB*
-1.361	ENST00000449753	immunoresponsive 1 homolog (mouse)	*ENST00000449753*
-1.347	NM_004244	CD163 molecule	*CD163*
-1.344	NM_002988	chemokine (C-C motif) ligand 18 (pulmonary and activation-regulated)	*CCL18*
-1.241	NR_026875	Neuralized homolog 3 (Drosophila) pseudogene	*NEURL3*
-1.229	NM_058173	mucin-like 1	*MUCL1*
-1.095/ -1.035	NM_000619	interferon gamma	*IFNG*
-1.087/ -1.029	NM_006274	chemokine (C-C motif) ligand 19	*CCL19*
-1.082	NM_001017986	Fc fragment of IgG high affinity Ib receptor (CD64)	*FCGR1B*
-1.054	NM_006658	chromosome 7 open reading frame 16	*C7orf16*
-1.053	NM_005064	chemokine (C-C motif) ligand 23	*CCL23*

Values b/a from oligo b/oligo a.

Up-regulated genes by TCDD in PBMCs

Disregarding FDR-cutoff, the most effectively up-regulated gene in PBMCs responding to TCDD-treatment for 24 h was *CYP1A1* (NM_000499; lfc = 1.798). One further AhR-related representative tended to be up-regulated in this regard: *AHRR* (NM_020731; lfc = 1.042) (see table 51).

Chemokine (C-C motif) ligand 1 (*CCL1*, NM_002981; lfc = 1.585) encodes a cytokine representing a small glycoprotein, which is secreted by activated T-lymphocytes and possesses chemotactic properties towards monocytes. CCL1 further binds to C-C chemokine receptor 8 (CCR8) (Dimmer *et al.*, 2012; Miller and Krangel, 1992). *CCR8* (NM_005201) was not affected within this study by any treatment.

Armadillo repeat containing 9 (*ARMC9*, NM_025139; lfc = 1.055) is annotated to the cellular component ‘extracellular vesicular exosome’ (GO:0070062). This component is defined as ‘A membrane-bounded vesicle that is released into the extracellular region by fusion of the limiting endosomal membrane of a multivesicular body with the plasma membrane’ (Binns *et al.*, 2009). Exosomes represent small membrane vesicle (50-90 nm in diameter), which are secreted by most hematopoietic cells (Caby *et al.*, 2005).

Another gene, which tended to be up-regulated by TCDD in PBMCs *in vitro*, was solute carrier family 16 member 6 (*SLC16A6*; NM_0046994; lfc = 1.023). The encoded protein, monocarboxylate transporter 7, catalyzes the rapid transport across the plasma membrane of many monocarboxylates such as lactate, pyruvate, branched-chain oxo-acids derived from leucine, valine and isoleucine, and ketone bodies such as acetoacetate, beta-hydroxybutyrate and acetate (Binns *et al.*, 2009; Dimmer *et al.*, 2012).

Besides, glucagon receptor (*GCGR*, NM_000160; lfc = 1.003) was directed towards up-regulation in TCDD-exposed PBMCs. In general, encoded G-protein coupled receptor for glucagon plays a central role in the regulation of blood glucose levels and glucose homeostasis. It further plays a role in signaling via a phosphatidylinositol-calcium second messenger system. Though known to be expressed on mononuclear blood cells, definite role(s) of the glucagon receptor with respect to these cells was barely examined (Binns *et al.*, 2009; Goldstein *et al.*, 1975).

Down-regulated genes by TCDD in PBMCs

Among down-regulated genes by TCDD-treatment in human PBMCs (see table 51), four genes encoded chemokines: chemokine (C-X-C motif) ligand 10 (*CXCL10*, NM_001565; lfc = -2.056), chemokine (C-C motif) ligand 18 (*CCL18*, NM_002988; lfc = -1.344), chemokine (C-C motif) ligand 19 (*CCL19*, NM_006274, lfc (max) = -1.087), and chemokine (C-C motif) ligand 23 (*CCL23*, NM_005064; lfc = -1.053). They are chemotactic for T-lymphocytes (CCL10, CCL18, CCL19, and CCL23), monocytes (CCL10, CCL23), B-lymphocytes (CCL19), and neutrophils (CCL23) (Binns *et al.*, 2009; Dimmer *et al.*, 2012).

Down-regulated complement factor B (*CFB*, NM_001710; lfc = -1.463) is part of the alternate pathway of the complement system, and has been implicated in proliferation and differentiation of preactivated B-lymphocytes due to inhibitory effects on the proliferation of preactivated B lymphocytes (Binns *et al.*, 2009; Dimmer *et al.*, 2012).

Suppressed *CD163* (NM_004244; lfc = -1.347) encodes CD163, which represents a hemoglobin scavenger receptor expressed in the monocyte-macrophage system. CD163 is an acute phase-regulated receptor involved in clearance and endocytosis of hemoglobin/haptoglobin complexes as well as in scavenging of components of damaged cells, and thus is implicated in protection of tissues from free hemoglobin-mediated oxidative damage, for instance. The receptor was discussed to play an anti-inflammatory role correlated with macrophage activation and response of monocytes (Binns *et al.*, 2009; Buechler *et al.*, 2000; Moestrup and Møller, 2004).

IFNG (NM_000619; lfc (max) = -1.095) also tended to be down-regulated by TCDD-treatment in PBMCs. IFN-γ is produced by activated lymphocytes promoting Th1-specific immune responses including response of CTLs, potentially activates macrophages, and further was discussed to bear antiproliferative effects on transformed cells (Dimmer *et al.*, 2012; Garbe *et al.*, 1990; Jetten, 2009).

The putatively down-regulated Fc fragment of IgG high affinity Ib receptor (*FCGR1B*, NM_001017986; lfc = -1.082) encodes the protein high affinity immunoglobulin gamma Fc receptor IB (IgG Fc receptor IB). Binding with lower affinity to the Fc region of immunoglobulins gamma, FCGR1B might play an important role in mechanisms by which Fc gamma receptors participate in the humoral immune response (Binns *et al.*, 2009; Porges *et al.*, 1992).

Another potentially down-regulated gene listed in table 51, chromosome 7 open reading frame 16 (*C7orf16*, NM_006658; lfc = -1.054), encodes a protein with serine/threonine protein phosphatase inhibitor activity (GO:0004865) (Binns *et al.*, 2009; Dimmer *et al.*, 2012).

Down-regulated mucin-like 1 (*MUCL1*, NM_058173; lfc = 1.229) is annotated to the biological process ‘O-glycan processing’ (GO:0016266), and is related to ‘O-linked glycosylation of mucins’ (REACT_115606) (Binns *et al.*, 2009; Dimmer *et al.*, 2012).

4.3.2.4. Human whole genome microarray analysis – TCDD+LPS

Disregarding FDR, *in vitro* treatment of human PBMCs with TCDD (10 nM) combined with LPS (1 µg/mL) resulted in three genes tendentially up-regulated and 15 genes tending to be inhibited after 24 h. In table 52, respective genes are presented.

Table 52: Human whole genome microarray analysis. Up-, and down-regulated genes in human PBMCs treated with TCDD (10 nM) + LPS (1 µg/mL), *in vitro*, 24 h, n = 3. Descending order each. Cutoff values: A ≥ 27, lfc ≥ 1, p-value < 0.05. FDR disregarded.

TCDD + LPS lfc	Gene systematic name	Gene description	PBMCs Gene name
up			
1.671	NM_000499	cytochrome P450, family 1, subfamily a, polypeptide 1	*CYP1A1*
1.07	NM_015508	TCDD-inducible poly(ADP-ribose) polymerase	*TIPARP*
1.059	NM_003246	thrombospondin 1	*THBS1*
down			
-1.576	NM_007286	synaptopodin	*SYNPO*
-1.498	ENST00000 449753	immunoresponsive 1 homolog (mouse)	*ENST00000449753*
-1.434	NM_001565	chemokine (C-X-C motif) ligand 10	*CXCL10*
-1.397	NM_005623	chemokine (C-C motif) ligand 8	*CCL8*
-1.378	NM_138456	basic leucine zipper transcription factor ATF-like 2	*BATF2*
-1.362	NM_002988	chemokine (C-C motif) ligand 18 (pulmonary and activation-regulated)	*CCL18*
-1.314	NM_001710	complement factor B	*CFB*
-1.279/ -1.105	NM_006274	chemokine (C-C motif) ligand 19	*CCL19*
-1.173	NM_058173	mucin-like 1	*MUCL1*
-1.167	NR_026875	neuralized homolog 3 (Drosophila) pseudogene	*NEURL3*
-1.152	NM_014398	lysosomal-associated membrane protein 3	*LAMP3*
-1.14	NM_005064	chemokine (C-C motif) ligand 23	*CCL23*
-1.131- (-1.002)	NM_001040058	secreted phosphoprotein 1	*SPP1*
-1.075	NM_001017986	Fc fragment of IgG high affinity Ib receptor (CD64)	*FCGR1B*
-1.06	NM_004244	CD163 molecule	*CD163*

Values b/a from oligo b/oligo a; values a-n: value range of more than two (n) oligos.

Up-regulated genes by TCDD+LPS in PBMCs

Two of three up-regulated genes in human PBMCs treated with TCDD (10 nM) + LPS (1 µg/mL) represented AhR-responsive targets: *CYP1A1*, and *TIPARP* (table 52).

The third gene, which was tended to be up-regulated along with this experiment, was thrombospondin 1 (*THBS1*, NM_003246; lfc = 1.059). The protein TSP-1 represents an inhibitor of angiogenesis, which is able to limit vessel density in normal tissues and to reduce tumor growth. This process, as well as related TSP-1-induced apoptosis in endothelial cells, was suggested to be dependent on CD36 (Dawson *et al.*, 1997; Jiménez *et al.*, 2000). TSP-1 can further be involved in the activation of latent TGF-β, and is induced at sites of tissue damage, where it co-occurs with endoplasmatic reticulum (ER) stress response. There, TSP-1 was reported to augment and protect ER function, by which protein production and resolution of misfolded proteins is regulated in case of ER stress response (Lynch *et al.*, 2012; Murphy-Ullrich and Poczatek, 2000).

Synaptopodin (*SYNPO*, NM_007286; lfc = -1.576) tended to be most effectively down-regulated by TCDD+LPS-treatment in human PBMCs. Encoded, actin-associated protein may play a role in modulating actin-based shape and motility of dendritic spines and is involved in synaptic plasticity (Binns *et al.*, 2009; Dimmer *et al.*, 2012). Further, SYNPO recently was shown to be expressed in endothelial cells in response to laminar shear stress and to participate in the mediation of accompanied wound healing process (Mun *et al.*, 2014).

Down-regulated genes by TCDD+LPS in PBMCs

Regarding potentially down-regulated genes by TCDD+LPS-treatment (see table 52), several genes encoding chemokines appeared. Besides those mentioned with respect to down-regulation by TCDD-treatment already (*CXCL10*, *CCL18*, *CCL19*, and *CCL23*), *CCL8* (NM_005623; lfc = -1.397) occurred additionally in this regard. Encoded monocyte chemotactic protein 2 (MCP-2) attracts monocytes, lymphocytes, basophils and eosinophils (Binns *et al.*, 2009; Dimmer *et al.*, 2012).

The protein encoding down-regulated basic leucine zipper transcription factor ATF-like 2 (*BATF2*, NM_138456; lfc = -1.378) represents an activating protein-1 (AP-1) family transcription factor, which participates in the control of differentiation of immune cells, and is an important regulator of gene expression in leukocytes (Foletta *et al.*, 1998). *BATF2* is inducible by type I interferon,

whereas down-regulated expression was found to be associated with a poor prognosis in hepatocellular carcinoma (Dimmer *et al.*, 2012; Ma *et al.*, 2011).

Further implicated with type I immunity was the protein osteopontin, which is encoded by the down-regulated secreted phosphoprotein 1 (*SPP1*, NM_001040058; lfc (max) = -1.131). Osteopontin, which appears to be essential in the pathway leading to type I immunity, acts as a cytokine and participates in the enhanced production of IFN-γ and IL-12, as well as in the reduction of IL-10 production (Binns *et al.*, 2009; Dimmer *et al.*, 2012).

Lysosomal-associated membrane protein 3 (*LAMP3*, NM_014398; lfc = -1.152), which was down-regulated in the course of the study in hand by TCDD+LPS-treatment *in vitro* in PBMCs, was found to progressively be induced during DC-differentiation on protein level, as well as upon activation with LPS, or TNF-α. It was suggested that LAMP3 might impact lysosome function after transfer of peptide-MHC class II molecules to the surface of DCs (De Saint-Vis *et al.*, 1998). LAMP3 was further reported to be expressed in B lymphocytes on protein level (Duchez *et al.*, 2011).

The remaining genes (*CFN*, *MUCL1*, *FCGR1B*, and *CD163*) were also implemented with respect to potential down-regulating effects on gene expression by TCDD-treatment of PBMCs (see table 51 and corresponding text below).

4.3.2.5. Human whole genome microarray analysis – TCDD+PHA

With respect to treatment of human PBMCs with TCDD+PHA, 16 genes were up-, and three genes were down-regulated in due consideration of FDR. Since regarding the incubations with TCDD alone as well as the combined incubation with TCDD+LPS, cutoffs were chosen less stringent with respect to disregarding FDR, this examination was also applied regarding TCDD+PHA-treatment.

Hence, 32 up-regulated and twelve down-regulated genes were obtained. Respective gene-list with potentially up-regulated genes is shown in table 53. Values, which accomplished the more stringent FDR-cutoff, were marked within the table.

Table 53: Human whole genome microarray analysis. 32 up-regulated genes in human PBMCs treated with TCDD (10 nM) + PHA (1.5%) *in vitro*, 24 h, n = 3. Descending order. Cutoff values: A ≥ 27, lfc ≥ 1, p-value < 0.05. *: In due consideration of FDR.

TCDD + PHA lfc	Gene systematic name	Gene description	PBMCs Gene name
up			
2.599	NM_000499	cytochrome P450, family 1, subfamily a, polypeptide 1	*CYP1A1**
2.342-1.259	NM_003246	thrombospondin 1	*THBS1*
2.225	NM_002522	neuronal pentraxin I	*NPTX1**
2.084	NM_020731	aryl-hydrocarbon receptor repressor	*AHRR**
1.936	NM_000361	thrombomodulin	*THBD*
1.846	NM_000784	cytochrome P450, family 27, subfamily a, polypeptide 1	*CYP27A1**
1.734	NM_016150	ankyrin repeat and SOCS box containing 2	*ASB2**
1.64	NM_015508	TCDD-inducible poly(ADP-ribose) polymerase	*TIPARP**
1.608-1.036	NM_000222	v-kit Hardy-Zuckerman 4 feline sarcoma viral oncogene homolog	*KIT**
1.574-1.561	NM_000104	cytochrome P450, family 1, subfamily b, polypeptide 1	*CYP1B1**
1.55	NM_002775	HtrA serine peptidase 1	*HTRA1*
1.537	NM_001432	epiregulin	*EREG*
1.477	NM_003485	G protein-coupled receptor 68	*GPR68**
1.454	NM_138375	Cdk5 and Abl enzyme substrate 1	*CABLES1**
1.431-1.384	NM_004994	matrix metallopeptidase 9 (gelatinase B)	*MMP9*
1.358-1.307	NM_002982	chemokine (C-C motif) ligand 2	*CCL2*
1.318	NM_176798	pyrimidinergic receptor P2Y	*P2RY6**
1.298	NM_138356	Src homology 2 domain containing F	*SHF**
1.273	NM_016205	platelet derived growth factor C	*PDGFC*
1.233	NM_002575	serpin peptidase inhibitor	*SERPINB2**
1.188-1.172	NM_001185156	interleukin 24	*IL24*
1.16	NM_130848	chromosome 5 open reading frame 20	*C5orf20*
1.159	NM_005767	lysophosphatidic acid receptor 6	*LPAR6*
1.154	NM_138788	transmembrane protein 45B	*TMEM45B*
1.139	NM_013451	myoferlin	*MYOF**
1.129	NM_001268	regulator of chromosome condensation (RCC1) and BTB (POZ) domain containing protein 2	*RCBTB2**
1.118	NM_023037	furry homolog	*FRY*
1.082	NM_012282	KCNE1-like	*KCNE1L*
1.06	NM_033120	naked cuticle homolog 2	*NKD2**
1.04	NM_014331	solute carrier family 7 member 11	*SLC7A11*
1.027	NM_002993	chemokine (C-X-C motif) ligand 6	*CXCL6*
1.022	NM_080747	keratin 72	*KRT72*

Values a-n: value range of more than two (n) oligos.

Up-regulated genes by TCDD+PHA in PBMCs

Four members of a proposed AhR-gene batterie, including *CYP1A1* (NM_000499; lfc = 2.599), *AHRR* (NM_020731; lfc = 2.084), *TIPARP* (NM_015508; lfc = 1.64), and *CYP1B1* (NM_000104; lfc (max) = 1.574), were up-regulated genes by treatment of PBMCs with TCDD+PHA (24 h), and even were within the FDR-cutoff (table 53).
A further up-regulated gene related to response to xenobiotics was *CYP27A1* (NM_000784; lfc = 1.846), as the encoded protein was annotated to the biological process 'xenobiotic metabolic process' (GO:0006805). CYP27A1 catalyzes the first step in the oxidation of the side chain in sterol intermediates, and possesses cholestanetriol 26-monooxygenase-, cholesterol 26-, and calcidiol 25-hydroxylase activity (Binns *et al.*, 2009; Dimmer *et al.*, 2012).

In addition to *CYP1A1*, *AHRR*, *TIPARP*, and to one gene, which as well was probably up-regulated by TCDD+LPS (*THBS1*, NM_003246; lfc (max) = 2.342), the genes occurring in table 53 were not affected in response to the other investigated PBMC-treatments.
Among these genes, two chemokines were present: *CCL2* (NM_002982; lfc (max) = 1.358), and *CXL6* (NM_002993; lfc = 1.027). Encoded chemokines attract monocytes and basophiles (*CCL2*), or neutrophil granulocytes (*CXL6*). Besides, the latter possesses antibacterial activity against gram-positive and negative bacteria.

The up-regulated genes are implicated in several and diverging processes. Ubiquitination and subsequent proteasomal degradation of target proteins represents a mechanism correlated with ankyrin repeat and SOCS box containing 2 (*ASB2*, NM_016150; lfc = 1.734), and naked cuticle homolog 2 (*NKD2*, NM_033120; lfc = 1.06). The latter was reported to be an inducible Wnt/β-catenin signaling pathway antagonist. Wnt/β-catenin signals are crucial in development and neoplasia, and aberrant activation of the pathway is often correlated with overexpression of the *c-myc* oncogene. Respective processes include Wnt/β-catenin promoted proliferation of cells as well as c-Myc induced apoptosis (Binns *et al.*, 2009; Dimmer *et al.*, 2012; You *et al.*, 2002; Zeng *et al.*, 2000; Zhang *et al.*, 2012).
Further genes up-regulated by TCDD+PHA-treatment related to apoptotic processes were Cdk5 and Abl enzyme substrate 1 (*CABLES1*, NM_138375; lfc = 1.454), Neuronal pentraxin I (*NPTX1*, NM_002522; lfc = 2.225), and serpin peptidase inhibitor (*SERPINB2*, NM_002575; lfc = 1.233). Serpin 2 represents a major product of macrophages in response to endotoxin and inflammatory cytokines, which is able to inhibit TNF-α induced apoptosis (Binns *et al.*, 2009; Dickinson *et al.*,

1995; Dimmer *et al.*, 2012). *NPTX1* further is annotated to the biological processs ‘cellular response to glucose stimulus’ (GO:0071333).

Glucose metabolism constitutes a regulated process in lymphocytes affecting immune cell function and survival, and is required to maintain immune homeostasis. Beyond, pyrimidinergic receptor P2Y (*P2RY6*, NM_176798; lfc = 1.318) which was up-regulated in PBMCs subsequent to TCDD+PHA-treatment, is a gene encoding a receptor for extracellular UDP, UTP, and ATP. Its activity is mediated by G-proteins which activate a phosphatidyinositol (PI)-calcium second messenger system.

A biological process, to which *P2RY6* hence is annotated is ‘phospholipase C-activating G-protein coupled receptor signaling pathway’ (GO:0007200). Potentially, if a growth factor or cytokine binds to its receptor on a T cell’s surface, phosphatidyinositol-3 kinase (PI-3K) is activated. Thus, PI is converted to PI 3,4,5-triphosphate (PIP3), subsequently recruiting Akt to the cell’s surface. There it becomes activated and in turn up-regulates GLUT-1 expression, glucose uptake, and glycolysis (Binns *et al.*, 2009; Communi *et al.*, 1996; Dimmer *et al.*, 2012; MacIver *et al.*, 2008).

Among further potentially up-regulated genes by TCDD+PHA in PBMCs, several were of diverging function. Serine protease HTRA1, which is encoded by potentially up-regulated HtrA serine peptidase 1 (*HTRA1*, NM_002775; lfc = 1.55), is involved in the regulation of insulin-like growth factors (IGFs) by cleaving IGF-binding proteins.

Implicated in the stimulation of localized cell proliferation and angiogenesis is epiregulin (*EREG*, NM_001432, lfc = 1.537), as the encoded protein represents a ligand of the EGF receptor (Komurasaki *et al.*, 1997).

MMP-9, which is encoded by matrix metallopeptidase 9 (*MMP9*, NM_004994; lfc (max) = 1.431), was proposed to play a role in leukocyte migration and in local proteolysis of the extracellular matrix (Tschesche *et al.*, 1992).

Platelet derived growth factor C (*PDGFC*, NM_016205; lfc = 1.273), which encodes PDGF-C is involved in wound healing in terms of inflammation, proliferation, and remodeling, as well as in fibrotic diseases. PDGF-C was further reported to participate in induction of liver fibrosis, steatosis, and hepatocellular carcinoma (Campbell *et al.*, 2005).

A cysteine/glutamate receptor is encoded by solute carrier family 7 member 11 (*SLC7A11*, NM_014331; lfc = 1.04). Interestingly, the gene was annotated to the biological process ‘response to toxic substance’ (GO:0009636). The annotation was due to findings by Flach *et al.* (2007). The authors found up-regulated *LC7A11* mRNA-levels in acute cholera patients (Flach *et al.*, 2007).

Thrombomodulin is a specific endothelial cell receptor, which is involved in coagulation mechanisms by reducing the amount of thrombin generated (*THBD*, NM_000361; lfc = 1.936) (Binns *et al.*, 2009; Dimmer *et al.*, 2012).

The twelve putatively down-regulated genes in PBMCs after treatment with TCDD+PHA, setting less stringent cutoffs (FDR disregarded), is presented in table 54. Values, which accomplished the more stringent FDR-cutoff, were marked within the table.

Table 54: Human whole genome microarray analysis. Twelve down-regulated genes in human PBMCs treated with TCDD (10 nM) + PHA (1.5%) *in vitro*, 24 h. Descending order. Cutoff values: A ≥ 27, lfc ≥ 1, p-value < 0.05. *: In due consideration of FDR.

TCDD + PHA lfc	Gene systematic name	Gene description	PBMCs Gene name
down			
-1.61- (-1.544)	NM_000619	interferon gamma	*IFNG*
-1.285- (-1.088)	NM_001955	endothelin 1	*EDN1*
-1.258	NM_005064	chemokine (C-C motif) ligand 23	*CCL23*
-1.21	NM_001955	endothelin 1	*EDN1*
-1.198	NM_024021	membrane-spanning 4-domains subfamily A member 4	*MS4A4A**
-1.155	NM_006658	chromosome 7 open reading frame 16	*C7orf16*
-1.152	NM_001775	CD38 molecule	*CD38*
-1.148	NM_001710	complement factor B	*CFB**
-1.042	NM_017414	ubiquitin specific peptidase 18	*USP18*
-1.023	NM_058173	mucin-like 1	*MUCL1**
-1.012	NM_002988	chemokine (C-C motif) ligand 18 (pulmonary and activation-regulated)	*CCL18*
-1.004	NM_006274	chemokine (C-C motif) ligand 19	*CCL19*

Values a-n: value range of more than two (n) oligos.

Down-regulated genes by TCDD+PHA in PBMCs

Within the table of down-regulated genes by TCDD+PHA-treatment in PBMCs (table 54), several were also down-regulated by TCDD alone (see table 51): *IFNG*, *CCL18*, *CCL19*, *CFB*, and *MUCL1*, and by TCDD+LPS-treatment (see table 52) with respect to the chemokines.

A further down-regulated gene by TCDD+PHA-treatment was Endothelin-1 (*EDN-1*, NM_001955; lfc (max) = -1.285), which was annotated to biological processes ‘protein kinase C deactivation’ (GO:0042313), and ‘nitric oxide transport’ (GO:0030185). In this regard, elevated endothelin-1 levels were correlated with impaired nitric oxide homeostasis through a PKC-dependent pathway (Ramzy *et al.*, 2006).

The protein encoding chromosome 7 open reading frame 16 (*C7orf16*, NM_006658; lfc = -1.155) potentially inhibits phosphatase activities of protein phosphatase 1 (PP1) and protein phosphatase 2A (PP2A) complexes.

CD38 (*CD38*, NM_001775; lfc = -1.152) is implicated in the synthesis of second messengers (cyclic ADP-ribose and nicotinate-adenine dinucleotide phosphate) involved in glucose-induced insulin secretion. Further, CD38 was annotated to the biological process ‘positive regulation of B cell proliferation’ (GO:0030890) since its diverging expression in B cell chronic lymphocytic leukemia was discussed in terms of involvement in cell proliferation (Joshi *et al.*, 2007).

Ubiquitin specific peptidase 18 (*USP18*; NM_017414; lfc = -1.042) is implicated in maintaining balance of specialized proteins. The encoded Ubl carboxyl-terminal hydrolase 18 is involved in the hydrolysis of ester-, thioester-, amide-, and peptide bonds formed by the C-terminal Gly of ubiquitin (Binns *et al.*, 2009; Dimmer *et al.*, 2012).

The protein encoded by *MS4A4A* (CD20 antigen-like 1; *MS4A4A*, NM_024021; lfc = -1.198) is an integral membrane-component, which might be involved in signal transduction as a component of a multimeric receptor complex. *MS4A4A* belongs to the *MS4A* gene family, of which *MS4A1* (NM_152866) encodes the B lymphocyte antigen CD20, which is indicated to be involved in the regulation of B cell activation and proliferation (Binns *et al.*, 2009; Dimmer *et al.*, 2012). *MS4A1* itself was not regulated by any investigated treatment of human PBMCs in this study, whereas other members of this gene family (27 probes present on array slides in total) were enormously below cutoff-level for signal-intensity: *MS4A6A* (NM_152852; lfc = -1.069, A = $2^{3.49}$), *MS4A8B* (NM_031457; lfc = -1.018, A = $2^{2.41}$), and *MS4A10* (NM_206893; lfc = -1.069, $2^{3.66}$), regarding TCDD+PHA-treatment, and *MS4A2* (NM_000139; lfc = -1.386, A = $2^{4.21}$), *MS4A3* (NM_006138; lfc = -1.447, A = $2^{4.59}$), *MS4A6A* (NM_152852; lfc = 1.885, A = $2^{3.49}$), *MS4A13* (NM_001012417; lfc = -1.395, A = $2^{3.07}$), with respect to TCDD+LPS-treatment.

4.3.2.6. Human whole genome microarray analysis – 'target' & several genes

In a further step, human whole genome microarray data was analyzed in terms of probale TCDD-mediated impact on transcription of eight 'potential' AhR-target genes (*CYP1A1*, *CYP1A2*, *CYP1B1*, *AHRR*, *TIPARP*, *ALDH3A1*, *CD36*, and *HSD17B2*), and of several cytokines (*IL2*, *IL4*, *IL5*, *IL6*, *IL10*, *IL12*, *IL13*, *IL17A*, *IL17F*, *IL18*, *IL21*, *IL22*, *IL23*, *IFNG*), and of the transcription factor FoxP3 (*FOXP3*) with specific roles in T cell lineage specification (reviewed in Jetten, 2009). Further examined was the expression of *TDO2*. IDO1, IDO2, and TDO degrade L-tryptophan to L-kynurenine and were proposed to be correlated with Treg differentiation and with AhR-dependent antitumor immune responses (Nguyen *et al.*, 2010; Mezrich *et al.*, 2010; Opitz *et al.*, 2011).

To approach to this objective, three different considerations of human whole genome microarray data were focused:
Firstly, presented data for n = 3 (individuals 1, 2, and 3) was further investigated with view of these genes. This data gives information on differentially regulated genes in response to the tree implemented treatments: TCDD, TCDD+LPS, and TCDD+PHA.
Secondly, each individual (individuals 1-4) was regarded separately.
The third examination combined gender-specific results to gain a female vs. male consideration.

Due to the limited volume of data, both the individual-specific and the female vs. male-consideration were only realizable by consolidation of the three treatment groups. With respect to these three considerations, the cutoff was eased. The false discovery rate (FDR), representing a method for identification of false positive hypotheses, was disregarded (Benjamini and Hochberg, 1995). Principally, the remaining cutoffs were set: $\left|\text{lfc}\right| \geq 1$, p-value < 0.05, A-mean value $\geq 2^7$.

The data is presented in table 55. In case a value accomplished more stringent cutoff(s), or if a value was below the lfc-cutoff or the A-mean-value cutoff, the value was marked accordingly.

Table 55: Human whole genome microarray analysis. Impact of TCDD on eight 'potential' target genes, and on genes implicated in T cell lineage specification. Treatment groups: TCDD (10 nM); TCDD+LPS (1 µg/mL), and TCDD+PHA (1.5%). Considerations: Individuals (i1-i4; treatment groups consolidated), female (f) vs. male (m) (treatment groups consolidated), and n = 3 (i1-3). PBMCs *in vitro*, 24 h; up-(↑), and down-regulation (↓) of genes. Cutoff values: A ≥ 27, │lfc│ ≥ 1, p-value < 0.05. FDR disregarded; *: in due consideration of FDR. Values in brackets: below A-mean value cutoff, and/or lfc-cutoff (new cutoff │lfc│ ≥ 0.585; 1.5-fold).

	Individuals				Female vs. male		n = 3		
Gene	i1 (f)	i2 (m)	i3 (m)	i4 (f)	f	m	TCDD	TCDD +LPS	TCDD +PHA
‚Target' Genes									
CYP1A1	↑	↑	↑	↑	↑	↑*	↑	↑	↑*
CYP1A2			(↑)						(↑)
CYP1B1	↑	↑	(↑)	(↑)	(↑)	↑*	(↑)	(↑)	↑*
AHRR	↑	↑	↑	(↑)	↑	↑	↑	(↑)	↑*
TIPARP	↑	↑	↑	(↑)	↑*	↑*	(↑)	↑	↑*
ALDH3A1			(↓)	(↑)	(↑)				
CD36			(↑) (↓)	(↓)					
HSD17B2	(↑) (↓)		(↑)	(↑) (↓)	(↑)	(↑) (↓)	(↑) (↓)	(↓)	(↑) (↓)
Genes implicated in T cell lineage specification									
IL2	(↓)	(↓)	(↓)	(↑) (↓)	(↓)	(↓)	(↓)	(↑) (↓)	(↓)
IL4			(↓)			(↓)			(↓)
IL5	(↑)						(↑)		
IL6		(↓)							(↓)
IL12				(↑) (↓)	(↓)			(↑)	(↓)
IL17A				(↓)					
IL18	(↓)	(↓)	(↓)	(↓)	(↓)	(↓)	(↓)	(↓)	(↓)
IL21				(↓)		(↓)			(↓)
IL23	(↓)			(↓)	(↓)				
IFNG	(↓)	(↓)	(↓)	(↓)	↓	↓	↓	(↓)	↓
FOXP3				(↓)					
TDO2	(↑)	(↓)	(↑)	(↑)	(↑)		(↑)		(↑)

As shown in table 55, one TCDD-responsive gene in human PBMCs was discovered obviously, constantly, and for each individual, namely *CYP1A1*. Inter-individual variations were as follows: lfc (i1) = 2.105, lfc (i2) = 2.107, lfc (i3) = 1.857, and lfc (i4) = 1.027. Apart from that, *CYP1B1*, *AHRR*, and *TIPARP* were as well clearly induced by TCDD with diverging specifity and statistical significance, dependent on the individual or treatment. Response with respect to *CYP1A2* was

minor and of low statistical relevance. TCDD-mediated effects on *ALDH3A1*, *CD36*, and *HSD17B2* were low and undirected.

Regarding the female vs. male consideration, the male-group on the most part was more responsive compared to the female-group with respect to all investigated genes except for *ALDH3A1*, *IL12*, and *IL23*. This was very likely most prominently due to effects in PBMCs from individual 4 (f). As indicated before, this individual differed from the others to the greatest extent regarding TCDD-dependent effects on gene expression in PBMCs. Response with respect to 'potential' AhR-target genes generally was weaker compared to the other individuals, whereas regarding genes implicated in T cell lineage specification, cells from individual 4 slightly tended to be affected to greater extent.

Impact of TCDD on transcription of genes involved in T cell lineage specification overall was limited and was accompanied by moderate inter-individual differences. Most prominently, and throughout the whole investigation presented in table 55, *IFNG* was down-regulated by treatment of human PBMCs with TCDD. Further, *IL18*, which encodes the formerly termed 'IFN-γ inducing factor', was also down-regulated by tendency.

TCDD's impact on *IL12*-transcription appeared not clearly directional and was supposedly dependent on the treatment: The interleukin tendentially was up-regulated after TCDD+LPS-treatment, and down-regulated subsequent to TCDD+PHA-incubation.
Regarding TCDD's proposed impact on further interleukins, *IL2* was lightly but not distinctly directed to down-regulation. Slight indications for down-regulation by TCDD were given with respect to *IL4*, *IL6*, *IL17A*, *IL21*, and *IL23*. *IL5* tended to be up-regulated by TCDD. Gene expression of *FOXP3* encoding the transcription factor FoxP3 tended to be down-regulated only in TCDD-treated PBMCs from individual 4.
Little evidence of a TCDD-mediated dysregulating effect on expression on *TDO2*, which was directing towards up-, or down-regulation dependent on the individual and on treatment, was given.

Probable effects on transcription of further genes implicated in T cell lineage specification (*IL1A*, *IL1B*, *IL10*, *IL13*, *IL17F*, *IL22*, *TGFB1*, *TNF*, *STAT3*, *STAT4*, *STAT5*, *STAT6*, *TBX21*, *GATA3*, *RORA*, and *RORC*) were as well investigated. These genes were not differentially regulated by any treatment, in PBMCs of any individual, or in view of the female vs. male consideration, respectively.

4.3.2.7. Human whole genome microarray analysis – summary

According to characterization by flow cytometry, human PBMC-suspensions contained 70 (±12)% $CD3^+$-cells (T lymphocytes), 6.0 (±1.0)% $CD19^+$-cells (B lymphocytes), and 10 (±3)% $CD14^+$-cells (monocytes/macrophages). These cells were treated with TCDD (10 nM), TCDD and LPS (10 nM TCDD + 1 µg/mL LPS), or TCDD combined with PHA (10 nM TCDD + 1.5% PHA) for 24 h. Corresponding control-treatments were DMSO (0.1%), LPS (1 µg/mL LPS), or PHA (1.5%), to which respective TCDD-treatment was correlated.

Inter-individual differences

Viewing whole genome microarray data obtained by treatment of freshly isolated PBMCs with either TCDD alone, together with LPS, or together with PHA, the results in total were very limited. Results varied markedly among the four investigated individuals (2 f, 2 m), leading to low clusters of accordant effects between the individuals. In this regard, impact induced by individual 4 (f) differed to the greatest extent from the three other individuals, which was further evident in view of the individual-specific, as well as the female vs. male consideration used for closer examination of TCDD's impact on several specific genes.

Efficacies regarding differential regulation of 'potential' AhR-target genes were constantly lowered compared to those in other individuals, whereas more genes involved in T cell lineage specification tended to be down-regulated in PBMCs from individual 4. Thus, corresponding data was excluded from most of further investigations to lightly increase correlance between the individuals and to yield statistically more reliable data.

Samples from male vs. samples from female individuals

The male-group on the most part was more responsive compared to the female-group with respect to all investigated genes except for *ALDH3A1*, *IL12*, and *IL23*. This was very likely most prominently due to effects in PBMCs from individual 4 (f). As indicated before, this individual differed from the others to the greatest extent regarding TCDD-dependent effects on gene expression in PBMCs. Response with respect to 'potential' AhR-target genes generally was weaker compared to the other individuals, whereas regarding genes implicated in T cell lineage specification, cells from individual 4 slightly tended to be more affected

Numbers of genes affected by TCDD and AhR-dependent genes

Setting cutoff-values as they were applied in mouse whole genome microarray analysis ($A \geq 2^7$, logarithmic (log2) fold change $|lfc| \geq 1$, and p-value < 0.05; in due consideration of FDR), only regarding one of three treatments, namely the TCDD+PHA-treatment, a small amount of genes was obtained to be significantly differentially regulated (16↑ 3↓). Hence, one of the cutoffs was loosened in order to gain an insight with respect to potential tendencies of TCDD or TCDD+LPS-treatment-derived effects on gene expression in human PBMCs. The false discovery rate (FDR), which represents a method for identification of false positive hypotheses, was disregarded to approach to this objective (Benjamini and Hochberg, 1995).

By ease of this cutoff, a few genes were found to potentially be differentially regulated in response to the treatments with TCDD alone (7↑ 12↓), as well as regarding combined treatment with TCDD+LPS (3↑ 15↓). The number of genes affected by TCDD+PHA-treatment increased (32↑ 12↓) due to this consideration. For the treatments with TCDD alone, down-regulating effects prevailed, whereas a reversed situation was observed for the treatment TCDD+PHA.
Among affected genes, *CYP1A1* was up-regulated for all three treatments. As further members of the AhR gene battery, *TIPARP* occurred in the list of up-regulated genes regarding TCDD+LPS-treatment, whereas *AHRR* was up-regulated by TCDD alone in human PBMCs. Regarding incubation with TCDD+PHA, both *AHRR* and *TIPARP* were induced. Further, *CYP1B1* was up-regulated with respect to TCDD+PHA-treatment.

TCDD's potential impact on genes involved in immune response

Search of potentially relevant genes with respect to a better understanding of TCDD's mode(s) of action on cells of the immune system proved to be difficult due to small amounts of relatively diverging genes affected.

→ TCDD

Taking view on unstimulated PBMCs treated with TCDD, mRNA of one chemokine was up-regulated (*CCL1*), and four (C*XCL10*, *CCL18*, *CCL19*, and *CCL23*) were down-regulated. By tendency, chemotaxis might be affected directed to inhibition with respect to T lymphocytes (C*XCL10*, *CCL18*, *CCL19*, and *CCL23*), B lymphocytes (*CCL19*), and neutrophils (*CCL23*). With respect to chemotactic properties towards monocytes, hints both enhancing (*CCL1*) as well as inhibiting effects were given (*XCL10*, *CCL23*). Further paths of potentially inhibited immune responses by TCDD included Th1-specific immune responses and response of CTLs (*IFNG*),

humoral immune response (*FCGR1B*), and macrophage activation as well as response of monocytes (*CD163*). One up-regulated gene might indicate a role of TCDD on signaling via a phosphatidylinositol-calcium second messenger system (*GCGR*).

→ TCDD+LPS

Regarding stimulation of PBMCs with LPS and concurrent incubation with TCDD, the majority of differentially regulated genes was down-regulated. Out of 15 down-regulated genes, five encoded chemokines. Besides the four chemokines as well inhibited by TCDD alone (C*XCL10*, *CCL18*, *CCL19*, and *CCL23*), *CCL8* was down-regulated. Altogether, down-regulation of these chemokines might indicate inhibited chemotactic properties towards T lymphocytes (*CCL8*, C*XCL10*, *CCL18*, *CCL19*, and *CCL23*), B lymphocytes (*CCL19*), monocytes (*CCL8*, *CCL23*), neutrophils (*CCL23*), as well as basophils and eosinophils (*CCL8*). Besides, possibly inhibited immune reactions due to TCDD-treatment might be type I immunity (*SPP1*), humoral immune response (*FCGR1B*), and macrophage activation as well as response of monocytes (*CD163*).

→ TCDD+PHA

Regarding PHA-stimulated PBMCs, several differentially regulated genes indicated an impact of TCDD on apoptosis (*CABLES1*, *NPTX1*, *SERPINB2*, and *NKD2*). *NKD2* represents an inducible Wnt/β-catenin signaling pathway antagonist, which might suggest a role of TCDD with respect to *c-myc* expression. *C-myc* itself was not regulated along with the PBMC microarray experiment.

Of chemokines regulated by TCDD+PHA-treatment in human PBMCs, two were up-regulated, which might indicate an augmented chemotaxis towards monocytes and basophiles (*CCL2*), and neutrophil granulocytes (*CXL6*).

The down-regulated chemokines on the other hand hinted directing inhibited chemotactic properties towards T lymphocytes (*CCL18*, *CCL19*, and *CCL23*), B lymphocytes (*CCL19*), as well as monocytes and neutrophils (*CCL23*). Further impact indicated TCDD-mediated inhibitory effects on Th1-specific immune responses and response of CTLs (*IFNG*), and on the regulation of B cell activation and proliferation (*MS4A4A*, *CD38*). Implicated in altered glucose-dependent immune homeostasis were *NPTX1*, *HTRA1*, and *CD38*, whereas up-regulated *P2RY6* might reflect an involvement in a phosphatidyinositol-calcium second messenger system.

TCDD's effect on 'potential' AhR-target genes in PBMCs

Reflecting the eight 'potential' AhR-target genes investigated along with the whole genome micorarray experiment using human PBMCs, *CYP1A1* proved to be constantly, although varying with respect to efficacy of induction, up-regulated by TCDD for all treatments (TCDD; TCDD+LPS; TCDD+PHA) and every individual. As well clearly induced by TCDD were *CYP1B1*, *AHRR*, and *TIPARP*. From statistic point of view, highest relevance was attributed to the TCDD+PHA-treatment, followed by TCDD alone for *AHRR*, and the TCDD+LPS-treatment regarding *TIPARP*. Whereas TCDD-mediated impact on *CYP1A2*-expression was minor, its effects on *ALDH3A1*, *CD36*, and *HSD17B2* were low and undirected.

TCDD's potential impact on genes involved in T cell lineage specification

Accompanied by inter-individual differences, transcription of genes involved in T cell lineage specification was limitedly impacted by TCDD in human PBMCs. A bunch of involved genes (*IL1A*, *IL1B*, *IL10*, *IL13*, *IL17F*, *IL22*, *TGFB1*, *TNF*, *STAT3*, *STAT4*, *STAT5*, *STAT6*, *TBX21*, *GATA3*, *RORA*, and *RORC*) was not regulated by any TCDD-treatment or in any individual.

Distinct down-regulation of *IFNG* in response to every TCDD-treatment, as well as tendencies to lightly suppressed transcription of *IL18* was observed. With respect to *IL2*, and *IL12*, inter-individual and/or 'inter-treatment' differences were obtained concerning direction of differential regulation. In general, *IL2* tended to be down-regulated by TCDD, whereas with respect to the TCDD+LPS-treatment, as well es regarding individual 4 (f), different probes on the microarray slides provided evidence for both up-, and down-regulation of *IL2*. Similarly, *IL12* tendentially was down-regulated by treatment of PBMCs with TCDD+PHA, and within the female-group, but was up-regulated by TCDD+LPS-treatment and showed both up-and down-regulating effects in cells from individual 4. With generally low impact and statistical significance, *IL4*, *IL6*, *IL17A*, *IL21*, *IL23*, and *FOXP3* tended to be down-regulated by TCDD. Transcription of *IL5*, and *TDO2* was slightly directed towards up-regulation, though not for every individual with respect to the latter. In total, TCDD's impact on transcription of genes in human PBMCs involved in T cell lineage specification was minor and of statistical low significance.

Overall, the human whole genome microarray experiment investigating effects of TCDD with and without stimuli gave an insight into probable impact of the congener towards immune cells. Still, due to the intricate situation regarding statistics and generally few effects and as well as with respect to inter-individual differences, referred results needed to be considered critically.

4.3.3. Quantitative real-time PCR – human PBMCs

Eight 'potential' AhR-target genes were chosen in the course of SYSTEQ project: *CYP1A1*, *CYP1A2*, *CYP1B1*, *AHRR*, *TIPARP*, *ALDH3A1*, *CD36*, and *HSD17B2*. In addition to the global investigations of TCDD on gene expression in freshly isolated human PBMCs by means of whole genome microarray analysis, these target genes were examined by qRT-PCR.

As used for microarray analysis, treatments (24 h) of interest were TCDD (10 nM), TCDD (10 nM) + LPS (1 µg/mL), or TCDD (10 nM) + PHA (1.5%) as well as accordant controls; DMSO (0.1%), LPS (1 µg/mL), or PHA (1.5%). Samples of all four individuals, two of them female and two of them male, were implemented and respective results were presented individually to study potential inter-individual differences. In accordance with observations obtained by microarray analysis, individual 4 (f) was excluded from statistical investigations.

4.3.3.1. QRT-PCR human PBMCs – *CYP1A1*

As well-investigated AhR-target gene, *CYP1A1* was analyzed in cDNA-samples of PBMCs, which were treated with either TCDD alone, with TCDD+LPS, or with TCDD+PHA. Measurement of *ACTB* as housekeeping gene was implemented. QRT-PCR-results obtained by measurement of respective cDNA-samples regarding *CYP1A1* are presented in figure 70.

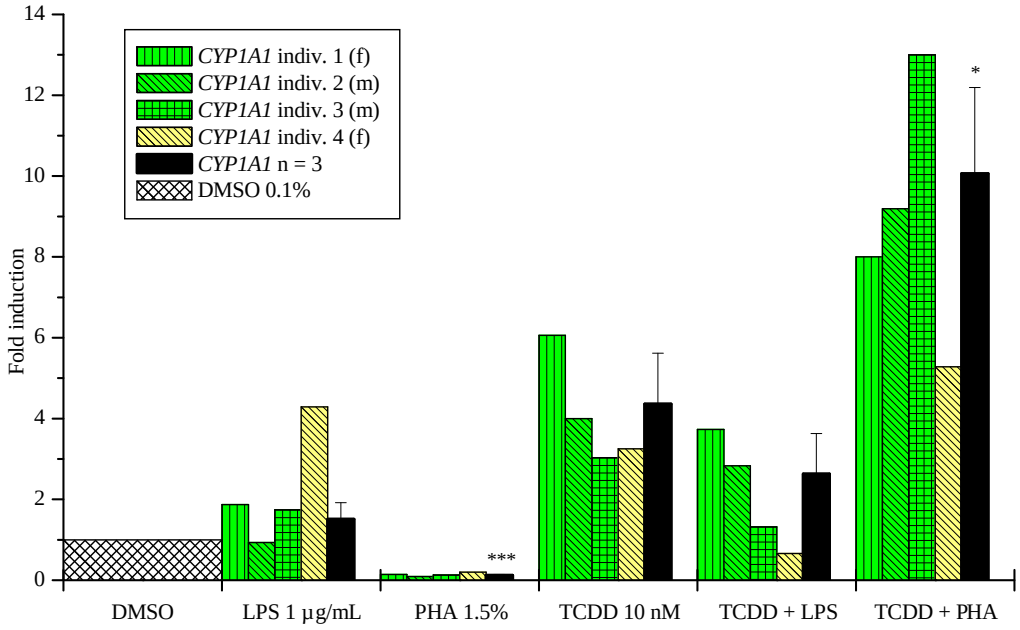

Figure 70: QRT-PCR (*CYP1A1*) human PBMCs. Cells treated with TCDD (10 nM), TCDD + LPS (1 µg/mL), or TCDD + PHA (1.5%) for 24 h. Abscissa: Treatment; ordinate: Fold induction (referred to *ACTB* mRNA-levels). Results from four individuals (indiv.; see legend). Two-tailed unpaired t-test (control vs. treatment group). Female, f; male, m. *: p-value < 0.05, ***: p-value < 0.001.

Principally, *CYP1A1* was inducible in response to treatment with TCDD in human PBMCs on mRNA-level (figure 70).
Highest *CYP1A1*-induction was obtained by treatment of cells with TCDD+PHA, adding up to 13-fold induction for individual 3 (m), and to 10(±2)-fold for n = 3, being statistically significant (p-value < 0.05). Incubation of PBMCs with TCDD alone led to a maximal *CYP1A1*-induction of 8.0-fold (individual 1, f), with a mean value for individuals 1 to 3 of 4.4(±1.3)-fold, which statistically was not considered significant. Among the three different treatments using TCDD, transcription of *CYP1A1*-mRNA was least efficiently induced by TCDD+LPS-treatment, amounting to 2.6(±1.3)-fold induction for n = 3, and maximally achieving a 3.7-fold induction for individual 1 (f).

Interestingly, expression of *CYP1A1* lightly appeared to be inhibited by treatment with PHA (1.5%) alone. The maximum effect (0.09-fold) was obtained by investigation cDNA-samples from individual 2 (m), averaging 0.1(±0.2)-fold for n = 3, which statistically was extremely significant (p-value < 0.001).

Among individuals 1, 2, and 3, light inter-individual differences were obtained regarding induction of *CYP1A1*-mRNA in PBMCs in respond to TCDD. Still, fold-inductions were fairly comparable and lay within an order of magnitude.
By contrast, the response in PBMCs obtained from individual 4 (f) mostly distinguished from the other individuals. Admittedly, treatment with TCDD alone led to a conformable *CYP1A1*-mRNA induction (3.2-fold), and highest *CYP1A1*-induction for individual 4 was measured in the sample from TCDD+PHA-treated PBMCs. Though, the latter was notably lowered (5.3-fold) compared to the remaining individuals.
The greatest difference regarding response of PBMCs from individual 4 contrasted with individuals 1 to 3 was revealed by treatments implying LPS: *CYP1A1*-mRNA was induced by LPS (1 µg/mL) alone (4.3-fold), but was slightly inhibited (0.7-fold ‘induction’) by combined incubation with TCDD (TCDD+LPS-treatment).

4.3.3.2. QRT-PCR human PBMCs – *CYP1A2*

Relative mRNA-expression levels of *CYP1A2* were analyzed in cDNA-samples obtained from PBMCs, which were treated with TCDD alone or in combination with the stimuli LPS, or PHA. *ACTB* served as housekeeping gene. Results of this investigation are presented in figure 71.

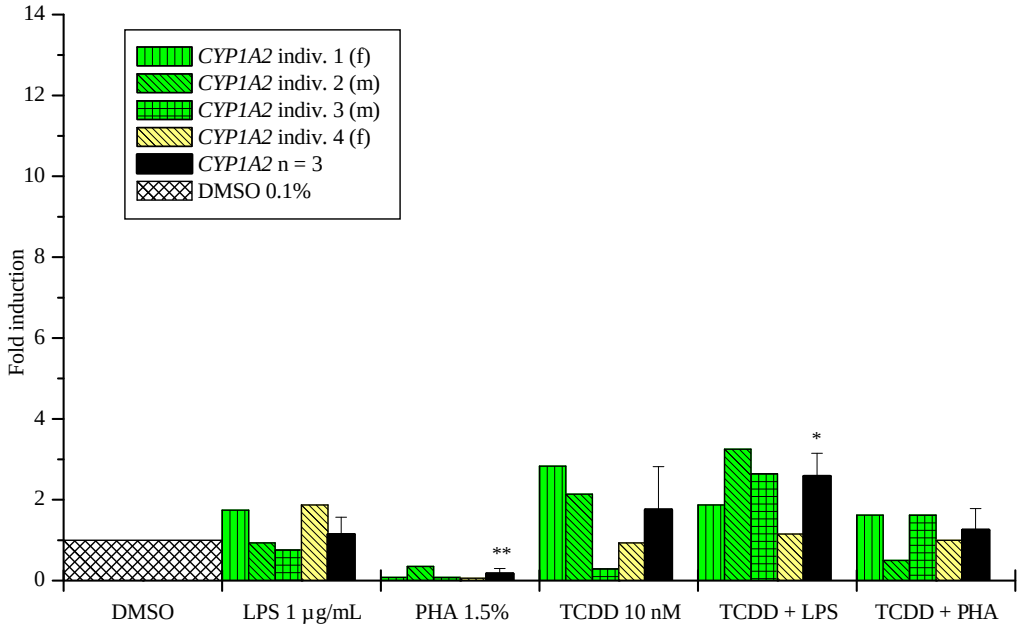

Figure 71: QRT-PCR (*CYP1A2*) human PBMCs. Cells treated with TCDD (10 nM), TCDD + LPS (1 µg/mL), or TCDD + PHA (1.5%) for 24 h. Abscissa: Treatment; ordinate: Fold induction (referred to *ACTB* mRNA-levels). Results from four individuals (indiv.; see legend). Two-tailed unpaired t-test (control vs. treatment group). Female, f; male, m. *: p-value < 0.05, **: p-value < 0.01.

Overall, responsiveness of *CYP1A2* was limited in PBMCs with respect to given conditions (figure 71). Highest inductive impact was obtained by treatment of PBMCs with TCDD+LPS, accounting for 2.6(±0.6)-fold induction for n = 3. This effect statistically was considered significant (p-value < 0.05).

Most responsive individuals were individual 2 regarding incubation of PBMCs with TCDD+LPS (3.2-fold induction), and individual 1 with respect to treatment with TCDD alone (2.8-fold induction).

Treatment with PHA alone inhibited expression of *CYP1A2*-mRNA in PBMC-samples from all four individuals. Values ranged from 0.4-, to 0.06-fold 'induction', and averaged 0.2(±0.1)-fold for n = 3, which statistically was considered very significant (p-value < 0.01).

4.3.3.3. QRT-PCR human PBMCs – *CYP1B1*

Effects of chosen treatments on human PBMCs involving TCDD as well as LPS or PHA with respect to *CYP1B1*-induction on mRNA-level were examined. Findings obtained in association with measurement of *ACTB* as housekeeping gene are summarized in figure 72.

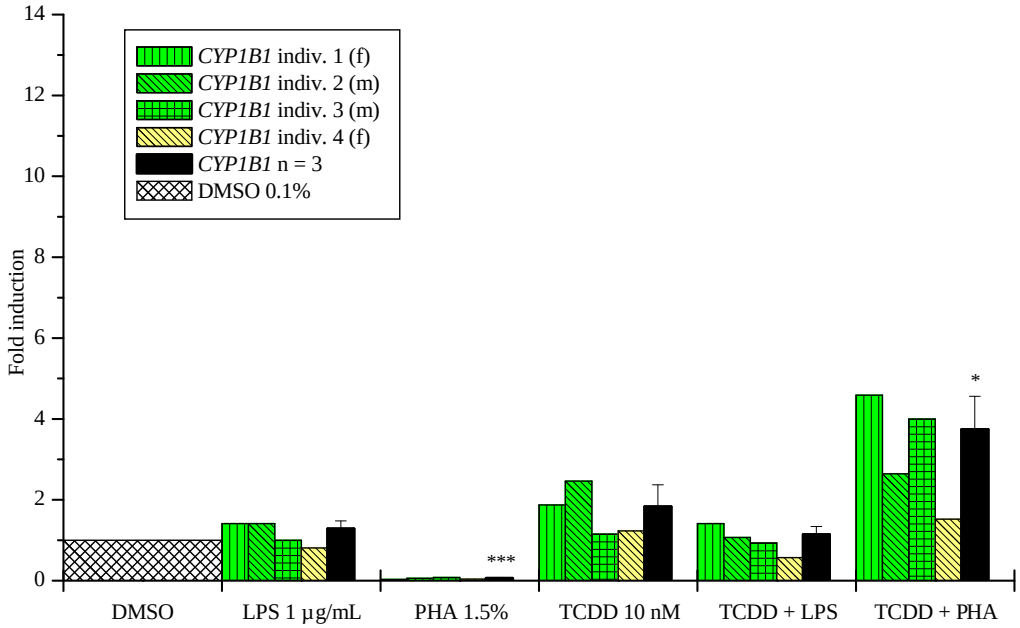

Figure 72: QRT-PCR (*CYP1B1*) human PBMCs. Cells treated with TCDD (10 nM), TCDD + LPS (1 µg/mL), or TCDD + PHA (1.5%) for 24 h. Abscissa: Treatment; ordinate: Fold induction (referred to *ACTB* mRNA-levels). Results from four individuals (indiv.; see legend). Two-tailed unpaired t-test (control vs. treatment group). Female, f; male, m. *: p-value < 0.05, ***: p-value < 0.001.

CYP1B1-mRNA was lightly inducible in human PBMCs in this study (figure 72). *CYP1B1*-mRNA most effectively was induced by treatment of cells with TCDD+PHA. This 3.7(±0.8)-fold induction was statistically considered significant (p-value < 0.05; n = 3). Though statistically not significant and to a quite low extent, transcription of *CYP1B1* was also induced by treatment with TCDD alone (1.8±0.5-fold), followed by combined treatment of TCDD+LPS (1.4±1.1-fold). *CYP1B1* was inhibited (0.06±0.2-fold) by treatment of PBMCs with PHA alone, implicating a statistically extreme significance (p-value < 0.001).

Inter-individually, the strongest distinction among andividuals was obtained regarding individual 4 (f). With respect to TCDD+PHA-treatment, the lowest inductive effect on *CYP1B1* was yielded among individuals (1.5-fold). Beyond, treatment of PBMCs from individual 4 had a lightly inhibitory effect (0.6-fold) on *CYP1B1* gene expression in PBMCs contrasting the up-regulating effects in PBMCs from individuals 1 to 3.

4.3.3.4. QRT-PCR human PBMCs – *AHRR*

As putative AhR-responsive representative, the AhR repressor encoded by *AHRR* was implemented in the *in vitro* studies studying TCDD-mediated response in human PBMCs. Gene expression was examined and referred to measurements of *ACTB*, which served as housekeeping gene. Obtained results are shown in figure 73.

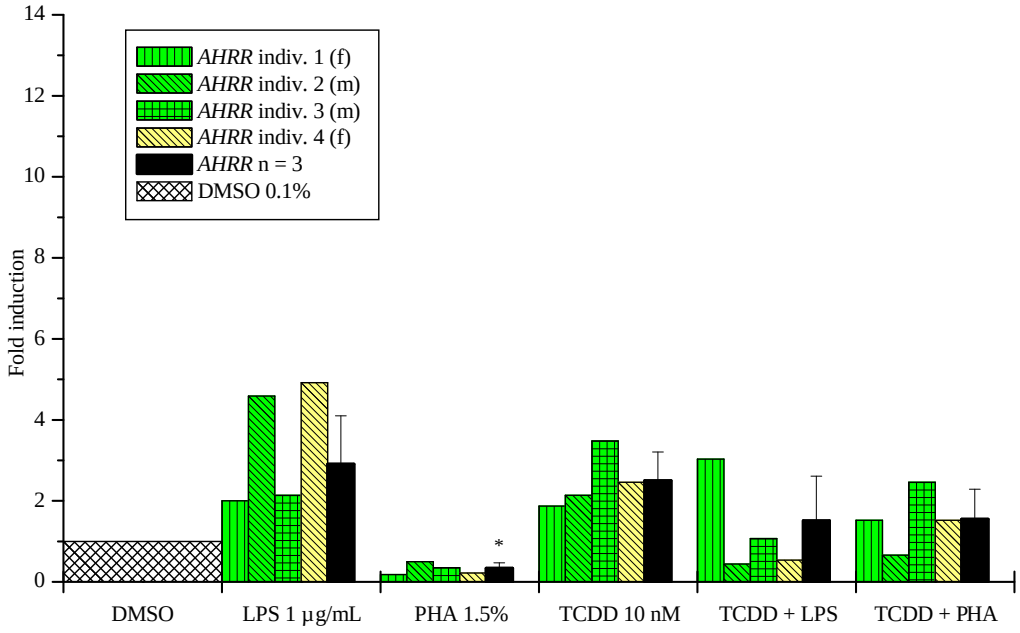

Figure 73: QRT-PCR (*AHRR*) human PBMCs. Cells treated with TCDD (10 nM), TCDD + LPS (1 µg/mL), or TCDD + PHA (1.5%) for 24 h. Abscissa: Treatment; ordinate: Fold induction (referred to *ACTB* mRNA-levels). Results from four individuals (indiv.; see legend). Two-tailed unpaired t-test (control vs. treatment group). Female, f; male, m. *: p-value < 0.05.

Except for inhibition of *AHRR*-transcription by PHA-treatment, no obvious or consensual effect on *AHRR* gene expression was revealed by investigation of chosen PBMC-treatments (figure 73). Sole statistically significant (p-value < 0.05) effect was due to aforementioned PHA-treatment (0.3±0.1-fold; n = 3).

Results hinted towards lightly up-regulating effects by TCDD-treatment alone (2.5±0.7-fold; n = 3), as well by LPS alone (2.9±1.2-fold; n = 3).

Overall, apparently undirected inter-individual differences dominated effects for all treatments regarding expression of *AHRR*.

4.3.3.5. QRT-PCR human PBMCs – *TIPARP*

Impact of treatment with TCDD, TCDD+LPS, or TCDD+PHA on transcription of *TIPARP* in human PBMCs was investigated by qRT-PCR. Accordant results including respective control-measurements are shown in figure 74.

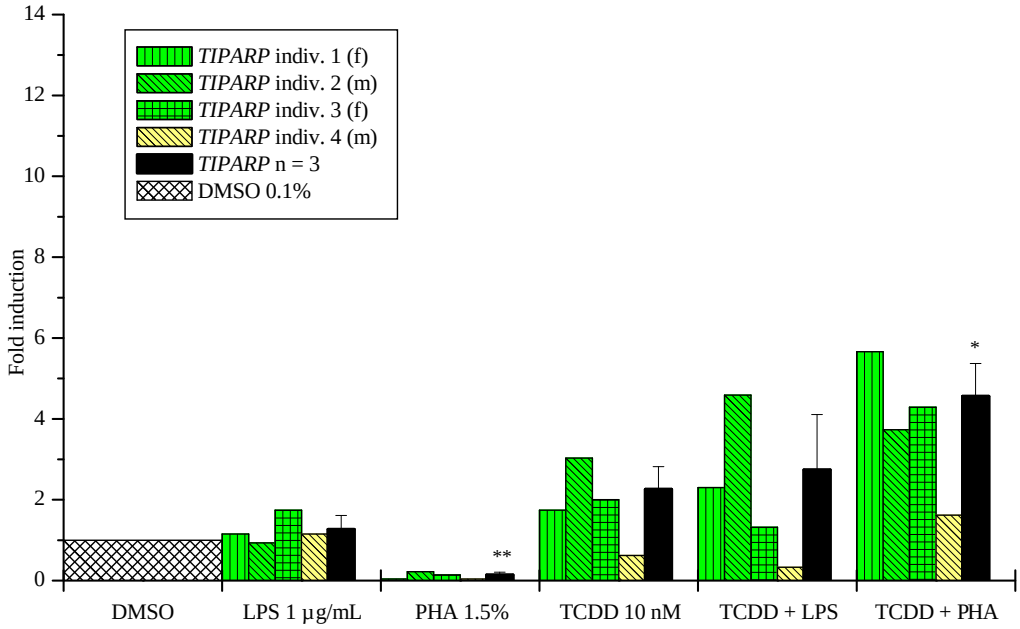

Figure 74: QRT-PCR (*TIPARP*) human PBMCs. Cells treated with TCDD (10 nM), TCDD + LPS (1 µg/mL), or TCDD + PHA (1.5%) for 24 h. Abscissa: Treatment; ordinate: Fold induction (referred to *ACTB* mRNA-levels). Results from four individuals (indiv.; see legend). Two-tailed unpaired t-test (control vs. treatment group). Female, f; male, m. *: p-value < 0.05, **: p-value < 0.01.

Statistically significant (p-value < 0.05) induction of *TIPARP* in human PBMCs responding to treatment with TCDD+PHA was found (figure 74). In this regard, a light induction value of 4.6(±0.8)-fold for n = 3 was revealed.
Slight, but not considered statistically significant *TIPARP*-inductions were as well obtained with respect to TCDD-treatment (2.3±0.6-fold; n = 3), and TCDD+LPS-treatment (2.7±1.4-fold; n = 3).

Inter-individual variations were not as prominent as regarding the other investigated genes with the exception of individual 4 (f). Incubation of PBMCs led to a statistically very significant down-regulation of *TIPARP* (0.14±0.07-fold; n = 3; p-value < 0.05).

4.3.3.6. QRT-PCR human PBMCs – *ALDH3A1*

As a further potential AhR-target gene, *ALDH3A1*-gene expression in PBMCs was investigated. Implicating measurements of *ACTB* serving as housekeeping gene, the respective results are presented in figure 75.

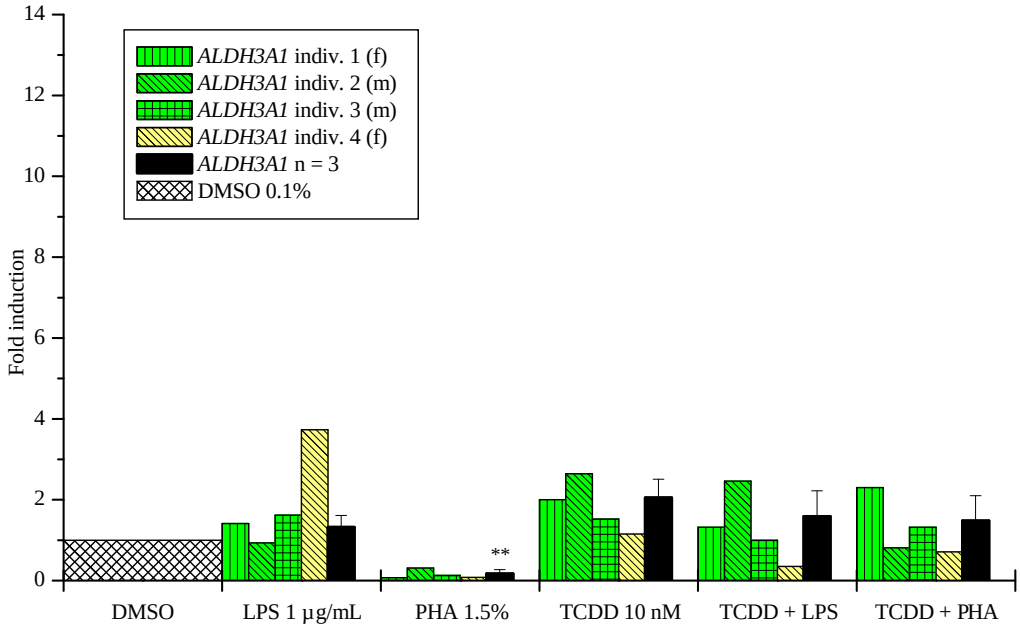

Figure 75: QRT-PCR (*ALDH3A1*) human PBMCs. Cells treated with TCDD (10 nM), TCDD + LPS (1 µg/mL), or TCDD + PHA (1.5%) for 24 h. Abscissa: Treatment; ordinate: Fold induction (referred to *ACTB* mRNA-levels). Results from four individuals (indiv.; see legend). Two-tailed unpaired t-test (control vs. treatment group). Female, f; male, m. **: p-value < 0.01.

ALDH3A1-gene expression was statistically very significantly (p-value < 0.01) down-regulated (0.2±0.1-fold; n = 3) by treatment with PHA in PBMCs (figure 75). Apart from that, no distinct impact due to any treatment was obtained. Results might indicate a slight up-regulating effect by treatment with TCDD (2.1±0.7-fold; n = 3).

Overall, inter-individual variations were predominating within this examination.

4.3.3.7. QRT-PCR human PBMCs – *CD36*

Results of qRT-PCR measurements of *CD36* with respect to samples from human PBMCs treated for 24 h with TCDD (10 nM), TCDD (10 nM) + LPS (1 µg/mL), or TCDD (10 nM) + PHA (1.5%), and appropriate controls, are depicted in figure 76.

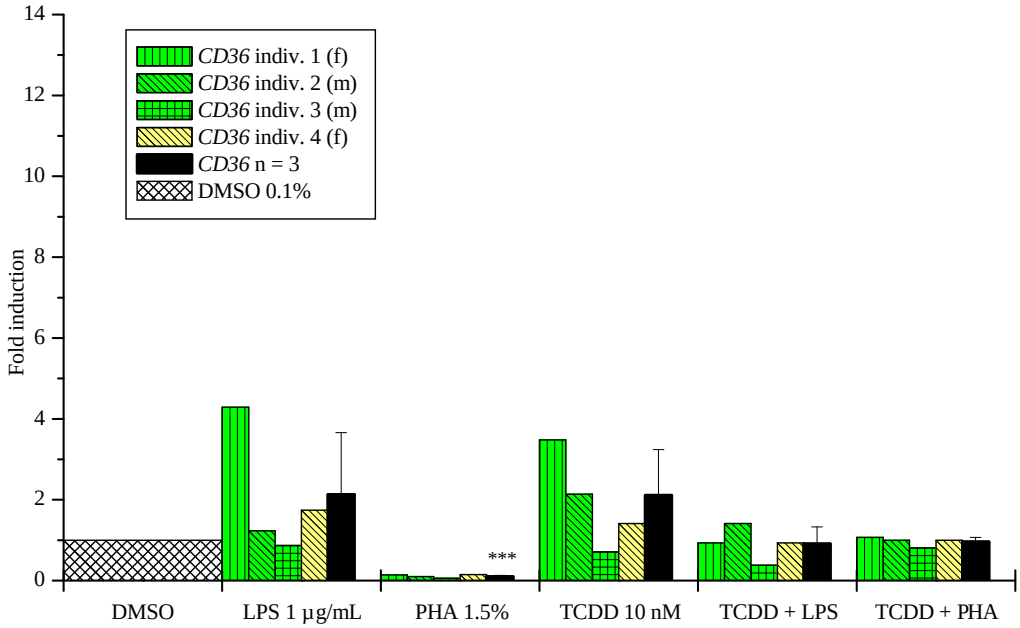

Figure 76: QRT-PCR (*CD36*) human PBMCs. Cells treated with TCDD (10 nM), TCDD + LPS (1 µg/mL), or TCDD + PHA (1.5%) for 24 h. Abscissa: Treatment; ordinate: Fold induction (referred to *ACTB* mRNA-levels). Results from four individuals (indiv.; see legend). Two-tailed unpaired t-test (control vs. treatment group). Female, f; male, m. ***: p-value < 0.001.

As obtained with respect to aforementioned and measured potential AhR-target genes, treatment of PBMCs with PHA led to down-regulation (0.1±0.03-fold; n = 3) of *CD36*-gene transcription (figure 76). The effect statistically was considered extremely significant (p-value < 0.001).

Remarkable were great variations of individual results. Cells from individuals tended to bear similar effects, at least compared among individuals, almost independent from treatment. PBMCs from individual 1 (f) were quite responsive to LPS-(4.3-fold), or TCDD (3.5-fold)-treatment, which was similar regarding individual 2 (m) with respect to TCDD-treatment (2.1-fold) but occured with lower extent.

4.3.3.8. QRT-PCR human PBMCs – *HSD17B2*

PBMCs incubated with TCDD, LPS, PHA, or an appropriate combination, were examined regarding impact of treatments on *HSD17B2*-expression. Results implicating measurements of *ACTB* as housekeeping gene are illustrated in figure 77.

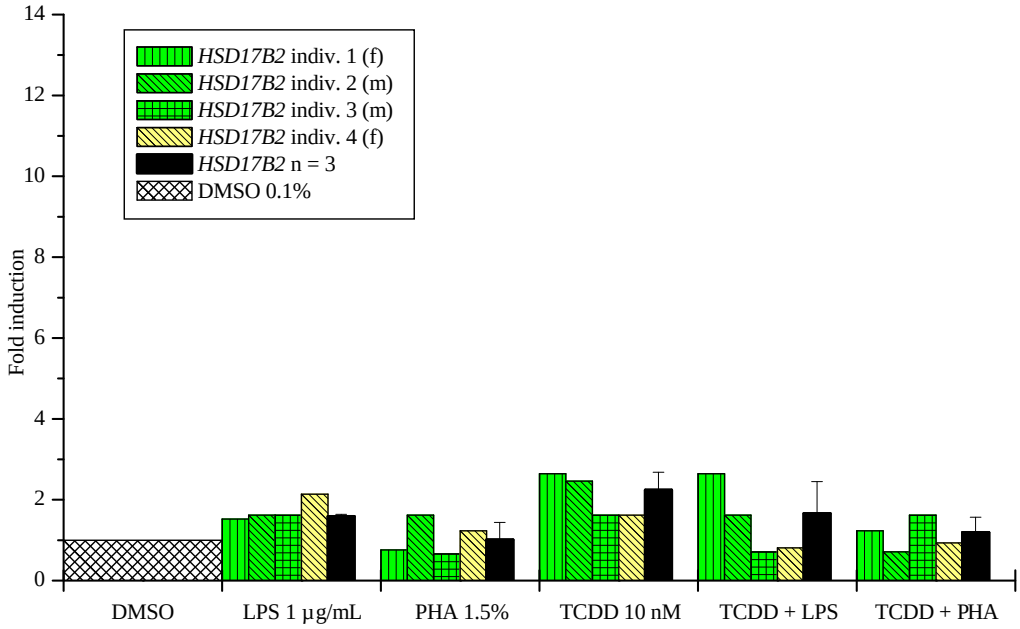

Figure 77: QRT-PCR (*HSD17B2*) human PBMCs. Cells treated with TCDD (10 nM), TCDD + LPS (1 µg/mL), or TCDD + PHA (1.5%) for 24 h. Abscissa: Treatment; ordinate: Fold induction (referred to *ACTB* mRNA-levels). Results from four individuals (indiv.; see legend). Two-tailed unpaired t-test (control vs. treatment group). Female, f; male, m.

Overall, any treatment had an effect on *HSD17B2*-gene expression in human PBMCs subsequent to 24 h of incubation (figure 77). With one exception, no obvious trend was distinguishable in this regard. A value of 2.2(±0.4)-fold induction by TCDD-incubation might lightly direct towards an up-regulating effect due to this treatment.

Even inter-individual differences were less prominent regarding impact on *HSD17B2*-gene transcription.

4.3.3.9. QRT-PCR human PBMCs – summary

In human PBMCs, *in vitro* gene expression of a set of 'potential' AhR-target genes was analyzed by qRT-PCR. Hence, expression of *CYP1A1*, *CYP1A2*, *CYP1B1*, *AHRR*, *TIPARP*, *ALDH3A1*, *CD36*, and *HSD17B2* using incubations with TCDD (TCDD, 10 nM; TCDD, 10 nM + LPS, 1 µg/mL; or TCDD, 10 nM + PHA, 1.5%), and respective controls (DMSO, 0.1%; LPS 1 µg/mL; or PHA, 1.5%) was assessed.
Overall, effects of TCDD and combined incubations with the stimuli LPS or PHA on gene expression in human PBMCs was impacted greatly by inter-individual differences.

Highest, but also highly varying inductions of gene transcription were obtained regarding *CYP1A1*-expression by TCDD-treatments, whereas only the treatment TCDD+PHA led to a statistically significant result. Comparable findings but with lower efficacy were revealed regarding *CYP1B1*. The least responsive gene among CYPs was represented by *CYP1A2*. In this regard, impact enforced by TCDD+LPS-treatment solely was considered statistically significant among examined TCDD-treaments.

Investigations concerning *TIPARP* yielded similar results to those obtained for *CYP1B1*. In fact, treatments with TCDD, or with TCDD+LPS, led to an even higher, although statistically not significant gene expression with respect to *TIPARP*-induction contrastet with results obtained for *CYP1B1*.
Concerning further investigated genes *AHRR*, *ALDH3A1*, *CD36*, and *HSD17B2*, no significant response was reported by treatment with TCDD or combined incubations with LPS or PHA.

Interestingly, PHA (1.5%) constantly possessed statistically significant repressive effects on transcription of all investigated 'potential' target genes except for *HSD17B2*.

5
Discussion

5.1. Discussion – Mouse Whole Genome Microarray Analysis

Impact of DL-congeners on gene expression in mouse livers was primarily and with strongest significance correlated with enhanced xenobiotic metabolic processes. Followed by alterations towards lipid-, and carbohydrate metabolism, further implicated mechanisms were oxidative processes, apoptosis, and immune response. Dependent on the congener, these processes were involved to diverging degree.

PCB 118

Effects due to treatment with PCB 118 were mostly limited to drug metabolism in mouse livers. Slight indications with respect to the compound's impact on insulin receptor signaling, carbohydrate-induced expression of liver enzymes essential for *de novo* lipogenesis as well as glycolysis, and correlated glucose homeostasis were given.

Considering down-regulated genes by PCB 118, the congener might tend to be involved in immune response, as regarding type 2 immune response and B cell differentiation, or IFN-γ production and Th1-differentiation, for instance. Most notably concerning down-regulated genes, statistical significances with respect to appearance of clustered GO terms was limited, which complicated the interpretation of these microarray results even more.

Further, the number of clustered genes within significant ('Top 20') GO terms in total was low, even regarding the most obviously affected path of xenobiotic metabolism. Hence, properties of more than 300 up-, and down-regulated genes were difficult to predict, as less than 100 were clearly assigned.

1-PeCDD

Treatment of mice with 1-PeCDD led to most comparable effects regarding gene expression in livers compared to those obtained in TCDD-treated mice. The highest overlap regarding numbers of 'together' regulated genes with TCDD was received in this respect. Besides 'oxidation-reduction processes', which was the most significantly affected GO term by 1-PeCDD and implied xenobiotic metabolic processes, a dominating effect on lipid metabolism represented the congener's impact. 1-PeCDD further tended to be involved in altered carbohydrate- and glucose-metabolism.

4-PeCDF, PCB 126, and PCB 156

Effects by 4-PeCDF, PCB 126, and PCB 156 were highly concentrated on (xenobiotic) metabolism and reflected a huge amount of transcribed as well as processed genes. Overlap between regulated genes by 4-PeCDF and PCBs, including PCB 118 as well, was respectable.

Overlap among DL-congeners

Among all DL-congeners, overlap turned out to be limited to 22 up-, and five down-regulated genes – a conserved list mainly composed of genes related to xenobiotic metabolism, followed by genes involved in lipid metabolic processes. Excluding PCB 118 from respective examination of DL-congeners, genes of resulting gene-list (48↑ 19↓) principally participated in the same processes as it was observed for all DL-congeners together in the (22↑ 5↓) gene list.

The higher number of differentially regulated genes within these processes, which represented the decisive difference between these analyses, yielded in a higher significance with respect to involvement in xenobiotic metabolic processes and, even more pronounced, regarding lipid metabolism.

Even though the 'DL-overlap' tended to be limited, DL-congeners shared impact on gene expression in mouse livers with respect to (xenobiotic) metabolic processes as well as lipid metabolism, whereas correlance appeared with greater significance by exclusion of PCB 118 with respect to this investigation.

'Relative effect potencies' of congeners

Regarding investigations for estimation of REPs, for instance by measurement of genes involved in xenobiotic metabolism such as *Cyp1a1*, these facts quasi 'reflected' basis principles of a TEF-concept, by which these congeners were and are classified according to their potencies. By persuing this thought, potential difficulties associated with this system might become obvious.

Considering the DL-congeners implemented in the study in hand, three potentially possible options were represented considering results obtained within present study. As obtained, all of (examined) congeners consensually shared impact with respect to xenobiotic metabolism, as well as particularly regarding *Cyp1a1*, which potentially is measured for estimation of REPs. One might measure *Cyp1a1*-inductions with divergent REPs for congeners with diverging properties in this regard. This would thus reflect diverging impact on consensually affected xenobiotic metabolism and might reflect AhR-mediated effects, which hence would match with the basic idea of the TEF concept.

Potential difficulties in this regard might occur during assessment of both those congeners possessing small overlap with TCDD, like PCB 118 (overlap around 25% with respect to TCDD's effects), and those compounds bearing quite considerable overlap with TCDD, like 4-PeCDF (overlap around 50-75% with respect to TCDD's effects). Regarding the latter, a huge amount of genes was induced and repressed besides these TCDD-overlapping effects.
In percentage, a similar situation might be obtained regarding PCB 118 – Although sharing around 25% 'properties' referring to inductive effects on gene expression with TCDD, this overlap represents as few as 10% of PCB 118's substance-specific impact.

Hence, estimation of REPs in the course of TEF-investigations might well reflect congeners' AhR-dependent effects, but dependent on the congener, a considerable amount of information gets lost. Even if the relevance of such 'additional' congener-specific impact remains unclear for now, it might be relevant for the assessment of a congener's toxic potential.

5.2. Discussion – Liver Cell Systems

Rat liver cell systems are widely used and well established regarding their use in verification and differentiation of dioxin-like effects. With respect to the study in hand, a set of 13 DL-congeners (TCDD, 1-PeCDD, 1,6-HxCDD, 1,4,6-HpCDD, TCDF, 4-PeCDF, 1,4-HxCDF, 1,4,6-HpCDF, PCB 77, PCB 105, PCB 118, PCB 126, and PCB 156) and the NDL-PCB 153 were investigated with respect to their potential EROD-inducing effects, and on CYP1A1-induction on protein level via Western Blotting in H4IIE cells and primary rat hepatocytes (PRH) from Sprague Dawley rats. Subsequent to a screening experiment examining TCDD's impact on gene transcription of eight 'potential' target genes (*Cyp1a1*, *Cyp1a2*, *Cyp1b1*, *Aldh3a1*, *AhRR*, *Tiparp*, *Cd36*, and *Hsd17b2*) in H4IIE cells and PRH, a further selection was made due to responsiveness and concentration-dependence in both tested liver cell systems. Hence, the seven 'core' congeners, TCDD, 1-PeCDD, 4-PeCDF, PCB 118, PCB 126, PCB 156, and the NDL-PCB 153 were examined with respect to their impact on transcription of *Cyp1a1*, *Cyp1a2*, *Cyp1b1*, and *Aldh3a1* in both H4IIE cells and primary rat hepatocytes. An incubation time of 24 h was applied for all examinations.

H4IIE vs. primary rat hepatocytes

As obtained in several studies, H4IIE cells were constantly more sensitive towards dioxin-dependent effects (Schmitz *et al.*, 1995; Zeiger *et al.*, 2001). One exception was obtained in this regard – the 'potential' AhR-target gene *Aldh3a1* was induced in PRH more potently as well as with higher efficacy compared to effects in H4IIE cells.

Contrasting effects on *Cyp1a1* in H4IIE cells with impact on *Aldh3a1* in PRH by means of qRT-PCR measurements, TCDD-treatment yielded comparable efficacy and around 1.5 orders of magnitude lower potency in PHR compared with values in H4IIE cells, which was around three orders of magnitude lower potency, but around 30 times higher efficacy contrasted with *Cyp1a1*-induction in PRH.

By contrast, *Aldh3a1* was least responding in H4IIE cells, the actual more sensitive liver cell system. Thus, *Aldh3a1* was considered a gene, which was responsive to DL-compounds, whereas *Aldh3a1*-induction by these chemicals was suggested not be exclusively dependent on the AhR. Interestingly, *Aldh3a1* was also reported to be induced in livers by *in vivo*-treatment of mice with phenobarbital, which actually represents a chemical functioning via the receptors CAR and/or PXR (Gährs *et al.*, 2013; Pappas *et al.*, 2003; Xie *et al.*, 2000). An involvement of the AhR regarding *Aldh3a1*-induction was indicated, since potencies of all investigated congeners were comparable to those regarding *Cyp1a1*-induction, for instance.

Responsiveness of 'AhR-target genes'

For both liver cell systems (after 'removing' of *Aldh3a1* as an inconclusive AhR-dependent gene), *Cyp1a1* was the most responsive target gene, followed by *Cyp1b1*, and *Cyp1a2*, as obtained in literature as well (Lai *et al.*, 2006; Xu *et al.*, 2000).

Comparison of REPs between the two applied rat liver cell systems provided information concerning their sensitivity towards a specific compound. Regarding *Cyp1a1*-induction, REPs for 1-PeCDD were higher in PRH than those in H4IIE cells, indicating a higher sensitivity in PRH compared to H4IIE cells, whereas this effect was reversed for 4-PeCDF. Comparable findings were observed with respect to 1-PeCDD and its impact on *Cyp1a2*-induction, as well as for 4-PeCDF referring to REP (EC50). Further, 1-PeCDD appeared to be about twice as potent as was TCDD regarding *Cyp1a1*-and *Cyp1a2*-induction.

REPs vs. TEFs

With respect to REP-values gained by liver cell system investigations on EROD-induction, as well as on qRT-PCR-investigations (*Cyp1a1*, *Cyp1a2*, *Cyp1b1*, and *Aldh3a1*), the current TEFs were widely confirmed (Van den Berg *et al.*, 2006).

A REP (EC50) for 4-PeCDF of 0.14 regarding *Cyp1a2*-induction in primary hepatocytes from Spreague Dawley rats quite well matched the one obtained along with own investigations (REP (EC50, PRH) = 0.13). The REP (EC50) obtained for *Cyp1a1*-induction was distinctly lowered (0.03) compared to the one revealed in current study (0.56). Differences might be due to an extended incubation-time of 48 h, compared to 24 h-duration implemented in this study (Budinsky *et al.*, 2010).

Regarding EROD-investigations using PRH as well as H4IIE-cells, further slight deviations from current TEFs occurred. Regarding REP (EC20) for 1-PeCDD, and regarding REP (EC50) for 1,4,6-HpCDD, REPs were twice as high in H4IIE cells compared to those in PRH.

Besides, both REPs for effects in H4IIE cells mediated by TCDF were both lower than those observed for PRH and below the current TEF. This effect might be due to the flattened concentration-response curve corresponding to TCDF's impact.

AhR-dependent effects and chemical structures of congeners

Ranking orders regarding PCDDs, PCDFs, and PCBs, in correlation with chlorination pattern and probability to reach a planar conformation were comparable with observations obtained in literature (Budinsky *et al.*, 2010; De Voogt *et al.*, 1990; Zeiger *et al.*, 2001).

Higher chlorinated PCDD-congeners tended to yield lower REPs, which is suggested to be due to reduced binding affinities towards the AhR (Kafafi *et al.*, 1993; Mhin *et al.*, 2002). Further, non-*ortho*-substituted PCB-congeners (PCB 126, PCB 77) tended to gain higher effects with respect to EROD-induction and CYP1-induction in rat liver cells, though with lowered extent regarding PCB 77.

For the PCB-congeners, the chlorination pattern is of specific relevance, as it maintains the probability to reach a planar conformation, which further yields in higher binding affinities towards the AhR, since with respect to non-*ortho*-substituted PCBs, the two phenyl rings are able to rotate more easily about the shared bond (De Voogt *et al.*, 1990). This situation tends to be sterically hindered in mono-*ortho*-PCBs like PCB 118, or PCB 156, leading to a lower potency with respect to AhR-dependent examinations.

5.3. Discussion – Human Whole Genome Microarray Analysis and QRT-PCR

One aim of this study was to reveal probable TCDD-induced effects on human immune cells. To approach to this objective, freshly isolated human PBMCs were characterized by flow cytometry (70±12% $CD3^+$-cells, T lymphocytes; 6.0±1.0% $CD19^+$-cells, B lymphocytes; and 10±3% $CD14^+$-cells, monocytes/macrophages) and exposed to one of three TCDD-treatments for 24 h:

TCDD (10 nM)
TCDD and LPS (10 nM TCDD + 1 µg/mL LPS), or
TCDD combined with PHA (10 nM TCDD + 1.5% PHA).

Corresponding control-treatments were DMSO (0.1%), LPS (1 µg/mL LPS), or PHA (1.5%), to which respective TCDD-treatments were correlated. Integrity of isolated mRNA was checked (2100 Bioanalyzer, Agilent Technologies GmbH, Waldbronn, Germany), before the two-color microarray-based gene expression analysis was perfomed applying Human GE 4x44K v2 Microarray Kits (Agilent Technologies GmbH, Waghaeusel-Wiesental, Germany) by implementation of dye-swop procedures to reduce potential artifactual effects due to diverging dye properties.
The set of 'potential' AhR-target genes (*CYP1A1*, *CYP1A2*, *CYP1B1*, *AHRR*, *TIPARP*, *ALDH3A1*, *CD36*, and *HSD17B2*) was further investigated by qRT-PCR.

Human whole genome microarrays and inter-individual differences

A first view on normalized and statistically analyzed data (Bioconductor R package Limma; Smyth, 2004), as well as on principal component analyses (PCAs) and on individual-specific human whole genome microarray data, distinct inter-individual variations were obvious.
One individual, individual 4 (f), differed greatly from the others regarding TCDD-dependent effects on gene expression in PBMCs. As indicated examplarily in the human microarray results-chapter, response with respect to 'potential' AhR-target genes (*CYP1A1*, *CYP1B1*, *AHRR*, and *TIPARP*, in particular) generally was weaker compared to the other individuals, whereas regarding genes implicated in T cell lineage specification, cells from individual 4 slightly tended to be more affected towards down-regulation. Due to close examinations on raw data, individual 4 (f) was discarded from most of further investigations of the microarray analysis. Hence, clustering of data among individuals 1, 2, and 3 improved, as well as did statistical significance and thus reliablility of data regarding the complete human whole genome microarray experiment.

Human whole genome microarrays and numbers of TCDD-regulated genes

Initially, cutoff-values were set as they were applied in mouse whole genome microarray analysis ($A \geq 2^7$, logarithmic (log2) fold change $|lfc| \geq 1$, and p-value < 0.05; in due consideration of the false discovery rate, FDR).

Using these statistical limitations, only one out of three treatments investigated showed a response at all: In response to TCDD+PHA-treatment, a small amount of genes significantly was differentially regulated (16↑ 3↓). Subsequently, the FDR-cutoff was loosened in order to gain an insight into potential tendencies of TCDD-derived effects respecting the other two treatments (TCDD; TCDD+LPS). The FDR, which represents a method for identification of false positive hypotheses, was disregarded to approach to this objective (Benjamini and Hochberg, 1995).

The genes lists still were short. In total, highest number of genes was affected after TCDD+PHA-treatment (32↑ 12↓), followed by TCDD (7↑ 12↓), and TCDD+LPS (3↑ 15↓).

Hochstenbach *et al.* (2010) found higher numbers of differentially regulated genes in human PBMCs subsequent to 20 h of *in vitro* treatment with TCDD (1 µM; 10 µM) applying a metabolic activation system using an Agilent whole-genome 4 x 44K microarray system (106↑ 169↓, 1 µM TCDD; and 117↑ 195↓, 10 µM TCDD). For metabolic activation, the authors made use of a human liver S9-mix (10% of a 30% S9-fraction). Statistical cutoffs as well differed from those of the study in hand. Hochstenbach *et al.* implemented a cutoff of $|lfc| \geq 1.5$fold, using three of five donors (Hochstenbach *et al.*, 2010). In a more recent study by Hochstenbach *et al.* (2012), in a similarly constructed test-system, 878 (1 µM TCDD), or 1233 (10 µM TCDD) genes were differentially regulated in PBMCs, respectively (cutoff: $|lfc| \geq 1.5$fold, five donors; p-value < 0.05, t-test) (Hochstenbach *et al.*, 2012).

The different cutoffs as well as the use of a S9 metabolic activation system represent two major deviations, which might explain the varying numbers of differentially regulated genes the authors declared compared to those of the study in hand.

Differentially regulated genes – *CYP1A1*

Differentially regulated genes by all three TCDD-treatments (TCDD; TCDD+LPS; TCDD+PHA) were headed by *CYP1A1*. Though with diverging statistical relevance and efficacy, this AhR-responsive gene was up-regulated in PBMCs from every individual and throughout all TCDD-treatments in present microarray experiment.

Inter-individual variations were as follows: lfc (i1) = 2.105, lfc (i2) = 2.107, lfc (i3) = 1.857, and lfc (i4) = 1.027 (effects of all three TCDD-treatments consolidated), whereas *CYP1A1*-induction with respect to treatments accounted for lfc (TCDD) = 1.798, lfc (TCDD+LPS) = 1.671, and lfc (TCDD+PHA) = 2.599 (n = 3).

Highest, but also highly varying inductions of gene transcription were obtained regarding *CYP1A1*-expression by TCDD-treatments with respect to qRT-PCR results in this study, whereas again, only the treatment TCDD+PHA led to a statistically significant result for n = 3.

According to the literature, *CYP1A1* was shown to be constitutively expressed in human PMBCs (Krovat *et al.* 2000, Siest *et al.*, 2008). Further, and in correlance with the study in hand, CYP1A1-induction was obtained to be inducible in human PBMCs both on gene transcription and on protein level, exhibiting great inter-, and intra-individual variety and overall comparably low absolute induction values in most of the experiments (Kouri *et al.*, 1974; Nohara *et al.*, 2006; Vanden Heuvel *et al.*, 1993; Van Ede *et al.*, 2014b). Respective results deviated from ~3fold (100 nM TCDD, 6 h) over ~20fold (10 nM TCDD, 72 h), and ~60fold (10 nM TCDD, 48 h) to ~160fold (10 nM TCDD, 48 h) *CYP1A1*-induction on mRNA-level in primary human PBMCs (Nohara *et al.*, 2006; Vanden Heuvel *et al.*, 1993; Van Ede *et al.*, 2014b).

Differentially regulated genes – *CYP1B1*

To a lowered extent compared to *CYP1A1*-induction in PBMCs, *CYP1B1* was up-regulated with respect to TCDD+PHA-treatment (lfc = 1.574). Further, PBMCs received from male individuals showed *CYP1B1*-induction of statistical significance. By ease of cutoffs (FDR disregarded, $|\text{lfc}| \geq 1.5$fold), indications for up-regulation of this gene were also revealed with respect to TCDD (lfc = 0.823)-, and TCDD+LPS (lfc = 0.805)-treatment, as well as regarding every individual with diverging efficacy: lfc (i1) = 1.016, lfc (i2) = 1.161, lfc (i3) = 0.995, lfc (i4) = 0.747 (effects of all three TCDD-treatments consolidated).

Similar findings were revealed by qRT-PCR-investigations of *CYP1B1*. Variability among individuals combined with a low inducibility led to minor and to statistically least significant

TCDD-mediated effects in human PBMCs, indicating a less reliable marker for TCDD-derived effects compared to *CYP1A1*. Findings were comparable to those in literature. Whereas *CYP1B1* was reported to be constitutively expressed in human PMBCs, elevated mRNA-levels achieved after TCDD-treatment varied from ~2-3fold (5 nM, 6h; 5 nM, 72 h; or 10 nM, 48 h (with PHA 1.5%)), to around 5-8fold (1 nM, 48 h (with PHA 1.5%)) induction in PBMCs (De Waard *et al.*, 2008; Finnström *et al.*, 2002; Van Duursen *et al.*, 2005; Van Ede *et al.*, 2014b).

Further, *CYP1B1*-induction appeared to depend on the type of treatment in the present study. This effect might, at least in parts, be attributable to inductive effects by LPS itself since *CYP1B1* has been shown to be inducible by this stimulus in human peripheral blood monocytes and macrophages (1 µg/mL LPS, 24 h) (Baron *et al.*, 1998). This observation was not reproduced along with the study in hand. Since applied PBMCs contained 10 (±3)% monocytes/macrophages, this effects might have been minor with respect to the complete suspension of cells, which probably made an insufficient difference for detection. As LPS 'alone' might be able to lightly induce *CYP1B1*, the span between treatment and control might have become smaller, hence leading to a lower TCDD-mediated inductive effect.

Differentially regulated genes – *CYP1B1 and TIPARP*

Similar findings as for *CYP1B1* were obtained with respect to *TIPARP*-induction in human PBMCs in response to TCDD for both the microarray experiment and qRT-PCR examinations. Emphasized from statistical point of view was the treatment with TCDD+PHA (lfc = 1.64, n = 3; qRT-PCR: 3.7(±0.8)-fold induction, n = 3), as well as both gender-specific investigations.

Yet, *TIPARP* was correlated with TCDD-exposure in a microarray experiment (22K Human 1A (V2) Oligo Microarray, Agilent) human PBMCs, where similar results for *CYP1B1*-and *TIPARP*-induction were observed in response to incubation of cells with TCDD (500 pM, 48 h; n = 5), accounting for 1.40-fold (*CYP1B1*), and 1.73-fold (*TIPARP*) induction, respectively (De Waard *et al.*, 2008).

With respect to both microarray data and qRT-PCR results, no obvious gender-specific differences were obtained regarding *CYP1B1*-induction in PBMCs among the four investigated individuals studied along with present study. This could have been implicated since basal expression was proposed to be significantly higher in women than in men (Finnström *et al.*, 2002). Probable differences in basal levels might also have been overlayed by quite distinct inducing effects, or might have been masked within the microarray experiment, since for the gender-, and individual-specific consideration, treatment-specific results were consolidated.

Differentially regulated genes – *AHRR*

One more AhR-dependent gene was affected by TCDD in human PBMCs with respect to the whole genome microarray experiment, namely *AHRR*. A clear, from statistical point of view most reliable correlation was observed for treatment of cells with TCDD+PHA (lfc = 2.084; n = 3). Concerning TCDD-treatment (lfc = 1.042; n = 3) as well as TCDD+LPS-treatment (lfc = 0.947; n = 3) and gender-, as well as individual-specific analyses, indications regarding TCDD-mediated up-regulating effects towards *AHRR*-expression in human PBMCs were given by choose of less stringent cutoffs. Inter-individual differences were as follows: lfc (i1) = 1.474, lfc (i2) = 1.462, lfc (i3) = 1.137, and lfc (i4) = 0.691 (effects of all three TCDD-treatments consolidated).

Regarding qRT-PCR investigations, no obvious or consensual effect on *AHRR* gene expression was revealed by investigation of chosen PBMC-treatments. Apparently undirected inter-individual differences dominated effects for all treatments regarding expression of *AHRR*. Results hinted towards lightly up-regulating effects by TCDD (10 nM)-treatment alone (2.5±0.7-fold; n = 3), as well as by LPS (1 µg/mL) alone (2.9±1.2-fold; n = 3).

In literature, *AHRR* was also reported to be inducible in human PBMCs by DL-congeners. In this regard, around 10 to 14-fold maximal *AHRR*-induction by TCDD (10 nM, 48 h) was yielded on average in these cells (Van Ede *et al.*, 2014b).

Differentially regulated genes – *CYP1A2, ALDH3A1, CD36,* and *HSD17B2*

Response with respect to *CYP1A2* was minor and of low statistical relevance (TCDD+PHA-treatment, n = 3; individual 3 (m)). QRT-PCR-results varied greatly inter-individually, but exhibited a slight, but statistically significant *CYP1A2*-induction for treatment of PBMCs with TCDD+LPS (2.6±0.6-fold induction, p-value < 0.05; n = 3). *CYP1A2*-expression appeared to be detectable only sporadically and not in every individual-specific PBMC-sample.

On the basis of current information, CYP1A2 is also not inducible by AhR ligands *in vitro* in human blood cells (Baron *et al.*, 1998; Finnström *et al.*, 2002; Krovat *et al.* 2000, Siest *et al.*, 2008). In a study using NDL-PCBs, PCB 138 was shown to down-regulate transcription of *CYP1A2* in human PBMCs *in vitro* (Gosh *et al.*, 2001).

Besides, impact on ‘potential’ AhR-target genes, *ALDH3A1*, *CD36*, and *HSD17B2* was low and undirected with respect to both the human whole genome microarray experiment and qRT-PCR examinations.

TCDD's potential impact on PBMCs with respect to immune response

In order to gain a better understanding in terms of TCDD's potential mode(s) of action towards cells of the immune system, differentially regulated genes revealed by human whole genome microarray analysis were examined with respect to identification of probable relevant genes in this regard. The search of these potentially relevant genes proved to be difficult due to the limited amount of genes differentially regulated genes, which in addition clustered marginally among each other.

TCDD-treatment – Chemokines

Viewing results obtained by TCDD-treatment of human PBMCs without any stimulus, several genes encoding chemokines were differentially regulated. One was up-regulated (*CCL1*), whereas four members (C*XCL10*, *CCL18*, *CCL19*, and *CCL23*) were down-regulated. Hence, chemotaxis might be affected directing to inhibition with respect to T lymphocytes (C*XCL10*, *CCL18*, *CCL19*, and *CCL23*), B lymphocytes (*CCL19*), and neutrophils (*CCL23*). Regarding TCDD's properties towards monocytes, evidence was provided respecting both enhancing (*CCL1*) as well as inhibitory effects (*XCL10*, *CCL23*) (Binns *et al.*, 2009; Dimmer *et al.*, 2012).

CCL1 was reported to be up-regulated by PCB 126 (1 µM, 18 h) in human PBMCs in the course of microarray experiments, whereas C*XCL10* was observed to be down-regulated (Wens *et al.*, 2011; Wens *et al.*, 2013).

TCDD-treatment – T cell lineage specification

Further indications respecting TCDD's inhibitory impact on immune response might include Th1-specific immune responses and response of CTLs (*IFNG*↓), humoral immune response (*FCGR1B*↓), and macrophage activation as well as response of monocytes (*CD163*↓). One up-regulated gene might indicate a role of TCDD on signaling via a phosphatidylinositol-calcium second messenger system (*GCGR*↑) (Binns *et al.*, 2009; Dimmer *et al.*, 2012).

Regarding minor effects on several cytokines and other relevant proteins implicated in T cell lineage specification, *IL2*, and *IL18* slightly tended to be down-regulated, whereas *IL5*-mRNA was slightly elevated by TCDD. Similarly to IFN-γ, IL18 as 'IFN-γ inducing factor' plays an important role in Th1 response, primarily due to its IFN-γ inducing ability (Dinarello, 1999). Increased *IL5* on the other side might potentially reflect a facilitated Th2-response, whereas down-regulated *IL2* might indicate a slight repression of Treg differentiation (Jetten, 2009).

By tendency, *TDO2* was slightly up-regulated by TCDD in human PBMCs. TDO catabolizes L-tryptophan (Trp) to L-kynurenine (Kyn), which itself was shown to represent an AhR-ligand and has been correlated with AhR-dependent antitumor immune responses. Elevated Kyn-concentrations might further give an indication directing to a slightly facilitated Treg differentiation by TCDD (Nguyen *et al.*, 2010; Mezrich *et al.*, 2010, Opitz *et al.*, 2011).

In literature, several diverging findings are found in correlation to TCDD's potential effects towards T cell lineage specification. On the one hand side, Th1-differentiation was proposed to be facilitated by TCDD (Fujimaki *et al.*, 2002; Negishi *et al.*, 2005), whereas on the other hand side, data on TCDD-impacted IFN-γ secretion is controversial. IFN-γ secretion was found to be up-regulated in several studies (Fujimaki *et al.*, 2002; Jeong *et al.*, 2012; Negishi *et al.*, 2005; Vorderstrasse and Kerkvliet, 2001), as well as down-regulated (Prell *et al.*, 2000; Quintana *et al.*, 2008; Quintana *et al.*, 2010), whereby the latter might correlate with the further observed hyporesponsiveness of CTLs (De Krey and Kerkvliet, 1995; Prell *et al.*, 2000).

TCDD-treatment – 'Immunosuppressive effects'?!

A further potentially repressed immune reaction responding to TCDD-treatment could implicate macrophage activation and response of monocytes (*CD163*↓).

CD163 is an acute phase-regulated receptor involved in clearance and endocytosis of hemoglobin/haptoglobin complexes as well as in scavenging of components of damaged cells. Thus, CD163 is implicated in protection of tissues from free hemoglobin-mediated oxidative damage, for instance. The receptor was discussed to play an anti-inflammatory role correlated with macrophage activation and response of monocytes (Binns *et al.*, 2009; Buechler *et al.*, 2000; Moestrup and Møller, 2004). In an Agilent whole genome microarray experiment, *CD163* was as well reported to be down-regulated by TCDD (10 µM, 20 h; human liver S9-mix) in human PBMCs (Hochstenbach *et al.*, 2010).

Taken together, proposed immune responses mediated by TCDD 'alone' in human PBMCs might involve repressed Th1-responses, slightly facilitated Th2-response, controversial findings with respect to Th17/Treg-differentiation, and inhibited response of monocytes/macrophages. Chemotaxis is suggested to be affected directing towards inhibition with respect to T lymphocytes (C*XCL10*, *CCL18*, *CCL19*, and *CCL23*), B lymphocytes (*CCL19*), and neutrophils (*CCL23*).

TCDD+LPS-treatment – Chemokines

Regarding treatment of PBMCs with TCDD together with LPS, the majority of differentially regulated genes tended to be down-regulated. Besides four chemokines, which were as well inhibited by TCDD alone (C*XCL10*, *CCL18*, *CCL19*, and *CCL23*), *CCL8* was down-regulated in addition. Altogether, down-regulation of these chemokines might indicate inhibited chemotactic properties towards T lymphocytes (*CCL8*, C*XCL10*, *CCL18*, *CCL19*, and *CCL23*), B lymphocytes (*CCL19*), monocytes (*CCL8*, *CCL23*), neutrophils (*CCL23*), as well as basophils and eosinophils (*CCL8*) (Binns *et al.*, 2009; Dimmer *et al.*, 2012).

TCDD+LPS-treatment – T cell lineage specification / 'Immunosuppressive effects'?!

Potentially repressed immune reactions responding to TCDD+LPS-treatment could implicate type 1 immunity (*SPP1*↓), humoral immune response (*FCGR1B*↓), macrophage activation and response of monocytes (*CD163*↓) (Binns *et al.*, 2009; Buechler *et al.*, 2000; Dimmer *et al.*, 2012; Moestrup and Møller, 2004).

SPP1 encodes the protein osteopontin, which acts as a cytokine and participates in the enhanced production of IFN-γ and IL-12, as well as in the reduction of IL-10 production, appears to be essential in the pathway leading to type 1 immunity (Binns *et al.*, 2009; Dimmer *et al.*, 2012).

SPP1 as well as *CD163* (aforementioned with respect to impact by TCDD 'alone'), were as well down-regulated in another whole genome microarray experiment using human PBMCs incubated with TCDD (10 µM, 20 h, human liver S9-mix) (Hochstenbach *et al.*, 2010).

One further accordingly regulated gene within this study was thrombospondin 1 (*THBS1*). This gene was up-regulated and encodes an inhibitor of angiogenesis (TSP-1), which is able to limit vessel density in normal tissues and to reduce tumor growth. TSP-1 is induced at sites of tissue damage, where it co-occurs with endoplasmatic reticulum (ER) stress response. TSP-1 was shown to augment and protect ER function, by which protein production and resolution of misfolded proteins is regulated in case of ER stress response (Lynch *et al.*, 2012; Murphy-Ullrich and Poczatek, 2000).

Inhibited *IFNG*-transcription as well as associated slight indication of repressed *IL18*-expression reflected findings for the TCDD-treatment described above. The further hint of an induced transcription of *IL12*, proposed facilitated Th1-response, as it was obtained elsewhere (Fujimaki *et al.*, 2002; Negishi *et al.*, 2005). Contrary regarding Th1-response by TCDD+LPS was an indication given due to down-regulation of *SSP1*, which more hinted towards inhibited Th1-response.

TCDD+PHA-treatment – numbers of affected genes and apoptosis

Compared to the TCDD-, and the TCDD+LPS-treatment, results differed from those obtained for TCDD+PHA starting with greater statistical significance and higher numbers of genes differentially regulated (32↑ 12↓).

Among these genes, several were involved in apoptotic mechanisms (*CABLES1*↑, *NPTX1*↑, *SERPINB2*↑, and *NKD2*↑). *NKD2* represents an inducible Wnt/β-catenin signaling pathway antagonist. Aberrations of Wnt/β-catenin signals are often correlated with overexpression of the *c-myc* oncogene, which might suggest a role of TCDD with respect to *c-myc* expression (You *et al.*, 2002; Zeng *et al.*, 2000; Zhang *et al.*, 2012). *C-myc* was not regulated along with the PBMC microarray experiment in hand.

TCDD+PHA-treatment – Chemokines

Two genes encoding chemokines were up-regulated in response to TCDD+PHA-treatment: Up-regulated *CCL2* might hint directing to facilitated chemotaxis towards monocytes and basophiles, and towards neutrophil granulocytes regarding *CXL6*. By contrast, down-regulated chemokines gave indications with respect to inhibited chemotactic properties towards T lymphocytes (*CCL18*, *CCL19*, and *CCL23*), B lymphocytes (*CCL19*), as well as monocytes and neutrophils (*CCL23*) (Binns *et al.*, 2009; Dimmer *et al.*, 2012).

TCDD+PHA-treatment – T cell lineage specification / 'Immunosuppressive effects'?!

Further impact indicated TCDD-mediated inhibitory effects on Th1-specific immune responses and correlated response of CTLs (*IFNG*↓), and B cell activation and proliferation (*MS4A4A*↓, *CD38*↓). Implicated in altered glucose-dependent immune homeostasis were *NPTX1*(↑), *HTRA1*(↑), and *CD38*(↓), whereas up-regulated *P2RY6* might reflect an involvement in a phosphatidyinositol-calcium second messenger system (Binns *et al.*, 2009; Dimmer *et al.*, 2012).

With respect to cytokines involved in T cell lineage specification, besides aforementioned *IFNG*, *IL2*, *IL4*, *IL6*, *IL18*, and *IL21* tended to be down-regulated by TCDD+PHA. One of these findings theoretically might reflect and inhibitory effect of TCDD on Th2-response regarding reduced *IL4*, as it was shown in literature before in murine spleen cells (Fujimaki *et al.*, 2002).

Besides, Th1-, and CTL-response tended to be inhibited (*IFNG*, *IL18*), as seen in immune cells with TCDD before regarding *IFNG* (Dinarello, 1999; Prell *et al.*, 2000; Quintana *et al.*, 2008; Quintana *et al.*, 2010), and hyporesponsiveness of CTLs (De Krey and Kerkvliet, 1995; Prell *et al.*, 2000).

Controversial findings were obtained regarding Th17/Treg differentiation – down-regulated *IL2* would imply repressed Treg-differentiation, whereas *IL6*, and *IL21* might reflect repressed Th17-differentiation (Jetten, 2009). In mice, Treg-differentiation was proposed to be augmented by TCDD, whereas Th17-differentation was shown to be inhibited by the congener (Nguyen *et al.*, 2010; Quintana *et al.*, 2008).

By tendency, *TDO2* was up-regulated by TCDD+PHA-treatment as discussed by means of the TCDD-treatment in the beginning of this chapter. Up-regulated *TDO2* could indicate lightly facilitated Treg-differentiation, as revealed before (Nguyen *et al.*, 2010; Mezrich *et al.*, 2010), wherease TDO-generated Kyn was correlated with AhR-dependent antitumor immune responses (Opitz *et al.*, 2011).

Considering discussed data on treatment of human PBMCs with TCDD ‘alone’, with TCDD+LPS, or with TCDD+PHA, one needs to keep in mind that the statistical relevance of data was overall limited and inter-individual differences were great along with the experiment. Discussed indications represent suggested potential directions regarding TCDD-mediated impact on immune cells.

6

Conclusions

‚Dioxin-like' compounds represent a group of chemicals which are known to exert most, if not all, of their biological and toxic effects by activation of the AhR. With respect to the TEF-concept, properties of these congeners are defined by their interaction with the AhR. Thus, potentially relevant substance-specific attributes might be disregarded.

With respect to the mouse whole genome microarray experiment, impact of DL-congeners on gene expression in mouse livers was primarily and with strongest significance correlated with enhanced xenobiotic metabolic processes. Followed by alterations towards lipid-, and carbohydrate metabolism, further implicated mechanisms were oxidative processes, apoptosis, and immune response to a lowered extent.
Whereas 1-PeCDD's impact on gene expression in mouse livers correlated most prominently with TCDD-mediated effects, overlap between TCDD and the remaining DL-congeners was limited. Regarding all DL-compounds together, a small, conserved list of differentially regulated genes was observed. This list primarily was constituted of genes involved in xenobiotic metabolism.

Some of the congeners involved in mouse microarray investigations, namely PCB 126, PCB 156, and 4-PeCDF, revealed great impact on gene expression in mouse livers by differentially regulating an enormous number of up to 3000 (↑↓) affected genes, which might be due to a high-dose effect. Still, since overlap among DL-congeners remained limited, unresolved issue represents the role of AhR-independent genes. As, for instance, the overlap between TCDD and PCB 118 was low, three quarters of the amount of PCB 118-impacted genes did not correlate with TCDD's, thus appeared to be AhR-independent but likewise of not specified 'source'.

Reflecting investigations using human PBMCs including results of the human whole genome microarray experiment and qRT-PCR investigations, identification of TCDD-mediated impact was intricate. Excepting impact on known AhR-targets - CYP1A1, CYP1B1, TIPARP, and AHRR - minor effects accompanied by distinct inter-individual differences were observed. Slight, but not clearly directed immunomodulatory impact of TCDD was indicated.

With respect to establishment of potential biomarkers, the search of genes, which would be differentially regulated in both animal experiments as well as in *in vitro* investigations using human primary cells, would be of peculiar interest.

Thus, regulated genes from the human PBMC-experiment were looked up in mouse whole genome microarray data and checked on their regulation in response to treatment with DL-congeners. The overlap was restricted to members of the AhR-gene batterie, namely CYP1A1, CYP1B1, and TIPARP.

Taking these three representatives to compare them with results obtained by gene expression analysis with rat liver cells, only CYP1A1, and CYP1B1 remained to be reliably significant. Accordingly, liver cell systems analyzed in terms of CYP1A-induction, as it was applied in the course of this study, still give relevant indications of ‘dioxin-like’ impact of a chemical, even though investigations using human primary hepatocytes tend to gain in importance.

References

Abraham, K., Hille, A., Ende, M., and Helge, H. (1994). Intake and fecal excretion of PCDDs, PCDFs, HCB and PCBs (138, 153, 180) in a breast-fed and a formula-fed infant. *Chemosphere*, **29** (9), 2279-86.

Abraham, K., Knoll, A., Ende, M., Päpke, O., and Helge, H. (1996). Intake, fecal excretion, and body burden of polychlorinated dibenzo-*p*-dioxins and dibenzofurans in breast-fed and formula-fed infants. *Pediatr Res*, **40** (5), 671-9.

Abraham, K., Krowke, R., and Neubert, D. (1988). Pharmacokinetics and biological activity of 2,3,7,8-tetrachlorodibenzo-*p*-dioxin. *Arch Toxicol*, **62** (5), 359-68. Agency for Toxic Substances and Disease Registry, Division of Toxicology and Environmental Medicine, Atlanta, GA 30333.

Ahlborg, U. G., Becking, G. C., Birnbaum, L. S., Brouwer, A. A., Derks, H. J. G. M., Feeley, M., Golor, G., Hanberg, A., Larsen, J. C., Liem, A. K. D., Safe, S. H., Schlatter, C., Waem, F., Younes, M., and Yrjänheikki, E. (1994). Toxic equivalency factors for dioxin-like PCBs: Report on WHO-ECEH and IPCS consultation, December 1993. *Chemosphere*, **28** (6), 1049-67.

Ahmad, K., and Henikoff, S. (2002). The histone variant H3.3 marks active chromatin by replication-independent nucleosome assembly. *Mol Cell*, **9** (6), 1191-200.

Akira, S., Takeda, K., and Kaisho, T. (2001). Toll-like receptors: critical proteins linking innate and acquired immunity. *Nat Immunol*, **2** (8), 675-80.

Alexa, A., Rahnenführer, J., and Lengauer, T. (2006). Improved scoring of functional groups from gene expression data by decorrelating GO graph structure. *Bioinformatics*, **22** (13), 1600-7.

Alexander, D. L., Ganem, L. G., Fernandez-Salguero, P., Gonzalez, F., and Jefcoate, C. R. (1998). Aryl-hydrocarbon receptor is an inhibitory regulator of lipid synthesis and of commitment to adipogenesis. *J Cell Sci*, **111** (22), 3311-22.

Alhouayek, M., Masquelier, J., Cani, P. D., Lambert, D. M., and Muccioli, G. G. (2013). Implication of the anti-inflammatory bioactive lipid prostaglandin D2-glycerol ester in the control of macrophage activation and inflammation by ABHD6. *Proc Natl Acad Sci USA*, **110** (43), 17558-63.

Alison, M., Chaudry, Z., Baker, J., Lauder, I., and Pringle, H. (1994). Liver regeneration: a comparison of in situ hybridization for histone mRNA with bromodeoxyuridine labeling for the detection of S-phase cells. *J Histochem Cytochem*, **42** (12), 1603-8.

Allan, D., and Michell, R. H. (1974). Phosphatidylinositol cleavage in lymphocytes. Requirement for calcium ions at a low concentration and effects of other cations. *Biochem. J*, **142**, 599-604.

Al-Salman, F., and Plant, N. (2012). Non-coplanar polychlorinated biphenyls (PCBs) are direct agonists for the human pregnane-X receptor and constitutive androstane receptor, and activate target gene expression in a tissue-specific manner. *Toxicol Appl Pharmacol*, **263** (1), 7-13.

Amacher, D. E., Adler, R., Herath, A., and Townsend, R. R. (2005). Use of proteomic methods to identify serum biomarkers associated with rat liver toxicity or hypertrophy. *Clin Chem*, **51** (10), 1796-803.

Andersson, H., Garscha, U., and Brittebo, E. (2011). Effects of PCB126 and 17β-oestradiol on endothelium-derived vasoactive factors in human endothelial cells. *Toxicology*, **285** (1-2), 46-56.

Anzenbacher, P., and Anzenbacherova, E. (2001). Cytochromes P450 and metabolism of xenobiotics. *Cell Mol Life Sci*, **58** (5-6), 737-47.

Arulmozhiraja, S., and Morita, M. (2004). Structure-activity relationships for the toxicity of polychlorinated dibenzofurans: approach through density functional theory-based descriptors. *Chem Res Toxicol*, **17** (3), 348-56.

Ashburner, M., Ball, C. A., Blake, J. A., Botstein, D., Butler, H., Cherry, J. M., Davis AP, Dolinski K, Dwight SS, Eppig JT, Harris MA, Hill DP, Issel-Tarver L, Kasarskis A, Lewis S, Matese JC, Richardson JE, Ringwald M, Rubin GM, and Sherlock, G. (2000). Gene Ontology: tool for the unification of biology. *Nature genetics*, **25** (1), 25-29.

ATSDR (2012). Addendum to the Toxicological Profile for Chlorinated Dibenzo-*p*-dioxins (CDDs). Supplement to the 1998 Toxicological Profile for Chlorinated Dibenzo-*p*-Dioxins (CDDs).

Aylward, L. L., Brunet, R. C., Starr, T. B., Carrier, G., Delzell, E., Cheng, H., and Beall, C. (2005). Exposure Reconstruction for the TCDD‐Exposed NIOSH Cohort Using a Concentration‐and Age‐Dependent Model of Elimination. *Risk Anal*, **25** (4), 945-56.

Baars, A. J., Bakker, M. I., Baumann, R. A., Boon, P. E., Freijer, J. I., Hoogenboom, L. A. P., Hoogerbrugge, R., van Klaveren, J. D., Liem, A.K., Traag, W. A., and De Vries, J. (2004). Dioxins, dioxin-like PCBs and non-dioxin-like PCBs

in foodstuffs: occurrence and dietary intake in The Netherlands. *Toxicol Lett*, **151** (1), 51-61.

Baba, T., Mimura, J., Gradin, K., Kuroiwa, A., Watanabe, T., Matsuda, Y., Inazawa, J., Sogawa, K., and Fujii-Kuriyama, Y. (2001). Structure and expression of the Ah receptor repressor gene. *J Biol Chem*, **276** (35), 33101-10.

Baba, T., Mimura, J., Nakamura, N., Harada, N., Yamamoto, M., Morohashi, K. I., and Fujii-Kuriyama, Y. (2005). Intrinsic function of the aryl hydrocarbon (dioxin) receptor as a key factor in female reproduction. *Mol Cell Biol*, **25** (22), 10040-51.

Baban, B., Chandler, P. R., Sharma, M. D., Pihkala, J., Koni, P. A., Munn, D. H., and Mellor, A. L. (2009). IDO activates regulatory T cells and blocks their conversion into Th17-like T cells. *J Immunol*, **183** (4), 2475-2483.

Baccarelli, A., Giacomini, S. M., Corbetta, C., Landi, M. T., Bonzini, M., Consonni, D., Grillo, P., Patterson, D. G. Jr., Pesatori, A. C., and Bertazzi, P. A. (2008). Neonatal thyroid function in Seveso 25 years after maternal exposure to dioxin. *PLoS Med*, **5** (7), e161.

Baccarelli, A., Mocarelli, P., Patterson Jr, D. G., Bonzini, M., Pesatori, A. C., Caporaso, N., and Landi, M. T. (2002). Immunologic effects of dioxin: new results from Seveso and comparison with other studies. *Environ Health Perspect*, **110** (12), 1169-73.

Backlund, M., and Ingelman-Sundberg, M. (2004). Different structural requirements of the ligand binding domain of the aryl hydrocarbon receptor for high-and low-affinity ligand binding and receptor activation. *Mol Pharmacol*, **65** (2), 416-25.

Bacsi, S. G., Reisz-Porszasz, S., and Hankinson, O. (1995). Orientation of the heterodimeric aryl hydrocarbon (dioxin) receptor complex on its asymmetric DNA recognition sequence. *Mol Pharmacol*, **47** (3), 432-8.

Baker, A., Payne, C. M., Briehl, M. M., and Powis, G. (1997). Thioredoxin, a gene found overexpressed in human cancer, inhibits apoptosis *in vitro* and *in vivo*. *Cancer Res*, **57** (22), 5162-7.

Bandiera, S., Sawyer, T., Campbell, M. A., Robertson, L., and Safe, S. (1982). Halogenated biphenyls as AHH inducers: effects of different halogen substituents. *Life Sci*, **31** (6), 517-25.

Bandiera, S., Sawyer, T., Romkes, M., Zmudzka, B., Safe, L., Mason, G., Keys, B., and Safe, S. (1984). Polychlorinated dibenzofurans (PCDFs): Effects of structure on binding to the 2,3,7,8-TCDD cytosolic receptor protein, AHH induction and toxicity. *Toxicology*, **32** (2), 131-44.

Baron, J. M., Zwadlo-Klarwasser, G., Jugert, F., Hamann, W., Rübben, A., Mukhtar, H., and Merk, H. F. (1998). Cytochrome P450 1B1: a major P450 isoenzyme in human blood monocytes and macrophage subsets. *Biochem Pharmacol*, **56** (9), 1105-10.

Bates, G. J., Nicol, S. M., Wilson, B. J., Jacobs, A. M. F., Bourdon, J. C., Wardrop, J., Gregory, D. J., Lane, D. P., Perkins, N. D., and Fuller−Pace, F. V. (2005). The DEAD box protein p68: a novel transcriptional coactivator of the p53 tumour suppressor. *EMBO J*, *24*(3), 543-53.

Bauer, T. M., Jiga, L. P., Chuang, J. J., Randazzo, M., Opelz, G., and Terness, P. (2005). Studying the immunosuppressive role of indoleamine 2,3-dioxygenase: tryptophan metabolites suppress rat allogeneic T-cell responses in vitro and in vivo. *Transpl Int*, **18** (1), 95-100.

Becher, H., Flesch-Janys, D., Kauppinen, T., Kogevinas, M., Steindorf, K., Manz, A., and Wahrendorf, J. (1996). Cancer mortality in German male workers exposed to phenoxy herbicides and dioxins. *Cancer Cause Control*, **7** (3), 312-21.

Benjamini, Y., and Hochberg, Y. (1995). Controlling the false discovery rate: a practical and powerful approach to multiple testing. *J R Stat Soc Series B Stat Methodol*, **57**, 289-300.

Berggren, M. I., Husbeck, B., Samulitis, B., Baker, A. F., Gallegos, A., and Powis, G. (2001). Thioredoxin peroxidase-1 (peroxiredoxin-1) is increased in thioredoxin-1 transfected cells and results in enhanced protection against apoptosis caused by hydrogen peroxide but not by other agents including dexamethasone, etoposide, and doxorubicin. *Arch Biochem Biophys*, **392** (1), 103-9.

Bertazzi, P. A., Bernucci, I., Brambilla, G., Consonni, D., and Pesatori, A. C. (1998). The Seveso studies on early and long-term effects of dioxin exposure: a review. *Environ Health Perspect*, **106** (2), 625-33.

Bertazzi, P. A., Consonni, D., Bachetti, S., Rubagotti, M., Baccarelli, A., Zocchetti, C., and Pesatori, A. C. (2001). Health effects of dioxin exposure: a 20-year mortality study. *Am J Epidemiol*, **153** (11), 1031-44.

Bertazzi, P.A, Pesatori, AC. and Landi, M.T. (1996) Cancer mortality, 1976-1991, in the population exposed to 2,3,7,8-tetrachlorodibenzo-p-dioxin. *Organohalogen compounds*, **30**, 294-6.

Bertazzi, P.A, Pesatori, AC., Consonni, D., Tironi, A., Landi, M.T. and Zocchetti, C. (1993). Cancer incidence in a population accidentaly exposed to 2,3,7,8-tetrachlorodibenzo-paradioxin. *Epidemiology*, **4**, 398-406.

Bertos, N. R., Wang, A. H., and Yang, X. J. (2001). Class II histone deacetylases: structure, function, and regulation. *Biochem Cell Biol*, **79** (3), 243-252.

Bessede, A., Gargaro, M., Pallotta, M. T., Matino, D., Servillo, G., Brunacci, C., Bicciato, S., Mazza, E. M., Macchiarulo, A., Vacca, C., Iannitti, R., Tissi, L., Volpi, C., Belladonna, M. L., Orabona, C., Bianchi, R., Lanz, T. V., Platten, M., Della Fazia, M. A., Piobbico, D., Zelante, T., Funakoshi, H., Nakamura, T., Gilot, D., Denison, M. S., Guillemin, G. J., DuHadawy, J. B., Prendergast, G. C., Metz, R., Geffard, M., Boon, L., Pirro, M., Iorio, A., Veyret, B., Romani, L., Grohmann, U., Fallarino, F., and Puccetti, P. (2014). Aryl hydrocarbon receptor control of a disease tolerance defence pathway. *Nature*, **511** (7508), 184-90.

BFR (2010). Aufnahme von Umweltkontaminanten über Lebensmittel (Cadmium, Blei, Quecksilber, Dioxine und PCB). Ergebnisse des Forschungsprojektes LexUKon. Bundesinstitut für Risikobewertung. 1-60.

Bhusari, S. (2006). *Effects of fescue toxicosis and chronic heat stress on murine hepatic gene expression* (Doctoral dissertation, University of Missouri).

Bigelow, S. W., and Nebert, D. W. (1982). The Ah regulatory gene product. Survey of nineteen polycyclic aromatic compounds' and fifteen benzo[a]pyrene metabolites' capacity to bind to the cytosolic receptor. *Toxicol Lett*, **10** (1), 109-18.

Binns, D., Dimmer, E., Huntley, R., Barrell, D., O'Donovan, C., and Apweiler, R. (2009). QuickGO: a web-based tool for Gene Ontology searching. *Bioinformatics*, 25(22), 3045-6.

Birnbaum, L. S. (1994). The mechanism of dioxin toxicity: relationship to risk assessment. *Environ Health Perspect*, **102** (Suppl 9), 157-67.

Bjeldanes, L. F., Kim, J. Y., Grose, K. R., Bartholomew, J. C., and Bradfield, C. A. (1991). Aromatic hydrocarbon responsiveness-receptor agonists generated from indole-3-carbinol in vitro and in vivo: comparisons with 2,3,7,8-tetrachlorodibenzo-*p*-dioxin. *Proc Natl Acad Sci U S A*, **88** (21), 9543-7.

Boers, D., Portengen, L., Bueno-de-Mesquita, H. B., Heederik, D., and Vermeulen, R. (2010). Cause-specific mortality of Dutch chlorophenoxy herbicide manufacturing workers. *Occup Environ Med*, **67** (1), 24-31.

Bøyum, A. (1964). Separation of white blood cells. *Nature* **204**, 793-4.

Breivik, K., Sweetman, A., Pacyna, J. M., and Jones, K. C. (2002). Towards a global historical emission inventory for selected PCB congeners—a mass balance approach: 1. Global production and consumption. *Sci Total Environ*, **290** (1), 181-98.

Budinsky, R. A., LeCluyse, E. L., Ferguson, S. S., Rowlands, J. C., and Simon, T. (2010). Human and rat primary hepatocyte CYP1A1 and 1A2 induction with 2,3,7,8-tetrachlorodibenzo-*p*-dioxin, 2,3,7,8-tetrachlorodibenzofuran, and 2,3,4,7,8-pentachlorodibenzofuran. *Toxicol Sci*, **118** (1), 224-35.

Budinsky, R. A., Rowlands, J. C., Casteel, S., Fent, G., Cushing, C. A., Newsted, J., Giesy, J. P., Ruby, M. V., and Aylward, L. L. (2008). A pilot study of oral bioavailability of dioxins and furans from contaminated soils: Impact of differential hepatic enzyme activity and species differences. *Chemosphere*, **70** (10), 1774-86.

Buechler, C., Ritter, M., Orsó, E., Langmann, T., Klucken, J., and Schmitz, G. (2000). Regulation of scavenger receptor CD163 expression in human monocytes and macrophages by pro-and antiinflammatory stimuli. *J Leukoc Biol*, **67** (1), 97-103.

Bumpus, N. N., and Johnson, E. F. (2011). 5-Aminoimidazole-4-carboxyamide-ribonucleoside (AICAR)-Stimulated Hepatic Expression of Cyp4a10, Cyp4a14, Cyp4a31, and Other Peroxisome Proliferator-Activated Receptor α-Responsive Mouse Genes Is AICAR 5′-Monophosphate-Dependent and AMP-Activated Protein Kinase-Independent. *J Pharmacol Exp Ther*, **339** (3), 886-95.

Burka, L. T., McGown, S. R., and Tomer, K. B. (1990). Identification of the biliary metabolites of 2,3,7,8-tetrachlorodibenzofuran in the rat. *Chemosphere*, **21** (10), 1231-42.

Burke, M. D., and Mayer, R. T. (1974). Ethoxyresorufin: direct fluorimetric assay of a microsomal O-dealkylation which is preferentially inducible by 3-methylcholanthrene. *Drug Metab Dispos*, **2** (6), 583-8.

Bustos, O., Naik, S., Ayers, G., Casola, C., Perez-Lamigueiro, M. A., Chippindale, P. T., Pritham E. J., and de la Casa-Esperón, E. (2009). Evolution of the *Schlafen* genes, a gene family associated with embryonic lethality, meiotic drive, immune processes and orthopoxvirus virulence. *Gene*, **447** (1), 1-11.

Campbell, J. S., Hughes, S. D., Gilbertson, D. G., Palmer, T. E., Holdren, M. S., Haran, A. C., Odell, M. M., Bauer, R. L., Ren, H. P., Haugen, H. S., Yeh, M. M., and Fausto, N. (2005). Platelet-derived growth factor C induces liver fibrosis, steatosis, and hepatocellular carcinoma. *Proc Natl Acad Sci USA*, **102** (9), 3389-94.

Caramaschi, F., Del Corno, G., Favaretti, C., Giambelluca, S. E., Montesarchio, E., and Fara, G. M. (1981). Chloracne

following environmental contamination by TCDD in Seveso, Italy. *Int J Epidemiol*, **10** (2), 135-43.

Carlson, E. A., McCulloch, C., Koganti, A., Goodwin, S. B., Sutter, T. R., & Silkworth, J. B. (2009). Divergent transcriptomic responses to aryl hydrocarbon receptor agonists between rat and human primary hepatocytes. *Toxicol Sci*, **112** (1), 257-72.

Carrier, G., Brunet, R. C., and Brodeur, J. (1995a). Modeling of the toxicokinetics of Polychlorinated Dibenzo-*p*-dioxins and Dibenzofurans in mammalians, including humans. II: Nonlinear distribution of PCDD/PCDF body burden between liver and adipose tissues. *Toxicol Appl Pharmacol*, **131** (2), 253-66.

Carrier, G., Brunet, R. C., and Brodeur, J. (1995b). Modeling of the toxicokinetics of Polychlorinated Dibenzo-*p*-dioxins and Dibenzofurans in mammalians, including humans. II: Kinetics of absorption and disposition of PCDD/sPCDFs. *Toxicol Appl Pharmacol*, **131** (2), 267-76.

Carver, L. A., and Bradfield, C. A. (1997). Ligand-dependent interaction of the aryl hydrocarbon receptor with a novel immunophilin homolog in vivo. *J Biol Chem*, **272** (17), 11452-6.

Carver, L. A., LaPres, J. J., Jain, S., Dunham, E. E., and Bradfield, C. A. (1998). Characterization of the Ah receptor-associated protein, ARA9. *J Biol Chem*, **273** (50), 33580-7.

Castilla, A., Prieto, J., and Fausto, N. (1991). Transforming growth factors beta 1 and alpha in chronic liver disease. Effects of interferon alfa therapy. *N Engl J Med*, **324** (14), 933-40.

Caulin, C., Ware, C. F., Magin, T. M., and Oshima, R. G. (2000). Keratin-dependent, epithelial resistance to tumor necrosis factor-induced apoptosis. *J Cell Biol*, **149** (1), 17-22.

Cella, M., Fuchs, A., Vermi, W., Facchetti, F., Otero, K., Lennerz, J. K., Doherty, J. M., Mills, J. C., and Colonna, M. (2009). A human natural killer cell subset provides an innate source of IL-22 for mucosal immunity. *Nature*, **457** (7230), 722-5.

Chae, H. Z., Chung, S. J., and Rhee, S. G. (1994a). Thioredoxin-dependent peroxide reductase from yeast. *J Biol Chem*, **269** (44), 27670-8.

Chae, H.Z., Robison, K., Poole, L.B., Church, G., Storz, G., and Rhee, S. G. (1994b). Cloning and sequencing of thiol-specific antioxidant from mammalian brain: alkyl hydroperoxide reductase and thiol-specific antioxidant define a large family of antioxidant enzymes. *Proc Nat Acad Sci USA*, **91** (15), 7017-21.

Chahin, A., Peiffer, J., Olry, J. C., Crepeaux, G., Schroeder, H., Rychen, G., and Guiavarc'h, Y. (2013). EROD activity induction in peripheral blood lymphocytes, liver and brain tissues of rats orally exposed to polycyclic aromatic hydrocarbons. *Food Chem Toxicol*, **56**, 371-80.

Chen, C. Y., Hamm, J. T., Hass, J. R., and Birnbaum, L. S. (2001). Disposition of Polychlorinated Dibenzo-*p*-dioxins, Dibenzofurans, and non-*ortho* Polychlorinated Biphenyls in Pregnant Long Evans Rats and the Transfer to Offspring. *Toxicol Appl Pharmacol*, **173** (2), 65-88.

Chien, W., and Pei, L. (2000). A novel binding factor facilitates nuclear translocation and transcriptional activation function of the pituitary tumor-transforming gene product. *J Biol Chem*, **275** (25), 19422-7.

Chitturi, S., and Farrell, G. C. (2001). Etiopathogenesis of nonalcoholic steatohepatitis. *Semin Liver Dis*, **21** (1), 27-41.

Chopra, M., Dharmarajan, A. M., Meiss, G., and Schrenk, D. (2009). Inhibition of UV-C Light–Induced Apoptosis in Liver Cells by 2,3,7,8-Tetrachlorodibenzo-*p*-Dioxin. *Toxicol Sci*, **111** (1), 49-63.

Chopra, M., Gährs, M., Haben, M., Michels, C., and Schrenk, D. (2010a). Inhibition of apoptosis by 2,3,7,8-tetrachlorodibenzo-p-dioxin depends on protein biosynthesis. *Cell Biol Toxicol*, **26** (4), 391-401.

Chopra, M., Link, P., Michels, C., and Schrenk, D. (2010b). Characterization of ochratoxin A-induced apoptosis in primary rat hepatocytes. *Cell Biol Toxicol*, **26** (3), 239-54.

Chou, M. Y., Chang, A. L., McBride, J., Donoff, B., Gallagher, G. T., and Wong, D. T. (1990). A rapid method to determine proliferation patterns of normal and malignant tissues by H3 mRNA in situ hybridization. *Am J Pathol*, **136** (4), 729-33.

Chuang, P. C., Wu, M. H., Shoji, Y., and Tsai, S. J. (2009). Downregulation of CD36 results in reduced phagocytic ability of peritoneal macrophages of women with endometriosis. *J Pathol*, **219** (2), 232-41.

Chung, S. I., Lewis, M. S., and Folk, J. E. (1974). Relationships of the catalytic properties of human plasma and platelet transglutaminases (activated blood coagulation factor XIII) to their subunit structures. *J Biol Chem*, **249** (3), 940-50.

Clayton, A. L., Hazzalin, C. A., and Mahadevan, L. C. (2006). Enhanced histone acetylation and transcription: a dynamic perspective. *Mol Cell*, **23** (3), 289-96.

Clifford, J. I., and Rees, K. R. (1967). The action of aflatoxin B1 on the rat liver. *Biochem J*, **102** (1), 65-75.

Colonna, M. (2009). Interleukin-22-producing natural killer cells and lymphoid tissue inducer-like cells in mucosal immunity. *Immunity*, **31** (1), 15-23.

Communi, D., Parmentier, M., and Boeynaems, J. M. (1996). Cloning, Functional Expression and Tissue Distribution of the Human P2Y6 Receptor. *Biochem Biophys Res Commun*, **222** (2), 303-8.

Consonni, D., Pesatori, A. C., Zocchetti, C., Sindaco, R., D'Oro, L. C., Rubagotti, M., and Bertazzi, P. A. (2008). Mortality in a population exposed to dioxin after the Seveso, Italy, accident in 1976: 25 years of follow-up. *Am J Epidemiol*, **167** (7), 847-58.

Cornu, M., Oppliger, W., Albert, V., Robitaille, A. M., Trapani, F., Quagliata, L., Fuhrer, T., Sauer, U., Terracciano, L., and Hall, M. N. (2014). Hepatic mTORC1 controls locomotor activity, body temperature, and lipid metabolism through FGF21. *Proc Natl Acad Sci USA*, **111** (32), 11592-9.

Coutavas, E. E., Hsieh, C. M., Ren, M., Drivas, G. T., Rush, M. G., and D'Eustachio, P. (1994). Tissue-specific expression of Ran isoforms in the mouse. *Mamm Genome*, **5** (10), 623-28.

Dalgaard, L. T., Thams, P., Gaarn, L. W., Jensen, J., Lee, Y. C., and Nielsen, J. H. (2011). Suppression of FAT/CD36 mRNA by human growth hormone in pancreatic β-cells. *Biochem Biophys Res Commun*, **410** (2), 345-50.

Dash, R., Su, Z. Z., Lee, S. G., Azab, B., Boukerche, H., Sarkar, D., and Fisher, P. B. (2010). Inhibition of AP-1 by SARI negatively regulates transformation progression mediated by CCN1. *Oncogene*, **29** (31), 4412-23.

Dawson, D. W., Pearce, S. F. A., Zhong, R., Silverstein, R. L., Frazier, W. A., and Bouck, N. P. (1997). CD36 mediates the in vitro inhibitory effects of thrombospondin-1 on endothelial cells. *J Cell Biol*, *138*(3), 707-17.

De Krey, G. K., and Kerkvliet, N. I. (1995). Suppression of cytotoxic T lymphocyte activity by 2,3,7,8-tetrachlorodibenzo-*p*-dioxin occurs in vivo, but not in vitro, and is independent of corticosterone elevation. *Toxicology*, **97** (1), 105-12.

De Montellano, P. R. O. (Ed.). (2005). Cytochrome P450: structure, mechanism, and biochemistry. Kluwer Academic/Plenum Publishers, New York, Springer.

De Mul, A., Bakker, M. I., Zeilmaker, M. J., Traag, W. A., van Leeuwen, S. P., Hoogenboom, R. L., Boon, P. E., and Klaveren, J. D. V. (2008). Dietary exposure to dioxins and dioxin-like PCBs in The Netherlands anno 2004. *Regul Toxicol Pharmacol*, **51** (3), 278-87.

De Saint-Vis, B., Vincent, J., Vandenabeele, S., Vanbervliet, B., Pin, J. J., Ait-Yahia, S., Patel S, Mattei MG, Banchereau J, Zurawski S, Davoust J, Caux C, and Lebecque, S. (1998). A novel lysosome-associated membrane glycoprotein, DC-LAMP, induced upon DC maturation, is transiently expressed in MHC class II compartment. *Immunity*, **9** (3), 325-36.

De Voogt, P., Wells, D. E., Reutergårdh, L., and Brinkman, U. A. T. (1990). Review: biological activity, determination and occurrence of planar, mono-and di-ortho PCBs. *Intern J Environ Anal Chem*, **40** (1-4), 1-46.

De Waard, P. W., Peijnenburg, A. A., Baykus, H., Aarts, J. M., Hoogenboom, R. L., van Schooten, F. J., and de Kok, T. M. (2008). A human intervention study with foods containing natural Ah-receptor agonists does not significantly show AhR-mediated effects as measured in blood cells and urine. *Chem Biol Interact*, **176** (1), 19-29.

DeCaprio, A. P., McMartin, D. N., O'Keefe, P. W., Rej, R., Silkworth, J. B., and Kaminsky, L. S. (1986). Subchronic oral toxicity of 2,3,7,8-tetrachlorodibenzo-*p*-dioxin in the guinea pig: Comparisons with a PCB-containing transformer fluid pyrolysate. *Fundam Appl Toxicol*, **6** (3), 454-63.

Denier van der Gon, H., van het Bolscher, M., Visschedijk, A., and Zandveld, P. (2007). Emissions of persistent organic pollutants and eight candidate POPs from UNECE–Europe in 2000, 2010 and 2020 and the emission reduction resulting from the implementation of the UNECE POP protocol. *Atmos Environ*, **41** (40), 9245-61.

Denison, M. S., Fisher, J. M., and Whitlock, J. P. (1988). The DNA recognition site for the dioxin-Ah receptor complex. Nucleotide sequence and functional analysis. *J Biol Chem*, **263** (33), 17221-4.

Denison, M. S., Pandini, A., Nagy, S. R., Baldwin, E. P., and Bonati, L. (2002). Ligand binding and activation of the Ah receptor. *Chem Biol Interact*, **141** (1), 3-24.

Denison, M. S., Phelan, D., Winter, G. M., and Ziccardi, M. H. (1998). Carbaryl, a carbamate insecticide, is a ligand for the hepatic Ah (dioxin) receptor. *Toxicol Appl Pharmacol*, **152** (2), 406-14.

Denison, M. S., Soshilov, A. A., He, G., DeGroot, D. E., and Zhao, B. (2011). Exactly the same but different: promiscuity and diversity in the molecular mechanisms of action of the aryl hydrocarbon (dioxin) receptor. *Toxicol Sci*, **124** (1), 1-22.

Dere, E., Lee, A. W., Burgoon, L. D., and Zacharewski, T. R. (2011). Differences in TCDD-elicited gene expression profiles in human HepG2, mouse Hepa1c1c7 and rat H4IIE hepatoma cells. *BMC Genomics*, **12** (1), 193.

DeVito, M. J., Ross, D. G., Dupuy, A. E., Ferrario, J., McDaniel, D., and Birnbaum, L. S. (1998). Dose–response relationships for disposition and hepatic sequestration of polyhalogenated dibenzo-p-dioxins, dibenzofurans, and biphenyls following subchronic treatment in mice. *Toxicol Sci*, **46** (2), 223-34.

Dey, A., Parmar, D., Dayal, M., Dhawan, A., and Seth, P. K. (2001). Cytochrome P450 1A1 (CYP1A1) in blood lymphocytes evidence for catalytic activity and mRNA expression. *Life Sci*, **69** (4), 383-93.

Diliberto, J. J., Akubue, P. I., Luebke, R. W., and Birnbaum, L. S. (1995). Dose-response relationships of tissue distribution and induction of CYP1A1 and CYP1A2 enzymatic activities following acute exposure to 2, 3, 7, 8-tetrachlorodibenzo-*p*-dioxin (TCDD) in mice. *Toxicol Appl Pharmacol*, **130** (2), 197-208.

Diliberto, J. J., Burgin, D. E., and Birnbaum, L. S. (1999). Effects of CYP1A2 on Disposition of 2,3,7,8-Tetrachlorodibenzo-*p*-dioxin, 2,3,4,7,8-Pentachlorodibenzofuran, and 2,2′,4,4′,5,5′-Hexachlorobiphenyl in CYP1A2 Knockout and Parental (C57BL/6N and 129/Sv) Strains of Mice. *Toxicol Appl Pharmacol*, ***159*** (1), 52-64.

Diliberto, J. J., Burgin, D., and Birnbaum, L. S. (1997). Role of CYP1A2 in hepatic sequestration of dioxin: studies using CYP1A2 knock-out mice. *Biochem Biophys Res Commun*, **236** (2), 431-3.

Diliberto, J. J., DeVito, M. J., Ross, D. G., and Birnbaum, L. S. (2001). Subchronic exposure of [3H]-2,3,7,8-tetrachlorodibenzo-p-dioxin (TCDD) in female B6C3F1 mice: relationship of steady-state levels to disposition and metabolism. *Toxicol Sci*, **61** (2), 241-55.

Dimmer, E. C., Huntley, R. P., Alam-Faruque, Y., Sawford, T., O'Donovan, C., Martin, M. J., Bely B., Browne P., Mun Chan W., Eberhardt R., Gardner M., Laiho K., Legge D., Magrane M., Pichler K., Poggioli D., Sehra H., Auchincloss A., Axelsen K., Blatter M. C., Boutet E., Braconi-Quintaje S., Breuza L., Bridge A., Coudert E., Estreicher A., Famiglietti L., Ferro-Rojas S., Feuermann M., Gos A., Gruaz-Gumowski N., Hinz U., Hulo C., James J., Jimenez S., Jungo F., Keller G., Lemercier P., Lieberherr D., Masson P., Moinat M., Pedruzzi I., Poux S., Rivoire C., Roechert B., Schneider M., Stutz A., Sundaram S., Tognolli M., Bougueleret L., Argoud-Puy G., Cusin I., Duek-Roggli P., Xenarios I., Apweiler R., and Bougueleret, L. (2012). The UniProt-GO annotation database in 2011. *Nucleic Acids Res*, 40 (D1), D565-70.

Dinarello, C. A. (1999). Interleukin-18. *Methods*, **19** (1), 121-32.

DiNatale, B. C., Murray, I. A., Schroeder, J. C., Flaveny, C. A., Lahoti, T. S., Laurenzana, E. M., Omiecinski, C. J., and Perdew, G. H. (2010). Kynurenic acid is a potent endogenous aryl hydrocarbon receptor ligand that synergistically induces interleukin-6 in the presence of inflammatory signaling. *Toxicol Sci*, **115** (1), 89-97.

Dörr, A. (2010). Beeinflussung der Ah-Rezeptorabhängigen CYP1A-Aktivität durch dioxinartige Verbindungen in der humanen Hepatomzelllinie HepG2. Diploma thesis, TU Kaiserslautern, Germany.

Dragan, Y. P., and Schrenk, D. (2000). Animal studies addressing the carcinogenicity of TCDD (or related compounds) with an emphasis on tumour promotion. *Food Addit Contam*, **17** (4), 289-302.

Duchez, S., Rodrigues, M., Bertrand, F., and Valitutti, S. (2011). Reciprocal polarization of T and B cells at the immunological synapse. *J Immunol*, **187** (9), 4571-80.

Egler, R. A., Fernandes, E., Rothermund, K., Sereika, S., de Souza-Pinto, N., Jaruga, P., Dizdaroglu, M., and Prochownik, E. V. (2005). Regulation of reactive oxygen species, DNA damage, and c-Myc function by peroxiredoxin 1. *Oncogene*, **24** (54), 8038-50.

Elsdale, T., and Bard, J. (1972). Collagen substrata for studies on cell behavior. *J Cell Biol*, **54** (3), 626-37.

Emond, C., Birnbaum, L. S., and DeVito, M. J. (2006). Use of a physiologically based pharmacokinetic model for rats to study the influence of body fat mass and induction of CYP1A2 on the pharmacokinetics of TCDD. *Environ Health Perspect*, 1394-400.

E-MTAB-599 – RNA-seq of mouse DBA/2J x C57BL/6J heart, hippocampus, liver, lung, spleen and thymus.
The ArrayExpress Archive of Functional Genomics Data.
Released on 04/09/2011.
http://www.ebi.ac.uk/arrayexpress/experiments/E-MTAB-599/. Accessed on 03/20/2013.

Eskenazi, B., Mocarelli, P., Warner, M., Samuels, S., Vercellini, P., Olive, D., Needham, L. L., Patterson, D. G., Brambilla, P., Gavoni, N., Casalini, S., Panazza, S., Turner, W., and Gerthoux, P. M. (2002). Serum dioxin concentrations and endometriosis: a cohort study in Seveso, Italy. *Environ Health Perspect*, **110** (7), 629-34.

Esser, C., Rannug, A., and Stockinger, B. (2009). The aryl hydrocarbon receptor in immunity. *Trends Immunol*, **30** (9), 447-54.

Evans, H. M., and Schulemann, W. (1914). The action of vital stains belonging to the benzidine group. *Science*, **39** (1004), 443-54.

Falahatpisheh, M. H., Nanez, A., and Ramos, K. S. (2011). AHR regulates WT1 genetic programming during murine nephrogenesis. *Mol Med*, **17** (11-12), 1275-84.

Fan, Y., Nikitina, T., Zhao, J., Fleury, T. J., Bhattacharyya, R., Bouhassira, E. E., Stein, A., Woodcock, C. L., and Skoultchi, A. I. (2005). Histone H1 depletion in mammals alters global chromatin structure but causes specific changes in gene regulation. *Cell*, **123** (7), 1199-1212.

Fattore, E., Fanelli, R., Turrini, A., and di Domenico, A. (2006). Current dietary exposure to polychlorodibenzo‐p‐dioxins, polychlorodibenzofurans, and dioxin‐like polychlorobiphenyls in Italy. *Mol Nutr Food Res*, **50** (10), 915-21.

Favreau, L. V., and Pickett, C. B. (1991). Transcriptional regulation of the rat NAD(P)H:quinone reductase gene. Identification of regulatory elements controlling basal level expression and inducible expression by planar aromatic compounds and phenolic antioxidants. *J Biol Chem*, **266** (7), 4556-61.

Fernandez-Salguero, P. M., Hilbert, D. M., Rudikoff, S., Ward, J. M., and Gonzalez, F. J. (1996). Aryl-hydrocarbon Receptor-Deficient Mice Are Resistant to 2,3,7,8-Tetrachlorodibenzo-*p*-dioxin-Induced Toxicity. *Toxicol Appl Pharmacol*, **140** (1), 173-9.

Fernandez-Salguero, P., Pineau, T., Hilbert, D. M., McPhail, T., Lee, S. S., Kimura, S., Nebert, D.W., Rudikoff, S., Ward, J. M., and Gonzalez, F. J. (1995). Immune system impairment and hepatic fibrosis in mice lacking the dioxin-binding Ah receptor. *Science*, **268** (5211), 722-6.

Fingerhut, M. A., Halperin, W. E., Marlow, D. A., Piacitelli, L. A., Honchar, P. A., Sweeney, M. H., Greife, A. L., Dill, P. A., Steenland, K., and Suruda, A. J. (1991). Cancer mortality in workers exposed to 2, 3, 7, 8-tetrachlorodibenzo-p-dioxin. *N Engl J Med*, **324** (4), 212-8.

Finnström, N., Ask, B., Dahl, M. L., Gadd, M., and Rane, A. (2002). Intra-individual variation and sex differences in gene expression of cytochromes P450 in circulating leukocytes. *Pharmacogenomics J*, **2** (2), 111-6.

Flach, C. F., Qadri, F., Bhuiyan, T. R., Alam, N. H., Jennische, E., Holmgren, J., and Lönnroth, I. (2007). Differential expression of intestinal membrane transporters in cholera patients. *FEBS Lett*, **581** (17), 3183-8.

Flaveny, C. A., Murray, I. A., Chiaro, C. R., and Perdew, G. H. (2009). Ligand selectivity and gene regulation by the human aryl hydrocarbon receptor in transgenic mice. *Mol Pharmacol*, **75** (6), 1412-20.

Floret, N., Mauny, F., Challier, B., Arveux, P., Cahn, J. Y., and Viel, J. F. (2003). Dioxin emissions from a solid waste incinerator and risk of non-Hodgkin lymphoma. *Epidemiology*, **14** (4), 392-8.

Frericks, M., Meissner, M., and Esser, C. (2007). Microarray analysis of the AHR system: tissue-specific flexibility in signal and target genes. *Toxicol Appl Pharmacol*, **220** (3), 320-2.

Frericks, M., Temchura, V. V., Majora, M., Stutte, S., and Esser, C. (2006). Transcriptional signatures of immune cells in aryl hydrocarbon receptor (AHR)-proficient and AHR-deficient mice. *Biol Chem*, **387** (9), 1219-26.

Fuhrmann, G. F.: Toxikologie für Naturwissenschaftler, 1. Auflage, B. G. Teubner Verlag / GWV Fachverlage GmbH, Wiesbaden 2006.

Fujigaki, H., Saito, K., Fujigaki, S., Takemura, M., Sudo, K., Ishiguro, H., and Seishima, M. (2006). The signal transducer and activator of transcription 1α and interferon regulatory factor 1 are not essential for the induction of indoleamine 2,3-dioxygenase by lipopolysaccharide: involvement of p38 mitogen-activated protein kinase and nuclear factor-κB pathways, and synergistic effect of several proinflammatory cytokines. *J Biochem*, **139** (4), 655-662.

Fujii-Kuriyama, Y., and Kawajiri, K. (2010). Molecular mechanisms of the physiological functions of the aryl hydrocarbon (dioxin) receptor, a multifunctional regulator that senses and responds to environmental stimuli. *Proc Jpn Acad Ser B Phys Biol Sci*, **86** (1), 40-53.

Fujimaki, H., Nohara, K., Kobayashi, T., Suzuki, K., Eguchi-Kasai, K., Tsukumo, S., Kijima, M., and Tohyama, C. (2002). Effect of a single oral dose of 2, 3, 7, 8-tetrachlorodibenzo-p-dioxin on immune function in male NC/Nga mice. *Toxicol Sci*, **66** (1), 117-24.

Fuller-Pace, F. V. (2013). The DEAD box proteins DDX5 (p68) and DDX17 (p72): multi-tasking transcriptional regulators. *Biochim Biophys Acta*, **1829** (8), 756-63.

Fung-Leung, W. P., Schilham, M. W., Rahemtulla, A., Kündig, T. M., Vollenweider, M., Potter, J., van Ewijk, W., and Mak, T. W. (1991). CD8 is needed for development of cytotoxic T but not helper T cells. *Cell*, **65** (3), 443-9.

Fung-Leung, W. P., Schilham, M. W., Rahemtulla, A., Kündig, T. M., Vollenweider, M., Potter, J., van Ewijk, W., and Mak, T. W. (1991). CD8 is needed for development of cytotoxic T but not helper T cells. *Cell*, *65*(3), 443-9.

Furihata, T., Hosokawa, M., Nakata, F., Satoh, T., and Chiba, K. (2003). Purification, molecular cloning, and functional expression of inducible liver acylcarnitine hydrolase in

C57BL/6 mouse, belonging to the carboxylesterase multigene family. *Arch biochem Biophys*, **416** (1), 101-9.

G4140-90050; protocol: Two-Color Microarray-Based Gene Expression Analysis, Low Input Quick Amp Labeling Kit; manual part number G4140-90050, version 6.5, May 2010; Agilent Technologies, Inc., Santa Clara, printed in USA.

Gährs, M., Roos, R., Andersson, P. L., and Schrenk, D. (2013). Role of the nuclear xenobiotic receptors CAR and PXR in induction of cytochromes P450 by non-dioxinlike polychlorinated biphenyls in cultured rat hepatocytes. *Toxicol Appl Pharmacol*, **272** (1), 77-85.

Garbe, C., Krasagakis, K., Zouboulis, C. C., Schröder, K., Krüger, S., Stadler, R., and Orfanos, C. E. (1990). Antitumor activities of interferon alpha, beta, and gamma and their combinations on human melanoma cells in vitro: changes of proliferation, melanin synthesis, and immunophenotype. *J Invest Dermatol*, **95**, 231S-7S.

Gasdaska, J. R., Berggren, M., and Powis, G. (1995). Cell growth stimulation by the redox protein thioredoxin occurs by a novel helper mechanism. *Cell Growth Differ*, **6** (12), 1643-50.

Gasiewicz, T. A., Geiger, L. E., Rucci, G., and Neal, R. A. (1983). Distribution, excretion, and metabolism of 2, 3, 7, 8-tetrachlorodibenzo-p-dioxin in C57BL/6J, DBA/2J, and B6D2F1/J mice. *Drug Metab Dispos*, **11** (5), 397-403.

Gentleman, R. C., Carey, V. J., Bates, D. M., Bolstad, B., Dettling, M., Dudoit, S., Ellis, B., Gautier, L., Ge, Y., Gentry, J., Hornik, K., Hothorn, T., Huber, W., Iacus, S., Irizarry, R., Leisch, F., Li, C., Maechler, M., Rossini, A.J., Sawitzki, G., Smith, C., Smyth, G., Tierney, L., Yang, J.Y., and Zhang, J. (2004). Bioconductor: open software development for computational biology and bioinformatics. *Genome Biol*, **5** (10), R80.

Geusau, A., Tschachler, E., Meixner, M., Päpke, O., Stingl, G., and McLachlan, M. (2001). Cutaneous elimination of 2,3,7,8-tetrachlorodibenzo-*p*-dioxin. *Br J Dermatol*, **145** (6), 938-43.

Ghosh, S., Zang, S., Mitra, P. S., Ghimbovschi, S., Hoffman, E. P., and Dutta, S. K. (2011). Global gene expression and Ingenuity biological functions analysis on PCBs 153 and 138 induced human PBMC *in vitro* reveals differential mode(s) of action in developing toxicities. *Environ Int*, **37** (5), 838-57.

Gibson, G. G., Orton, T. C., and Tamburini, P. P. (1982). Cytochrome P-450 induction by clofibrate. Purification and properties of a hepatic cytochrome P-450 relatively specific for the 12-and 11-hydroxylation of dodecanoic acid (lauric acid). *Biochem J*, **203** (1), 161-8.

Girolami, F., Spalenza, V., Carletti, M., Perona, G., Sacchi, P., Rasero, R., and Nebbia, C. (2011). Gene expression and inducibility of the aryl hydrocarbon receptor-dependent pathway in cultured bovine blood lymphocytes. *Toxicol Lett*, **206** (2), 204-9.

Glynn, D., Bortnick, R. A., and Morton, A. J. (2003). Complexin II is essential for normal neurological function in mice. *Hum Mol Genet*, **12** (19), 2431-48.

Goldsworthy, M., Absalom, N. L., Schröter, D., Matthews, H. C., Bogani, D., Moir, L., Long, A., Church, C., Hugill, A., Anstee, Q. M., Goldin, R., Thursz, M., Hollfelder, F., and Cox, R. D. (2013). Mutations in Mll2, an H3K4 methyltransferase, result in insulin resistance and impaired glucose tolerance in mice. *PloS One*, **8** (6), e61870.

Gonzalez, R. J., and Tarloff, J. B. (2001). Evaluation of hepatic subcellular fractions for Alamar blue and MTT reductase activity. *Toxicol In Vitro*, **15** (3), 257-9.

Green, M. R., Monti, S., Dalla-Favera, R., Pasqualucci, L., Walsh, N. C., Schmidt-Supprian, M., Kutok, J. L., Rodig, S. J., Neuberg, D. S., Rajewski, K., Golub,T. R., Alt, F. W., Shipp, M. A., and Manis, J. P. (2011). Signatures of murine B-cell development implicate Yy1 as a regulator of the germinal center-specific program. *Proc Natl Acad Sci USA*, **108** (7), 2873-8.

Grogan, T. M., Fenoglio-Prieser, C., Zeheb, R., Bellamy, W., Frutiger, Y., Vela, E., Stemmerman, G., Macdonald, J., Richter, L., Gallegos, A., and Powis, G. (2000). Thioredoxin, a putative oncogene product, is overexpressed in gastric carcinoma and associated with increased proliferation and increased cell survival. *Human Pathol*, **31** (4), 475-81.

Hake, S. B, and Allis, C. D. (2006). Histone H3 variants and their potential role in indexing mammalian genomes: the "H3 barcode hypothesis". *Proc Natl Acad Sci U S A*, **103** (17), 6428-35.

Hake, S. B., Garcia, B. A., Duncan, E. M., Kauer, M., Dellaire, G., Shabanowitz, J., Bazett-Jones, D. P., Allis, C. D., and Hunt, D. F. (2006). Expression patterns and post-translational modifications associated with mammalian histone H3 variants. *J Biol Chem*, **281** (1), 559-68.

Hakk, H., and Dilberto, J. J. (2002). Comparison of overall metabolism of 2,3,7,8-TCDD in CYP1A2 (-/-) knockout and C57BL/6N parental strains of mice. *Organohalogen compounds*, **55**, 461-4.

Hakk, H., and Dilberto, J. J. (2003). Comparison of overall metabolism of 1,2,3,7,8-PeCDD in CYP1A2 (-/-) knockout and C57BL/6N parental strains of mice. *Organohalogen compounds*, **64**, 293-6.

Hakk, H., Diliberto, J. J., and Birnbaum, L. S. (2009). The effect of dose on 2, 3, 7, 8-TCDD tissue distribution, metabolism and elimination in CYP1A2 (-/-) knockout and C57BL/6N parental strains of mice. *Toxicol Appl Pharmaco*, **241** (1), 119-26.

Hanieh, H. (2014). Toward Understanding the Role of Aryl Hydrocarbon Receptor in the Immune System: Current Progress and Future Trends. *Biomed Res Int*, **2014** (520763), 1-14.

Hankinson, O. (1995). The aryl hydrocarbon receptor complex. *Annu Rev Pharmacol Toxicol*, **35** (1), 307-40.

Hankinson, O. (2005). Role of coactivators in transcriptional activation by the aryl hydrocarbon receptor. *Arch Biochem Biophys*, **433** (2), 379-86.

Hardwick, J. P., Song, B. J., Huberman, E., and Gonzalez, F. J. (1987). Isolation, complementary DNA sequence, and regulation of rat hepatic lauric acid omega-hydroxylase (cytochrome P-450LA omega). Identification of a new cytochrome P-450 gene family. *J Biol Chem*, **262** (2), 801-10.

Harrad, S., Wang, Y., Sandaradura, S., and Leeds, A. (2003). Human dietary intake and excretion of dioxin-like compounds. *J Environ Monit*, **5** (2), 224-8.

Harris, M. W., Moore, J. A., Vos, J. G., and Gupta, B. N. (1973). General biological effects of TCDD in laboratory animals. *Environ Health Perspect*, **5**, 101-9.

Harris, M., Zacharewski, T., Piskorska-Pliszczynska, J., Rosengren, R., and Safe, S. (1990). Structure-dependent induction of aryl hydrocarbon hydroxylase activity in C57BL6 mice by 2, 3, 7, 8-tetrachlorodibenzo-*p*-dioxin and related congeners: Mechanistic studies. *Toxicol Appl Pharmacol*, **105** (2), 243-53.

Haws, L. C., Su, S. H., Harris, M., DeVito, M. J., Walker, N. J., Farland, W. H., Finley, B., and Birnbaum, L. S. (2006). Development of a refined database of mammalian relative potency estimates for dioxin-like compounds. *Toxicol Sci*, **89** (1), 4-30.

He, J., Lee, J. H., Febbraio, M., and Xie, W. (2011). The emerging roles of fatty acid translocase/CD36 and the aryl hydrocarbon receptor in fatty liver disease. *Exp Biol Med (Maywood)*, **236** (10), 1116-21.

Heath-Pagliuso, S., Rogers, W. J., Tullis, K., Seidel, S. D., Cenijn, P. H., Brouwer, A., & Denison, M. S. (1998). Activation of the Ah receptor by tryptophan and tryptophan metabolites. *Biochemistry*, **37** (33), 11508-15.

Heilier, J. F., Nackers, F., Verougstraete, V., Tonglet, R., Lison, D., and Donnez, J. (2005). Increased dioxin-like compounds in the serum of women with peritoneal endometriosis and deep endometriotic (adenomyotic) nodules. *Fertil Steril*, **84** (2), 305-12.

Heintz, N., Sive, H. L., and Roeder, R. G. (1983). Regulation of human histone gene expression: kinetics of accumulation and changes in the rate of synthesis and in the half-lives of individual histone mRNAs during the HeLa cell cycle. *Mol Cell Biol*, **3** (4), 539-50.

Hernández-Ochoa, I., Karman, B. N., and Flaws, J. A. (2009). The role of the aryl hydrocarbon receptor in the female reproductive system. *Biochem Pharmacol*, **77** (4), 547-59.

Heuser, M., Yap, D. B., Leung, M., de Algara, T. R., Tafech, A., McKinney, S., Dixon, J., Thresher, R., Colledge, B., Carlton, M., Humphris, R. K., and Aparicio, S. A. (2009). Loss of MLL5 results in pleiotropic hematopoietic defects, reduced neutrophil immune function, and extreme sensitivity to DNA demethylation. *Blood*, **113** (7), 1432-43.

Hochstenbach, K., van Leeuwen, D. M., Gmuender, H., Stølevik, S. B., Nygaard, U. C., Løvik, M., Granum, B., Namork, E., van Delft, J. H., and van Loveren, H. (2010). Transcriptomic profile indicative of immunotoxic exposure; in vitro studies in peripheral blood mononuclear cells. *Toxicol Sci*, **118** (1), 19-30.

Hochstenbach, K., van Leeuwen, D. M., Gottschalk, R. W., Gmuender, H., Stølevik, S. B., Nygaard, U. C., Løvik, M., Granum, B., Namork, E., van Loveren, H., and van Delft, J. H. M. (2012). Transcriptomic fingerprints in human peripheral blood mononuclear cells indicative of genotoxic and non-genotoxic carcinogenic exposure. *Mutat Res*, **746** (2), 124-34.

Hollingshead, B. D., Beischlag, T. V., DiNatale, B. C., Ramadoss, P., and Perdew, G. H. (2008). Inflammatory signaling and aryl hydrocarbon receptor mediate synergistic induction of interleukin 6 in MCF-7 cells. *Cancer Res*, **68** (10), 3609-17.

Homberger, E., Reggiani, G., Sambeth, J., and Wipf, H. K. (1979). The Seveso accident: its nature, extent and consequences. *Ann occup Hyg*, **22** (4), 327-70.

Hooived, M., Heederik, D. J., Kogevinas, M., Boffetta, P., Needham, L. L., Patterson, D. G., & Bueno-de-Mesquita, H. B. (1998). Second follow-up of a Dutch cohort occupationally exposed to phenoxy herbicides, chlorophenols, and contaminants. *Am J Epidemiol*, **147** (9), 891-9.

http://wetten.overheid.nl/BWBR0003081: Dutch government websites http://www.overheid.nl.

Hu, W., Sorrentino, C., Denison, M. S., Kolaja, K., and Fielden, M. R. (2007). Induction of cyp1a1 is a nonspecific biomarker of aryl hydrocarbon receptor activation: results of large scale screening of pharmaceuticals and toxicants in vivo and in vitro. *Mol Pharmacol*, **71** (6), 1475-86.

Hunt, M. C., Yang, Y. Z., Eggertsen, G., Carneheim, C. M., Gåfvels, M., Einarsson, C., and Alexson, S. E. (2000). The peroxisome proliferator-activated receptor α (PPARα) regulates bile acid biosynthesis. *J Biol Chem*, **275** (37), 28947-53.

IARC (1987). Overall evaluations of carcinogenicity: an updating of IARC Monographs volumes 1 to 42. *IARC Monogr Eval Carcinog Risks Hum Suppl*, **18** (7), 1-440.

IARC (1997). Polychlorinated dibenzo-para-dioxins and polychlorinated dibenzofurans. *IARC Monogr Eval Carcinog Risks Hum*, **69**, 1–631.

IARC (2012). 2,3,7,8-Tetrachlorodibenzo-*para*-Dioxin, 2,3,4,7,8-Pentachlorodibenzofuran, and 3,3',4,4',5-Pentachlorobiphenyl. *IARC Monogr Eval Carcinog Risks Hum Suppl*, **100F**, 339-78.

IARC-List of classifications 2014. Agents Classified by the IARC Monographs, Volumes 1-108. http://monographs.iarc.fr/ENG/Classification/ClassificationsAlphaOrder.pdf; Accessed on 05/12/2014.

Ichinose, A., and Davie, E. W. (1988). Characterization of the gene for the a subunit of human factor XIII (plasma transglutaminase), a blood coagulation factor. *Proc Natl Acad Sci U S A*, **85** (16), 5829-33.

Iida, T., Hirakawa, H., Matsueda, T., Nagayama, J., and Nagdata, T. (1999). Polychlorinated dibenzo-*p*-dioxins and related compounds: correlations of levels in human tissues and in blood. *Chemosphere*, **38** (12), 2767-74.

Iizuka, K., Bruick, R. K., Liang, G., Horton, J. D., and Uyeda, K. (2004). Deficiency of carbohydrate response element-binding protein (ChREBP) reduces lipogenesis as well as glycolysis. *Proc Natl Acad Sci USA*, **101** (19), 7281-6.

Ikuta, T., Eguchi, H., Tachibana, T., Yoneda, Y., and Kawajiri, K. (1998). Nuclear localization and export signals of the human aryl hydrocarbon receptor. *J Biol Chem*, **273** (5), 2895-904.

Ikuta, T., Tachibana, T., Watanabe, J., Yoshida, M., Yoneda, Y., and Kawajiri, K. (2000). Nucleocytoplasmic shuttling of the aryl hydrocarbon receptor. *J Biochem*, **127** (3), 503-9.

Inouye, K., Pan, X., Imai, N., Ito, T., Takei, T., Tohyama, C., and Nohara, K. (2005). T cell-derived IL-5 production is a sensitive target of 2,3,7,8-tetrachlorodibenzo-*p*-dioxin (TCDD). *Chemosphere*, **60** (7), 907-13.

Ishihara, K., and Hirano, T. (2002). IL-6 in autoimmune disease and chronic inflammatory proliferative disease. *Cytokine Growth Factor Rev*, **13** (4), 357-68.

Ito, T., Inouye, K., Fujimaki, H., Tohyama, C., and Nohara, K. (2002). Mechanism of TCDD-induced suppression of antibody production: effect on T cell-derived cytokine production in the primary immune reaction of mice. *Toxicol Sci*, **70** (1), 46-54.

Iwahara, S., Satoh, H., Song, D.-X., Webb, J., Burlingame, A. L., Nagae, Y., and Muller-Eberhard, U. (1995). Purification, characterization, and cloning of a heme-binding protein (23 kDa) in rat liver cytosol. *Biochemistry*, **34**, 13398-406.

Iwasaki, Y., Hosoya, T., Takebayashi, H., Ogawa, Y., Hotta, Y., and Ikenaka, K. (2003). The potential to induce glial differentiation is conserved between Drosophila and mammalian glial cells missing genes. *Development*, *130*(24), 6027-6035.

Jaiswal, A. K. (1991). Human NAD(P)H:quinone oxidoreductase (NQO1) gene structure and induction by dioxin. *Biochemistry*, **30** (44), 10647-53.

JECFA (2001). Summary of the fifty-seventh meeting of the Joint FAO/WHO-Expert Committee on Food Additives, Rome, 5-14 June 2001. 24-40.

Jeong, K. T., Hwang, S. J., Oh, G. S., and Park, J. H. (2012). FICZ, a tryptophan photoproduct, suppresses pulmonary eosinophilia and Th2-type cytokine production in a mouse model of ovalbumin-induced allergic asthma. *Int Immunopharmacol*, **13** (4), 377-85.

Jetten, A. M. (2009). Retinoid-related orphan receptors (RORs): critical roles in development, immunity, circadian rhythm, and cellular metabolism. *Nucl Recept Signal*, 7 (e003), 1-32.

Jiang, G., and Zhang, B. B. (2003). Glucagon and regulation of glucose metabolism. *Am J Physiol Endocrinol Metab*, **284** (4), E671-8.

Jiang, H., Shukla, A., Wang, X., Chen, W. Y., Bernstein, B. E., and Roeder, R. G. (2011). Role for Dpy-30 in ES cell-fate specification by regulation of H3K4 methylation within bivalent domains. *Cell*, **144** (4), 513-25.

Jiménez, B., Volpert, O. V., Crawford, S. E., Febbraio, M., Silverstein, R. L., and Bouck, N. (2000). Signals leading to apoptosis-dependent inhibition of neovascularization by thrombospondin-1. *Nat Med*, **6** (1), 41-8.

Jin, C., Zang, C., Wei, G., Cui, K., Peng, W., Zhao, K., and Felsenfeld, G. (2009). H3. 3/H2A. Z double variant–containing nucleosomes mark 'nucleosome-free regions' of active promoters and other regulatory regions. *Nat Genet*, **41** (8), 941-45.

Joffre, O., Nolte, M. A., and Spörri, R. (2009). Inflammatory signals in dendritic cell activation and the induction of adaptive immunity. *Immunol Rev*, **227** (1), 234-47.

Joshi, A. D., Hegde, G. V., Dickinson, J. D., Mittal, A. K., Lynch, J. C., Eudy, J. D., Armitage, J. O., Bierman, P. J., Bociek, R. G., Devetten, M. P., Vose, J. M., and Joshi, S. S. (2007). ATM, CTLA4, MNDA, and HEM1 in High versus Low CD38-Expressing B-Cell Chronic Lymphocytic Leukemia. *Clin Cancer Res*, **13** (18), 5295-304.

Jux, B., Kadow, S., and Esser, C. (2009). Langerhans cell maturation and contact hypersensitivity are impaired in aryl hydrocarbon receptor-null mice. *J Immunol*, **182** (11), 6709-17.

Kadowaki, T., Goldfarb, D., Spitz, L. M., Tartakoff, A. M., and Ohno, M. (1993). Regulation of RNA processing and transport by a nuclear guanine nucleotide release protein and members of the Ras superfamily. *EMBO J*, **12** (7), 2929-37.

Kafafi, S. A., Afeefy, H. Y., Ali, A. H., Said, H. K., and Kafafi, A. G. (1993). Binding of polychlorinated biphenyls to the aryl hydrocarbon receptor. *Environ Health Perspect*, **101** (5), 422-28.

Kafafi, S. A., Afeefy, H. Y., Said, H. K., and Hakimi, J. M. (1992a). A new structure-activity model for Ah receptor binding. Polychlorinated dibenzo-*p*-dioxins and dibenzofurans. *Chem Res Toxicol*, **5** (6), 856-62.

Kafafi, S. A., Said, H. K., Mahmoud, M. I., and Afeefy, H. Y. (1992b). The electronic and thermodynamic aspects of Ah receptor binding. A new structure-activity model: I. The polychlorinated dibenzo-*p*-dioxins. *Carcinogenesis*, **13** (9), 1599-605.

Kalmes, M., Hennen, J., Clemens, J., and Blömeke, B. (2011). Impact of aryl hydrocarbon receptor (AhR) knockdown on cell cycle progression in human HaCaT keratinocytes. *Biol Chem*, **392** (7), 643-51.

Kang, H. K., Dalager, N. A., Needham, L. L., Patterson, D. G., Lees, P. S., Yates, K., and Matanoski, G. M. (2006). Health status of Army Chemical Corps Vietnam veterans who sprayed defoliant in Vietnam. *Am J Ind Med*, **49** (11), 875-84.

Karlaganis, G., Marioni, R., Sieber, I., and Weber, A. (2001). The elaboration of the 'Stockholm convention'on persistent organic pollutants (POPs): a negotiation process fraught with obstacles and opportunities. *Environ Sci & Pollut Res*, **8** (3), 216-21.

Kawai, M., and Hosaki, S. (1990). Clinical usefulness of malate dehydrogenase and its mitochondrial isoenzyme in comparison with aspartate aminotransferase and its mitochondrial isoenzyme in sera of patients with liver disease. *Clin Biochem*, **23** (4), 327-34.

Kawano, Y., Nishiumi, S., Tanaka, S., Nobutani, K., Miki, A., Yano, Y., Seo, Y., Kutsumi, H., Ashida, H., Azuma, T., and Yoshida, M. (2010). Activation of the aryl hydrocarbon receptor induces hepatic steatosis via the upregulation of fatty acid transport. *Arch Biochem Biophys*, **504** (2), 221-7.

Kazlauskas, A., Poellinger, L., and Pongratz, I. (1999). Evidence that the co-chaperone p23 regulates ligand responsiveness of the dioxin (Aryl hydrocarbon) receptor. *J Biol Chem*, **274** (19), 13519-24.

Keller, H., Dreyer, C., Medin, J., Mahfoudi, A., Ozato, K., and Wahli, W. (1993). Fatty acids and retinoids control lipid metabolism through activation of peroxisome proliferator-activated receptor-retinoid X receptor heterodimers. *Proc Natl Acad Sci U S A*, **90** (6), 2160-4.

Kennedy, S. W., Lorenzen, A., James, C. A., and Collins, B. T. (1993). Ethoxyresorufin-*O*-deethylase and Porphyrin Analysis in Chicken Embryo Hepatocyte Cultures with a Fluorescence Multiwell Plate Reader. *Anal Biochem*, **211** (1), 102-12.

Kerkvliet, N. I., Shepherd, D. M., and Baecher-Steppan, L. (2002). T Lymphocytes Are Direct, Aryl Hydrocarbon Receptor (AhR)-Dependent Targets of 2,3,7,8-Tetrachlorodibenzo-*p*-dioxin (TCDD): AhR Expression in Both $CD4^+$ and $CD8^+$ T Cells Is Necessary for Full Suppression of a Cytotoxic T Lymphocyte Response by TCDD. *Toxicol Appl Pharmacol*, **185** (2), 146-52.

Kidd, P. (2003). Th1/Th2 Balance: The Hypothesis, its Limitations, and Implications for Health and Disease. *Altern Med Rev*, **8** (3), 223-46.

Kikuchi, M., Nakao, M., Inoue, Y., Matsunaga, K., Shichijo, S., Yamana, H., and Itoh, K. (1999). Identification of a SART−1-derived peptide capable of inducing HLA-A24-restricted and tumor−specific cytotoxic T lymphocytes. *Int J Cancer*, **81** (3), 459-66.

Kim, H., Lee, T. H., Park, E. S., Suh, J. M., Park, S. J., Chung, H. K., Kwon, O. Y., Kim, Y. K., Ro H. K., and Shong, M. (2000). Role of peroxiredoxins in regulating intracellular hydrogen peroxide and hydrogen peroxide-induced apoptosis in thyroid cells. *J Biol Chem*, **275** (24), 18266-70.

Kim, S. Y., Kim, T. J., and Lee, K. Y. (2008). A novel function of peroxiredoxin 1 (Prx-1) in apoptosis signal-regulating kinase 1 (ASK1)-mediated signaling pathway. *FEBS lett*, **582** (13), 1913-8.

Kim, Y. C., Masutani, H., Yamaguchi, Y., Itoh, K., Yamamoto, M., and Yodoi, J. (2001). Hemin-induced activation of the thioredoxin gene by Nrf2. A differential regulation of the antioxidant responsive element by a switch of its binding factors. *J Biol Chem*, **276** (21), 18399-406.

Kimura, A., Naka, T., Nakahama, T., Chinen, I., Masuda, K., Nohara, K., Fujii-Kuriyama, Y., and Kishimoto, T. (2009). Aryl hydrocarbon receptor in combination with Stat1 regulates LPS-induced inflammatory responses. *J Exp Med*, **206** (9), 2027-35.

Kimura, A., Naka, T., Nohara, K., Fujii-Kuriyama, Y., and Kishimoto, T. (2008). Aryl hydrocarbon receptor regulates Stat1 activation and participates in the development of Th17 cells. *Proc Natl Acad Sci USA*, **105** (28), 9721-6.

Kitamura, K., Nagao, M., Hayatsu, H., and Morita, M. (2005). Effect of chlorophyllin-chitosan on excretion of dioxins in a healthy man. *Environ Sci Technol*, **39** (4), 1084-91.

Kliewer, S. A., Umesono, K., Noonan, D. J., Heyman, R. A., and Evans, R. M. (1992). Convergence of 9-cis retinoic acid and peroxisome proliferator signalling pathways through heterodimer formation of their receptors. *Nature*, 358 (6389), 771-4.

Kobayashi, A., Sogawa, K., and Fujii-Kuriyama, Y. (1996). Cooperative interaction between AhR· Arnt and Sp1 for the drug-inducible expression of CYP1A1 gene. *J Biol Chem*, **271** (21), 12310-6.

Kociba, R. J., Keeler, P. A., Park, C. N., and Gehring, P. J. (1976). 2,3,7,8-Tetrachlorodibenzo-*p*-dioxin (TCDD): Results of a 13-week oral toxicity study in rats. *Toxicol Appl Pharmacol*, **35** (3), 553-74.

Kociba, R. J., Keyes, D. G., Beyer, J. E., Carreon, R. M., Wade, C. E., Dittenber, D. A., Kalnins, R. P., Frauson, L. E., Park, C. N., Barnard, S. D., Hummel, R. A., and Humiston, C. G. (1978). Results of a two-year chronic toxicity and oncogenicity study of 2,3,7,8-tetrachlorodibenzo-*p*-dioxin in rats. *Toxicol Appl Pharmacol*, **46** (2), 279-303.

Kogevinas, M., Becher, H., Benn, T., Bertazzi, P. A., Boffetta, P., Bueno-de-Mesqurta, H. B., Coggon, D., Colin, D., Flesch-Janys, D., Fingerhut, M., Green, L., Kauppinen, T., Littorin, Lynge, E., Mathews, J. D., Neuberger, M., Pearce, N., and Saracci, R. (1997). Cancer mortality in workers exposed to phenoxy herbicides, chlorophenols, and dioxins an expanded and updated international cohort study. *Am J Epidemiol*, **145** (12), 1061-75.

Komura, K., Hayashi, S. I., Makino, I., Poellinger, L., and Tanaka, H. (2001). Aryl hydrocarbon receptor/dioxin receptor in human monocytes and macrophages. *Mol Cell Biochem*, **226** (1-2), 107-17.

Komurasaki, T., Toyoda, H., Uchida, D., and Morimoto, S. (1997). Epiregulin binds to epidermal growth factor receptor and ErbB-4 and induces tyrosine phosphorylation of epidermal growth factor receptor, ErbB-2, ErbB-3 and ErbB-4. *Oncogene*, **15** (23), 2841-8.

Kouri, R. E., Ratrie, H. 3rd, Atlas, S. A., Niwa, A., and Nebert, D. W. (1974). Aryl hydrocarbon hydroxylase induction in human lymphocyte cultures by 2,3,7,8-tetrachlorodibenzo-*p*-dioxin. *Life Sci*, **15** (9), 1585-95.

Krey, G., Braissant, O., L'Horset, F., Kalkhoven, E., Perroud, M., Parker, M. G., and Wahli, W. (1997). Fatty acids, eicosanoids, and hypolipidemic agents identified as ligands of peroxisome proliferator-activated receptors by coactivator-dependent receptor ligand assay. *Mol Endocrinol*, **11** (6), 779-91.

Krovat, B. C., Tracy, J. H., and Omiecinski, C. J. (2000). Fingerprinting of cytochrome P450 and microsomal epoxide hydrolase gene expression in human blood cells. *Toxicol Sci*, **55** (2), 352-60.

Kuroki, H., Haraguchi, K., and Masuda, Y. (1990). Metabolism of polychlorinated dibenzofurans (PCDFs) in rats. *Chemosphere*, **20** (7), 1059-64.

Laemmli, U. K. (1970). Cleavage of structural proteins during the assembly of the head of bacteriophage T4. *Nature*, **227** (5259), 680-5.

Lahvis, G. P., Lindell, S. L., Thomas, R. S., McCuskey, R. S., Murphy, C., Glover, E., Bentz,M., Southard, J., and Bradfield, C. A. (2000). Portosystemic shunting and persistent fetal vascular structures in aryl hydrocarbon receptor-deficient mice. *Proc Natl Acad Sci USA*, **97** (19), 10442-7.

Lahvis, G. P., Pyzalski, R. W., Glover, E., Pitot, H. C., McElwee, M. K., and Bradfield, C. A. (2005). The aryl hydrocarbon receptor is required for developmental closure of the ductus venosus in the neonatal mouse. *Mol Pharmacol*, **67** (3), 714-20.

Lai, K. P., Mak, N. K., Wei, X., Wong, R. N. S., Wong, M. H., and Wong, C. K. (2006). Bifunctional modulating effects of an indigo dimer (bisindigotin) to CYP1A1 induction in H4IIE cells. *Toxicology*, **226** (2), 188-196.

Landi, M. T., Bertazzi, P. A., Baccarelli, A., Consonni, D., Masten, S., Lucier, G., Mocarelli, P., Needham, L., Caporaso, N., and Grassman, J. (2003). TCDD-mediated alterations in

the AhR-dependent pathway in Seveso, Italy, 20 years after the accident. *Carcinogenesis*, **24** (4), 673-80.

Lauby-Secretan, B., Loomis, D., Grosse, Y., El Ghissassi, F., Bouvard, V., Benbrahim-Tallaa, L., Guha, N., Baan, R., Mattock, H., and Straif, K. (2013). Carcinogenicity of polychlorinated biphenyls and polybrominated biphenyls. *Lancet Oncol*, **14** (4), 287-8.

Lawrence, B. P., Leid, M., and Kerkvliet, N. I. (1996). Distribution and behavior of the Ah receptor in murine T lymphocytes. *Toxicol Appl Pharmacol*, **138** (2), 275-84.

Leclercq, I. A., Farrell, G. C., Field, J., Bell, D. R., Gonzalez, F. J., and Robertson, G. R. (2000). CYP2E1 and CYP4A as microsomal catalysts of lipid peroxides in murine nonalcoholic steatohepatitis. *J Clin Invest*, **105** (8), 1067-75.

Lee, J. H., Wada, T., Febbraio, M., He, J., Matsubara, T., Lee, M. J., Gonzalez, F. J., and Xie, W. (2010). A novel role for the dioxin receptor in fatty acid metabolism and hepatic steatosis. *Gastroenterology*, **139** (2), 653-663.

Lee, S. S., Pineau, T., Drago, J., Lee, E. J., Owens, J. W., Kroetz, D. L., Fernandez-Salguero, P. M., Westphal, H., and Gonzalez, F. J. (1995). Targeted disruption of the alpha isoform of the peroxisome proliferator-activated receptor gene in mice results in abolishment of the pleiotropic effects of peroxisome proliferators. *Mol Cell Biol*, **15** (6), 3012-22.

Letcher, R. J., Klasson-Wehler, E., and Bergman, A. (2000). Methyl sulfone and hydroxylated metabolites of polychlorinated biphenyls. In *Volume 3 Anthropogenic Compounds Part K. The Handbook of Environmental Chemistry* (pp. 315-59); Paasivirta, J., ed. Springer, Heidelberg, Germany.

Li, C., Wang, Y., Wang, S., Wu, B., Hao, J., Fan, H., Ju, Y., Ding, Y., Chen, L., Chu, X., Liu, W., Ye, X., and Meng, S. (2013). Hepatitis B Virus mRNA-mediated miR-122 inhibition upregulates PTTG1-binding protein, which promotes hepatocellular carcinoma tumor growth and cell invasion. *J Virol*, **87** (4), 2193-205.

Li, J., Malaby, A. W., Famulok, M., Sabe, H., Lambright, D. G., and Hsu, V. W. (2012). Grp1 plays a key role in linking insulin signaling to glut4 recycling. *Dev Cell*, **22** (6), 1286-98.

Li, Y., Innocentin, S., Withers, D. R., Roberts, N. A., Gallagher, A. R., Grigorieva, E. F., Wilhelm, C., and Veldhoen, M. (2011). Exogenous stimuli maintain intraepithelial lymphocytes via aryl hydrocarbon receptor activation. *Cell*, **147** (3), 629-40.

Liem, A. K., Fürst, P., and Rappe, C. (2000). Exposure of populations to dioxins and related compounds. *Food Addit Contam*, **17** (4), 241-59.

Lincoln, D. T., Emadi, E. M., Tonissen, K. F., and Clarke, F. M. (2003). The thioredoxin-thioredoxin reductase system: over-expression in human cancer. *Anticancer Res*, **23** (3B), 2425-33.

Lindl T.: Zell- und Gewebekultur: Einführung in die Grundlagen sowie ausgewählte Methoden und Anwendungen, 5., überarbeitete und erweiterte Auflage **2002**, Spektrum Akademischer Verlag GmbH, Heidelberg, Germany.

Lohr, C (2013). Effects of Polychlorinated Dibenzo-*p*-Dioxins, Polychlorinated Dibenzofurans, and Polychlorinated Biphenyls in Human Liver Cell Models (*in vitro*) and in Mice (*in vivo*). Doctoral Thesis. University of Kaiserslautern.

Luecke, S., Backlund, M., Jux, B., Esser, C., Krutmann, J., and Rannug, A. (2010). The aryl hydrocarbon receptor (AHR), a novel regulator of human melanogenesis. *Pigment Cell Melanoma*, **23** (6), 828-33.

Luger, K., Mäder, A. W., Richmond, R. K., Sargent, D. F., and Richmond, T. J. (1997). Crystal structure of the nucleosome core particle at 2.8 Å resolution. *Nature*, **389** (6648), 251-60.

Luo, L., Wang, Y., Feng, Q., Zhang, H., Xue, B., Shen, J., Ye, Y., Han, X., Ma, H., Xu, J., Chen, D., and Yin, Z. (2009). Recombinant protein glutathione-*S*-transferases P1 attenuates inflammation in mice. *Mol Immunol*, **46** (5), 848-57.

Lutz, R. J., Dedrick, R. L., Tuey, D., Sipes, I. G., Anderson, M. W., and Matthews, H. B. (1984). Comparison of the pharmacokinetics of several polychlorinated biphenyls in mouse, rat, dog, and monkey by means of a physiological pharmacokinetic model. *Drug Metab Dispos*, **12** (5), 527-35.

Lynch, J. M., Maillet, M., Vanhoutte, D., Schloemer, A., Sargent, M. A., Blair, N. S., Lynch, K. A., Okada, T., Aronow, B. J., Osinska, H., Prywes, R., Lorenz, J. N., Mori, K., Lawler, J., Robbins, J., and Molkentin, J. D. (2012). A thrombospondin-dependent pathway for a protective ER stress response. *Cell*, **149** (6), 1257-68.

Ma, H., Liang, X., Chen, Y., Pan, K., Sun, J., Wang, H., Li, Y., Zhao, J., Li, J., Chen, M., and Xia, J. (2011). Decreased expression of BATF2 is associated with a poor prognosis in hepatocellular carcinoma. *Int J Cancer*, **128** (4), 771-7.

Ma, Q., and Baldwin, K. T. (2000). 2,3,7,8-Tetrachlorodibenzo-*p*-dioxin-induced Degradation of Aryl Hydrocarbon Receptor (AhR) by the Ubiquitin-Proteasome

Pathway. Role of the transcription activation and DNA binding of the AhR. *J Biol Chem*, **275** (12), 8432-8.

Ma, Q., and Whitlock, J. P. (1996). The aromatic hydrocarbon receptor modulates the Hepa 1c1c7 cell cycle and differentiated state independently of dioxin. *Mol Cell Biol*, **16** (5), 2144-50.

Ma, Q., and Whitlock, J. P. (1997). A novel cytoplasmic protein that interacts with the Ah receptor, contains tetratricopeptide repeat motifs, and augments the transcriptional response to 2,3,7,8-tetrachlorodibenzo-*p*-dioxin. *J Biol Chem*, **272** (14), 8878-84.

Ma, Q., Baldwin, K. T., Renzelli, A. J., McDaniel, A., and Dong, L. (2001). TCDD-Inducible Poly (ADP-ribose) Polymerase: A Novel Response to 2,3,7,8-Tetrachlorodibenzo-*p*-dioxin. *Biochem Biophys Res Commun*, **289** (2), 499-506.

Machala, M., Neca, J., and Vondrácek, J. (2004). Antiestrogenic Effects of Environmental Pollution in Human Blood and Placenta. *Epidemiology*, **15** (4), S117.

Marcus, R. S., Holsapple, M. P., and Kaminski, N. E. (1998). Lipopolysaccharide activation of murine splenocytes and splenic B cells increased the expression of aryl hydrocarbon receptor and aryl hydrocarbon receptor nuclear translocator. *J Pharmacol Exp Ther*, **287** (3), 1113-8.

Marin, S., Villalba, P., Diaz-Ferrero, J., Font, G., and Yusà, V. (2011). Congener profile, occurrence and estimated dietary intake of dioxins and dioxin-like PCBs in foods marketed in the Region of Valencia (Spain). *Chemosphere*, **82** (9), 1253-61.

Marrs, W. R., Blankman, J. L., Horne, E. A., Thomazeau, A., Lin, Y. H., Coy, J., Bodor, A. L., Muccioli, G. G., Hu, S. S., Woodruff, G., Fung, S., Lafourcade, M., Alexander, J. P., Long, J. Z., Li, W., Xu, C., Möller, T., Mackie, K., Manzoni, O. J., Cravatt, B. F., and Stella, N. (2010). The serine hydrolase ABHD6 controls the accumulation and efficacy of 2-AG at cannabinoid receptors. *Nature Neurosci*, **13** (8), 951-7.

Martey, C. A., Baglole, C. J., Gasiewicz, T. A., Sime, P. J., and Phipps, R. P. (2005). The aryl hydrocarbon receptor is a regulator of cigarette smoke induction of the cyclooxygenase and prostaglandin pathways in human lung fibroblasts. *Am J Physiol Lung Cell Mol Physiol*, **289** (3), L391-9.

Melchior, F., Paschal, B., Evans, J., and Gerace, L. (1993). Inhibition of nuclear protein import by nonhydrolyzable analogues of GTP and identification of the small GTPase Ran/TC4 as an essential transport factor. *J Cell Biol*, **123** (6), 1649-59.

Meller, N., Liu, Y. C., Collins, T. L., Bonnefoy-Berard, N., Baier, G., Isakov, N., and Altman, A. (1996). Direct interaction between protein kinase C theta (PKC theta) and 14-3-3 tau in T cells: 14-3-3 overexpression results in inhibition of PKC theta translocation and function. *Mol Cell Biol*, **16** (10), 5782-91.

Meunier, B., De Visser, S. P., and Shaik, S. (2004). Mechanism of oxidation reactions catalyzed by cytochrome P450 enzymes. *Chem Rev*, **104** (9), 3947-80.

Meyer, B. K., Pray-Grant, M. G., Vanden Heuvel, J. P., and Perdew, G. H. (1998). Hepatitis B virus X-associated protein 2 is a subunit of the unliganded aryl hydrocarbon receptor core complex and exhibits transcriptional enhancer activity. *Mol Cell Biol*, **18** (2), 978-88.

Mezrich, J. D., Fechner, J. H., Zhang, X., Johnson, B. P., Burlingham, W. J., and Bradfield, C. A. (2010). An interaction between kynurenine and the aryl hydrocarbon receptor can generate regulatory T cells. *J Immunol*, **185** (6), 3190-8.

Mhin, B. J., Lee, J. E., and Choi, W. (2002). Understanding the congener-specific toxicity in polychlorinated dibenzo-p-dioxins: chlorination pattern and molecular quadrupole moment. *J Am Chem Soc*, **124** (1), 144-8.

Milbrath, M. O., Wenger, Y., Chang, C. W., Emond, C., Garabrant, D., Gillespie, B. W., and Jolliet, O. (2009). Apparent half-lives of dioxins, furans, and polychlorinated biphenyls as a function of age, body fat, smoking status, and breast-feeding. *Environ Health Perspect*, **117** (3), 417-25.

Miller, M. D., and Krangel, M. S. (1992). The human cytokine I-309 is a monocyte chemoattractant. *Proc Natl Acad Sci USA*, **89** (7), 2950-4.

Mimura, J., Yamashita, K., Nakamura, K., Morita, M., Takagi, T. N., Nakao, K., Ema, M., Sogawa, K., Yasuda, M., Katsuki, M., and Fujii-Kuriyama, Y. (1997). Loss of teratogenic response to 2,3,7,8-tetrachlorodibenzo-*p*-dioxin (TCDD) in mice lacking the Ah (dioxin) receptor. *Genes Cells*, **2** (10), 645-54.

Mire-Sluis, A. R., Wickremasinghe, R. G., Hoffbrand, A. V., Timms, A. M., and Francis, G. E. (1987). Human T lymphocytes stimulated by phytohaemagglutinin undergo a single round of cell division without a requirement for interleukin-2 or accessory cells. *Immunology*, **60** (1), 7-12.

Mitchell, K. A., and Elferink, C. J. (2009). Timing is everything: consequences of transient and sustained AhR activity. *Biochem Pharmacol*, **77** (6), 947-56.

Mito, Y., Henikoff, J. G., and Henikoff, S. (2005). Genome-scale profiling of histone H3.3 replacement patterns. *Nat Genet*, **37** (10), 1090-7.

Moennikes, O., Loeppen, S., Buchmann, A., Andersson, P., Ittrich, C., Poellinger, L., and Schwarz, M. (2004). A constitutively active dioxin/aryl hydrocarbon receptor promotes hepatocarcinogenesis in mice. *Cancer Res*, **64** (14), 4707-10.

Moestrup, S. K., and Møller, H. J. (2004). CD163: a regulated hemoglobin scavenger receptor with a role in the anti-inflammatory response. *Ann Med*, **36** (5), 347-54.

Monteiro, P., Gilot, D., Le Ferrec, E., Rauch, C., Lagadic-Gossmann, D., and Fardel, O. (2008). Dioxin-mediated up-regulation of aryl hydrocarbon receptor target genes is dependent on the calcium/calmodulin/CaMKIα pathway. *Mol Pharmacol*, **73** (3), 769-77.

Morinobu, A., Gadina, M., Strober, W., Visconti, R., Fornace, A., Montagna, C., Feldman, G. M., Nishikomori, R., and O'Shea, J. J. (2002). STAT4 serine phosphorylation is critical for IL-12-induced IFN-γ production but not for cell proliferation. *Proc Natl Acad Sci USA*, **99** (19), 12281-6.

Morrison, D. K. (2009). The 14-3-3 proteins: integrators of diverse signaling cues that impact cell fate and cancer development. *Trends Cell Biol*, **19** (1), 16-23.

Moser, G. A., and McLachlan, M. S. (2001). The influence of dietary concentration on the absorption and excretion of persistent lipophilic organic pollutants in the human intestinal tract. *Chemosphere*, **45** (2), 201-11.

Moser, M., and Leo, O. (2010). Key concepts in immunology. *Vaccine*, **28S**, C2-C13.

Muerhoff, A. S., Griffin, K. J., and Johnson, E. F. (1992). The peroxisome proliferator-activated receptor mediates the induction of CYP4A6, a cytochrome P450 fatty acid omega-hydroxylase, by clofibric acid. *J Biol Chem*, **267** (27), 19051-3.

Mun, G. I., Park, S., Kremerskothen, J., and Boo, Y. C. (2014). Expression of synaptopodin in endothelial cells exposed to laminar shear stress and its role in endothelial wound healing. *FEBS Lett*, **588** (6), 1024-30.

Munn, D. H., Shafizadeh, E., Attwood, J. T., Bondarev, I., Pashine, A., and Mellor, A. L. (1999). Inhibition of T cell proliferation by macrophage tryptophan catabolism. *J Exp Med*, **189** (9), 1363-72.

Murphy-Ullrich, J. E., and Poczatek, M. (2000). Activation of latent TGF-β by thrombospondin-1: mechanisms and physiology. *Cytokine Growth Factor Rev*, **11** (1), 59-69.

Muskhelishvili, L., Latendresse, J. R., Kodell, R.L., and Henderson, E. B. (2003). Evaluation of cell proliferation in rat tissues with BrdU, PCNA, Ki-67 (MIB-5) immunohistochemistry and in situ hybridization for histone mRNA. *J Histochem Cytochem*, **51** (12), 1681-8.

Nagai, H., Takei, T., Tohyama, C., Kubo, M., Abe, R., and Nohara, K. (2005). Search for the target genes involved in the suppression of antibody production by TCDD in C57BL/6 mice. *Int Immunopharmacol*, **5** (2), 331-43.

Nair, S. C., Toran, E. J., Rimerman, R. A., Hjermstad, S., Smithgall, T. E., and Smith, D. F. (1996). A pathway of multi-chaperone interactions common to diverse regulatory proteins: estrogen receptor, Fes tyrosine kinase, heat shock transcription factor Hsf1, and the aryl hydrocarbon receptor. *Cell Stress Chaperones*, **1** (4), 237-50.

Namba, R., Maglione, J. E., Young, L. J., Borowsky, A. D., Cardiff, R. D., MacLeod, C. L., and Gregg, J. P. (2004). Molecular characterization of the transition to malignancy in a genetically engineered mouse-based model of ductal carcinoma *in situ*. *Mol Cancer Res*, **2** (8), 453-63.

National Toxicology Program (NTP). (1982). Carcinogenesis Bioassay of 2,3,7,8-Tetrachlorodibenzo-*p*-dioxin (CAS No. 1746-01-6) in Osborne-Mendel Rats and B6C3F1 Mice (Gavage Study). *National Toxicology Program technical report series*, **209**, 1-211.

Nebert, D. W., and Gelboin, H. V. (1968a). Substrate-inducible microsomal aryl hydroxylase in mammalian cell culture I. Assay and properties of induced enzyme. *J Biol Chem*, **243** (23), 6242-9.

Nebert, D. W., and Gelboin, H. V. (1968b). Substrate-inducible microsomal aryl hydroxylase in mammalian cell culture II. Cellular responses during enzyme induction. *J Biol Chem*, **243** (23), 6250-61.

Nebert, D. W., Levitt, R. C., Orlando, M. M., and Felton, J. S. (1977). Effects of environmental chemicals on the genetic regulation of microsomal enzyme systems. *Clin Pharmacol Ther*, **22**, 640-58.

Nebert, D. W., Robinson, J. R., Niwa, A., Kumari, K., and Poland, A. P. (1975). Genetic expression of aryl hydrocarbon hydroxylase activity in the mouse. *J Cell Physiol*, **85** (S1), 393-414.

Nebert, D. W., Roe, A. L., Dieter, M. Z., Solis, W. A., Yang, Y. I., and Dalton, T. P. (2000). Role of the aromatic hydrocarbon receptor and [Ah] gene battery in the oxidative stress response, cell cycle control, and apoptosis. *Biochem Pharmacol*, **59** (1), 65-85.

Needham, L. L., Gerthoux, P. M., Patterson, D. G., Brambilla, P., Turner, W. E., Beretta, C., Pirkle, J. L., Colombo, L., Sampson, E. J., Tramacere, P.L., Signorini, S., Meazza, L., Carreri, V., Jackson, R. J., Mocarelli, P. (1997/98). Serum dioxin levels in Seveso, Italy, population in 1976. *Teratog Carcinog Mutagen*, **17** (4-5), 225-40.

Negishi, T., Kato, Y., Ooneda, O., Mimura, J., Takada, T., Mochizuki, H., Yamamoto, M., Fujii-Kuriyama, Y., and Furusako, S. (2005). Effects of aryl hydrocarbon receptor signaling on the modulation of TH1/TH2 balance. *J Immunol*, **175** (11), 7348-56.

Nelson, D. R., Kamataki, T., Waxman, D. J., Guengerich, F. P., Estabrook, R. W., Feyereisen, R., Gonzalez, F. J., Coon, M. J., Gunsalus, I.C., Gotoh, O., Okuda, K., and Nebert, D. W. (1993). The P450 superfamily: update on new sequences, gene mapping, accession numbers, early trivial names of enzymes, and nomenclature. *DNA Cell Biol*, **12** (1), 1-51.

Neuberger, M., Rappe, C., Bergek, S., Cai, H., Hansson, M., Jäger, R., Kundi, M., Lim, C. K., Wingfors, H., and Smith, A. G. (1999). Persistent health effects of dioxin contamination in herbicide production. *Environ Res*, **81** (3), 206-14.

Neuhold, L. A., Shirayoshi, Y., Ozato, K., Jones, J. E., and Nebert, D. W. (1989). Regulation of mouse CYP1A1 gene expression by dioxin: requirement of two cis-acting elements during induction. *Mol Cell Biol*, **9** (6), 2378-86.

Nguyen, N. T., Kimura, A., Nakahama, T., Chinen, I., Masuda, K., Nohara, K., Fujii-Kuriyama, Y., and Kishimoto, T. (2010). Aryl hydrocarbon receptor negatively regulates dendritic cell immunogenicity via a kynurenine-dependent mechanism. *Proc Natl Acad Sci USA*, **107** (46), 19961-6.

Nohara, K., Ao, K., Miyamoto, Y., Ito, T., Suzuki, T., Toyoshiba, H., and Tohyama, C. (2006). Comparison of the 2,3,7,8-tetrachlorodibenzo-*p*-dioxin (TCDD)-induced CYP1A1 gene expression profile in lymphocytes from mice, rats, and humans: Most potent induction in humans. *Toxicology*, **225** (2), 204-13.

O'Brien, J., Wilson, I., Orton, T., Pognan, F. (2000), Investigation of the Alamar Blue (resazurin) fluorescent dye for the assessment of mammalian cell cytotoxicity. *Eur J Biochem*, **267**, 5421-6.

Ogura, I. (2004). Half-life of each dioxin and PCB congener in the human body. *Organohalogen Compounds*, **66**, 3376-84.

Okey, A. B., and Vella, L. M. (1982). Binding of 3-Methylcholanthrene and 2,3,7,8-Tetrachlorodibenzo-*p*-dioxin to a Common *Ah* Receptor Site in Mouse and Rat Hepatic Cytosols. *Eur J Biochem*, **127** (1), 39-47.

Opitz, C. A., Litzenburger, U. M., Sahm, F., Ott, M., Tritschler, I., Trump, S., Schumacher, T., Jestaedt, L., Schrenk, D., Weller, M., Jugold, M., Guillemin, G. J., Miller, C. L., Lutz, C., Radlwimmer, B., Lehrmann, I., von Deimling A., Wick W., and Platten, M. (2011). An endogenous tumour-promoting ligand of the human aryl hydrocarbon receptor. *Nature*, **478** (7368), 197-203.

Osada, H., Tatematsu, Y., Saito, H., Yatabe, Y., Mitsudomi, T., and Takahashi, T. (2004). Reduced expression of class II histone deacetylase genes is associated with poor prognosis in lung cancer patients. *Int J Cancer*, **112** (1), 26-32.

Oshima, M., Mimura, J., Sekine, H., Okawa, H., and Fujii-Kuriyama, Y. (2009). SUMO modification regulates the transcriptional repressor function of aryl hydrocarbon receptor repressor. *J Biol Chem*, **284** (17), 11017-26.

Oshima, M., Mimura, J., Yamamoto, M., and Fujii-Kuriyama, Y. (2007). Molecular mechanism of transcriptional repression of AhR repressor involving ANKRA2, HDAC4, and HDAC5. *Biochem Biophys Res Commun*, **364** (2), 276-82.

Ott, M. G., and Zober, A. (1996). Cause specific mortality and cancer incidence among employees exposed to 2,3,7,8-TCDD after a 1953 reactor accident. *Occup Environ Med*, **53** (9), 606-12.

Owens, I. S. (1977). Genetic regulation of UDP-glucuronosyltransferase induction by polycyclic aromatic compounds in mice. Co-segregation with aryl hydrocarbon (benzo (alpha) pyrene) hydroxylase induction. *J Biol Chem*, **252** (9), 2827-33.

Pappas, P., Sotiropoulou, M., Karamanakos, P., Kostoula, A., Levidiotou, S., and Marselos, M. (2003). Acute-phase response to benzo [a] pyrene and induction of rat ALDH3A1. *Chem Biol Interact*, **143**, 55-62.

Patterson Jr, D. G., Needham, L. L., Pirkle, J. L., Roberts, D. W., Bagby, J., Garrett, W. A., Andrews, J. S. Jr., Falk, H., Bernet, J. T., Sampson, E. J., and Houk, V. N. (1988). Correlation between serum and adipose tissue levels of 2,3,7,8-tetrachlorodibenzo-*p*-dioxin in 50 persons from Missouri. *Arch Environ Contam Toxicol*, **17** (2), 139-43.

Pei, L., and Melemed, S. (1997). Isolation and characterization of a pituitary tumor-transforming gene (PTTG). *Mol Endocrinol*, **11**, 433-41.

Pelclová, D., Prázný, M., Škrha, J., Fenclová, Z., Kalousová, M., Urban, P., Navrátil, T., Šenholdová, Z., and Šmerhovský, Z. (2007). 2, 3, 7, 8-TCDD exposure, endothelial dysfunction and impaired microvascular reactivity. *Hum Exp Toxicol*, **26** (9), 705-13.

Peng, C. Y., Graves, P. R., Thoma, R. S., Wu, Z., Shaw, A. S., and Piwnica-Worms, H. (1997). Mitotic and G2 checkpoint control: regulation of 14-3-3 protein binding by phosphorylation of Cdc25C on serine-216. *Science*, **277** (5331), 1501-5.

Perdew, G. H. (1988). Association of the Ah receptor with the 90-kDa heat shock protein. *J Biol Chem*, **263** (27), 13802-5.

Perdew, G. H., and Babbs, C. F. (1991). Production of ah receptor ligands in rat fecal suspensions containing tryptophan or indole-3-carbinol. *Nutr Cancer* **16** (3-4), 209-18.

Pesatori, A. C., Consonni, D., Rubagotti, M., Grillo, P., and Bertazzi, P. A. (2009). Cancer incidence in the population exposed to dioxin after the "Seveso accident": twenty years of follow-up. *Environ Health*, **8** (39), 1-11.

Pesatori, A. C., Consonni, D., Rubagotti, M., Grillo, P., and Bertazzi, P. A. (2009). Cancer incidence in the population exposed to dioxin after the "Seveso accident": twenty years of follow-up. *Environ Health*, **8** (39), 1-11.

Pfaffl, M. W. (2001). A new mathematical model for relative quantification in real-time RT–PCR. *Nucleic Acids Res*, **29** (9), e45.

Phelan, D., Winter, G. M., Rogers, W. J., Lam, J. C., and Denison, M. S. (1998). Activation of the Ah receptor signal transduction pathway by bilirubin and biliverdin. *Arch Biochem Biophys*, **357** (1), 155-63.

Piper, W. N., Rose, J. Q., and Gehring, P. J. (1973). Excretion and tissue distribution of 2,3,7,8-tetrachlorodibenzo-*p*-dioxin in the rat. *Environ Health Perspect*, **5**, 241-4.

Pitot, H. C., Peraino, C., Morse Jr, P. A., and Potter, V. R. (1964). Hepatomas in tissue culture compared with adapting liver in vivo. *Natl Cancer Inst Monogr*, **13**, 229-45.

Plíšková, M., Vondráček, J., Canton, R. F., Nera, J., Kočan, A., Petrík, J., Trnovec, T., Sanderson, T., van den Berg, M., and Machala, M. (2005). Impact of polychlorinated biphenyls contamination on estrogenic activity in human male serum. *Environ Health Perspect*, **113** (10) 1277-84.

Plumb, M., Stein, J., and Stein, G. (1983). Coordinate regulation of multiple histone mRNAs during the cell cycle in HeLa cells. *Nucleic Acids Res*, **11** (8), 2391-410.

Podolak, I., Galanty, A., and Sobolewska, D. (2010). Saponins as cytotoxic agents: a review. *Phytochem Rev*, 9 (3), 425-74.

Poiger H. and Buser H.R., In: Banbury Report IB (1984). Courtesy of the Banbury Reports Collection, Cold Spring Harbor Laboratory Archives.

Poiger, H., and Schlatter, C. (1986). Pharmacokinetics of 2, 3, 7, 8-TCDD in man. *Chemosphere*, **15** (9), 1489-94.

Poiger, H., Buser, H. R., Weber, H., Zweifel, U., and Schlatter, C. (1982). Structure elecidation of mammalian TCDD-metabolites. *Experientia*, **38** (4), 484-6.

Poiger, H., Pluess, N., and Buser, H. R. (1989). The metabolism of selected PCDFs in the rat. *Chemosphere*, **18** (1), 259-64.

Poland, A., Glover, E., and Kende, A. S. (1976). Stereospecific, high affinity binding of 2,3,7,8-tetrachlorodibenzo-*p*-dioxin by hepatic cytosol. Evidence that the binding species is receptor for induction of aryl hydrocarbon hydroxylase. *J Biol Chem*, **251** (16), 4936-46.

Pollard, J. W. (2004). Tumour-educated macrophages promote tumour progression and metastasis. *Nat Rev Cancer*, **4** (1), 71-8.

Porges, A. J., Redecha, P. B., Doebele, R., Pan, L. C., Salmon, J. E., and Kimberly, R. P. (1992). Novel Fc gamma receptor I family gene products in human mononuclear cells. *J Clin Invest*, **90** (5), 2102-9.

Poso, A., Tuppurainen, K., Ruuskanen, J., and Gynther, J. (1993). Binding of some dioxins and dibenzofurans to the Ah receptor. A QSAR model based on comparative molecular field analysis (CoMFA). *J Mol Struct (Theochem)*, **282** (3), 259-64.

Post, S. M., Duez, H., Gervois, P. P., Staels, B., Kuipers, F., and Princen, H. M. (2001). Fibrates Suppress Bile Acid Synthesis via Peroxisome Proliferator–Activated Receptor-α–Mediated Downregulation of Cholesterol 7α-Hydroxylase and Sterol 27-Hydroxylase Expression. *Arterioscler Thromb Vasc Biol*, **21** (11), 1840-5.

Potapovich, A. I., Lulli, D., Fidanza, P., Kostyuk, V. A., De Luca, C., Pastore, S., and Korkina, L. G. (2011). Plant polyphenols differentially modulate inflammatory responses of human keratinocytes by interfering with activation of transcription factors NFκB and AhR and EGFR–ERK pathway. *Toxicol Appl Pharmacol*, **255** (2), 138-49.

Prell, R. A., Dearstyne, E., Steppan, L. G., Vella, A. T., and Kerkvliet, N. I. (2000). CTL Hyporesponsiveness Induced by 2,3,7,8-Tetrachlorodibenzo-*p*-dioxin: Role of Cytokines and Apoptosis. *Toxicol Appl Pharmacol*, **166** (3), 214-21.

Puga, A., Ma, C., and Marlowe, J. L. (2009). The aryl hydrocarbon receptor cross-talks with multiple signal transduction pathways. *Biochem Pharmacol*, **77** (4), 713-22.

Püschel, A. W. (1999). Divergent properties of mouse netrins. *Mech Dev*, **83** (1), 65-75.

Quintana, F. J., Basso, A. S., Iglesias, A. H., Korn, T., Farez, M. F., Bettelli, E., Caccamo, M., Oukka, M., and Weiner, H. L. (2008). Control of Treg and TH17 cell differentiation by the aryl hydrocarbon receptor. *Nature*, **453** (7191), 65-71.

Quintana, F. J., Murugaiyan, G., Farez, M. F., Mitsdoerffer, M., Tukpah, A. M., Burns, E. J., and Weiner, H. L. (2010). An endogenous aryl hydrocarbon receptor ligand acts on dendritic cells and T cells to suppress experimental autoimmune encephalomyelitis. *Proc Natl Acad Sci USA*, **107** (48), 20768-73.

Ramadoss, P., and Perdew, G. H. (2004). Use of 2-azido-3-[125I] iodo-7,8-dibromodibenzo-*p*-dioxin as a probe to determine the relative ligand affinity of human versus mouse aryl hydrocarbon receptor in cultured cells. *Mol Pharmacol*, **66** (1), 129-36.

Ramsey, J. C., Hefner, J. G., Karbowski, R. J., Braun, W. H., and Gehring, P. J. (1982). The *in vivo* biotransformation of 2,3,7,8-tetrachlorodibenzo-*p*-dioxin (TCDD) in the rat. *Toxicol Appl Pharmacol*, **65** (1), 180-4.

Ramzy, D., Rao, V., Tumiati, L. C., Xu, N., Sheshgiri, R., Miriuka, S., and Ross, H. J. (2006). Elevated endothelin-1 levels impair nitric oxide homeostasis through a PKC-dependent pathway. *Circulation*, **114** (1 suppl), I-319-26.

Rawlings, J. S., Rosler, K. M., and Harrison, D. A. (2004). The JAK/STAT signaling pathway. *J Cell Sci*, **117** (8), 1281-3.

Ray, S., and Swanson, H. I. (2009). Activation of the aryl hydrocarbon receptor by TCDD inhibits senescence: a tumor promoting event? *Biochem Pharmacol*, **77** (4), 681-8.

Rendic, S., and Di Carlo, F. J. (1997). Human cytochrome P450 enzymes: a status report summarizing their reactions, substrates, inducers, and inhibitors. *Drug Metab Rev*, **29** (1-2), 413-580.

Robertson, L. W., and Ruder, A. (2009). Polychlorinated biphenyls (PCBs). In *IARC/NORA: Identification of research needs to resolve the carcinogenicity of highpriority IARC carcinogens. Views and Expert opinions of an IARC/NORA expert group meeting Lyon, France*, **30**, 166-83.

Rocak, S., and Linder, P. (2004). DEAD-box proteins: the driving forces behind RNA metabolism. *Nat Rev Mol Cell Biol*, **5** (3), 232-41.

Rodríguez de Fonseca, F., Del Arco, I., Bermudez-Silva, F. J., Bilbao, A., Cippitelli, A., Navarro, M. (2004) The endocannabinoid system: physiology and pharmacology. *Alcohol Alcohol*, **40** (1), 2-14.

Rohde, S., Moser, G. A., Päpke, O., and McLachlan, M. S. (1999). Clearance of PCDD/Fs via the gastrointestinal tract in occupationally exposed persons. *Chemosphere*, **38** (14), 3397-410.

Rohde, S., Moser, G. A., Päpke, O., and McLachlan, M. S. (1999). Clearance of PCDD/Fs via the gastrointestinal tract in occupationally exposed persons. *Chemosphere*, **38** (14), 3397-410.

Roos, R. (2011). Einfluss hochreiner, nicht dioxin-artiger polychlorierter Biphenyle auf ausgewählte fremdstoffmetabolisierende Enzyme der Leber im Nager und in Zellkulturmodellen (Impact of highly pure, non dioxin like polychlorinated biphenyls on selected xenobiotic metabolizing liver enzymes in rodents and in cell culture models). Doctoral dissertation, University Library, University of Kaiserslautern.

Rose, J. Q., Ramsey, J. C., Wentzler, T. H., Hummel, R. A., and Gehring, P. J. (1976). The fate of 2,3,7,8-tetrachlorodibenzo-*p*-dioxin following single and repeated oral doses to the rat. *Toxicol Appl Pharmacol*, **36** (2), 209-26.

Rous, P., and Jones, F. S. (1916). The protection of pathogenic microorganisms by living tissue cells. *J Exp Med*, **23** (5), 601-12.

Ruby, C. E., Funatake, C. J., and Kerkvliet, N. I. (2004). 2,3,7,8-Tetrachlorodibenzo-*p*-dioxin (TCDD) directly enhances the maturation and apoptosis of dendritic cells *in vitro*. *J Immunotoxicol*, **1** (3), 159-66.

Rushmore, T. H., and Pickett, C. B. (1990). Transcriptional regulation of the rat glutathione S-transferase Ya subunit gene. Characterization of a xenobiotic-responsive element controlling inducible expression by phenolic antioxidants. *J Biol Chem*, **265** (24), 14648-53.

Russell, R. C., Fang, C., and Guan, K. L. (2011). An emerging role for TOR signaling in mammalian tissue and stem cell physiology. *Development*, **138** (16), 3343-56.

Rustici, G., Kolesnikov, N., Brandizi, M., Burdett, T., Dylag, M., Emam, I., Farne, A., Hastings, E., Ison, J., Keays, M., Kurbatova, N., Malone, J., Mani, R., Mupo, A., Pereira, R. P., Pilicheva, E., Rung, J., Sharma, A., Tang, Y. A., Ternent, T., Tikhonov, A., Welter, D., Williams, E., Brazma, A., Parkinson, H., and Sarkans, U. (2013). ArrayExpress update - trends in database growth and links to data analysis tools. *Nucleic Acids Res*, **41**, D987-90.

Safe, S. (2001). Molecular biology of the Ah receptor and its role in carcinogenesis. *Toxicol Lett*, **120** (1), 1-7.

Safe, S. H. (1994). Polychlorinated biphenyls (PCBs): environmental impact, biochemical and toxic responses, and implications for risk assessment. *Crit Rev Toxicol*, **24** (2), 87-149.

Safe, S., Fujita, T., Romkes, M., Piskorska-Pliszczynska, J., Homonko, K., and Denomme, M. A. (1986). Properties of the 2,3,7,8-TCDD receptor - a QSAR approach. *Chemosphere*, **15** (9), 1657-63.

Sakaguchi, S., Yamaguchi, T., Nomura, T., and Ono, M. (2008). Regulatory T cells and immune tolerance. *Cell*, **133** (5), 775-87.

Santos-Rosa, H., Schneider, R., Bannister, A. J., Sherriff, J., Bernstein, B. E., Emre, N. T., Schreiber, S. L., Mellor, J., and Kouzarides, T. (2002). Active genes are tri-methylated at K4 of histone H3. *Nature*, **419** (6905), 407-11.

Santostefano, M. J., Johnson, K. L., Whisnant, N. A., Richardson, V. M., DeVito, M. J., and Birnbaum, L. S. (1996). Subcellular localization of TCDD differs between the liver, lungs, and kidneys after acute and subchronic exposure: Species/dose comparisons and possible mechanism. *Fundam Appl Toxicol*, **34** (2), 265-75.

Saurabh, K., Sharma, A., Yadav, S., and Parmar, D. (2010). Polycyclic aromatic hydrocarbon metabolizing cytochrome P450s in freshly prepared uncultured rat blood lymphocytes. B*iochem Pharmacol*, **79** (8), 1182-8.

Saurat, J. H., Kaya, G., Saxer-Sekulic, N., Pardo, B., Becker, M., Fontao, L., Zennegg, M., Schmid, P., Schaad, O., Descombes, P., and Sorg, O. (2012). The cutaneous lesions of dioxin exposure: lessons from the poisoning of Victor Yushchenko. *Toxicol Sci*, **125** (1), 310-7.

Sawyer, T., and Safe, S. (1982). PCB isomers and congeners: Induction of aryl hydrocarbon hydroxylase and ethoxyresorufin *O*-deethylase enzyme activities in rat hepatoma cells. *Toxicol Lett*, **13** (1), 87-93.

Sawyer, T., Bandiera, S., Safe, S., Hutzinger, O., and Olie, K. (1983). Bioanalysis of polychlorinated dibenzofuran and dibenzo-*p*-dioxin mixtures in fly ash. *Chemosphere*, **12** (4/5), 529-36.

SCF (2000). Opinion of the SCF on the risk assessment of dioxins and dioxin-like PCBs in food. European Commission, Brussels, Adopted on 22 November 2000. 1-141.

SCF (2001). Opinion of the SCF on the risk assessment of dioxins and dioxin-like PCBs in food. European Commission, Brussels, Update based on new scientific information available since the adoption of the SCF opinion of 22nd November 2000. Adopted on 30 May 2001. 1-29.

Schecter, A., Päpke, O., Ball, M., and Ryan, J. J. (1991). Partitioning of dioxins and dibenzofurans: whole blood, blood plasma and adipose tissue. *Chemosphere*, **23** (11), 1913-9.

Schiaffonati, L., and Tiberio, L. (1997). Gene expression in liver after toxic injury: analysis of heat shock response and oxidative stress-inducible genes. *Liver*, **17** (4), 183-91.

Schlenstedt, G., Saavedrat, C., Loeb, J. D. L., Colet, C. N, and Silver, P. A. (1995). The GTP-bound form of the yeast Ran/TC4 homologue blocks nuclear protein import and appearance of poly(A)+ RNA in the cytoplasm. *Proc Natl Acad Sci USA*, **92**, 225-9.

Schlosburg, J. E., Blankman, J. L., Long, J. Z., Nomura, D. K., Pan, B., Kinsey, S. G., Nguyen, P. T., Ramesh, D., Booker, L., Burston, J. J., Thomas, E. A., Selley, D. E., Sim-Selley, L. J., Liu, Q. S., Lichtman, A. H., and Cravatt, B. F. (2010). Chronic monoacylglycerol lipase blockade causes functional antagonism of the endocannabinoid system. *Nature Neurosci*, **13** (9), 1113-9.

Schlummer, M., Moser, G. A., and McLachlan, M. S. (1998). Digestive tract absorption of PCDD/Fs, PCBs, and HCB in humans: mass balances and mechanistic considerations. *Toxicol Appl Pharmacol*, **152** (1), 128-37.

Schmidt, J. V., Su, G. H., Reddy, J. K., Simon, M. C., and Bradfield, C. A. (1996). Characterization of a murine Ahr null allele: involvement of the Ah receptor in hepatic growth and development. *Proc Natl Acad Sci U S A*, **93** (13), 6731-6.

Schmitz, H. J., Hagenmaier, A., Hagenmaier, H. P., Bock, K. W., and Schrenk, D. (1995). Potency of mixtures of polychlorinated biphenyls as inducers of dioxin receptor-regulated CYP1A activity in rat hepatocytes and H4IIE cells. *Toxicology*, **99** (1), 47-54.

Schrenk, D., Karger, A., Lipp, H. P., and Bock, K. W. (1992). 2,3,7,8-Tetrachlorodibenzo-*p*-dioxin and ethinylestradiol as co-mitogens in cultured rat hepatocytes. *Carcinogenesis*, **13** (3), 453-6.

Schrenk, D., Stilven, T., Gohl, G., Viebahn, R., and Bock, K. W. (1995). Induction of CYP1A and glutathione S-transferase activities by 2,3,7,8-tetrachlorodibenzo-p-dioxin in human hepatocyte cultures. *Carcinogenesis*, **16** (4), 943-6.

Schrey, P., Wittsiepe, J., Mackrodt, P., and Selenka, F. (1998). Human fecal PCDD/F-excretion exceeds the dietary intake. *Chemosphere*, **37** (9), 1825-831.

Schwab., K., Patterson, L. T., Aronow, B. J., Luckas, R., Liang H. C., and Potter, S.S. (2003). A catalogue of gene expression in the developing kidney. *Kidney Int*, **64**, 1588-604.

Seefeld, M. D., Corbett, S. W., Keesey, R. E., & Peterson, R. E. (1984). Characterization of the wasting syndrome in rats treated with 2,3,7,8-tetrachlorodibenzo-*p*-dioxin. *Environ Health Perspect*, **73** (2), 311-22.

Seglen P. O. (1972): Preparation of rat liver cells. *Expl Cell Res*, **74**; 450-4.

Seidel, S. D., Winters, G. M., Rogers, W. J., Ziccardi, M. H., Li, V., Keser, B., and Denison, M. S. (2001). Activation of the Ah receptor signaling pathway by prostaglandins. *J Biochem Mol Toxicol*, **15** (4), 187-96.

Senft, A. P. (2002). *Aromatic Hydrocarbon Receptor-dependent Mitochondrial Oxidative Stress* (Doctoral dissertation, University of Cincinnati).

Sérée, E., Villard, P. H., Pascussi, J. M., Pineau, T., Maurel, P., Nguyen, Q. B., Fallone, F., Martin, P.-M., Champion, S., Lacarelle, B., Savouret, J.-F, and Barra, Y. (2004). Evidence for a new human CYP1A1 regulation pathway involving PPAR-α and 2 PPRE sites. *Gastroenterology*, **127** (5), 1436-45.

Shaban, Z., El-Shazly, S., Abdelhady, S., Fattouh, I., Muzandu, K., Ishizuka, M., Kimura, K., Kazusaka, A., and Fujita, S. (2004a). Down regulation of hepatic PPARalpha function by AhR ligand. *J Vet Med Sci*, **66** (11), 1377-86.

Shaban, Z., El-Shazly, S., Ishizuka, M., Kimura, K., Kazusaka, A., and Fujita, S. (2004b) PPARalpha-dependent modulation of hepatic CYP1A by clofibric acid in rats. *Arch Toxicol*, **78** (9), 496-507.

Sharma, M. D., Baban, B., Chandler, P., Hou, D. Y., Singh, N., Yagita, H., Azuma, M., Blazar, B. R., Mellor, A., L., and Munn, D. H. (2007). Plasmacytoid dendritic cells from mouse tumor-draining lymph nodes directly activate mature Tregs via indoleamine 2, 3-dioxygenase. *J Clin Invest*, **117** (9), 2570-82.

Sharma, R., Lake, B. G., and Gibson, G. G. (1988). Co-induction of microsomal cytochrome P-452 and the peroxisomal fatty acid β-oxidation pathway in the rat by clofibrate and di-(2-ethylhexyl) phthalate: dose-response studies. *Biochem Pharmacol*, **37** (7), 1203-6.

Shen, E. S., and Whitlock, J. P. (1992). Protein-DNA interactions at a dioxin-responsive enhancer. Mutational analysis of the DNA-binding site for the liganded Ah receptor. *J Biol Chem*, **267** (10), 6815-9.

Shen, X., and Gorovsky, M. A. (1996). Linker histone H1 regulates specific gene expression but not global transcription in vivo. *Cell*, **86** (3), 475-83.

Sherr, D. H., and Monti, S. (2013). The role of the aryl hydrocarbon receptor in normal and malignant B cell development. *Semin Immunopathol*, 35 (6), 705-16

Siest, G., Jeannesson, E., Marteau, J. B., Samara, A., Marie, B., Pfister, M., and Visvikis-Siest, S. (2008). Transcription factor and drug-metabolizing enzyme gene expression in lymphocytes from healthy human subjects. *Drug Metab Dispos*, **36** (1), 182-9.

Silkworth, J. B., Koganti, A., Illouz, K., Possolo, A., Zhao, M., and Hamilton, S. B. (2005). Comparison of TCDD and PCB CYP1A induction sensitivities in fresh hepatocytes from human donors, sprague-dawley rats, and rhesus monkeys and HepG2 cells. *Toxicol Sci*, **87** (2), 508-19.

Sirot, V., Tard, A., Venisseau, A., Brosseaud, A., Marchand, P., Le Bizec, B., and Leblanc, J. C. (2012). Dietary exposure to polychlorinated dibenzo-*p*-dioxins, polychlorinated dibenzofurans and polychlorinated biphenyls of the French population: Results of the second French Total Diet Study. *Chemosphere*, **88** (4), 492-500.

Smith, F. A., Schwetz, B. A., and Nitschke, K. D. (1976). Teratogenicity of 2, 3, 7, 8-tetrachlorodibenzo-*p*-dioxin in CF-1 mice. *Toxicol Appl Pharmacol*, **38** (3), 517-23.

Smyth, G. K. (2004). Linear models and empirical Bayes methods for assessing differential expression in microarray experiments. *Stat Appl Genet Mol Biol*, Volume **3**, Article 3.

Smyth, G. K. (2005). Limma: linear models for microarray data. In *Bioinformatics and computational biology solutions using R and Bioconductor* (Gentleman, R., Carey, V., Dudoit, S., Irizarry R., and Huber W. (eds), pp. 397-420. Springer, New York.

Song, J., Clagett-Dame, M., Peterson, R. E., Hahn, M. E., Westler, W. M., Sicinski, R. R., and DeLuca, H. F. (2002). A ligand for the aryl hydrocarbon receptor isolated from lung. *Proc Natl Acad Sci USA*, **99** (23), 14694-9.

Sorg, O., Zennegg, M., Schmid, P., Fedosyuk, R., Valikhnovskyi, R., Gaide, O., V Kniazevych, and Saurat, J. H. (2009). 2,3,7,8-tetrachlorodibenzo-*p*-dioxin (TCDD) poisoning in Victor Yushchenko: identification and measurement of TCDD metabolites. *Lancet*, **374** (9696), 1179-85.

Soulat, D., Bürckstümmer, T., Westermayer, S., Goncalves, A., Bauch, A., Stefanovic, A., Hantschel, O., Bennett, K. L., Decker, T., and Superti-Furga, G. (2008). The DEAD−box helicase DDX3X is a critical component of the TANK−

binding kinase 1-dependent innate immune response. *EMBO J*, **27** (15), 2135-46.

Sparschu, G. L., Dunn, F., and Rowe, V. K. (1971). Study of the teratogenicity of 2,3,7,8-tetrachiorodibenzo-*p*-dioxin in the rat. *Food Cosmet Toxicol*, **9** (3), 405-12.

Spencer, D. L., Masten, S. A., Lanier, K. M., Yang, X., Grassman, J. A., Miller, C. R., Sutter, T. R., Lucier, G. W., and Walker, N. J. (1999). Quantitative analysis of constitutive and 2, 3, 7, 8-tetrachlorodibenzo-p-dioxin-induced cytochrome P450 1B1 expression in human lymphocytes. *Cancer Epidemiol Biomarkers Prev*, **8** (2), 139-46.

Srere, P. A., and Bhaduri, A. (1962). Incorporation of radioactive citrate into fatty acids. *Biochim Biophys Acta*, **59** (2), 487-9.

Staels, B., van Tol, A., Andreu, T., and Auwerx, J. (1992). Fibrates influence the expression of genes involved in lipoprotein metabolism in a tissue-selective manner in the rat. *Arterioscler Thromb Vasc Biol*, **12** (3), 286-294.

Staels, B., Vu-Dac, N. G. O. V., Kosykh, V. A., Saladin, R., Fruchart, J. C., Dallongeville, J., and Auwerx, J. (1995). Fibrates downregulate apolipoprotein C-III expression independent of induction of peroxisomal acyl coenzyme A oxidase. A potential mechanism for the hypolipidemic action of fibrates. *J Clin Invest*, **95** (2), 705-12.

Steenland, K., Deddens, J., and Piacitelli, L. (2001). Risk assessment for 2,3,7,8-tetrachlorodibenzo-*p*-dioxin (TCDD) based on an epidemiologic study. *Am J Epidemiol*, **154** (5), 451-8.

Steenland, K., Piacitelli, L., Deddens, J., Fingerhut, M., and Chang, L. I. (1999). Cancer, heart disease, and diabetes in workers exposed to 2,3,7,8-tetrachlorodibenzo-p-dioxin. *J Natl Cancer Inst*, **91** (9), 779-86.

Steenland, K., Piacitelli, L., Deddens, J., Fingerhut, M., and Chang, L. I. (1999). Cancer, heart disease, and diabetes in workers exposed to 2, 3, 7, 8-tetrachlorodibenzo-p-dioxin. *J Natl Cancer Inst*, **91** (9), 779-86.

Su, E. J., Cheng, Y. H., Chatterton, R. T., Lin, Z. H., Yin, P., Reierstad, S., Innes, J., and Bulun, S. E. (2007). Regulation of 17-beta hydroxysteroid dehydrogenase type 2 in human placental endothelial cells. *Biol Reprod*, **77** (3), 517-25.

Su, J., Lin, M., and Napoli, J. L. (1999). Complementary Deoxyribonucleic Acid Cloning and Enzymatic Characterization of a Novel 17β/3α-Hydroxysteroid/Retinoid Short Chain Dehydrogenase/Reductase 1. *Endocrinology*, **140** (11), 5275-84.

Sugihara, K., Okayama, T., Kitamura, S., Yamashita, K., Yasuda, M., Miyairi, S., Minobe, Y., and Ohta, S. (2008). Comparative study of aryl hydrocarbon receptor ligand activities of six chemicals in vitro and in vivo. *Arch Toxicol*, **82** (1), 5-11.

Sulentic, C. E., Holsapple, M. P., and Kaminski, N. E. (1998). Aryl hydrocarbon receptor-dependent suppression by 2,3,7,8-tetrachlorodibenzo-*p*-dioxin of IgM secretion in activated B cells. *Mol Pharmacol*, **53** (4), 623-9.

Suskind, R. R. (1985). Chloracne, the hallmark of dioxin intoxication. *Scand J Work Environ Health*, **11** (3), 165-71.

Suskind, R. R. (1985). Chloracne, the hallmark of dioxin intoxication. *Scand J Work Environ Health*, **11** (3), 165-71.

Sutter, T. R., and Greenlee, W. F. (1992). Classification of members of the Ah gene battery. *Chemosphere*, **25** (1-2), 223-6.

Swanson, S. E., Rappe, C., Malmström, J., and Kringstad, K. P. (1988). Emissions of PCDDs and PCDFs from the pulp industry. *Chemosphere*, **17** (4), 681-91.

Tai, H. L., McReynolds, J. H., Goldstein, J. A., Eugster, H. P., Sengstag, C., Alworth, W. L., and Olson, J. R. (1993). Cytochrome-P4501A1 Mediates the Metabolism of 2,3,7,8-Tetrachlorodibenzofuran in the Rat and Human. *Toxicol Appl Pharmacol*, **123** (1), 34-42.

Tamburini, P. P., Masson, H. A., Bains, S. K., Makowski, R. J., Morris, B., and Gibson, G. G. (1984). Mutiple forms of hepatic cytochrome P-450. Purification, characterization and comparison of a novel clofibrate-induced isoenzyme with other major forms of cytochrome P-450. *Eur J Biochem*, **139** (2), 235-46.

Tanaka, G., Kanaji, S., Hirano, A., Arima, K., Shinagawa, A., Goda, C., Yasanuga, S., Ikizawa, K., Yanagihara, Y., Kubo, M., Kuriyama-Fujii, Y., Sugita, Y., Inokuchi, A., and Izuhara, K. (2005). Induction and activation of the aryl hydrocarbon receptor by IL-4 in B cells. *Int Immunol*, **17** (6), 797-805.

Tard, A., Gallotti, S., Leblanc, J. C., and Volatier, J. L. (2007). Dioxins, furans and dioxin-like PCBs: occurrence in food and dietary intake in France. *Food Addit Contam*, **24** (9), 1007-17.

Taylor, M. W., and Feng, G. S. (1991). Relationship between interferon-gamma, indoleamine 2, 3-dioxygenase, and tryptophan catabolism. *FASEB J*, **5** (11), 2516-22.

Thatcher, T. H., and Gorovsky, M. A. (1994). Phylogenetic analysis of the core histones H2A, H2B, H3, and H4. *Nucleic Acids Res*, **22** (2), 174-9.

Thoma, H., Mücke, W., and Kauert, G. (1990). Comparison of the polychlorinated dibenzo-p-dioxin and dibenzofuran in human tissue and human liver. *Chemosphere*, **20** (3), 433-42.

Thomas, M. E., Harris, K. P., Walls, J., Furness, P. N., and Brunskill, N. J. (2002). Fatty acids exacerbate tubulointerstitial injury in protein-overload proteinuria. *Am J Physiol Renal Physiol*, **283** (4), F640-7.

Thömke, F., Jung, D., Besser, R., Röder, R., Konietzko, J., and Hopf, H. C. (1999). Increased risk of sensory neuropathy in workers with chloracne after exposure to 2,3,7,8-polychlorinated dioxins and furans. *Acta Neurol Scand*, **100** (1), 1-5.

Tillitt, D. E., Giesy, J. P., and Ankley, G. T. (1991). Characterization of the H4IIE rat hepatoma cell bioassay as a tool for assessing toxic potency of planar halogenated hydrocarbons in environmental samples. *Environ Sci Technol*, **25** (1), 87-92.

Timsit, Y. E., and Negishi, M. (2007). CAR and PXR: the xenobiotic-sensing receptors. *Steroids*, **72** (3), 231-46.

Törnkvist, A., Glynn, A., Aune, M., Darnerud, P. O., and Ankarberg, E. H. (2011). PCDD/F, PCB, PBDE, HBCD and chlorinated pesticides in a Swedish market basket from 2005–levels and dietary intake estimations. *Chemosphere*, **83** (2), 193-9.

Towbin, H., Staehelin, T., and Gordon, J. (1979). Electrophoretic transfer of proteins from polyacrylamide gels to nitrocellulose sheets: procedure and some applications. *Proc Natl Acad Sci*, **76** (9), 4350-4.

Trnovec, T., Bencko, V., Langer, P., van den Berg, M., Kočan, A., Bergman, A., and Hustak, M. (2004). Study design, objectives, hypotheses, main findings, health consequences for the population exposed, rationale of future research. *Organohalogen Compounds*, **66**, 3573-9.

Trnovec, T., Jusko, T. A., Šovčíková, E., Lancz, K., Chovancová, J., Patayová, H., Palkovičová, L., Drobná, B., Langer, P., van den Berg, M., Dedik, L., and Wimmerová, S. (2013). Relative effect potency estimates of dioxin-like activity for dioxins, furans, and dioxin-like PCBs in adults based on two thyroid outcomes. *Environ Health Perspect*, **121** (8), 886-92.

Truffinet, V., Pinaud, E., Cogné, N., Petit, B., Guglielmi, L., Cogné, M., and Denizot, Y. (2007). The 3' *IgH* locus control region is sufficient to deregulate a c-*myc* transgene and promote mature B cell malignancies with a predominant Burkitt-like phenotype. *J Immunol*, **179**, 6033-42.

Tschesche, H. V. S. J. R. H., Knäuper, V., Krämer, S., Michaelis, J., Oberhoff, R., & Reinke, H. (1991). Latent collagenase and gelatinase from human neutrophils and their activation. *Matrix Suppl*, **1** , 245-55.

Tsuchiya, Y., Nakajima, M., and Yokoi, T. (2003). Critical enhancer region to which AhR/ARNT and Sp1 bind in the human CYP1B1 gene. *J Biochem*, **133** (5), 583-92.

Tsuchiya, Y., Nakajima, M., Kyo, S., Kanaya, T., Inoue, M., and Yokoi, T. (2004). Human CYP1B1 is regulated by estradiol via estrogen receptor. *Cancer Res*, **64** (9), 3119-25.

Tsun, Z. Y., Bar-Peled, L., Chantranupong, L., Zoncu, R., Wang, T., Kim, C., Spooner, E., Sabatini, D. M. (2013). The folliculin tumor suppressor is a GAP for the RagC/D GTPases that signal amino acid levels to mTORC1. *Mol Cell*, **52** (4), 495-505.

Tucker, A. N., Vore, S. J., and Luster, M. I. (1986). Suppression of B cell differentiation by 2,3,7,8-tetrachlorodibenzo-*p*-dioxin. *Mol Pharmacol*, **29** (4), 372-7.

Tugwood, J. D., Issemann, I., Anderson, R. G., Bundell, K. R., McPheat, W. L., and Green, S. (1992). The mouse peroxisome proliferator activated receptor recognizes a response element in the 5'flanking sequence of the rat acyl CoA oxidase gene. *EMBO J*, **11** (2), 433-9.

Tulp, M. T. M., and Hutzinger, O. (1978). Rat metabolism of polychlorinated dibenzo-p-dioxins. *Chemosphere*, **7** (9), 761-8.

Tuominen, R., Warholm, M., Möller, L., and Rannug, A. (2003). Constitutive *CYP1B1* mRNA expression in human blood mononuclear cells in relation to gender, genotype, and environmental factors. *Environ Res*, **93** (2), 138-48.

UNECE (2010). The Protocol on the regional UNECE Convention on Long-Range Transboundary Air Pollution (CLRTAP) on POPs: The 1998 Aarhus protocol on POPs Including the Amendments Adopted by the Parties on 18 December 2009. ECE/EB.AIR/104. 21 April 2010.

UNEP (2013). The Stockholm convention on POPs. Persistent Organic Pollutants Review Committee, ninth meeting, Rome 14-18 October 2013; UNEP/POPS/POPRC.9/13. 28 November 2013.

Van Birgelen, A. P. J. M., van der Kolk, J., Fase, K.M., Bol, I., Poiger, H., Brouwer, A., and van den Berg, M. (1995). Subchronic dose-response study of 2,3,7,8-tetrachlorodibenzo-*p*-dioxin in female Sprague Dawley rats. *Toxicol Appl Pharmacol*, **132**, 1-13.

Van Birgelen, A., and Van den Berg, M. (1998). Toxicokinetics. Draft Monograph for the WHO Consultation on the assessment of the health effects of dioxins: re-

evaluation of the Tolerable Daily Intake. 25-29 May 1998, Geneva, Switzerland.

Van den Berg, M., Birnbaum, L. S., Bosveld, A. T., Brunström, B., Cook, P., Feeley, M., Giesy J. P., Hanberg A., Hasegawa R., Kennedy S. W., Kubiak T., Larsen J. C., van Leeuwen F. X., Liem A. K., Nolt C., Peterson R. E. , Poellinger L., Safe S., Schrenk D., Tillitt D., Tysklind M., Younes M., Waern F., and Zacharewski, T. (1998). Toxic equivalency factors (TEFs) for PCBs, PCDDs, PCDFs for humans and wildlife. *Environ Health Perspect*, **106** (12), 775-92.

Van den Berg, M., Birnbaum, L. S., Denison, M., De Vito, M., Farland, W., Feeley, M., Fiedler, H., Hakansson, H., Hanberg, A., Haws, L., Rose, M., Safe, S., Schrenk, D., Tohyama, C., Tritscher, A., Tuomisto, J., Tysklind, M., Walker, N., and Peterson, R. E. (2006). The 2005 World Health Organization of human and mammalian toxic equivalency factors for dioxins and dioxin-like compounds. *Toxicol Sci*, **93** (2), 223-41.

Van den Berg, M., De Jongh, J., Poiger, H., and Olson, J. R. (1994). The toxicokinetics and metabolism of polychlorinated dibenzo-p-dioxins (PCDDs) and dibenzofurans (PCDFs) and their relevance for toxicity. *Crit Rev Toxicol*, **24** (1), 1-74.

Van Duursen, M. B., Sanderson, J. T., and van den Berg, M. (2005). Cytochrome P450 1A1 and 1B1 in human blood lymphocytes are not suitable as biomarkers of exposure to dioxin-like compounds: polymorphisms and interindividual variation in expression and inducibility. *Toxicol Sci*, **85** (1), 703-12.

Van Ede, K. I., Andersson, P. L., Gaisch, K. P., van den Berg, M., and van Duursen, M. B. (2014a). Comparison of intake and systemic relative effect potencies of dioxin-like compounds in female rats after a single oral dose. *Arch Toxicol*, **88** (3), 637-46.

Van Ede, K. I., Aylward, L. L., Andersson, P. L., van den Berg, M., and van Duursen, M. (2013b). Tissue distribution of dioxin-like compounds: Potential impacts on systemic relative potency estimates. *Toxicol Lett*, **220** (3), 294-302.

Van Ede, K. I., Gaisch, K. P. J., Andersson, P. L., van den Berg, M., van Duursen, M. B. M. (2011). "Induction of CYP1A1 and AhRR Gene Expression in Female Mouse and Rat Lymphocytes by TCDD, 4-PeCDF and PCB126: Uptake Versus Systemic Dose Levels". Proceedings of Dioxin 2011. *Organohalogen Compounds*, **73**, 476-79.

Van Ede, K. I., Gaisch, K. P., van den Berg, M., and van Duursen, M. (2014b). Differential relative effect potencies of some dioxin-like compounds in human peripheral blood lymphocytes and murine splenic cells. *Toxicol Lett*, **226** (1), 43-52.

Van Leeuwen, F. X., Feeley, M., Schrenk, D., Larsen, J. C., Farland, W., and Younes, M. (2000). Dioxins: WHO's tolerable daily intake (TDI) revisited. *Chemosphere*, **40** (9), 1095-101.

Van Leeuwen, F. X., Feeley, M., Schrenk, D., Larsen, J. C., Farland, W., and Younes, M. (2000). Dioxins: WHO's tolerable daily intake (TDI) revisited. *Chemosphere*, **40** (9), 1095-101.

Vanden Heuvel, J. P. (1999). Peroxisome proliferator-activated receptors (PPARS) and carcinogenesis. *Toxicol Sci*, **47** (1), 1-8.

Vanden Heuvel, J. P., Clark, G. C., Thompson, C. L., McCoy, Z., Miller, C. R., Lucier, G. W., and Bell, D. A. (1993). CYP1A1 mRNA levels as a human exposure biomarker: use of quantitative polymerase chain reaction to measure CYP1A1 expression in human peripheral blood lymphocytes. *Carcinogenesis*, **14** (10), 2003-6.

Varvas, K., Kurg, R., Hansen, K., Järving, R., Järving, I., Valmsen, K., Lõhelaid H, and Samel, N. (2009). Direct evidence of the cyclooxygenase pathway of prostaglandin synthesis in arthropods: genetic and biochemical characterization of two crustacean cyclooxygenases. *Insect Biochem Mol Biol*, **39** (12), 851-60.

Veerkamp, W., Wever, J., and Hutzinger, O. (1981). The metabolism of some chlorinated dibenzofurans by rats. *Chemosphere*, **10** (4), 397-403.

Veldhoen, M., Hirota, K., Westendorf, A. M., Buer, J., Dumoutier, L., Renauld, J. C., and Stockinger, B. (2008). The aryl hydrocarbon receptor links TH17-cell-mediated autoimmunity to environmental toxins. *Nature*, ***453*** (7191), 106-9.

Vogel, C. F., Goth, S. R., Dong, B., Pessah, I. N., and Matsumura, F. (2008). Aryl hydrocarbon receptor signaling mediates expression of indoleamine 2,3-dioxygenase. *Biochem Biophys Res Commun*, **375** (3), 331-5.

Vorderstrasse, B. A., and Kerkvliet, N. I. (2001). 2,3,7,8-Tetrachlorodibenzo-*p*-dioxin Affects the Number and Function of Murine Splenic Dendritic Cells and Their Expression of Accessory Molecules. *Toxicol Appl Pharmacol*, **171** (2), 117-25.

Wahli, W., Braissant, O., and Desvergne, B. (1995). Peroxisome proliferator activated receptors: transcriptional regulators of adipogenesis, lipid metabolism and more…. *Chem Biol*, **2** (5), 261-6.

Waller, C. L., and McKinney, J. D. (1992). Comparative molecular field analysis of polyhalogenated dibenzo-*p*-

dioxins, dibenzofurans, and biphenyls. *J Med Chem*, **35** (20), 3660-6.

Waller, C. L., and McKinney, J. D. (1995). Three-dimensional quantitative structure-activity relationships of dioxins and dioxin-like compounds: model validation and Ah receptor characterization. *Chem Res Toxicol*, **8** (6), 847-58.

Wang, C., Xu, C. X., Krager, S. L., Bottum, K. M., Liao, D. F., and Tischkau, S. A. (2011). Aryl hydrocarbon receptor deficiency enhances insulin sensitivity and reduces PPAR-α pathway activity in mice. *Environ Health Perspect*, **119** (12), 1739-44.

Wang, X., Santostefano, M. J., Evans, M. V., Richardson, V. M., Diliberto, J. J., and Birnbaum, L. S. (1997). Determination of parameters responsible for pharmacokinetic behavior of TCDD in female Sprague–Dawley rats. *Toxicol Appl Pharmacol*, **147** (1), 151-68.

Watanabe, H., Suzuki, A., Kobayashi, M., Lubahn, D. B., Handa, H., and Iguchi, T. (2003). Similarities and differences in uterine gene expression patterns caused by treatment with physiological and non-physiological estrogens. *J Mol Endocrinol*, **31**, 487-97.

Watanabe, M. X., Kunisue, T., Ueda, N., Nose, M., Tanabe, S., and Iwata, H. (2013). Toxicokinetics of dioxins and other organochlorine compounds in Japanese people: Association with hepatic CYP1A2 expression levels. *Environ Int*, **53**, 53-61.

Wei, P., Zhang, J., Dowhan, D. H., Han, Y., and Moore, D. D. (2002). Specific and overlapping functions of the nuclear hormone receptors CAR and PXR in xenobiotic response. *Pharmacogenomics J*, **2** (2), 117-26.

Weis, K. (2003). Regulating access to the genome: Nucleocytoplasmic transport throughout the cell cycle. *Cell*, **112**, 441-51.

Weistrand, C., and Norén K. (1998). Polychlorinated naphthalenes and other organochlorine contaminants in human adipose and liver tissue. *J Toxicol Environ Health A*, *53*(4), 293-311.

Wendling, J. M., Orth, R. G., and Poiger, H. (1990). Determination of [^{3}H]-2,3,7,8-tetrachlorodibenzo-p-dioxin in human feces to ascertain its relative metabolism in man. *Anal Chem*, **62** (8), 796-800.

Wens, B., De Boever, P., Maes, M., Hollanders, K., and Schoeters, G. (2011). Transcriptomics identifies differences between ultrapure non-dioxin-like polychlorinated biphenyls (PCBs) and dioxin-like PCB126 in cultured peripheral blood mononuclear cells. *Toxicology*, **287** (1), 113-23.

Wens, B., De Boever, P., Verbeke, M., Hollanders, K., and Schoeters, G. (2013). Cultured human peripheral blood mononuclear cells alter their gene expression when challenged with endocrine-disrupting chemicals. *Toxicology*, **303**, 17-24.

Whitlock, J. P., Jr. (1993). Mechanistic aspects of dioxin action. *Chem Res Toxicol*, **6**, 754-63.

WHO (2000). Consultation on assessment of the health risk of dioxins; re-evaluation of the tolerable daily intake (TDI): executive summary. *Food Addit Contam*, **17** (4), 223-40.

WHO, 2000. Assessment of the health risk of dioxins: re-evaluation of the tolerable daily intake (TDI): executive summary. *Food Add Contam*, **17**, 223-40.

Windal, I., Vandevijvere, S., Maleki, M., Goscinny, S., Vinkx, C., Focant, J. F., Eppe, G., Hanot, V., Van Loco, J. (2010). Dietary intake of PCDD/Fs and dioxin-like PCBs of the Belgian population. *Chemosphere*, **79** (3), 334-40.

Wirbelauer, C., Bell, O., and Schübeler, D. (2005). Variant histone H3. 3 is deposited at sites of nucleosomal displacement throughout transcribed genes while active histone modifications show a promoter-proximal bias. *Genes Dev*, **19** (15), 1761-6.

Wortham, N. C., Ahamed, E., Nicol, S. M., Thomas, R. S., Periyasamy, M., Jiang, J., Ochocka, A. M., Shousha, S., Huson, L., Bray, S. E., Coombes, R. C., Ali, S., Fuller-Pace, F. V., and Fuller-Pace, F. V. (2009). The DEAD-box protein p72 regulates ERα-/oestrogen-dependent transcription and cell growth, and is associated with improved survival in ERα-positive breast cancer. *Oncogene*, **28** (46), 4053-64.

Wroblewski, V. J., and Olson, J. R. (1985). Hepatic metabolism of 2,3,7,8-tetrachlorodibenzo-*p*-dioxin (TCDD) in the rat and guinea pig. *Toxicol Appl Pharmacol*, **81** (2), 231-40.

Xie, W., Barwick, J. L., Simon, C. M., Pierce, A. M., Safe, S., Blumberg, B., Guzelian, P. S., and Evans, R. M. (2000). Reciprocal activation of xenobiotic response genes by nuclear receptors SXR/PXR and CAR. *Genes Dev*, **14** (23), 3014-23.

Xu, L., Li, A. P., Kaminski, D. L., and Ruh, M. F. (2000). 2, 3, 7, 8 Tetrachlorodibenzo-*p*-dioxin induction of cytochrome P4501A in cultured rat and human hepatocytes. *Chem Biol Interact*, **124** (3), 173-89.

Yaffe, M. B., Rittinger, K., Volinia, S., Caron, P. R., Aitken, A., Leffers, H., Gamblin, S. J., Smerdon, S. J., and Cantley, L. C. (1997). The structural basis for 14-3-3: phosphopeptide binding specificity. *Cell*, **91** (7), 961-71.

Yanagawa, T., Ishikawa, T., Ishii, T., Tabuchi, K., Iwasa, S., Bannai, S., Omura, K., Suzuki, H., and Yoshida, H. (1999) Peroxiredoxin I expression in human thyroid tumors. *Cancer Lett*, **145** (1-2), 127-32.

Yanagida, A., Sogawa, K., Yasumoto, K. I., and Fujii-Kuriyama, Y. (1990). A novel cis-acting DNA element required for a high level of inducible expression of the rat P-450c gene. *Mol Cell Biol*, **10** (4), 1470-5.

Yang, X. J., and Grégoire, S. (2005). Class II histone deacetylases: from sequence to function, regulation, and clinical implication. *Mol Cell Biol*, **25** (8), 2873-84.

Yang, Y., Kim, A. H., Yamada, T., Wu, B., Bilimoria, P. M., Ikeuchi, Y., de la Iglesia, N., Shen, J., and Bonni, A. (2009). A Cdc20-APC ubiquitin signaling pathway regulates presynaptic differentiation. *Science*, **326** (5952), 575-8.

Yao, H., Ashihara, E., Strovel, J. W., Nakagawa, Y., Kuroda, J., Nagao, R., Tanaka, R., Yokota, A., Takeuchi, M., Hayashi, Y., Shimazaki, C., Taniwaki, M., Strand, K., Padia, J., Hirai, H., Kimura, S., and Maekawa, T. (2011). AV-65, a novel Wnt/β-catenin signal inhibitor, successfully suppresses progression of multiple myeloma in a mouse model. *Blood Cancer J*, **1** (11), e43.

Yasen, M., Mizushima, H., Mogushi, K., Obulhasim, G., Miyaguchi, K., Inoue, K., Nakahara, I., Ohta, T., Aihara, A., Tanaka, S., Arii, S., and Tanaka, H. (2009). Expression of Aurora B and alternative variant forms in hepatocellular carcinoma and adjacent tissue. *Cancer Sci*, **100** (3), 472-80.

Yoshida, T., Katsuya, K., Oka, T., Koizumi, S. I., Wakita, D., Kitamura, H., and Nishimura, T. (2012). Effects of AhR ligands on the production of immunoglobulins in purified mouse B cells. *Biomed Res*, **33** (2), 67-74.

Zeiger, M., Haag, R., Höckel, J., Schrenk, D., and Schmitz, H. J. (2001). Inducing effects of dioxin-like polychlorinated biphenyls on CYP1A in the human hepatoblastoma cell line HepG2, the rat hepatoma cell line H4IIE, and rat primary hepatocytes: comparison of relative potencies. *Toxicol Sci*, **63** (1), 65-73.

Zeng, W., Wharton, K. A., Mack, J. A., Wang, K., Gadbaw, M., Suyama, K., Klein, P. S., and Scott, M. P. (2000). naked cuticle encodes an inducible antagonist of Wnt signalling. *Nature*, **403** (6771), 789-95.

Zha, J., Harada, H., Yang, E., Jockel, J., and Korsmeyer, S. J. (1996). Serine Phosphorylation of Death Agonist BAD in Response to Survival Factor Results in Binding to 14-3-3 Not BCL-X_L. *Cell*, **87** (4), 619-28.

Zhang, L., Li, J., Liu, X., Zhao, Y., Li, X., Wen, S., and Wu, Y. (2013). Dietary intake of PCDD/Fs and dioxin-like PCBs from the Chinese total diet study in 2007. *Chemosphere*, **90** (5), 1625-30.

Zhang, L., Savas, Ü., Alexander, D. L., and Jefcoate, C. R. (1998). Characterization of the mouse CYP1B1 gene Identification of an enhancer region that directs aryl hydrocarbon receptor-mediated constitutive and induced expression. *J Biol Chem*, **273** (9), 5174-83.

Zhang, P. J., Wei, R., Wen, X. Y., Ping, L., Wang, C. B., Dong, Z. N., Deng, X.X., Bo, W., Bin, C., and Tian, Y. P. (2012). Genes expression profiling of peripheral blood cells of patients with hepatocellular carcinoma. *Cell Biol Int*, **36** (9), 803-9.

Zhang, S., Li, Y., Wu, Y., Shi, K., Bing, L., and Hao, J. (2012). Wnt/β-Catenin Signaling Pathway Upregulates c−Myc Expression to Promote Cell Proliferation of P19 Teratocarcinoma Cells. *Anat Rec (Hoboken)*, **295** (12), 2104-13.

Zhang, Z., Schwartz, S., Wagner, L., and Miller,W. (2000). A greedy algorithm for aligning DNA sequences, *J Comput Biol*; **7** (1-2), 203-14.

Zhang, Z., Yamashita, H., Toyama, T., Sugiura, H., Omoto, Y., Ando, Y., Mita, K., Hamaguchi, M., Hayashi, S., and Iwase, H. (2004). HDAC6 expression is correlated with better survival in breast cancer. *Clin Cancer Res*, **10** (20), 6962-8.

Zhao J., Chen, J., Lu, B., Dong, L., Wang, H., Bi, C., Wu, G., Guo, H., Wu, M., Guo, Y.. (2008a). TIP30 induces apoptosis under oxidative stress through stabilization of p53 messenger RNA in human hepatocellular carcinoma. *Cancer Res*, **68** (11), 4133-41.

Zhao, Y. Y., Tao, F. M., and Zeng, E. Y. (2008b). Theoretical study of the quantitative structure–activity relationships for the toxicity of dibenzo-*p*-dioxins. *Chemosphere*, **73** (1), 86-91.

Zieve, L., Anderson, W. R., Dozeman, R., Draves, K., and Lyftogt, C. (1985). Acetaminophen liver injury: sequential changes in two biochemical indices of regeneration and their relationship to histologic alterations. *J Lab Clin Med*, **105** (5), 619-24.

Attachments

I. Supplemental tables

Table 56: Mouse whole genome microarray analysis. Top 20 genes accordantly down-regulated in mouse livers by 1-PeCDD (25 µg/kg bw, three days), and TCDD (25 µg/kg bw, three days). TCDD-raw data by courtesy of Christiane Lohr (Lohr, 2013). Cutoff values: A ≥ 27, lfc ≤ -1, p-value < 0.05.

1-PeCDD & TCDD lfc	lcf	Gene systematic name	Gene description	**Gene name**
-1.320	-2.846	NM_013692	Kruppel-like factor 10	*Klf10*
-2.535/ -2.537	-2.573/ -2.488	BC031891/ NR_002861	serine (or cysteine) peptidase inhibitor clade A member 4 pseudogene 1	*Serpina4-ps1*
-2.244- -2.138	-2.276- -2.141	NM_207655	epidermal growth factor receptor	*Egfr*
-2.797- -2.009	-2.125- -1.545	NM_007706	suppressor of cytokine signaling 2	*Socs2*
-1.323	-2.025	NM_144942	cysteine sulfinic acid decarboxylase	*Csad*
-1.312	-1.886	NM_009744	B-cell leukemia/lymphoma 6	*Bcl6*
-1.889	-1.821	XM_001003154	similar to Glucose phosphate isomerase 1 transcript variant 2	*LOC676974*
-1.865	-1.806	NM_130450	ELOVL family member 6 elongation of long chain fatty acids (yeast)	*Elovl6*
-1.429	-1.734	NM_010390	histocompatibility 2 Q region locus 1	*H2-Q1*
-1.242	-1.694	NM_001081212	insulin receptor substrate 2	*Irs2*
-1.650- -1.372	-1.689- -1.594	NM_029720	cysteine-rich with EGF-like domains 2	*Creld2*
-1.281	-1.675	NM_144796	sushi domain containing 4	*Susd4*
-1.616	-1.669	NM_183257	hepcidin antimicrobial peptide 2	*Hamp2*
-1.556	-1.649	XM_886827	predicted gene EG622384	*Fabp5l2*
-1.894	-1.557	NM_009723	ATPase Ca++ transporting plasma membrane 2	*Atp2b2*
-1.843	-1.538	NM_175475	cytochrome P450 family 26 subfamily b polypeptide 1	*Cyp26b1*
-1.566	-1.531	NAP114472-1	Unknown	*NAP114472-1*
-1.495	-1.525	NM_010634	fatty acid binding protein 5 epidermal	*Fabp5*
-2.087	-1.502	NM_001111110	cytidine monophospho-N-acetylneuraminic acid hydroxylase transcript variant 2	*Cmah*
-1.560	-1.481	NM_028769	synovial apoptosis inhibitor 1 synoviolin	*Syvn1*

Values b/a from oligo b/oligo a; values a-n: value range of more than two (n) oligos.

Table 57: Mouse whole genome microarray analysis. Top 20 genes accordantly up-regulated in mouse livers by 4-PeCDF (250 µg/kg bw, three days), and TCDD (25 µg/kg bw, three days). TCDD-raw data by courtesy of Christiane Lohr (Lohr, 2013). Cutoff values: A ≥ 27, lfc ≥ 1, p-value < 0.05.

4-PeCDF & TCDD lfc	lcf	Gene systematic name	Gene description	**Gene name**
5.994	9.478	NM_009992	cytochrome P450 family 1 subfamily a polypeptide 1	*Cyp1a1*
2.926	5.169	NM_009994	cytochrome P450 family 1 subfamily b polypeptide 1	*Cyp1b1*
2.414	3.985	NM_009993	cytochrome P450 family 1 subfamily a polypeptide 2	*Cyp1a2*
3.052	3.582	NM_010210	fragile histidine triad gene	*Fhit*
1.880	3.379	NM_017379	tubulin alpha 8	*Tuba8*
3.413	3.103	NM_027872	solute carrier family 46 member 3	*Slc46a3*
3.240	2.903	NM_178892	TCDD-inducible poly(ADP-ribose) polymerase	*Tiparp*
2.705	2.819	NM_008181	glutathione S-transferase alpha 1 (Ya)	*Gsta1*
1.580	2.722	XM_001477458	predicted gene ENSMUSG00000054044	*Gm9933*
1.796	2.678	NM_016865	HIV-1 tat interactive protein 2 homolog (human)	*Htatip2*
1.054	2.518	NM_025557	Purkinje cell protein 4-like 1	*Pcp4l1*
1.724	2.153	NM_023440	transmembrane protein 86B	*Tmem86b*
1.510	2.123	NM_026791	F-box and WD-40 domain protein 9	*Fbxw9*
1.397	1.978	NM_028747	RIKEN cDNA 0610012H03 gene	*0610012H03Rik*
1.629/ 1.941	1.857/ 1.362	NM_013541	glutathione S-transferase pi 1	*Gstp1*
2.925/ 2.197	1.853/ 1.036	NM_001122660	predicted gene 10639	*Gm10639*
1.455	1.762	NM_001163577	prominin 1	*Prom1*
4.227	1.758	NM_007643	CD36 antigen transcript variant 2	*Cd36*
1.232	1.702	NM_007689	chondroadherin	*Chad*
3.055/ 3.085	1.696/ 1.650	NM_145603	carboxylesterase 2	*Ces2*

Values b/a from oligo b/oligo a.

Table 58: Mouse whole genome microarray analysis. Top 20 genes accordantly down-regulated in mouse livers by 4-PeCDF (250 µg/kg bw, three days), and TCDD (25 µg/kg bw, three days). TCDD- raw data by courtesy of Christiane Lohr (Lohr, 2013). Cutoff values: A ≥ 27, lfc ≤ -1, p-value < 0.05.

4-PeCDF & TCDD lfc	lcf	Gene systematic name	Gene description	**Gene name**
-6.185/ -6.176	-2.573/ -2.488	BC031891/ NR_002861	serine (or cysteine) peptidase inhibitor clade A member 4 pseudogene 1	*Serpina4-ps1*
-2.026- -1.742	-2.125- -2.003	NM_007706	suppressor of cytokine signaling 2	*Socs2*
-2.089	-1.890	XM_001475897	similar to myosin XV	*LOC100046261*
-3.233	-1.821	XM_001003154	similar to Glucose phosphate isomerase 1 transcript variant 2	*LOC676974*
-1.551	-1.694	NM_001081212	insulin receptor substrate 2	*Irs2*
-1.063	-1.675	NM_144796	sushi domain containing 4	*Susd4*
-2.335	-1.645	ENSMUST0000 0111752	Homeobox protein cut-like 2	*Cux2*
-1.551	-1.560	ENSMUST0000 0006786	Sodium-dependent phosphate transport protein 3 (Sodium/phosphate cotransporter 3)(Na(+)/PI cotransporter 3) (Solute carrier family 17 member 2)	*Slc17a2*
-1.477	-1.557	NM_009723	ATPase Ca++ transporting plasma membrane 2	*Atp2b2*
-3.971	-1.502	NM_001111110	cytidine monophospho-N-acetylneuraminic acid hydroxylase	*Cmah*
-3.753	-1.439	NM_001081141	gamma-aminobutyric acid (GABA) B receptor 2	*Gabbr2*
-3.042	-1.432	NM_007606	carbonic anhydrase 3	*Car3*
-1.048	-1.425	NM_008061	glucose-6-phosphatase catalytic	*G6pc*
-3.525	-1.423	NM_134037	ATP citrate lyase	*Acly*
-3.371	-1.387	AK017236	adult male pituitary gland	*5330406M23Rik*
-4.422- -4.290	-1.387- -1.328	NM_009692	apolipoprotein A-I	*Apoa1*
-2.090	-1.378	AK017143	11 days pregnant adult female ovary and uterus cDNA	*5031425E22Rik*
-1.610/ -1.701	-1.374/ -1.328	NM_027147	energy homeostasis associated	*Enho*
-2.076	-1.335	NM_019423	elongation of very long chain fatty acids (FEN1/Elo2 SUR4/Elo3 yeast)-like 2	*Elovl2*
-1.853	-1.309	AK050412	adult male liver tumor cDNA	*1810008I18Rik*

Values b/a from oligo b/oligo a; values a-n: value range of more than two (n) oligos.

Table 59: Mouse whole genome microarray analysis. Twelve genes accordantly down-regulated in mouse livers by PCB 118 (150000 µg/kg bw, three days), and TCDD (25 µg/kg bw, three days). TCDD-raw data by courtesy of Christiane Lohr (Lohr, 2013). Cutoff values: A ≥ 27, lfc ≤ -1, p-value < 0.05.

PCB 118 & TCDD lfc	lcf	Gene systematic name	Gene description	**Gene name**
-1.383	-2.846	NM_013692	Kruppel-like factor 10	*Klf10*
-1.023	-1.890	XM_001475897	similar to myosin XV (LOC100046261)	*LOC100046261*
-2.119	-1.886	NM_009744	B-cell leukemia/lymphoma 6	*Bcl6*
-1.636	-1.821	XM_001003154	similar to Glucose phosphate isomerase 1 transcript variant 2 (LOC676974)	*LOC676974*
-2.255	-1.694	NM_001081212	insulin receptor substrate 2	*Irs2*
-1.044	-1.675	NM_144796	sushi domain containing 4	*Susd4*
-1.879	-1.425	NM_008061	glucose-6-phosphatase catalytic	*G6pc*
-2.033	-1.387	AK017236	adult male pituitary gland cDNA RIKEN full-length enriched library	*5330406M23Rik*
-1.265 -1.235	-1.387- -1.328	NM_009692	apolipoprotein A-I	*Apoa1*
-1.209	-1.113	XM_001471861	hypothetical protein LOC100044148	*Etnk2*
-1.003	-1.103	XM_001481023	hypothetical protein LOC100043770	*Gm4635*
-1.035	-1.055	NM_001081065	zinc finger protein 707	*Zfp707*

Value range of more than two (n) oligos: values a-n.

Table 60: Mouse whole genome microarray analysis. Top 20 genes accordantly up-regulated in mouse livers by PCB 126 (250 µg/kg bw, three days), and TCDD (25 µg/kg bw, three days). TCDD-raw data by courtesy of Christiane Lohr (Lohr, 2013). Cutoff values: A ≥ 27, lfc ≥ 1, p-value < 0.05.

PCB 126 & TCDD lfc	lcf	Gene systematic name	Gene description	**Gene name**
6.292	9.478	NM_009992	cytochrome P450 family 1 subfamily a polypeptide 1	*Cyp1a1*
2.557	5.169	NM_009994	cytochrome P450 family 1 subfamily b polypeptide 1	*Cyp1b1*
2.555	3.985	NM_009993	cytochrome P450 family 1 subfamily a polypeptide 2	*Cyp1a2*
2.056	3.582	NM_010210	fragile histidine triad gene	*Fhit*
1.767	3.379	NM_017379	tubulin alpha 8	*Tuba8*
3.172	3.103	NM_027872	solute carrier family 46 member 3	*Slc46a3*
1.431	2.903	NM_178892	TCDD-inducible poly(ADP-ribose) polymerase	*Tiparp*
3.095	2.819	NM_008181	glutathione S-transferase alpha1 (Ya)	*Gsta1*
1.134	2.678	NM_016865	HIV-1 tat interactive protein 2 homolog (human)	*Htatip2*
1.451	2.518	NM_025557	Purkinje cell protein 4-like 1	*Pcp4l1*
2.542	2.153	NM_023440	transmembrane protein 86B	*Tmem86b*
1.423	2.123	NM_026791	F-box and WD-40 domain protein 9	*Fbxw9*
1.159/ 2.161	1.857/ 1.362	NM_013541	glutathione S-transferase pi 1	*Gstp1*
3.049/ 2.144	1.853/ 1.036	NM_001122660	predicted gene 10639	*Gm10639*
1.464	1.762	NM_001163577	prominin 1	*Prom1*
2.282	1.758	NM_007643	CD36 antigen	*Cd36*
2.860/ 2.770	1.696/ 1.650	NM_145603	carboxylesterase 2	*Ces2*
1.035	1.653	NM_001166250	monoglyceride lipase	*Mgll*
3.250	1.630	NM_198171	cDNA sequence BC015286	*BC015286*
1.381/ 2.045	1.621/ 1.211	NM_025341	abhydrolase domain containing 6	*Abhd6*

Values b/a from oligo b/oligo a.

Table 61: Mouse whole genome microarray analysis. Top 20 genes accordantly down-regulated in mouse livers by PCB 126 (250 µg/kg bw, three days), and TCDD (25 µg/kg bw, three days). TCDD-raw data by courtesy of Christiane Lohr (Lohr, 2013). Cutoff values: A ≥ 27, lfc ≤ -1, p-value < 0.05.

PCB 126 & TCDD lfc	TCDD lcf	Gene systematic name	Gene description	Gene name
-4.502/ -4.480	-2.573/- 2.488	BC031891/ NR_002861	serine (or cysteine) peptidase inhibitor clade A member 4 pseudogene 1	*Serpina4-ps1*
-1.345	-1.890	XM_001475897	similar to myosin XV	*LOC100046261*
-1.479	-1.821	XM_001003154	similar to Glucose phosphate isomerase 1	*LOC676974*
-2.174	-1.502	NM_001111110	cytidine monophospho-N-acetylneuraminic acid hydroxylase	*Cmah*
-1.879	-1.439	NM_001081141	gamma-aminobutyric acid (GABA) B receptor 2	*Gabbr2*
-1.230	-1.432	NM_007606	carbonic anhydrase 3	*Car3*
-2.087	-1.425	NM_008061	glucose-6-phosphatase catalytic	*G6pc*
-1.873	-1.423	NM_134037	ATP citrate lyase	*Acly*
-1.809	-1.387	AK017236	adult male pituitary gland cDNA	*5330406M23Rik*
-3.308- -3.260	-1.387- -1.328	NM_009692	apolipoprotein A-I	*Apoa1*
-1.068/ -1.067	-1.295/ -1.229	NM_009569	zinc finger protein multitype 1	*Zfpm1*
-1.259	-1.276	NM_145368	acyl-coenzyme A amino acid N-acyltransferase 2	*Acnat2*
-1.091	-1.214	NM_144836	solute carrier family 17 (sodium phosphate) member 2	*Slc17a2*
-2.283	-1.154	NM_198414	progestin and adipoQ receptor family member IX	*Paqr9*
-1.214	-1.150	NM_198649	actin binding LIM protein family member 3	*Ablim3*
-1.964	-1.135	ENSMUST00000099683	Unknown	*ENSMUST0000 0099683*
-1.051	-1.113	XM_001471861	hypothetical protein LOC100044148	*Etnk2*
-2.885	-1.103	XM_001481023	hypothetical protein LOC100043770	*Gm4635*
-1.894/ -1.951	-1.092/ -1.001	ENSMUST00000099050	Unknown	*ENSMUST0000 0099050*
-1.743	-1.073	ENSMUST00000099046	Unknown	*ENSMUST0000 0099046*

Values b/a from oligo b/oligo a; values a-n: value range of more than two (n) oligos.

Table 62: Mouse whole genome microarray analysis. Top 20 genes accordantly up-regulated in mouse livers by PCB 156 (150000 µg/kg bw, three days), and TCDD (25 µg/kg bw, three days). TCDD-raw data by courtesy of Christiane Lohr (Lohr, 2013). Cutoff values: A ≥ 27, lfc ≥ 1, p-value < 0.05.

PCB 156 & TCDD lfc	**TCDD** lcf	Gene systematic name	Gene description	**Gene name**
7.467	9.478	NM_009992	cytochrome P450 family 1 subfamily a polypeptide 1	*Cyp1a1*
3.652	5.169	NM_009994	cytochrome P450 family 1 subfamily b polypeptide 1	*Cyp1b1*
3.402	3.985	NM_009993	cytochrome P45 family 1 subfamily a polypeptide 2	*Cyp1a2*
3.861	3.582	NM_010210	fragile histidine triad gene	*Fhit*
2.352	3.379	NM_017379	tubulin alpha 8	*Tuba8*
2.845	3.103	NM_027872	solute carrier family 46 member 3	*Slc46a3*
1.331	2.903	NM_178892	TCDD-inducible poly(ADP-ribose) polymerase	*Tiparp*
4.006	2.819	NM_008181	glutathione S-transferase alpha 1 (Ya)	*Gsta1*
1.033	2.722	XM_001477458	predicted gene ENSMUSG00000054044	*Gm9933*
2.494	2.678	NM_016865	HIV-1 tat interactive protein 2 homolog (human)	*Htatip2*
1.359	2.518	NM_025557	Purkinje cell protein 4-like 1	*Pcp4l1*
1.016	2.386	NM_013872	phosphomannomutase 1	*Pmm1*
2.236	2.153	NM_023440	transmembrane protein 86B	*Tmem86b*
2.067	2.123	NM_026791	F-box and WD-40 domain protein 9	*Fbxw9*
1.720	1.978	NM_028747	RIKEN cDNA 0610012H03 gene	*0610012H03Rik*
1.900/ 1.174	1.931/ 1.039	NM_007618	serine (or cysteine) peptidase inhibitor clade A member 6	*Serpina6*
2.309/ 2.269	1.857/ 1.362	NM_013541	glutathione S-transferase pi 1	*Gstp1*
3.939/ 2.268	1.853/ 1.036	NM_001122660	predicted gene 10639	*Gm10639*
2.622	1.758	NM_007643	CD36 antigen	*Cd36*
1.556	1.702	NM_007689	chondroadherin	*Chad*

Values b/a from oligo b/oligo a.

Table 63: Mouse whole genome microarray analysis. Top 20 genes accordantly down-regulated in mouse livers by PCB 156 (150000 µg/kg bw, three days), and TCDD (25 µg/kg bw, three days). TCDD-raw data by courtesy of Christiane Lohr (Lohr, 2013). Cutoff values: A ≥ 27, lfc ≤ -1, p-value < 0.05.

PCB 156 & lfc	TCDD lcf	Gene systematic name	Gene description	Gene name
-1.423	-2.846	NM_013692	Kruppel-like factor 10	*Klf10*
-4.279/ -4.481	-2.573/ -2.488	BC031891/ NR_002861	serine (or cysteine) peptidase inhibitor clade A member 4 pseudogene 1	*Serpina4-ps1*
-2.005- -2.089	-2.276- -2.141	NM_207655	epidermal growth factor receptor	*Egfr*
-1.549	-1.890	XM_001475897	similar to myosin XV	*LOC100046261*
-2.090	-1.886	NM_009744	B-cell leukemia/lymphoma 6	*Bcl6*
-2.953	-1.821	XM_001003154	similar to Glucose phosphate isomerase 1	*LOC676974*
-1.002	-1.734	NM_010390	histocompatibility 2 Q region locus 1	*H2-Q1*
-2.591	-1.694	NM_001081212	insulin receptor substrate 2	*Irs2*
-1.619	-1.675	NM_144796	sushi domain containing 4	*Susd4*
-1.374	-1.669	NM_183257	hepcidin antimicrobial peptide 2	*Hamp2*
-1.451	-1.560	ENSMUST0000 0006786	ens|Sodium-dependent phosphate transport protein 3 (Sodium/phosphate cotransporter 3)(Na(+)/PI cotransporter 3)(Solute carrier family 17 member 2)	*Slc17a2*
-1.311	-1.557	NM_009723	ATPase Ca++ transporting plasma membrane 2	*Atp2b2*
-2.491	-1.502	NM_001111110	cytidine monophospho-N-acetylneuraminic acid hydroxylase (Cmah) transcript variant 2	*Cmah*
-2.730	-1.439	NM_001081141	gamma-aminobutyric acid (GABA) B receptor 2	*Gabbr2*
-2.945	-1.432	NM_007606	carbonic anhydrase 3	*Car3*
-3.060	-1.425	NM_008061	glucose-6-phosphatase catalytic	*G6pc*
-3.297/ -1.584	-1.423/ -1.313	NM_134037	ATP citrate lyase (Acly) mRNA [NM_134037]	*Acly*
-3.509	-1.387	AK017236	adult male pituitary gland cDNA RIKEN full-length enriched library clone:5330406M23 product:unclassifiable full insert sequence	*5330406M23Rik*
-2.821- -2.710	-1.387- -1.328	NM_009692	apolipoprotein A-I	*Apoa1*

Values b/a from oligo b/oligo a; values a-n: value range of more than two (n) oligos.

Table 64: Mouse whole genome microarray analysis. 48 accordantly up-regulated genes in mouse livers by treatment with DL-congeners TCDD, 1-PeCDD, 4-PeCDF, PCB 126, or PCB 156. Listed in descending order according to TCDD-derived effects. TCDD-raw data by courtesy of Christiane Lohr (Lohr, 2013). Cutoff values: A ≥ 27, │lfc│ ≥ 1, p-value < 0.05.

	Gene	DL-congeners excepting PCB 118	
lfc (TCDD)	systematic name	Gene description	**Gene name**
9.478	NM_009992	cytochrome P450 family 1 subfamily a polypeptide 1	*Cyp1a1*
5.169	NM_009994	cytochrome P450 family 1 subfamily b polypeptide 1	*Cyp1b1*
3.985	NM_009993	cytochrome P450 family 1 subfamily a polypeptide 2	*Cyp1a2*
3.582	NM_010210	fragile histidine triad gene	*Fhit*
3.379	NM_017379	tubulin alpha 8	*Tuba8*
3.103	NM_027872	solute carrier family 46 member 3	*Slc46a3*
2.903	NM_178892	TCDD-inducible poly(ADP-ribose) polymerase	*Tiparp*
2.819	NM_008181	glutathione S-transferase alpha 1 (Ya)	*Gsta1*
2.678	NM_016865	HIV-1 tat interactive protein 2 homolog (human)	*Htatip2*
2.518	NM_025557	Purkinje cell protein 4-like 1	*Pcp4l1*
2.153	NM_023440	transmembrane protein 86B	*Tmem86b*
1.857/1.362	NM_013541	glutathione S-transferase pi 1	*Gstp1*
1.853	NM_001122660	predicted gene 10639	*Gm10639*
1.758	NM_007643	CD36 antigen	*Cd36*
1.696/1.65	NM_145603	carboxylesterase 2	*Ces2*
1.653	NM_001166250	monoglyceride lipase	*MgII*
1.63	NM_198171	cDNA sequence BC015286	*BC015286*
1.621/1.211	NM_025341	abhydrolase domain containing 6	*Abhd6*
1.602	NM_010902	nuclear factor erythroid derived 2 like 2	*Nfe2l2*
1.559	NM_181796	glutathione S-transferase pi 2	*Gstp2*
1.499	NM_026428	dicarbonyl L-xylulose reductase	*Dcxr*
1.481	NM_008030	flavin containing monooxygenase 3	*Fmo3*
1.441	NM_009150	selenium binding protein 1	*Selenbp1*
1.441	NM_009150	selenium binding protein 1	*Selenbp1*
1.423	NM_011099	pyruvate kinase muscle	*Pkm2*
1.394	NM_172881	UDP glucuronosyltransferase 2 family polypeptide B35	*Ugt2b35*
1.391	NM_009466	UDP-glucose dehydrogenase	*Ugdh*
1.316	NM_009768	basigin	*Bsg*
1.297	NM_008182	glutathione S-transferase alpha 2 (Yc2)	*Gsta2*
1.286	NM_001145875	RIKEN cDNA 9530008L14 gene	*9530008L14Rik*
1.282	XM_129965	Mus musculus gene model 1833	*Gm1833*
1.259	NM_001081372	predicted gene 5158	*Gm5158*
1.247/1.209	NM_008278	hydroxyprostaglandin dehydrogenase 15 (NAD)	*Hpgd*
1.244	NM_145953	cystathionase (cystathionine gamma-lyase)	*Cth*
1.198	NM_019771	destrin	*Dstn*
1.181	A_55_P2168781	Unknown	*A_55_P2168781*
1.156	NM_008828	phosphoglycerate kinase 1	*Pgk1*
1.15	NM_011671	uncoupling protein 2 (mitochondrial)	*Ucp2*
1.136	NM_020008	C-type lectin domain family 7	*Clec7a*
1.127	NAP096647-001	MUSXPGK phosphoglycerate kinase	*NAP096647-001*
1.111	NM_019749	gamma-aminobutyric acid receptor associated protein	*Gabarap*
1.105	NM_025797	cytochrome b-5	*Cyb5*
1.094	NM_009811	caspase 6	*Casp6*
1.093	NM_009801	carbonic anhydrase 2	*Car2*
1.069	NM_026185	abhydrolase domain containing 15	*Abhd15*
1.034	NM_001081036	predicted gene 9294	*Gm9294*
1.002	NM_025911	coiled-coil domain containing 91	*Ccdc91*

Values b/a from oligo b/oligo a; values a-n: value range of more than two (n) oligos.

Table 65: Mouse whole genome microarray analysis. 19 accordantly down-regulated genes in mouse livers by treatment with DL-congeners TCDD, 1-PeCDD, 4-PeCDF, PCB 126, or PCB 156. Listed in descending order according to TCDD-derived effects. TCDD-raw data by courtesy of Christiane Lohr (Lohr, 2013). Cutoff values: $A \geq 2^7$, $|lfc| \geq 1$, p-value < 0.05.

		DL-congeners excepting PCB 118	
lfc (TCDD)	Gene systematic name	Gene description	**Gene name**
-2.573/ -2.488	BC031891/ NR_002861	serine (or cysteine) peptidase inhibitor clade A member 4 pseudogene 1	*Serpina4-ps1*
-1.821	XM_001003154	similar to Glucose phosphate isomerase 1 transcript variant 2	*LOC676974*
-1.502	NM_001111110	cytidine monophospho-N-acetylneuraminic acid hydroxylase	*Cmah*
-1.439	NM_001081141	gamma-aminobutyric acid (GABA) B receptor	*Gabbr2*
-1.432	NM_007606	carbonic anhydrase 3	*Car3*
-1.425	NM_008061	glucose-6-phosphatase catalytic	*G6pc*
-1.423	NM_134037	ATP citrate lyase	*Acly*
-1.387- -1.328	NM_009692	apolipoprotein A-I	*Apoa1*
-1.276	NM_145368	acyl-coenzyme A amino acid N-acyltransferase 2	*Acnat2*
-1.15	NM_198649	actin binding LIM protein family	*Ablim3*
-1.135	ENSMUST0000 0099683	Unknown	*ENSMUST00000 099683*
-1.113	XM_001471861	hypothetical protein LOC100044148	*Etnk2*
-1.103	XM_001481023	hypothetical protein LOC100043770	*Gm4635*
-1.092	ENSMUST0000 0099050	Unknown	*ENSMUST00000 099050*
-1.073	ENSMUST0000 0099046	Unknown	*ENSMUST00000 099046*
-1.064	NM_011169	prolactin receptor	*Prlr*
-1.035	NM_021041	ATP-binding cassette	*Abcc9*
-1.031	ENSMUST0000 0099035	Q4YHF0_PLABE (Q4YHF0) Pb-fam-2 protein (Fragment)	*ENSMUST00000 099035*
-1.028	XM_914710	similar to EF-hand Ca2+ binding protein p22 (LOC638627)	*LOC638627*

Values b/a from oligo b/oligo a; values a-n: value range of more than two (n) oligos.

II. Curriculum Vitae **Sylke Neser**

Education

University of Kaiserslautern, Food Chemistry and Toxikology (since 2004)

- Research work (2008):
  'The impact of TCDD on DNA-methylation in primary rat hepatocytes'
- First state exam in food chemistry (2008)
- Diploma thesis (2009)

  „Impact of apple juice extracts and apple juice ingredients on the formation of reactive oxygen species *in vitro*" in the course of the Federal Ministry of Education and Research (Bundesministerium für Bildung und Forschung, BMBF)-funded Nutrition Net "Role of dietary components on the genesis of intestinal disorders and possibilities of their prevention by nutritional intervention"
- Degree: Qualified Food Chemist (Dipl.-LMChem.)

PhD

05/2009-10/2012	Research assistant in the department of chemistry, division of food chemistry and toxicology at the University of Kaiserslautern; Working group: Prof. Dr. Dr. Dieter Schrenk: Investigations on the impact of dioxins and dioxin-like polychlorinated biphenyls on gene expression *in vitro* und *in vivo* within the framework of the EU project SYSTEQ, which was funded under the Seventh Framework Programme of the European Commission.
Since 10/2012	Draft of the doctoral dissertation to acquire the doctoral degree in Natural Sciences; Dr. rer. nat.

Further education

Since 2009	Participation in the postgraduate education program of the German Society for experimental and clinical Pharmacology and Toxicology (Deutsche Gesellschaft für experimentelle und klinische Pharmakologie und Toxikologie e.V., DGPT) and the Helmholtz Center Munich to graduate as toxicologist (DGPT)

Publications

Article	Neser and Schrenk: ‘Use of palmitoylethanolamide for pain therapy – a safe dietary food for special medical purposes? (Palmitoylethanolamid gegen Schmerzen – Ein sicheres diätetisches Lebensmittel für medizinische Zwecke?)’ Deutsche Apothekerzeitung 2012, Ausgabe 22
Poster	Neser *et al.*: Dioxin 2011 (31st International Symposium on Halogenated Persistent Organic Pollutants), Brussels ’Induction of CYP1A activity in *in vitro* models as a basis for derivation of systemic TEFs’
Poster	Schrenk *et al.*: Dioxin 2011, Brüssel ’Applying TEFs in Risk Assessment (An Update on SYSTEQ, II)’
Poster	Neser *et al.*: Regionalverbandstagung der Lebensmittelchemischen Gesellschaft (LChG) der Gesellschaft Deutscher Chemiker (GDCh) 2012, Kaiserslautern ’Gene regulating effects in mouse liver subsequent to treatment with selected dioxin-like compounds and PCB 153 using whole genome microarray analysis’
Poster	Neser *et al.*: 78. Jahrestagung der Deutschen Gesellschaft für experimentelle und klinische Pharmakologie und Toxikologie e.V. (DGPT) 2012, Dresden ’Gene regulating effects in mouse liver subsequent to treatment with selected dioxin-like compounds and PCB 153 using whole genome microarray analysis’
Poster	Lohr *et al.*: 78. Jahrestagung der DGPT 2012, Dresden „Whole genome microarray analysis of the effects of TCDD and PCB 153 in human hepatic cell models“

Kaiserslautern, 7th of November 2014

III. Eidesstattliche Erklärung

Hiermit erkläre ich an Eides statt, dass ich die eingereichte Dissertation eigenständig verfasst, die für die Arbeit benutzten Hilfsmittel und Quellen genannt und die Ergebnisse beteiligter Mitarbeiter sowie anderer Autoren klar gekennzeichnet habe. Ich habe weder die Dissertation oder Teile der Disseration als Prüfungsarbeit bei einem anderen Fachbereich eingereicht noch ein Promotionsverfahren bei einer anderen Hochschule beantragt.

Kaiserslautern, 7. November 2014